December 2019

Part I: A Concise Asymmetric Synthesis of Microtubule Inhibitor Tryprostatin B Part II: Synthesis and Biological Assessment of Histone Deacetylase (HDAC) Inhibitors Part III: Acid Catalyzed Reactions of Aromatic Ketones with Ethyl Diazoacetate

Md Mizzanoor Rahaman
University of Wisconsin-Milwaukee

PART I: A CONCISE ASYMMETRIC SYNTHESIS OF MICROTUBULE INHIBITOR TRYPROSTATIN B

PART II: SYNTHESIS AND BIOLOGICAL ASSESSMENT OF HISTONE DEACETYLASE INHIBITORS

PART III: ACID CATALYZED REACTIONS OF AROMATIC KETONES WITH ETHYL DIAZOACETATE

by

Mizzanoor Rahaman

A Dissertation Submitted in

Partial Fulfillment of the

Requirements for the Degree of

Doctor of Philosophy

in Chemistry

at

The University of Wisconsin-Milwaukee

December 2019

ABSTRACT

PART I: A CONCISE ASYMMETRIC SYNTHESIS OF MICROTUBULE INHIBITOR TRYPROSTATIN B

PART II: SYNTHESIS AND BIOLOGICAL ASSESSMENT OF HISTONE DEACETYLASE INHIBITORS

PART III: ACID CATALYZED REACTIONS OF AROMATIC KETONES WITH ETHYL DIAZOACETATE

by

Mizzanoor Rahaman

The University of Wisconsin-Milwaukee, 2019
Under the Supervision of Professor M. Mahmun Hossain

PART I: A CONCISE ASYMMETRIC SYNTHESIS OF MICROTUBULE INHIBITOR TRYPROSTATIN B

Tryprostatin (TPS) A and B, microtubule inhibitor, are the members of a family of prenylated Trp-Pro diketopiperzine alkaloids. These two natural products were isolated in 1995 from the fermentation broth of *Aspergillus fumigatus* BM939 by Osada and coworkers. TPS and related diketopiperazine containing compounds such as phenylahistins, spirotryprostatins, and cyclotryprostatins are inhibitors of the mammalian cell cycle. They prevent cell cycle progression at the G2/M phase through a unique mechanism consisting of inhibiting the interaction between microtubule assisted proteins (MAP-2) and the C-terminal end of tubulin. TPS A and B hold great potential because they were found to have inhibitory activity on the cell cycle progression of mouse tsFT210 cells with minimum inhibitory concentration (MIC) values of 16.4 μM for TPS A and 4.4 μM for TPS B, respectively. The poor abundance of TPS A and B in nature and long synthetic

procedure have limited their development as viable anti-cancer therapeutics. On the other hand, their interesting biological activity and simple structure have drawn attention from the synthetic community, and several total syntheses have been reported. Herein, a concise and efficient total synthesis of tryprostatin B was described. The key step was the preparation of a diprenylated gramine salt where the prenyl group was incorporated at the 2-position of the indole moiety by direct lithiation of the Boc-protected gramine. We also developed and optimized the asymmetric phase-transfer-catalyzed reaction with diprenylated gramine salt to provide the C2-prenyl tryptophan intermediate resulting in 93% enantiomeric excess (ee) and 65% yield. The total synthesis of tryprostatin B was done in six steps with 35% overall yield.

PART II: SYNTHESIS AND BIOLOGICAL ASSESSMENT OF HISTONE DEACETYLASE INHIBITORS

Histone acetylation and deacetylation in eukaryotic cells is delicately maintained by histone acetyltransferases (HAT) and histone deacetylases (HDAC). These enzymes are responsible for the modifications to chromatin structures and regulation of transcription. In general HAT activity leads to an increase in gene transcription through the opening of the chromatin framework by adding acetyl groups. In contrast, HDAC catalyze the removal of the acetyl groups on lysine residues located on the NH_2 terminal tails of core histones, which leads to gene repression by chromatin condensation. As a result, inhibition of HDAC activity can result in a general hyperacetylation of histones, which is followed by the transcriptional activation of certain genes through relaxation of the DNA conformation. These posttranslational modifications are essential for the regulation of many cellular processes. Natural product-based HDAC inhibitors such as

vorinostat (SAHA), romidepsin (FK228) are usually very potent, moderately isoform-selective, but are often associated with poor solubility, ineffective against solid tumors and excessive cytotoxicity. To overcome these limitations of the market drugs, a group of HDAC inhibitors were synthesized based on market drug FK228. One of our synthetic compounds was found to be active against class I HDAC and possibly effective against Alzheimer's disease. Further investigations, including microsomal assays and pharmacokinetic studies, are currently underway.

PART III: ACID CATALYZED REACTIONS OF AROMATIC KETONES WITH ETHYL DIAZOACETATE

3-Hydroxyacrylates or 3-oxo-esters are useful precursors for synthesizing important biologically active and pharmaceutically important compounds due to their multiple functionality and preferable substrate scope. These synthons are also applied for the construction of quaternary carbon center containing compounds due to the presence of an active prochiral center. In 1998 and later in 2004, our group reported the unprecedented reactions of aromatic aldehydes with ethyl diazoacetate (EDA) in the presence of the iron Lewis acid and the Brønsted type acid, respectively. This novel reaction formed 3-hydroxyacrylates by an unusual 1, 2-aryl shift. In this project, we extended this method for less reactive aromatic ketones with EDA using Brønsted acid catalyst to produce the 3-hydroxyacrylates. 3-hydroxyacrylates and 3-oxo-esters were isolated from the reactions by 1,2-aryl/alkyl shifts. The products from these reactions can be applied to make all-carbon quaternary center containing natural products.

To

My Beloved Parents

And

My Cute Daughter, Rain

TABLE OF CONTENTS

PART I: A CONCISE ASYMMETRIC SYNTHESIS OF MICROTUBULE INHIBITOR TRYPROSTATIN B

PART II: SYNTHESIS AND BIOLOGICAL ASSESSMENT OF HISTONE DEACETYLASE INHIBITORS

PART III: ACID CATALYZED REACTIONS OF AROMATIC KETONES WITH ETHYL DIAZOACETATE

LIST OF FIGURES

PART I: A CONCISE ASYMMETRIC SYNTHESIS OF MICROTUBULE INHIBITOR TRYPROSTATIN B

PART II: SYNTHESIS AND BIOLOGICAL ASSESSMENT OF HISTONE DEACETYLASE INHIBITORS

PART III: ACID CATALYZED REACTIONS OF AROMATIC KETONES WITH ETHYL DIAZOACETATE

LIST OF SCHEMES

PART I: A CONCISE ASYMMETRIC SYNTHESIS OF MICROTUBULE INHIBITOR TRYPROSTATIN B

PART III: ACID CATALYZED REACTIONS OF AROMATIC KETONES WITH ETHYL DIAZOACETATE

LIST OF TABLES

PART I: A CONCISE ASYMMETRIC SYNTHESIS OF MICROTUBULE INHIBITOR TRYPROSTATIN B

PART III: ACID CATALYZED REACTIONS OF AROMATIC KETONES WITH ETHYL DIAZOACETATE

ACKNOWLEDGEMENTS

LIST OF ABBREVIATIONS

ACN	Acetonitrile
Boc	*t*-Butyloxycarbonyl
DCM	Dichloromethane
DCE	1, 2-Dichloroethane
DEA	Diethylamine
DIPEA	*N, N*-Diisopropylethylamine
DMAP	4-Dimethylaminopyridine
DMF	Dimethylformamide
DME	Dimethoxyethane
EDA	Ethyl diazoacetate
EtOAc	Ethyl acetate
Et$_2$O	Diethyl ether
HAT	Histone acetyltransferase
HDAC	Histone deacetylase
*i*PrOH	Isopropyl alcohol
MeOH	Methanol
MTT	3-(4,5-Dimethylthiazol-2-yl)-2,5-diphenyltetrazolium bromide
PTC	Phase-transfer catalyst
PyBOP	Benzotriazol-1-yl-oxytripyrrolidinophosphonium hexafluorophosphate
TEA	Triethylamine
THF	Tetrahydrofuran

PART I: A CONCISE ASYMMETRIC SYNTHESIS OF MICROTUBULE INHIBITOR TRYPROSTATIN B

1.1. INTRODUCTION

1.1.1. Microtubules

Microtubules are ropelike polymers of tubulin proteins, found in all eukaryotic cells and they are key components of the cytoskeleton (Figure 1.1).[1] They are formed by the polymerization of a dimer of two globular proteins, *alpha (α)-* and *beta (β)*-tubulin into protofilaments that can then associate laterally to form a hollow tube, the microtubule.[2] The most common form of a microtubule consists of 13 parallel rows and can grow as long as 50 micrometers in the tubular arrangement.[3,4] The outer diameter of microtubule is about 24 nm and the inner diameter is about 12 nm.[4,5] Microtubules are long, hollow cylinders made up of polymerized $α$- and $β$-tubulin dimers in eukaryotes cells. These two tubulin proteins join back to back and make polymers.[6] Microtubules have a distinct polarity that is critical for their biological function. When $α$-tubulin exposed it is called negative end and when $β$-tubulin exposed it is called positive end. While microtubule elongation can occur at both the positive end and negative ends, it is significantly more rapid at the positive end.[7] Microtubule inhibitor binds to $β$-tubulin to stop polymerization. Microtubules are important for the function of cellular processes. They are involved in maintaining the shape and size of the cell, and transport materials in the cell.[8] Microtubules are also involved in cell division system by mitosis and meiosis and are the major constituents of mitotic spindles, which are used to pull eukaryotic chromosomes apart.[9]
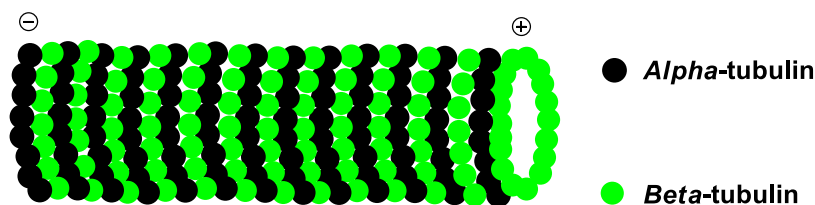
Figure 1.1: Structure of Microtubule

1.1.2. Microtubules in Cell Division

The cell cycle is the vital process where a single cell divides into two different cells. It is the series of events by which a cell duplicates its DNA (DNA replication) and divides of cytoplasm and organelles to produce two daughter cells.[10] After formation of daughter cells, each of the daughter cell begin the process of new cell cycle.[11] Actually, the cell cycle is broken down into four phases (Figure 1.2). In Gap 1 phase, also known as G1 phase, cells increase in size and make sure everything is ready for DNA replication and go to the synthesis (S) phase. In the S-phase where DNA replication occurs. In the Gap 2 phase, also known as G2 phase, the cells increase in size and ensures that cell is ready to enter the Mitosis (M) phase. In the Mitosis (M) phase, cells growth stops and divide into two daughter cells.[12-13]
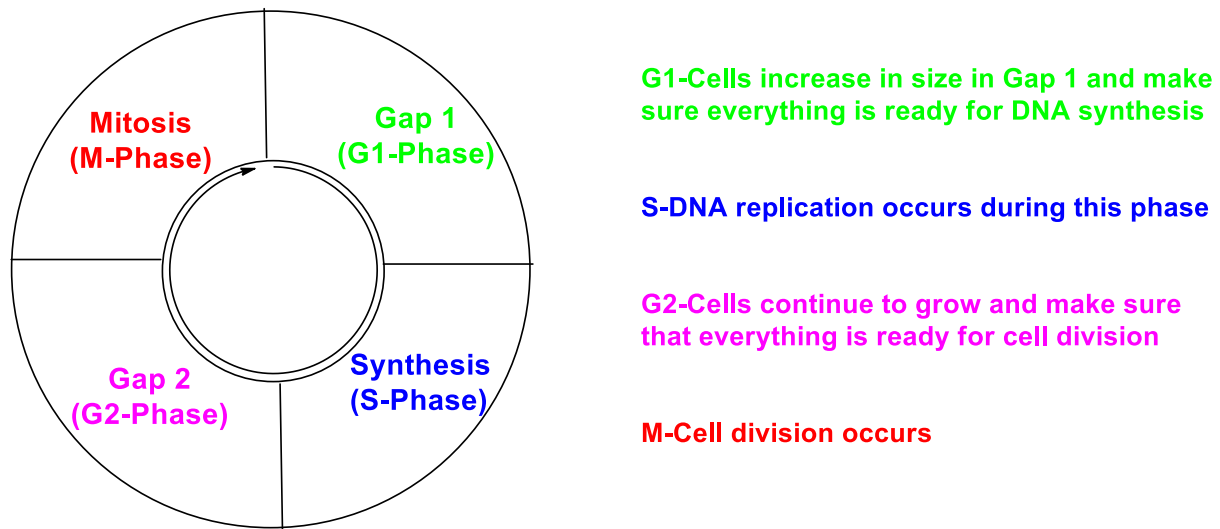
Figure 1.2: Schematic Diagram of Cell Division with Four Different Phases

1.1.3. How Microtubule Inhibitors Work

In the cell cycle process, cells are entered the four different phases; G1 phase, S-phase, G2-phase, and M-phase. There are two different check points in the cell cycle, G1/S check point and G2/M check point (Figure 1.3). In the mitosis (M) phase, there are four different sub-phases; prophase, metaphase, anaphase, and telophase (Figure 1.4).[11-13] The earliest sub-phase in mitosis phase is prophase, in this phase early stage spindle formation occurs. The condensation of the chromatin and the disappearance of the nucleolus are the two main function in prophase.[13] Anti-cancer drugs are designed based on these two check points, some drugs control the G1/S check point and stop DNA replication, and other drugs control the G2/M check point and stop cell division. Microtubule inhibitors bind with beta-tubulin at the G2/M check point and stop the early-stage spindle formation at metaphase stage.[14]
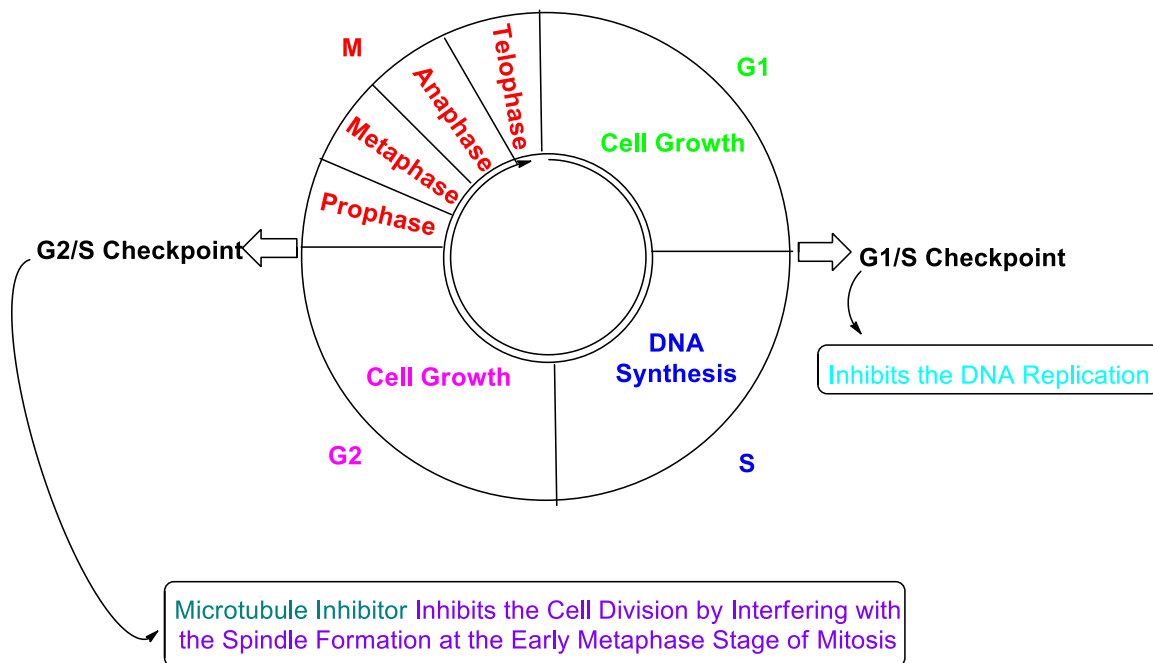
Figure 1.3: Cell cycle with Two Check Points

Mitotic spindles sometimes called the spindle apparatus is used by nearly all eukaryotic cells to separate their chromosomes during cell division. This includes the microtubule-associated proteins (MAPs) and the microtubule organization center (MTOC).[15] Cytoskeletal drugs are small molecules that interact with action or tubulin. Some drugs destabilize the microtubules, and others prevent polymerization. Microtubule inhibitors such as tryprostatins bind to actin monomers and prevents polymerization of actin filaments and stop pomerization.[16] Microtubule inhibitors have been also able to bind to tubulin protein and change its activation site, for this reason the microtubule dynamics are manipulated. By the interference of spindle formation, microtubule inhibitor can prevent a cell from going into a cell cycle and can lead to programmed cell death or apoptosis.[17] Microtubule dynamics can be suppressed by both microtubule stabilizer and destabilizers. The taxane family, for example, paclitaxel act as stabilizer anti-cancer drug that stabilize the microtubule, preventing it from disassembling, and on the other hands, vinca alkaloids, for example, vinblastine-vincristine have the opposite effect, and these destabilize the microtubule (Figure 1.4).
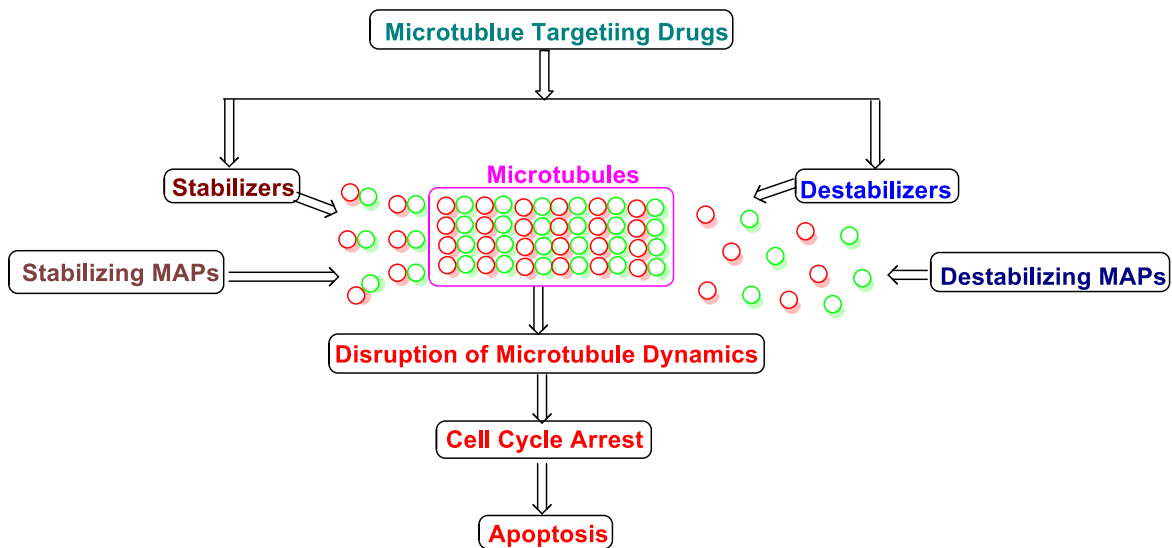
Figure 1.4: Block Diagram of Microtubule Drugs Function

1.1.4. Microtubule Inhibitors

Microtubule inhibitors such as vinca alkaloids (vinblastine, vincristine), taxanes (paclitaxel), and indole based diketopiperazine (tryprostatins) compounds destabilize microtubules and suppress microtubule dynamics proper mitotic function, effectively blocking cell cycle progression and resulting in apoptosis (Figure 1.5).[19,20] To elucidate the biological function of a cellular factor, development of specific inhibitors is a successful approach. There are many examples applying inhibitors to elucidate the regulatory mechanism of the cell cycle. Specific and effective inhibitors of the cell cycle should be useful tools for the investigation of the cell cycle mechanism and good candidates for cancer chemotherapy.[21]

Vinblastine

Vincristine

Paclitaxel
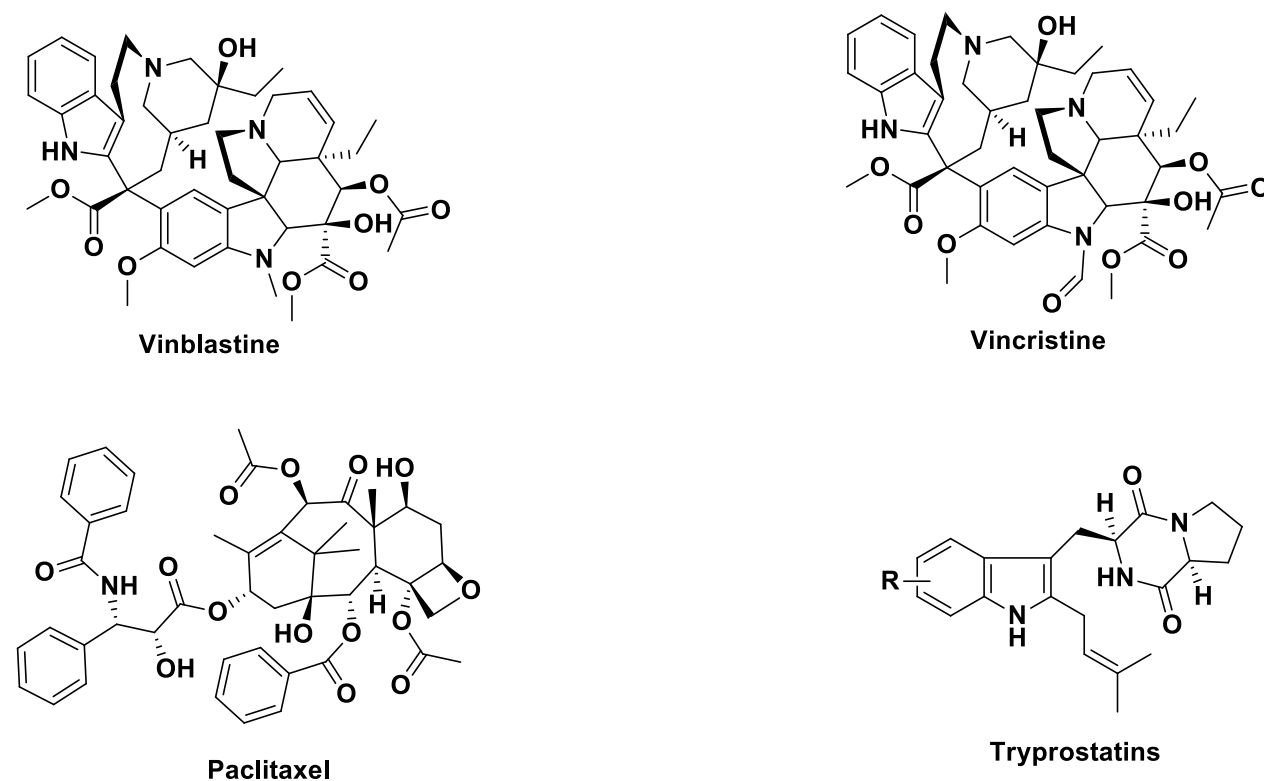
Tryprostatins

Figure 1.5: Examples of Some Microtubule Inhibitors

1.2. Isolation and Background of Tryprostatin A and B

Tryprostatin (TPS) A and B (Figure 1.6) are members of a family of prenylated Trp-Pro diketopiperzine alkaloids. These two natural products were isolated in 1995 from the fermentation broth of *Aspergillus fumigatus* BM939 by Osada and coworkers.[22] These two compounds operate through a mode of action by inhibiting multiple-drug resistance, which is a major obstacle in chemotherapy, showing promise as anti-cancer anti-mitotic agents. TPS and related diketopiperazine ring containing compounds such as phenylahistins, spirotryprostatins, and cyclotryprostatins are inhibitors of the mammalian cell cycle.[23-25] It was found that tryprostatins A **1** and B **2** completely inhibited cell cycle progression of tsFT210n cells in the G/2M phase at a final concentration of 50 µg/ml of **1** and 12.5 µg/ml of **2**, respectively.[25] They prevent cell cycle progression at the G2/M phase through a unique mechanism consisting of inhibiting the interaction between microtubule-assisted proteins (MAP-2) and the C-terminal end of tubulin. TPS A and B have great potential because they were found to have inhibitory activity on the cell cycle progression of mouse tsFT210 cells with minimum inhibitory concentration (MIC) values: 16.4 µM for TPS A and 4.4 µM for TPS B, respectively.[23,26] Multidrug resistance (MDR) in human cancers is one of the major causes of failure in chemotherapy. Fungal secondary metabolite Tryprostatin A (TPS-A) was analyzed with regard to its potency to reverse the Breast Cancer Resistance Protein (BCRP) mediated drug resistance. No cytotoxicity was seen at effective concentrations, indicating that TPS-A is a novel BCRP inhibitor. The scarcity of TPS A and B in nature and long, low-yielding synthetic procedures have limited their development as viable anticancer therapeutics.[27-33]

TPS A and B contain a 2-prenylindole moiety and diketopiperazine unit.[34]
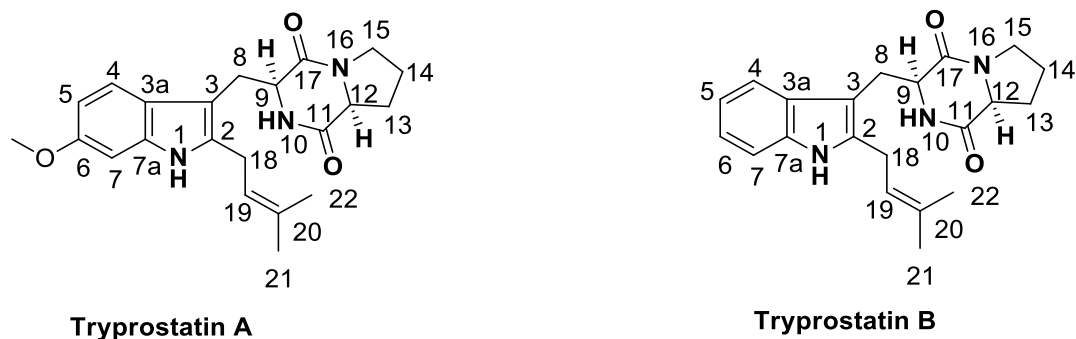
Figure 1.6: Structure of Microtubule Inhibitor, Tryprostatin A and B

Like TPS A and B, there are a lot of natural products are reported which contain 2-prenylindole moiety and diketopiperazine units such as spirotryprostatin A and B (Figure 1.7). These two are isolated from *Aspergillus fumigatus* is a species of fungus of sea sediment. Like several other indolic alkaloids, they have been found to have anti-mitotic properties, and as such they have become of great interest as anti-cancer drugs.

Figure 1.7: Structure of Spirotryprostatin A and B

Osada *et al.* isolated TPS A and B, spirotryprostatin A and B, and new compounds called the cyclotryprostatins A-D which belong to the family of Fumitregorins.[35] Cyclotryprostatins A-D also prevent cell cycle progression at the G2/M phase. They inhibited cell cycle progression of tsFT210 cells in the G2/M phase with IC_{50} values of 5.6µM, 19.5µM, 23.4µM, and 25.3µM, respectively (Figure 1.8).[36-37] Fumitremorgins A-C, that belong to a class of naturally diketopiperazines, are tremorogenic metabolites of *Aspergillus* and *Penicillium*.[38]

R=H, Cyclotryprostatin A
R=CH$_3$, Cyclotryprostatin B

Cyclotryprostatin C

Cyclotryprostatin D

Fumitremorgin A

Fumitremorgin B

Fumitremorgin C
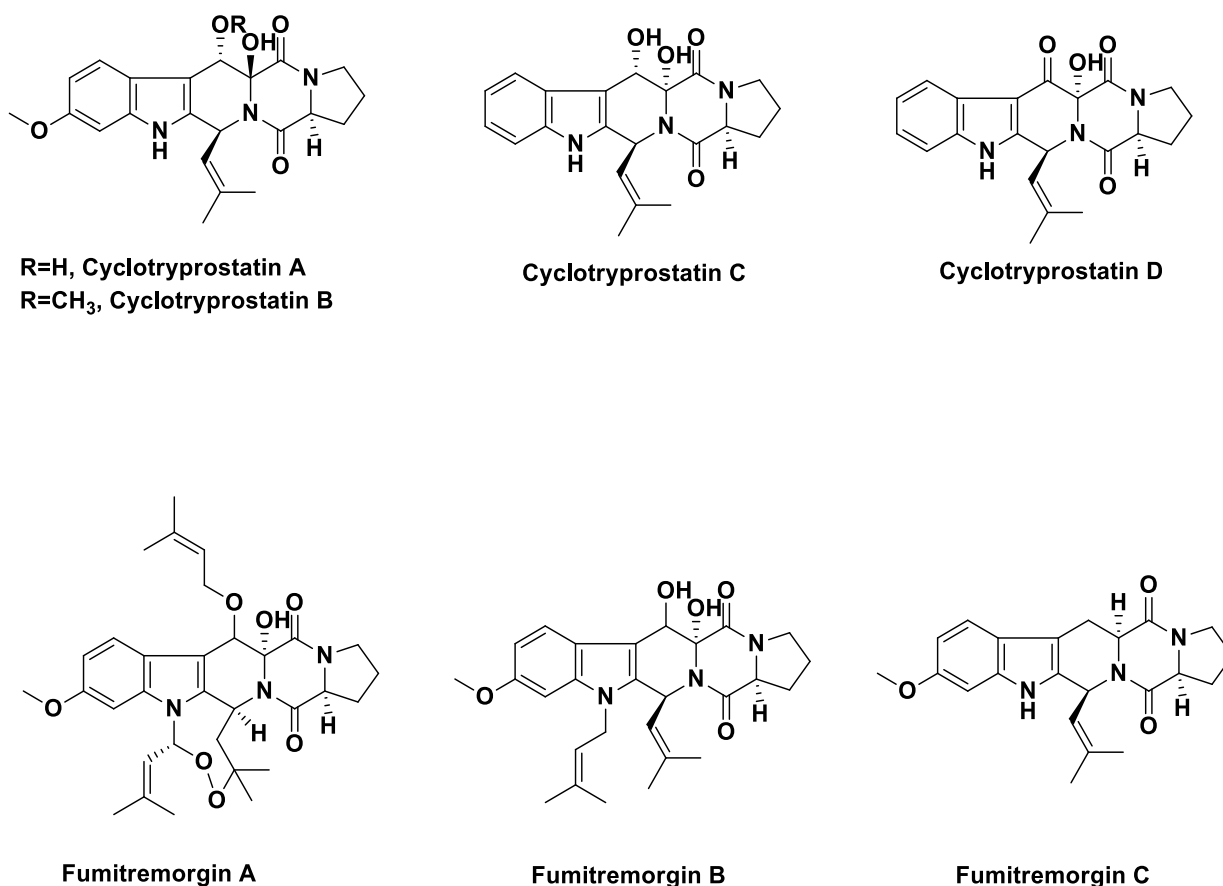
Figure 1.8: Example of Trp-Pro Diketopiperzine Alkaloids

Tryprostatins are important compounds for treating cancer, via microtubule inhibition. Microtubules are promising targets for stopping the cell division of cancer cells.[39,40] The interesting biological activity of these alkaloids has stimulated interest in their total synthesis. The scarcity of TPS A and B in nature and long, low-yielding synthetic procedures have limited their development as viable anticancer therapeutics. On the other hand, their interesting biological activity and simple structure have drawn attention from the synthetic community, and several total syntheses have been reported.[41-52] The first total synthesis of the Tryprostatin B was reported by Danishefsky et al. via the chloroindolenine/borane approach. Illustrated by the scheme below.[41]

1.2.1. Danishefsky's Synthesis of Tryprostatin B in 1996

In the Danishefsky's synthesis of tryprostatin B in 1996, the *N*-phthaloyl-*L*-tryptophan methyl ester was treated with tert-butyl hypochlorite to generate the chloroindolenine intermediate at 0 °C. This intermediate was then treated with tri-*n*-butylprenyl stannane and followed by rapid addition of boron trichloride (two equivalents) to provide the desired 2-prenyl tryptophan derivative. This is the way to introduce a prenyl function at the 2-position of a 3-substituted indole. Removal of the *N*-phthaloyl protecting group generated the required *L*-2-prenyltryptophan methyl ester. The coupling reaction between the 2-prenyl tryptophan and the *N*-Boc-*L*-proline acid fluoride to afford dipeptide. The Boc-protecting group was removed on treatment of material with trimethylsilyl iodide in acetonitrile to afford the free amine. When the free amine was stirred in a solution of ammonia/methanol for 24 h, the formation of the diketopiperazine unit resulted in Tryprostatin B identical to the natural material (Scheme 1.1).
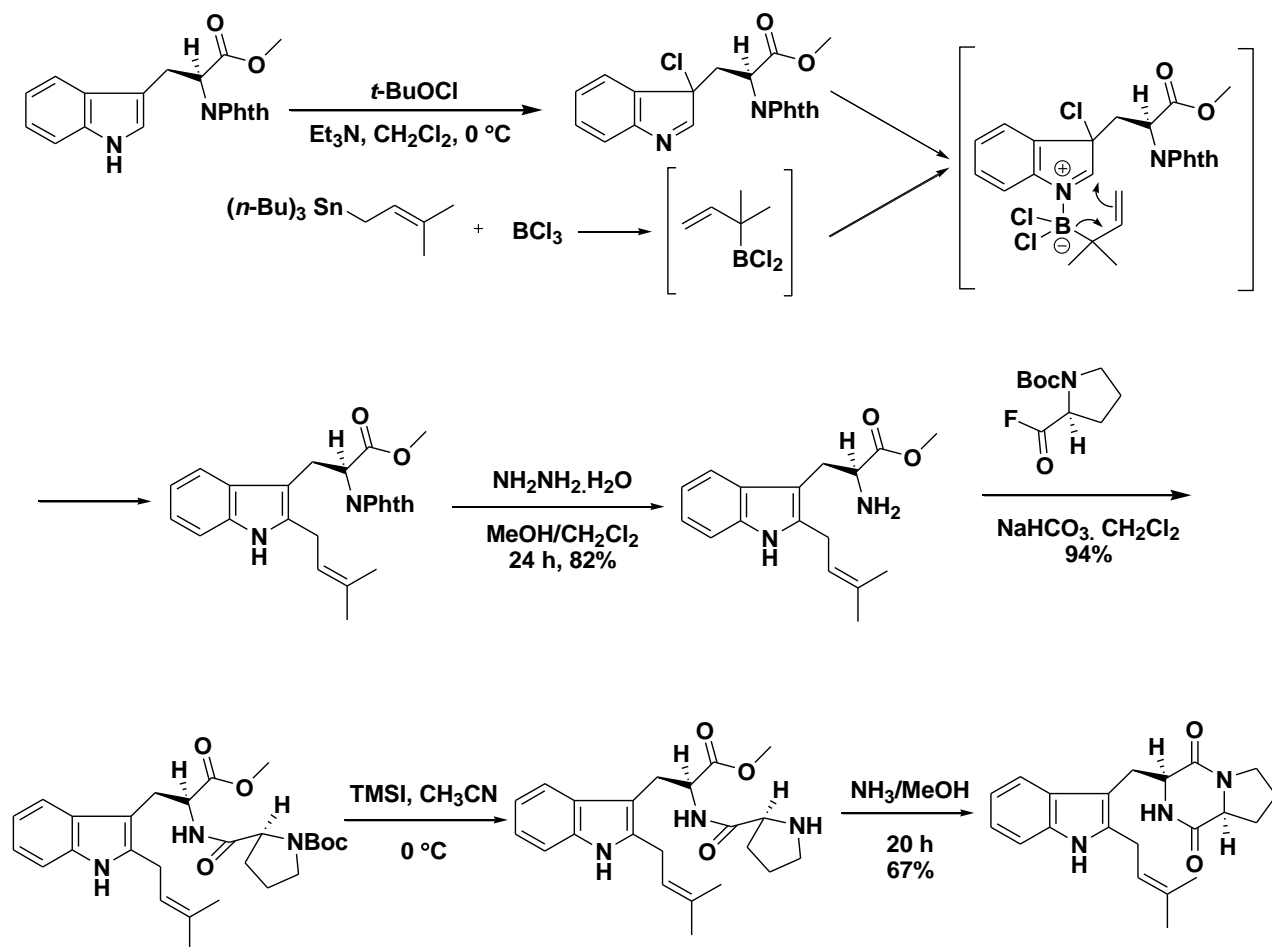
Scheme 1.1: Danishefsky's Synthesis of Tryprostatin B

1.2.2. Synthesis of Tryprostatin A by Cook et al. in 1997

The first total synthesis of tryprostatin A was completed by Cook and his coworkers *via* a regiospecific bromination process coupled with the Schöllkopf chiral auxiliary.[42-44] The regiospecific bromination of 3-methylindoles were achieved at the indole 2-position via an electrophilic process or at the 3-methyl position under free radical conditions, this method appeared to be useful for the preparation of a 2-prenyltryptophans and later tryprostatins.

The synthesis began with the Fischer indole cyclization via a Japp-Klingmann azo-ester intermediate (Scheme 1.2). The azo-ester intermediate was formed when *m*-anisidine was treated with sodium nitrite and concentrated aqueous HCl at 0 °C, followed by the addition of ethyl α-ethylacetoacetate, this intermediate was heated in a solution of 3 N ethanolic HCl, the desired ethyl 6-methoxy-3-methylindole- 2-carboxylate was obtained. Alkaline hydrolysis of the ester under yielded the corresponding carboxylic acid which was converted into 6-methoxy-3-methyl indole in excellent yield via the subsequent copper/quinoline-mediated decarboxylation sequence. To protect indole N(H) moiety, 6-methoxyindole was treated with di-tert-butyl decarbonate in presence dimethoxyamonopyridine. The protected 3-methylindole was then reacted with N-bromosuccinamide (NBS) in carbon tetrachloride to provide the 2-bromoindole as illustrated in Scheme 2. When 2-bromoindole was reacted with NBS under free radical conditions, azobisisobutyronitrile (AIBN), dibromide indole was obtained in 93% yield. Dibromide was coupled with the Schöllkopf chiral auxiliary at -78 °C, a pyrazine compound was obtained in 91% yield. The pyrazine was treated with *n*-butyllithium at -78 °C, followed by addition of prenyl bromide, 2-isoprenylpyrazine was isolated in 86% yield. The pyrazine group was removed under acidic conditions (aqueous HCl, THF) in 94% yield to provide D-valine ethyl ester and the 2-prenyltryptophan. The 6-methoxy-2-prenyltryptophan was stirred with *N*-(trichloroethoxy carbonyl)(Troc)-*L*-prolyl chloride in the presence of triethylamine in CH$_2$Cl$_2$ at 0 °C, the desired dipeptide was obtained. The Troc protecting group was removed by heating with Zn (dust) in refluxing MeOH. Finally, formation of the diketopiperazine unit and removal of Boc-protecting group from the indole N(H) function were achieved when dipeptide was heated at 160 °C (neat) to furnish tryprostatin A in 50% overall yield (Scheme 1.2).
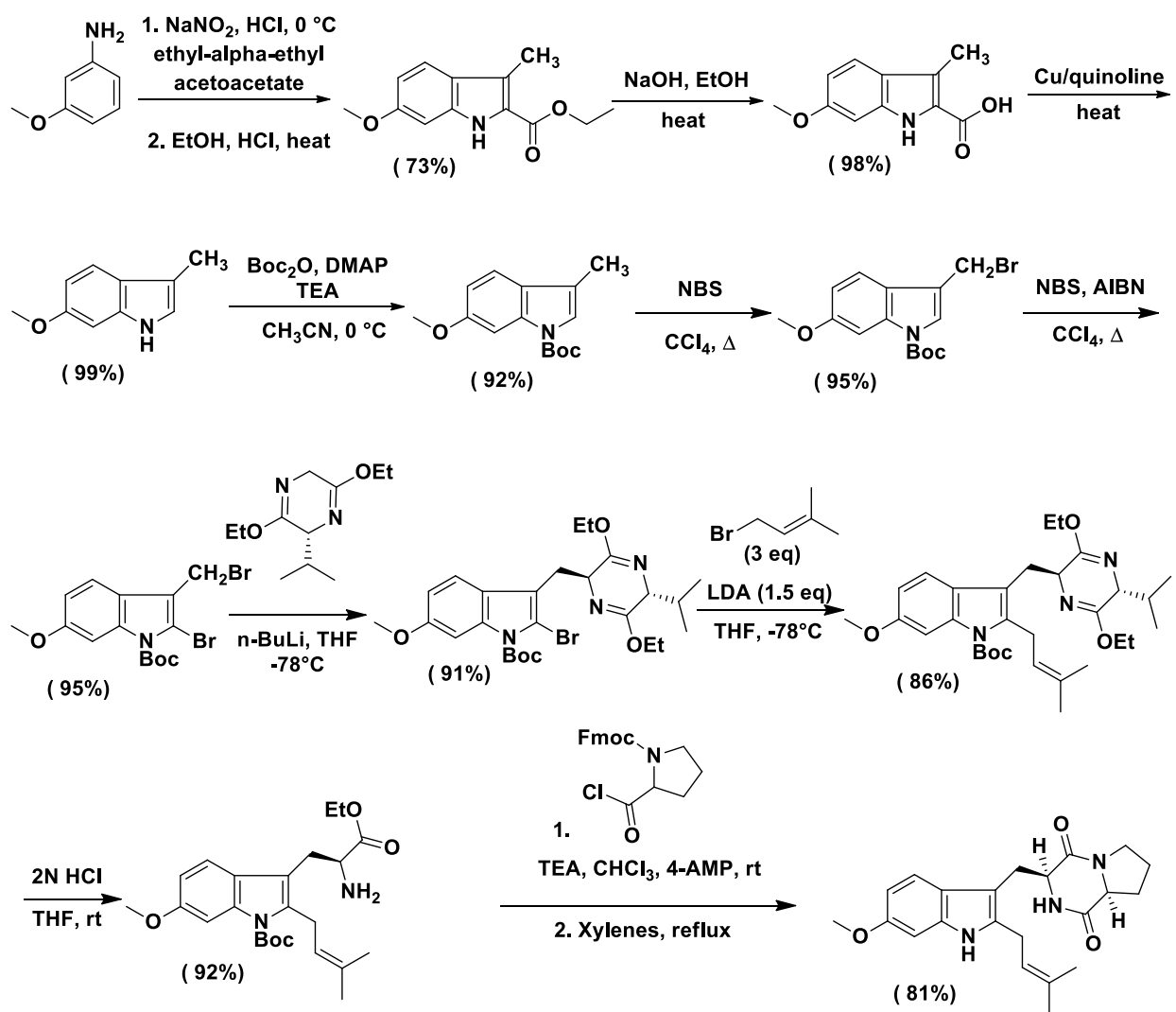
Scheme 1.2. Cook's Synthesis of Tryprostatin A

Later the synthesis of tryprostatin A and B as well as their enantiomers was developed by Cook (Scheme 1.3).[44] In order to introduce the prenyl group at the indole C-2 position of and decrease the number of steps earlier reported by Cook *et al.* LDA was employed to form the anion at C(2). The indole was stirred with LDA at -78 ˚C followed by the addition of dry, pure prenyl bromide to furnish 2-prenylpyrazine. This was an improvement over the synthesis of 2-prenylpyrazine, and this procedure was use for tryprostatin B.

Tryptophan preparation for the synthesis of tryprostatin A and B

R = OMe
R =H
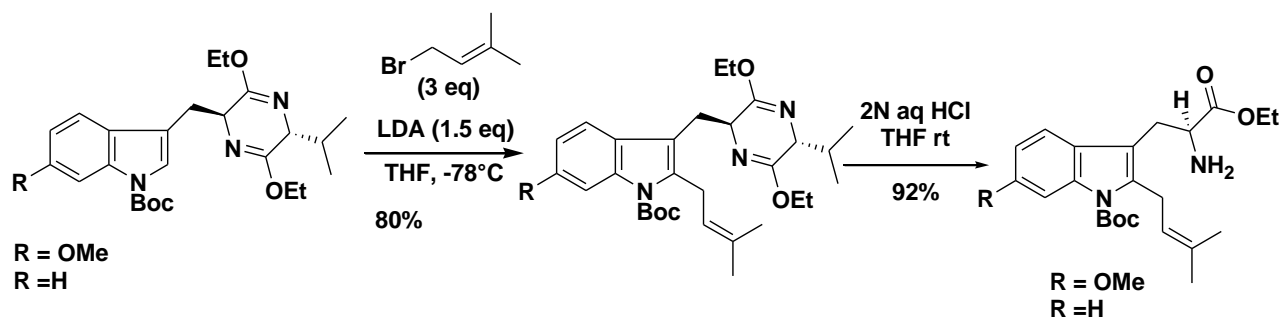
Tryptophan preparation for the synthesis of 9-epimer tryprostatin A and B

R = OMe
R =H
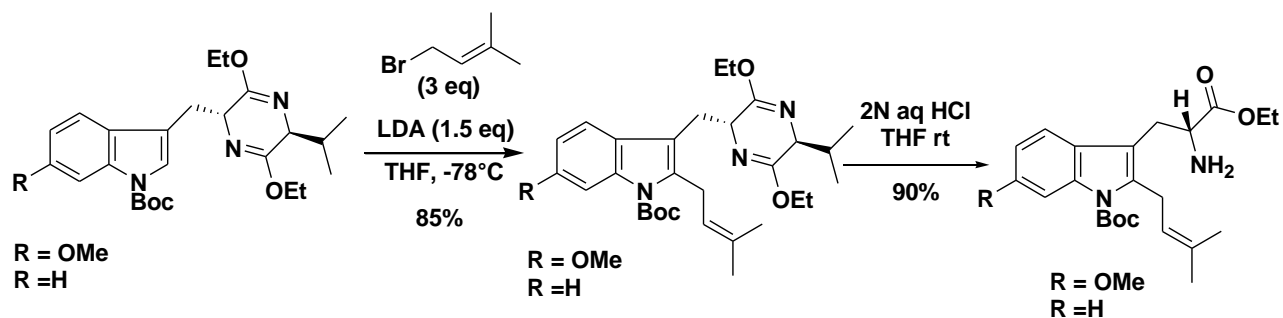
Scheme 1.3. Synthesis Enantiomers of Tryptophans by Cook et al.

With the key 2-prenyltryptophan derivatives in hand, the diketopiperazine unit was built on as illustrated, 2-prenyl-tryptophans were stirred with *N*-Fmoc-*L*-prolyl chloride in the presence of triethylamine in chloroform at room temperature. The Fmoc-protecting group was removed by addition of diethylamine (DEA) in acetonitrile. Formation of the diketopiperazine as well as the removal of the Boc-protecting group from the indole N(H) were achieved by heating in refluxing xylenes in high dilution. A stereospecific, enantiospecific total synthesis of tryprostatin A and B was accomplished *via* alkylation of the corresponding 2-lithioindole derivatives. This procedure was also applied to the enantiomers of tryprostatin A and tryprostatin B (Scheme 1.4). The optical rotations of the natural products and the enantiomers agreed with those reported by Osada *et al.* for the natural products. This route was used for the total synthesis of the mismatched pairs of tryprostatin A and B for biological screening.

R = OMe Typrostatin A
$[\alpha]^{27}{}_D$ = -65.9° (c = 0.97, in CHCl$_3$)
R =H Tryprostatin B
$[\alpha]^{26}{}_D$ = -70.9° (c = 0.80, in CHCl$_3$)

R = OMe enantiomer of Tryprostatin A
$[\alpha]^{28}{}_D$ = 70.3° (c = 1.0, in CHCl$_3$)
R =H enantiomer of Tryprostatin B
$[\alpha]^{26}{}_D$ = 71.9° (c = 1.1, in CHCl$_3$)

R = OMe, ds1-try A
R =H, ds1-try B

R = OMe, ds2-try A
R =H, ds2-try B
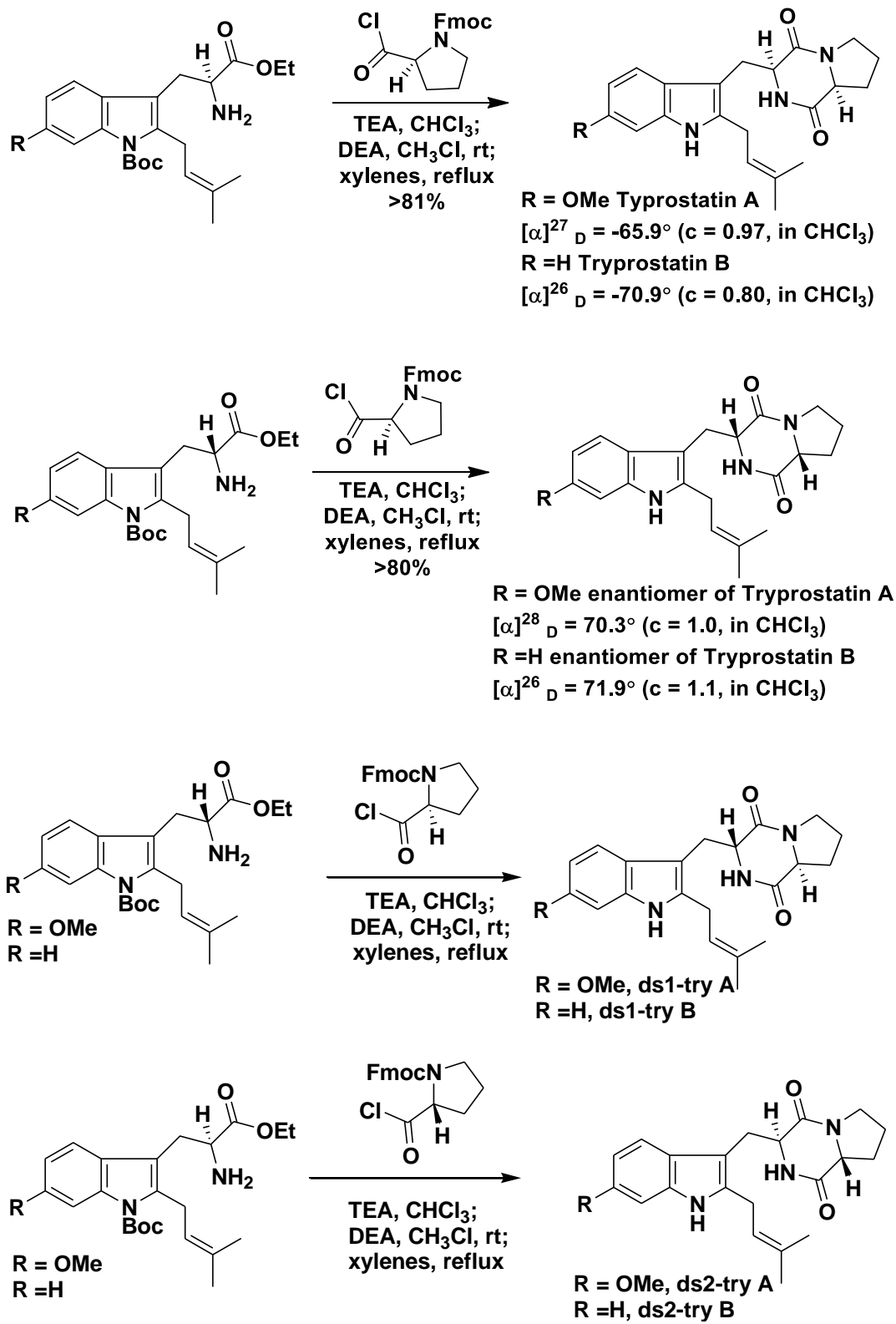
Scheme 1.4. Synthesis of Enantiomers and Diastereomers of Tryprostatin A and B.

15

1.2.3. Fukuyama's Most Recent Synthesis of Tryprostatin A and B in 2010

Fukuyama and his coworkers synthesized TPS A and B from the Garner aldehyde.[51,52] The Garner aldehyde was treated with carbon tetrabromide, triphenyl phosphine in presence of triethyl amine followed by Grignard reagent ethyl magnesium bromide at 0 °C formed alkyne which was went to the Sonogashira coupling with 2-iodoformanilide, partial reduction of the triple bond was examined by the treatment with $Zn/LiCuBr_2$ in ethanol gave the desired product along with the corresponding amine in 2,2,2-trifluoroethanol as the solvent to suppress the undesired solvolysis with 99% yield. Subsequent dehydration with bis(trichloromethyl) carbonate (triphosgene) gave the ortho-alkenyl isocyanide and thus set the stage for a radical-mediated cyclization where 2,2'-azobis(4- methoxy-2,4-dimethylvaleronitrile) (V-70, 20) acts as a radical initiator with a lower decomposition temperature. Thus, we established reliable conditions for imidoyl-radical-mediated indole synthesis. When this method was applied to the radical cyclization of the isocyanide, complete selectivity was observed for the cyclization of the imidoyl radical to give the 2-stannylindole and by Stille-type coupling reaction. The desired 2-prenyl indole product was obtained in only 82% yield with prenyl acetate as the coupling partner in presence of triphenylarsine, lithium chloride, and [Pd2(dba)3] as the catalyst. The 2-prenyl indole moiety N(H) was protected with a Boc group, hydrolysis of the acetonide, and oxidation of the resulting alcohol to the carboxylic acid with 2,2,6,6-tetramethylpiperidin-1-oxyl (TEMPO). Under reflux in N-methylpyrrolidinone (NMP) conditions, spontaneous cyclization occurred to give tryprostatin B (2) in 89% yield. Thus, tryprostatin B was synthesized by Fukuyama and coworkers in 11 steps from Garner aldehyde in 33% overall yield on a half-gram scale. By following the similar method, tryprostatin A was synthesized in 30% overall yield (Scheme 1.5).
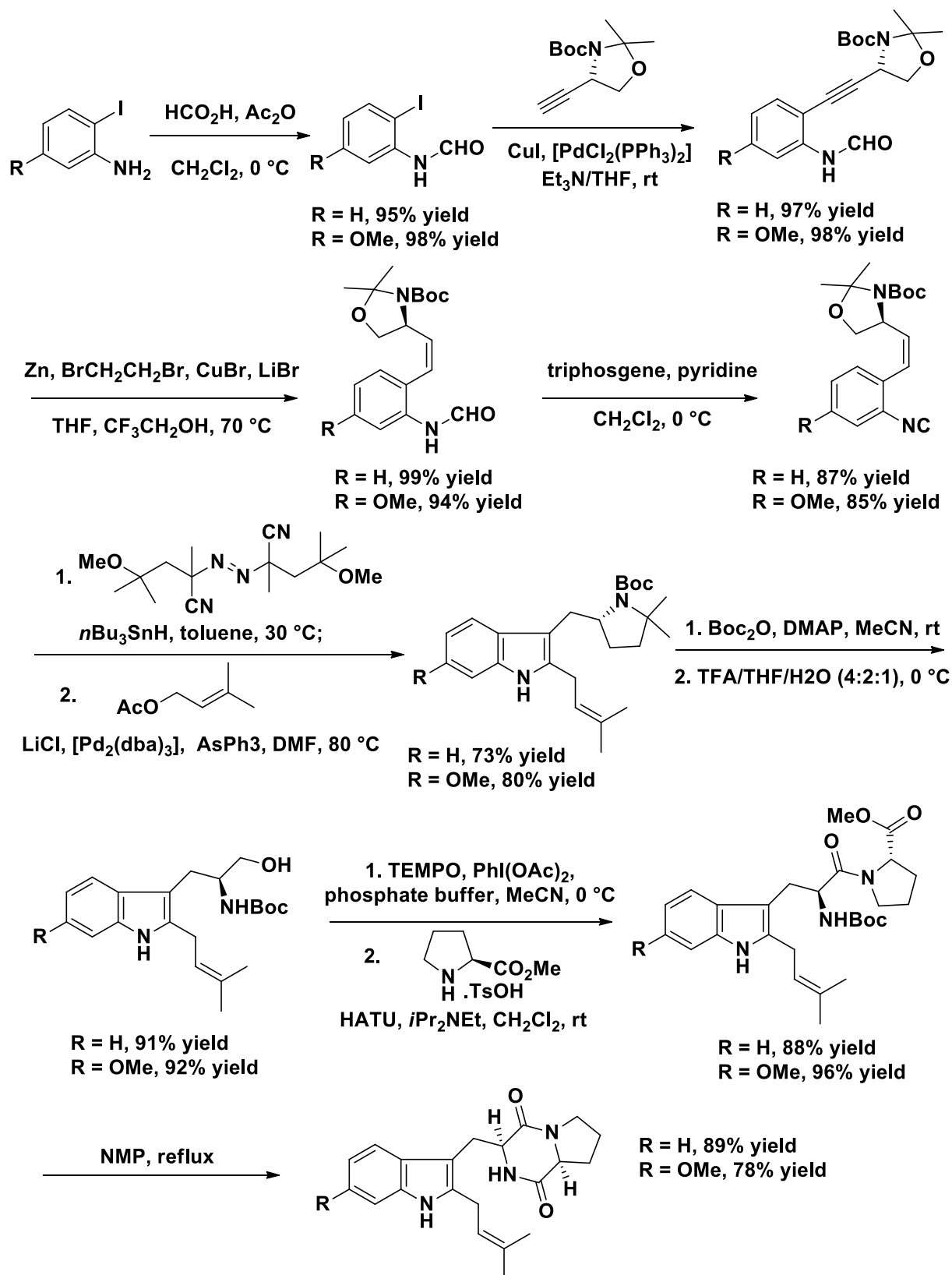
Scheme 1.5. Fukuyama's Synthesis of Tryprostatin A and B

1.3. Background of Our Synthesis of Tryprostatin B

1.3.1. Synthesis of Tryptophan from Acrylate via Gramine

In 1998, Professor Hossain group discovered an unprecedented reaction for the formation of 3-hydroxyacrylate from commercially available aldehydes and ethyl diazoacetate (EDA) in presence of iron Lewis acid catalyst by a unique 1,2-aryl shift (Scheme 1.6).[53] Later, in 2004, same group explored catalyst scopes of the reactions with Brønsted type acids, specifically HBF$_4$·OEt$_2$, for the formation of 3-hydroxyacrylates from the corresponding aldehydes and EDA (Scheme 1.6).[54]
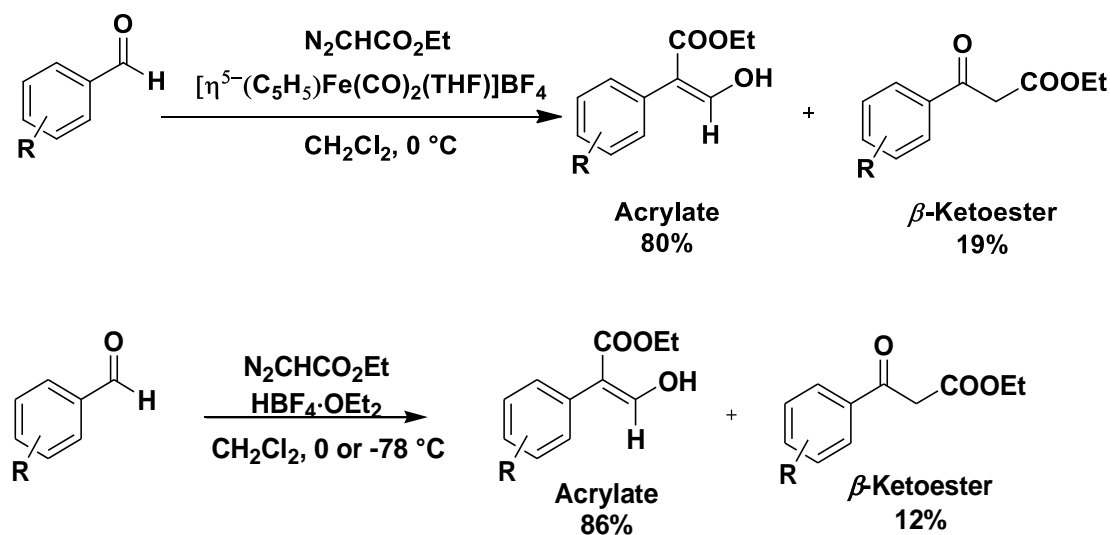
Scheme 1.6. Synthesis of Acrylates by Hossain et al.

3-Hydroxyacrylates are very important synthon for synthesizing important biologically active and pharmaceutically important compounds due to the multiple functionality.[55,56] Hossain group reported a lot of synthesis of biological active compounds including active building blocks such as benzofuran, indole, gramine and so on from the 3-hydroxyacylates.[57,58] Synthesis of gramine from commercially available aldehydes are illustrated below (Scheme 1.7):
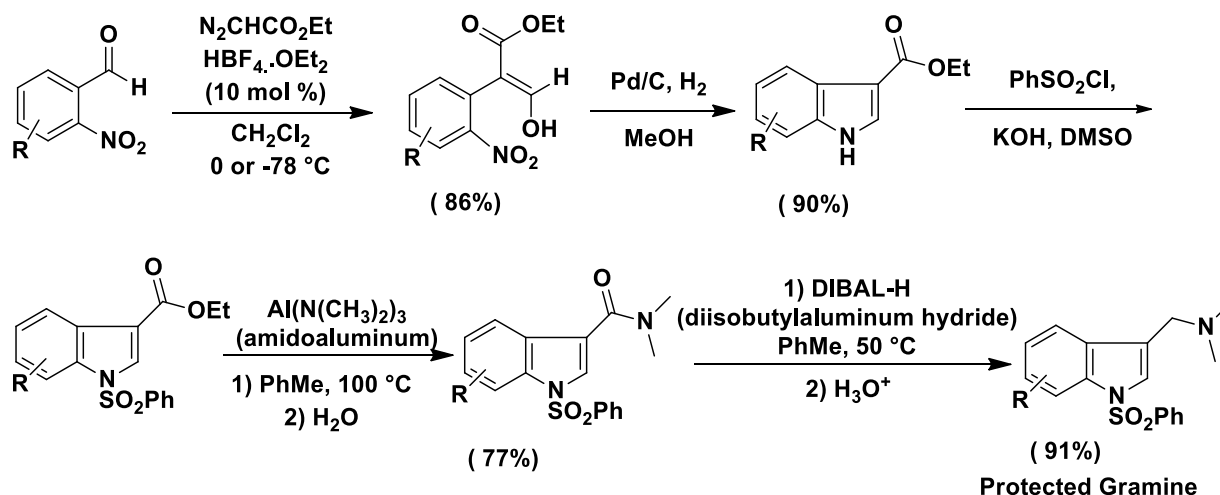
Scheme 1.7. Synthesis of Gramine from Acrylates

After synthesis of several substituted gramine, our group wondered if it would be possible to make enatiopure-pure tryptophan using a chiral phase transfer catalyst (PTC). Our group thought that this would be interesting chemistry and would be likely to find industrial use of this method as tryptophans are important building blocks novel indole-based class of compounds.[59] Then, the Hossain group developed the following reaction to make tryptophan (Scheme 1.8).[60]
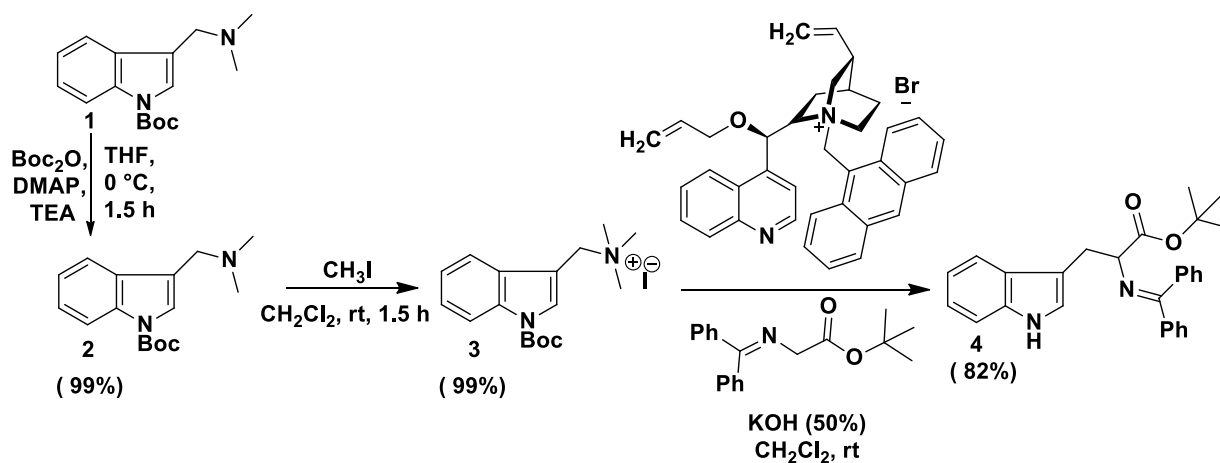
Scheme 1.8: Synthesis of Chiral Tryptophan from Gramine

Hossain and coworkers synthesized several substituted chiral tryptophan from substituted gramine in their laboratory.[60] Here are some examples in Figure 1.9.

(80% yield, 92% ee)

(73% yield, 90% ee)

(75% yield, 91% ee)

(65% yield, 95% ee)
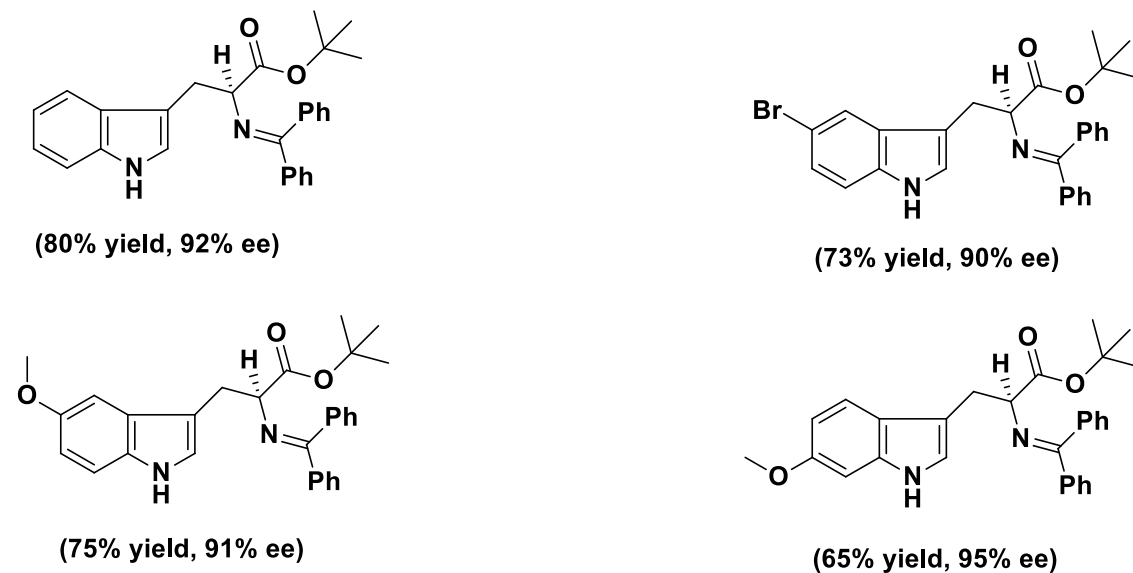
Figure 1.9: Examples of Some Protected Chiral Tryptophans

When we had chiral tryptophans in our hand, we designed a retrosynthetic scheme for the synthesis of tryprostatin B from gramine. The retrosynthetic scheme is illustrated below (Scheme 1.9):

Tryprostatin B

Gramine
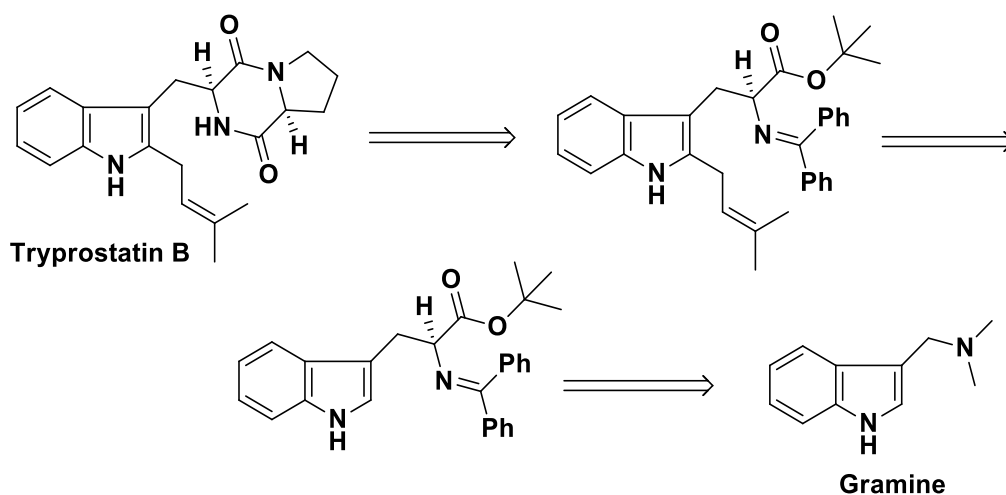
Scheme 1.9: Retrosynthetic Scheme of Tryprostatin B

20

1.3.2. Phase-Transfer-Catalysis (PTC): General Concepts and Mechanism

In order to endorse the successful alkylation of C2-prenylated protected tryptophan, a basic understanding of the phase transfer catalyzed (PTC) reaction is required. In 1971, Starks introduced the term phase transfer catalysis where he described a little organic quaternary salt dramatically increase the rate of reaction (Scheme 1.10). Reaction between an organic solution of an alkyl halide and an inorganic solution of sodium cyanide in presence of tetralkylammonium or tetralkylphosphonium salt produced product faster.[63]
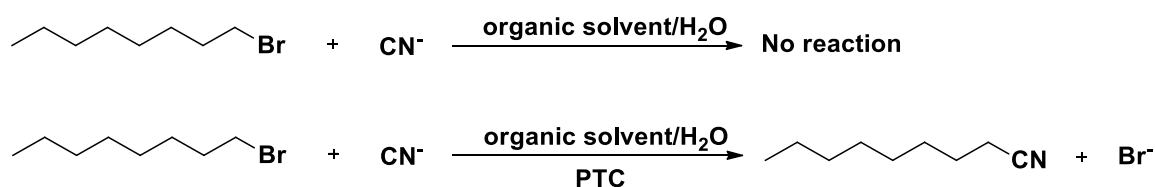
Scheme 1.10. Phase-Transfer-Catalyzed Reactions Reported by Starks

Cyanide ion is insoluble in organic solvent, so the reaction was unable to continue without the presence of phase transfer catalyst (PTC). PTC carry the nucleophilic cyanide ion from aqueous phase to organic phase and exchange the ion with phase transfer catalyst at the interface. The new ion pair then travel to the organic phase and reacts with nucleophile (Figure 1.10).
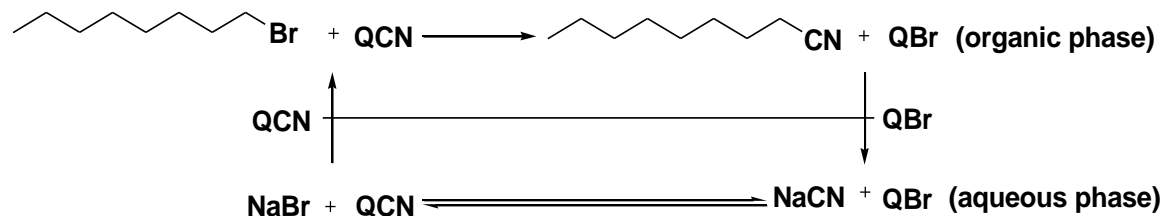
Figure 1.10: Mechanistic Presentation of Phase-Transfer-Catalyzed Reaction

1.3.3. Prenylation at the C2-Position of Indole Ring in Other Groups

Tryprostatin (TPS) A and B contain a 2-prenylindole moiety and diketopiperazine unit. The prenylation at the C2 position of the indole ring is a big challenge for synthetic chemists; several steps have been described in several procedures to introduce the prenyl groups. In these schemes, prenylation of C2 position at indole ring are discussed by Danishefsky, Cook, and Fukuyama respectively (Scheme 1.11).[41, 42, 51]
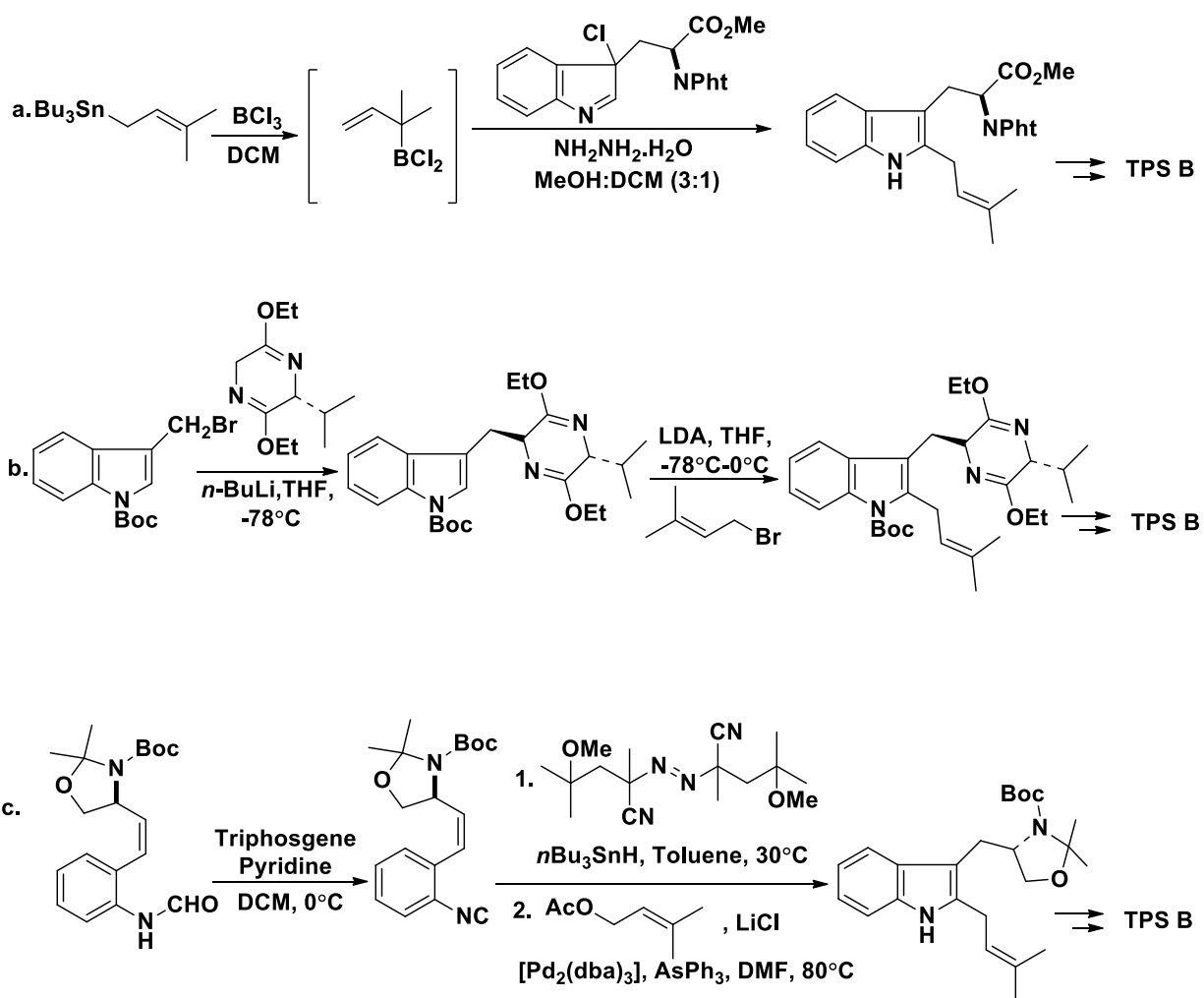
Scheme 1.11. Previous Syntheses of C2-Prenyl Indole Moiety

22

1.3.4. Prenylation at the C2-Position of Indole Ring in Other Groups

In order to prepare the intermediate prenyl tryptophan, our strategy envisaged the installation of the prenyl group at the C2 position of the indole ring of chiral tryptophan [61] Consequently, tryptophan was Boc-protected and treated with prenyl bromide in the presence of n-butyllithium or lithium diisopropylamide (LDA), the attempts of prenylation were unsuccessful (Scheme 1.12).
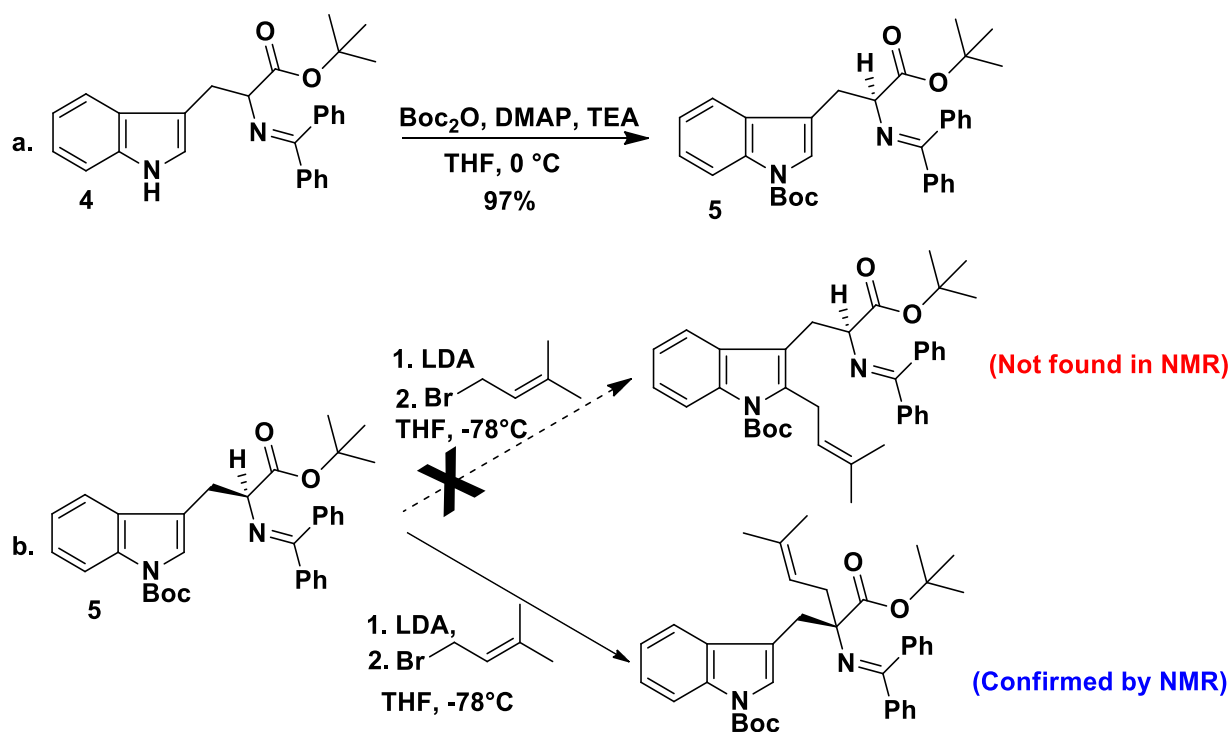
Scheme 1.12: Attempt to Synthesize of *C2*-Prenyl Tryptophan from Tryptophan

Receiving important data from the reactions, we decided that the prenyl group containing the indole moiety of the target compound could be constructed before the PTC reaction. To incorporate the prenyl group at the C2 position, we first reacted the Boc-protected gramine with one equivalent of prenyl bromide in the presence of *n*-butyllithium, and the reaction provided exclusively *N*-prenylated gramine salt with 88% yield (Scheme 1.13 and 1.14); no C2-prenylation was observed.
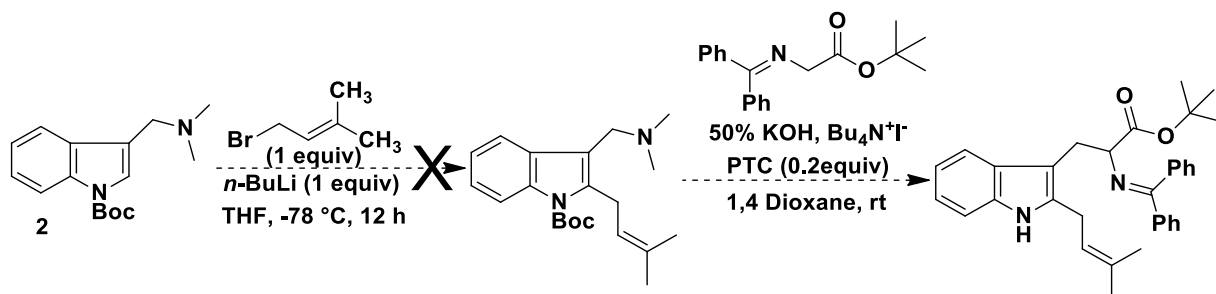
Scheme 1.13: Attempt to Synthesize of C2-Prenyl Tryptophan from Gramine
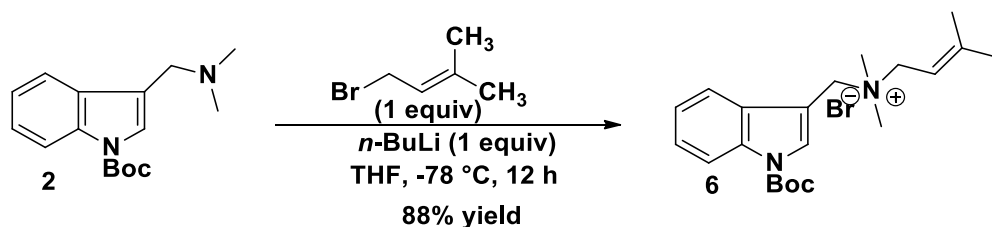
Scheme 1.14: Synthesis of *N*-Prenylated Tryptophan

N-Prenylated gramine salt was found to undergo a PTC reaction with Schiff base in the presence

of 50% KOH to provide the tryptophan 3 (Scheme 1.15). The formation of compound **4** revealed

that the N-prenylated gramine salt is also viable for a PTC reaction, and later, it gave a comparable

yield (75%) to the previously reported reaction involving N-trifluoromethoxybenzyl gramine salt.
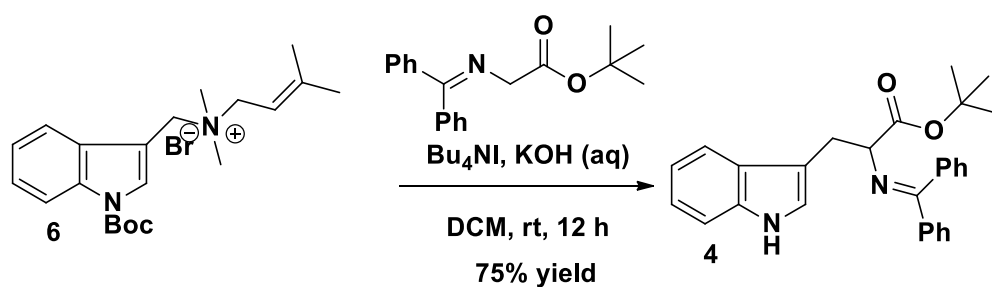
Scheme 1.15: Formation of Tryptophan from *N*-Prenylated Gramine Salt

To our surprise, we observed during our investigation that using two equivalents of *n*-butyllithium and excess of prenyl bromide (4.5 equiv) led to the formation of the C2, N-diprenylated gramine salt in 92% yield. These findings open a new window to synthesize C2 prenylated indole moiety in only two steps from gramine. To the best of our knowledge, this is the easiest way to incorporate the prenyl group at the C2 position of the indole moiety (Scheme 1.16).
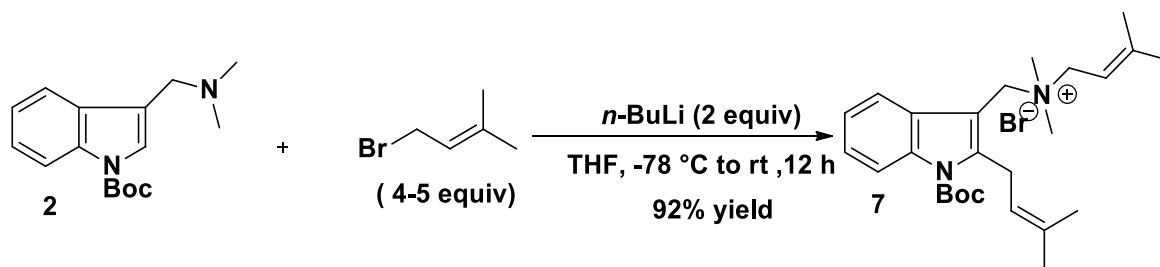
Scheme 1.16: Formation of *C2, N*-Diprenylated Gramine Salt

To see if the C2 alkylation of indole ring also feasible for other alkyl groups, we reacted Boc-protected gramine with benzyl bromide. This finding concluded that to synthesize C2 alkylated indole moiety in only two steps from gramine, any suitable electrophile could be used for further syntheses. The reaction was done with 73% yield (Scheme 1.17).
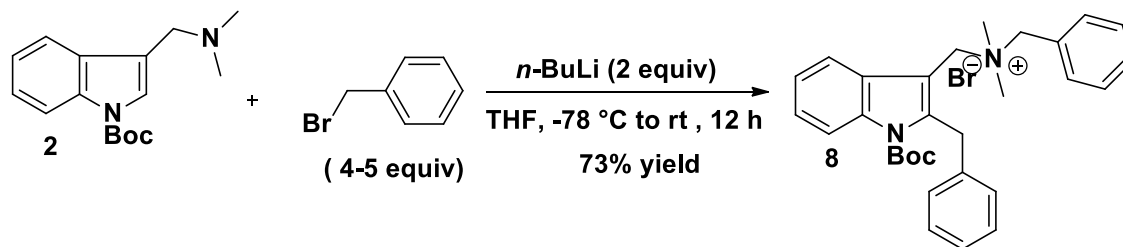
Scheme 1.17: Formation of *C2, N*-Dibenzylated Gramine Salt

The structure of C2, N-diprenylated salt was confirmed by X-ray diffractrometry (Figure 1.11).[62]

Blocks grown using slow diffusion method: Ethyl Acetate/Hexane

Analyzed by X-ray diffraction at UCSD with Arnold L. Rheingold

Unit Cell Dimensions: a=8.5784(2) Å; b=12.9668(3) Å; c=13.5267(3) Å

$$\alpha=109.266(2)°; \beta=103.084(2)°; \gamma=107.596(2)°$$

Triclinic lattice, P1 space group, $Z = 2$ molecules per unit cell. R1 = 4.39%
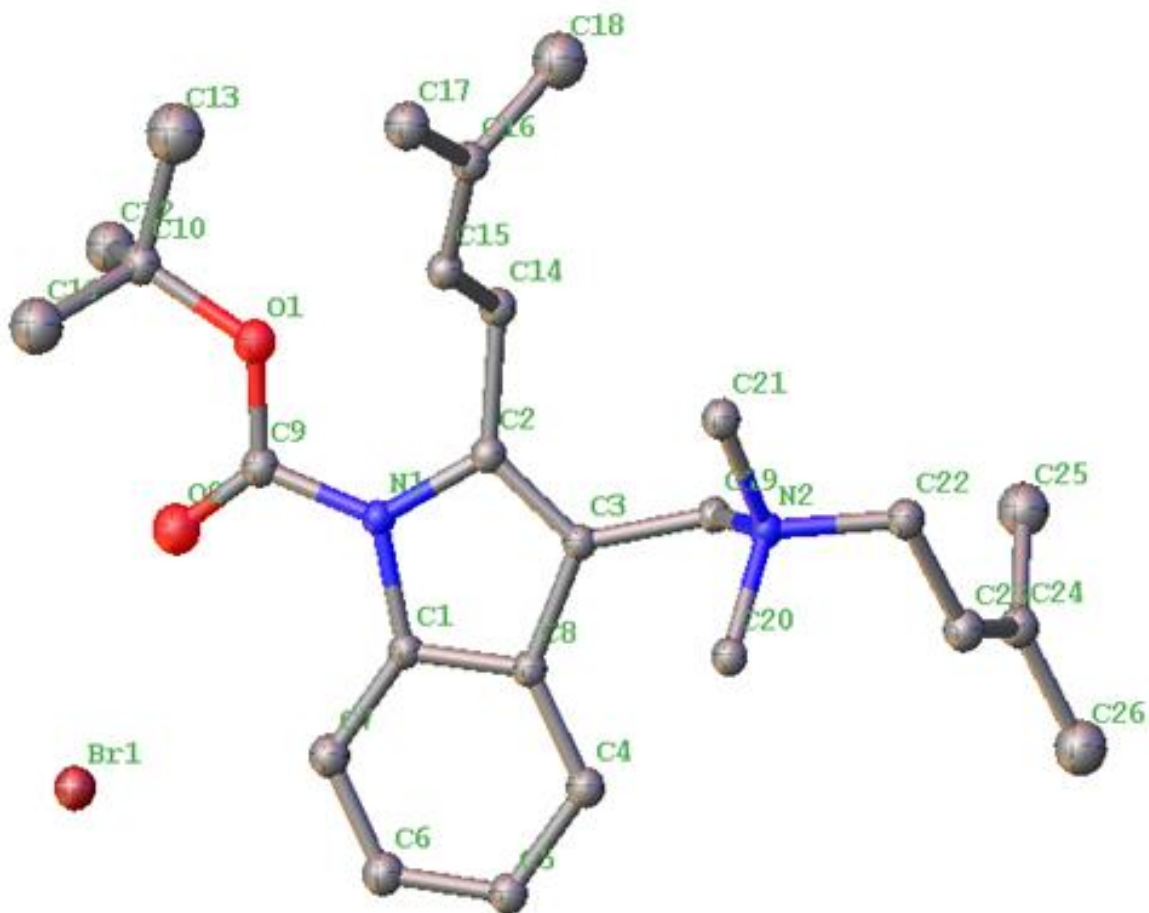
Figure 1.11. Crystal Structure of *C2, N*-Diprenylated Gramine Salt

With the C2 prenyl group containing diprenylated gramine salt, we planned to investigate the PTC reaction with Schiff base. By performing a racemic PTC reaction of diprenylated, the desired C2-prenyl tryptophan was isolated in 82% yield (Scheme 1.18).
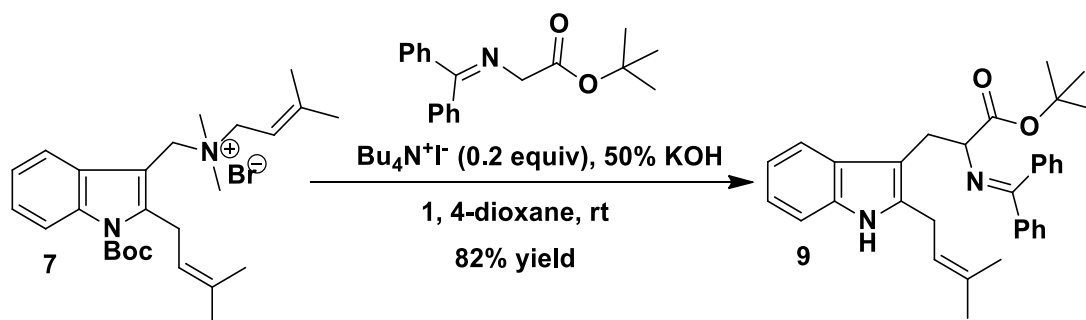
Scheme 1.18: Racemic PTC Reaction of *C2, N*-Diprenylated Gramine Salt

By using a PTC reaction process, it can be easily achieved faster reactions which make fewer byproducts and eliminate the need for expensive or dangerous solvents and expensive raw materials. This process needs two solvents to dissolve all the reactants in organic phase and catalyst and base in aqueous phase. The mechanism of PTC reaction is shown below in Figure 1.12:
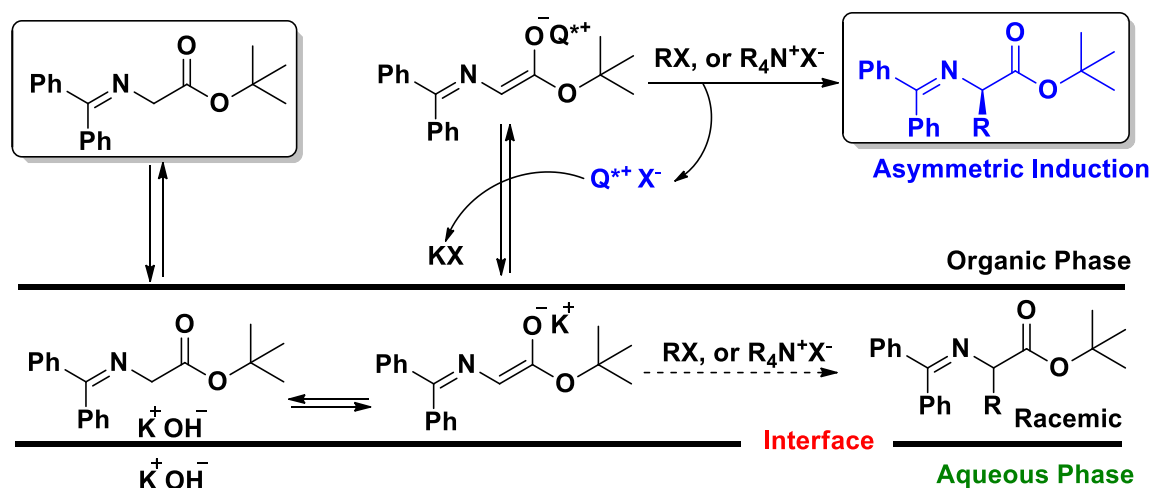
Figure 1.12: Mechanism of Phase-Transfer-Catalyzed Alkylation of Schiff Base.

1.3.5. Optimization of Phase-Transfer-Catalyzed (PTC) Reaction

Encouraged by the results from a racemic PTC reaction, we then turned our attention to the asymmetric PTC reaction of the diprenylated gramine salt to prepare chiral C2-prenyl tryptophan. We did several reactions with different phase transfer catalysts, and we chose Chinchona catalysts as well as recently developed Maruoka catalyst (Figure 1.13) as the PTC.[60] All the time same amounts of reactants, catalyst, base, and solvent were taken. Reactions were run for the same reaction time for all the reaction (Scheme 1.19).
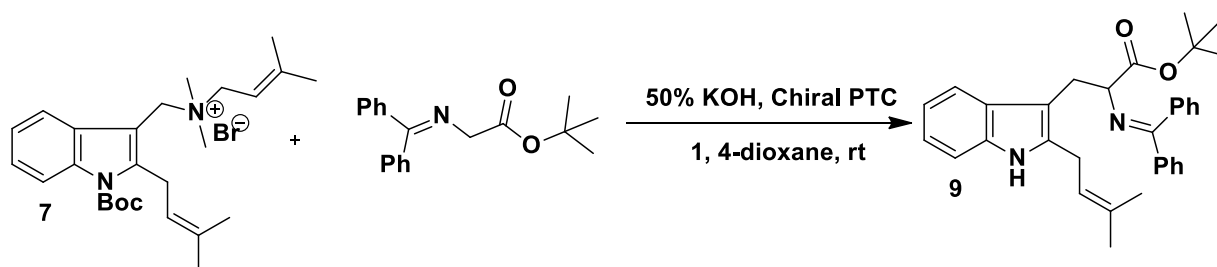
Scheme 1.19: Chiral PTC Reaction of *C2, N*-Diprenylated Gramine Salt

To optimize the reaction conditions for higher asymmetric induction, we investigated the effects of catalysts as well as systematic variations in the solvents, mixed solvent systems, temperature, and time on enantiodiscrimination. In order to find the best catalyst for high enantiomeric excess (ee), several catalysts were screened as presented in Table 1.1. Chiral stationary HPLC showed that *O*-allyl-*N*-(9-anthracenylmethyl) cinchonidinium bromide (A), which was an effective catalyst for enantioselectivity, as observed by our previous studies (Figure 1.13).[60]

Table 1.1: Optimization of PTC Reaction by Catalyst Screening

Rxn #	Catalyst	% Conversion	% ee
		Catalyst Loading	
1	A	100	61
2	B	100	39
3	C	100	39
4	D	100	Rac
5	E	100	ND

We performed several reactions with different phase transfer catalysts, and we chose Chinchona catalysts as well as recently developed Maruoka catalyst as the PTC (Figure 1.13).
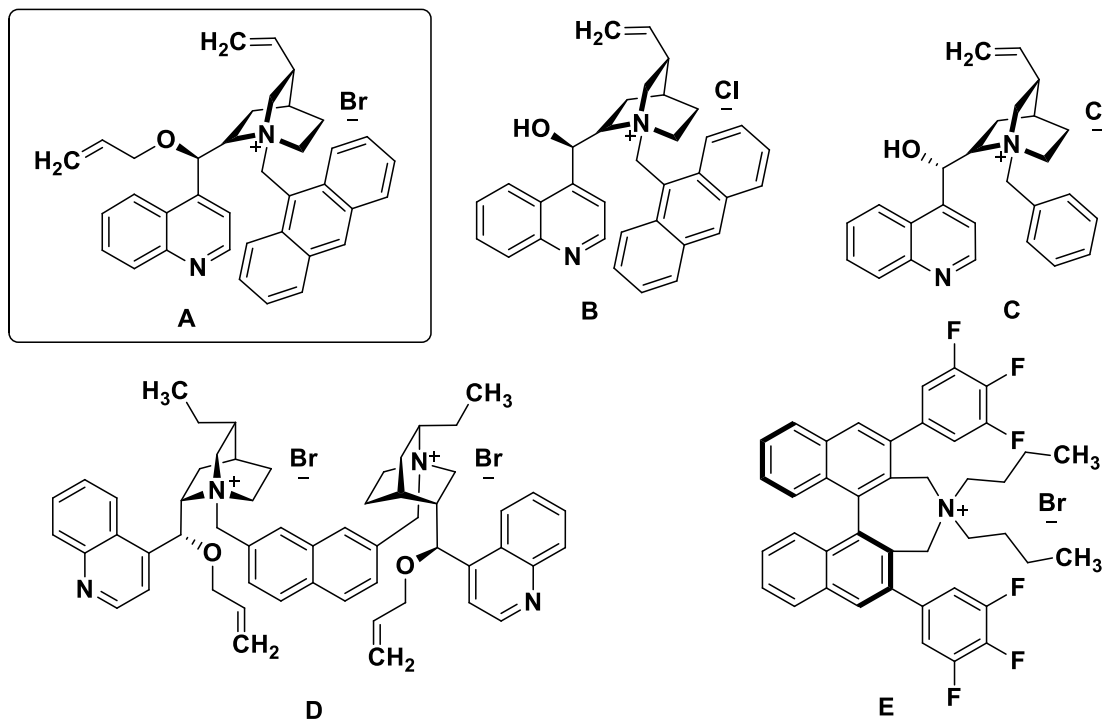
Figure 1.13: Examples of Some Phase-Transfer Catalysts

In order to find the best solvent for high enantiomeric excess (ee), several solvents were examined as presented in Table 1.2. Chiral stationary HPLC showed that polar solvents such as dichloromethane (56% ee), 1,4-dioxane (61% ee), dimethoxyethane (60% ee), and 1,2-dicholoroethane (50%) worked well at room temperature (Table 1.2, entries 1-3, 10, and 15).

Table 1.2: Optimization of PTC Reaction by Solvent Screening

Solvent Screening				
Rxn #	Solvent	Equiv. cat.	% Conversion	% ee
1	DCM	0.2	100	56
2	1,4-Dioxane	0.2	100	61
3	THF	0.2	95	52
4	Toluene	0.2	90	38
5	EtOAc	0.2	80	30
6	Xylene	0.2	75	18
7	Chloroform	0.2	NR	N/A
8	ACN	0.2	100	5
9	Ether	0.2	80	5
10	DME	0.2	100	60
11	DMF	0.2	85	Rac
12	Methylcyclohexane	0.2	80	Rac
13	Hexane	0.2	75	Rac
14	Mesitylene	0.2	80	Rac
15	1,2-Dichloroethane	0.2	100	50

Less polar solvents like toluene did not have a satisfactory result due to poor solubility of the Boc protected diprenylated gramine salt. To improve the asymmetric induction, we investigated mixed solvent systems in different ratios, but no significant improvement was observed at room temperature. However, lowering the temperature from 25 °C to 0 °C resulted in an increase of enantioselectivity (Table 1, entries 5 and 8). Better enantiomeric excess (88% ee) was obtained in a dioxane-chloroform mixture (10:1 ratio) at 0 °C (Table 1.3, entry 8).

Table 1.3: Optimization of PTC Reaction by Mixture of Solvent Screening

	Solvent Screening				
Rxn #	Solvents	Time (hrs)	Temp. (°C)	% Conversion	% ee
1	Dioxane:Chloroform (1:1)	18	rt	35	73
2	Dioxane:Chloroform (2:1)	18	-10	65	84
3	Dioxane:Chloroform (4:1)	18	rt	72	71
4	Dioxane:Chloroform (5:1)	36	0	70	85
5	Dioxane:Chloroform (10:1)	18	rt	63	62
6	Dioxane:Chloroform (10:1)	36	10	100	78
7	Dioxane:Chloroform (10:1)	18	0	62	87
8	Dioxane:Chloroform (10:1)	36	0	100	88
9	Dioxane:Chloroform (10:1)	36	-10	NR	NA
10	Dioxane:Chloroform (20:1)	18	rt	66	63

We were not able to carry out lower temperature reactions with this mixture because of the relatively high freezing point of dioxane. Other mixed solvent systems at lower temperature did not provide promising results compared to the single solvent system at the same temperature. Then we turn our attention to use single solvent at lower temperature. 1, 4-Dioxane, dimethoxyethane, dichlomethane, and tetrahydrofuran were selected for lower temperature. By further cooling to -20 °C, dichloromethane improved the enantioselection up to 93% (Table 1.4, entry 9). During our study, it was revealed that a longer reaction length gave a higher conversion to product.

Table 1.4: Optimization of PTC Reaction by Temperature Screening

Temperature Screening					
Rxn #	Solvent	Time (hrs)	Temperature (^{0}C)	% Conversion	%ee
1	1,4-Dioxane	18	10	100	81
2	1,4-Dioxane	18	0	NR	NA
3	DME	18	10	100	66
4	DME	18	0	95	72
5	DME	18	-10	78	71
6	DME	36	-20	80	85
7	DCM	18	0	96	60
8	DCM	18	-10	90	80
9	DCM	36	-20	85	93
10	THF	18	0	92	65
11	THF	18	-10	95	70
12	THF	36	-20	90	88

With the optimized reaction conditions (DCM, -20 °C, 72 hrs, 93% ee, and 65 % isolated yield) in hand, we then focused on the total synthesis of tryprostatin B from protected chiral protected tryptophan. The diphenylmethylene group was removed from protected tryptophan under acidic conditions (aqueous HCl, THF) in 97% yield to provide the 2-prenyl tryptophan *tert*-butyl ester **10** (Scheme 1.20).[64]
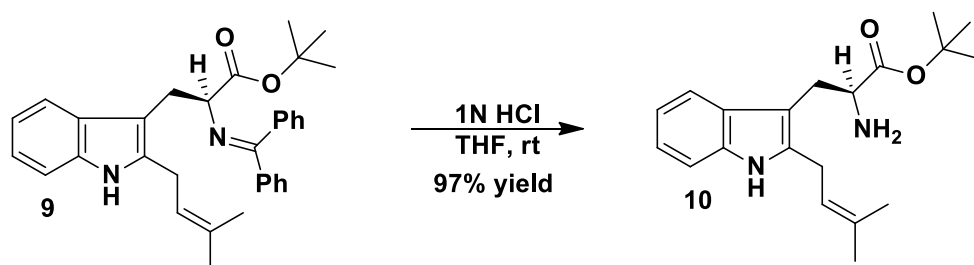
Scheme 1.20: Deprotection of C2-Prenylated Protected Tryptophan

Reaction of **10** with the *N*-Fmoc-*L*-prolyl chloride in the presence of trimethylamine yielded Fmoc-protected dipeptide **11** (Scheme 1.21).[42]
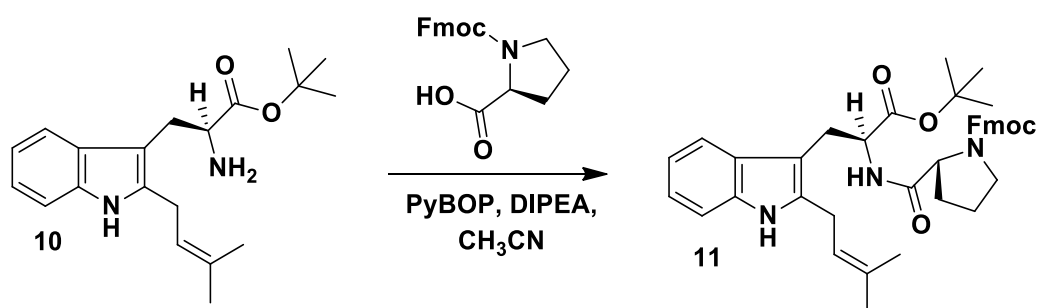
Scheme 1.21: Coupling Reaction of C2-Prenylated Tryptophan *t*-Butyl Ester

The Fmoc protecting group was deprotected with piperidine in dimethylformamide (DMF) provided dipeptide in 76% yield (Scheme 1.22).[42]
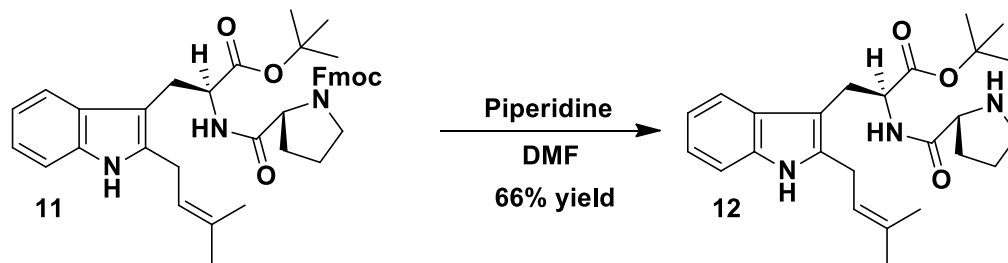
Scheme 1.22: Deprotection of Fmoc-Group from Amide Compound

1.3.6. Cyclization of Amide Compound

Lastly, to synthesize TPS B, we performed the cyclization reaction for the formation of bicyclic diketopiperazine unit in dipeptide **12**. At the outset of the program, we undertook a study to identify an efficient method for cyclization. Initially, to prepare tryprostatin B, we refluxed compound **12** in xylene/neat heat following a procedure described by Cook et al (Scheme 1.23).[42-44]
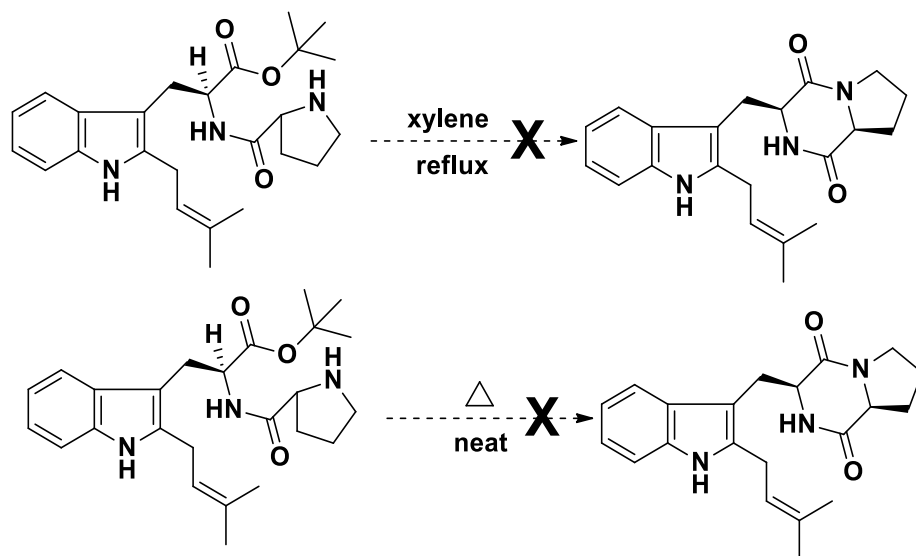
Scheme 1.23: Attempt to Cyclize for Making Diketopiperazine by Xylene Reflux and Neat Heat

We refluxed compound **12** in N-methyl-2-pyrrolidone (NMP) by following a procedure described by Fukuyama et al (Scheme 1.24).[51,52]
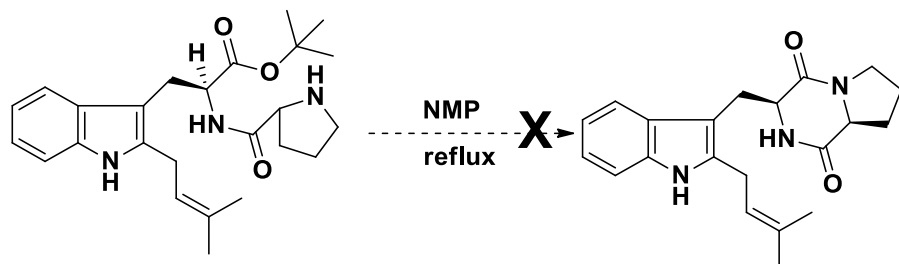
Scheme 1.24: Attempt to Cyclize for Making Diketopiperazine by NMP Reflux

Their ethyl ester substrate was easily cyclized in reflux condition, whereas our *tert*-butyl ester substrate was difficult to cyclize. We applied an alternative procedure reported by Carvalho and coworkers by reacting dipeptide with 20% piperidine in DMF followed by the addition of DIPEA in CH₃CN at room temperature (Scheme 1.25). However, no desired product resulted from this reaction.[65]
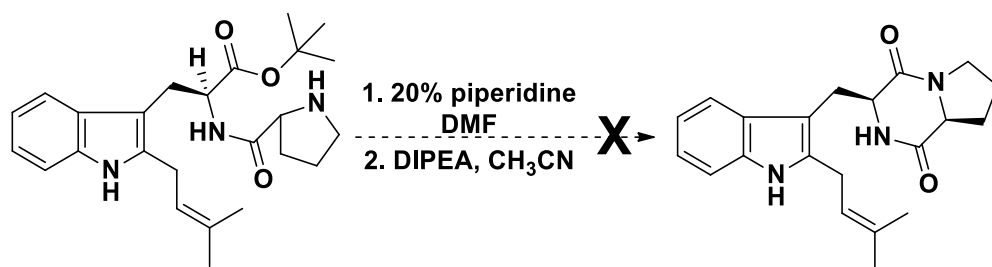
Scheme 1.25: Attempt to Cyclize for Making Diketopiperazine by Piperidine

Later, cyclization as described by Williams using 2-hydroxypyridine in toluene under reflux was also unsuccessful with dipeptide compound (Scheme 1.26).[66]
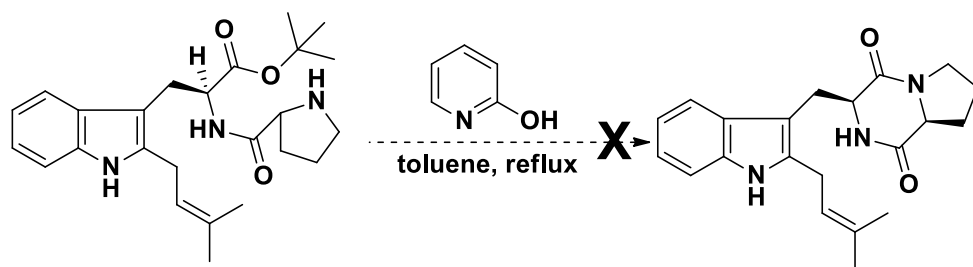
Scheme 1.26: Attempt to Cyclize for Making Diketopiperazine by 2-Hydroxypyridine Reflux

Later, cyclization as described by Danishefsky using ammonia in methanol under reflux was also

unsuccessful with dipeptide compound **12** (Scheme 1.27).[51,52]
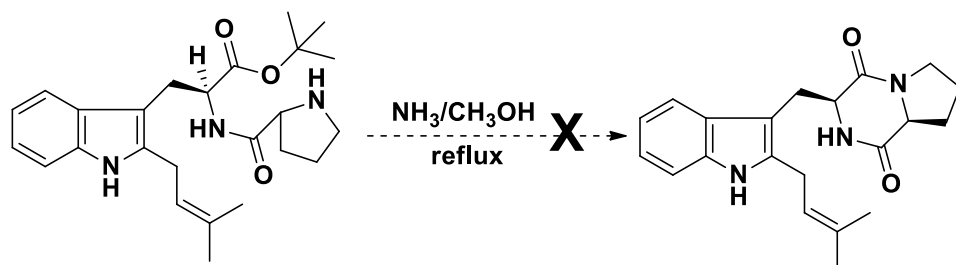
Scheme 1.27: Attempt to Cyclize for Making Diketopiperazine by Ammonia/Methanol Reflux

1.3.7. Microwave Reaction

In seeking a workable solution to the goal of cyclization involving a *tert*-butyl ester group, we

applied the microwave method which was developed by Rios et al..[67] First, we developed a model

microwave experiment with a *tert*-butyl ester group containing compound **14** (Scheme 1.28).
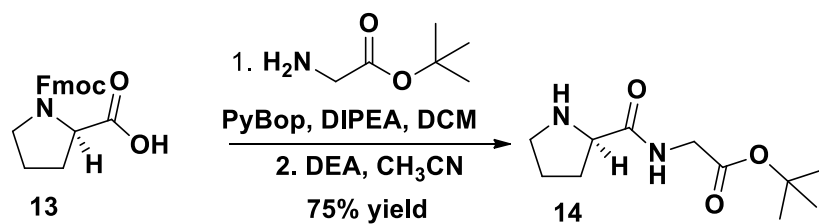
Scheme 1.28: Synthesis of *t*-Butyl Containing Amide

Compound 13 was synthesized from Fmoc-proline and glycine *tert*-butyl ester through a coupling reaction. The model compound was heated in water for 10 min at 250 ℃ and 150 psi using a CEM Discover microwave at 250 W. The desired bicyclo[4.3.0]-2,5-diketopiperazine **15** was obtained in high yield and NMR was matched with the reported values in the literature (Scheme 1.29).[68]
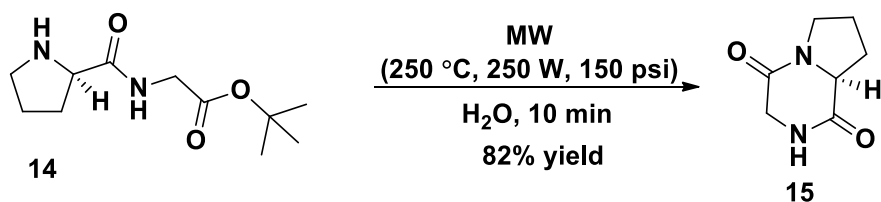
Scheme 1.29: Model Microwave Reaction for Diketopiperazine

Encouraged by this successful reaction involving the *tert*-butyl ester group, we turned our interest to the dipeptide **12**. Under the above-mentioned microwave conditions, spontaneous cyclization occurred to give tryprostatin B in 81% yield.[69] The proton and carbon NMR spectra of the final com-pound matched with the published data (Scheme 1.30).[51]
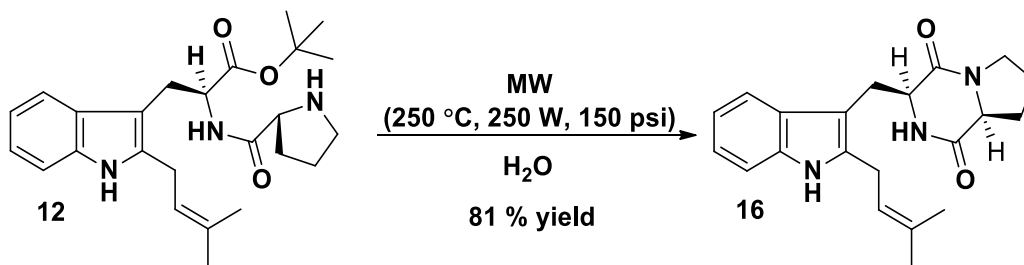
Scheme 1.30: Synthesis of Tryprostatin B by Microwave Reaction

From our developed method, TPS B was synthesized from the commercially available gramine in six steps in 35% overall yield (Scheme 1.31).[69]

1.4. Total Synthesis of Tryprostatin B[69]
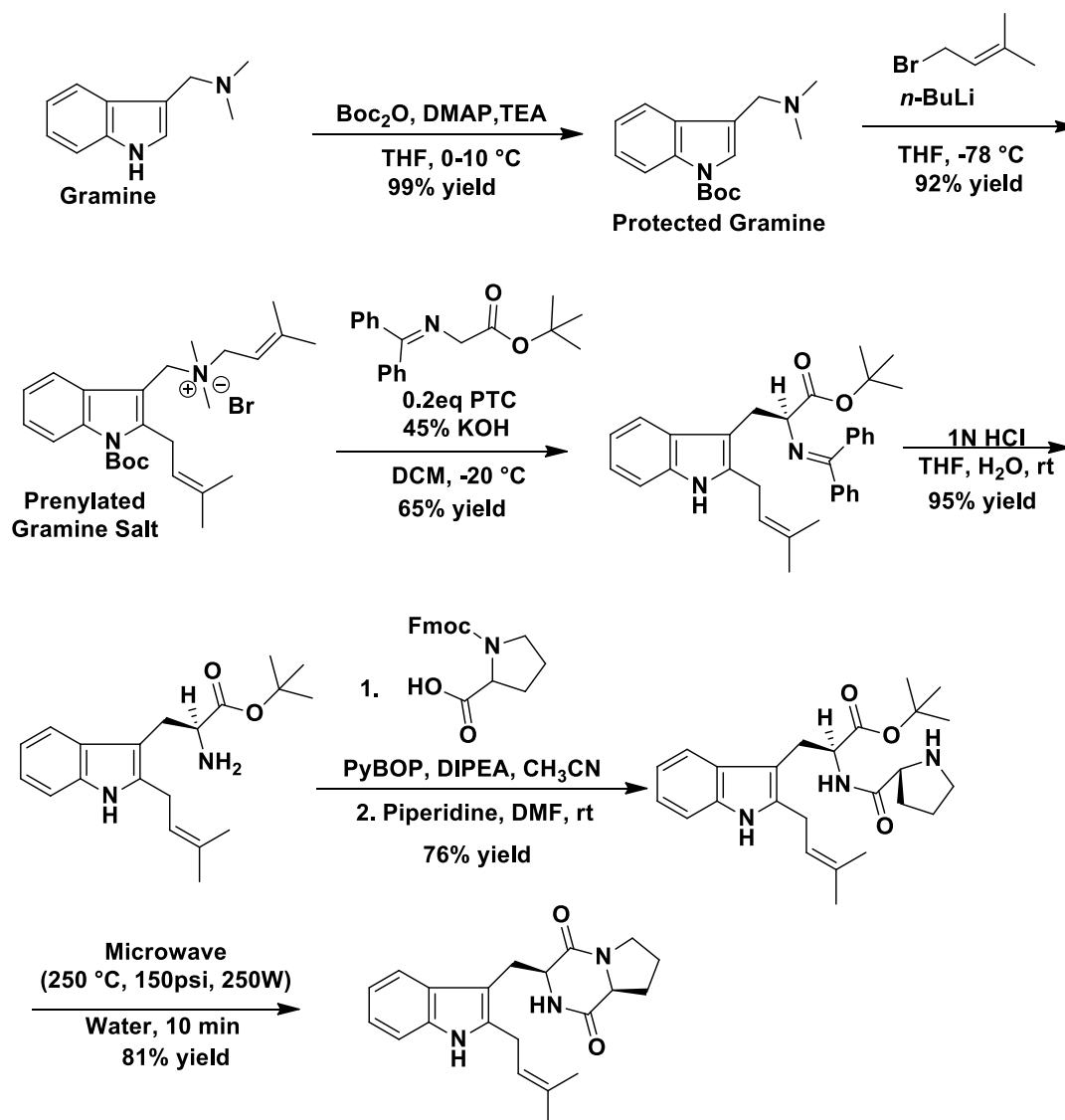
Scheme 1.31: Total Synthesis of Tryprostatin B

By following our developed method, we tried to synthesize the total synthesis of TPS A. We already synthesize four steps of total synthesis of tryprostatin A which are shown in Scheme 1.32.

1.5. Partial Synthesis of Tryprostatin A
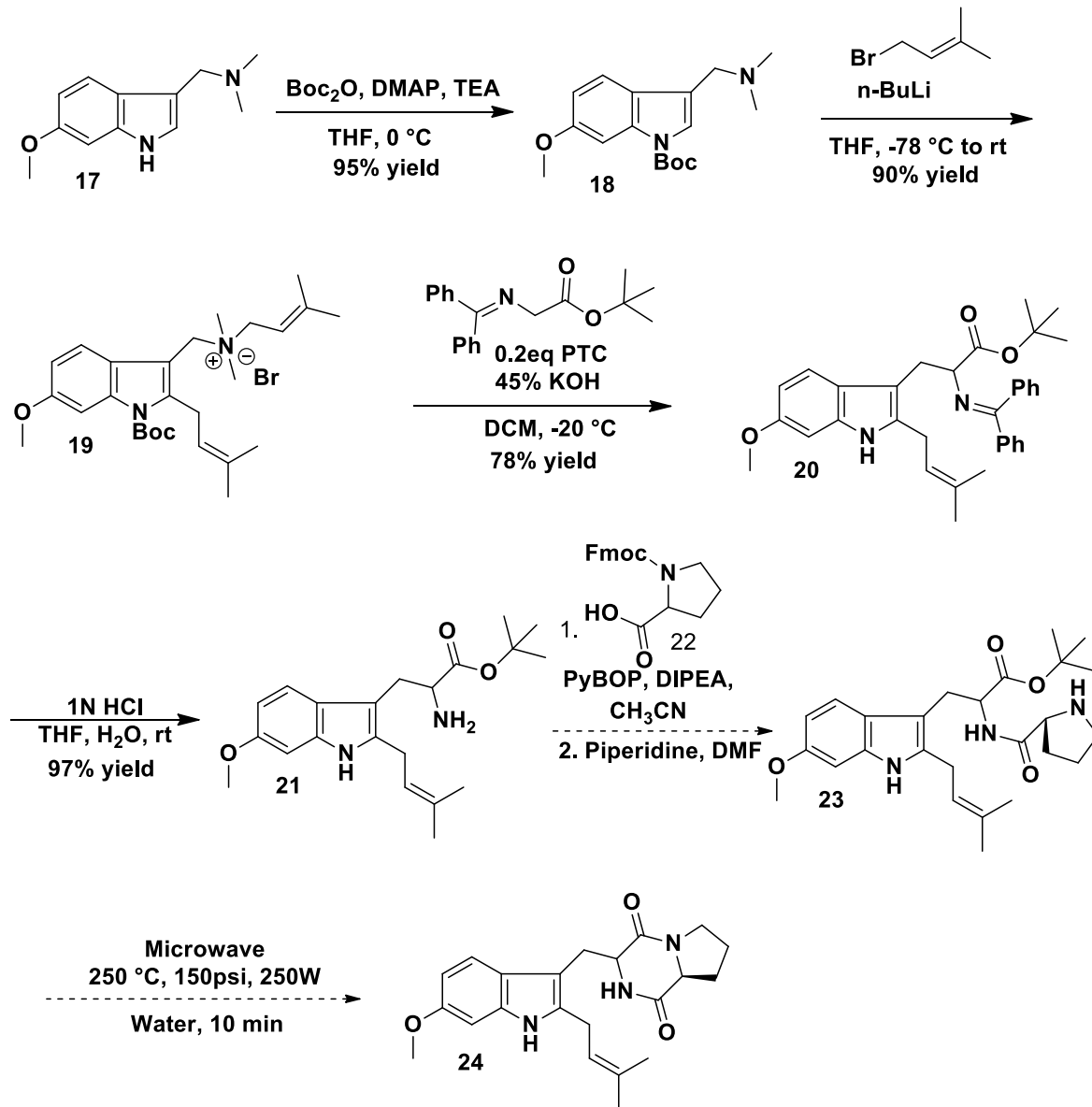
Scheme 1.32: Partial Synthesis of Tryprostatin A

By following our developed method, we tried to synthesize the total synthesis of TPS A. These

four steps are already done and next two steps are currently underway.

1.6. Conclusion

In summary, Tryprostatin (TPS) A and B have great potential because they were found to have inhibitory activity on the cell cycle progression of mouse tsFT210 cells. Their interesting biological activity and simple structure have drawn attention from the synthetic community, and several total syntheses have been reported. We described a concise and efficient asymmetric synthesis of tryprostatin B. The key steps involved first, the preparation of C2 prenyl gramine salt by direct lithiation from Boc protected gramine. This is most unique process by which one can incorporate any electrophile at the C2 position of gramine. This method opens a new window for the indole based synthetic chemists as well as organic chemists. Second, the asymmetric phase transfer catalyzed (PTC) reaction of the prenylated gramine salt. By the PTC reaction, our method was most effective because it produced less waste with minimum number of chemicals. The PTC reaction was optimized by changing the solvent, temperature, and time. From our developed method, C2 prenylated indole was synthesized with only on two steps from gramine and TPS B was synthesized in six steps with 35% overall yield. By changing the substituent, our group have planned to synthesis of analogs of tryprostatins, and after making the analogs (Figure 1.14) our group will see the activity of new synthetic compounds against breast cancer.[70,71] Further investigations into the synthesis of TPS A and their analogs are under way.
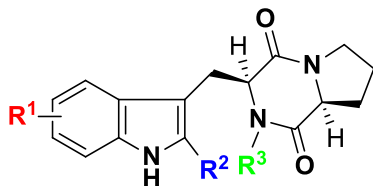
Figure 1.14: Different Analogs of Tryprostatins

1.7. General Methods and Experimental

1.7.1. General Consideration

All reactions were performed under a dry nitrogen atmosphere using standard Schlenk techniques unless otherwise noted. All reaction vessels were flame dried under vacuum and filled with nitrogen prior to use. Reagents and solvents were purchased from Sigma-Aldrich, Milwaukee. All ^1H and ^{13}C NMR spectra were recorded in $CDCl_3$ (internal standard: 7.26 ppm, ^1H; 77.16 ppm, ^{13}C) at room temperature with a Burker 300 MHz and 500 MHz spectrometers. The chemical shifts (δ) are given in parts per million (ppm) and the coupling constants in Hertz (Hz). The following abbreviations are used: *s*-singlet, *d*-doublet, *t*-triplet, *q*-quartet, *m*-multiplet. Previously reported compounds were identified by ^1H NMR. All new compounds were additionally characterized by ^1H NMR, ^{13}C NMR and high-resolution mass spectrometry (HRMS). HRMS were obtained using electrospray ionization (ESI) technique. For column chromatography, silica gel (35-70 microns) was used. Thin layer chromatography (TLC) was performed on aluminium backed plates pre-coated (0.25 mm) with Silica Gel 60 F254 with a suitable solvent system and was visualized using UV fluorescence and/or iodine chamber. Enantioselectivity was obtained via chiral high-performance liquid chromatography (HPLC) using a Waters setup including an In-Line Degasser AF, 2998 photodiode array (PDA) detector, and 1525 binary HPLC pump equipped with Breeze software. This was equipped with a Chiralcel OD (column no. OD00CE-FF071) column eluting with *i*PrOH/hexane with 0.5 mL/min flow rate at ambient temperature. HPLC grade solvents were used in all HPLC analyses. HPLC retention times (tR) of enantiomers are quoted in minutes and were determined by comparison to racemic materials. Microwave reaction was done at 250 °C, 250 W, and 150 psi using a CEM Discover Microwave synthesizer.

41

1.7.2. Experimental Methods

Tert-butyl 3-((dimethylamino)methyl)-1H-indole-1-carboxylate (2)
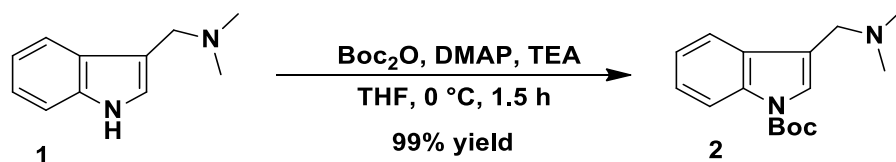
A solution of Boc anhydride (Boc$_2$O) (3.0 g, 13.8 mmol), 4-dimethylaminopyridine (DMAP) (0.14 g, 1.1 mmol), trimethylamine (TEA) (0.122 mL, 0.88 mmol) in THF (50 mL) was maintained at 0 °C for 30 min. A solution of gramine **1** (2.0 g, 11.5 mmol) in THF (15 mL) was added dropwise through the dropping funnel over a period of 30 min at 0 °C. The reaction mixture was stirred at 0 °C for 1.5 hours under nitrogen atmosphere. After consumption of starting material, as judged by TLC analysis, water (20 mL) was added to the reaction mixture. The aqueous layer was extracted with ether (3 x 15 mL), washed with brine (1 x 15 mL). The combined organic layer was dried over anhydrous Na$_2$SO$_4$. The crude product was purified with column chromatography on silica gel (hexane/EtOAc = 7/3) to give product **2** as a light brown solid (3.1 g, 99%). **^{1}H NMR (CDCl$_3$, 300 MHz):** δ 8.17 (d, J = 9.0 Hz, 1H), 7.70 (d, J = 9.0 Hz, 1H), 7.55 (s, 1H), 7.36-7.24 (m, 2H), 3.60 (s, 2H), 2.33 (s, 6H), 1.69 (s, 9H); **^{13}C NMR (CDCl$_3$, 75 MHz):** δ 149.8, 135.6, 130.6, 124.6, 124.4, 122.6, 119.6, 117.8, 115.1, 83.5, 54.5, 45.4, 28.2; **HRMS (ESI+):** Calculated (m/z) for C$_{16}$H$_{23}$N$_2$O$_2$ (M+H)$^+$: 275.1754, Found 275.1752.

***Tert*-butyl-3-(3-(tert-butoxy)-2-((diphenylmethylene)amino)-3-oxopropyl)-1H-indole-1-carboxylate (5)**
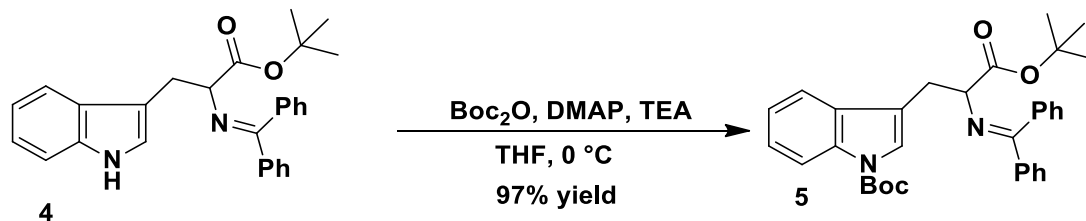
A solution of Boc anhydride (Boc₂O) (0.62 g, 2.8 mmol), 4-dimethylaminopyridine (DMAP) (0.029 g, 0.24 mmol), trimethylamine (TEA) (0.039 mL, 0.28 mmol) in THF (15 mL) was maintained at 0 °C for 30 min. A solution of tryptophan **4** (1.0 g, 2.4 mmol) in THF (25 mL) was added dropwise through the dropping funnel over a period of 30 min at 0 °C. The reaction mixture was stirred at 0 °C for 1.5 hours under nitrogen atmosphere. After consumption of starting material, as judged by TLC analysis, water (15 mL) was added to the reaction mixture. The aqueous layer was extracted with ether (3 x 15 mL), washed with brine (1 x 10 mL). The combined organic layer was dried over anhydrous Na₂SO₄. The crude product was purified with column chromatography on silica gel (hexane/EtOAc = 25/1) to give Boc-protected product **5** as a white solid (1.19 g, 97%).

¹H NMR (CDCl₃, 300 MHz): δ 8.16 (d, *J* = 9.0 Hz, 1H), 7.63 (d, *J* = 6.0 Hz, 2H), 7.40-7.23 (m, 9H), 7.12 (t, *J* = 7.5 Hz, 1H), 6.79 (d, *J* = 6.0 Hz, 2H), 4.32 (dd, *J* = 9.0, 6.0 Hz, 1H), 3.37 (dd, *J* = 13.5, 4.5 Hz, 1H), 4.32 (dd, *J* = 13.5, 7.5 Hz, 1H), 1.64 (s, 9H), 1.49 (s, 9H); **¹³C NMR (CDCl₃, 75 MHz):** δ 170.9, 170.5, 149.7, 139.6, 136.2, 135.4, 130.7, 130.2, 128.8, 128.3, 128.2, 127.9, 127.7, 124.2, 124.1, 122.2, 119.2, 117.0, 115.0, 83.2, 81.2, 66.1, 28.9, 28.2, 28.1; **HRMS (ESI+):** Calculated (m/z) for C₃₃H₃₇N₂O₄ (M+H)⁺ : 525.2748, Found 525.2740.

N-((1-(tert-butoxycarbonyl)-1H-indol-3-yl)methyl)-N,N,3-trimethylbut-2-en-1-aminium bromide (6)
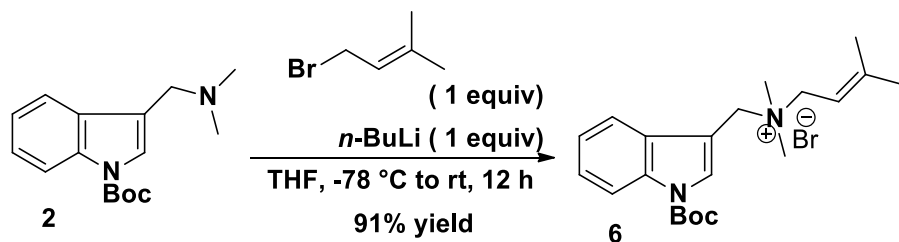
A solution of **2** (1.5 g, 5.5 mmol) in THF (15 mL) was taken in three necked round bottomed flask and nitrogen was bubbled through the solution for 20 min. This mixture was cooled to -78 °C and *n*-butyl lithium (2.2 mL, 2.5 M, 5.5 mmol) was added dropwise to the reaction mixture maintaining a temperature -78 °C over a period of 1 h under nitrogen atmosphere. Prenyl bromide (0.63 mL, 5.5 mmol) was added to the reaction dropwise through the dropping funnel over a period of 30 min. The reaction mixture was allowed to warm to room temperature and was stirred overnight. After consumption of the starting material, as judged by TLC analysis, water (15 mL) was added to the reaction mixture and THF was removed under reduced pressure. The mixture was then extracted with CH_2Cl_2 (3 x 15 mL), the combined organic layers were washed with brine solution (1 x 10 mL) and dried over anhydrous Na_2SO_4 and evaporated *in vacuo* to obtain crude product. The residue was purified with flash column chromatography on silica gel (DCM/MeOH = 20/1) to afford **6** as off-white solid (2.1 g, 91 %). **^{1}H NMR (CDCl$_3$, 300 MHz):** δ 8.11 (d, *J* = 9.0 Hz, 2H), 8.02 (d, *J* = 6.0 Hz, 1H), 7.94 (s, 1H), 7.29-7.16 (m, 2H), 5.32 (t, *J* = 7.5 Hz, 1H), 5.22 (s, 2H), 4.38 (d, *J* = 9.0 Hz, 2H), 3.15 (s, 6H), 1.81 (s, 3H), 1.76 (s, 3H), 1.59 (s, 9H); **^{13}C NMR (CDCl$_3$, 75 MHz):** δ 148.9, 148.8, 135.0, 130.5, 129.8, 125.2, 123.8, 120.3, 115.2, 110.9, 107.6, 85.0, 61.5, 58.6, 48.4, 28.1, 26.4, 19.5; **HRMS (ESI+):** Calculated (m/z) for $C_{21}H_{31}N_2O_2$ [M]$^+$: 343.2380, Found: 343.2363.

***Tert*-butyl 2-((diphenylmethylene)amino)-3-(1H-indol-3-yl)propanoate (4)**
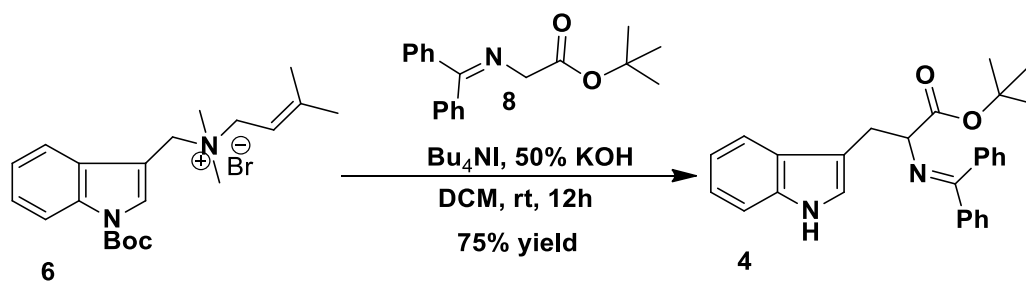
A solution of **7** (1g, 2.4 mmol), *N*-(diphenylmethylene) glycine tert-butyl ester **6** (0.70 g, 2.4 mmol) and tetrabutylammonium iodide (0.18 g 0.47 mmol) in dry DCM (20 mL) was maintained at -20 °C for 30 minutes. 50% aqueous KOH (1.3 g, 24 mmol) was added to the reaction. Then the reaction was stirred overnight. After consumption of the starting material, as judged by TLC, water was added, and the aqueous layer was extracted with CH_2Cl_2 (3 x 25 mL). The combined organic layers were dried over anhydrous Na_2SO_4; the solvent was evaporated *in vacuo*. The residue was purified with flash column chromatography on silica gel (hexane/EtOAc = 10/1) to afford **3** as a light-yellow oil (0.75 mg, 75%). Compound **4** was confirmed[3] by comparing spectra to known NMR. **^{1}H NMR (CDCl₃, 500 MHz):** δ 7.99 (brs, 1H), 7.64 (d, *J* = 5.0 Hz, 2H), 7.39 (t, *J* = 7.5 Hz, 1H), 7.33-7.27 (m, 5H), 7.18-7.14 (m, 3H), 7.01-6.96 (m, 2H), 6.44 (d, *J* = 5.0 Hz, 2H), 4.29 (dd, *J* = 10.0, 5.0 Hz, 1H), 3.45 (dd, *J* = 15.0, 5.0 Hz, 1H), 3.27 (dd, *J* = 15.0, 10.0 Hz, 1H), 1.45 (s, 9H); **^{13}C NMR (CDCl₃, 125 MHz):** δ 171.3, 170.1, 139.7, 136.2, 136.0, 130.1, 128.8, 128.1, 128.0, 127.9, 127.8, 127.6, 123.0, 121.7, 119.1, 119.0, 112.3, 110.8, 80.9, 66.7, 29.1, 28.1.

N-((1-(tert-butoxycarbonyl)-2-(3-methylbut-2-en-1-yl)-1H-indol-3-yl)methyl)-N,N,3-trimeth-ylbut-2-en-1-aminium bromide (7)
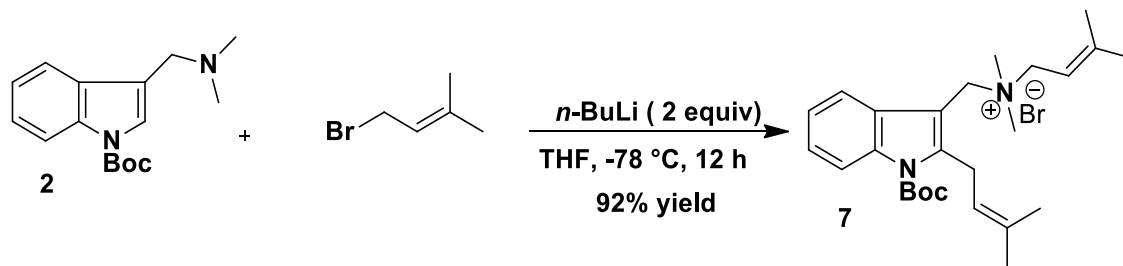
A solution of **2** (1.5 g, 5.5 mmol) in THF (25 mL) was taken in three necked round bottomed flask

and nitrogen was bubbled through the solution for 20 min. This mixture was cooled to -78 °C and

n-butyl lithium (4.4 mL, 2.5 M, 10.9 mmol) was added dropwise to the reaction mixture

maintaining a temperature -78 °C over a period of 1 h under nitrogen atmosphere. Prenyl bromide

(2.8 mL, 24.4 mmol) was added to the reaction dropwise through the dropping funnel over a period

of 30 min. The reaction mixture was allowed to warm to room temperature and was stirred

overnight. After consumption of the starting material, as judged by TLC analysis, water (20 mL)

was added to the reaction mixture and THF was removed under reduced pressure. The mixture

was then extracted with CH_2Cl_2 (3 x 15 mL), the combined organic layers were washed with brine

solution (1 x 10 mL) and dried over anhydrous Na_2SO_4 and evaporated *in vacuo* to obtain crude

product. The residue was purified with flash column chromatography on silica gel (DCM/MeOH

= 20/1) to afford **7** as a brown solid (2.48 g, 92 %). **^{1}H NMR (CDCl$_3$, 300 MHz):** δ 8.08 (d, *J* =

9.0 Hz, 2H), 7.32 (dd, *J* = 9.0 Hz, 6.0 Hz, 2H), 5.38 (t, *J* = 7.5 Hz, 1H), 5.27 (s, 2H), 5.04 (s, 1H),

4.56 (d, *J* = 6.0 Hz, 2H), 3.91 (s, 2H), 3.17 (s, 6H), 1.93 (s, 3H), 1.88 (s, 3H), 1.80 (s, 3H), 1.67

(s, 12H); **^{13}C NMR (CDCl$_3$, 75 MHz):** δ 149.6, 148.7, 144.1, 135.8, 134.1, 129.0, 124.4, 123.6,

120.3, 119.8, 114.9, 111.2, 106.0, 85.0, 61.8, 58.1, 48.4, 27.9, 26.8, 26.4, 25.4, 19.5, 18.7; **HRMS**

(ESI+): Calculated (m/z) for $C_{26}H_{39}N_2O_2$ [M]$^+$: 411.3006, Found: 411.2993.

N-benzyl-1-(2-benzyl-1-(tert-butoxycarbonyl)-1*H*-indol-3-yl)methyl)-*N*,*N*-dimethylmethan-aminium bromide (8)
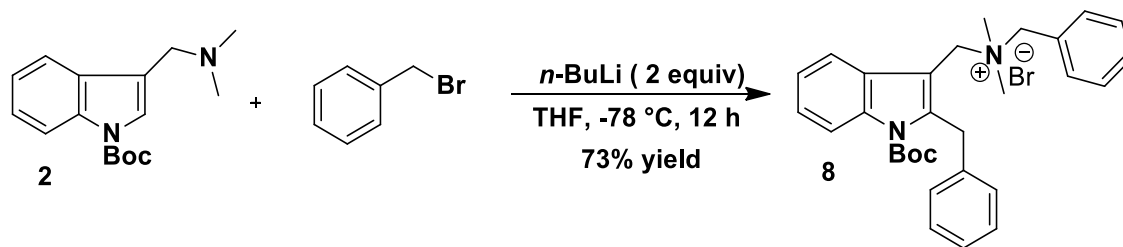
A solution of **2** (1.0 g, 3.6 mmol) in THF (20 mL) was taken in three necked round bottomed flask and nitrogen was bubbled through the solution for 20 min. This mixture was cooled to -78 °C and *n*-butyl lithium (2.9 mL, 2.5 M, 7.3 mmol) was added dropwise to the reaction mixture maintaining a temperature -78 °C over a period of 1 h under nitrogen atmosphere. Benzyl bromide (2.0 mL, 16.4 mmol) was added to the reaction dropwise through the dropping funnel over a period of 30 min. The reaction mixture was allowed to warm to room temperature and was stirred overnight. After consumption of the starting material, as judged by TLC analysis, water 15 mL) was added to the reaction mixture and THF was removed under reduced pressure. The mixture was then extracted with CH_2Cl_2 (3 x 15 mL), the combined organic layers were washed with brine solution (1 x 10 mL) and dried over anhydrous Na_2SO_4 and evaporated *in vacuo* to obtain crude product. The residue was purified with flash column chromatography on silica gel (DCM/MeOH = 20/1) to afford **8** as a brown solid (1.41g, 73 %). **¹H NMR (CDCl₃, 300 MHz):** δ 8.19 (d, *J* = 9.0 Hz, 1H), 8.09 (d, *J* = 9.0 Hz, 1H), 7.63 (d, *J* = 6.0 Hz, 2H), 7.29-7.21 (m, 5H), 7.07 (t, *J* = 7.5 Hz, 2H), 7.00-6.92 (m, 3H), 5.39 (s, 2H), 5.32 (s, 2H), 4.78 (s, 2H), 3.02 (s, 6H), 1.31 (s, 9H); **¹³C NMR (CDCl₃, 75 MHz):** δ 149.4, 142.3, 138.6, 136.2, 133.4, 130.3, 129.1, 128.9, 128.4, 127.9, 127.6, 126.1, 124.8, 123.9, 120.1, 115.2, 107.9, 85.1, 66.9, 58.8, 48.1, 32.8, 27.5.; **HRMS (ESI+):** Calculated (m/z) for $C_{30}H_{35}N_2O_2$ [M]⁺: 455.2693, Found: 455.2624.

(S)-*tert*-butyl-2-((diphenylmethylene)amino)-3-(2-(3-methylbut-2-en-1-yl)-1H-indol-3-yl)-propanoate (9)
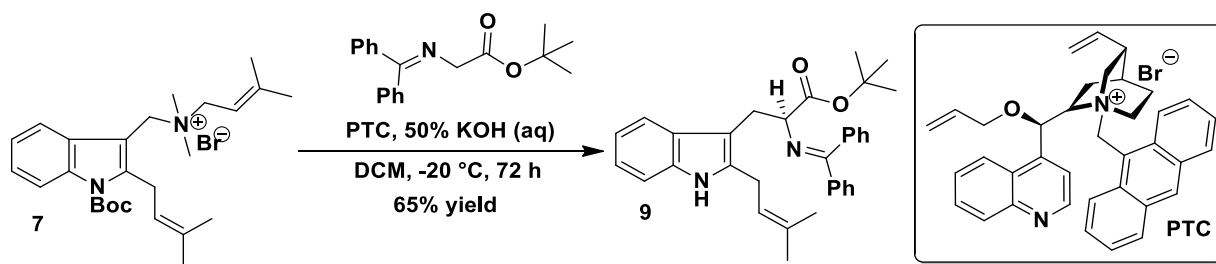
A solution of **7** (500 mg, 1.01 mmol), *N*-(diphenylmethylene) glycine tert-butyl ester (300 mg, 1.01 mmol) and *O*-allyl-*N*-(9-anthracenylmethyl) cinchonidinium bromide **PTC** (123 mg 0.203 mmol) in dry DCM (10 mL) was maintained at -20 °C for 30 minutes. 50% aqueous KOH (86 mg, 15 mmol) was added to the reaction by maintaining the temperature -20 °C. Reaction was stirred vigorously with mechanical stirrer for 72 h. After consumption of the starting material, as judged by TLC, water was added, and the aqueous layer was extracted with CH$_2$Cl$_2$ (3 x 10 mL). The combined organic layers were dried over anhydrous Na$_2$SO$_4$; the solvent was evaporated *in vacuo*. The residue was purified with flash column chromatography on silica gel (hexane/EtOAc = 20/1) to afford **9** as a light brown solid (326 mg, 65%). **^{1}H NMR (CDCl$_3$, 300 MHz):** δ 7.75 (s, 1H), 7.62 (d, *J* = 9.0 Hz, 2H), 7.37-7.28 (m, 3H), 7.23-7.20 (m, 3H), 7.06 (q, *J* = 9.0 Hz, 3H), 6.91 (t, *J* = 9.0 Hz, 1H), 6.41 (d, *J* = 6.0 Hz, 2H), 5.10 (t, *J* = 6.0 Hz, 1H), 4.26 (dd, *J* = 10.5 Hz, 4.5 Hz, 1H), 3.39 (dd, *J* = 19.5 Hz, 4.5 Hz, 1H), 3.28 (dd, *J* = 15.0 Hz, 9.0 Hz, 1H), 1.68 (s, 3H), 1.65 (s, 3H), 1.48 (s, 9H); **^{13}C NMR (CDCl$_3$, 75 MHz):** δ 171.5, 169.6, 139.5, 136.0, 135.5, 134.9, 134.3, 129.9, 129.2, 128.7, 127.8, 127.7, 127.6, 120.8, 120.6, 119.0, 118.4, 110.0, 107.2, 80.8, 66.7, 28.1, 27.9, 25.7, 25.1, 17.7; **HRMS (ESI+):** Calculated (m/z) for C$_{33}$H$_{37}$N$_2$O$_2$ [M+H]$^+$: 493.2850, Found: 493.2845. **HPLC:** 93% *ee*, Chiralcel OD column (25 cm x 0.46 cm, ID), 2 % *i*-PrOH in hexane, 0.5 mL/min, 25.27 min (major), 29.34 min (minor).

(S)-*tert*-butyl 2-amino-3-(2-(3-methylbut-2-en-1-yl)-1H-indol-3-yl) propanoate (10)
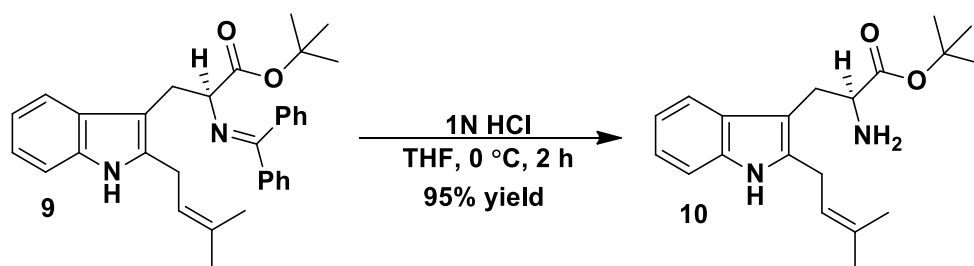
A solution of **9** (200 mg, 0.41 mmol) THF (6 mL) and 1N hydrochloric acid (4 mL) was maintained in cold water bath for 2 h under nitrogen atmosphere. After consumption of the starting material, as judged by TLC analysis, the mixture was extracted with hexane (3 x 5 mL) then the aqueous layer was basified using saturated $NaHCO_3$ and extracted with CH_2Cl_2 (3 x 5 mL), washed with brine (1 x 5 mL). The combined organic layer was dried over anhydrous $MgSO_4$ and the solvent was evaporated under *in vacuo*. The crude product was purified by silica gel column chromatography (DCM/MeOH = 20:1) to afford **10** as a light yellow solid (126 mg, 95% yield). **^{1}H NMR (CDCl$_3$, 300 MHz):** δ 8.52 (brs, 1H), 7.59 (d, J = 9.0 Hz, 1H), 7.26 (d, J = 6.0, 1H), 7.15-7.08 (m, 2H), 5.34 (t, J = 7.5 Hz, 1H), 3.75 (dd, J = 9.0, 3.0 Hz, 1H), 3.49 (d, J = 6.0 Hz, 2H), 3.25 (dd, J = 15.0, 6.0 Hz, 1H), 2.91 (dd, J = 15.0, 9.0 Hz, 1H), 1.96 (brs, 2H), 1.78 (s, 6H), 1.46 (s, 9H),.; **^{13}C NMR (CDCl$_3$, 75 MHz):** δ 174.6, 136.0, 135.4, 134.1, 128.8, 121.1, 120.7, 119.2, 118.2, 110.6, 106.6, 81.0, 55.9, 30.5, 28.0, 25.8, 25.3, 18.0; **HRMS (ESI+):** Calculated (m/z) for $C_{20}H_{29}N_2O_2$ [M+H]$^+$: 329.2224, Found: 329.2220.

(S)-tert-butyl-3-(2-(3-methylbut-2-en-1-yl)-1H-indol-3-yl)-2-((S)-pyrrolidine-2-carboxami-do)propanoate (12)
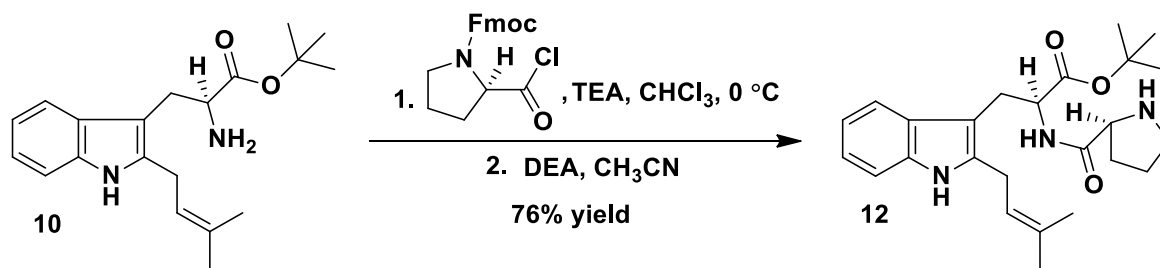
N-Fmoc-*L*-prolyl chloride (101 mg, 0.3 mmol) was dissolved in dry CHCl₃ (5 mL). This solution was added dropwise at 0 °C to a solution of **10** (100 mg, 0.2 mmol) and triethylamine (0.106 mL, 0.76 mmol) in dry CHCl₃ (2 mL). The mixture that resulted was stirred at 0 °C for 0.5 h, and then at room temperature for overnight. After consumption of the starting material, as judged by TLC analysis, the reaction was concentrated under reduced pressure. The residue was then dissolved in CH₃CN (5 mL) and stirred via a stir bar until it made a homogeneous solution. To this solution diethyl amine (10 mL) was added dropwise to the reaction flask using an addition funnel. The reaction was let stir overnight and progress was monitored by TLC. The solvent was removed under reduced pressure and the residue was purified with column chromatography on silica gel (DCM/MeOH = 50/1) to afford the product **12** as a brown solid (94 mg, 76% yield). **¹H NMR (CDCl₃, 300 MHz):** δ 8.02 (d, *J* = 9.0 Hz, 1H), 7.96 (s, 1H), 7.55 (d, *J* = 9.0 Hz, 1H), 7.28-7.24 (m, 1H), 7.11-7.03 (m, 2H), 5.35 (t, *J* = 7.5 Hz, 1H), 4.72 (q, *J* = 7.5 Hz, 1H), 3.71 (q, *J* = 7.5 Hz, 1H), 3.50 (t, *J* = 7.5 Hz, 2H), 3.28-3.11 (m, 2H), 3.04-2.87 (m, 2H), 2.09-1.99 (m, 1H), 1.80 (s, 3H), 1.78 (s, 3H), 1.70-1.61 (m, 3H), 1.36 (s, 9H); **¹³C NMR (CDCl₃, 75 MHz):** δ 173.6, 171.3, 135.7, 135.0, 134.9, 129.1, 121.0, 120.1, 119.1, 118.4, 110.3, 105.9, 81.6, 60.2, 53.5, 47.0, 30.4, 27.9, 27.2, 25.8, 25.2, 17.9; **HRMS (ESI+):** Calculated (m/z) for $C_{25}H_{36}N_3O_3$ [M+H]⁺: 426.2751, Found: 426.2745.

Synthesis of Model Compound, (*S*)-hexahydropyrrolo[1,2-a]pyrazine-1,4-dione (15)
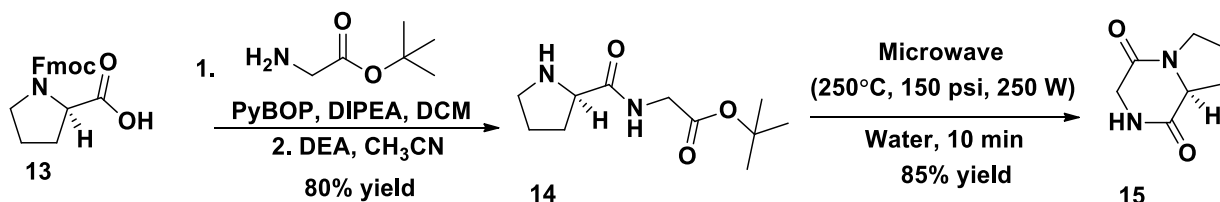
PyBOP (1.84 g, 3.55 mmol) and DIPEA (1.55 mL, 8.88 mmol) were added to a solution of Fmoc-*L*- proline **13** (1.0 g, 2.96 mmol) and *tert*-butyl ester glycine (0.414 g, 2.96 mmol) in CH_3CN (25 mL). The reaction was stirred overnight, and progress was monitored by TLC. After consumption of the starting material, as judged by TLC analysis, the reaction was concentrated under reduced pressure. The residue was then dissolved in CH_3CN (10 mL) and stirred via a stir bar until it made a homogeneous solution. To this solution diethyl amine (10 mL) was added dropwise using an addition funnel and the reaction was let stir overnight. Next day, the solvent was removed under reduced pressure and was extracted with hexane (3 x 15 mL). The residue was passed through flash column chromatography on silica gel (DCM/MeOH = 50/1) to afford the Fmoc removal dipeptide **14**. Then, the dipeptide **14** (100 mg, 0.22 mmol) was suspended in water (1 mL) and heated during 10 minutes at 250 °C and 150 psi, using a CEM Discover Microwave apparatus at 250 W. The resulting suspension was filtered through a Hirsch funnel and washed with water (5 mL), the solid was dried under high vacuum and the residue was purified with column chromatography on silica gel (DCM/MeOH = 50/1) to afford the product **15** as a white solid (57 mg, 85% yield). Compound **17** was confirmed[68] by comparing spectra to known NMR. **^{1}H NMR (CDCl$_3$, 300 MHz):** δ 7.10 (s, 1H), 4.10 (d, *J* = 15.0 Hz, 1H), 3.90 (dd, *J* = 15.0, 5.0 Hz, 1H), 3.69-3.52 (m, 2H), 2.42-2.34 (m, 1H), 2.14-2.01 (m, 2H), 1.95-1.87 (m, 2H). **^{13}C NMR (CDCl$_3$, 75 MHz):** δ 170.1, 163.5, 58.5, 46.6, 45.3, 28.5, 22.4.

Synthesis of Tryprostatin B (16)
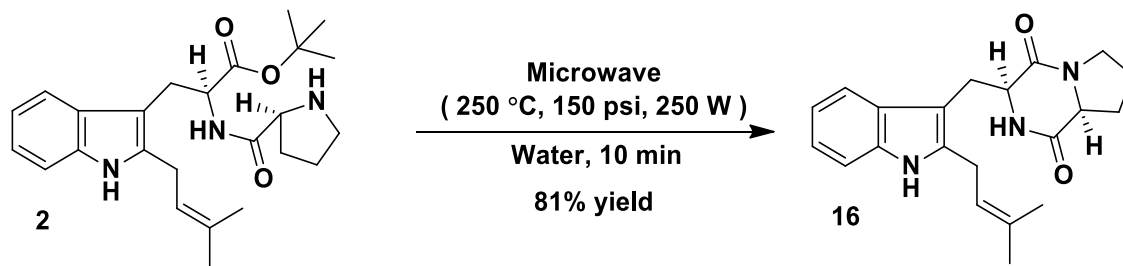
The dipeptide product **13** (50 mg, 0.12 mmol) was suspended in water (1 mL) and heated for 10 minutes at 250 °C and 150 psi, using a CEM Discover Microwave apparatus at 250 W. The resulting suspension was filtered through a Hirsch funnel and washed with water (5 mL). Then, the solid was dried under high vacuum and the residue was purified with column chromatography on silica gel (DCM/MeOH = 50/1) to afford the product **1** as yellow solid (33 mg, 81% yield). Compound **1** was confirmed[52] by comparing spectra to known NMR. **^{1}H NMR (CDCl$_3$, 500 MHz):** δ 8.03 (brs, 1H), 7.50 (d, J = 10.0 Hz, 1H), 7.34 (d, J = 5.0 Hz, 1H), 7.18 (t, J = 7.5 Hz, 1H), 7.12 (t, J = 7.5 Hz, 1H), 5.66 (s, 1H), 5.33 (t, J = 7.5 Hz, 1H), 4.39 (dd, J = 10.0, 5.0 Hz, 1H), 4.08 (t, J = 7.5 Hz, 1H), 3.72-3.67 (m, 2H), 3.63-3.59 (m, 1H), 3.49 (t, J = 7.5 Hz, 2H), 3.00-2.91 (m, 1H), 2.38-2.33 (m, 1H), 2.08-2.02 (m, 2H), 1.96-1.90 (m, 1H), 1.81 (s, 3H), 1.78 (s, 3H); **^{13}C NMR (CDCl$_3$, 125 MHz):** δ 169.4, 165.8, 136.4, 135.5, 135.4, 128.0, 121.9, 119.9, 119.7, 117.8, 110.8, 104.7, 59.3, 54.6, 45.4, 28.4, 25.8, 25.6, 25.1, 22.7, 18.0; **HRMS (ESI+):** Calculated (m/z) for C$_{21}$H$_{26}$N$_3$O$_2$ [M+H]$^+$: 352.2020, Found: 352.2035.

***Tert*-butyl 3-((dimethylamino)methyl)-6-methoxy-1H-indole-1-carboxylate (18)**
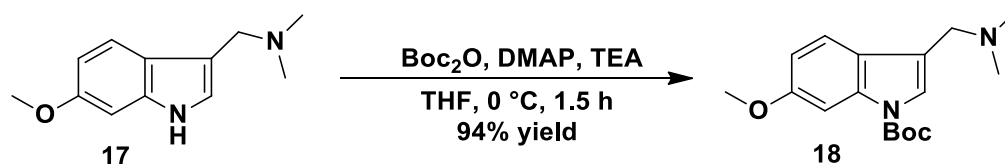
A solution of Boc anhydride (Boc$_2$O) (2.6.0 g, 14.7 mmol), 4-dimethylaminopyridine (DMAP) (0.12 g, 0.98 mmol), trimethylamine (TEA) (0.120 mL, 1.17 mmol) in THF (50 mL) was maintained at 0 °C for 30 min. A solution of 6-methoxy gramine (2.0 g, 9.8 mmol) in THF (15 mL) was added dropwise through the dropping funnel over a period of 30 min at 0 °C. The reaction mixture was stirred at 0 °C for 1.5 hours under nitrogen atmosphere. After consumption of starting material, as judged by TLC analysis, water (20 mL) was added to the reaction mixture. The aqueous layer was extracted with ether (3 x 15 mL), washed with brine (1 x 15 mL). The combined organic layer was dried over anhydrous Na$_2$SO$_4$. The crude product was purified with column chromatography on silica gel (hexane/EtOAc = 3/2) to give product **18** as a light brown solid (2.8 g, 94%). **^{1}H NMR (CDCl$_3$, 300 MHz):** δ 7.76 (s, 1H), 7.54 (d, *J* = 9.0 Hz, 1H), 7.39 (s, 1H), 6.88 (d, *J* = 9.0 Hz, 1H), 3.86 (s, 3H), 3.49 (s, 2H), 2.27 (s, 6H), 1.66 (s, 9H); **^{13}C NMR (CDCl$_3$, 75 MHz):** δ 157.9, 149.8, 136.6, 124.3, 123.0, 120.2, 118.1, 111.9, 99.3, 83.2, 55.5, 54.7, 45.5, 28.2; **HRMS (ESI+):** Calculated (m/z) for C$_{17}$H$_{25}$N$_2$O$_3$ (M+H)$^+$: 305.1860, Found 305.1850.

N-((1-(tert-butoxycarbonyl)-6-methoxy-2-(3-methylbut-2-en-1-yl)-1H-indol-3-yl)methyl)-N,N,3-trimeth -ylbut-2-en-1-aminium bromide (19)
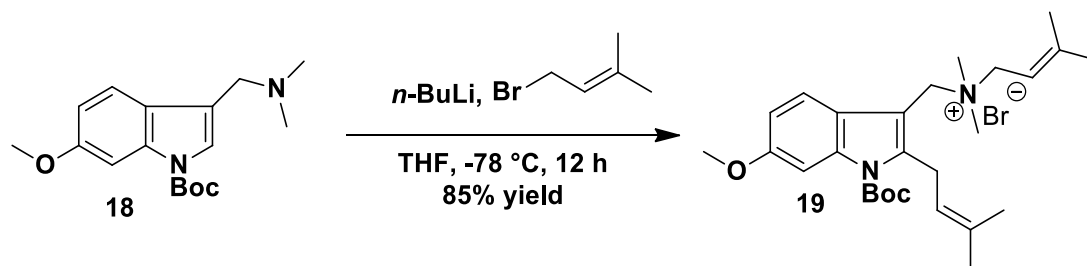

A solution of Boc-protected 6-methoxy gramine **18** (2.0 g, 6.6 mmol) in THF (25 mL) was taken in three necked round bottomed flask and nitrogen was bubbled through the solution for 20 min. This mixture was cooled to -78 °C and *n*-butyl lithium (5.3 mL, 2.5 M, 13.2 mmol) was added dropwise to the reaction mixture maintaining a temperature -78 °C over a period of 1 h under nitrogen atmosphere. Prenyl bromide (3.0 mL, 26.3 mmol) was added to the reaction dropwise through the dropping funnel over a period of 30 min. The reaction mixture was allowed to warm to room temperature and was stirred overnight. After consumption of the starting material, as judged by TLC analysis, water (20 mL) was added to the reaction mixture and THF was removed under reduced pressure. The mixture was then extracted with CH_2Cl_2 (3 x 15 mL), the combined organic layers were washed with brine solution (1 x 10 mL) and dried over anhydrous Na_2SO_4 and evaporated *in vacuo* to obtain crude product. The residue was purified with flash column chromatography on silica gel (DCM/MeOH = 20/1) to afford **19** as a brown solid (2.9 g, 85 %).

^{1}H NMR (CDCl$_3$, 300 MHz): δ 7.94 (d, *J* = 9.0 Hz, 1H), 7.57 (s, 1H), 6.82 (t, *J* = 6.0 Hz, 1H), 5.31 (t, *J* = 7.5 Hz, 1H), 5.07 (s, 2H), 4.95 (s, 1H), 4.42 (d, *J* = 6.0 Hz, 1H), 3.75 (s, 6H), 3.05 (s, 6H), 1.80 (s, 3H), 1.76 (s, 3H), 1.67 (s, 3H), 1.57 (s, 12H); **^{13}C NMR (CDCl$_3$, 75 MHz):** δ 157.7, 149.7, 148.7, 142.6, 136.9, 133.9, 122.8, 120.6, 120.4, 112.5, 111.2, 106.0, 99.6, 84.9, 61.8, 58.3, 55.5, 48.3, 27.8, 26.8, 26.4, 25.4, 19.4, 18.6; **HRMS (ESI+):** Calculated (m/z) for $C_{27}H_{41}N_2O_3$ [M]$^+$: 441.3112, Found: 441.3102.

***Tert*-butyl-2-((diphenylmethylene)amino)-3-(6-methoxy)-(2-(3-methylbut-2-en-1-yl)-1H-indol-3-yl)- 1*H*-indol-3-propanoate (2)**
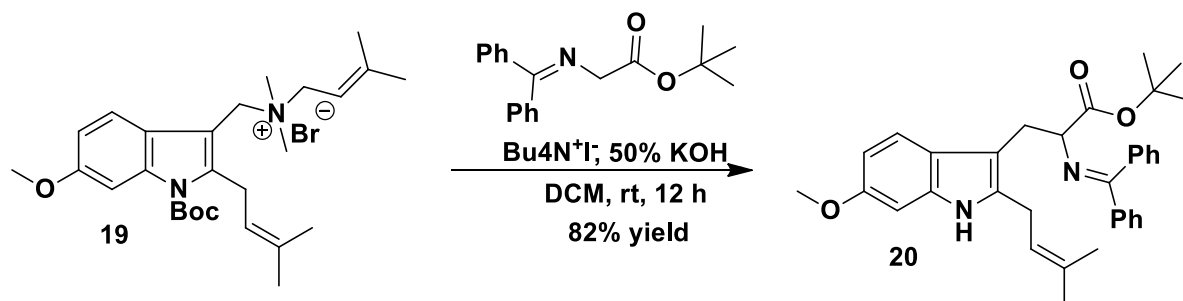
A solution of C2, N-diprenylated-6-methoxy gramine salt **19** (1.0 g, 1.9 mmol), *N*-(diphenylmethylene) glycine tert-butyl ester (680 mg, 2.3 mmol) and tetrabutylammonium bromide (232 mg 0.383 mmol) in dry DCM (10 mL) was maintained at -20 °C for 30 minutes. 50% aqueous KOH (1.0 g, 19.0 mmol) was added to the reaction by maintaining at the room temperature. Reaction was stirred vigorously with mechanical stirrer for 12 h. After consumption of the starting material, as judged by TLC, water was added, and the aqueous layer was extracted with CH_2Cl_2 (3 x 10 mL). The combined organic layers were dried over anhydrous Na_2SO_4; the solvent was evaporated *in vacuo*. The residue was purified with flash column chromatography on silica gel (hexane/EtOAc = 20/1) to afford as a light yellow solid **20** (820 mg, 82%). **^{1}H NMR (CDCl₃, 300 MHz):** δ 7.75 (d, *J* = 6.0 Hz, 3H), 7.35-7.31 (m, 2H), 7.26-7.20 (m, 3H), 7.07 (t, *J* = 7.5 Hz , 3H), 6.77 (d, *J* = 3.0 Hz, 1H), 6.57 (dd, *J* = 9.0 Hz, 3.0 Hz, 1H), 6.43 (d, *J* = 9.0 Hz, 2H), 5.06 (t, *J* = 7.5 Hz, 1H), 4.21 (dd, *J* = 9.0 Hz, 3.0 Hz, 1H), 3.83 (s, 3H), 3.33 (dd, *J* = 19.5 Hz, 4.5 Hz, 3H), 3.22 (dd, *J* = 15.0 Hz, 9.0 Hz, 1H), 1.66 (s, 3H), 1.63 (s, 3H), 1.46 (s, 9H); **^{13}C NMR (CDCl₃, 75 MHz):** δ 171.4, 169.5, 155.7, 139.5, 136.0, 135.5, 134.2, 134.1, 129.9, 128.7, 127.8, 127.7, 127.6, 123.7, 120.8, 119.0, 108.4, 107.1, 94.2, 80.8, 66.7, 55.8, 28.1, 27.9, 25.7, 25.1, 17.7; **HRMS (ESI+):** Calculated (m/z) for $C_{34}H_{39}N_2O_3$ [M+H]$^+$: 523.2955, Found: 523.3072.

Tert-butyl-2-amino-3-(6-methoxy)-(2-(3-methylbut-2-en-1-yl)-1H-indol-3-yl)   propanoate (21)
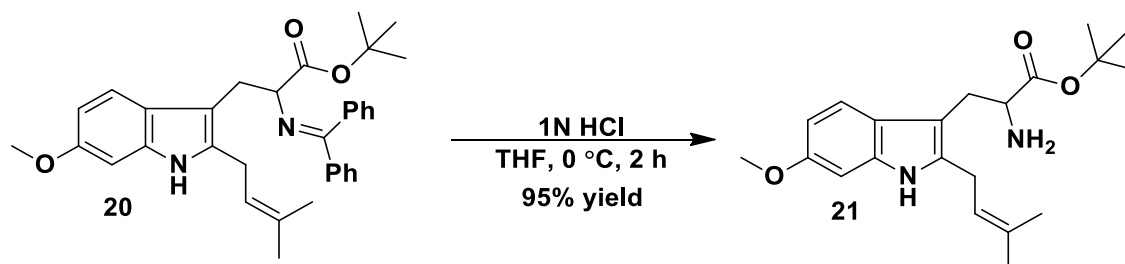

A solution of **20** (500 mg, 0.96 mmol) THF (10 mL) and 1N hydrochloric acid (5 mL) was maintained in cold water bath for 2 h under nitrogen atmosphere. After consumption of the starting material, as judged by TLC analysis, the mixture was extracted with hexane (3 x 10 mL) then the aqueous layer was basified using saturated $NaHCO_3$ and extracted with CH_2Cl_2 (3 x 10 mL), washed with brine (1 x 5 mL). The combined organic layer was dried over anhydrous $MgSO_4$ and the solvent was evaporated under *in vacuo*. The crude product was purified by silica gel column chromatography (DCM/MeOH = 20:1) to afford **21** as a light yellow solid (307 mg, 90% yield).

^{1}H NMR (CDCl$_3$, 300 MHz): δ 7.87 (brs, 1H), 7.44 (d, J = 5.0 Hz, 1H), 6.82 (s, !H), 6.77 (d, J = 5.0, 1H), 3.84 (s, 3H), 3.68 (d, J = 10.0 Hz, 1H), 3.47 (d, J = 10.0 Hz, 2H), 3.18 (dd, J = 15.0, 5.0 Hz, 1H), 2.85 (dd, J = 15.0, 10.0 Hz, 1H), 1.79 (s, 3H), 1.77 (s, 1H), 1.44 (s, 9H),; **^{13}C NMR (CDCl$_3$, 75 MHz):** δ 174.7, 155.9, 136.0, 134.4, 134.4, 123.3, 120.6, 118.9, 108.7, 106.7, 94.6, 80.9, 55.9, 55.8, 30.6, 28.0, 25.8, 25.2, 17.9; **HRMS (ESI+):** Calculated (m/z) for $C_{21}H_{31}N_2O_3$ [M+H]$^+$: 359.2329, Found: 359.2404.

1.8. References

1. Beese, L.; Stubbs, G.; Cohen, C. Microtubule structure at 18 A resolution. *J. Mol. Biol*. **1987**, *194*, 257-264.

2. de Pablo, P. J.; Schaap, I. A. T.; MacKintosh, F. C.; Schmidt, C. F. Deformation and collapse of microtubules on the nanometer scale. *Phys. Rev. Lett*. **2003**, *91*, 98-101.

3. Chrétien, D.; Wade, R. H. New data on the microtubule surface lattice. *Biol. Cell* **1991**, *71*, 161-174.

4. Pampaloni, F.; Florin, E. Microtubule architecture: inspiration for novel carbon nanotube-based biomimetic materials. *Trends Biotechnol*. **2008**, *26*, 302-310.

5. Odde, D. J. Ma, L.; Briggs, A. H.; DeMarco, A.; Kirschner, M. W. Microtubule bending and breaking in living fibroblast cells. *J. Cell. Sci*. **1999**, *112*, 3283-3288.

6. Chrétien, D.; Fuller, S. D. Microtubules switch occasionally into unfavorable configurations during elongation. *J. Mol. Biol*. **2000**, *298*, 663-676.

7. Chrétien, D.; Flyvbjerg, H.; Fuller, S. D. Limited flexibility of the inter-protofilament bonds in microtubules assembled from pure tubulin. *Eur. Biophys. J*. **1998**, *27*, 490-500.

8. Rochlin, M. W.; Dailey, M. E.; Bridgman, P. C. Polymerizing microtubules activate site-directed F-actin assembly in nerve growth cones. *Mol. Biol. Cell* **1999**, *10*, 2309–2327.

9. Pilhofer, M.; Ladinsky, M. S.; McDowall, A. W.; Petroni, G.; Jensen, G. J. Microtubules in Bacteria: Ancient Tubulins Build a Five-Protofilament Homolog of the Eukaryotic Cytoskeleton. *PLos Biol.* **2011**, *9*, e1001213.

10. Wang, J. D.; Levin, P. A. Metabolism, cell growth and the bacterial cell cycle. *Nat. Rev. Microbiol*. **2009**, *7*, 822–827.

11. Ubersax J. A.; Woodbury, E. L.; Quang, P. N.; Paraz, M.; Blethrow, J. D.; Shah, K.; Shokat, K. M.; Morgan, D. O. Targets of the cyclin-dependent kinase Cdk1. *Nature* **2003**, *425*, 859-864.

12. Morgan, D. O. Review of The Cell Cycle: Principles of Control. *Cell Div*. **2007**, *2*, 27-32.

13. Colin P. C. De Souza, C. P. C.; Osmani, S. A. Mitosis, Not Just Open or Closed. *Eukaryot Cell.* **2007**, *6*, 1521–1527.

14. Barnum, K. J.; O'Connell, M. J. Cell Cycle Regulation by Checkpoints. *Methods Mol Biol.* **2014**, *1170*, 29–40.

15. Campbell, N. A.; Reece, J. B. Biology San Francisco: Benjamin Cummings. **2005**, *7*, 221–224.

16. Manandhar, G. F.; Schatten, H.; Sutovsky, P. Centrosome reduction during gametogenesis and its significance. *Biol. Reprod*. **2005**, *72*, 2–13.

17. Matson, D. R.; Stukenberg, P. T. Spindle Poisons and Cell Fate: A Tale of Two Pathways. *Molecular Interventions* **2011**, *11*, 141–150.

18. van der Heijden, R.; Jacobs, D. I.; Snoeijer, W.; Hallard, D.; Verpoorte, R. The Catharanthus alkaloids: Pharmacognosy and biotechnology. *Current Med. Chem*. **2004**, *11*, 607–628.

19. Sears, J. E.; Boger, D. L. Total Synthesis of Vinblastine, Related Natural Products, and Key Analogues and Development of Inspired Methodology Suitable for the Systematic Study of Their Structure-Function Properties. *Accounts of Chemical Research*. **2015**, *48*, 653–662.

20. Kuboyama, T.; Yokoshima, S.; Tokuyama, H.; Fukuyama, T. Stereocontrolled total synthesis of (+)-vincristine. *Proceedings of the National Academy of Sciences of the United States of America.* **2004**, *101*, 11966–11970.

21. Takimoto, C. H.; Calvo, E. Chapter 3: Principles of Oncologic Pharmacotherapy". In Pazdur, R.; Wagman, L. D.; Camphausen, K. A.; Hoskins, W. J. Cancer Management: A Multidisciplinary Approach. **2008**, *11*.

22. Cui, C. -B.; Kayeya, H.; Okada, G.; Onose, R.; Ubukata, M.; Takahashi, I.; Isono, K.; Osada, H. J. Tryprostatins A and B, Novel Mammalian Cell Cycle Inhibitors Produced. *Antibiot.* **1995**, *48*, 1382-1384.

23. Cui, C.-B.; Kayeya, H.; Osada, H. Novel Mammalian Cell Cycle lnhibitors, Spirotryprostatins A and B, Produced by Aspergillusfumigatus, Which Inhibit Mammalian Cell Cycle at G2/M Phase. *Tetrahedron* **1996**, *52*, 12651-12666.

24. Cui, C. -B.; Kayeya, H.; Osada, H. Novel MammalianCell Cycle Inhibitors, Tryprostatins A, B and Other Diketopiperazines Produced by Aspergillus fumigatus I. Taxonomy, Fermentation, Isolation and Biological Properties. *J. Antibiot*. **1996**, *49*, 527-533.

25. Cui, C. -B.; Kayeya, H.; Osada, H. Novel MammalianCell Cycle Inhibitors, Tryprostatins A, B and Other Novel MammalianCell Cycle Inhibitors, Tryprostatins A, B and Other Diketopiperazines Produced by Aspergillus fumigatus II. Physico-chemical Properties and Structures. *J. Antibiot*. **1996**, *49*, 534-540.

26. Osada, H.; Cui, C. -B.; Onose, R.; Hanaoka, F. Screening of Cell Cycle Inhibitors from Microbial Metabolites by a Bioassay Using a Mouse cdc2 Mutant Cell Line, tsFr210. *Bioorg. Med. Chem*. **1997**, *5*, 193-203.

27. Usui, T.; Kondoh, M.; Cui, C.; Mayumi, T.; Osada, H. Tryprostatin A, a specific and novel inhibitor of microtubule assembly. *Biochem. J*. **1998**, *333*, 543-548.

28. Usui, T.; Nakazawa, J.; Osada, H. Studies on inhibitory mechanism of microtubule inhibitors. *Riken Rev*. **2001**, *41*, 92-93.

29. Zhao, S.; Smith, K. S.; Deveau, A. M.; Dieckhaus, C. M.; Johnson, M. A.; Macdonald, T. L.; Cook, J. M. Biological Activity of the Tryprostatins and Their Diastereomers on Human Carcinoma Cell Lines. *J. Med. Chem*. **2002**, *45*, 1559-1562.

30. Caballero, E.; Avendaño, C.; Menéndez, J. C. Brief Total Synthesis of the Cell Cycle Inhibitor Tryprostatin B and Related Preparation of Its Alanine Analogue. *J. Org. Chem*. *2003*, *68*, 6944-6951.

31. Woehlecke, H.; Osada, H.; Herrmann. A.; Lage, H. Reversal of Breast Cancer Resistance Protein-Mediated Druc Resistance by Tryprostatin A. *Int. J. Cancer* **2003**, *107*, 721-728.

32. Jain, H.; Zhang, C.; Zhou, S.; Zhou, H.; Ma, J.; Liu, X.; Liao, X.; Deveau, A.; Dieckhaus, C.; Johnson, M.; Smith, K.; Macdonald T.; Kakeya, H.; Osada, H.; Cook, J. M. Synthesis and Structure-Activity Relationship Studies on Tryprostatin A, A Potent Inhibitor of Breast Cancer Resistance Protein. *Bioorg. Med. Chem*. **2008**, *16*, 4626-4651.

33. Maiya, S.; Grundmann, A.; Li, S.-M.; Turner, G. Improved tryprostatin B production by heterologous gene expression in Aspergillus nidulans. *Fungal Genetics and Biology* **2009**, *46*, 436–440.

34. Sanz-Cervera, J. F.; Stocking, E. M.; Usui, T.; Osada, H.; Williams, R. M. Synthesis and Evaluation of Microtubule Assembly Inhibition and Cytotoxicity of Prenylated Derivatives of cyclo-L-Trp-L-Pro. *Bioorg. Med. Chem*. **2000**, *8*, 2407-2415.

35. Pommier, Y. Topoisomerase I inhibitors: camptothecins and beyond. *Nat. Rev. Cancer*.

2006, *6*, 789-802.

36. Keen, N.; Taylor, S. Aurora-Kinase Inhibitors as Anticancer Agents. *Nat. Rev. Cancer* **2004**, *4*, 927-936.

37. Jordan, M. A.; Wilson, L. Microtubules as a Target for Anticancer Drugs. *Nat. Rev. Cancer* **2004**, *4*, 253-265.

38. Gallagher, R. T.; Latch, G. C. M. Production of the Tremorgenic Mycotoxins Verruculogen and Fumitremorgin B by *Penicillium piscarium* Westling. *Appl Environ Microbiol.* **1977***, 33*, 730–731.

39. Mukhtar, E.; Adhami, V. M.; Mukhtar, H. Targeting Microtubules by Natural Agents for Cancer Therapy. *Mol Cancer Ther*. **2014**, *13*, 275–284.

40. Dumontet, C.; Jordan, M. A. Microtubule-binding agents: a dynamic field of cancer therapeutics. *Nat. Rev. Drug Discov*. **2010**, *9*, 790–803.

41. Depew, K. M.; Danishefsky, S. J.; Rosen, N.; Sepp-Lorenzino, L. J. Total Synthesis of Tryprostatin B: Generation of a Nucleophilic Prenylating Species from a Prenylstannane. *J. Am. Chem. Soc*. **1996**, *118*, 12463-12464.

42. Gan, T.; Liu, R.; Yu, P.; Zhao, S.; Cook, J. M. Enantiospecific Synthesis of Optically Active 6-Methoxytryptophan Derivatives and Total Synthesis of Tryprostatin A. *J. Org. Chem.* **1997**, *62*, 9298-9304.

43. Gan, T. Cook, J. M. Enantiospecific Total Synthesis of Tryprostatin A. *Tetrahedron Lett*. **1997**, *38*, 1301-1304.

44. Zhao, S.; Gan, T.; Yu, P.; Cook, J. M. Total Synthesis of Tryprostatin A and B As Well As Their Enantiomers. *Tetrahedron Lett*. **1998**, *39*, 7009-7012.

45. Schkeryantz, J. M.; Woo, J. C. G.; Siliphaivanh, P.; Depew, K. M.; Danishefsky, S. J. Total Synthesis of Gypsetin, Deoxybrevianamide E, Brevianamide E, and Tryprostatin B: Novel Constructions of 2,3 Disubstituted Indoles. *J. Am. Chem. Soc*. **1999**, *121*, 11964-11975.

46. Cardoso, A. S.; Lobo, A. M.; Prabhakar, S. Studies in the aza-Cope reaction: a formal highly enantioselective synthesis of tryprostatin B. *Tetrahedron Lett.* **2000**, *41*, 3611–3613.

47. Wang, H.; Usui, T.; Osada, H.; Ganesan, A. J. Synthesis and Evaluation of Tryprostatin B and Demethoxyfumitremorgin C Analogues. *J. Med. Chem*. **2000**, *43*, 1577-1585.

48. Wang, B.; Chen, L.; Kim, K. Preparation of novel 2-(trialkylsilyl)ethyl linkers and first synthesis of Tryprostatin B on solid phase. *Tetrahedron Lett*. **2001**, *42*, 1463–1466.

49. Cardoso, A. S. P.; Marques, M. M. B.; Srinivasan, N.; Prabhakar, S.; Lobo, A. M.; Rzepa, H. S. Studies in sigmatropic rearrangements of N-prenylindole derivatives – a formal enantiomerically pure synthesis of tryprostatin B. *Org. Biomol. Chem*. **2006**, *4*, 3966-3972.

50. Wagger, J.; Svete, J.; Stanovnik, B. Synthesis of Unsaturated Tryprostatin B Analogues and Determination of Their Enantiomeric Purity with (S)-1-Benzyl-6-methylpiperazine-2,5-dione. *Synthesis* **2008**, *9*, 1436–1442.

51. Yamakawa, T.; Ideue, E.; Shimokawa, J.; Fukuyama, T. Total Synthesis of Tryprostatins A and B. *Angew. Chem. Int. Ed*. **2010**, *49*, 9262-9265.

52. Yamakawa, T.; Ideue, E.; Iwaki, Y.; Sato, A.; Tokuyama, H.; Shimokawa, J.; Fukuyama, T. Total Synthesis of Tryprostatins A and B. *Tetrahedron* **2011**, *67*, 6547-6560.

53. Mahmood S., Hossain M. M. Iron Lewis Acid Catalyzed Reactions of Aromatic Aldehydes with Ethyl Diazoacetate: Unprecedented Formation of 3-Hydroxy-2-arylacrylic Acid Ethyl Esters by a Unique 1,2-Aryl Shift. *J. Org. Chem*. **1998**, *63*, 3333-3336.

54. Dudley M., Morshed M., Brennan C., Islam S., Ahmad S., Atuu M., Branstetter B., Hossain M. M. Acid-Catalyzed Reactions of Aromatic Aldehydes with Ethyl Diazoacetate: An Investigation on the Synthesis of 3-Hydroxy-2-arylacrylic Acid Ethyl Esters. *J. Org. Chem.* **2004**, *69*, 7599-7608.

55. Mahmood, S. J.; Brennan, C.; Hossain, M. M. A Convenient New Synthesis of a Naproxen Precursor. *Synthesis* **2002**, *13*, 1807-1809.

56. Morshed, M. M.; Wang, Q.; Islam, S.; Hossain, M. M. Convenient Synthesis of 5-Aryl Uracils. *Synth. Commun.* **2007**, *37*, 4173–4181.

57. Islam S.; Brennan C.; Wang Q.; Hossain M. M. Convenient Method of Synthesizing 3-Ethoxycarbonyl Indoles. *J. Org. Chem.* **2006**, *71*, 4675-4677.

58. Todd, R.; Hossain M. M. A Practical Synthesis of Indole-Based Heterocycles Using an Amidoaluminum-Mediated Strategy. *Synthesis* **2009**, *11*, 1846-1850.

59. Ma, C.; Liu, X.; Li, X.; Flippen-Anderson, J.; Yu, S.; Cook, J. M. Efficient Asymmetric Synthesis of Biologically Important Tryptophan Analogues via a Palladium-Mediated Heteroannulation Reaction. *J. Org. Chem.* **2001**, *66*, 4525-4542.

60. Todd, R.; Huisman, M.; Uddin, N.; Oehm, S.; Hossain, M. M. One Pot Enantioselective Synthesis of Tryptophan Derivatives via Phase- Transfer Catalytic Alkylation of Glycine Using a Cinchona-Derived Catalyst. *Synlett* **2012**, *23*, 2687-2691.

61. Wang, F.; Fang, Y.; Zhu, T.; Zhang, M. Lin, A.; Gu, Q.; Zhu, W. Seven new prenylated indole diketopiperazine alkaloids from holothurianderived fungus Aspergillus fumigatus. *Tetrahedron* **2008**, *64*, 7986–7991.

62. Huisman, M; Oehm, S; Rheingold, A; Hossain, M, *CSD Communication*, **2016**.

63. Starks, C. M. Phase-transfer catalysis. I. Heterogeneous reactions involving anion transfer by quaternary ammonium and phosphonium salts. *J. Am. Chem. Soc*. **1971**, *93*, 195-199.

64. Zheng, B.-H.; Ding, C.-H.; Hou, X.-L.; Dai, L.-X. Ag-Catalyzed Diastereo- and Enantioselective Synthesis of β-Substituted Tryptophans from Sulfonylindoles. *Org. Lett*. **2010**, *12*, 1688-1691.

65. Campo, V. L.; Martins, M. B.; da Silva, C. H. T. P.; Carvalho, I. Novel and facile solution-phase synthesis of 2,5-diketopiperazines and O-glycosylated analogs. *Tetrahedron* **2009**, *65*, 5343-5349.

66. Stocking, E.; Sanz-Cervera, J.; Williams, R. Total Synthesis of VM55599. Utilization of an Intramolecular Diels−Alder Cycloaddition of Potential Biogenetic Relevance. *J. Am. Chem. Soc.* **2000**, *122*, 1675-1683.

67. Pérez-Picaso, L.; Escalante, J.; Olivo, H. F; Rios, M. Y. Efficient Microwave Assisted Syntheses of 2,5-Diketopiperazines in Aqueous Media. *Molecules* **2009**, *14*, 2836-2849.

68. Furtado, N. A. J. C.; Pupo, M. T.; Carvalho, I.; Campo, V. L. C.; Duarte, M. C. T.; Bastos, J. K. Diketopiperazines Produced by an Aspergillus fumigatus Brazilian Strain. *J. Braz. Chem. Soc*. **2005**, *16*, 1448-1453.

69. Huisman, M.; Rahaman, M.; Asad, S.; Oehm, S.; Novin, S.; Rheingold, A. L.; Hossain, M. M. Total Synthesis of Tryprostatin B: Synthesis and Asymmetric Phase-Transfer-Catalyzed Reaction of Prenylated Gramine Salt. *Org. Lett*. **2019**, *21*, 134−137.

70. Fani, N.; Bordbar, A. K.; Ghayeb, Y.; Sepehric, S. Computational design of Tryprostatin-A derivatives as novel αβ-tubulin inhibitors. *J. Biomol. Struct. Dynam*. **2014**, *20*, 37-41.

71. Van, T. N.; Claes, P.; Kimpe, N. D. Setyternthesis of Functionalized Diketopiperazines as Cyclotryprostatin and Tryprostatin Analogues. *Synlett* **2013**, *24*, 1006–1010.

PART II: SYNTHESIS AND BIOLOGICAL ASSESSMENT OF HISTONE DEACETYLASE INHIBITORS

2.1. Introduction

2.1.1. Histone

Histones are most abundant highly alkaline proteins found in eukaryotic cell nuclei.[1,2] Five major families of histones are H1/H5, H2A, H2B, H3, and H4. Histones H2A, H2B, H3 and H4 are known as the core histones, while histones H1/H5 are known as the linker histones.[3-5] Histone H2A and H2B make a dimer and later dimer of dimer, and H3 and H4 make dimer and later tetramer, all these core histones then combine and form octamer of histones.[6-8] This histone octamer rapped by deoxyribonucleic acid (DNA) and makes nucleosome.[9] They are the chief protein components of chromatin and playing a role in gene regulation. This interaction is largely regulated by the modification of lysine residues.[10]

2.1.2. Histone Deacetylase (HDAC)

Histone deacetylases (HDAC), also called lysine deacetylases (KDAC), are a class of enzymes which eliminate acetyl groups ($O=C-CH_3$) from an N-acetyl lysine amino acid on a histone, permitting the histone to wrap the DNA more strongly.[11-15] Its action is opposite to that of histone acetyltransferase (HAT) which replace acetyl groups ($O=C-CH_3$) to the lysine amino acid on a histone.[16-20] Acetyl CoA transfers the acetyl group to the lysine terminal of the histone (Figure 2.1).[21-25] Acetylation/deacetylation process is important because it regulates many protein functions in cells.[26-30] DNA is wrapped around histones, and DNA expression, protein stability, and protein-protein interactions are regulated by acetylation and de-acetylation.[31-35] HAT/HDAC inhibition and posttranslational modifications are essential for the regulation of many cellular processes such as transcription, cell division, cell survival and differentiation.[36-40]
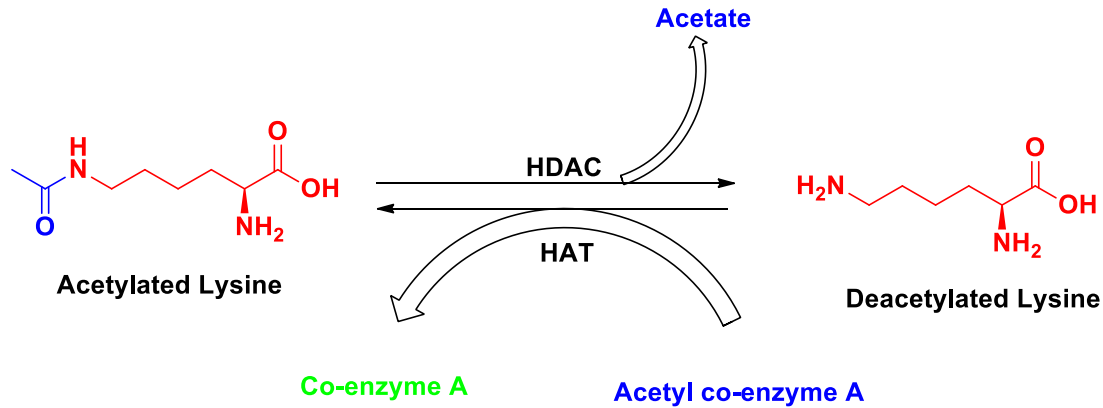
Figure 2.1: Mode of Action of HDAC and HAT

HATs and HDACs enzymes are responsible for amendments to chromatin structures that can regulate gene transcription.[41-45] In general, HAT acetylation activity leads to an increase in gene transcription by neutralizing the positive charge on lysine residuals of histones, which relaxes their interactions with the negatively charged DNA backbone, leading to form a more active chromatin framework.[46, 47] In contrast, HDACs catalyze the removal of the acetyl groups on lysine residuals located on the amino-terminal tails of core histones, which leads to gene repression by chromatin condensation, leading to form an inactive chromatin framework.[48] As a result, inhibition of HATs leads to a gene that is always deactivated and produced oncogene, while inhibition of HDACs leads to general hyperacetylation of histones, which is followed by the transcriptional activation of certain genes through relaxation of the DNA conformations and produced antioncogene.[49-52] Usually, cancer is considered to initiate from a wide variety of genetic and genomic modifications, such as mutations, deletions, rearrangements, and amplifications, leading to abnormal expression of tumor suppressor genes and oncogenes. Gathering evidence indicates that cancer is associated with abnormal cell functions that include apoptosis, autophagy, cell motility, and DNA repair. These cell functions are controlled at least in part by HDACs.[53-56]

2.1.3. Classification of HDAC proteins

Based on their size, number of catalytic sites, subcellular localization, and their sequence homology to yeast counterparts, there are total eighteen known human HDACs proteins that are divided into four classes (Figure 2.2).[57] HDACs 1, 2, 3 and 8 are classified as Class I which are found in nucleus, HDACs 4, 5, 7, and 9 are classified as Class IIa and found in nucleus and cytoplasm. HDACs 6 and 10 are classified as Class IIb and found in cytoplasm. HDAC 11 is known as class IV and found in both nucleus and cytoplasm. All these HDACs are Zn^{2+} dependent enzymes. Class III proteins, also known as sirtuins, (SIRTs 1–7) are defined by their dependency on the coenzyme, electron transporter, nicotinamide adenine dinucleotide (NAD^+), found in nucleus and cytoplasm.[58-60]

Class	Name	Location in Cell	Location in Body	Group
Class I	HDAC1 HDAC2 HDAC3 HDAC8	Nucleus	Ubiquitous	Zn Dependent
Class IIA	HDAC4 HDAC5 HDAC7 HDAC9	Nucleus/Cytoplasm	Tissue	Zn Dependent
Class IIB	HDAC6 HDAC10	Cytoplasm	Tissue	Zn Dependent
Class III	SIRT (1-7)	Nucleus/Cytoplasm	Tissue	NAD Dependent
Class IV	HDAC11	Nucleus/Cytoplasm		Zn Dependent

Figure 2.2: Classification of HDAC

2.1.4. HDAC Involvement with Different Types of Cancers and Memory Loss

Cancer is a group of diseases involving abnormal cell growth which is a complex process that is influenced by multiple factors and progresses in multiple steps.[61] This unwanted cell growth in one place spreads out to other parts of the body. A typical characteristic of human cancer is the deregulation of histone acetylation which has the fatal consequence of gene transcription.[62] The decrease of histone acetylation is the reason for cancer, for example gastrointestinal tumors. It is well established and reported by scientists that the acetylation/deacetylation state of histones has an important effect on the biological activity of a cell.[63] Any imbalance in the levels of acetylation/deacetylation can encourage abnormal outgrowth and cell death. HDACs are expressed at much higher rates than normal cells in numerous types of cancers. Due to the overexpression of HDAC, it creates different types of cancer such as prostate, ovarian (HDAC1, HDAC2, and HDAC3), colorectal, lung cancers (HDAC1 and HDAC3), gastric pancreatic (HDAC2) and hepatocellular carcinomas. The overexpression is only found in cancer cells, but are not found in normal, resting endothelial cells and normal organs.[64] Solid and hematological tumors are the cause of unusual expression of classical (class I, II, and IV) HDACs. HDACs has been connected to a variety of malignancies, including with advanced disease and poor outcomes in patients. It has been reported that high expression of HDAC1, 2, and 3 are related with poor outcomes in gastric and ovarian cancers, and high expression of HDAC8 correlates with advanced-stage disease and poor survival in neuroblastoma. HDACs have also been found broadly dysregulated in multiple myeloma (MM) and overexpression of class I HDACs, particularly HDAC1, is associated with inferior patient outcomes.[65] HDAC2 and 3 are responsible for blocking neural plasticity and impair memory, and HDAC inhibitors increase histone acetylation and enhance both memory and synaptic plasticity.[66-68]

2.2. HDAC Inhibitors

Over the last decade, there has been extensive research and devolvement of many HDACi which has led to very promising results in treating cancer cells and other various diseases.[69-83] Several HDACi drugs are in clinical trials for treatment of cancers and diseases (Figure 2.3).[84-89] The first HDACi, suberoyl anilide hydroxamic acid (SAHA, Vorinostat) was approved by the Food and Drug Administration (FDA) for treatment of T-Cell lymphoma (CTCL) in the early 2000s.[90-93] Then, in 2009 the FDA approved romidepsin/FK-228 also for CTCL.[94-96] SAHA is considered to be a pan-inhibitor, which means it has no selective to any class or specific HDAC protein and inhibits the majority of the 11-zinc dependent HDAC isoforms. However, FK-228 is considered a class I selective inhibitor (inhibiting only HDAC1 and HDAC2). Valproic acid and trichostatin A are in preclinical trials.[74, 98]

Class	HDAC Inhibitor	Target HDAC Class	Clinical Status
Hydroxamic Acids	Trichostatin A	Pan Inhibitor	Preclinical
	SAHA	Pan Inhibitor	Approved for Cutaneous T-Cell Lymphoma
	Belinostat	Pan Inhibitor	Approved for Cutaneous T-Cell Lymphoma
	Panabiostat	Pan Inhibitor	Approved for Multiple Myeloma
Short Chain Fatty Acids	Valproic Acid	HDAC1 and HDACIIA	Approved for Epilepsia, Bipolar Disorders, and Migrane
Benzamide	Entinostat	HDAC1	Phase III Clinical Trial
Cyclic Tetrapeptide	Romidepsin	HDAC1	Approved for Cutaneous T-Cell Lymphoma

Figure 2.3: Overview of Selected HDAC Inhibitors

There are many different types of HDAC inhibitors but the four most promising classes of HDACi are usually classified based on their chemical structure such as 1) hydroxamic acids, 2) cyclic peptides, 3) short-chain fatty acids, and 4) benzamide/ketone derivatives (Figure 2.4).[99-108]
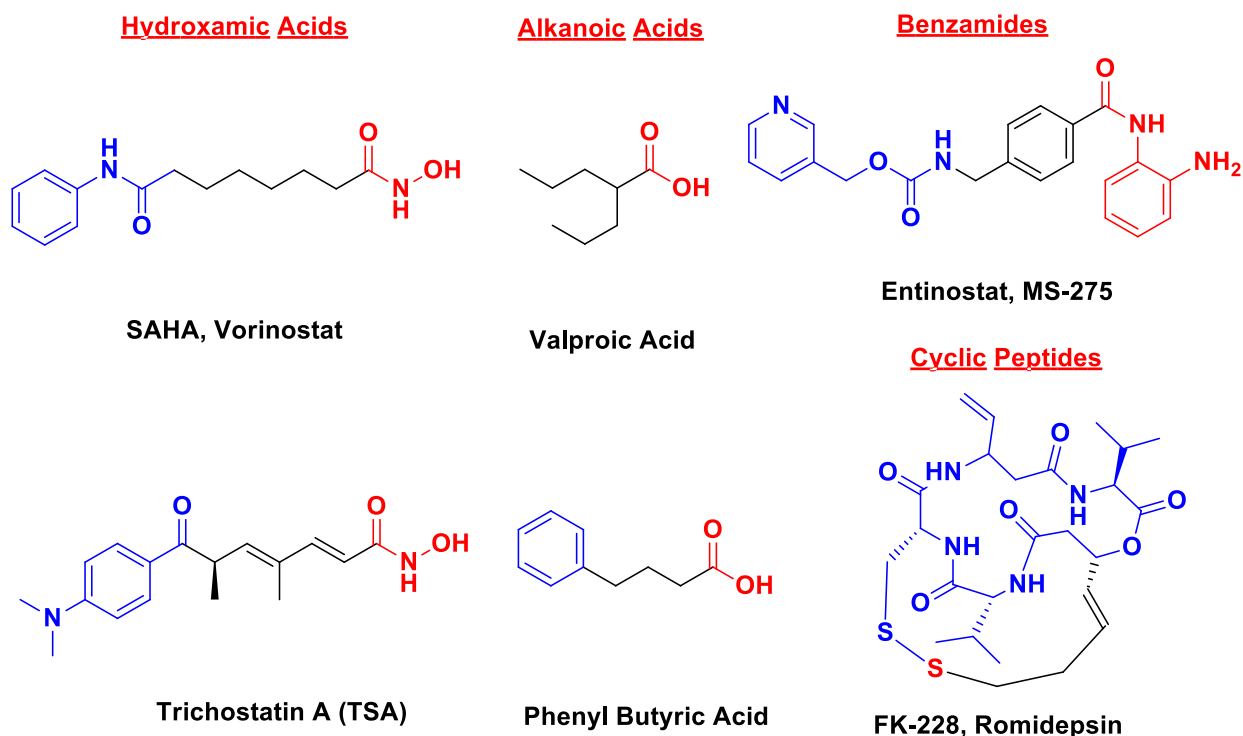
Figure 2.4: Types of HDAC Inhibitors

All the four groups of HDAC inhibitors have similar trends structurally. The structure of HDACi are characterized by these main features: a coordinating group/zinc binding group (ZBG) (such as a thiol or hydroxamic acid) to chelate to Zn^{2+} in the active site, a hydrophobic region (capping group), and a five to seven carbon linker that connects the cap group to ZBG (Figure 2.5). In HDAC inhibitors, linker connects a cap region and a ZBG.[109-123] The cap is relatively flexible and mediates surface-to-surface interactions between drug and protein target; the ZBG is critical for HDAC inhibitory activity by chelating a zinc ion in the catalytic center of HDACs.[124-151]

2.2.1. Mechanism of HDAC Inhibition

To understand how HDAC inhibitors bind to their enzymes, the first experiments were carried out to study in 1999.[152] The structure of the complexes of TSA and SAHA with histone deacetylase-like protein were clearly measured to 2.0 angstroms (Å) resolution. For further development of more potent and specific HDAC specific inhibitors, analysis of the X-ray crystal revealed that the region interacting with TSA or SAHA of histone deacetylase-like protein contains three main features 1) a surface recognition section, 2) a tube-like, 11 Å deep channel, and 3) a 14 Å long, tapered pocket which attaches to the channel.[153] Structure-activity relationship showed that inhibitors such as TSA and SAHA were able to block the HDAC activity through chelation of the zinc ion using a polar moiety such as hydroxamic acid or benzamide groups and in the similar way, romidepsin FK228 were able to block the HDAC activity through chelation of zinc ion using thiol group.[154] HDAC inhibitors are one of the most promising targets for the development of anti-cancer drugs. Results from several studies and market demand of drugs have encouraged further development of more HDAC inhibitors for use in cancer therapy.[155] HDAC inhibitors have been used in many clinical trials for that can target both hematological and solid malignancies are in progress. However, the mechanism of action by which they are employed to the HDAC pocket and mediate corresponding cellular activities is still mysterious. A better understanding of the nature of the molecular basis of the selectivity of the HDAC inhibitors will enable the development of more effective and specific agents to treat cancer.[156-158]
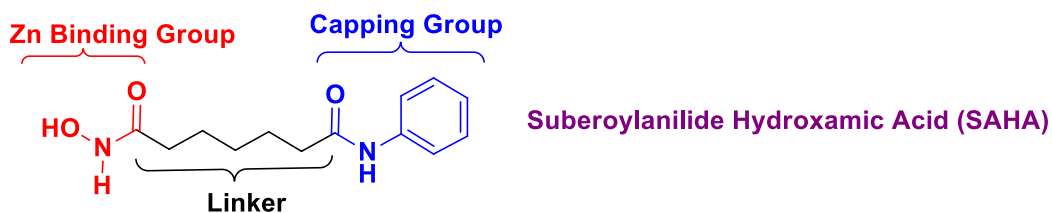
Figure 2.5: HDAC Inhibitor with Three Different Parts

2.2.2. Shortfalls and solution of current drugs

Current HDAC inhibitors used in cancer are toxic with many side effects to patients. They have lack specificity and affect several types of HDAC, and they have poor solubility.[159, 160] In order to obtain new compound derivatives or fragments that could reduce cytotoxicity but still retain adequate HDAC inhibitory activity as well as antitumor activity, we thought we would design some compounds which would be less toxic, more soluble, and better specificity toward specific HDAC types. Our goal was to synthesize small molecules which will be easy to synthesize from inexpensive commercially available starting materials. New analogs would have promising effects on cervical cancer, breast cancer, colon cancer, prostate cancer, and renal cancer cell lines. To keep thiol group as binding site, our group designed some amide compounds as HDAC inhibitors based on the Romidepsin, FK228 (Figure 2.6).
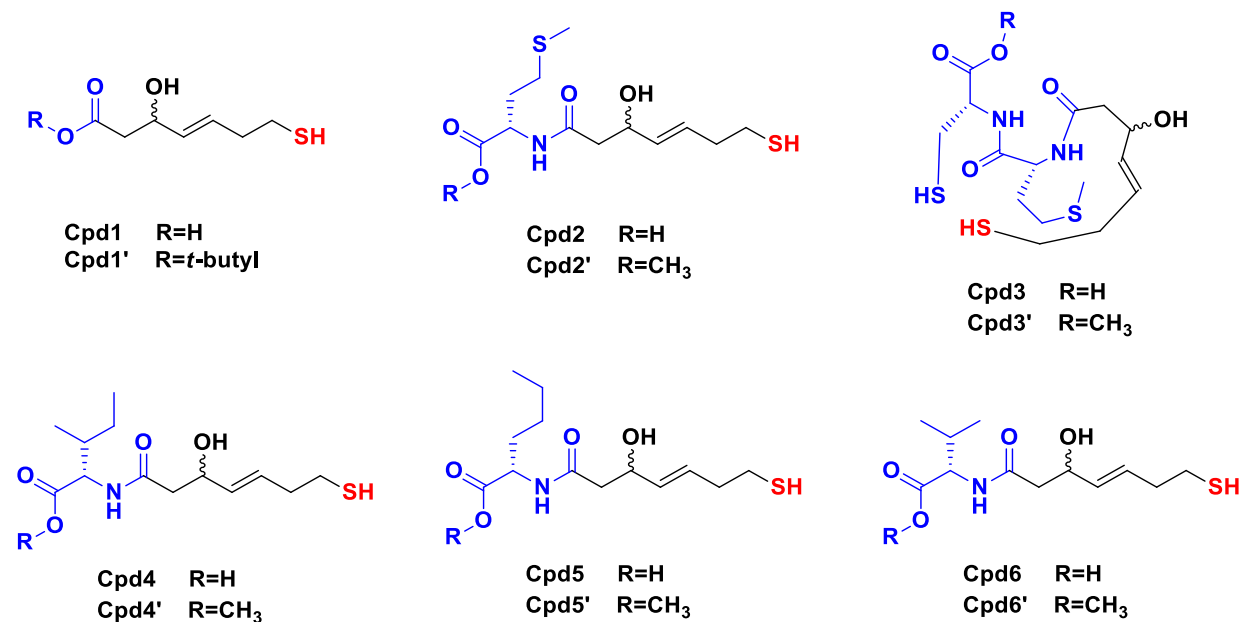
Figure 2.6: HDAC Inhibitors Prepared for the SAR Study

2.3. Cell lines, Reagents, and Animals

A human prostate cancer line (DU145) purchased from ATCC (Manassas, VA) and cultured in DMEM medium (Life Technologies, Grand Island, NY), supplemented with 10% fetal bovine serum (Atlanta Biologicals, Flowery Branch, GA), 100 U/ml penicillin, 100 μg/ml streptomycin and 2mM L-Glutamine (all from ThermoFisher Scientific) in Dr. Douglas Steeber's laboratory. Cell counts and viability were determined using a hemocytometer following appropriate dilution in trypan blue exclusion dye. The 4T1 cells were grown in RPMI 1640 media that was supplemented as above along with addition of 55 μM 2-mercaptoethanol (Life Technologies, Grand Island, NY). Cpd1' and Cpd5 were synthesized and purified by high performance liquid chromatography (HPLC) as described. The food and drug administration (FDA)-approved drugs romidepsin (FK228) were purchased commercially (Selleckchem, Houston, TX) and used as positive controls for comparison purposes. Dimethyl sulfoxide (DMSO, ThermoFisher) was used to dissolve the drugs and served as vehicle controls for all experiments. 3-(4,5-Dimethylthiazol-2-yl)-2,5-diphenyltetrazolium bromide (MTT) was purchased from Sigma Aldrich and was used as a colorimetric reagent to determine cell proliferation. Live cells actively convert MTT into a purple insoluble formazan product, while dead cells do not, and this change can be measured spectrophotometrically after being dissolved in DMSO. Wild type BALB/c mice and C57BL/6J (B6) mice were originally purchased from the Jackson Laboratories (Bar Harbor, ME) and further housed and bred in a specific pathogen-free facility at the University of Wisconsin-Milwaukee and screened regularly for pathogens. Mice behavioral study for Alzheimer's disease was done in Dr. Karyn Frick's laboratory. All procedures were approved by the Animal Care and Use Committee of the University of Wisconsin-Milwaukee.

2.3.1. MTT Cellular Assay

3-(4,5-dimethylthiazol-2-yl)-2,5-diphenyltetrazolium bromide (MTT), a yellow tetrazole is reduced to purple formazan in living cells, shows the color after the assay where increasing amounts of cells resulted in increased purple coloring (Figure 2.7).[161] For the assay, cells were allowed to adhere for 24 hours at 37 °C with 5% CO_2. All of the synthetic compounds, FK228, and DMSO control concentrations were diluted in series with supplemented Dulbecco's Modified Eagle Medium (DMEM) sterilely. The media was aspirated off the 96 well plate and the drug, or control, concentrations were added to the plate in triplicate. The cells were then incubated with the drugs or DMSO controls for 48 hours. The drug and control treatments were removed and 200 µg/mL of MTT diluted in supplemented DMEM was added to each well. Cells were incubated with the MTT for 4 hours at 37 °C with 5% CO_2. The MTT concentration was aspirated off and 200 µL DMSO was added to each well after 4 hours. The plate was mixed on a rotator for 10 minutes at a moderate pace and then with a pipettor to dissolve all the MTT in each well. The plate was read at 570 nM with the reference wavelength at 690 nM on a Molecular Devices Versamax plate reader (San Jose, CA). The reference wavelength absorbance for each well was subtracted. The average for the triplicate blank wells was calculated and subtracted from each well. The % viability of each concentration was calculated by dividing the average absorbance for each drug concentration by the DMSO control for that concentration.
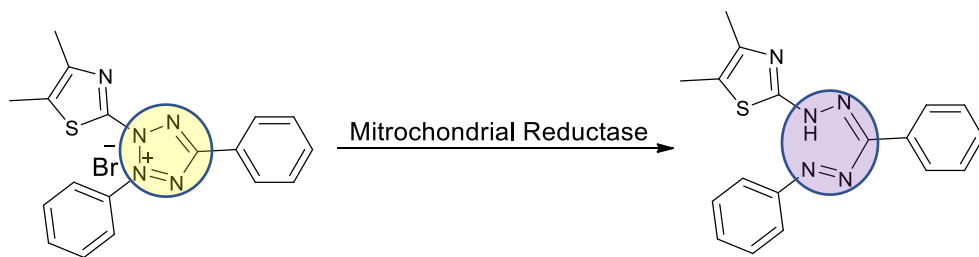
Figure 2.7: MTT, a Yellow Tetrazole, is Reduced to Purple Formazan in Living Cells

2.3.2. H3 Acetylation Assay

For H3 acetylation assay, DU145 cells were cultured as above. Cells were counted and resuspended at 60,000 cells/mL in supplemented DMEM. 1 mL of cells at 60,000 cells/mL were added to wells of a 24 well plate. The cells were allowed to adhere for 24 hours at 37 °C with 5% CO_2. The media was aspirated and Cpd 1' at 50, 5, or 0.5 μM concentrations, or DMSO controls, in supplemented DMEM were added to the wells in duplicate. The plate was incubated at 37 °C with 5% CO_2 for 24 hours. Cells were fixed with 350-500 μL 4% paraformaldehyde for 10 minutes at room temperature after the 24-hour incubation. 400-500 μL tris-buffered saline (TBS) with 0.1% Tween 20 and 1% bovine serum albumin (TBS-T w/ 1% BSA) was added to each well for 1 hour at 4 °C for permeabilization. TBS-T w/ 1% BSA was removed and 350 to 500 μL rabbit anti-acetyl-Histone H3 (Lys9/Lys14) antibody (Cell Signaling Technology, Danvers, MA) at a 1:2000 dilution in TBS-T w/1% BSA was added to each well. The primary antibody was incubated with the cells overnight at 4 °C. The primary antibody was removed and goat anti-rabbit IgG AlexaFluor™ 488 (Jackson ImmunoResearch, West Grove, PA) at a 1:500 dilution was added to each well and incubated for 1.5 hours at 4 °C. The Plate was removed from the fridge and 350-500 μL of 4′,6-diamidino-2-phenylindole (DAPI) at 0.3 μg/mL was added to each well. DAPI was incubated in dark at room temperature for 15 minutes, and wells were imaged with the fluorescence microscope (Figure 2.8).[162]
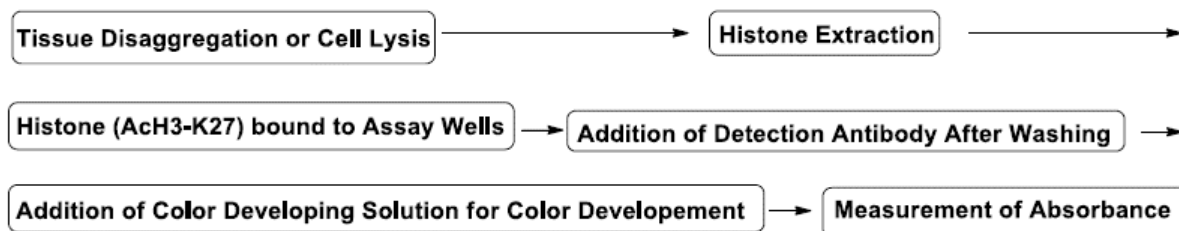
Figure 2.8: Block Diagram of H3-Acetylation Assay

2.3.3. Memory Enhancement Study

The present study was designed to evaluate the effect of our synthetic compound on memory of mice for Alzheimer's disease. Mice were housed in a conventional animal vivarium and were given free access to food and water. All studies and procedures were approved by the Animal Care and Use Committee of the University of Wisconsin, Milwaukee. Each animal was initially weighed using a digital scale and then intraperitoneally (IP) injected with the compounds. The effects on hippocampal memory in rodents was assessed in spatial tasks such as object location/placement and in object recognition tasks.[163] Effect of drugs on learning and memory of mice was evaluated by these behavioral study as well as by IP injection. From the study is has been shown that our drug has significant effect and drugs found in hippocampus study. Hippocampus is a small portion on the brain which develop the memory (Figure 2.9). A single mouse was given a single IP dose of 40 mg/kg, body weight and a second mouse received a dose of 20 mg/kg. Later, brains were collected, separated the hippocampus, and mass of the compound was investigated by single quadrupole liquid chromatography-mass spectrometry (LC-MS) and triple quadrupole LC-MS/MS analysis.
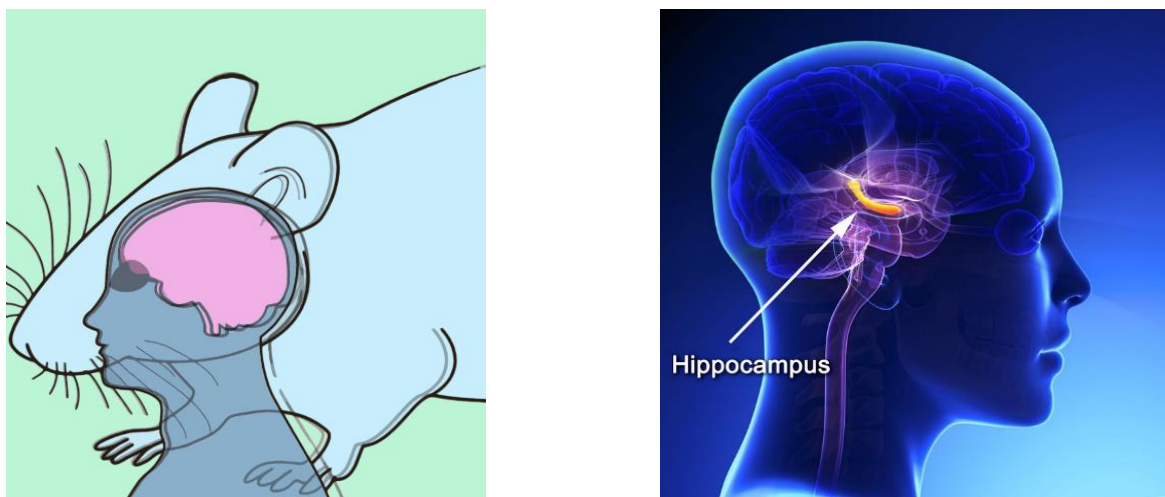
Figure 2.9: Memory Enhancement Study in the Hippocampus of the Brain of Mice

2.4. Results and Discussion

2.4.1. Results from MTT Assay

One of our synthetic compounds were found to be active against prostate cancer cell line. We performed MTT assay, a colorimetric assay for assessing cell metabolic activity, reflects the number of viable cells present. MTT, a yellow tetrazole, is reduced to purple formazan in living cells and increasing amounts of cells resulted in increased purple coloring. Cpd 1, Cpd 1', Cpd 5, and Cpd 5' were tested for MTT assay with DU-145 prostate cancer line. The result showed that Cpd 1, Cpd 5 and Cpd 5' are not active which were shown from the cell viability. The cell viability was compared with market drug FK228 (Figure 2.10)
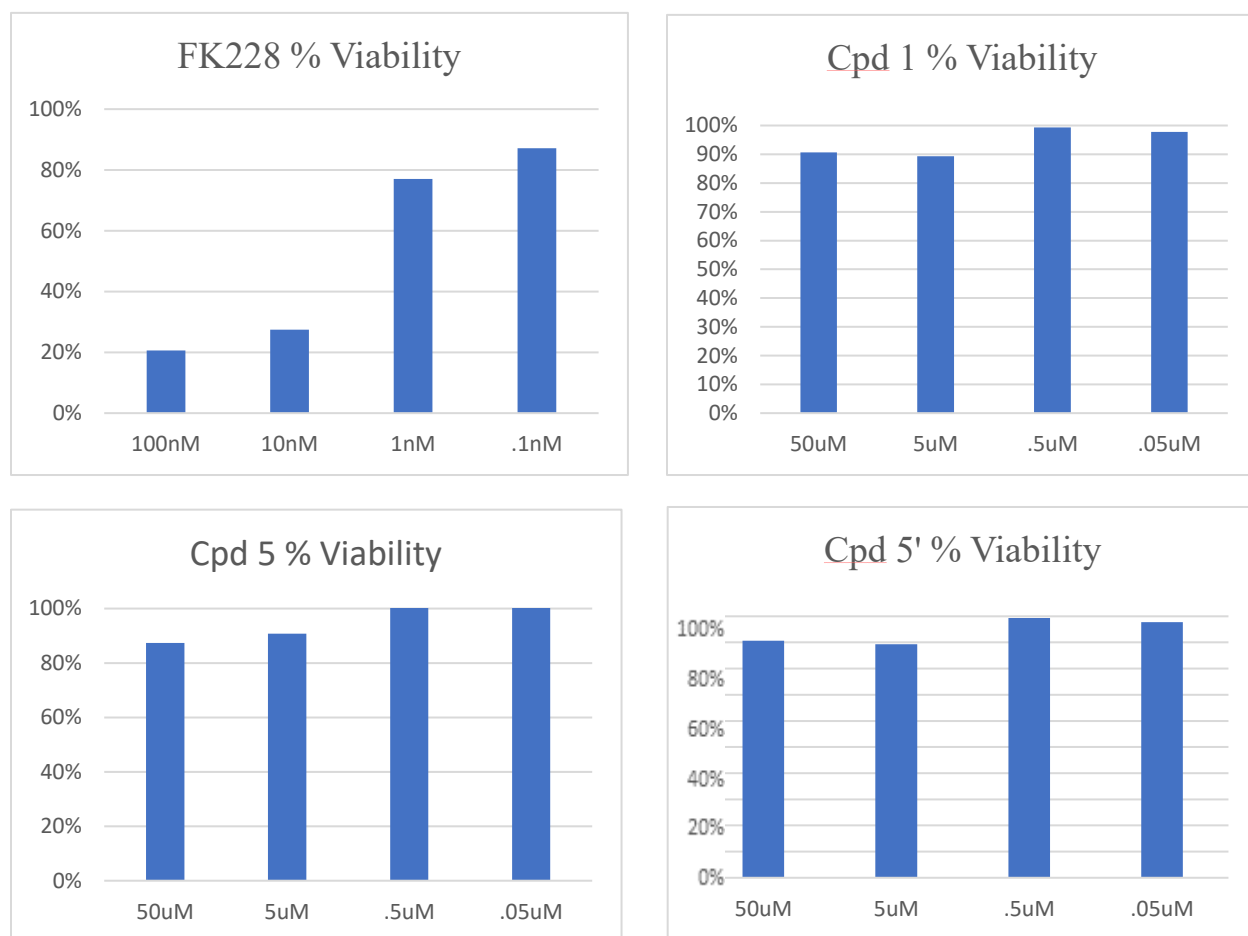
Figure 2.10: Activity Measurement by Cell Viability of Cpd 1, Cpd 5, and Cpd 5'

When our synthetic compounds were not active, we thought this is due to the purity. To make purer, the mixture was first purified by Hi-Flash Column (ODS-C18, 3.0x16.5 cm, 50 um, Yamazen A1-580), 0-20min 20-100% ACN/H2O 20ml/min and the detection wave length was set at 210 nm. The peak was collected at 8-12min. Then this peak was injected in HPLC (Varian ProStar) with the column (Prep-C18, 21.2x250 mm, 10 um) system and 35 % ACN/H$_2$O was used to elute the column under the flow rate of 8ml/min (Figure 2.11).
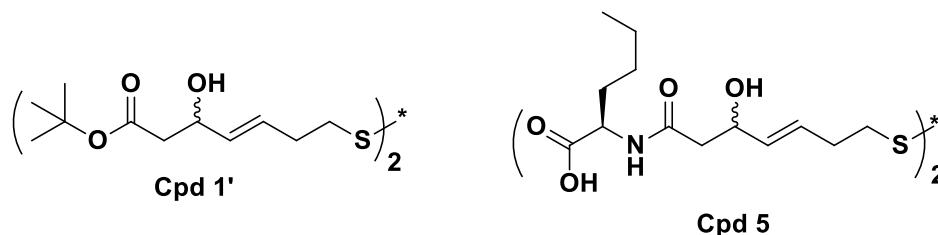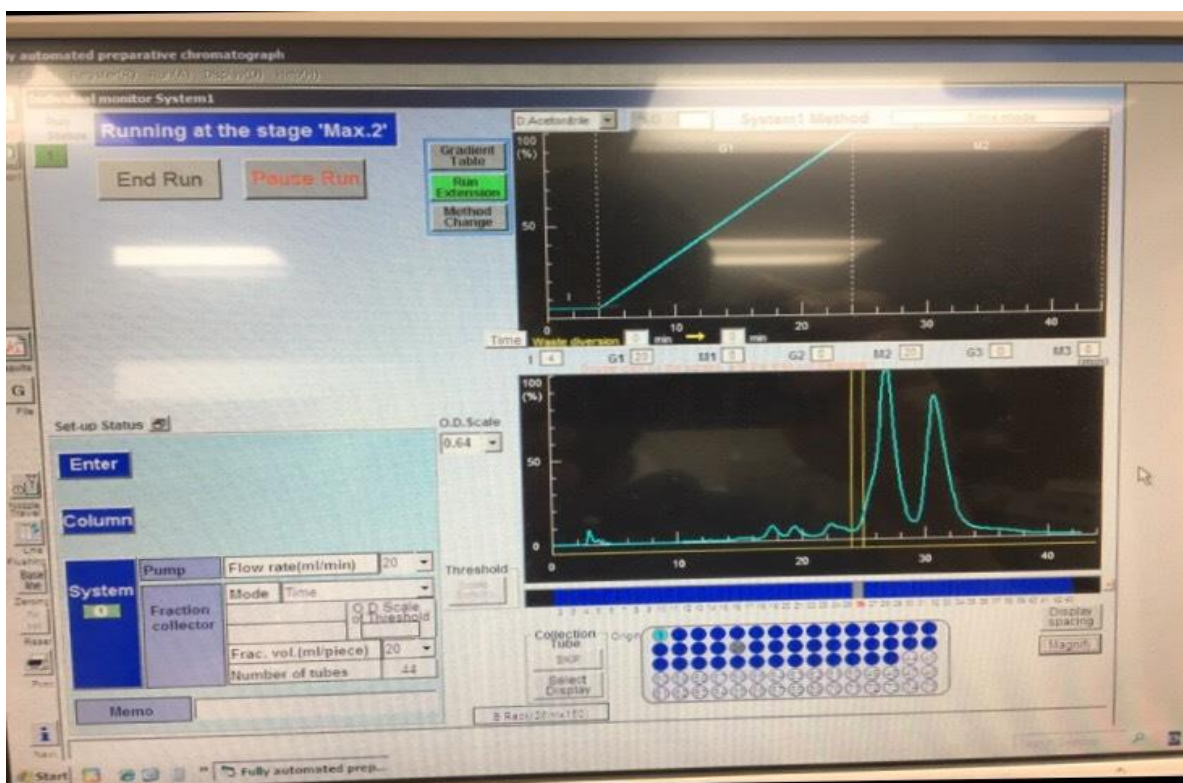
Figure 2.11: Purification of Cpd 1' and Cpd 5 by Yamazen Flash Column and HPLC

We separated two diestereoisomers of our synthetic compounds by silica gel column chromatography. After collecting pure product, activity of the compounds were tested, and this time also two diesteromeres of compound 5 were not active (Figure 2.12);
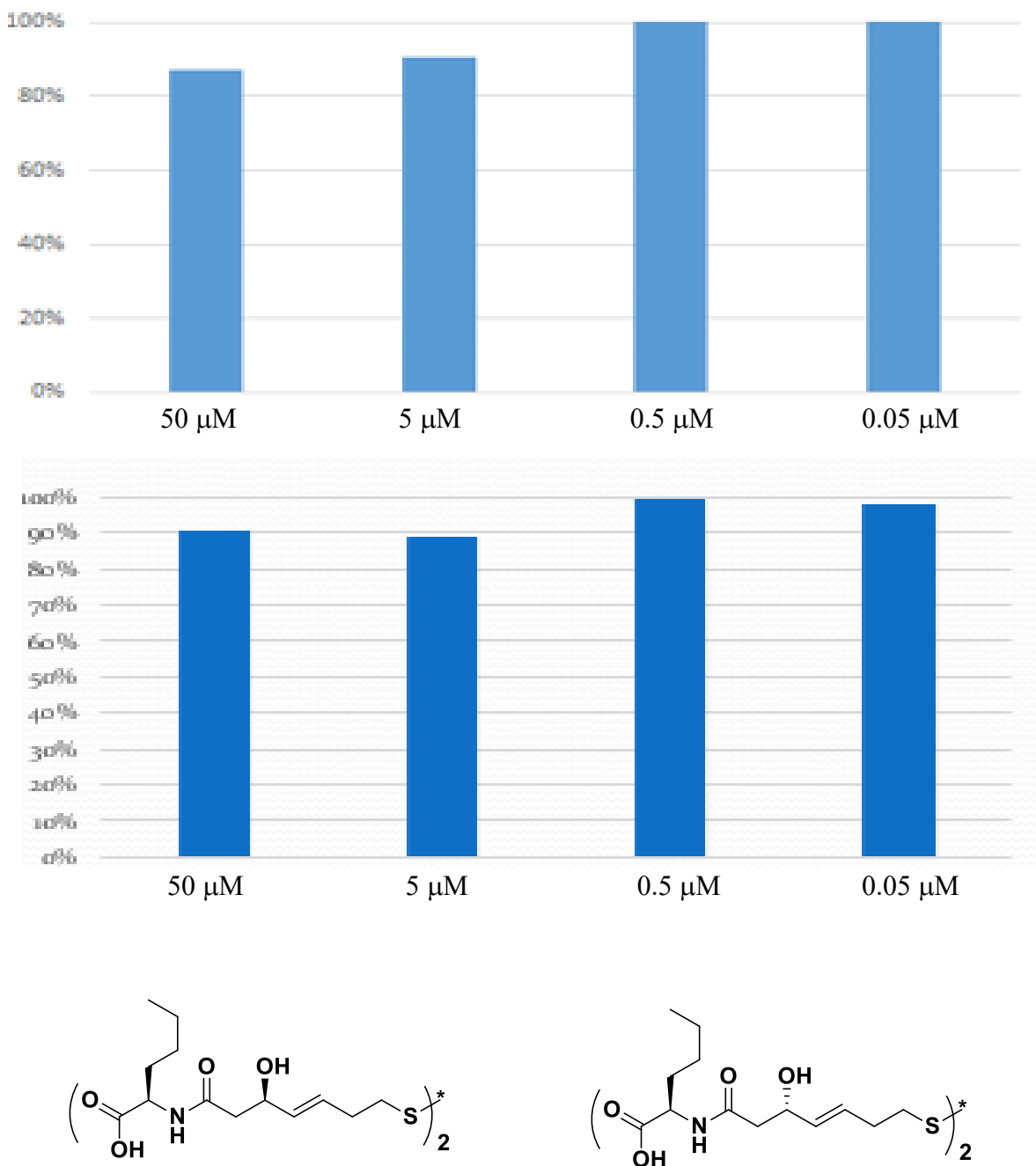
Figure 2.12: Activity Measurement by Cell Viability of Diastereomers A and B of Cpd 5

When Cpd 1, Cpd 5, and Cpd 5' did not show any activity against, we tested Cpd 1' for the same assay with similar line. Surprisingly we found that Cpd 1' has activity in MTT assay (Figure 2.13). When 3.1 μM solution of Cpd 1' was used for the assay, it showed there was no cell death, all cells are viable. The statement was almost true for 6.2 μM and 12.5 μM solution of Cpd 1', cells are viable 90% and 80%, respectively. When 25μM solution was tested it was found that 1lmost 80% cells are death and 20% cells are viable. So, the Cpd 1' was active against prostate cancer cell line.
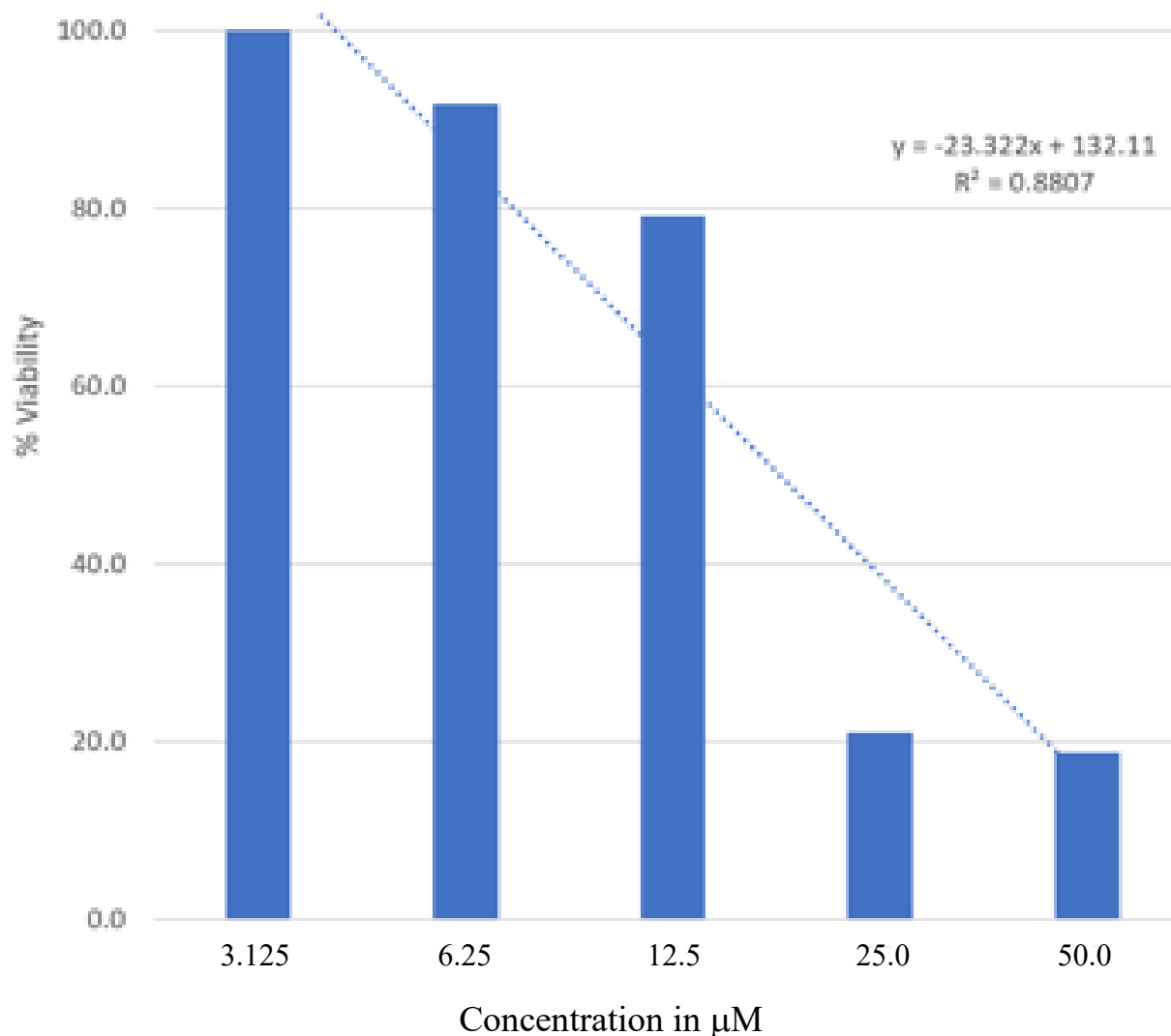
Figure 2.13: Activity of Cpd 1' in DU-145 Prostate Cancer Cell Line

2.4.2. Results from H3 Acetylation Assay

We found that Cpd 1' is active, and more than 80% cell are dead in MTT assay. But we wanted to make sure the cell death is due to our synthetic compound or other reason. To make sure our compound is active, and it can acetylase the histones, we performed H3-acetylation assay. From the H3-acetylation assay, we confirmed that our synthetic compound Cpd 5 and Cpd 5' are not active in H3-acetylation assay (Figure 2.14). All results are compared with DMSO control, and blue colors are shown as non-acetylated histone and green colors are acetylated histones.

DMSO control   Cpd 5 in 25 μM

Cpd 5' in 50 μM   Cpd 5 in 50 μM
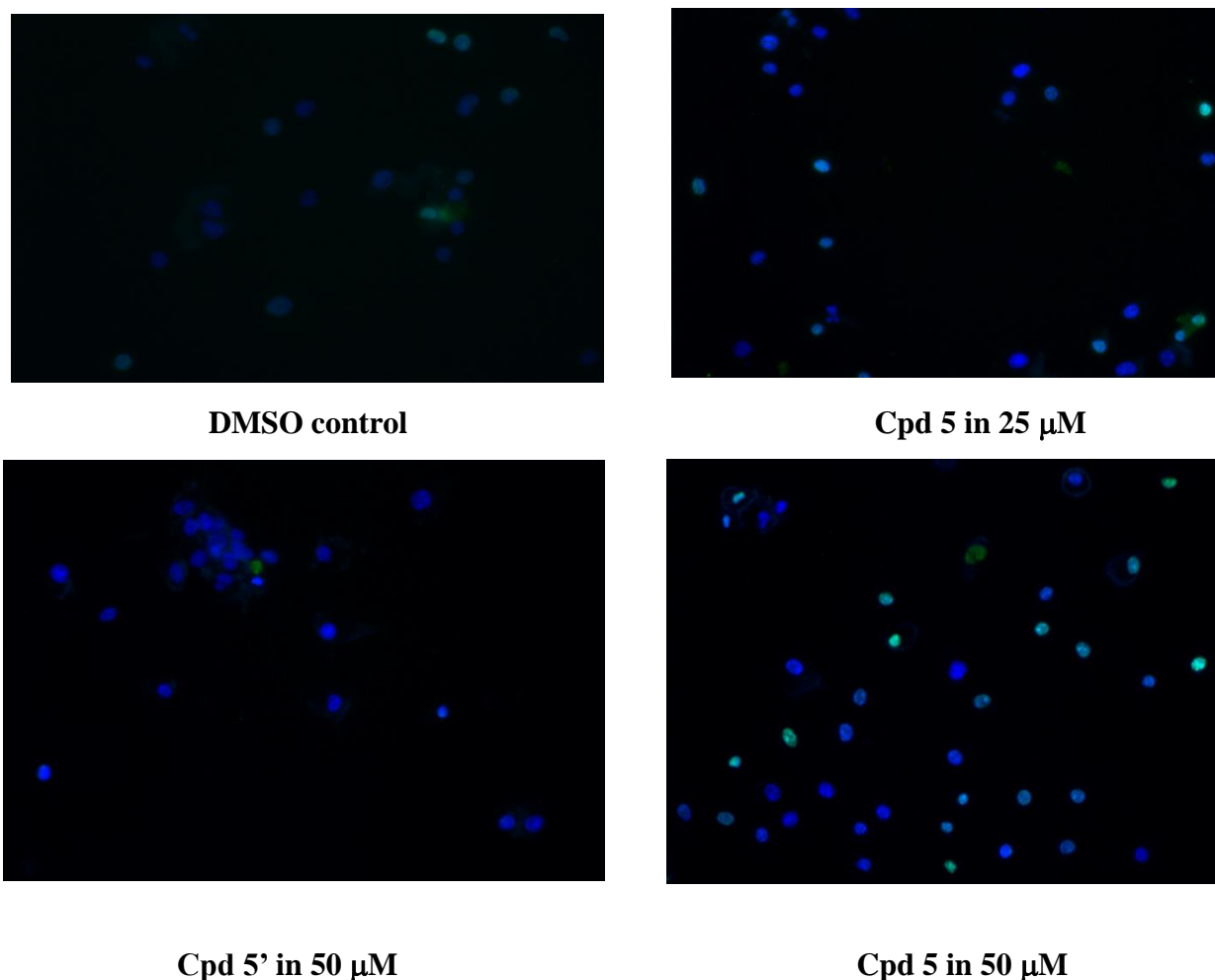
Figure 2.14: Activity of Cpd 5 and Cpd 5' in DU-145 Prostate Cancer Cell Line

In H3-acetylation assay, Cpd 1 and Cpd 1' were also tested and found that Cpd 1' is also active in this assay (Figure 2.15). All results are compared with DMSO control, and blue colors are shown as nuclear stain (non-acetylated histone) and green colors are acetylated histones.

Blank

DMSO

Cpd 1 in 50 μM

Cpd 1' in 50 μM
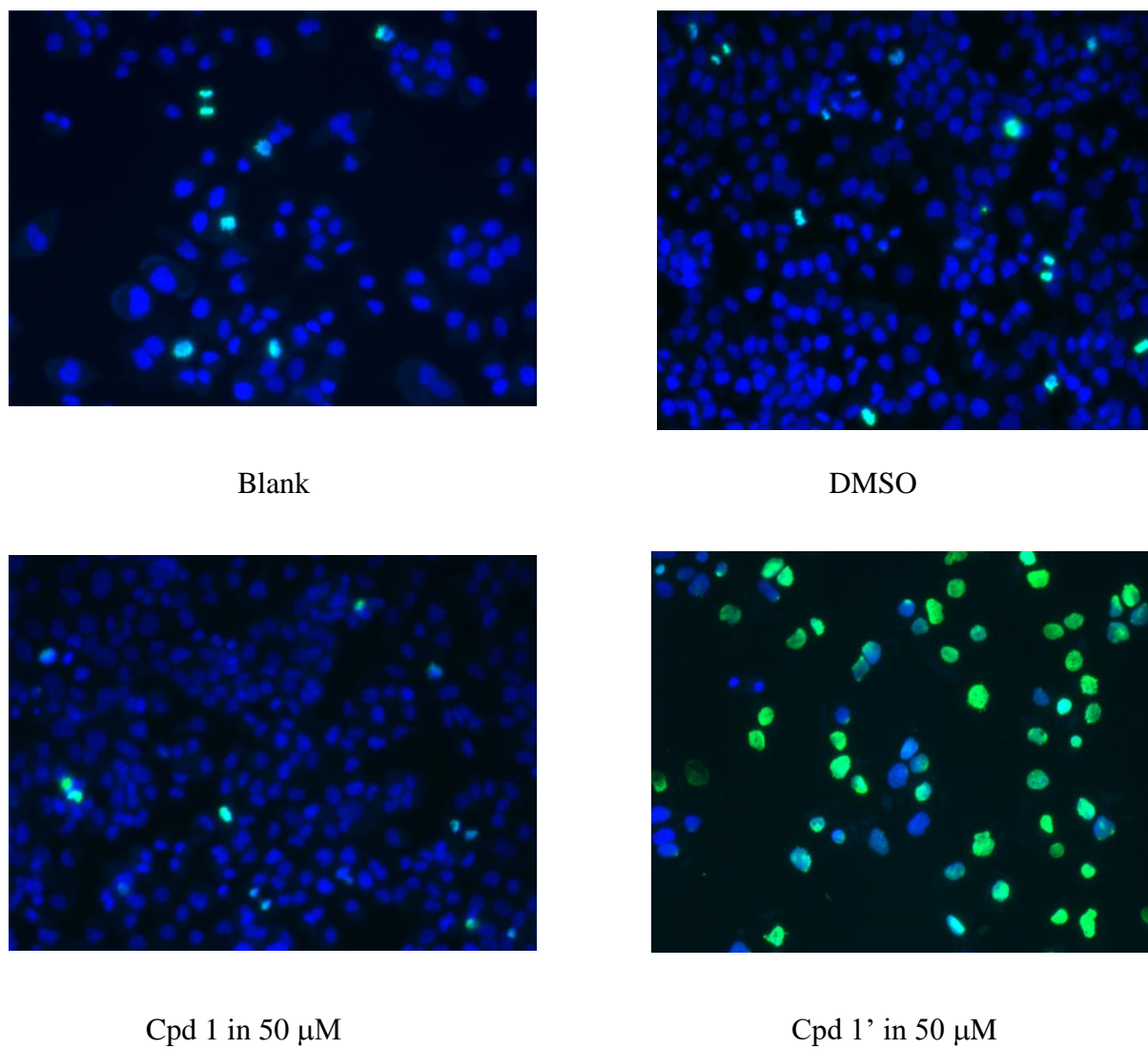
Figure 2.15: Activity of Cpd 1 and Cpd 1' active in DU-145 Prostate Cancer Cell Line

When it was shown that Cpd 1' was active and it acetylated the histone in 50 solution, then it was also tested with lower concentration of Cpd 1'. All the results are compared with market drug FK 228 (Figure 2.16). It was found that Cpd 1' had medium acetylation with the concentration 12.5 μM and 25 μM. Deep green color indicated that higher acetylation, and light green indicated medium acetylation.
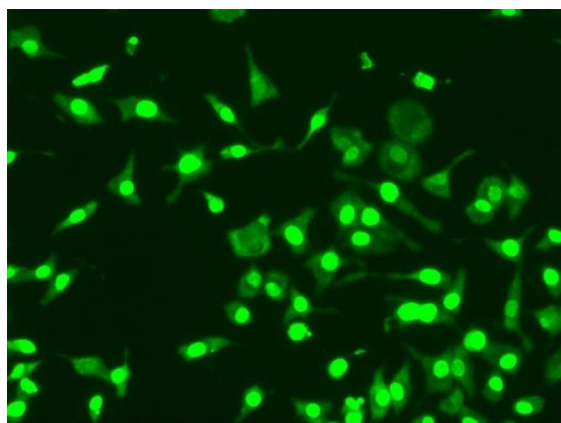
FK 228 in 10 nM   Cpd 1' in 12.5 μM
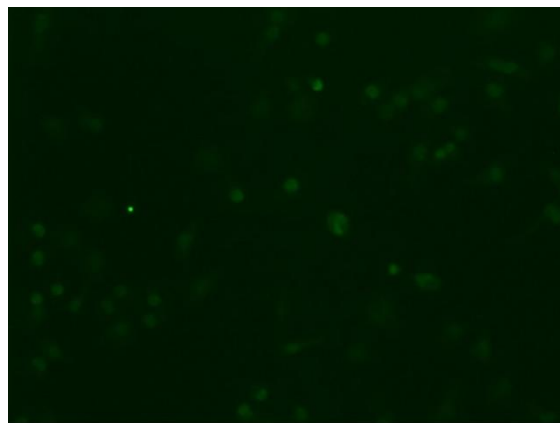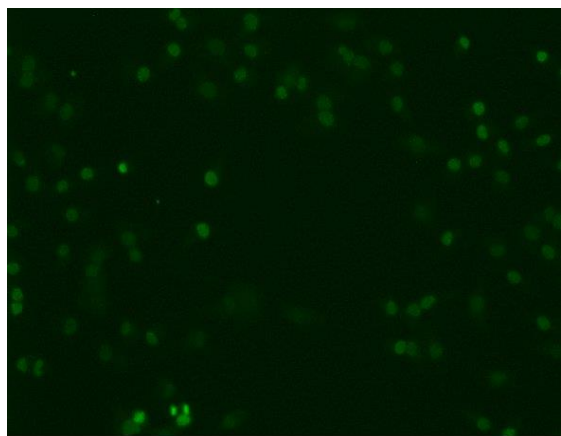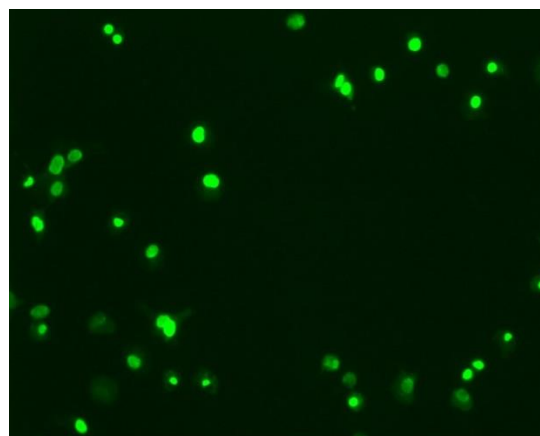
Cpd 1' in 25 μM   Cpd 1' in 50 μM

Figure 2.16: Activity of Cpd 1' in Different Concentration in DU-145 Prostate Cancer Cell Line

2.4.3. Results from *In-Vivo* Studies

Our synthetic compound 1' was also tested for memory enhancement study in mice. It is known that if the compound enters the hippocampus of the brain and inhibit HDAC activity, then memory enhancement could occur. Because HDAC 2 and HDAC 3 blocks neural plasticity and impair memory. From the behavioral study of mice and *in vivo* test, it was shown that our compound can increase the memory. It was found from the *ip* injection of mice that; our compound was present in the hippocampus for 10 min with 40 mg/kg and 20 mg/kg dose respectively (Figure 2.17). Our synthetic compound was identified with respect to internal standard 4, 5-diphenyl imidazole.
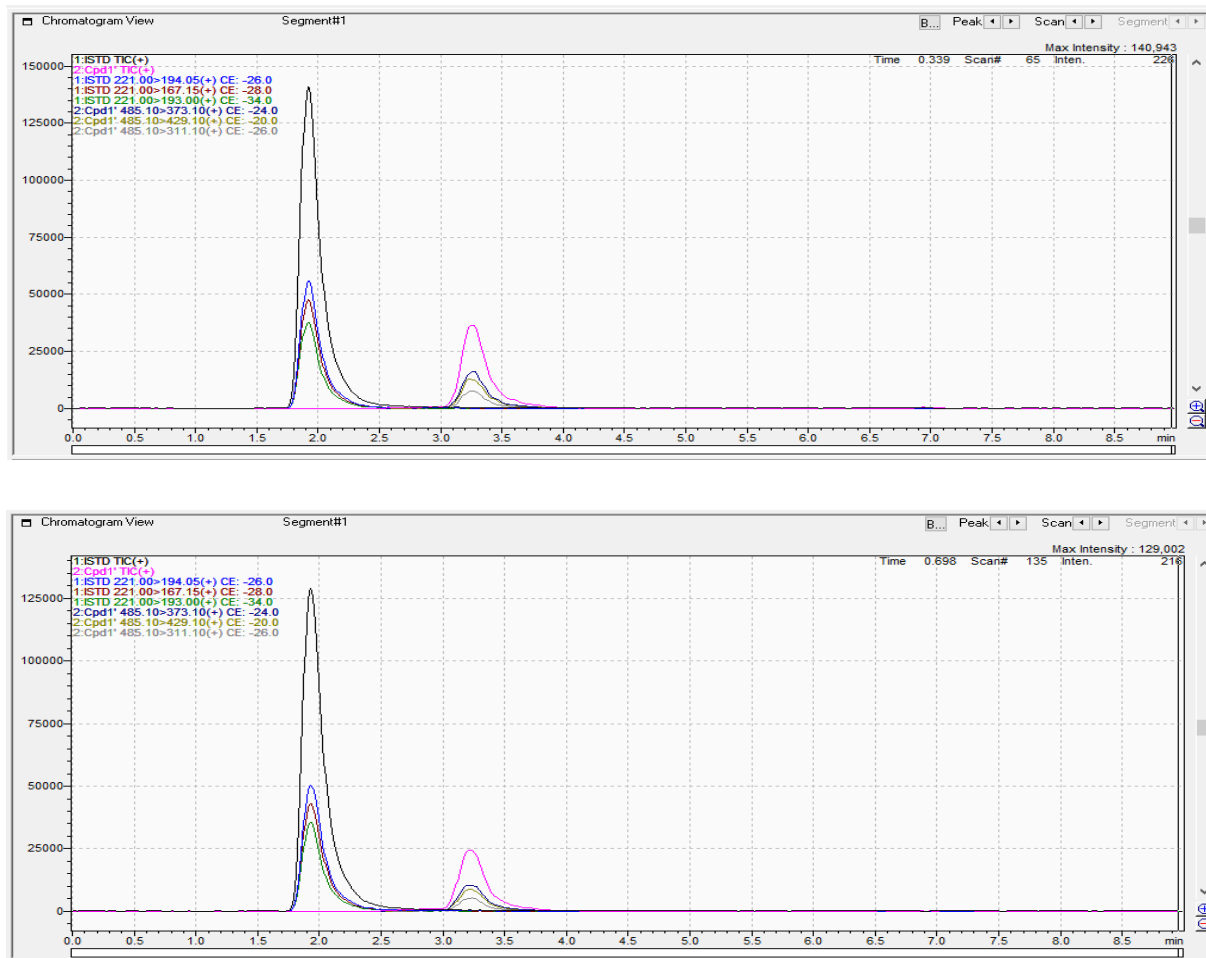
Figure 2.17: Compound was Found in Hippocampus *In Vivo* Study with Cpd1'

It was also found from the *ip* injection of mice that; our synthetic compound Cpd 1' was present in the other parts of the brain for *in vivo* 10 min with 40 mg/kg and 20 mg/kg dose respectively (Figure 2.18). Our synthetic compound was identified with respect to internal standard 4, 5-diphenyl imidazole which are shown on left peak of the figure (Figure 2.18).
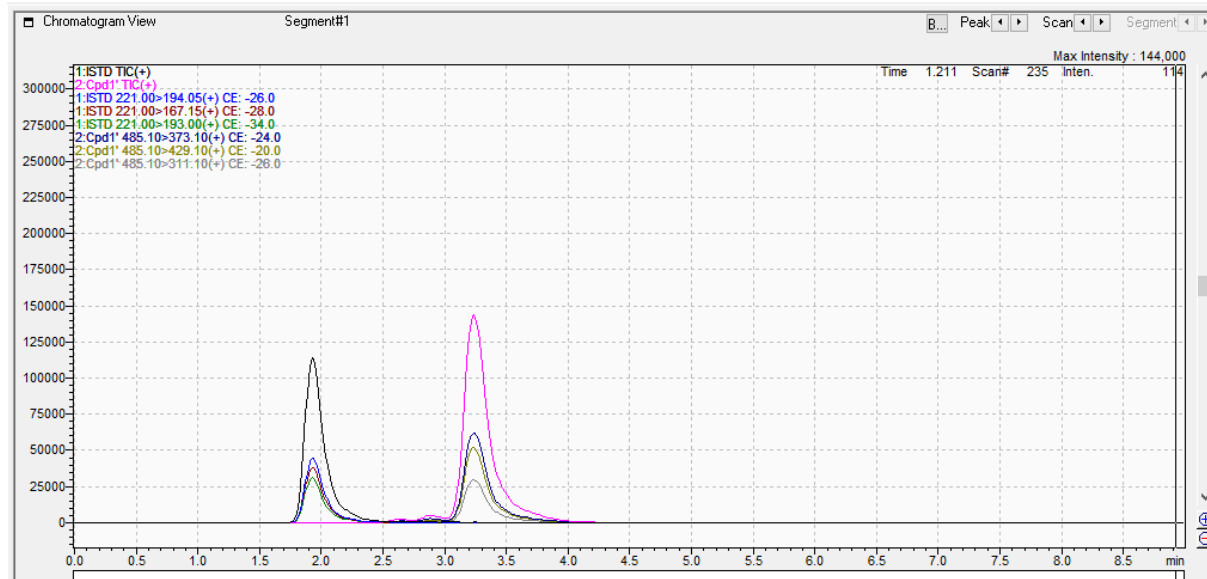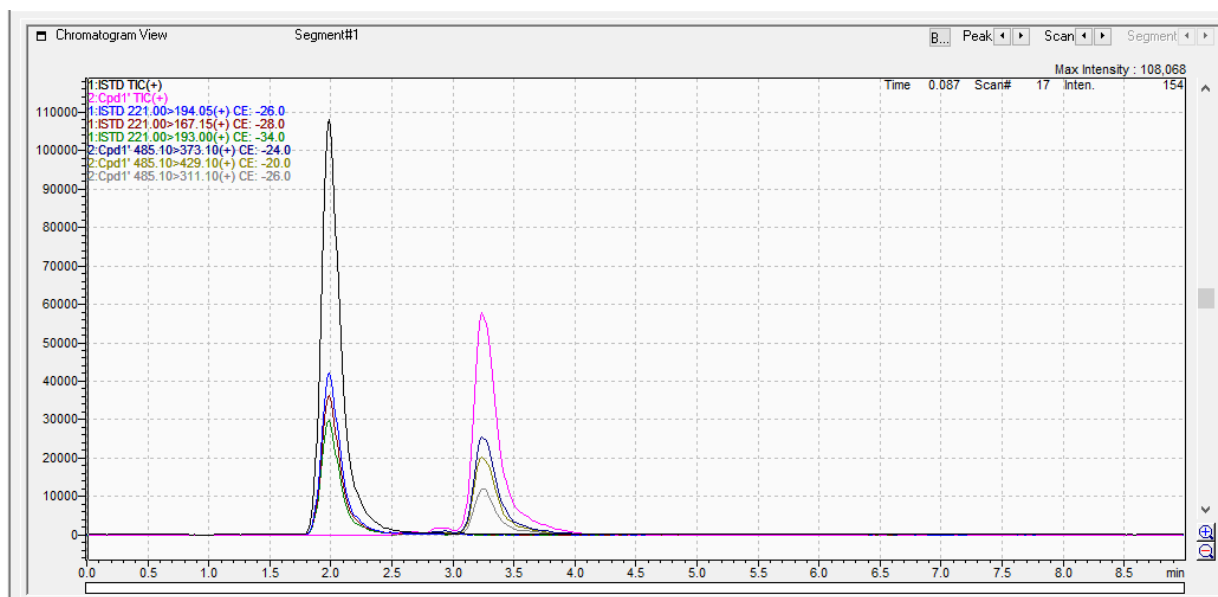
Figure 2.18: Compound was Found in Other Parts of the Brain *In Vivo* Study with Cpd1'

Several in vivo studies were done with our synthetic compound, Cpd 1' was done with the collaboration of Biology department and Psychology Department. All the *in vivo* studies are found to be positive. The compound is detectable in blood, brain, and liver (Figure 2.19). Our synthetic compound was identified with respect to internal standard 4, 5-diphenyl imidazole which are shown on the figure using average area ratio of compound and internal standard (Figure 2.19).
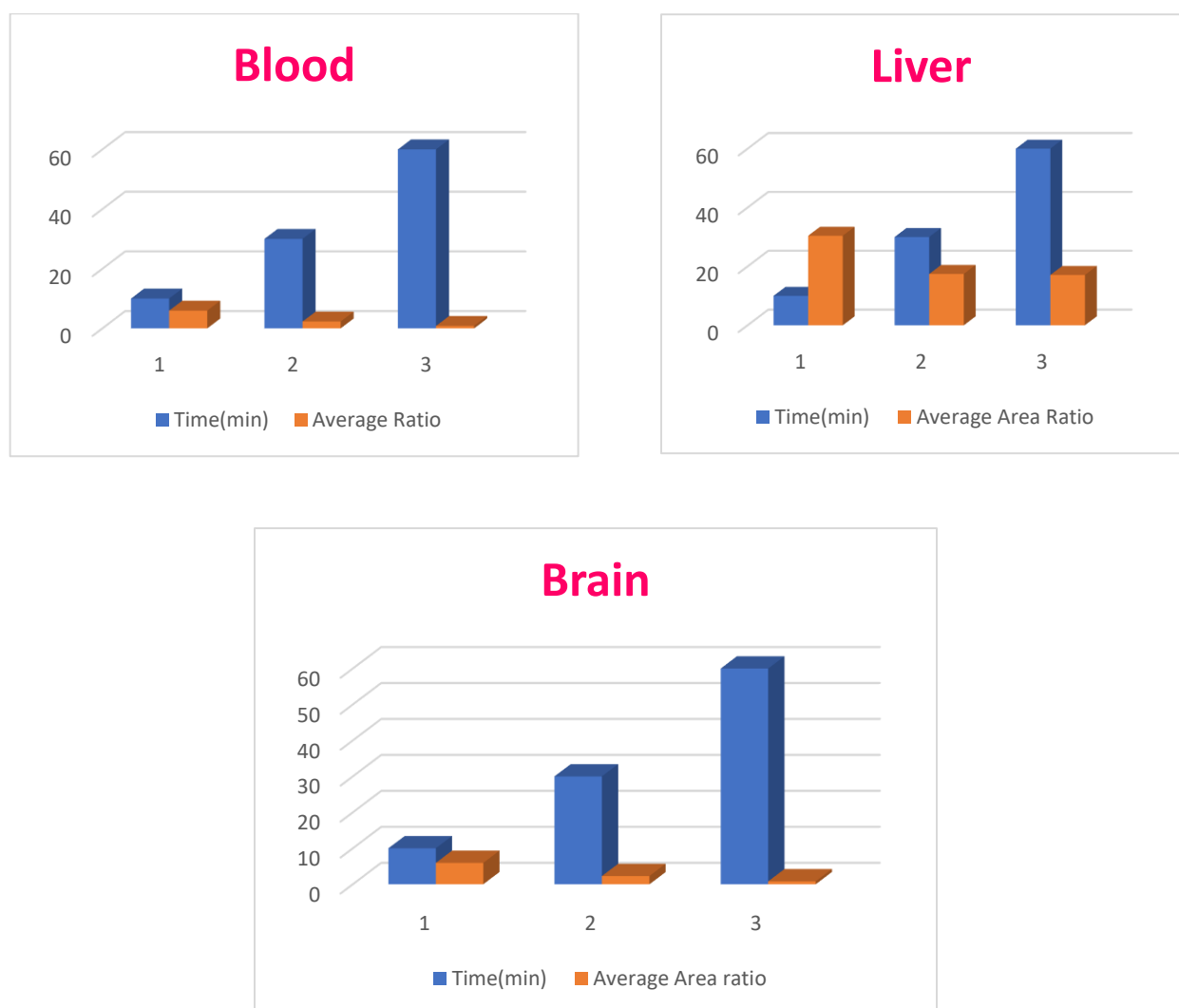
Figure 2.19: Presence of Cpd 1'in Blood, Brain, and Liver

The plasma stability assay (PSA) is to measure the degradation of compounds in plasma. This is the in vitro absorption, distribution, metabolism, and elimination (ADME) screening system. It was also found from PSA study that our synthetic compound Cpd 1' was present it was found that our compound is stable with 8.9 hours half-life (Figure 2.20).
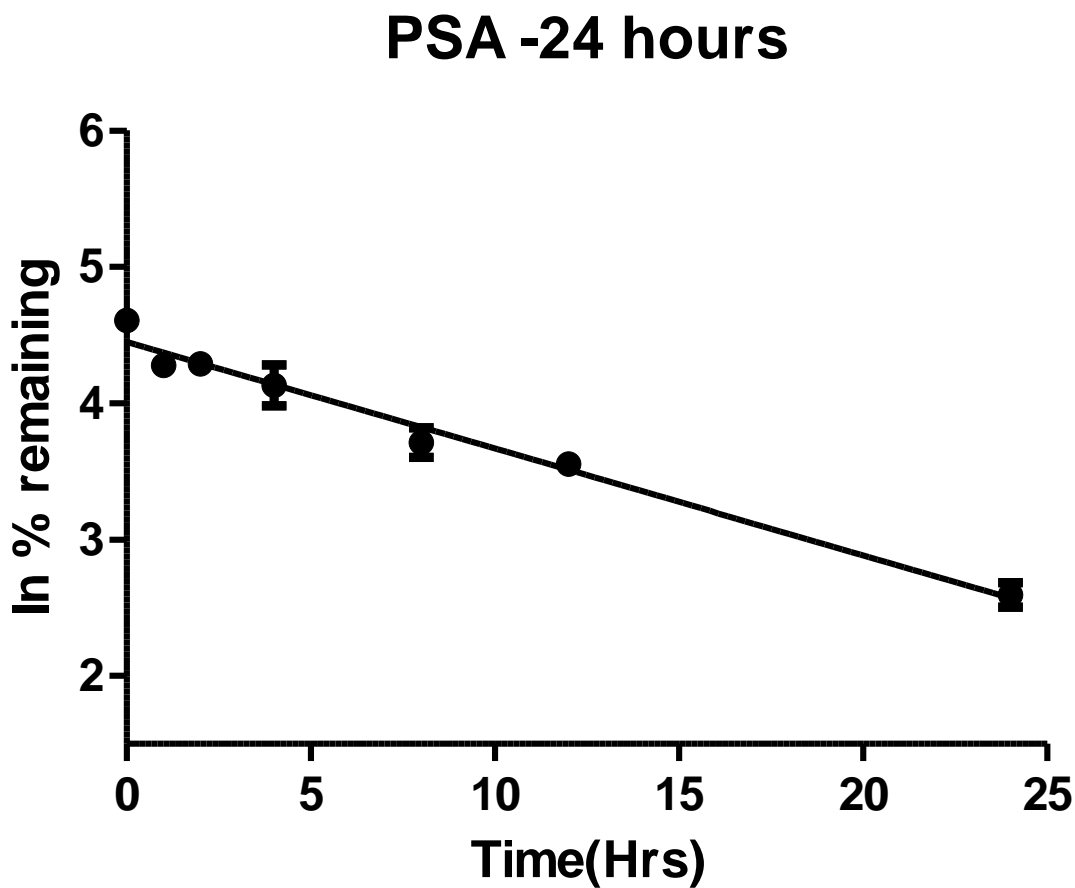
Figure 2.20: Plasma Stability Assay (PSA) with Cpd1'

2.5. Conclusion

In conclusion, histone deacetylase inhibitors are an exciting new class of medicines with broad applications. We synthesized a set of compounds based on the scaffold of the FK228 in our lab, among them Cpd 1' was found to be active against DU-145 prostate cancer cell line. Comprehensive pharmacokinetic studies, more behavioral study on mice are currently underway. Our group has been making different analogs of Cpd 1'as well as the modification of Cpd 1' to have a most active compound as anti-cancer agent as well Alzheimer's disease.
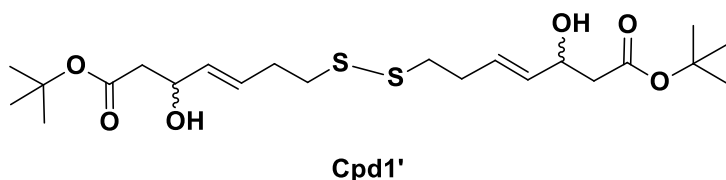
Cpd1'

Our group has been planning to make a best drug by the following changes in future;

1. By making the monomer of our synthetic compound Cpd 1'
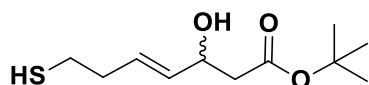
2. By the reduction of double for making the longer chain of Cpd 1'
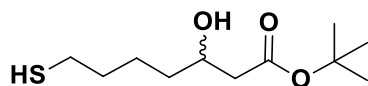
3. By making R/S enantiomer by the kinetic resolution of Cpd 1'

R-Cpd1'   *S*-Cpd1'
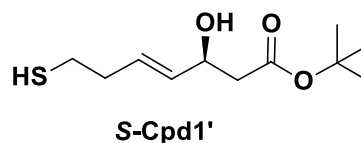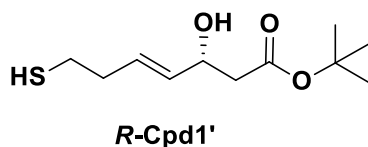
2.6. General Methods and Experimental

2.6.1. General Consideration

All reactions were performed under a dry nitrogen atmosphere using standard Schlenk techniques unless otherwise noted. All reaction vessels were flame dried under vacuum and filled with nitrogen prior to use. Reagents and solvents were purchased from Sigma-Aldrich, Milwaukee. All ^{1}H and ^{13}C NMR spectra were recorded in $CDCl_3$ (internal standard: 7.26 ppm, ^{1}H; 77.16 ppm, ^{13}C) at room temperature with a Burker 300 MHz and 500 MHz spectrometers. The chemical shifts (δ) are given in parts per million (ppm) and the coupling constants in Hertz (Hz). The following abbreviations are used: *s*-singlet, *d*-doublet, *t*-triplet, *q*-quartet, *m*-multiplet. Previously reported compounds were identified by ^{1}H NMR. All new compounds were additionally characterized by ^{1}H NMR, ^{13}C NMR and high-resolution mass spectrometry (HRMS). HRMS were obtained using electrospray ionization (ESI) technique. For column chromatography, silica gel (35-70 microns) was used. Thin layer chromatography (TLC) was performed on aluminium backed plates pre-coated (0.25 mm) with Silica Gel 60 F254 with a suitable solvent system and was visualized using UV fluorescence and/or iodine chamber. The crude reaction mixture was first purified by Hi-Flash Column (ODS-C18, 3.0x16.5 cm, 50 um, Yamazen A1-580), 0-20min 20-100% ACN/H_2O 20ml/min and the detection wave length was set up at 210 nm. The peak was collected at 8-12min. Then this peak was injected in the high-performance liquid chromatography (HPLC) (Varian ProStar) with the column (Prep-C18, 21.2x250 mm, 10 um) system and 40 % ACN/H_2O was used to elute the column under the flow rate of 8 ml/min.

2.6.2. Experimental:

3-(Tritylthio)propanal, 3:
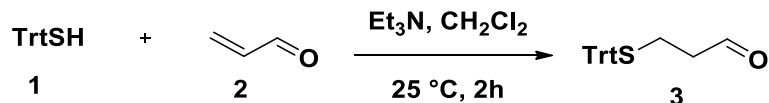
A round bottom flask was charged with triphenylmethanethiol (5.0 g, 18.1 mmol). The flask was put under argon and the contents of the flask were dissolved in dichloromethane (50 mL). Triethylamine (3.0 mL, 21.7 mmol, 1.2 equiv.) was added to the mixture and was stirred for additional 10 minutes. Acrolein (1.2 mL, 18.1 mmol) was added to the mixture dropwise and was stirred for 2 hours and was then concentrated in vacuo. The crude product was purified by flash column chromatography with a 25% ethyl acetate/hexane solution until the product spot eluted. The product, 3-(tritylthio)propanal was purified by recrystallization with toluene and collected 5.3 g with 88% yield **3**. Compound **3** was confirmed[164] by comparing spectra to known NMR. **^{1}H NMR (CDCl$_3$, 500 MHz):** δ (ppm) 9.59 (s, 1H), 7.47 (d, J = 10.0 Hz, 6H), 7.47 (q, J = 7.5 Hz, 6H), 7.26 (t, J = 5.0 Hz, 3H), 2.51 (t, J = 7.5 Hz, 2H), 2.41 (t, J = 7.5 Hz, 2H); **^{13}C NMR (CDCl$_3$, 125 MHz):** δ (ppm) 200.4, 144.5, 129.6, 128.0, 126.8, 67.0, 42.7, 24.4.

(*E*)-5-(tritylthio)pent-2-enal, 6:
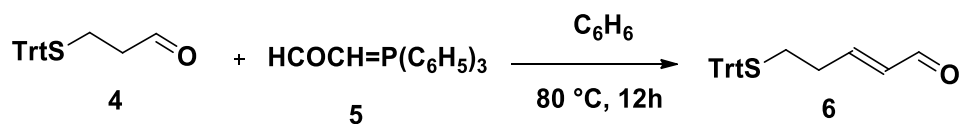
A round bottom flask was charged with 3-(tritylthio)propanal (5.0 g, 15.0 mmol, 1 equiv.) and 2-(triphenylphosphoranylidene) (5.3 g, 16.6 mmol, 1.1 equiv.). The flask was put under argon and

the contents of the flask were dissolved in benzene (100 mL). The solution was then refluxed overnight. When all starting materials were found to be disappeared, the reaction mixture was allowed to cool to room temperature and was then concentrated in *vacuo*. The crude product was separated via column chromatography and the column was run with a 20% ethyl acetate/hexane solution until the product spot eluted. And then the product was purified by recrystallization with toluene to give 3.8 g (70%) of pure product **6**. Compound **6** was confirmed[164] by comparing spectra to known NMR. **^{1}H NMR (CDCl$_3$, 500 MHz):** δ (ppm) 9.46 (q, $J = 7.5$ Hz, 1H), 7.47 (d, $J = 5.0$ Hz, 6H), 7.33 (d, $J = 5.0$ Hz, 6H), 7.26 (d, $J = 5.0$ Hz, 3H), 6.68-6.63 (m, 1H), 6.02 (dd, $J = 15.0$, 5.0 Hz, 1H), 2.39-2.33 (m, 4H); **^{13}C NMR (CDCl$_3$, 125 MHz):** δ (ppm) 193.8, 155.8, 144.6, 133.7, 129.6, 128.0, 126.8, 67.0, 31.8, 30.1.

(*E*)-tert-butyl 3-hydroxy-7-(tritylthio)hept-4-enoate, 9:
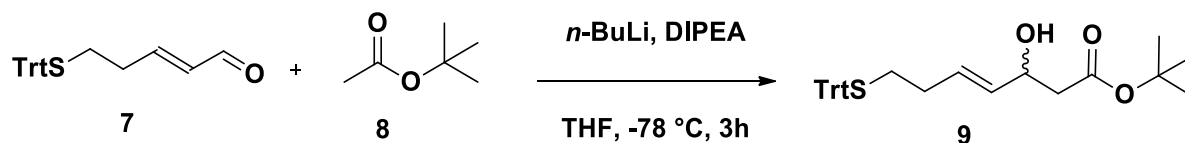
A round bottom flask was charged with THF (50 mL) and cooled to -78 °C under nitrogen. Later, diisopropylethylamine (DIPEA) (9.4 mL, 53.8 mmol, 5.5 equiv.) and *n*-butyllithium (21.5 mL, 53.8 mmol, 5.5 equiv.) were added dropwise at -78°C and was stirred for 1 hour. *Tert*-butyl acetate (6.6 mL, 48.9 mmol, 5 equiv.) was added at -78°C and was allowed to stir for additional 1 hour. Lastly, (E)-5-(tritylthio)pent-2-enal (3.5 g, 9.8 mmol, 1 equiv.) was added and the mixture was stirred for 45 min at -78°C. The reaction was quenched with a saturated solution of NH$_4$Cl (25 mL) and then concentrated in *vacuo* to remove the organic solvent. Then dichloromethane was added to aqueous mixture and the two phases were separated. After collecting the bottom organic

layer, the aqueous layer was extracted two more times with dichloromethane and the organic layers were combined. The organic layer was washed with $NaHCO_3$ solution, brine, then dried over anhydrous Na_2SO_4, and concentrated in *vacuo*. The residue was purified with flash column chromatography on silica gel (ethyl acetate/ hexane, 1:9) to afford 3.6 g (78%) of product, (E)-1-tert-butoxy-4-hydroxy-8-(tritylthio)oct-5-en-2-one as a white solid **9**. **^{1}H NMR (CDCl$_3$, 500 MHz):** δ (ppm) 7.46 (d, J = 5.0 Hz, 6H), 7.32 (t, J = 7.5 Hz, 6H), 7.25 (t, J = 7.5 Hz, 3H), 5.64-5.58 (m, 1H), 5.45 (dd, J = 15.0, 5.0 Hz, 1H), 4.43 (s, 1H), 3.09 (s, 1H), 2.48-2.42 (m, 2H), 2.25 (t, J = 5.0 Hz, 2H), 2.13 (t, J = 7.0 Hz, 2H), 149 (s, 9H); **^{13}C NMR (CDCl$_3$, 125 MHz):** δ (ppm) 171.8, 144.9, 132.1, 129.9, 129.6, 127.9, 126.6, 81.3, 68.7, 66.6, 42.4, 31.5, 31.4, 28.2. **HRMS (ESI+):** Calculated (m/z) for $C_{30}H_{34}O_3S$ (M+Na)$^+$: 497.2121, Found 497.2129.

(*E*)-3-hydroxy-7-(tritylthio)hept-4-enoic acid, 10:
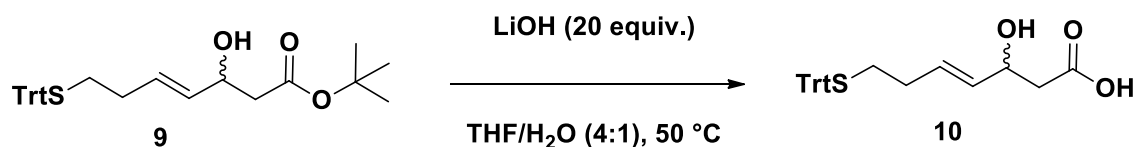
(E)-tert-butyl 3-hydroxy-7-(tritylthio)hept-4-enoate (3.0 g, 6.3 mmol, 1.0 equiv.) was dissolved in a 4:1 ratio of THF/water (50 mL). Next, lithium hydroxide (3.0 g, 126.5 mmol, 25 equiv.) was added. The solution was then heated to 50 °C and stirred for 12 hours. The reaction was then diluted with water (20 mL) and then acidified to a pH of 4-5 with $KHSO_4$. The aqueous layer was extracted with ethyl acetate (20 mL) four times. The organic layers were combined and washed with water, brine, dried over anhydrous sodium sulfate, and concentrated in *vacuo*. The residue was purified with flash column chromatography on silica gel (ethyl acetate/ hexane, 9:10) and obtained 2.5 g (95%) of product as a white solid, **10**. Compound **10** was confirmed[164] by comparing spectra to

known NMR. **^{1}H NMR (CDCl$_3$, 300 MHz):** δ (ppm) 7.43 (d, J = 6.0 Hz, 6H), 7.30 (t, J = 7.5 Hz, 6H), 7.25 (t, J = 6.0 Hz, 3H), 5.66-5.57 (m, 1H), 5.44 (dd, J = 15.0, 6.0 Hz, 1H), 4.48 (q, J = 6.0 Hz, 1H), 2.56 (d, J = 6.0 Hz, 2H), 2.25 (t, J = 7.5 Hz, 2H), 2.11 (q, J = 6.0 Hz, 2H); **^{13}C NMR (CDCl$_3$, 75 MHz):** δ (ppm) 177.3, 144.9, 131.6, 130.7, 129.6, 127.9, 126.7, 68.5, 66.7, 41.3, 31.4, 31.3.

(4E,4'E)-di-tert-butyl 7,7'-disulfanediylbis(3-hydroxyhept-4-enoate), Cpd 1':
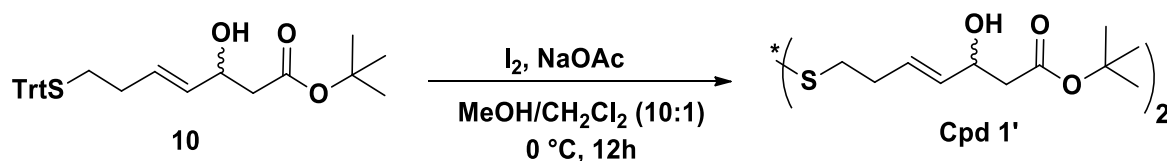
Iodine (0.27 g, 2.1 mmol, 1.0 equiv.) and sodium acetate (0.17 g, 0.464 mmol, 2.0 equiv.) were dissolved in a 10:1 solution of CH$_2$Cl$_2$/MeOH (15 mL) at 0 °C. (E)-tert-butyl 3-hydroxy-7-(tritylthio)hept-4-enoate (1.0 g, 2.1 mmol, 1.0 equiv.) was dissolved in a 10:1 solution of CH$_2$Cl$_2$/MeOH (10 mL) and was added dropwise over 20 minutes to the first solution containing iodine and sodium acetate. This solution was then allowed to stir for additional 2 hour. The reaction was quenched by adding a saturated sodium thiosulfate (Na$_2$S$_2$O$_3$) solution until the mixture turned clear. Then, brine (5 mL) was added and the phases were separated. The aqueous layer was extracted with dichloromethane (3 x 15 mL) and then with ethyl acetate (3 x 15 mL). The organic layers were combined, dried over Na$_2$SO$_4$, and concentrated in *vacuo*. The crude reaction mixture was first purified by Hi-Flash Column (ODS-C18, 3.0x16.5 cm, 50 um, Yamazen A1-580), 0-20min 20-100% ACN/H$_2$O 20ml/min and the detection wave length was set up at 210 nm. The peak was collected at 15-20 min. Then this peak was injected in the HPLC (Varian ProStar) with

the column (Prep-C18, 21.2x250 mm, 10 um) system and 70 % ACN/H_2O was used to elute the column under the flow rate of 8 ml/min. The wavelength was set at 200 nm to detect the compound and 0.66 g of the pure compound **Cpd 1'** was collected at 22-25 min. (68 % yield). The residue was purified with flash column chromatography on silica gel (hexane/ethyl acetate, 7:3) using triethyl amine (TEA) with similar yield. **^{1}H NMR (CDCl$_3$, 300 MHz):** δ (ppm) 5.70-5.60 (m, 1H), 5.48 (dd, J = 15.0, 6.0 Hz, 1H), 4.38 (q, J = 6.0 Hz, 1H), 3.3 (s, 1H), 2.64 (t, J = 7.5 Hz, 2H), 2.38-2.31 (m, 4H), 1.38 (s, 9H); **^{13}C NMR (CDCl$_3$, 125 MHz):** δ (ppm) 171.6, 132.8, 129.1, 81.2, 68.7, 42.5, 38.1, 31.8, 28.1. **HRMS (ESI+):** Calculated (m/z) for $C_{22}H_{38}O_6S_2Na$ (M+Na)$^+$: 485.2002, Found 485.1995.

(4E, 4'E)-7,7'-disulfanediylbis(3-hydroxyhept-4-enoic acid), Cpd 1:
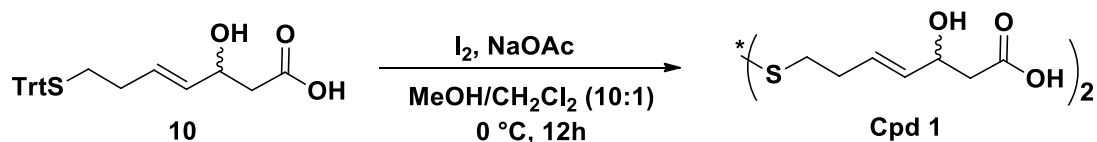
Iodine (0.30 g, 2.4 mmol, 1 equiv.) and sodium acetate (0.20 g, 2.4 mmol, 1.0 equiv.) were taken in round bottomed flask and then dissolved in a 10:1 solution of CH$_2$Cl$_2$/MeOH (15 mL) at 0 °C. (E)-3-hydroxy-7-(tritylthio)hept-4-enoic acid (1.0 g, 2.4 mmol, 1 equiv.) was dissolved in a 10:1 solution of CH$_2$Cl$_2$/MeOH (10 mL) and was added dropwise over 20 minutes to the solution containing iodine and sodium acetate. This solution was then allowed to stir for additional 2 hour. The reaction was quenched by adding a saturated sodium thiosulfate (Na$_2$S$_2$O$_3$) solution until the reaction mixture turned clear. Brine (5 mL) was added and the phases were separated. The aqueous layer was extracted with dichloromethane (3 x 15 mL) and then with ethyl acetate (3 x 15 mL). The organic layers were combined, dried over Na$_2$SO$_4$, and concentrated in *vacuo*. The

residue was purified with flash column chromatography on silica gel with 100% ethyl acetate. 0.50

g pure product **Cpd 1** was obtained with 70% yield. **^{1}H NMR (CD$_3$OD, 300 MHz):** δ (ppm) 5.80-

5.71 (m, 1H), 5.62 (dd, *J* = 15.0, 6.0 Hz, 1H), 4.48 (q, *J* = 6.0 Hz, 1H), 2.76 (t, *J* = 7.5 Hz, 2H),

2.49-2.43 (m, 4H); **^{13}C NMR (CD$_3$OD, 75 MHz):** δ (ppm) 173.7, 133.3, 128.7, 68.6, 42.1, 37.7,

31.6.

(2*S*)-methyl 2-((E)-3-hydroxy-7-(tritylthio)hept-4-enamido)hexanoate, 11:
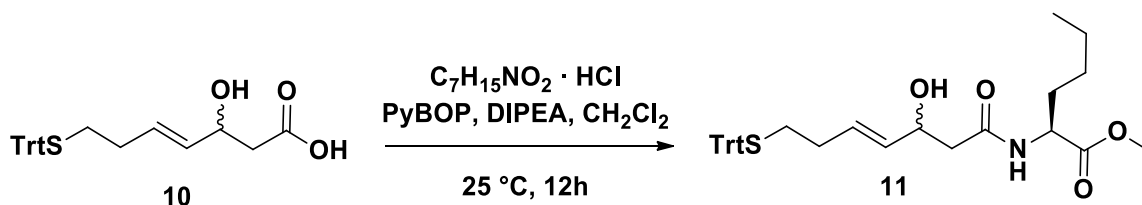
(*E*)-3-hydroxy-7-(tritylthio)hept-4-enoic acid (2.0 g, 4.8 mmol, 1 equiv.) and D-methionine methyl

ester hydrochloride salt (0.87 g, 4.8 mmol, 1.0 equiv.) were dissolved in anhydrous

dichloromethane (50 mL) under nitrogen. The reaction was cooled to 0 ºC and then benzotriazol-

1-yl-oxytripyrrolidinophosphonium hexafluorophosphate (PyBOP) (3.0 mg, 5.7 mmol, 1.2 equiv.)

was added. The solution stirred for 20 min and then DIPEA (3.3 mL, 19.0 mmol, 4.0 equiv.) was

added to the solution. The reaction was allowed to warm to 25 ºC and stirred for 12 hr. It was then

quenched with a saturated NH$_4$Cl, extracted with dichloromethane (3 x 15 mL), washed with brine,

dried over Na$_2$SO$_4$, and then concentrated in *vacuo*. The residue was purified with flash column

chromatography on silica gel (hexane/ethyl acetate, 3:2) and obtained 2.2 g (81%) of product **11**

as a white solid. Compound **11** was confirmed[164] by comparing spectra to known NMR. **^{1}H NMR**

(CDCl$_3$, 300 MHz): δ (ppm) 7.43 (d, *J* = 10.0 Hz, 6H), 7.30 (t, *J* = 7.5 Hz, 6H), 7.24 (d, *J* = 10.0

Hz, 3H), 6.43 (d, *J* = 5.0 Hz, 1H), 5.62-5.56 (m, 1H), 5.45 (dd, *J* = 15.0, 5.0 Hz, 1H), 4.64-4.60

(m, 1H), 4.44 (s, 1H), 3.76 (s, 3H), 3.50 (s, 1H), 2.45 (dd, $J = 15.0, 5.0$ Hz, 1H), 2.37 (dd, $J = 15.0$,

10.0 Hz, 1H), 2.24 (t, $J = 7.5$ Hz, 2H), 2.11 (t, $J = 5.0$ Hz, 1H), 1.87-1.83 (m, 1H), 1.68 (d, $J = 5.0$

Hz, 1H), 1.33 (d, $J = 5.0$ Hz, 4H), 0.92 (t, $J = 7.5$ Hz, 3H); **^{13}C NMR (CDCl$_3$, 75 MHz):** δ (ppm)

173.1, 171.5, 144.9, 132.2, 130.2, 129.6, 127.9, 126.6, 69.1, 66.6, 52.4, 52.1, 42.6, 32.1, 31.5, 31.4,

27.4, 22.3, 13.9.

(2S)-2-((E)-3-hydroxy-7-(tritylthio)hept-4-enamido)hexanoic acid, 12:
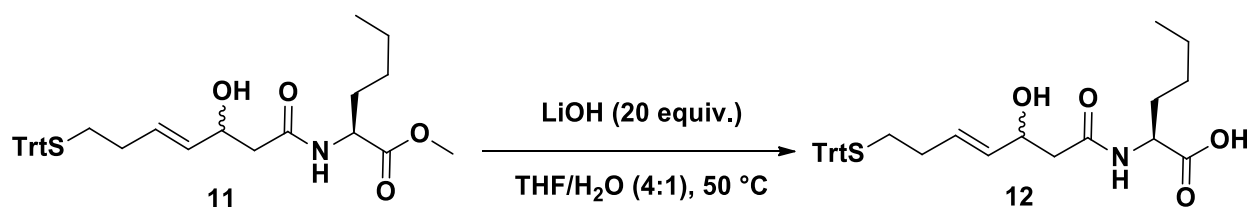
(2S)-methyl 2-((E)-3-hydroxy-7-(tritylthio)hept-4-enamido)hexanoate (2.0 g, 3.7 mmol, 1.0

equiv.) was dissolved in a 4:1 ratio of THF/water (25 mL). Next was added lithium hydroxide (2.2

mg, 91.7 mmol, 25 equiv.). The solution was then heated to 50°C and stirred for 12 hr. The reaction

was then diluted with 20 mL of water and then acidified to a pH of 4-5 with KHSO$_4$. The aqueous

layer was extracted with ethyl acetate (36 x 15 mL). The organic layers were combined and washed

with water, brine, dried over anhydrous Na$_2$SO$_4$, and concentrated in *vacuo*. The residue was

purified with flash column chromatography on silica gel (ethyl acetate/hexane, 1:1) and obtained

1.8 g (92%) of product as a white solid **12**. Compound 12 was confirmed[164] by comparing spectra

to known NMR. **^{1}H NMR (CDCl$_3$, 300 MHz):** δ (ppm) 7.43 (d, $J = 10.0$ Hz, 6H), 7.30 (t, $J = 7.5$

Hz, 6H), 7.24 (t, $J = 7.5$ Hz, 3H), 6.68 (d, $J = 5.0$ Hz, 1H), 6.57 (d, $J = 5.0$ Hz, 1H), 5.61-5.56 (m,

1H), 5.47-5.41 (m, 1H), 4.57-4.44 (m, 1H), 4.46 (t, $J = 10.0$ Hz, 1H), 2.46-2.36 (m, 2H), 2.23 (t, J

$= 7.5$ Hz, 2H), 2.10 (t, $J = 10.0$ Hz, 1H), 1.91-1.87 (m, 1H), 1.72-1.68 (m, 1H), 1.35 (s, 4H), 1.29

(s, 1H), 0.92 (t, $J = 5.0$ Hz, 3H); **^{13}C NMR (CDCl$_3$, 75 MHz):** δ (ppm) 175.6, 172.3, 146.9, 144.9, 129.6, 127.9, 127.3, 126.7, 69.2, 66.7, 52.3, 42.7, 31.7, 31.5, 31.4, 27.4, 22.3, 13.9.

(2*S*,2'*S*)-dimethyl-2,2'-(((4*E*,4'*E*)-7,7'-disulfanediylbis(3-hydroxyhept-4-enoyl))bis(azanediyl))dihexanoate, Cpd 5':
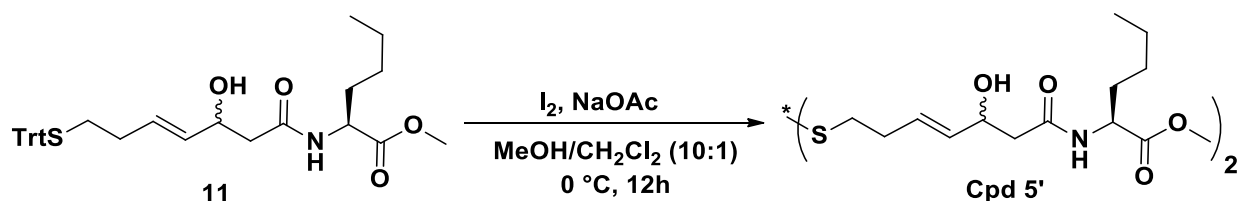
 Iodine (0.70 g, 2.8 mmol, 1 equiv.) and sodium acetate (0.45 g, 5.5 mmol, 2 equiv.) were dissolved in a 10:1 solution of CH$_2$Cl$_2$/MeOH (15 mL) at 0°C. (2*S*)-methyl 2-((*E*)-3-hydroxy-7-(tritylthio)hept-4-enamido)hexanoate (1.5 g, 2.8 mmol, 1 equiv.) was dissolved in a 10:1 solution of CH$_2$Cl$_2$/MeOH (10 mL) and was added dropwise over 20 minutes to the first solution containing iodine and sodium acetate. This solution was then allowed to stir for 2 hr. The reaction was quenched by adding a saturated sodium thiosulfate (Na$_2$S$_2$O$_3$) solution until the reaction mixture turned clear. Then brine (15 mL) was added and the phases were separated. The aqueous layer was extracted with dichloromethane (3 x 15 mL) and then with ethyl acetate (3 x 15 mL). The organic layers were combined, dried over Na$_2$SO$_4$, and concentrated in *vacuo.* The residue was purified with column chromatography on silica gel (ethyl acetate, 100%) in presence of triethylamine (TEA) and 1.2 g product was obtained with 75 % yield of **Cpd 5'**. **^{1}H NMR (CDCl$_3$, 500 MHz):** δ (ppm) 6.67 (d, $J = 10.0$ Hz, 1H), 5.79-5.73 (m, 1H), 5.60 (dd, $J = 15.0, 5.0$ Hz, 1H), 4.49 (q, $J = 5.0$ Hz, 1H), 4.51 (s, 1H), 3.90 (brs, 1H), 3.75 (s, 3H), 2.74 (t, $J = 7.5$ Hz, 2H), 2.51-2.41 (m, 4H), 1.88-1.81 (m, 1H), 1.71-1.65 (m, 1H), 1.35-1.28 (m, 4H), 0.89 (t, $J = 7.5$ Hz, 3H);

13C NMR (CDCl₃, 125 MHz): δ (ppm) 173.3, 171.8, 132.9, 129.3, 69.2, 52.4, 52.2, 42.9, 38.2, 31.8, 31.7, 27.5, 22.2, 13.8. **HRMS (ESI+):** Calculated (m/z) for $C_{28}H_{51}N_2O_8S_2$ (M+H)$^+$: 605.2925, Found 605.2914.

(2S,2'S)-2,2'-(((4E,4'E)-7,7'-disulfanediylbis(3-hydroxyhept-4-enoyl))bis(azanediyl)) dihexanoic acid, Cpd 5:
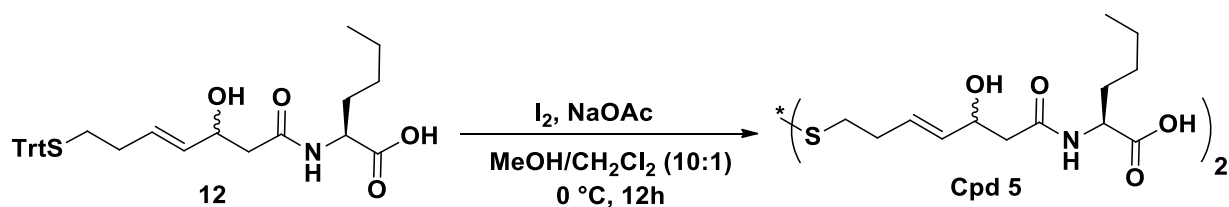
Iodine (0.24 g, 1.8 mmol, 1 equiv.) and sodium acetate (0.23g, 3.8 mmol, 2 equiv.) were dissolved in a 10:1 solution of CH₂Cl₂/MeOH (15 mL) at 0°C. (2S)-2-((E)-3-hydroxy-7-(tritylthio)hept-4-enamido)hexanoic acid (1.0 g, 1.8 mmol, 1 equiv.) was dissolved in a 10:1 solution of CH₂Cl₂/MeOH (10 mL) and was added dropwise over 20 minutes to the first solution containing iodine and sodium acetate. This solution was then allowed to stir for 2 hr. The reaction was quenched by adding a saturated sodium thiosulfate (Na₂S₂O₃) solution until the reaction mixture turned clear. Then brine (15 mL) was added and the phases were separated. The aqueous layer was extracted with dichloromethane (3 x 15 mL) and then with ethyl acetate (3 x 15 mL). The organic layers were combined, dried over Na₂SO₄, and concentrated in *vacuo*. The crude reaction mixture was first purified by Hi-Flash Column (ODS-C18, 3.0x16.5 cm, 50 um, Yamazen A1-580), 0-20min 20-100% ACN/H₂O 20ml/min and the detection wave length was set at 210 nm. The peak was collected at 8-12min. Then this peak was injected in HPLC (Varian ProStar) with the column (Prep-C18, 21.2x250 mm, 10 um) system and 35 % ACN/H₂O was used to elute the

column under the flow rate of 8ml/min. The wavelength was set at 200 nm to detect the compound and 0.55 g of the pure compound was collected at 16-20 min. (55 % yield). The residue was purified with column chromatography on silica gel (dichloromethane/methanol, 20:1) with 84% yield of **Cpd 5**. **^{1}H NMR (CD$_3$OD, 500 MHz):** δ (ppm) 5.80-5.71 (m, 1H), 5.62 (dd, J = 15.0, 5.0 Hz, 1H), 4.45 (q, J = 7.5 Hz, 1H), 4.27 (q, J = 3.0 Hz, 1H), 3.76 (t, J = 7.5 Hz, 2H), 2.45 (t, J = 7.5 Hz, 4H), 1.85 (t, J = 7.5 Hz, 1H), 1.68 (q, J = 6.0 Hz, 1H), 1.36 (s, 4H), 0.93 (t, J = 3.0 Hz, 3H); **^{13}C NMR (CD$_3$OD, 125 MHz):** δ (ppm) 177.9, 171.4, 133.6, 128.5, 69.0, 54.9, 43.6, 37.7, 32.4, 31.6, 27.6, 22.3, 13.0. **HRMS (ESI+)**: Calculated (m/z) for C$_{26}$H$_{44}$N$_2$O$_8$S$_2$ (M+H)$^+$: 577.2612, Found 577.2610.

(E)-3-hydroxy-N-phenyl-7-(tritylthio)hept-4-enamide, 13:
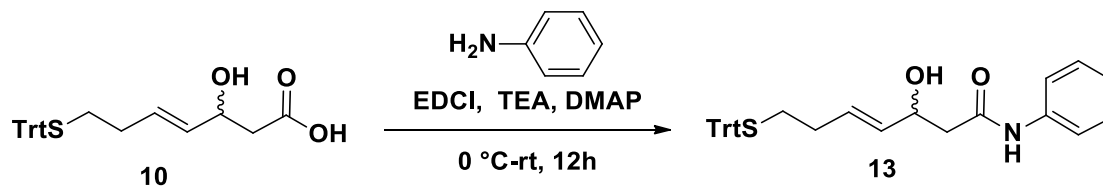
(E)-3-hydroxy-7-(tritylthio)hept-4-enoic acid (200 mg, 0.48 mmol, 1 equiv.) and aniline (45 μL, 0.48 mmol, 1.0 equiv.) were dissolved in anhydrous dichloromethane (10 mL) under nitrogen. The reaction was cooled to 0 ℃. Then, 1-Ethyl-3-(3-dimethylaminopropyl)carbodiimide (EDC, EDAC or EDCI) (82 mg, 53 mmol, 1.2 equiv.) and 4-dimethylaminopyridinewas (DMAP) (86 mg, 0.12 mmol, 0.25 equiv. were added to the solution of carboxylic acid and aniline. The reaction was allowed to warm to 25℃ and stirred for 12 hr. It was then quenched with a saturated NaHCO$_3$ (10 mL), extracted with dichloromethane (3 x 15 mL), washed with brine, dried over Na$_2$SO$_4$, and then concentrated in *vacuo*. The residue was purified with column chromatography on silica gel

(hexane/ethylacetate, 3:2) and obtained 189 mg of pure product **13** with 80% yield. **^{1}H NMR (CDCl$_3$, 500 MHz):** δ (ppm) 7.96 (brs, 1H), 7.50 (d, J = 9.0 Hz, 2H), 7.43 (d, J = 9.0 Hz, 6H), 7.35-7.20 (m, 11H), 7.14 (d, J = 9.0 Hz, 1H), 5.66-5.57 (m, 1H), 6.02 (dd, J = 15.0, 6.0 Hz, 1H), 4.52 (s, 1H), 3.15 (s, 1H), 2.53 (t, J = 4.5 Hz, 2H), , 2.24 (t, J = 6.0 Hz, 2H), 2.11 (t, J = 6.0 Hz, 2H); **^{13}C NMR (CDCl$_3$, 125 MHz):** δ (ppm) 169.9, 144.9, 137.6, 132.2, 130.5, 129.6, 129.0, 127.9, 126.7, 124.5, 120.1, 69.3, 66.7, 43.9, 31.4, 31.3. **HRMS (ESI+):** Calculated (m/z) for C$_{32}$H$_{31}$N$_2$O$_2$S (M+H)$^+$: 492.2003, Found 492.1930.

(4E,4'E)-7,7'-disulfanediylbis(3-hydroxy-N-phenylhept-4-enamide), Cpd 7:

Iodine (26 mg, 0.20 mmol, 1.0 equiv.) and sodium acetate (33 mg, 0.40 mmol, 2.0 equiv.) were dissolved in a 10:1 solution of CH$_2$Cl$_2$/MeOH (5 mL) at 0°C. (E)-3-hydroxy-N-phenyl-7-(tritylthio)hept-4-enamide (100 mg, 0.20 mmol, 1.0 equiv.) was dissolved in a 10:1 solution of CH$_2$Cl$_2$/MeOH (5 mL) and was added dropwise over 20 minutes to the first solution containing iodine and sodium acetate. This solution was then allowed to stir for 2 hr. The reaction was quenched by adding a saturated sodium thiosulfate (Na$_2$S$_2$O$_3$) solution until the reaction mixture turned clear. Then, brine (5 mL) was added and the phases were separated. The aqueous layer was extracted with dichloromethane (3 x 5 mL) and then with ethyl acetate (3 x 5 mL). The organic layers were combined, dried over Na$_2$SO$_4$, and concentrated in *vacuo.* The residue was purified with column chromatography on silica gel (dichloromethane/methanol, 50:1) and obtained 65 mg white solid with 65.5 % yield of **Cpd 7**. **^{1}H NMR (CD$_3$OD, 300 MHz):** δ (ppm) 7.55 (d, J = 6.0

Hz, 2H), 7.31 (t, J = 7.5 Hz, 2H), 7.10 (t, J = 7.5 Hz, 1H), 5.81-5.71 (m, 1H), 5.64 (dd, J = 15.0, 6.0 Hz, 1H), 4.56 (q, J = 6.0 Hz, 1H), 2.68 (t, J = 7.5 Hz, 2H), 2.56 (t, J = 7.5 Hz, 2H), 2.41 (q, J = 6.0 Hz, 2H); **^{13}C NMR (CD$_3$OD, 75 MHz):** δ (ppm) 170.4, 138.3, 133.4, 128.9, 128.4, 123.8, 119.9, 69.2, 44.5, 37.7, 31.5. **HRMS (ESI+):** Calculated (m/z) for $C_{26}H_{32}N_2O_4S_2$ (M-H)$^-$: 499.1731, Found 499.1656.

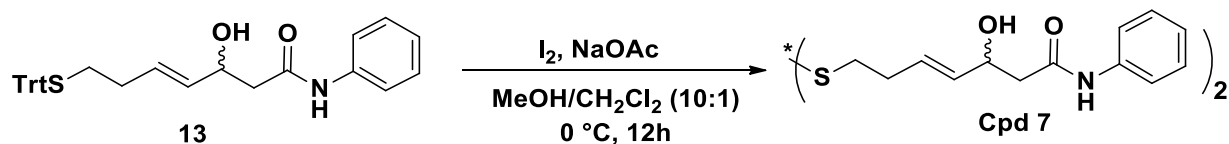**(E)-N-(tert-butyl)-3-hydroxy-7-(tritylthio)hept-4-enamide, 14:**
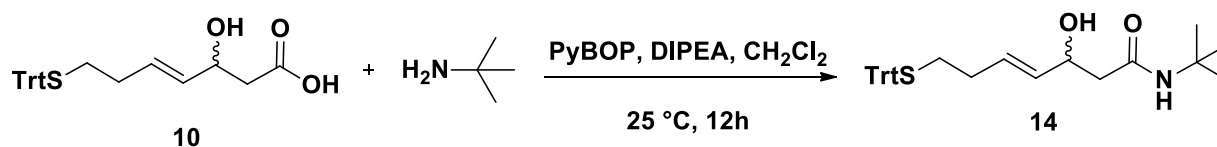
(E)-3-hydroxy-7-(tritylthio)hept-4-enoic acid (500 mg, 1.2 mmol, 1.0 equiv.) and tertiary butyl amine (125 μm, 1.2 mmol, 1.0 equiv.) were dissolved in anhydrous dichloromethane (15 mL) under nitrogen. The reaction mixture was cooled to 0 ℃ and then benzotriazol-1-yl-oxytripyrrolidinophosphonium hexafluorophosphate (PyBOP) (746 mg, 1.4 mmol, 1.2 equiv.) was added. The solution stirred for 20 min and then DIPEA (832 μL, 1.19 mmol, 4 equiv.) was added. The reaction was allowed to warm to 25℃ and stirred for 12 hr. It was then quenched with a saturated NH$_4$Cl, extracted with dichloromethane (3 x 5 mL), washed with brine, dried over Na$_2$-SO$_4$, and then concentrated in *vacuo*. The residue was purified with column chromatography on silica gel (hexane/ethylacetate, 1:1) and obtained 407 mg white solid with 72 % yield of **14**. **^{1}H NMR (CDCl$_3$, 500 MHz):** δ (ppm) 7.43 (d, J = 10.0 Hz, 6H), 7.30 (t, J = 7.5 Hz, 6H), 7.23 (t, J = 7.5 Hz, 3H), 5.66 (brs, 1H), 5.60-5.54 (m, 1H), 5.42 (dd, J = 15.0, 5.0 Hz, 1H), 4.40 (t, J = 7.5 Hz, 1H), 3.15, 3.92 (s, 1H), 2.31-2.21 (m, 4H), 2.12-2.07 (m, 2H), 1.35 (s, 9H); **^{13}C NMR (CDCl$_3$, 125 MHz):** δ (ppm) 171.3, 144.9, 132.4, 129.7, 129.6, 127.9, 126.6, 69.3, 66.6, 51.4, 43.2, 31.5,

31.4, 28.8. **HRMS (ESI+)**: Calculated (m/z) for $C_{30}H_{35}NO_2S$ (M+Na)$^+$: 496.2281, Found 496.2390.

(4E,4'E)-7,7'-disulfanediylbis(N-(tert-butyl)-3-hydroxyhept-4-enamide), Cpd 8:
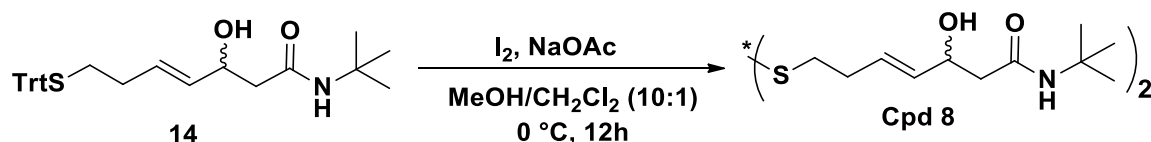
Iodine (107 mg, 0.85 mmol, 1.0 equiv.) and sodium acetate (69 mg, 1.7 mmol, 2.0 equiv.) were dissolved in a 10:1 solution of CH_2Cl_2/MeOH (15 mL) at 0°C. (*E*)-N-(tert-butyl)-3-hydroxy-7-(tritylthio)hept-4-enamide (400 mg, 0.85 mmol, 1.0 equiv.) was dissolved in a 10:1 solution of CH_2Cl_2/MeOH (5 mL) and was added dropwise over 20 minutes to the first solution containing iodine and sodium acetate. This solution was then allowed to stir for 2 hr. The reaction was quenched by adding a saturated sodium thiosulfate ($Na_2S_2O_3$) solution until the reaction mixture turned clear. Then, brine (5 mL) was added and the phases were separated. The aqueous layer was extracted with dichloromethane (3 x 10 mL) and then with ethyl acetate (3 x 10 mL). The organic layers were combined, dried over Na_2SO_4, and concentrated in *vacuo*. The residue was purified with column chromatography on silica gel (dichloromethane/methanol, 20:1) and obtained 264 mg white solid with 68 % yield. **^{1}H NMR (CDCl₃, 500 MHz):** δ (ppm) 5.93 (s, 1H), 5.75-5.70 (m, 1H), 5.56 (dd, *J* = 15.0, 5.0 Hz, 1H), 4.45 (s, 1H), 4.22 (s, 1H), 2.74 (t, *J* = 7.5 Hz, 2H), 2.68 (q, *J* = 10.0 Hz, 2H), 2.33-2.25 (m, 2H), 1.35 (s, 9H); **^{13}C NMR (CDCl₃, 125 MHz):** δ (ppm) 171.4, 133.1, 129.0, 69.3, 51.4, 43.2, 38.3, 31.8, 28.8.

2.7. References

1. Youngson, R. M. *Collins Dictionary of Human Biology*. **2006**, Glasgow: HarperCollins

2. Cox, M.; Nelson, D. R.; Lehninger, A. L. Lehninger Principles of Biochemistry. **2005**, San Francisco: W.H. Freeman.

3. Tessarz, P.; Kouzarides, T. Histone core modifications regulating nucleosome structure and dynamics. *Nat. Rev. Mol. Cell Biol*. **2014**, *15*, 703–708.

4. Venkatesh, S.; Workman, J. L. Histone exchange, chromatin structure and the regulation of transcription. *Nat. Rev. Mol. Cell Biol*. **2015**, *16*, 178–189.

5. Redon, C.; Pilch, D.; Rogakou, E.; Sedelnikova, O.; Newrock, K.; Bonner, W. Current *Opinion in Genet. Develop*. **2002**, *12*, 162-169.

6. Bhasin, M.; Reinherz, E. L.; Reche, P A. Recognition and Classification of Histones Using Support Vector Machine. *J. Comput. Biol*. **2006**, *13*, 102-112.

7. Mariño-Ramírez, L.; Kann, M. G.; Shoemaker, B. A.; Landsman, D. Histone structure and nucleosome stability. Expert Rev. Proteomics **2005**, *2*, 719-729.

8. Cutter, A.; Hayes, J. J. A Brief Review of Nucleosome Structure. *FEBS Lett*. **2015**, *7*, 2914–2922.

9. Shuaib, M. Epigenetic mechanism of CENP-A loading to centromeres. Biochemistry, Molecular Biology. Université de Strasbourg, **2012**. English.

10. Jaenisch, R.; Bird, A. Epigenetic regulation of gene expression: how the genome integrates intrinsic and environmental signals. *Nat. Genet*. **2003**, *33*, 245–254.

11. Bottomley M. J.; Lo Surdo, P.; Di Giovine, P.; Cirillo, A.; Scarpelli, R.; Ferrigno, F.; Jones, P.; Neddermann, P.; De Francesco, R.; Steinkühler, C.; Gallinari, P.; Carfi, A.

"Structural and functional analysis of the human HDAC4 catalytic domain reveals a regulatory structural zinc-binding domain. *J. Biol. Chem.* **2008**, *283*, 26694–26704.

12. Choudhary, C.; Kumar, C.; Gnad, F.; Nielsen, M. L.; Rehman, M.; Walther, T. C.; Olsen, J. V.; Mann, M. Lysine acetylation targets protein complexes and co-regulates major cellular functions. *Science* **2009**, *325*, 834–840

13. Haberland, M.; Montgomery, R. L.; Olson, E. N. The many roles of histone deacetylases in development and physiology: Implications for disease and therapy. *Nat. Rev. Genet.* **2009**, *10*, 32−42.

14. Verdin, E.; Dequiedt, F.; Kasler, H. Class II Histone Deacetylases Versatile Regulators. *Trends Genet.* **2003**, *19*, 286−293.

15. Fass, D. M.; Kemp, M. M.; Schroeder, F. A.; Wagner, F. F.; Wang, Q.; Holson, E. B. Histone Acetylation and Deacetylation. In Epigenetic Regulation and Epigenomics: Advances in Molecular Biology and Medicine; *Wiley-VCH Vrlag & Co. KGaA: Weinheim*, **2012**, 515−561.

16. de Ruijter, A. J. M.; Van Gennip, A. H.; Caron, H. N.; Kemp, S.; Van Kuilenburg, A. B. P. Histone deacetylases (HDACs): characterization of the classical HDAC family. *Biochem. J.* **2003**, *370*, 737−749.

17. Witt, O.; Deubzer, H. E.; Milde, T.; Oehme, I. HDAC family: What is the cancer relevant targets. *Cancer Lett.* **2009**, *277*, 8−21.

18. Zou, H.; Wu, Y.; Navre, M.; Sang, B.-C. Characterization of the two catalytic domains in histone deacetylase 6. Biochem. Biophys. *Res. Commun.* **2006**, *341*, 45−50.

19. Zhang, Y.; Gilquin, B.; Khochbin, S.; Matthias, P. Two catalytic domains are required for protein deacetylation. *J. Biol. Chem.* **2006**, *281*, 2401−2404.

20. Weichert, W.; Röske, A.; Niesporek, S.; Noske, A.; Buckendahl, A.-C.; Dietel, M.; Gekeler, V.; Boehm, M.; Beckers, T.; Denkert, C. Class I histone deacetylase expression has independent prognostic impact on human colorectal cancer: Specific role of class I histone deacetylases in vitro and in vivo. *Clin. Cancer Res*. **2008**, *14*, 1669−1677.

21. Seidel, C.; Schnekenburger, M.; Dicato, M.; Diederich, M. Histone deacetylase modulators provided by Mother Nature. *Genes and Nutrition* **2012**, *7*, 357-367.

22. Rikimaru, T.; Taketomi, A.; Yamashita, Y.; Shirabe, K.; Hamatsu, T.; Shimada, M.; Maehara, Y. Clinical significance of histone deacetylase 1 expression in patients with hepatocellular carcinoma. *Oncology* **2007**, *72*, 69−74.

23. López, J. E.; Sullivan, E. D.; Fierke, C. A. Metal-dependent deacetylases: Cancer and epigenetic regulators. *ACS Chem. Biol.* **2016**, *11*, 706–716.

24. Ropero, S.; Esteller, M. The role of histone deacetylases (HDACs) in human cancer.; *Molecular Oncology* **2007**, *1*, 19–22.

25. Seto, E.; Yoshida, M. Erasers of Histone Acetylation: The Histone Deacetylase Enzymes. *Cold Spring Harb Perspect Biol.* **2014**, *6*, a018713.

26. Mahlknecht, U.; Hoelzer, D. Histone acetylation modifiers in the pathogenesis of malignant disease. *Mol. Med*. **2000**, *6*, 623–644.

27. Clayton, A. L.; Hazzalin, C. A.; Mahadevan, L. C. Enhanced Histone Acetylation and Transcription: A Dynamic Perspective. *Molecular Cell*. **2006**, 289–296.

28. Gräff, J.; Tsai, L.-H. Histone acetylation: molecular mnemonics on the chromatin. *Nat. Rev. Neurosci.* **2013**, *14*, 97–111.

29. Kuo, M. H.; Allis, C. D. Roles of histone acetyltransferases and deacetylases in gene regulation. *BioEssays*. **1998**, 615–626.

30. Legube, G.; Trouche, D. Regulating histone acetyltransferases and deacetylases. *EMBO Rep.* **2003**, *4*, 944–947.

31. Marks, P. A.; Miller, T.; Richon, V. M. Histone deacetylases. *Current Opinion in Pharmacology*. **2003**, 344–351.

32. Peserico, A.; Simone, C. Physical and functional HAT/HDAC interplay regulates protein acetylation balance. *J. Biomed. Biotech*. **2010**, *2011*, 1-10.

33. Icardi, L.; De Bosscher, K.; Tavernier, J. The HAT/HDAC interplay: Multilevel control of STAT signaling. *Cytokine and Growth Factor Reviews*. **2012**, 283–291.

34. Toussirot, E.; Abbas, W.; Khan, K. A.; Tissot, M.; Jeudy, A.; Baud, L.; Bertolini, E.; Wendling, D.; Herbein, G. Imbalance between HAT and HDAC Activities in the PBMCs of Patients with Ankylosing Spondylitis or Rheumatoid Arthritis and Influence of HDAC Inhibitors on TNF Alpha Production. *PLoS One* **2013**, *8*, e70939.

35. Lin, H. Y.; Chen, C. S.; Lin, S. P.; Weng, J. R.; Chen, C. S. Targeting histone deacetylase in cancer therapy. *Med. Research Rev*. **2006**, 397–413.

36. Gray, S. G.; Ekström, T. J. The human histone deacetylase family. *Exp. Cell Res*. **2001**, *262*, 75–83.

37. Gregoretti, I. V.; Lee, Y. M.; Goodson, H. V. Molecular evolution of the histone deacetylase family: Functional implications of phylogenetic analysis. *J. Mol. Biol*. **2004**, *338*, 17–31.

38. Hu, E.; Chen, Z.; Fredrickson, T.; Zhu, Y.; Kirkpatrick, R.; Zhang, G. F.; Johanson, K.; Sung, C. M.; Liu, R.; Winkler, J. Cloning and characterization of a novel human class I histone deacetylase that functions as a transcription repressor. *J. Biol. Chem*. **2000**, *275*, 15254–15264.

39. Verdin, E.; Dequiedt, F.; Kasler, H. G. Class II histone deacetylases: Versatile regulators. *Trends in Genetics*. **2003**, 286–293.

40. Fischle, W.; Kiermer, V.; Dequiedt, F.; Verdin, E. The emerging role of class II histone deacetylases. *Biochem Cell Biol.* **2001**, *79*, 337–348.

41. Yang, X.-J.; Grégoire, S. Class II histone deacetylases: from sequence to function, regulation, and clinical implication. *Mol. Cell. Biol*. **2005**, *25*, 2873–2884.

42. North, B. J.; Verdin, E. Sirtuins: Sir2-related NAD-dependent protein deacetylases. *Genome Biol*. **2004**, *5*, 224-228.

43. Martin, M.; Kettmann, R.; Dequiedt, F. Class IIa histone deacetylases: regulating the regulators. *Oncogene* **2007**, *26*, 5450–5467.

44. Parra, M. Class IIa HDACs - New insights into their functions in physiology and pathology. *FEBS J.* **2015**, *282*, 1736–1744.

45. Bertos, N. R.; Wang, A. H.; Yang, X. J. Class II histone deacetylases: structure, function, and regulation. *Biochem. Cell Biol*. **2001**, *79*, 243–252.

46. Jones, P.; Altamura, S.; De Francesco, R.; Gallinari, P.; Lahm, A.; Neddermann, P.; Rowley, M.; Serafini, S.; Steinkühler, C. Probing the elusive catalytic activity of vertebrate class IIa histone deacetylases. *Bioorg. Med. Chem. Lett*. **2008**, *18*, 1814–1819.

47. Tong, J. J.; Liu, J.; Bertos, N. R.; Yang, X.-J. Identification of HDAC10, a novel class II human histone deacetylase containing a leucine-rich domain. *Nucleic Acids Res*. **2002**, *30*, 1114–1123.

48. Ropero, S.; Esteller, M. The role of histone deacetylases (HDACs) in human cancer. *Molecular Oncology*. **2007**, 19–25.

49.   Singh, B. N.; Zhang, G.; Hwa, Y. L.; Li, J.; Dowdy, S. C.; Jiang, S.-W. Nonhistone protein acetylation as cancer therapy targets. Expert Rev. *Anticancer Ther*. **2010**, *10*, 935–954.

50.   Osada, H.; Tatematsu, Y.; Saito, H.; Yatabe, Y.; Mitsudomi, T.; Takahashi, T. Reduced expression of class II histone deacetylase genes is associated with poor prognosis in lung cancer patients. *Int. J. Cancer* **2004**, *112*, 26–32.

51.   Choudhary, C.; Weinert, B. T.; Nishida, Y.; Verdin, E.; Mann, M. The growing landscape of lysine acetylation links metabolism and cell signalling. *Nat. Rev. Mol. Cell. Biol.* **2014**, *15*, 536–550.

52.   Caron, C.; Boyault, C.; Khochbin, S. Regulatory cross-talk between lysine acetylation and ubiquitination: Role in control of protein stability. *BioEssays*. **2005**, 408–415.

53.   Matus, D. Q.; Lohmer, L. L.; Kelley, L. C.; Schindler, A. J.; Kohrman, A. Q.; Barkoulas, M.; Zhang, W.; Chi, Q.; Sherwood, D. R. Invasive Cell Fate Requires G1 Cell-Cycle Arrest and Histone Deacetylase-Mediated Changes in Gene Expression. *Dev. Cell* **2015**, *35*, 162–174.

54.   Grunstein, M. Histone acetylation in chromatin structure and transcription. *Nature* **1997**, *389*, 349–352.

55.   Bannister, A. J.; Kouzarides, T. Regulation of chromatin by histone modifications. *Cell Res*. **2011**, *21*, 381–395.

56.   Venkatesh, S.; Workman, J. L. Histone exchange, chromatin structure and the regulation of transcription. *Nat. Rev. Mol. Cell Biol*. **2015**, *16*, 178–189.

57.   Lakshmaiah, K. C.; Jacob, L. A.; Aparna, S.; Lokanatha, D.; Saldanha, S. C. Epigenetic therapy of cancer with histone deacetylase inhibitors. *J. Cancer Res. Ther.* **2014**, *10*, 469-478.

58. Tandon, N.; Ramakrishnan, V.; Kumar, S. K. Clinical use and applications of histone deacetylase inhibitors in multiple myeloma. Clinical Pharmacology: Advances and Applications, **2016**, *8*, 35-44.

59. Licciardi, P. V.; Ververis, K.; Hiong, A.; Karagiannis, T. C. Histone deacetylase inhibitors (HDACIs): multitargeted anticancer agents. *Biologics: Targets and Therapy*, **2013**, *7*, 47-60.

60. Zhou, W.; Zhu, W.-G. The Changing Face of HDAC Inhibitor Depsipeptide. *Current Cancer Drug Targets* **2009**, *9*, 91–100.

61. Jones, R. G.; Thompson, C. B. Tumor suppressors and cell metabolism: a recipe for cancer growth. *Genes Dev*. **2009**, *23*, 537–548.

62. Bernstein, B. E., Meissner, A., and Lander, E. S. The mammalian epigenome, *Cell* **2007**, *128*, 669-681.

63. Spange, S.; Wagner, T.; Heinzel, T.; Kramer, O. H. Acetylation of non-histone proteins¨ modulates cellular signalling at multiple levels. *Int. J. Biochem. Cell Biol.* **2009**, *41*, 185−198.

64. Jaenisch, R.; Bird, A. Epigenetic regulation of gene expression: how the genome integrates intrinsic and environmental signals. *Nat. Genet*. **2003**, *33*, 245–254.

65. Zhang, J.; Zhong, Q. Histone deacetylase inhibitors and cell death. Cellular and molecular life sciences: *CMLS*. **2014**, 3885–3901.

66. Guan, J.-S.; Haggarty, S. J.; Giacometti, E.; Dannenberg, J.-H.; Joseph, N.; Gao, J.; Nieland, T. J. F.; Zhou, Y.; Wang, X.; Mazitschek, R.; Bradner, J. E.; DePinho, R. A.; Jaenisch, R.; Tsai, L.-H. HDAC2 negatively regulates memory formation and synaptic plasticity. *Nature* **2009**, *459*, 55−60.

67. McQuown, S. C.; Barrett, R. M.; Matheos, D. P.; Post, R. J.; Rogge, G. A.; Alenghat, T.; Mullican, S. E.; Jones, S.; Rusche, J. R.; Lazar, M. A.; Wood, M. A. HDAC3 is a critical negative regulator of long-term memory formation. *J. Neurosci*. **2011**, *31*, 764−774.

68. Weïwer, M.; Lewis, M. C.; Wagner, F. F.; Holson, E. B. Therapeutic potential of isoform selective HDAC inhibitors for the treatment of schizophrenia. *Future Med. Chem*. **2013**, *5*, 1491–1508.

69. Bolden, J. E.; Peart, M. J.; Johnstone, R. W. Anticancer activities of histone deacetylase inhibitors. *Nat. Rev. Drug Discovery* **2006**, *5*, 769−784.

70. Emanuele, S.; Lauricella, M.; Tesoriere, G. Histone deacetylase inhibitors: Apoptotic effects and clinical implications. *Int. J. Oncol*. **2008**, *33*, 637−646.

71. Minucci, S.; Pelicci, P. G. Histone deacetylase inhibitors and the promise of epigenetic (and more) treatments for cancer. *Nature Rev. Cancer* **2006,** *6*, 38−51.

72. Marks, P. A., Histone deacetylase inhibitors: a chemical genetics approach to understanding cellular functions. *Biochim Biophys Acta* **2010**, *1799*, 717-725.

73. Wiech NL, Fisher JF, Helquist P, Wiest O: Inhibition of histone deacetylases: a pharmacological approach to the treatment of non-cancer disorders. *Curr Top Med Chem* **2009**, *9*, 257-271.

74. Wagner JM, Hackanson B, Lübbert M, Jung M: Histone deacetylase (HDAC) inhibitors in recent clinical trials for cancer therapy. *Clin Epigenetics* **2010**, *1*, 117-136.

75. Marks, P. A.; Richon, V. M.; Miller, T.; Kelly, W. K. Histone Deacetylase Inhibitors. *Adv. Can. Res*. **2004**, *91*, 137−168.

76. Glaser, K. B.; Staver, M. J.; Waring, J. F.; Stender, J.; Ulrich, R. G.; Davidsen, S. K. Gene expression profiling of multiple histone deacetylase (HDAC) inhibitors: defining a

common gene set produced by HDAC inhibition in T24 and MDA carcinoma cell lines. *Mol. Cancer Ther*. **2003**, *2*, 151−163.

77. Bertrand, P. Inside HDAC with HDAC inhibitors. *European Journal of Medicinal Chemistry*. **2010**, *45*, 2095-2116.

78. Bolden, J. E.; Peart, M. J.; Johnstone, R. W. Anticancer activities of histone deacetylase inhibitors. *Nature Rev. Drug Discovery* **2006**, *5*, 769−784.

79. Chuang, D. M.; Leng, Y.; Marinova, Z.; Kim, H. J.; Chiu, C. T. Multiple roles of HDAC inhibition in neurodegenerativeconditions. *Trends Neurosci*. **2009**, *32*, 591−601.

80. Rotilli, D.; Simonetti, G.; Savarino, A.; Palamara, A. T.; Migliaccio, A. R.; Mai, A. Non-cancer uses of histone deacetylase inhibitors: effects on infectious diseases and beta-hemoglobinopathies. *Curr. Top. Med. Chem*. **2009**, *9*, 272−291.

81. Andrews, K. T.; Haque, A.; Jones, M. K. HDAC inhibitors in parasitic diseases. *Immunol. Cell Biol*. **2012**, *90*, 66−77.

82. Johnstone, R. W. Histone-deacetylase inhibitors: novel drugs for the treatment of cancer. *Nat. Rev. Drug Discovery*. **2002**, *1*, 287−299.

83. Dokmanovic, M.; Clarke, C.; Marks, P. A. Histone deacetylase inhibitors: Overview and perspectives. *Mol. Cancer Res*. **2007**, *5*, 981− 989.

84. Furlan, A.; Monzani, V.; Reznikov, L. L.; Leoni, F.; Fossati, G.; Modena, D.; Mascagni, P.; Dinarello, C. A. Pharmacokinetics, safety and inducible cytokine responses during a phase 1 trial of the oral histone deacetylase inhibitor ITF2357 (givinostat). *Mol. Med*. **2011**, *17*, 353–362.

85. Galli, M.; Salmoiraghi, S.; Golay, J.; Gozzini, A.; Crippa, C.; Pescosta, N.; Rambaldi, A. A phase II multiple dose clinical trial of histone deacetylase inhibitor ITF2357 in patients with relapsed or progressive multiple myeloma. *Ann. Hematol*. **2010**, *89*, 185–190.

86. Andreu-Vieyra, C. C. V; Berenson, J. J. R. The potential of panobinostat as a treatment option in patients with relapsed and refractory multiple myeloma. *Ther. Adv. Hematol*. **2014**, *5*, 197–210.

87. Morabito, F.; Voso, M. T.; Hohaus, S.; Gentile, M.; Vigna, E.; Recchia, A. G.; Iovino, L.; Benedetti, E.; Lo-Coco, F.; Galimberti, S. Panobinostat for the treatment of acute myelogenous leukemia. *Expert Opin. Investig*. *Drugs* **2016**, 1117-1131.

88. Prince, H. M.; Bishton, M. J.; Johnstone, R. W. Panobinostat (LBH589): a potent pan-deacetylase inhibitor with promising activity against hematologic and solid tumors. *Future Oncol*. **2009**, *5*, 601–612.

89. Shao, W.; Growney, J. D.; Feng, Y.; O'Connor, G.; Pu, M.; Zhu, W.; Yao, Y. M.; Kwon, P.; Fawell, S.; Atadja, P. Activity of deacetylase inhibitor panobinostat (LBH589) in cutaneous T-cell lymphoma models: Defining molecular mechanisms of resistance. *Int. J. Cancer* **2010**, *127*, 2199–2208.

90. Grant, S.; Easley, C.; Kirkpatrick, P. Vorinostat. *Nat. Rev. Drug Discovery*. **2007**, *6*, 21−22.

91. Marks, P. a; Breslow, R. Dimethyl sulfoxide to vorinostat: development of this histone deacetylase inhibitor as an anticancer drug. *Nat. Biotechnol*. **2007**, *25*, 84–90.

92. Duvic, M.; Talpur, R.; Ni, X.; Zhang, C.; Hazarika, P.; Kelly, C.; Chiao, J. H.; Reilly, J. F.; Ricker, J. L.; Richon, V. M.; et al. Phase 2 trial of oral vorinostat (suberoylanilide

hydroxamic acid, SAHA) for refractory cutaneous T-cell lymphoma (CTCL). *Blood* **2007**, *109*, 31–39.

93.   Richon, V. M. Cancer biology: mechanism of antitumour action of vorinostat (suberoylanilide hydroxamic acid), a novel histone deacetylase inhibitor. *Br. J. Cancer* **2006**, *95*, S2–S6.

94.   Jain, S.; Zain, J. Romidepsin in the treatment of cutaneous T-cell lymphoma. *J. Blood Med*. **2011**, *2*, 37–47.

95.   Campas-Moya, C. Romidepsin for the treatment of cutaneous T-cell lymphoma. *Drugs Today (Barc)*. **2009**, *45*, 787–795.

96.   Bertino, E. M.; Otterson, G. a. Romidepsin: a novel histone deacetylase inhibitor for cancer. *Expert Opin. Investig. Drugs* **2011**, *20*, 1151–1158.

97.   Yoshida, M.; Kijima, M.; Akita, M.; Beppu, T. Potent and specific inhibition of mammalian histone deacetylase both in vivo and in vitro by trichostatin A. *J. Biol. Chem*. **1990**, *265*, 17174–17179.

98.   Vanommeslaeghe, K.; Van Alsenoy, C.; De Proft, F.; Martins, J. C.; Tourwé, D.; Geerlings, P. Ab initio study of the binding of Trichostatin A (TSA) in the active site of histone deacetylase like protein (HDLP). *Org. Biomol. Chem*. **2003**, *1*, 2951–2957.

99.   Weichert, W.; Röske, A.; Gekeler, V.; Beckers, T.; Stephan, C.; Jung, K.; Fritzsche, F. R.; Niesporek, S.; Denkert, C.; Dietel, M.; Kristiansen, G. Histone deacetylases 1, 2 and 3 are highly expressed in prostate cancer and HDAC2 expression is associated with shorter PSA relapse time after radical prostatectomy. *Br. J. Cancer* **2008**, *98*, 604− 610.

100. Lane, A. A.; Chabner, B. A. Histone deacetylase inhibitors in cancer therapy. *J. Clin. Oncol*. **2009**, *27*, 5459−5468.

101. Karagiannis, T. C.; El-Osta, A. Will broad-spectrum histone deacetylase inhibitors be superseded by more specific compounds? *Leukemia* **2007**, *21*, 61−65.

102. Wiech NL, Fisher JF, Helquist P, Wiest O: Inhibition of histone deacetylases: a pharmacological approach to the treatment of non-cancer disorders. *Curr Top Med Chem* **2009**, *9*, 257-271.

103. Wagner JM, Hackanson B, Lübbert M, Jung M: Histone deacetylase (HDAC) inhibitors in recent clinical trials for cancer therapy. *Clin Epigenetics* **2010**, *1*, 117-136.

104. Porter, N. J.; Mahendran, A.; Breslow, R.; Christianson, D. W. Unusual zinc-binding mode of HDAC6-selective hydroxamate inhibitors. *PNAS* **2017**, *114*, 13459-13464.

15. Falkenberg, K. J.; Johnstone, R. W. Histone deacetylases and their inhibitors in cancer, neurological diseases and immune disorders. *Nat. Rev. Drug Discov.* **2014**, *13*, 673–691.

106. Dokmanovic, M.; Clarke, C.; Marks, P. A. Histone deacetylase inhibitors: Overview and perspectives. *Mol. Cancer Res*. **2007**, *5*, 981–989.

107. Ganai, S. A.; Ramadoss, M.; Mahadevan, V. Histone deacetylase (HDAC) inhibitors– Emerging roles in neuronal memory, learning, synaptic plasticity and neural regeneration. Curr *Neuropharmacol* **2016**, *14*, 55–71.

108. Hancock, W. W.; Akimova, T.; Beier, U. H.; Liu, Y.; Wang, L. HDAC inhibitor therapy in autoimmunity and transplantation. *Annals of the Rheum. Diseases* **2012**, *71*, i46–i54.

109. Li, Y.; Seto, E. HDACs and HDAC Inhibitors in Cancer Development and Therapy. *Cold Spring Harb Perspect Med*. **2016**, *6*, a026831.

110. Kaushik, d.; Vashistha, V.; Isharwal, S.; Sediqe, S. A.; Lin, M.-F. Histone deacetylase inhibitors in castration-resistant prostate cancer: molecular mechanism of action and recent clinical trials. *Ther Adv Urol*. **2015**, *7*, 388–395.

111. Lakshmaiah, K. C.; Jacob, L. A.; Aparna, S.; Lokanatha, D.; Saldanha, S. C. Epigenetic therapy of cancer with histone deacetylase inhibitors. *J. Cancer Res. Ther*. **2014**, *10*, 469-478.

112. Eckschlager, T.; Plch, J.; Stiborova, M.; Hrabeta, M. Histone Deacetylase Inhibitors as Anticancer Drugs. *Int. J. Mol. Sci*. **2017**, *18*, 1414-1435.

113. De Souza, C.; Chatterji, B. P. HDAC Inhibitors as Novel Anti-Cancer Therapeutics. *Recent Pat Anticancer Drug Discov*. **2015**, *10*, 145-162.

114. Drummond, D. C.; Noble, C. O.; Kirpotin, D. B.; Guo, Z.; Scott, G. K.; Benz, C. C. clinical Development of Histone Deacetylase Inhibitors as Anticancer Agents. *Annu. Rev. Pharmacol. Toxicol.* **2005**. *45,* 495–528.

115. Suraweera, A.; O'Byrne, K. J.; Richard, D. J. Combination Therapy with Histone Deacetylase Inhibitors (HDACi) for the Treatment of Cancer: Achieving the Full Therapeutic Potential of HDACi. *Front. Oncol*. **2018**, *8*, 1-15.

116. Cincinelli, R.; Musso, L.; Artali, R.; Guglielmi, M. B.; La Porta, I.; Melito, C.; Colelli, F.; Cardile, F.; Signorino, G.; Fucci, A.; Frusciante, M.; Pisano, C.; Dallavalle, S. Hybrid topoisomerase I and HDAC inhibitors as dual action anticancer agents. *PLoS One* **2018**, *13*, e0205018.

117. Damaskos, C.; Valsami, S.; Kontos, M.; Spartalis, E.; Kalampokas, T.; Kalampokas, E.; Athanasiou, A.; Moris, D.; Daskalopoulou, A.; Davakis, S.; Tsourouflis, G.; Kontzoglou, K.; Perrea, D.; Nikiteas, N.; Dimitroulis, D. Histone Deacetylase Inhibitors: An Attractive Therapeutic Strategy Against Breast Cancer. *Anticancer Research* **2017**, *37*, 35-46.

118. Liu, L.; Sun, X.; Xie, Y.; Zhuang, Y.; Yao, R.; Xu, K. Anticancer effect of histone deacetylase inhibitor scriptaid as a single agent for hepatocellular carcinoma. *Bioscience Reports* **2018**, *38*, BSR20180360.

119. Tan, J.; Cang, S.; Ma, Y.; Petrillo, R. L.; Liu, D. Novel histone deacetylase inhibitors in clinical trials as anti-cancer agents. *J. Hematology & Oncol*. **2010**, *3*, 1-13.

120. Huang, M.; Zhang, J.; Yan, c.; Li, X.; Zhang, J.; Ling, R. Small molecule HDAC inhibitors: Promising agents for breast cancer treatment. *Bioinorg. Chem.* **2019**, 103184.

121. Schobert, R.; Biersack, B. Multimodal HDAC Inhibitors with Improved Anticancer Activity. *Current Cancer Drug Targets* **2018**, *18*, 39-56.

122. Yadav, R.; Mishra, P.; Yadav, D. Histone Deacetylase Inhibitors: A Prospect in Drug Discovery. *Turk. J. Pharm. Sci.* **2019**, *16*, 101-114.

123. Pan, L. N.; Lu, J.; Huang, B. HDAC inhibitors: a potential new category of anti-tumor agents. *Cell. Mol. Immunol*. **2007**, *4*, 337–343.

124. Smith, L. T.; Otterson, G. A.; Plass, C. Unraveling the epigenetic code of cancer for therapy. *Trends in Genetics*. **2007**, 449–456.

125. Kim, D. H.; Kim, M.; Kwon, H. J. Histone deacetylase in carcinogenesis and its inhibitors as anti-cancer agents. *J. Biochem. Mol. Biol*. **2003**, *36*, 110-115.

126. Marks, P. A.; Xu, W.-S. Histone deacetylase inhibitors: Potential in cancer therapy. *J Cell Biochem*. **2009**, *107*, 600–608.

127. Dokmanovic, M.; Marks, P. A. Prospects: Histone deacetylase inhibitors. *J. Cell. Biochem*. 2005, *96*, 293–304.

128. Marks, P. A.; Richon, V. M.; Breslow, R.; Rifkind, R. A. Histone deacetylase inhibitors as new cancer drugs. *Curr. Opin. Oncol*. **2001**, *13*, 477–483.

129. Falkenberg, K. J.; Johnstone, R. W. Histone deacetylases and their inhibitors in cancer, neurological diseases and immune disorders. *Nat. Rev. Drug Discov*. **2014**, *13*, 673–691.

130. Xu, W. S.; Parmigiani, R. B.; Marks, P. A. Histone deacetylase inhibitors: molecular mechanisms of action. *Oncogene* **2007**, *26*, 5541–5552.

131. Lane, A. A.; Chabner, B. A. Histone deacetylase inhibitors in cancer therapy. *J. Clin. Oncol*. **2009**, *27*, 5459–5468.

132. Rosato, R. R.; Grant, S. Histone deacetylase inhibitors: insights into mechanisms of lethality. *Expert Opin. Ther. Targets* **2005**, *9*, 809–824.

133. Bolden, J. E.; Peart, M. J.; Johnstone, R. W. Anticancer activities of histone deacetylase inhibitors. *Nat. Rev. Drug Discov*. **2006**, *5*, 769–784.

134. Ververis, K.; Hiong, A.; Karagiannis, T. C.; Licciardi, P. V. Histone deacetylase inhibitors (HDACIS): Multitargeted anticancer agents. *Biologics: Targets and Therapy*. **2013**, 47–60.

135. Liu, T.; Kuljaca, S.; Tee, A.; Marshall, G. M. Histone deacetylase inhibitors: Multifunctional anticancer agents. *Cancer Treatment Reviews*. **2006**, 157–165.

136. Walkinshaw, D. R.; Yang, X. J. Histone deacetylase inhibitors as novel anticancer therapeutics. *Curr. Oncol*. **2008**, *15*, 237–243.

137. Alvarez, A. A.; Field, M.; Bushnev, S.; Longo, M. S.; Sugaya, K. The Effects of Histone Deacetylase Inhibitors on Glioblastoma-Derived Stem Cells. *J. Mol. Neurosci*. **2014**, *55*, 7–20.

138. Kong, D.; Ahmad, A.; Bao, B.; Li, Y.; Banerjee, S.; Sarkar, F. H. Histone Deacetylase Inhibitors Induce Epithelial-to-Mesenchymal Transition in Prostate Cancer Cells. *PLoS One* **2012**, *7*, e45045.

139. Marks, P. A.; Richon, V. M.; Rifkind, R. A. Histone Deacetylase Inhibitors: Inducers of Differentiation or Apoptosis of Transformed Cells. *J. Natl. Cancer Inst*. **2000**, *92*, 1210-1216.

140. Ocker, M. Deacetylase inhibitors - focus on non-histone targets and effects. *World J. Biol. Chem*. **2010**, *1*, 55–61.

141. Bolden, J. E.; Shi, W.; Jankowski, K.; Kan, C.-Y.; Cluse, L.; Martin, B. P.; MacKenzie, K. L.; Smyth, G. K.; Johnstone, R. W. HDAC inhibitors induce tumor-cell-selective pro-apoptotic transcriptional responses. *Cell Death Dis*. **2013**, 4, e519.

142. Matthews, G. M.; Newbold, A.; Johnstone, R. W. Intrinsic and extrinsic apoptotic pathway signaling as determinants of histone deacetylase inhibitor antitumor activity. *Adv. Cancer Res.* **2012**, *116*, 165–197.

143. Stevens, F. E.; Beamish, H.; Warrener, R.; Gabrielli, B. Histone deacetylase inhibitors induce mitotic slippage. *Oncogene* **2008**, *27*, 1345–1354.

144. Gammoh, N.; Lam, D.; Puente, C.; Ganley, I.; Marks, P. A.; Jiang, X. Role of autophagy in histone deacetylase inhibitor-induced apoptotic and nonapoptotic cell death. *Proc. Natl. Acad. Sci*. *U. S. A*. **2012**, *109*, 6561–6565.

145. Zhang, J.; Ng, S.; Wang, J.; Zhou, J.; Tan, S. H.; Yang, N.; Lin, Q.; Xia, D.; Shen, H. M. Histone deacetylase inhibitors induce autophagy through FOXO1-dependent pathways. *Autophagy* **2015**, *11*, 629–642.

146. Ariffin, J. K.; das Gupta, K.; Kapetanovic, R.; Iyer, A.; Reid, R. C.; Fairlie, D. P.; Sweet, M. J. Histone Deacetylase Inhibitors Promote Mitochondrial Reactive Oxygen Species Production and Bacterial Clearance by Human Macrophages. *Antimicrob. Agents Chemother.* **2016**, *60*, 1521–1529.

147. Rosato, R. R.; Almenara, J. A.; Maggio, S. C.; Coe, S.; Atadja, P.; Dent, P.; Grant, S. Role of histone deacetylase inhibitor-induced reactive oxygen species and DNA damage in LAQ-824/fludarabine antileukemic interactions. *Mol. Cancer Ther*. **2008**, *7*, 3285–3297.

148. Ellis, L.; Hammers, H.; Pili, R. Targeting tumor angiogenesis with histone deacetylase inhibitors. *Cancer Letters*. **2009**, 145–153.

149. Weis, S. M.; Cheresh, D. A. Tumor angiogenesis: molecular pathways and therapeutic targets. *Nat. Med*. **2011**, *17*, 1359–1370.

150. Marchion, D.; Münster, P. Development of histone deacetylase inhibitors for cancer treatment. *Expert Rev. Anticancer Ther*. **2007**, *7*, 583–598.

151. Dokmanovic, M.; Clarke, C.; Marks, P. a. Histone deacetylase inhibitors: overview and perspectives. *Mol. Cancer Res*. **2007**, *5*, 981–989.

152. Hancock, W. W.; Akimova, T.; Beier, U. H.; Liu, Y.; Wang, L. HDAC inhibitor therapy in autoimmunity and transplantation. Annals of the Rheum. Diseases, 2012, *71*, i46–i54.

153. Hai, Y.; Christianson, D. W. Histone deacetylase 6 structure and molecular basis of catalysis and inhibition. *Nat. Chem. Biol*. **2016**, *12*, 741–747.

154. Finnin, M. S., Donigian, J. R., Cohen, A., Richon, V. M., Rifkind, R. A., Marks, P. A., Breslow, R. Pavletich, N. P., Structures of a histone deacetylase homologue bound to the TSA and SAHA inhibitors. *Nature* **1999**, *401*, 188-193.

155. Bose, P.; Dai, Y.; Grant, S. Histone deacetylase inhibitor (HDACI) mechanisms of action: emerging insights. *Pharmacol Ther*. **2014**, *143*, 323–336.

156. Bantscheff, M.; Hopf, C.; Savitski, M. M.; Dittmann, A.; Grandi, P.; Michon, A. M.; Schlegl, J.; Abraham, Y.; Becher, I.; Bergamini, G.; et al. Chemoproteomics profiling of

HDAC inhibitors reveals selective targeting of HDAC complexes. *Nat Biotechnol* **2011**, *29*, 255–265.

157. Bertrand, P. Inside HDAC with HDAC inhibitors. *Eur. J. Med. Chem*. **2010**, 2095–2116.

158. Khan, O.; La Thangue, N. B. HDAC inhibitors in cancer biology: emerging mechanisms and clinical applications. *Immunol. Cell Biol*. **2012**, *90*, 85–94.

159. Gryder, B. E.; Sodji, Q. H.; Oyelere, A. K. Targeted cancer therapy: giving histone deacetylase inhibitors all they need to succeed. *Future Med Chem*. **2012**, *4*, 505–524.

160. Benedetti, R.; Conte, M.; Altucci, L. Targeting Histone Deacetylases in Diseases: Where Are We? *Antioxid Redox Signal*. **2015**, *23*, 99-126.

161. Stockert, J. C. Horobin, R. W.; Colombo, L. L.; Blázquez-Castro, A. Tetrazolium salts and formazan products in Cell Biology: Viability assessment, fluorescence imaging, and labeling perspectives. *Acta Histochem*. **2018**, *120*, 159-167.

162. Zhang, B.; West, E. J.; Van, K. C.; Gurkoff, G. G.; Zhou, J.; Zhang, X-M.; Kozikowski, A. P.; Lyeth, B. G. HDAC inhibitor increases histone H3 acetylation and reduces microglia inflammatory response following traumatic brain injury in rats. *Brain Res*. **2008**, *1226*, 181–191.

163. Frick, K. M. Molecular mechanisms underlying the memory-enhancing effects of estradiol. *Horm Behav*. **2015**, *74*, 4–18.

164. Ulicki, J. S. "Part I: Synthesis and Biological Evaluations of Potent Class L Selective Histone Deacetylase Inhibitors Part II: Aqueous Complexes for Efficient Sizebased Separation of Americium from Curium Part III: Designing Strong Chiral Bronsted Acids and Their Application for Oxaxinanones Derivatization and the Aza-henry Reaction" (**2014**). *Theses and Dissertations.* Paper 771.

PART III: ACID CATALYZED REACTIONS OF AROMATIC KETONES WITH ETHYL DIAZOACETATE

3.1. INTRODUCTION

3.1.1. 3-Hydroxyacrylates:

3-Hydroxyacrylates and their related 3-oxo-esters are useful precursor to synthesize important biologically active compounds[1-5], drugs compounds[6-8], natural products[9,10], quaternary carbon center containing compounds[11-14], and common monomer in polymer[15-17] industry because of their multifunctional groups reactivity. In organic syntheses, these monomers can also be utilized in Michael additions with enolates, amines, and thiols and enantioselective Michael and Mannich type reaction with β-keto esters.[18-22] Due to the multifunctionality, presence of a prochiral center, and preferable substrate scope; 3-hydroxyacrylates have tremendous potential for further downstream synthesis of important biologically active compounds.[23, 24] Therefore, increasing efforts have been devoted to the development of efficient protocols for the synthesis of this valuable scaffold by using commercially available starting materials in shorter steps.[25,26]

3.1.2. Lewis Acid Catalyzed Reaction:

Roskamp and his co-worker reacted carbonyl compounds and ethyl diazoacetate (EDA) in presence of commercial Lewis acids such as BF_3, $ZnCl_2$, $ZnBr_2$, $AlCl_3$, $SnCl_2$, $GeCl_2$, and $SnCl_4$, and they reported β-keto esters only.[27] In 1998, our group reported an unprecedented formation of 3-hydroxyacrylates from the reactions of aromatic aldehydes with EDA in the presence of iron Lewis acid $[\eta^5\text{-}(C_5H_5)Fe^+(CO)_2(THF)]BF_4$ **1** as a catalyst by a unique 1,2-aryl shift (Scheme 3.1).[28]
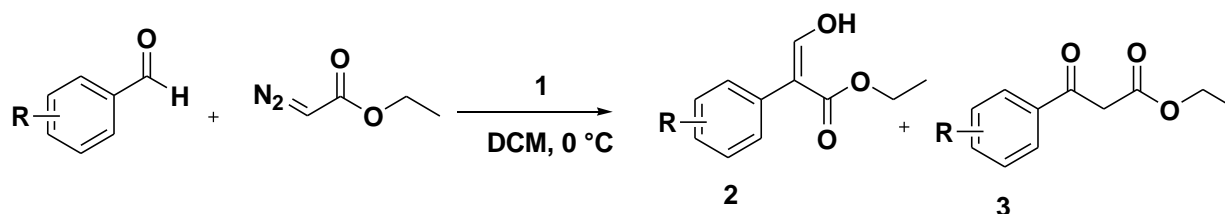
Scheme 3.1: Iron Lewis Acid Catalyzed Synthesis of 3-Hydroxyacrylates by Hossain et al.

In the presence of 10 mol% of iron Lewis acid, benzaldehyde was found to consume all the EDA to provide 58% of 3-hydroxyacrylate **2a** and 25% of *3*-oxo ester **3a** at room temperature. The mechanism of the reaction is shown in the following figure (Figure 3.1).
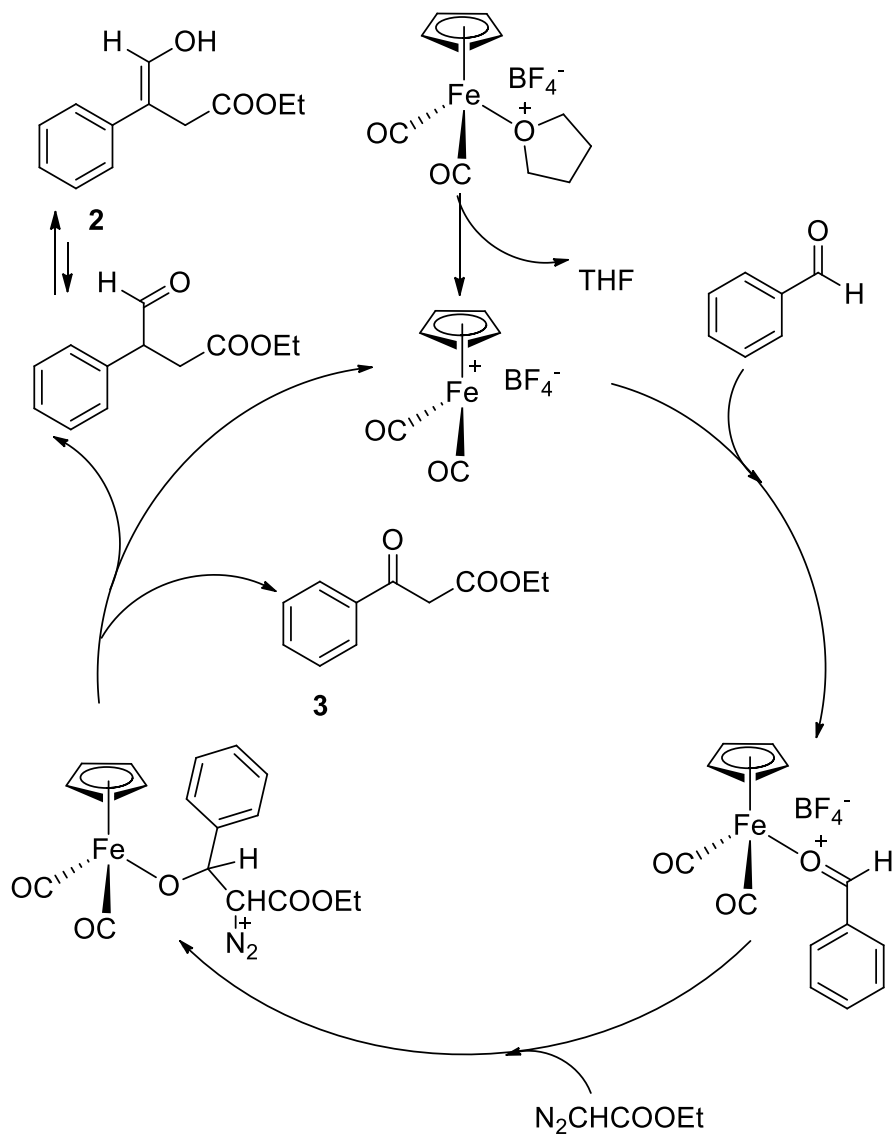
Figure 3.1: Mechanism of Formation of 3-Hydroxyacrylate Using Iron Lewis Acid

It was found that the yields of enol esters increased at lower temperatures than room temperature. For example, at 0 °C, the yield of the reaction of EDA and benzaldehyde increased to 70% yield of **2a** and 19% of **3a**. Surprisingly, when the reaction was run at lower temperature such as at -78 °C, the yield of 3-hydroxyacrylates remained the same. When EDA and aldehyde were treated without catalyst under the same reaction conditions, neither of the products was formed, and only starting materials were isolated from the reaction mixture. The effects of substituents on benzaldehyde upon formation of enol esters vs keto esters was determined by the reactions of other aromatic aldehydes were investigated. It was found that the yields of enol esters were observed to be dependent on the nature of the substituent on benzaldehyde. With electron- rich aldehydes, the only product isolated was 3-hydroxyacrylate; no formation of 3-oxo-ester was observed. However, in the presence of electron-withdrawing groups in the aldehyde the yield of 3-hydroxyacrylates were low. The reaction mechanism was not been fully investigated at that time.

Kanemasa et al. also described the similar results to ours by utilizing Lewis acid $ZnCl_2$ in the presence of chlorotrimethylsilane as catalyst (Scheme 3.2).[29] They also mentioned that the types of products depending upon the nature of Lewis acid catalysts employed. Reactions catalyzed by Lewis acids $SnCl_2$ and $SnCl_4$ yielded 3-oxo-ester via nucleophilic 1, 2-hydride migration.
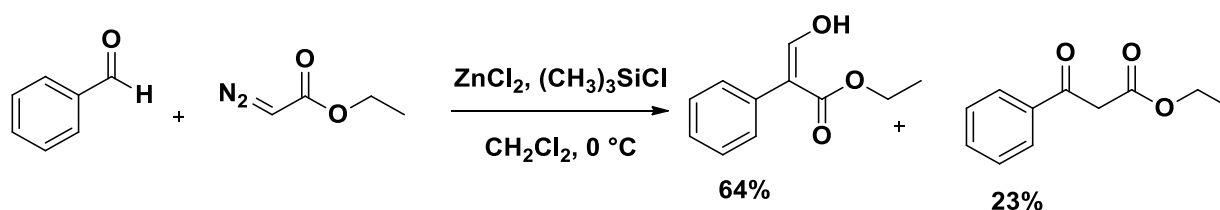
Scheme 3.2: Formation of 3-Hydroxyacrylate Using $ZnCl_2$ Lewis Acid

Kirchner and his coworkers reported iron(II) complexes bearing tridentate PNP (diphosphine–pyridine pincer ligand) type ligands, [Fe(PNP-Ph)(CH₃CN)₃](BF₄)₂, as catalysts for the selective formation of 3-hydroxyacrylates from aromatic aldehydes and EDA (Scheme 3.3).[30] They also

reported that the acrylate reaction is strongly dependent on the nature of the counterion, whereas with BF_4^- the reaction proceeds with conversions up to 90%, in the case of the counterions NO_3^-, CF_3COO^-, $CF_3SO_3^-$, SbF_6^-, and BAr'_4^- [Ar' = 3,5-$(CF_3)_2C_6H_3$] no reaction took place.[31]
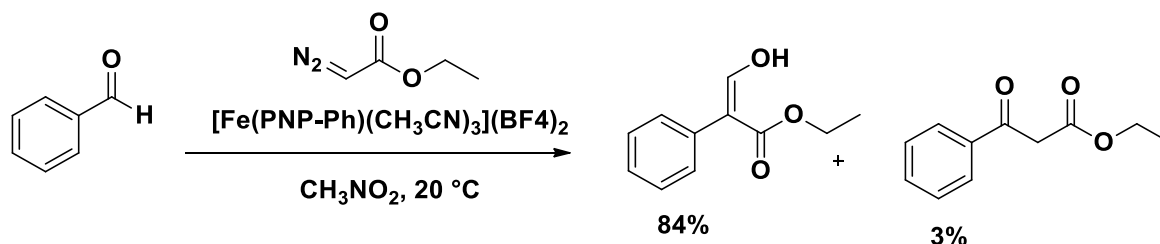
Scheme 3.3: Formation of 3-Hydroxyacrylate Using Fe-PNP Lewis Acid

Further work by Pe´rez and co-workers using gold-based catalysts of general formulae (NHC)AuCl (NHC = N-heterocyclic carbene ligand) for such transformations (Scheme 3.4).[32 -] They discovered the gold [IPrAu(NCMe)]BF$_4$ and used in aldehyde and EDA reaction as a catalyst and found that it worked really great for the production of 3-hydroxyacrylates.
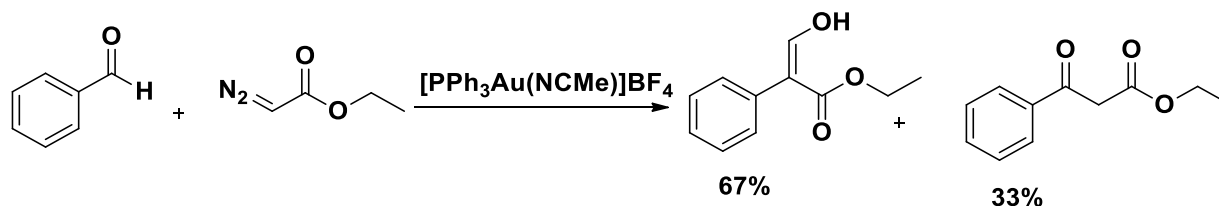
Scheme 3.4: Formation of 3-Hydroxyacrylate Using Gold Lewis Acid

Crowley et al. reported the click chemistry with azide type compounds where they used Au(SMe$_2$)Cl by immediately the treating of Ag(I) complex was resulting transmetallation provided the neutral 1,2,3-triazolylidene gold(I) chloride complex and used as a catalyst to synthesize acrylate. These gold(I) "click" carbene complexes used for the self-assembly of a metallomacrocycle and as precatalysts for gold(I)-catalysed reactions (Scheme 3.5).[33]
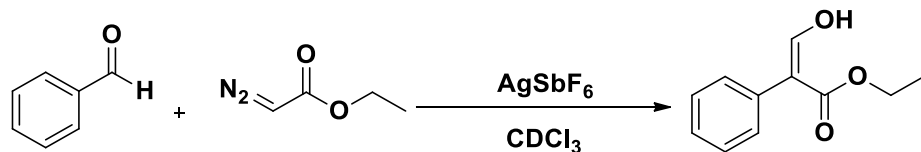
Scheme 3.5: Formation of 3-Hydroxyacrylate Using Ag-Lewis Acid

3.1.3. Brønsted Type Acid Catalyzed Reaction

It was found that formation of 3-hydroxyacrlates or related 3-oxo-esters were in presence of different types of Lewis acids catalysts, all the catalysts investigated gave a mixture of 3-hydroxyacrylate and 3-oxo-ester in different ratios. Some catalysts gave good overall yields in 3-hydroxyacrylates and others gave 3-oxo-esters in high yields. The most interesting results with respect to yield and ratio of products were those reactions catalyzed by $SnCl_2$, $HBF_4.OEt_2$, and $[\eta^5-(C_5H_5)Fe(CO)_2(THF)]BF_4$. For example, the main product observed from $SnCl_2$ and $SnCl_2.2H_2O$ is the 3-oxo-ester. In comparison, $[\eta^5-(C_5H_5)Fe(CO)_2(THF)]BF_4$ gave mainly 3-hydroxyacrylate.[4] Surprisingly, it was observed that $HBF_4.OEt_2$ also catalyzes the reaction between aromatic aldehydes and EDA to provide 3-hydroxyacrylates in good yields versus the corresponding 3-oxo-esters. The idea of using the $HBF_4.OEt_2$ acid as a catalyst came from the fact that $HBF_4.OEt_2$ is used in the synthesis of $[\eta^5-(C_5H_5)Fe(CO)_2(THF)]BF_4$.[4] Hossain and co-workers thought that acid impurities from $HBF_4.OEt_2$ could be a possible source of catalytic activity. To establish that $[\eta^5-(C_5H_5)Fe(CO)_2(THF)]BF_4$, and not $HBF_4.OEt_2$ impurities, was truly the catalyst in the reaction of aromatic aldehydes with EDA, the reaction was performed in the presence of proton sponge, 1,8-bis(dimethylamino)naphthalene. The activity of $[\eta^5-(C_5H_5)Fe(CO)_2(THF)]BF_4$ was not inhibited by the addition of proton sponge. Proton sponge experiment showed that with $HBF_4.OEt_2$, the reaction was almost completely inhibited by the addition of proton sponge and only the aldehyde starting material was recovered. From the inspiration of the proton sponge

127

experiment, in 1998, our group also explored the reactions with the Brønsted type, specifically HBF$_4$.OEt$_2$, to produce 3-hydroxyacrylates and 3-oxo-esters from the same starting materials (Scheme 3.6).[34]
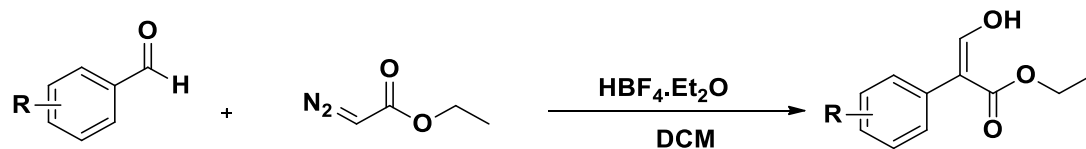
Scheme 3.6: Synthesis of 3-Hydroxyacrylates by Hossain et al.in 2004

It had been reported that substituents on the aromatic aldehyde play an important role in product distribution when reactions are catalyzed by iron Lewis acid, [η^5-(C$_5$H$_5$)Fe(CO)$_2$(THF)]BF$_4$ catalyst. Electron-donating groups favor the formation of 3-hydroxyacrylates, whereas electron-withdrawing groups favor the 3-oxo-ester. To prove the statement, several reactions were performed by using iron Lewis acid as well as Brønsted type acid, and all reactions were carried out at room temperature under the same conditions for comparison. Analysis of aromatic ketones such as acetophenone and trifluoroacetophenone showed that only acetophenone reacted with HBF$_4$.OEt$_2$, while no reaction was observed in the presence of iron Lewis acid, whereas trifluoroacetophenone was unreactive regardless of the catalyst used. From the inspiration of Brønsted type acid, HBF$_4$.OEt$_2$, it was investigated with other Brønsted type acids with varying acid strengths. It was found that yield was dependent on the following order: BF$_4^-$ > HSO$_4^-$ > NO$_3^-$ > ClO$_4^-$ > Cl$^-$ and CH$_3$COO$^-$. Those Brønsted acids with nonnucleophilic anions gave the best results, for example, sulfuric acid and HBF$_4$.OEt$_2$. In each case where a metal-halogen type catalyst (SnCl$_2$, AlCl$_3$) was utilized in the reaction, significantly produced more 3-oxo-esters than 3-hydroxyacrylate. Kanemasa and coworkers suggested that chelation transition state orients the migrating hydride (from the aldehyde) and leaving nitrogen (from EDA) anti to one another, and

this transition state reduces the steric interactions and facilitates 3-oxo-ester formation. The catalysts, other than those of the metal-halogen type, Brønsted type acid, $HBF_4.OEt_2$, bind to the aldehyde first and then the nucleophilic methine carbanion of EDA can attack either the *re-* or *si-* face of the aldehyde. In this situation, six Newman projections have been drawn and explained by Hossain and coworkers[34] (Figure 3.2).
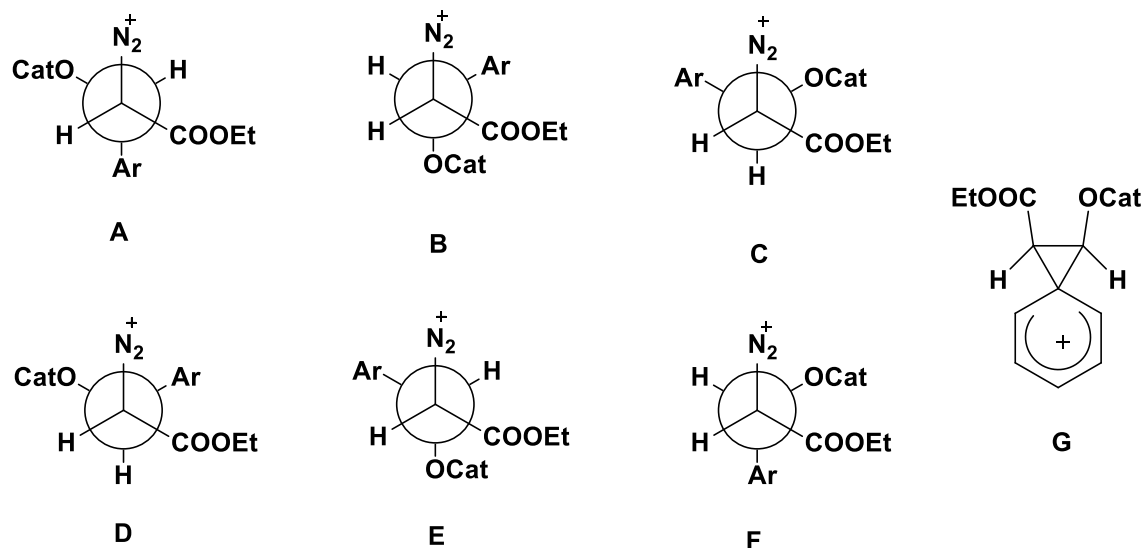
Figure 3.2: Stable and Unstable Rotamers of Benzaldehyde and EDA Reaction

Among all rotamers (Figure 3.2), 'A' and 'F' two rotamers have leaving group and aryl migrating are antiperiplanar but rotamer 'A' has less energy than 'F' because of less bulky group interaction, so product of 3-hydroxyacrylates were formed more from the rotamer 'A'. For 3-oxoesters, in rotamer 'C' and 'D', leaving group and hydride migrating group were antiperiplanar, but this rotamer 'C' has little higher energy by the comparison with rotamer 'D', for this reason oxo-ester yielded from rotamer 'D'. Actually, 3-hydroacrylates were more than 3-oxoesters because between rotamers 'A' and 'D', transition state of aryl migration from rotamer 'A' (Figure 3.2 "G") makes a lower energy stable state, so more acrylates products were formed than oxo-esters.

3.1.4. Base Catalysed Reaction

Wang et al. reported DBU-catalyzed condensation of ethyl diazoacetate (EDA) with aldehydes in pure water afforded corresponding β-hydroxy α-diazo carbonyl compounds, the β-hydroxy group was further converted into β-siloxy group and gave 1,2-aryl shift products predominantly by Rh(II)-catalyzed reaction (Scheme 3.7).[35]
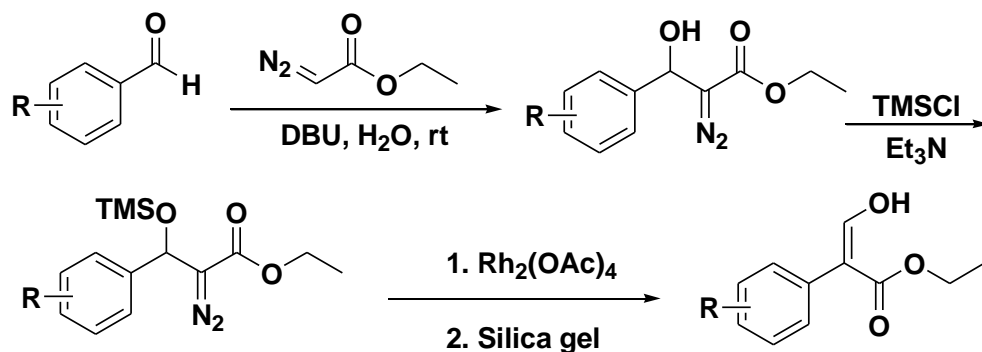
Scheme 3.7: Synthesis of 3-Hydroxyacrylates by Wang et al.

3.2. Application of 3-hydroxyacrylates

In 1998, Schmittel and his coworker reported a short and efficient preparation of 3,8-dialkylated or 3,8-diarylated 1,10-phenanthrolines-4,7-diones (Scheme 3.8). They used hydroxy acrylate as a one of the important starting materials. 1,10-Phenanthrolines have been used as important ligands for a vast amount of metal complexes.[36]
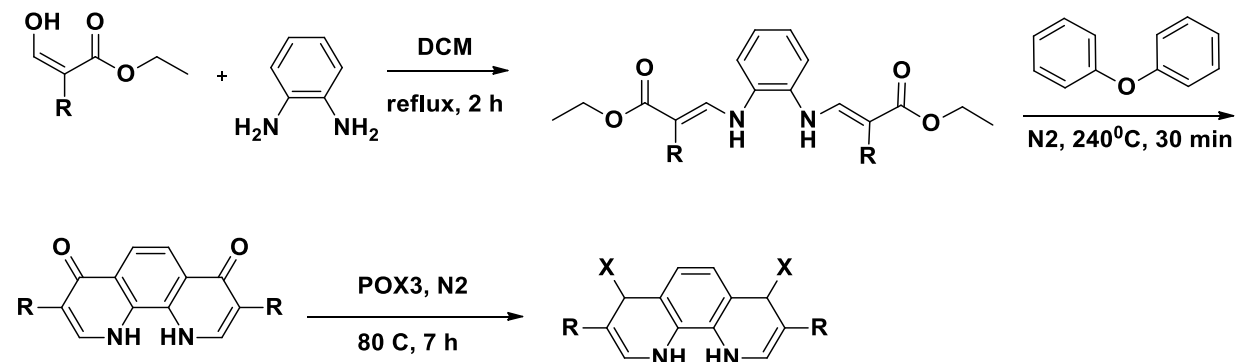
Scheme 3.8: Synthesis of Phenanthrolines from 3-Hydroxyacrylates

Naproxen, 2-(6-methoxy-2-naphthyl)propenoic acid was synthesized in good yield from commercially available 6-methoxy-2-naphthaldehyde in three steps. The synthesis includes an unprecedented one-step reduction of acrylic acid ethyl ester to propenoic acid ethyl ester in high yield (Scheme 3.9).[7] α-arylpropanoic acids is of great commercial interest as they are widely used as non-steroidal anti-inflammatory agents.
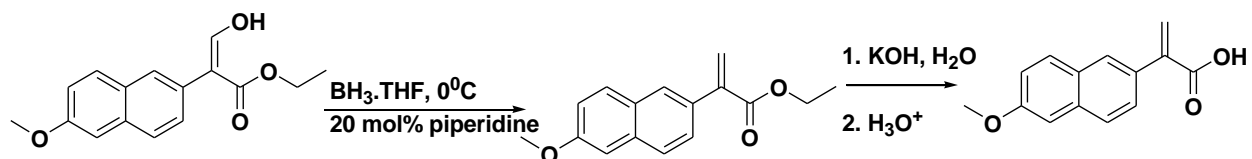
Scheme 3.9: Synthesis of Naproxen from 3-Hydroxyacrylates

Hossain et al. reported the first kinetic resolution of tropic acid ethyl ester (TAEE) with lipase PS and vinyl acetate as an acylating agent (Scheme 11).[1,2] The resulting (S)-(_)-3-acetoxy tropic acid ethyl ester and (R)-(+)-tropic acid ethyl ester is produced in high yields and in excellent ee (87–94%). The method has been extended to resolve a variety of tropic acid ester derivatives. In addition, an improved method for the preparation of racemic mixtures of tropic acid ethyl ester and its derivatives from 3-hydroxy-2-phenylacrylic acid ethyl ester using NaBH4 in methanol is reported. This procedure is better than the previous ones because it is cleaner, safer and can be worked up easily. An improved method of deacylating the chiral 3-acetoxy tropic acid ethyl ester without any loss of stereochemical integrity using HCl/CH₃OH is also reported. (S)-(-)-Tropic acid is an important building block for bio-logically active tropane alkaloids, such as hyoscyamine and scopolamine. The dynamic kinetic resolution of racemic mixtures of tropic acid ethyl ester under substrate racemizing conditions was studied using lipase PS with a ruthenium catalyst by Hossain et al. (Scheme 3.10).
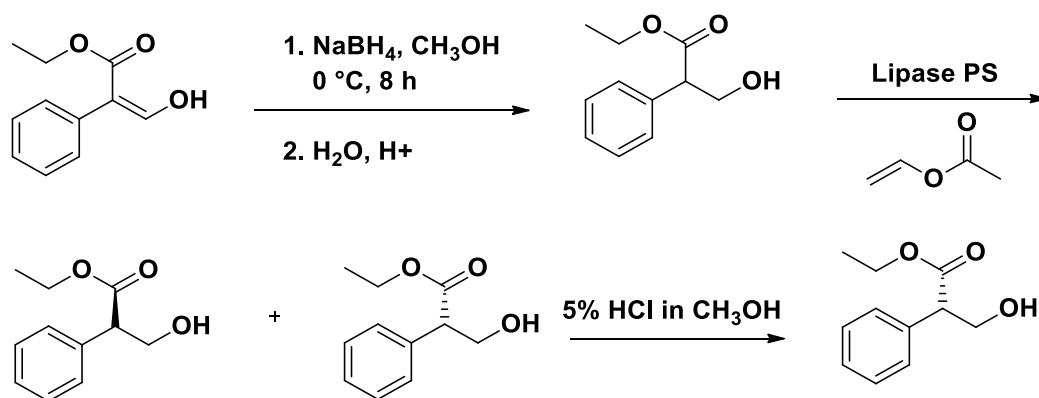
Scheme 3.10: Kinetic Resolution of Tropic Acid Ethyl Ester (TAEE)

Hossain group developed a convenient one-pot procedure for the synthesis of 3-ethoxycarbonylbenzofurans from commercially available salicylaldehydes and ethyl diazoacetate (Scheme 3.11).[24] The method is high-yielding, efficient, simple and selective. Benzofuran is a very pivotal precursor for the synthesis of many pharmaceutical and biologically active compounds.
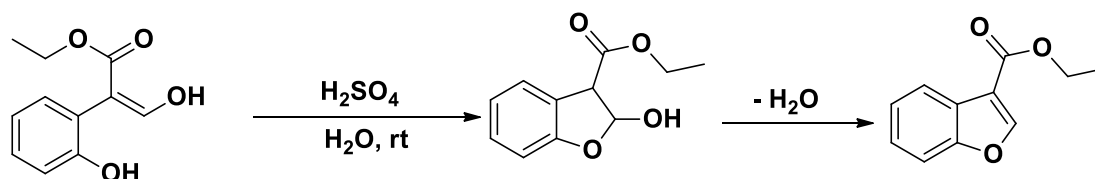
Scheme 3.11: Synthesis of 3-Ethoxycarbonylindole

A convenient one-step synthesis of 5-aryl uracils has been developed. The procedure involves heating ethyl 3-hydroxy-2-arylpropenate with urea followed by base-catalyzed cyclization. The method is simple and high yielding (Scheme 3.12).[6]
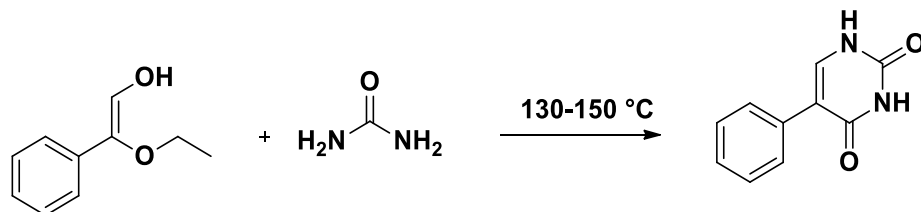
Scheme 3.12: Synthesis of 5-Aryl Uracils from 3-Hydroxyacrylate

A large number of biologically active compounds consist of an indole scaffolding. Because of this, chemists are continually searching for more efficient means through which to successfully synthesize the required alkaloids (Scheme 3.13).[23]
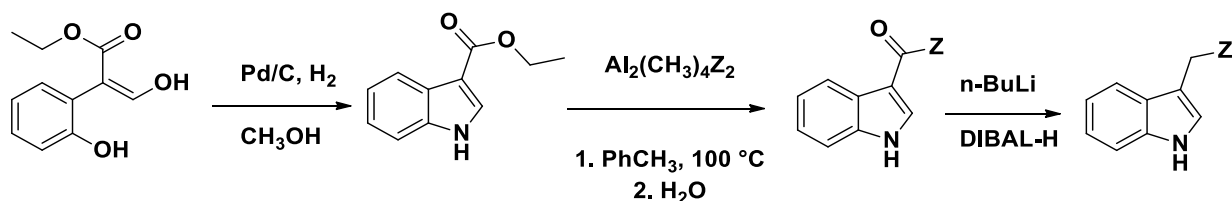
Scheme 3.13: Synthesis of Gramine from 3-Hydroxyacrylate

The formation of α-aryl quaternary carbon centers, pre-sent in a growing number of biologically active natural products and pharmaceutical agents, poses a unique challenge due to the steric congestion encountered during the C–C bond formation process. Generally, a quaternary aryl carbon center is formed using strongly basic lithium arenes. In 2010, Hossain at el. described a Claisen rearrangement process for generating α-aryl quaternary car-bon centers from 3-allyloxy-2-arylacrylates, made from arylhydroxyacrylates (Scheme 3.14). Although Claisen rearrangements have been used previously for making quaternary carbon centers.[11]
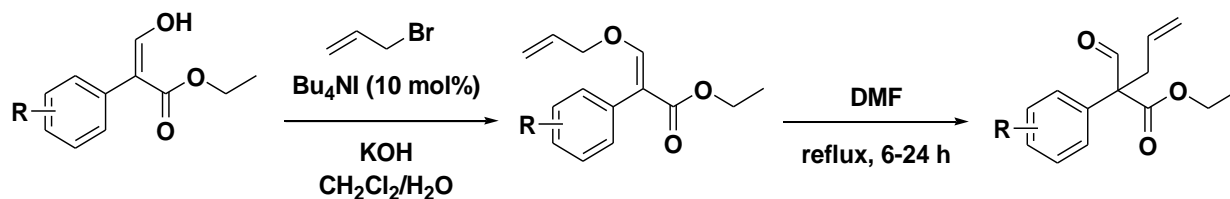
Scheme 3.14: Synthesis of α-Aryl Quaternary Carbon Centers

Later, Hossain and coworkers described a set of acyclic all-carbon α-aryl quaternary aldehydes by intermolecular palladium-catalyzed asymmetric allylic alkylation (Pd-AAA) in 2014 (Scheme 3.15). Hydroxyacrylates were used as unprecedented nucleophilic counterparts instead of widely used ketone substrates. This produced a very rare all- carbon quaternary aldehyde. Chiral ligand

(R,R)-L3 was found to be optimal in this Pd-AAA reaction and pro-vided good to excellent yields (75–99%) and enantioselectivities (75–94%) with a range of analogs.[12]
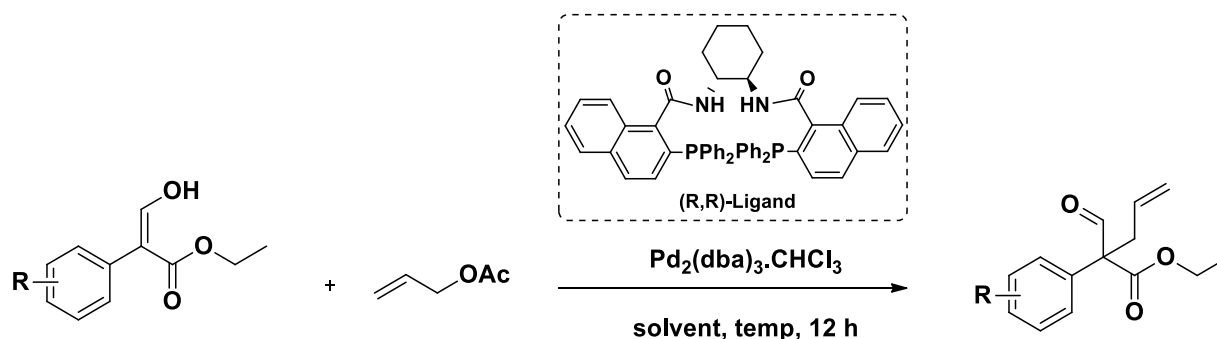
Scheme 3.15: Synthesis of Asymmetric α-Aryl Quaternary Carbon Centers by AAA Reaction

In 2015, Hossain at el. Reported a stereoselective synthesis of carbonates derived from 3-hydroxy-2-aryl acrylates that can form the *Z*- or *E*-stereoisomer in very high *Z/E* ratios (50:1 and 1:99, respectively) (Scheme 3.16). The stereochemical outcome depends on the choice of base, addition of TMEDA and reaction temperature. The *Z*- and *E*-stereoisomers have different reactivities towards the decarboxylative asymmetric allylic alkylation (DAAA) reaction, with the E-stereoisomer displaying both greater reactivity and enantiodifferentiation with chiral ligands. The DAAA of E-stereoisomer analogues takes place in excellent yields ranging from 96–99% and enantioselectivities ranging from 42–78% ee.[13]
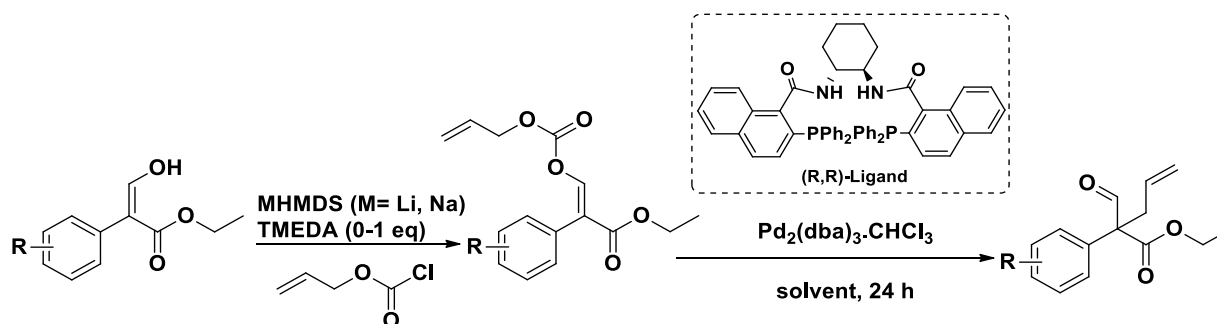
Scheme 3.16: Synthesis of Asymmetric α-Aryl quaternary Carbon Centers by DAAA Reaction

Later, in 2018, Hossain and coworkers reported the first palladium(0)-catalyzed asymmetric allylic alkylation (AAA) of allyl enol ether via p-allylpalladium intermediate using Trost chiral diphosphine (Scheme 3.17).[17] This unprecedented reaction produced very rare a-aryl quaternary aldehydes with multi-functional groups. The main novelty in the chemistry demonstrates that enol ethers can be used as precursors for p-allylpalladium intermediates, an observation that is certainly rare and to the best of our knowledge, perhaps without prior precedent. Chiral ligand (R, R)-L3 was found to be optimal in this Pd-AAA reaction and provided good to excellent yield (80–95%) and enantioselectivity (70–90%) with a range of analogs.[14]
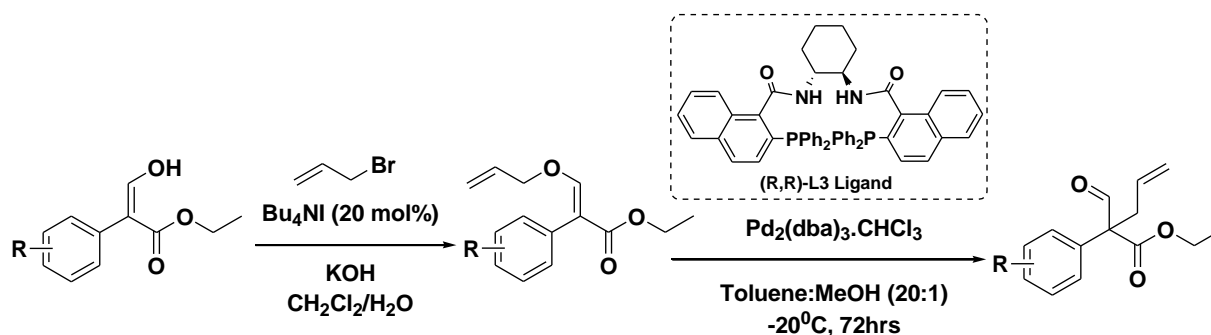
Scheme 3.17: Synthesis of Asymmetric Quaternary Carbon Centers from *O*-Allylated Enol-Ether

Hossain and coworkers developed a concise method of synthesizing racemic arylpropanoic acids, which have been widely used as nonsteroidal anti-inflammatory drugs (NSAIDs) (Scheme 3.18). The synthesis involves only four steps from commercially available benzaldehyde. The synthesis incorporates an unprecedented reduction reaction, conversion of 3-hydroxy-2-arylpropenoic acid ethyl ester to 2-arylpropenoic acid ethyl ester by $BH_3 \cdot THF$. The reduction reaction has been investigated and optimized.[3]
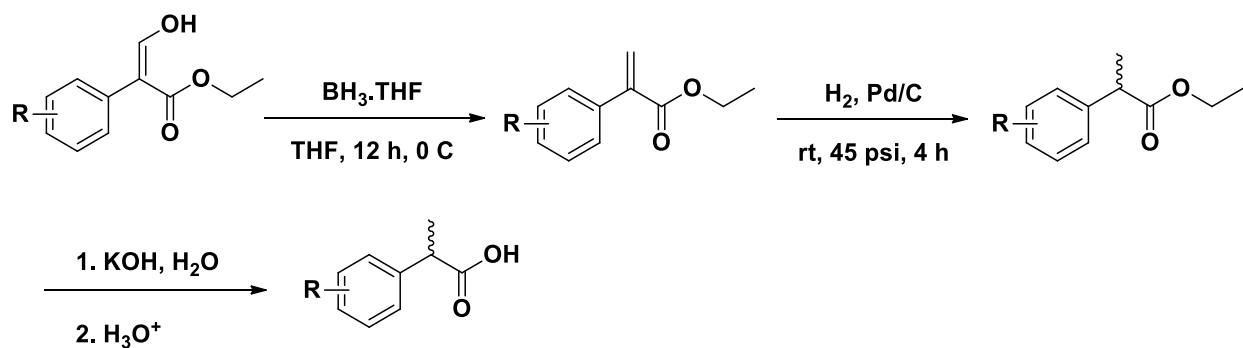
Scheme 3.18: Synthesis of Arylpropanoic Acids

Telvekar and coworkers synthesized N'-benzylidene ben-zofuran-3-carbohydrazides from 3-ethoxycarbonyl benzo-furans (Scheme 3.19).[20] All these compounds were found to be active against tuberculosis and showed antifungal activity against Candida albicans.[37]
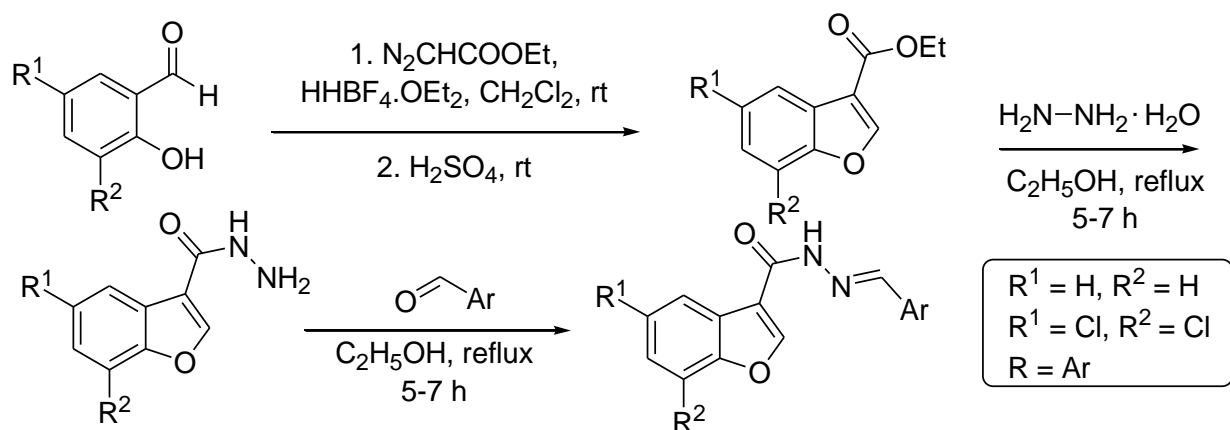
Scheme 3.19: Synthesis of N'-Benzylidene Benzofuran-3-Carbohydrazide

Eccles and coworkers synthesized several leukotriene A4 hydrolase (LTA4H) inhibitors from 3-ethoxycarbonyl benzofuran (Scheme 3.20).[21] LTA4H inhibitors are used in inflammatory diseases, such as bowel disease, rheumatoid arthritis, chronic obstructive pulmonary disease, and asthma.[38]
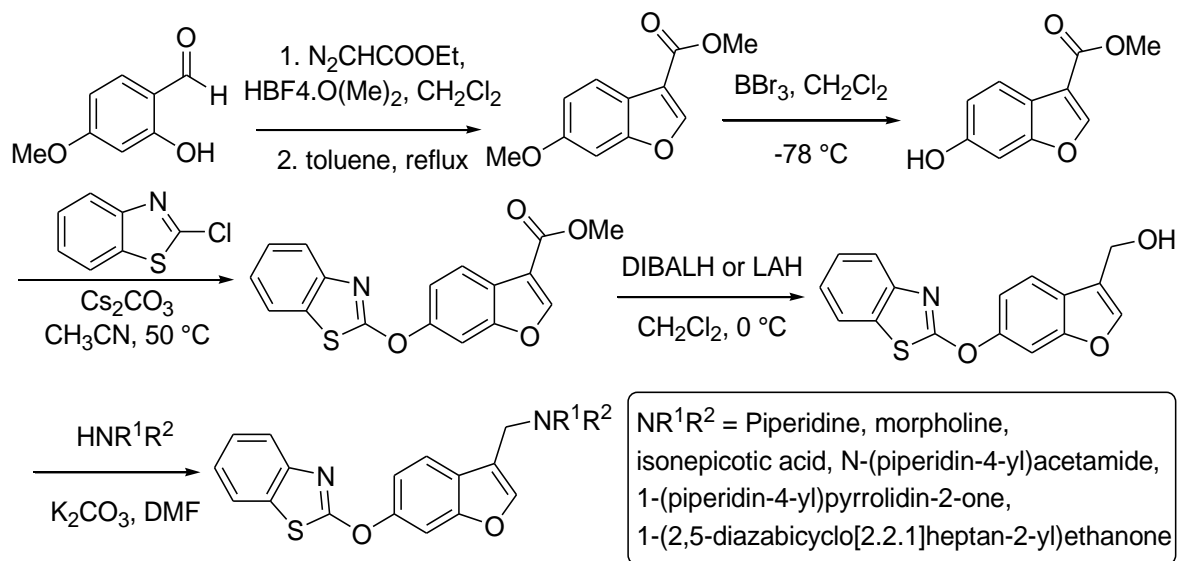
Scheme 3.20: Synthesis of Leukotriene A4 Hydrolase (LTA4H) Inhibitor

Morrow et al. synthesized pterocarpenes and coumestans type heterocycles by the Mitsunobu coupling of 3-hydroxymethylbenzofurans with *ortho*-iodophenols (Scheme 3.21). Pterocarpans group have been shown to exhibit broad spectrum activity against Gram-positive bacteria and vancomycin-resistant strains of enterococci. Coumestans such as coumestrol and flemmichapparin C have also been shown to display antibacterial, antifungal, and antimyotoxic effects.[39]
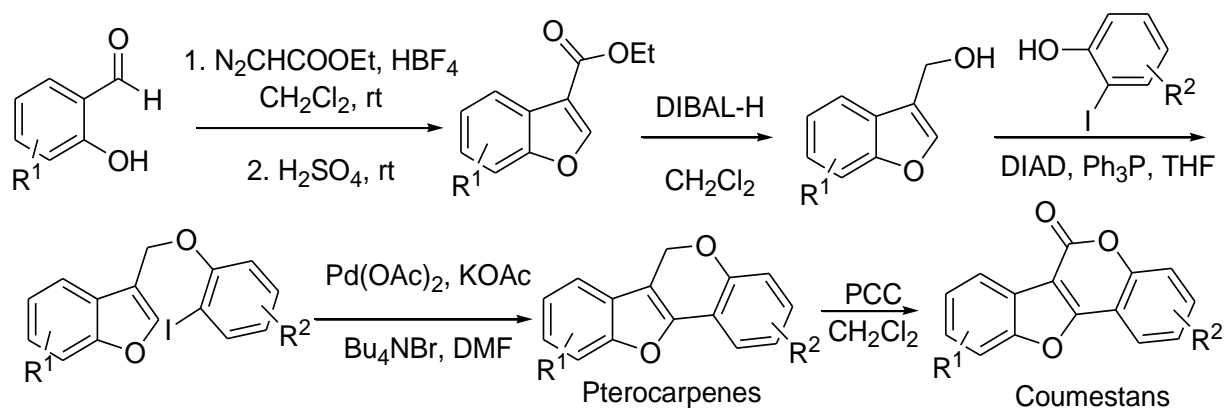
Scheme 3.21: Synthesis of Pterocarpenes and Coumestans

Tolstikov et al. reported several regioselective Diels–Alder reactions of Danishefsky's diene with 3-ethoxycarbonyl benzofurans (Scheme 3.22).[40] These reactions provided effective method for the construction of heterocyclic skeleton of hexahydrodibenzofuran-7-one and tetrahydrodibenzofuran-7-one. These tricyclic fragments are the structural motifs of many pharmacologically vital substances, such as plant alkaloids morphine, galanthamine, lycoramine, and lunarine, linderol A, and several selective estrogen receptor β agonists.
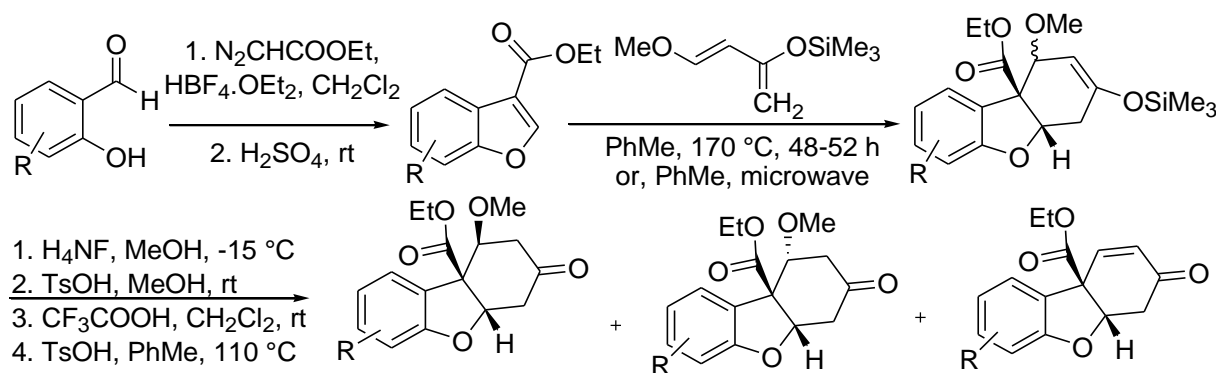
Scheme 3.22: Diels–Alder Reactions of 3-Ethoxycarbonyl Benzofuran

Elofssan and coworkers constructed a library based on 3-carboxy 2-aryl benzofuran scaffold from the 3-ethoxycarbonyl benzofuran (Scheme 3.23).[41] These two scaffolds are core components in many biologically active natural and synthetic compounds of which many display a wide range of activities including antiviral, antibacterial, anti-inflammatory, antiangiogenic, and antimitotic activities.
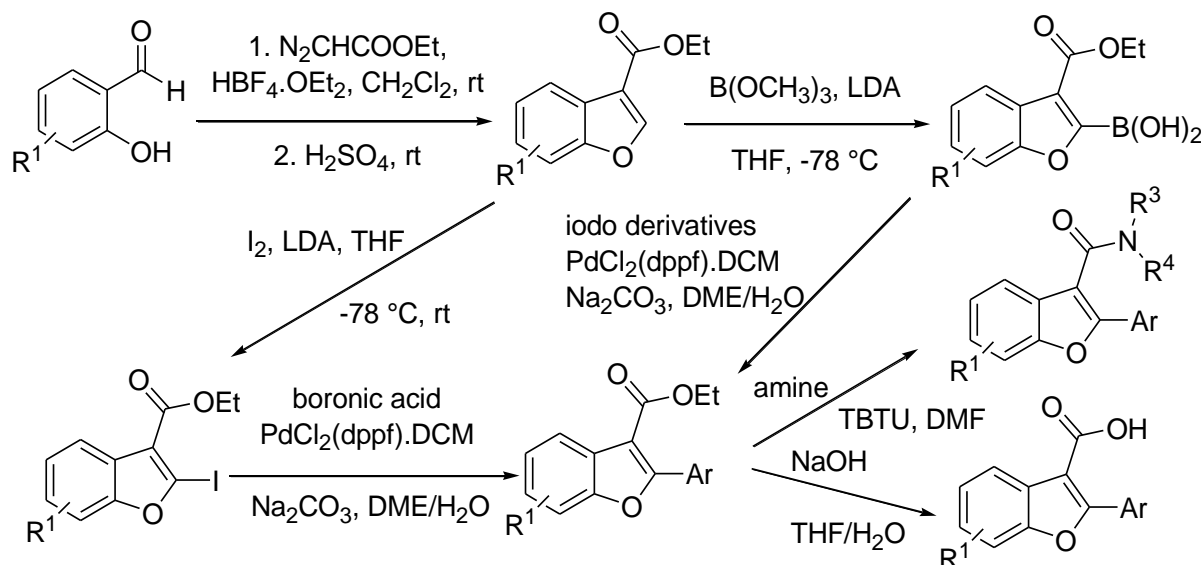
Scheme 3.23: Synthesis of 2-Arylbenzofuran-3-Carboxamide Derivatives

Zhao et al. reported a total synthesis of paeoveitol, the norditerpene natural product which has antidepressant ability, from 3-ethoxycarbonyl benzofuran (Scheme 3.24).[42] Our published procedure was employed to synthesize 3-ethoxycarbonyl benzofuran, which was reduced to Paeoveitol D. Paeoveitol was synthesize by an unusual intermolecular ortho-quinone methide cycloaddition with Paeoveitol D with excellent regio- and diastereoselectivity of the product.
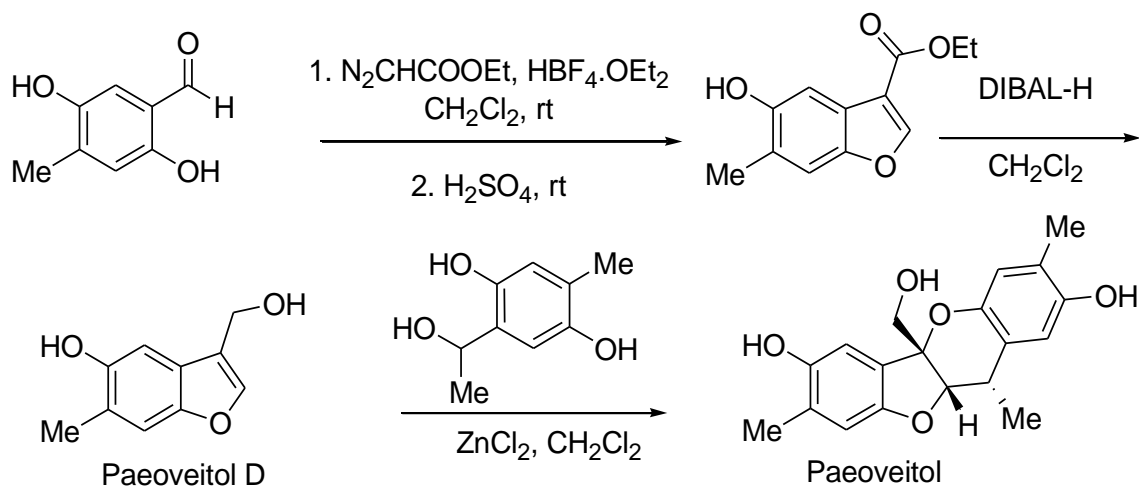
Scheme 3.24: Total Synthesis of Paeoveitol via Paeoveitol D

Chen and coworkers reported the first catalytic asymmetric total synthesis of (+)-paeoveitol and (-)-paeoveitol from 3-ethoxycarbonyl benzofuran via a biomimetic hetero-Diels-Alder reaction in the presence of chiral phosphoric acids as catalysts (Scheme 3.25).[43]
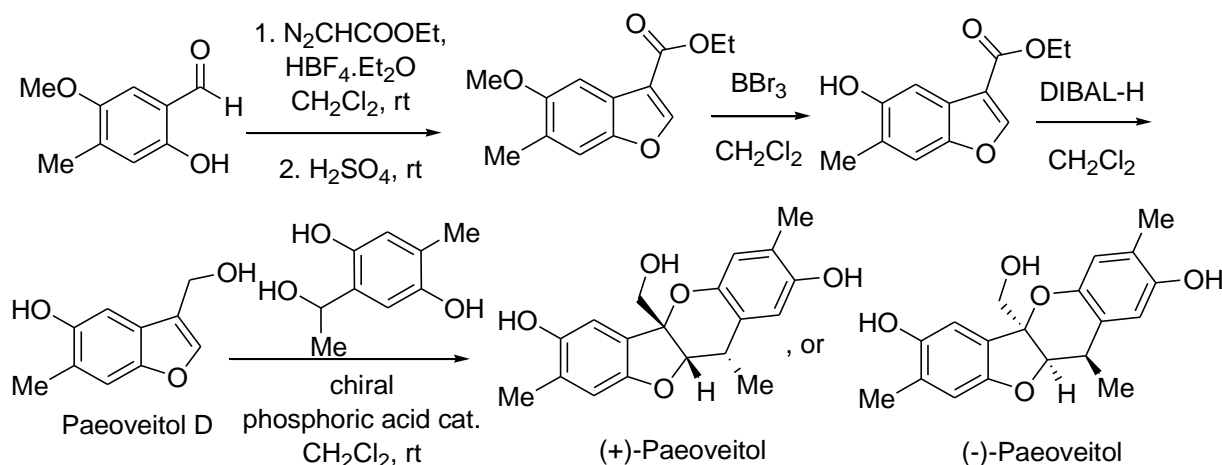
Scheme 3.25: Asymmetric Synthesis of (+)-Paeoveitol and (-)-Paeoveitol

Bongen et al. reported an efficient asymmetric synthesis of 7-benzoyl-2,3-dihydro-1-benzofuran-3-carboxylic acid, BRL-37959 (Scheme 3.26).[44] 3-Ethoxycarbonyl benzofuran was reduced by magnesium turnings to form 2,3-dihydrobenzofuran-3-carboxylic acid ethyl ester and resolved by dynamic kinetic resolution. Friedel-Crafts acylation of the enantiopure product followed by acidic hydrolysis produced (R)-BRL-37959 which acts as analgesic agents with low gas irritancy.
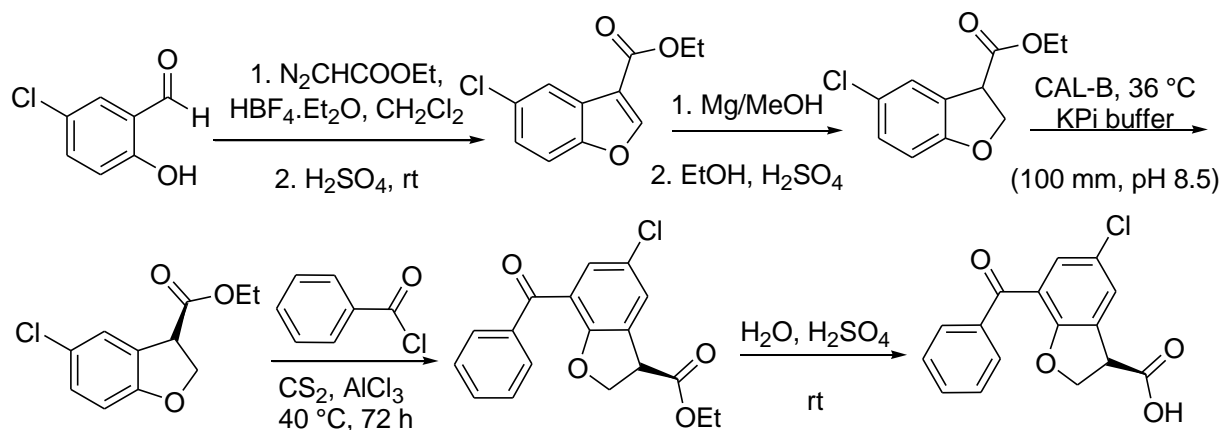
Scheme 3.26: Synthesis of Enantiopure (R)-BRL-37959

Recently, in 2018, our group reported the synthesis of 7-benzoyl-2,3-dihydro-1-benzofuran-3-carboxylic acid, BRL-37959 and its analogs from 3-ethoxycarbonyl benzofuran (Scheme 3.27).[45] To synthesize BRL-37959, incorporation of benzoyl group at the C-6 position of benzofuran ring by the Friedel-Crafts acylation reaction was main challenge. Our recent method demonstrates that bismuth (III) trifluoromethanesulfonate can be used as a catalyst for the Friedel-Crafts acylation reaction with good yield. It is reported in the synthetic procedure, 3-ethoxycarbonyl benzofuran was synthesized by our previous established method and reduced by a Mg/MeOH mixture followed by using as a catalyst to produce 7-benzoyl-2,3-dihydro-1-benzofuran-3-carboxylate. Basic hydrolysis of this carboxylate was converted to carboxylic acid and formed the desired product of BRL-37959. This efficient method allowed us for the production in high yields as well as the production of many possible analogs of BRL-37959.
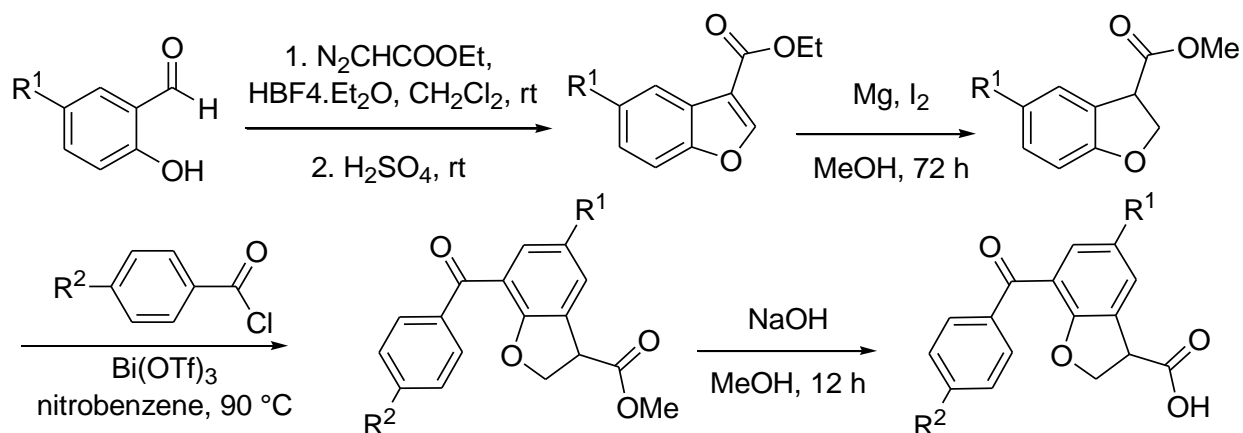
Scheme 3.27: Synthesis of BRL-37959 and Its Analogs

All the important medicinal syntheses of acrylates are discussed in our recent published discussion addendum.[46]

3.3. Present Synthesis of 3-Hydroxyacrylates

In our previous work, we studied the reaction of acetophenone with EDA, which yielded exclusively 3-hydroxyacrylate product (Scheme 3.28).[13] To expand the scope of this reaction, phenyl-alkyl ketones were employed as substrates in this transformation, and the results are summarized in Table 3.1.
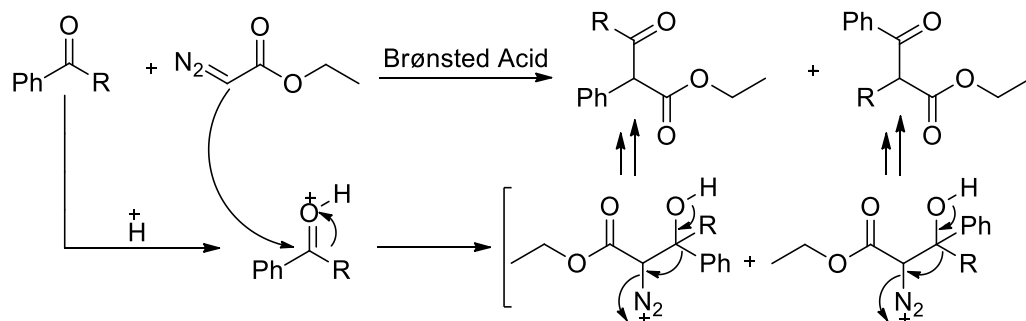
Scheme 3.28: Synthesis of 3-Hydroxyacrylates from Ketones

From the perceptive nature of phenyl and methyl groups of acetophenone, the reactions were extended to other aromatic ketones beyond acetophenone to examine the substrate scope for aromatic ketones with different alkyl groups. The results of these reactions are summarized in Table 3.1. When propiophenone was employed as a substrate for this transformation, the desired phenyl group migrated product, 3-hydroxyacrylate 3b along with ethyl group migrated product, 3-oxo-ester 3b' was obtained in 62% yield. The oxo-ester 3b' was isolated, and the structure was characterized by NMR and confirmed by comparison with the authentic compounds. This migratory tendency of different phenyl and alkyl groups from isolated yield of our synthetic products in this cate-gory were almost similar, (3-hydroxyacrylates/oxo-esters > 1.2:1) (3b-f). However, when the reaction was carried out with octanophenone as a substrate, the corresponding product 3g was obtained in lower yield (37% yield) with lower alkyl-migrated product.

Table 3.1. Migratory Aptitude of Alkyl-Phenyl Groups

3a, 64%   3b/3b' = 1.2:1, 62%   3c/3c' = 1.4:1, 60%   3d/3d' = 1.7:1, 45%

3e/3e' = 1.7:1, 55%   3f/3f' = 1.8:1, 48%   3g/3g' = 2:1, 37%
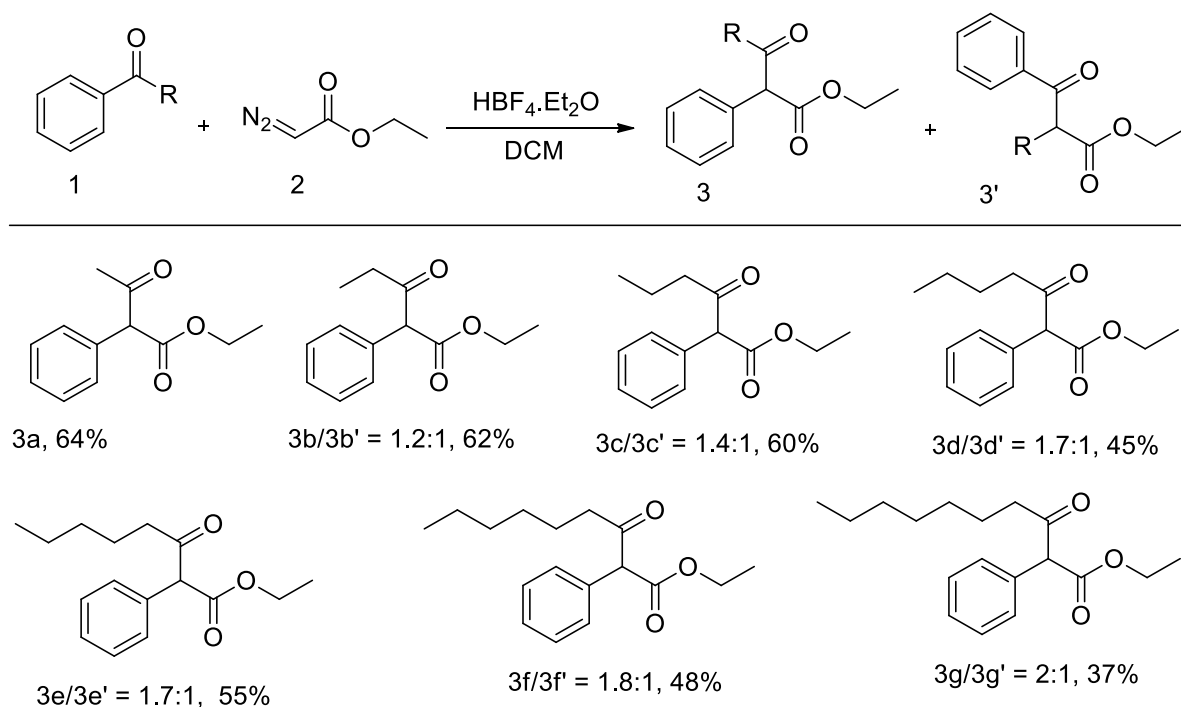
where, R = CH_3, C_2H_5, C_3H_7, C_4H_9, C_5H_{11}, C_6H_{13}, and C_7H_{15}.

To understand longer chain effects of phenyl-alkyl ketones, we next examined the substrate scope for aromatic ketones with different alkyl groups with EDA employed as the reaction partner. The results of these reactions are summarized in Table 3.1. From these reactions we found two types of products from two different migrations. From general studies on the relative migration aptitude, the following order has been found: tertiary alkyl > cyclo-hexyl > secondary alkyl > benzyl > phenyl > primary alkyl > cyclo-pentyl, cyclopropyl > methyl.

3.4. Conclusion and Future Works

Aldehydes and ethyl diazoacetate produced 3-hydroxy acrylates in presence of Lewis or Brønsted acid catalyst. Less reactive aromatic/aliphatic ketones and aldehydes also yielded the 3-hydroxy acrylates and 3-oxo-esters. A bunch of 3-hydroxy acrylates and related 3-oxo-esters are synthesized from different kinds carbonyl substrates. A large number of biological active compounds as well as quaternary carbon center containing compounds could be synthesized by using these two kinds of products (Figure 3.3).
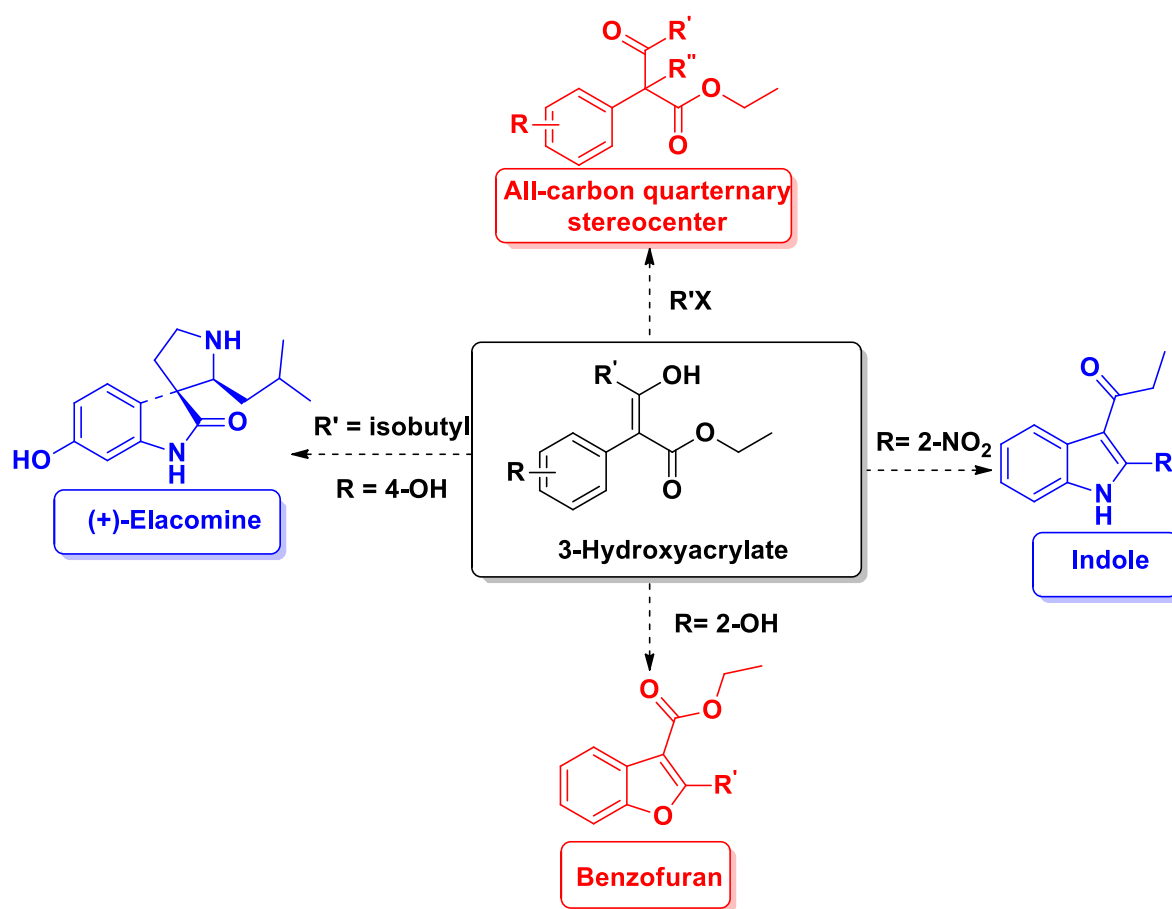
Figure 3.3: Probable Natural Products and Biological Active Compounds

3.5. General Consideration

All reactions were performed under a dry nitrogen atmosphere using standard Schlenk techniques unless otherwise noted. All reaction vessels were flame dried under vacuum and filled with nitrogen prior to use. Reagents and solvents were purchased from Sigma-Aldrich, Milwaukee. All ^1H and ^{13}C NMR spectra were recorded in $CDCl_3$ (internal standard: 7.26 ppm, ^1H; 77.16 ppm, ^{13}C) at room temperature with a Burker 300 MHz and 500 MHz spectrometers. The chemical shifts (δ) are given in parts per million (ppm) and the coupling constants in Hertz (Hz). All new compounds were additionally characterized by ^1H NMR, ^{13}C NMR and high-resolution mass spectrometry (HRMS). HRMS were obtained using electrospray ionization (ESI) technique. For column chromatography, silica gel (35-70 microns) was used. Thin layer chromatography (TLC) was performed on aluminum backed plates pre-coated (0.25 mm) with Silica Gel 60 F254 with a suitable solvent system and was visualized using UV fluorescence and/or iodine chamber.

3.5.1. General Procedure and Experimental

For each experiment, 1.5-5.0 mmol of the carbonyl compounds was dissolved in 15-25 mL of freshly distilled dichloromethane under nitrogen. A Brønsted acid, $HBF_4 \cdot OEt_2$ catalyst (0.1-0.2 equiv) of was added, and the reaction mixture was stirred for 1 hour. Ethyl diazoacetate (EDA) (1.2-2.0 equiv) was diluted in 5 mL of freshly distilled dichloromethane and added to the aldehyde over a period of 6-7 h. The reaction mixture was allowed to stir for an additional 36 h, and each reaction was quenched by adding THF. The reaction mixture was filtered through a silica plug and the solvent removed by rotary evaporation. Crude products were isolated by silica column chromatography with 0-10% ethyl acetate in hexane.
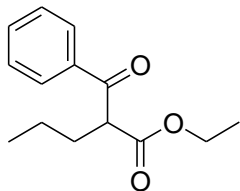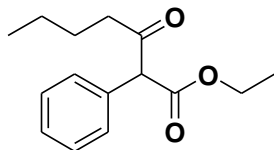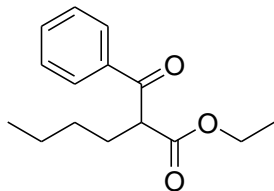
Ethyl 3-oxo-2-phenylbutanoate (keto-enol tautomer) as a colorless liquid (3a)
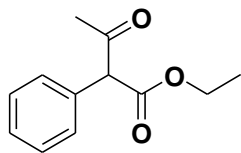
The title compound was prepared according to the general procedure and purified by silica gel column chromatography (hexane/ethyl acetate = 100:1) to afford **3a** as a colorless oil with 60% yield. Compound **3a** was confirmed by comparing to known NMR.

^{1}H NMR (CDCl$_3$, 300 MHz): δ 13.15 (s, 1H), 7.40-7.29 (m, 8H), 7.19-7.16 (m, 2H), 4.71 (s, 1H), 4.26-4.16 (m, 4H), 2.21 (s, 3H), 1.87 (s, 3H), 1.30 (t, J = 7.5 Hz, 3H), 1.21 (t, J = 7.5 Hz, 3H). **^{13}C NMR (CDCl$_3$, 125 MHz):** δ 201.6, 173.9, 172.6, 168.5, 135.3, 132.7, 131.2, 129.3, 128.9, 128.3, 128.0, 126.9, 104.4, 65.8, 61.6, 60.6, 28.8, 19.9, 14.2, 14.1. **HRMS (ESI+):** Calculated (m/z) for C$_{12}$H$_{15}$O$_3$ (M+H)$^+$: 207.1016, Found 207.0987.

Ethyl 3-oxo-2-phenylpentanoate (keto-enol tautomer) as a colorless liquid (3b)
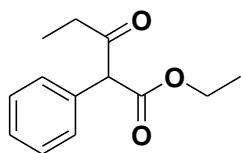
The title compound was prepared according to the general procedure and purified by silica gel column chromatography (hexane/ethyl acetate = 100:1) to afford **3b and 3b'** as a colorless oil with 62% yield.

^{1}H NMR (CDCl$_3$, 300 MHz): δ 13.23 (s, 1H), 7.37-28 (m, 8H), 7.18 (t, J = 4.5 Hz, 2H), 4.76 (s, 1H), 4.26-4.14 (m, 4H), 2.53 (q, J = 6.0 Hz, 2H), 2.15 (q, J = 6.0 Hz, 2H), 1.28 (t, J = 7.5 Hz, 3H), 1.18 (t, J = 7.5 Hz, 3H), 1.12-1.01 (m, 6H). **^{13}C NMR (CDCl$_3$, 75 MHz):** δ 204.2, 178.1, 172.8, 168.7, 135.2, 133.0, 131.2, 129.4, 128.8, 128.1, 128.0, 126.9, 103.6, 64.8, 61.5, 60.5, 34.9, 26.3, 14.2, 14.0, 11.1, 7.8. **HRMS (ESI+):** Calculated (m/z) for C$_{13}$H$_{17}$O$_3$ (M+H)$^+$: 221.1172, Found 221.1164.
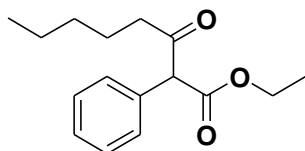
Ethyl 2-benzoylbutanoate (β-keto ester) as a colorless liquid (3b')
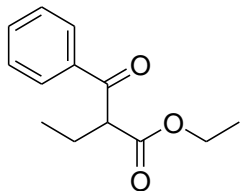
The compound was prepared according to the general procedure and purified by silica gel column chromatography (hexane/ethyl acetate = 100:1) to afford **3b and 3b'** as a colorless oil with 62% yield. Compound **5a'** was confirmed by comparing to known NMR.

¹H NMR (CDCl₃, 300 MHz): δ 7.98 (d, *J* = 9.0 Hz, 2H), 7.55 (t, *J* = 6.0 Hz, 1H), 7.48 (t, *J* = 6.0 Hz, 2H), 4.21 (t, *J* = 6.0 Hz, 1H), 4.12 (q, *J* = 9.0 Hz, 2H), 2.07-1.98 (m, 2H), 1.14 (t, *J* = 6.0 Hz, 3H), 0.98 (t, *J* = 7.5 Hz, 3H). **¹³C NMR (CDCl₃, 75 MHz):** δ 195.2, 169.9, 136.4, 133.4, 128.7, 128.5, 61.2, 55.8, 22.4, 14.0, 12.1.
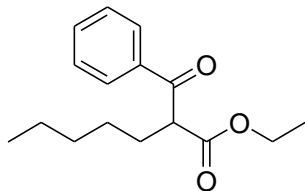
Ethyl 3-oxo-2-phenylhexanoate (keto-enol tautomer) as a colorless liquid (3c)
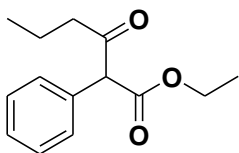
The compound was prepared according to the general procedure and purified by silica gel column chromatography (hexane/ethyl acetate = 100:1) to afford **3c and 3c'** as a colorless oil with 60% yield.

¹H NMR (CDCl₃, 300 MHz): δ 13.20 (s, 1H), 7.40-7.30 (m, 8H), 7.18 (d, *J* = 5.0 Hz, 2H), 4.74 (s, 1H), 4.27-4.17 (m, 4H), 2.48 (t, *J* = 7.5 Hz, 2H), 2.11 (t, *J* = 8.0 Hz, 2H), 1.63-1.55 (m, 4H), 1.29 (t, *J* = 6.0 HZ, 3H), 1.19 (t, *J* = 6.0 Hz, 3H), 0.89-0.83 (m, 6H). **¹³C NMR (CDCl₃, 75 MHz):** δ 203.7, 176.9, 172.9, 168.6, 135.2, 132.8, 131.4, 129.5, 128.8, 128.2, 128.0, 126.9, 104.3, 65.0, 61.6, 60.6, 43.5, 34.7, 20.1, 17.1, 14.2, 14.1, 13.8, 13.4. HRMS (ESI+): Calculated (m/z) for C₁₄H₁₉O₃ (M+H)⁺ : 235.1329, Found 235.1312.
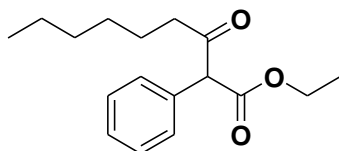
Ethyl 2-benzoylpentanoate (β-keto ester) as a colorless liquid (3c')

The compound was prepared according to the general procedure and purified by silica gel column chromatography (hexane/ethyl acetate = 100:1) to afford **3c and 3c'** as a colorless oil with 60% yield. Compound **3c'** was confirmed by comparing to known NMR.

¹H NMR (CDCl₃, 300 MHz): δ 7.98 (t, J = 4.5 Hz, 2H), 7.55 (t, J = 7.5 Hz, 1H), 7.48 (t, J = 7.5 Hz, 2H), 4.31 (t, J = 7.5 Hz, 1H), 4.15 (q, J = 6.0 Hz, 2H), 2.04-1.95 (m, 2H), 1.43-1.33 (m, 2H), 1.17 (t, J = 7.5 Hz, 3H), 0.95 (t, J = 7.5 Hz, 3H).
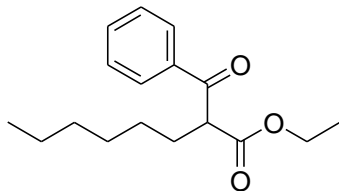
Ethyl 3-oxo-2-phenylheptanoate (keto-enol tautomer) as a colorless liquid (3d)

The compound was prepared according to the general procedure and purified by silica gel column chromatography (hexane/ethyl acetate = 100:1) to afford **3d and 3d'** as a colorless oil with 45% yield.

¹H NMR (CDCl₃, 300 MHz): δ 13.20 (s, 0.4H), 8.15 (d, J = 5.0 Hz, 1H), 7.51 (t, J = 5.0 Hz, 1H), 7.51-7.35 (m, 7H), 7.17 (d, t, J = 5.0 Hz, 1H), 4.73 (s, 1.3H), 4.30-4.16 (m, 4H), 2.49 (t, J = 7.5 Hz, 2H), 2.12 (t, J = 7.5 Hz, 2H), 1.56-1.53 (m, 4H), 1.30-1.24 (m, 7H), 1.22 (t, J = 4.5 Hz, 3H), 0.93-0.80 (m, 6H). ¹³C NMR (CDCl₃, 75 MHz): δ 203.6, 176.8, 172.8, 168.5, 135.1, 132.7, 131.3, 129.4, 128.8, 128.1, 127.9, 126.8, 104.2, 65.0, 61.5, 60.5, 43.4, 34.6, 20.0, 17.0, 14.2, 14.0, 13.7, 13.4. **HRMS (ESI+):** Calculated (m/z) for C₁₅H₂₁O₃ (M+H)⁺ : 249.1485; Found 249.1458.
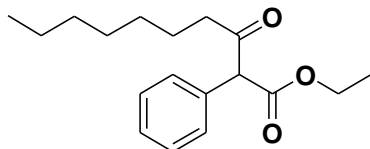
Ethyl 2-benzoylhexanoate (β-keto ester) as a colorless liquid (3d')

The compound was prepared according to the general procedure and purified by silica gel column chromatography (hexane/ethyl acetate = 100:1) to afford **3e and 3e'** as a colorless oil with 45% yield. Compound **3e'** was confirmed by comparing to known NMR.

^{1}H NMR (CDCl$_3$, 300 MHz): δ 8.01 (d, J = 9.0 Hz, 2H), 7.55 (d, J = 6.0 Hz, 1H), 7.48 (t, J = 7.5 Hz, 2H), 4.30 (t, J = 7.5 Hz, 1H), 4.12 (q, J = 15.9, 9.0 Hz, 2H), 2.03 (q, J = 12.0, 6.0 Hz, 2H), 1.36-1.28 (m, 4H), 1.19 (t, J = 7.5 Hz, 3H), 0.92 (t, J = 7.5 Hz, 3H). **^{13}C NMR (CDCl$_3$, 75 MHz):** δ 195.3, 170.1, 136.4, 133.4, 128.7, 128.6, 61.3, 54.4, 29.8, 28.7, 22.5, 14.0, 13.8.
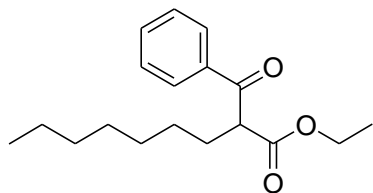
Ethyl 3-oxo-2-phenyloctanoate (keto-enol tautomer) as a colorless liquid (3e)

The compound was prepared according to the general procedure and purified by silica gel column chromatography (hexane/ethyl acetate = 100:1) to afford **3e and 3e'** as a colorless oil with 55% yield.

^{1}H NMR (CDCl$_3$, 300 MHz): δ 13.26 (s, 1H), 7.41-28 (m, 8H), 7.19 (t, J = 6.0 Hz,2H), 4.77 (s, 1H), 4.26-4.14 (m, 4H), 2.51 (t, J = 7.5 Hz, 2H), 2.14 (t, J = 7.5 Hz, 2H), 1.63-1.54 (m, 4H), 1.43-1.32 (m, 14H), 0.89-0.83 (m, 6H). **^{13}C NMR (CDCl$_3$, 75 MHz):** δ 203.6, 177.2, 172.8, 168.5, 135.2, 132.9, 131.3, 129.5, 128.7, 127.9, 126.9, 104.1, 65.0, 61.4, 60.5, 41.5, 32.7, 31.3, 31.1, 26.4, 23.3, 22.3, 22.3, 22.2, 14.1, 14.0. **HRMS (ESI+):** Calculated (m/z) for C$_{16}$H$_{23}$O$_3$ (M+H)$^{+}$: 263.1642; Found 263.1642.

Ethyl 2-benzoylheptanoate (β-keto ester) as a colorless liquid (3e')

The compound was prepared according to the general procedure and purified by silica gel column chromatography (hexane/ethyl acetate = 100:1) to afford **3e and 3e'** as a colorless oil with 55% yield.

^{1}H NMR (CDCl$_3$, 300 MHz): δ 8.01 (d, J = 9.0 Hz, 2H), 7.59 (t, J = 7.5 Hz, 1H), 7.46 (t, J = 7.5 Hz, 2H), 4.30 (t, J = 7.5 Hz, 1H), 4.16 (q, J = 7.5 Hz, 2H), 2.05-1.98 (m, 2H), 1.39-1.27 (m, 6H), 1.18 (t, J = 7.5 Hz, 3H). 0.88 (t, J = 7.5 Hz, 3H). **^{13}C NMR (CDCl$_3$, 75 MHz):** δ 195.3, 170.1, 136.4, 133.4, 128.7, 128.7, 128.6, 128.5, 61.3, 54.4, 31.6, 28.9, 27.3, 22.4, 13.9. **HRMS (ESI+):** Calculated (m/z) for C$_{16}$H$_{23}$O$_3$ (M+H)$^+$: 263.1642; Found 263.1649.

Ethyl 3-oxo-2-phenylnonanoate (keto-enol tautomer) as a colorless liquid (3f)

The compound was prepared according to the general procedure and purified by silica gel column chromatography (hexane/ethyl acetate = 100:1) to afford **3f and 3f'** as a colorless oil with 48% yield.

^{1}H NMR (CDCl$_3$, 300 MHz): δ 13.20 (s, 1H), 7.39-7.29 (m, 9H), 7.18-7.15 (m, 1H), 4.74 (s, 1H), 4.26-4.17 (m, 4H), 2.50 (t, J = 7.5 Hz, 3H), 2.12 (t, J = 7.5 Hz, 2H), 1.58-1.54 (m, 4H), 1.31-1.18 (m, 18H), 0.89-0.84 (m, 6H). **^{13}C NMR (CDCl$_3$, 75 MHz):** δ 203.7, 177.2, 172.9, 168.6, 135.2, 132.8, 131.3, 129.6, 129.4, 129.0, 128.8, 128.1, 128.0, 126.9, 104.1, 65.0, 61.5, 60.5, 41.9, 32.7, 31.5, 28.8, 28.5, 26.6, 23.6, 22.4, 14.2, 14.1, 14.0. **HRMS (ESI+):** Calculated (m/z) for C$_{17}$H$_{25}$O$_3$ (M+H)$^+$: 277.1798; Found 277.1783.

Ethyl 2-benzoyloctanoate (β-keto ester) as a colorless liquid (3f')

The compound was prepared according to the general procedure and purified by silica gel column chromatography (hexane/ethyl acetate = 100:1) to afford **3f and 3f'** as a colorless oil with 48% yield.

^{1}H NMR (CDCl$_3$, 300 MHz): δ 8.01 (d, J = 9.0 Hz, 2H), 7.60 (t, J = 6.0 Hz, 1H), 7.49 (t, J = 7.5 Hz, 2H), 4.30 (t, J = 7.5 Hz, 1H), 4.16 (q, J = 7.5 Hz, 2H), 2.03 (d, J = 3.0 Hz, 2H), 1.36-1.27 (m, 8H), 1.19 (t, J = 6.0 Hz, 3H), 0.88 (t, J = 6.0 Hz, 3H). **^{13}C NMR (CDCl$_3$, 75 MHz):** δ 195.3, 170.1, 136.4, 133.4, 128.7, 128.6, 61.3, 54.4, 31.5, 29.7, 29.1, 29.0, 27.6, 22.5, 14.0. **HRMS (ESI+):** Calculated (m/z) for C$_{17}$H$_{25}$O$_3$ (M+H)$^+$: 277.1798; Found 277.1860.

Ethyl 3-oxo-2-phenyldecanoate (keto-enol tautomer) as a colorless (3g)

The compound was prepared according to the general procedure and purified by silica gel column chromatography (hexane/ethyl acetate = 100:1) to afford **3g and 3g'** as a colorless oil with 37% yield.

^{1}H NMR (CDCl$_3$, 300 MHz): δ 13.18 (s, 1H), 7.37-28 (m, 8H), 7.16 (d, J = 6.0 Hz, 2H), 4.73 (s, 1H), 4.27-4.15 (m, 4H), 2.49 (t, J = 7.5 Hz, 2H), 2.11 (t, J = 7.5 Hz, 2H), 1.62-1.55 (m, 4H), 1.31-1.17 (m, 22H), 0.89-0.85 (m, 6H). **^{13}C NMR (CDCl$_3$, 75 MHz):** δ 203.8, 177.2, 172.9, 168.6, 135.2, 132.8, 131.3, 129.4, 128.8, 128.1, 127.9, 126.9, 104.1, 65.0, 61.5, 60.6, 41.6, 32.7, 31.6, 29.1, 28.9, 28.8, 26.7, 23.6, 22.6, 22.6, 14.2. **HRMS (ESI+):** Calculated (m/z) for C$_{18}$H$_{27}$O$_3$ (M+H)+ : 291.1955, Found 291.1945.

Ethyl 2-benzoylnonanoate (β-keto ester) as a colorless liquid (3g')

The compound was prepared according to the general procedure and purified by silica gel column chromatography (hexane/ethyl acetate = 100:1) to afford **3g and 3g'** as a colorless oil with 37% yield.

^{1}H NMR (CDCl$_3$, 300 MHz): δ 8.01 (d, J = 9.0 Hz, 2H), 7.59 (t, J = 7.5 Hz, 1H), 7.49 (t, J = 7.5 Hz, 2H), 4.29 (t, J = 7.5 Hz, 1H), 4.15 (q, J = 7.5 Hz, 2H), 2.03-1.98 (m, 2H), 1.34-1.27 (m, 10H), 1.18 (t, J = 7.5 Hz, 3H). 0.88 (t, J = 6.0 Hz, 3H). **^{13}C NMR (CDCl$_3$, 75 MHz):** δ 195.3, 170.1, 136.4, 133.4, 128.7, 128.5, 61.3, 54.4, 31.7, 29.4, 29.0, 29.0, 27.6, 22.6, 14.0, 14.0. **HRMS (ESI+):** Calculated (m/z) for C$_{18}$H$_{27}$O$_3$ (M+H)+ : 291.1955, Found 291.1988.

3.6. References

1. Atuu, M. R.; Mahmood, S. J.; Laib, F.; Hossain, M. M. Kinetic resolution of tropic acid ethyl ester and its derivatives by lipase PS. *Tetrahedron: Asymmetry* **2004**, *15*, 3091–3101.

2. Atuu, M. R.; Hossain, M. M. Dynamic kinetic resolution of racemic tropic acid ethyl ester and its derivatives. *Tetrahedron Lett*. **2007**, *48*, 3875–3878.

3. Islam, M. S.; Ahmad, S.; Atuu, M. S.; Foerstering, F. H.; Hossain, M. M. Concise Synthesis of 2-Arylpropanoic Acids and Study of Unprecedented Reduction of 3-Hydroxy-2-arylpropenoic Acid Ethyl Ester to 2-Arylpropenoic Acid Ethyl Ester by $BH_3 \cdot THF$. *Helv. Chim. Acta*. **2015**, *98*, 1273–1286.

4. Croisy, M.; Huel, C.; Bisagni, E. Synthesis of 3-(4-Methoxyphenyl)-5, 7-Dimethoxy(1H)-Quinolin-2- or 4-ones and Derivatives. *Heterocycles* **1997**, *45*, 683–690.

5. Kamaya, H.; Sato, M.; Kaneko, C. An Efficient Method for α-Monofluorination of Carbonyl Compounds with Molecular Fluorine: Use of α-Hydroxymethylene Substituent as Directing and Activating Groups. *Tetrahedron Lett*. **1997**, *38*, 587–590.

6. Morshed, M. M.; Wang, Q.; Islam, S.; Hossain, M. M. Convenient Synthesis of 5-Aryl Uracils. *Synth. Commun*. **2007**, *37*, 4173–4181.

7. Mahmood, S. J.; Brennan, C.; Hossain, M. M. A Convenient New Synthesis of a Naproxen Precursor. *Synthesis* **2002**, *13*, 1807-1809.

8. Sechi, M.; Sannia, L.; Carta, F.; Palomba, M.; Dallocchio, R.; Dessì, A.; Derudas, M.; Zawahir, Z.; Neamati, N. Design of novel bioisosteres of β-diketo acid inhibitors of HIV-1 integrase. *Antivir. Chem. Chemother*. **2005**, *16*, 41–61.

9. Lange, G. L.; Organ, M. G. Use of Cyclic β-Keto Ester Derivatives in Photoadditions. Synthesis of (±)-Norasteriscanolide. *J. Org. Chem*. **1996**, *61*, 5358–5361.

10. Sum, F. W.; Weiler, L. Synthesis of Isoprenoid Natural Products from β-keto Esters. *Tetrahedron* **1981**, *37*, 303–317.

11. Alberch, E.; Uddin, M.; Shevyrev, M.; Hossain, M. M. Synthesis of compounds containing *α*-aryl quaternary carbon centers. *Arkivoc* **2010**, 139–146.

12. Asad, S. A.; Ulicki, J.; Shevyrev, M.; Uddin, N.; Alberch, E.; Hossain, M. M. First Example of the Intermolecular Palladium-Catalyzed Asymmetric Allylic Alkylation of Hydroxyacrylates: Synthesis of All-Carbon α-Aryl Quaternary Aldehydes. *Eur. J. Org. Chem.* **2014**, 5695–5699.

13. Alberch, E.; Brook, C.; Asad, S. A.; Shevyrev, M.; Ulicki, J. S.; Hossain, M. M. Stereoselective Allyl Enol Carbonates for the Synthesis of Chiral Aldehydes Bearing All Carbon Quaternary Stereocenters via the Decarboxylative Asymmetric Allylic Alkylation (DAAA). *Synlett* **2015**, *26*, 388–392.

14. Uddin, N.; Rahaman, M.; Alberch, E.; Asad, S. A.; Hossain, M. M. Palladium (0)-catalyzed rearrangement of allyl enol ethers to form chiral quaternary carbon centers via asymmetric allylic alkylation. *Tetrahedron Lett.* **2018**, *59*, 3401–3404.

15. Nason, C.; Roper, T.; Hoyle, C.; Pojman, J. A. UV-Induced Frontal Polymerization of Multifunctional (Meth)acrylates. *Macromolecules* **2005**, *38*, 5506−5512.

16. Leng, X.; Nguyen, N. H.; Beusekom, B. V.; Wilson, D. A.; Percec, V. SET-LRP of 2-hydroxyethyl acrylate in protic and dipolar aprotic solvents. *Polym. Chem.* **2013**, *4*, 2995−3004.

17. Schmittel, M.; Ammon, H. A Short Synthetic Route to 4,7-Dihalogenated 1,10-Phenanthrolines with Additional Groups in 3,8-Position: Soluble Precursors for Macrocyclic Oligophenanthrolines. *Eur. J. Org. Chem.* **1998**, 785–792.

18. Berzosa, X.; Bellatriu, X.; Teixido, J.; Borrell, J. I. An Unusual Michael Addition of 3,3-Dimethoxypropanenitrile to 2-Aryl Acrylates: A Convenient Route to 4-Unsubstituted 5,6-Dihydropyrido[2,3-d]pyrimidines. *J. Org. Chem.* **2010**, *75*, 487−490.

19. Steunenberg, P.; Sijm, M.; Zuilhof, H.; Sanders, J. P. M.; Scott, E. L.; Franssen, M. C. R. Lipase-Catalyzed Aza-Michael Reaction on Acrylate Derivatives. *J. Org. Chem.* **2013**, *78*, 3802−3813.

20. Li, G.-Z.; Randev, R. K.; Soeriyadi, A. H.; Rees, G.; Boyer, C.; Tong, Z.; Davis, T. P.; Becer, C. R.; Haddleton, D. M. Investigation into thiol-(meth)acrylate Michael addition reactions using amine and phosphine catalysts. *Polym. Chem.* **2010**, *1*, 1196−1204.

21. Ooi, T.; Miki, T.; Taniguchi, M.; Shiraishi, M.; Takeuchi, M.; Maruoka, K. Highly enantioselective construction of quaternary stereocenters on beta-keto esters by phase-transfer catalytic asymmetric alkylation and Michael reaction. *Angew. Chem. Int. Ed.* **2003**, *42*, 3796–3798.

22. Neuvonen, A. J.; Pihko, P. M. Enantioselective Mannich Reaction of β-Keto Esters with Aromatic and Aliphatic Imines Using a Cooperatively Assisted Bifunctional Catalyst. *Org. Lett.* **2014**, *16*, 5152−5155.

23. Islam, M.S.; Brennan, C.; Wang, Q.; Hossain, M. M. Convenient Method of Synthesizing 3-Ethoxycarbonyl Indoles. *J. Org. Chem.* **2006**, *71*, 4675–4677.

24. Dudley, M. E.; Morshed, M. M; Hossain, M. M. A Convenient Method of Synthesizing 3-Ethoxycarbonylbenzofurans from Salicylaldehydes and Ethyl Diazoacetate. *Synthesis* **2006**, *10*, 1711–1714.

25. Hasegawa, K.; Arai, S.; Nishida, A. Synthesis of α-diazo-β-hydroxyesters through a one-pot protocol by phase-transfer catalysis: application to enantioselective aldol-type

reaction and diastereoselective synthesis of α-amino-β-hydroxyester derivatives. *Tetrahedron* **2006**, *62*, 1390–1401.

26. Liao, M.; Wang, J. CuSO4-catalyzed diazo decomposition in water: a practical synthesis of β-keto esters. *Tetrahedron Lett*. **2006**, *47*, 8859–8861.

27. Holmquist, C. R.; Roskamp, E. J. A Selective Method for Diazoacetate Catalyzed the Direct Conversion of Aldehydes into *β*-Keto Esters with Ethyl by Tin(I1) Chloride. *J. Org. Chem*. **1989**, *54*, 3258-3260.

28. Mahmood, S. J.; Hossain, M. M. Iron Lewis Acid Catalyzed Reactions of Aromatic Aldehydes with Ethyl Diazoacetate: Unprecedented Formation of 3-Hydroxy-2-arylacrylic Acid Ethyl Esters by a Unique 1,2-Aryl Shift. *J. Org. Chem*. **1998**, *63*, 3333–3336.

29. Kanemasa, S.; Kanai, T.; Araki, T.; Wada, E. Lewis Acid.Catalyzed Reactions of Ethyl Diazoacetate with Aldehydes. Synthesis of (α-Formyl Esters by a Sequence of AIdol Reaction and 1,2-Nucleophilic Rearrangement. *Tetrahedron Lett*. **1999**, *40*, 5055–5058.

30. Benito-Garagorri, D.; Wiedermann, J.; Pollak, M.; Mereiter, K.; Kirchner, K. Iron(II) Complexes Bearing Tridentate PNP Pincer-Type Ligands as Catalysts for the Selective Formation of 3-Hydroxyacrylates from Aromatic Aldehydes and Ethyldiazoacetate. *Organometallics* **2007**, *26*, 217–222.

31. Alves, L. G.; Dazinger, G.; Veiros, L. F.; Kirchner, K. Unusual Anion Effects in the Iron-Catalyzed Formation of 3-Hydroxyacrylates from Aromatic Aldehydes and Ethyl Diazoacetate. *Eur. J. Inorg. Chem*. **2010**, 3160–3166.

32. Fructos, M. R.; Dı´az-Requejo, M. M.; Pe´rez, P. J. Highly active gold-based catalyst for the reaction of benzaldehyde with ethyl diazoacetate. *Chem. Commun*. **2009**, 5153–5155.

33. Kilpin, K. J.; Paul, U. S. D.; Lee, A. L.; Crowley, J. D. Gold(I) ''click'' 1,2,3-triazolylidenes: synthesis, self-assembly and Catalysis. *Chem. Commun*. **2011**, *47*, 328–330.

34. Dudley, M. E.; Morshed, M. M.; Brennan, C. L.; Islam, M. S.; Ahmad, M. S.; Atuu, M. R.; Branstetter, B.; Hossain, M. M. Acid-Catalyzed Reactions of Aromatic Aldehydes with Ethyl Diazoacetate: An Investigation on the Synthesis of 3-Hydroxy-2-arylacrylic Acid Ethyl Esters. *J. Org. Chem*. **2004**, *69*, 7599–7608.

35. Xiao, F.; Liu, Y.; Wang, J. DBU-catalyzed condensation of acyldiazomethanes to aldehydes in water and a new approach to ethyl β-hydroxy α-arylacrylates. *Tetrahedron Lett.* **2007**, *48*, 1147–1149.

36. Schmittel, M.; Ammon, H. A Short Synthetic Route to 4,7-Dihalogenated 1,10 Phenanthrolines with Additional Groups in 3,8-Position: Soluble Precursors for Macrocyclic Oligophenanthrolines. *Eur. J. Org. Chem*. **1998**, 785-792

37. Telvekar, V. N.; Belubbi, A.; Bairwa, V. K.; Satardekar, K. *Bioorg*. Novel N′-benzylidene benzofuran-3-carbohydrazide derivatives as antitubercular and antifungal agents. *Med. Chem. Lett.* **2012**, *22*, 2343-2346.

38. Eccles, W.; Blevitt, J. M.; Booker, J. N.; Chrovian, C. C.; Crawford, S.; de Leon, A. R.; Deng, X.; Fourie, A. M.; Grice, C. A.; Herman, K.; Karlsson, L.; Kearney, A. M.; Lee-Dutra, A.; Liang, J.; Luna, R.; Pippel, D.; Rao, N.; Riley, J. P.; Santillán, A.; Savall, B.; Tanis, V. M.; Xue, X.; Young, A. L. Identification of benzofuran central cores for the inhibition of leukotriene A4 hydrolase. *Bioorg. Med. Chem. Lett*. **2013**, *23*, 811-815.

39. Fowler, K. J.; Ellis, J. L.; Morrow, G. W. 6-Endo Heck Cyclization of 3-(2-Iodophenoxy) methylbenzofurans: A Useful Approach to Pterocarpenes. *Synth. Commun*. **2013**, *43*, 1676–1682.

40. Kil'met'ev, A. S.; Shul'ts, E. E.; Shakirov, M. M.; Rybalova, T. V.; Tolstikov, G. A. Diels-alder reactions with ethyl 1-benzofuran-3-carboxylates. *Russ. J. Org. Chem.* **2013**, *49*, 872–885.

41. Qin, L.; Vo, D.-D.; Nakhai, A.; Andersson, D.; Elofsson, M. Diversity-Oriented Synthesis of Libraries Based on Benzofuran and 2,3-Dihydrobenzofuran Scaffolds. *ACS Comb. Sci.* **2017**, *19*, 370−376.

42. Xu, L.; Liu, F.; Xu, L.-W.; Gao, Z.; Zhao, Y.-M. A Total Synthesis of Paeoveitol. *Org. Lett*. **2016**, *18*, 3698−3701.

43. Li, T.-Z.; Geng, C.-A.; Yin, X.-J.; Yang, T.-H.; Chen, X.-L.; Huang, X.-Y.; Ma, Y.-B.; Zhang, X.-M.; Chen, J.-J. Catalytic Asymmetric Total Synthesis of (+)- and (−)-Paeoveitol via a Hetero-Diels–Alder Reaction. *Org. Lett.* **2017**, *19*, 429−431.

44. Bongen, P.; Pietruszka, J.; Simon, R. C. Dynamic Kinetic Resolution of 2,3-Dihydrobenzo[b]furans: Chemoenzymatic Synthesis of Analgesic Agent BRL 37959. *Chem. Eur. J.* **2012**, *18*, 11063–11070.

45. Ahmed, S. A.; Hinz, D. J.; Jellen, M. J.; Hossain, M. M. A Concise Synthesis of Potential COX Inhibitor BRL-37959 and Analogs Involving Bismuth(III) Catalyzed Friedel-Crafts Acylation. *Chem. Biodiversity* **2018**, *15*, e1800334.

46. Rahaman, M.; Hossain, M. M. Discussion Addendum for: Convenient Preparation of 3-Ethoxycarbonyl Benzofurans from Salicylaldehydes and Ethyl Diazoacetate. *Org. Synth*. **2019**, *96*, 98-109.

APPENDIX A

PART I: A CONCISE ASYMMETRIC SYNTHESIS OF MICROTUBULE INHIBITOR TRYPROSTATIN B

Copies of ^{1}H NMR, ^{13}C NMR, HRMS, and HPLC Spectral Data

^{1}H NMR Spectrum of Compound 2 in CDCl$_3$

1.69

2.33

3.60

7.24
7.26
7.28
7.31
7.34
7.36
7.55
7.68
7.71
8.15
8.18

9.08

6.19

2.08

2.34
1.00
1.05

1.05

ppm

^{13}C NMR Spectrum of Compound 2 in CDCl$_3$

28.23

45.44

54.45

76.64
77.07
77.27
77.49
83.54

115.15
117.75
119.63
122.56
124.37
124.63
130.57
135.60

149.76
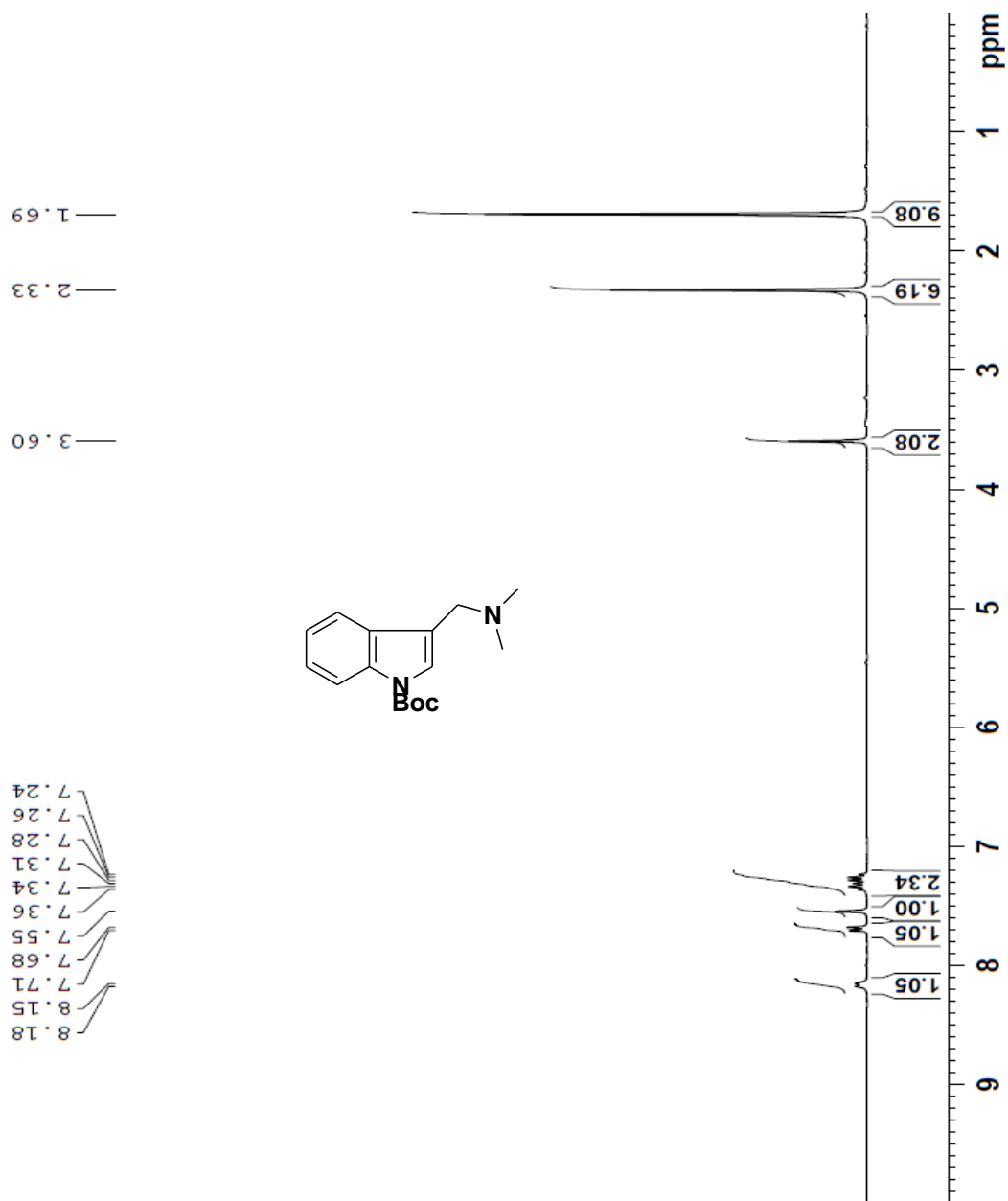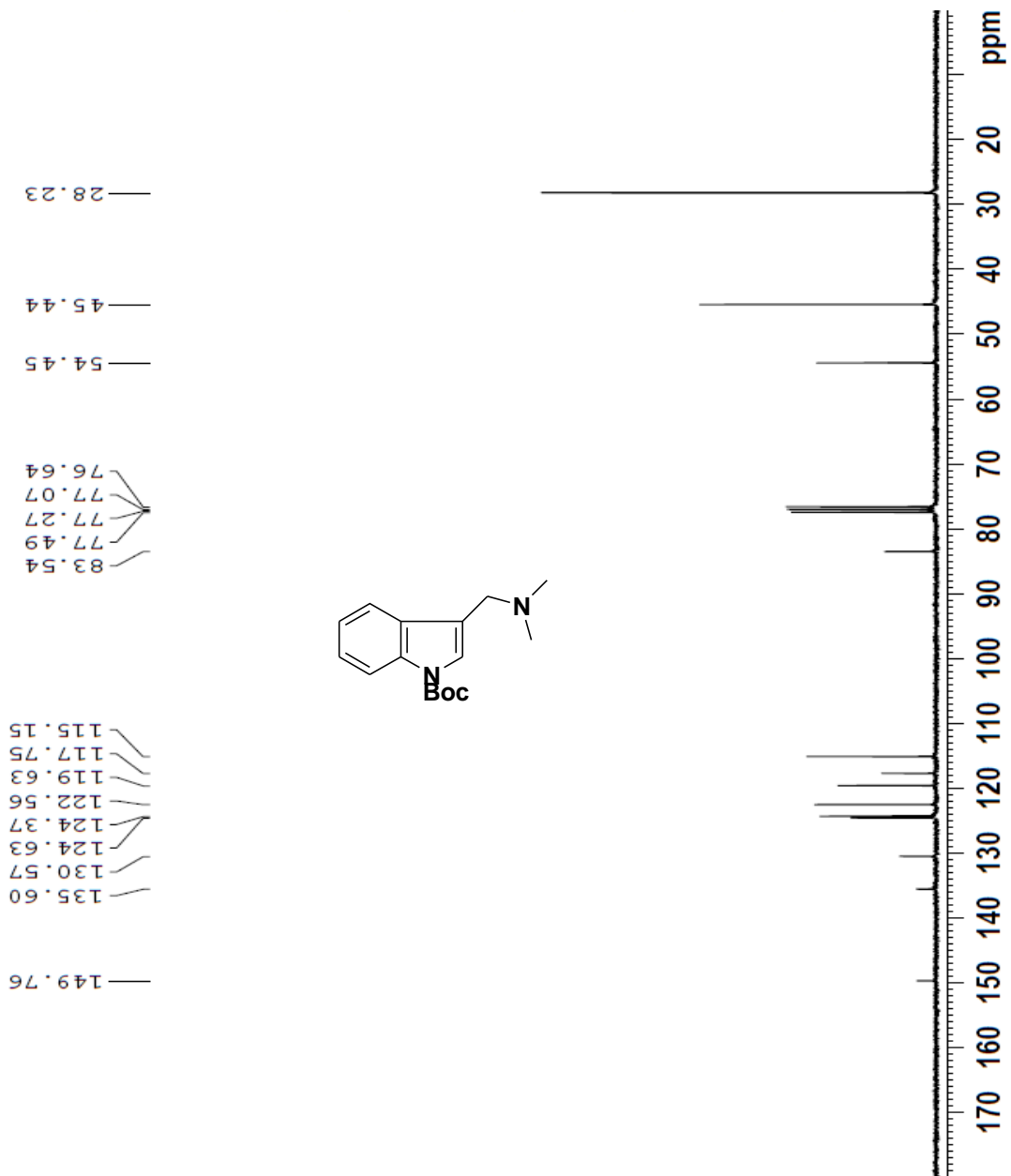
HRMS of Compound 2

Event#: 1 MS(E+)   Ret. Time : 0.293 -> 0.693 - 0.040 -> 0.092   Scan# : 45 -> 105 - 7 -> 15
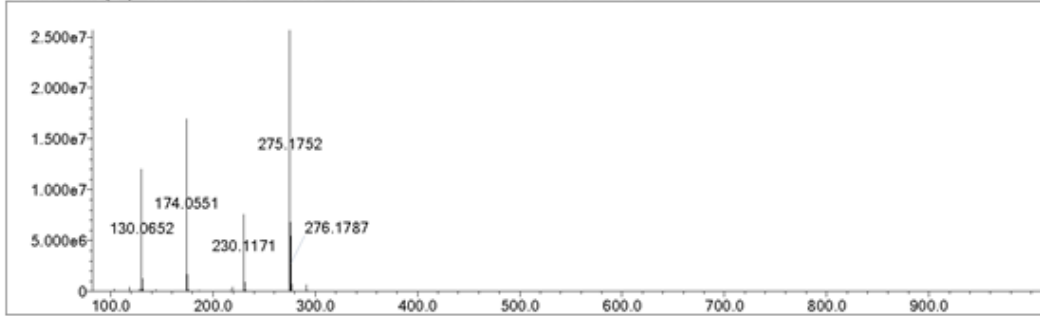
Measured region for 275.1752 m/z
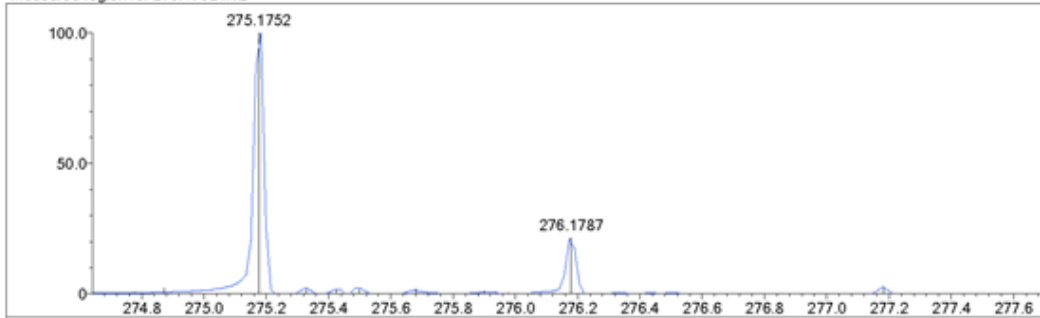
C16 H22 N2 O2 [M+H]+ : Predicted region for 275.1754 m/z
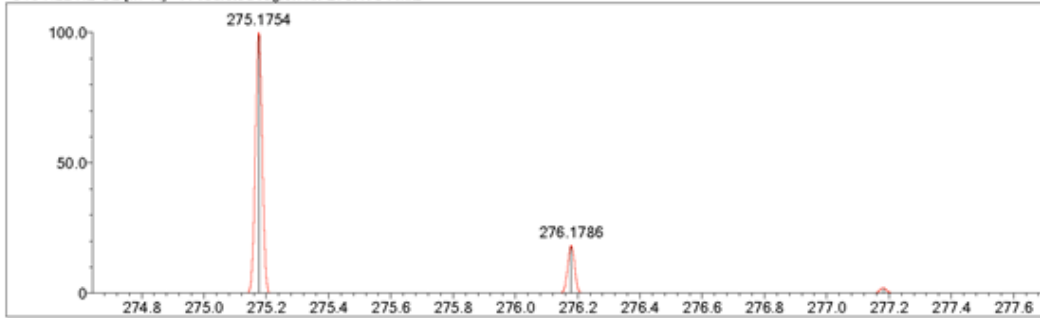
Rank	Score	Formula (M)	Ion	Meas. m/z	Pred. m/z	Df. (mDa)	Df. (ppm)	Iso	DBE
1	91.12	C16 H22 N2 O2	[M+H]+	275.1752	275.1754	-0.2	-0.73	91.12	7.0

^{1}H NMR Spectrum of Compound 4 in CDCl$_3$
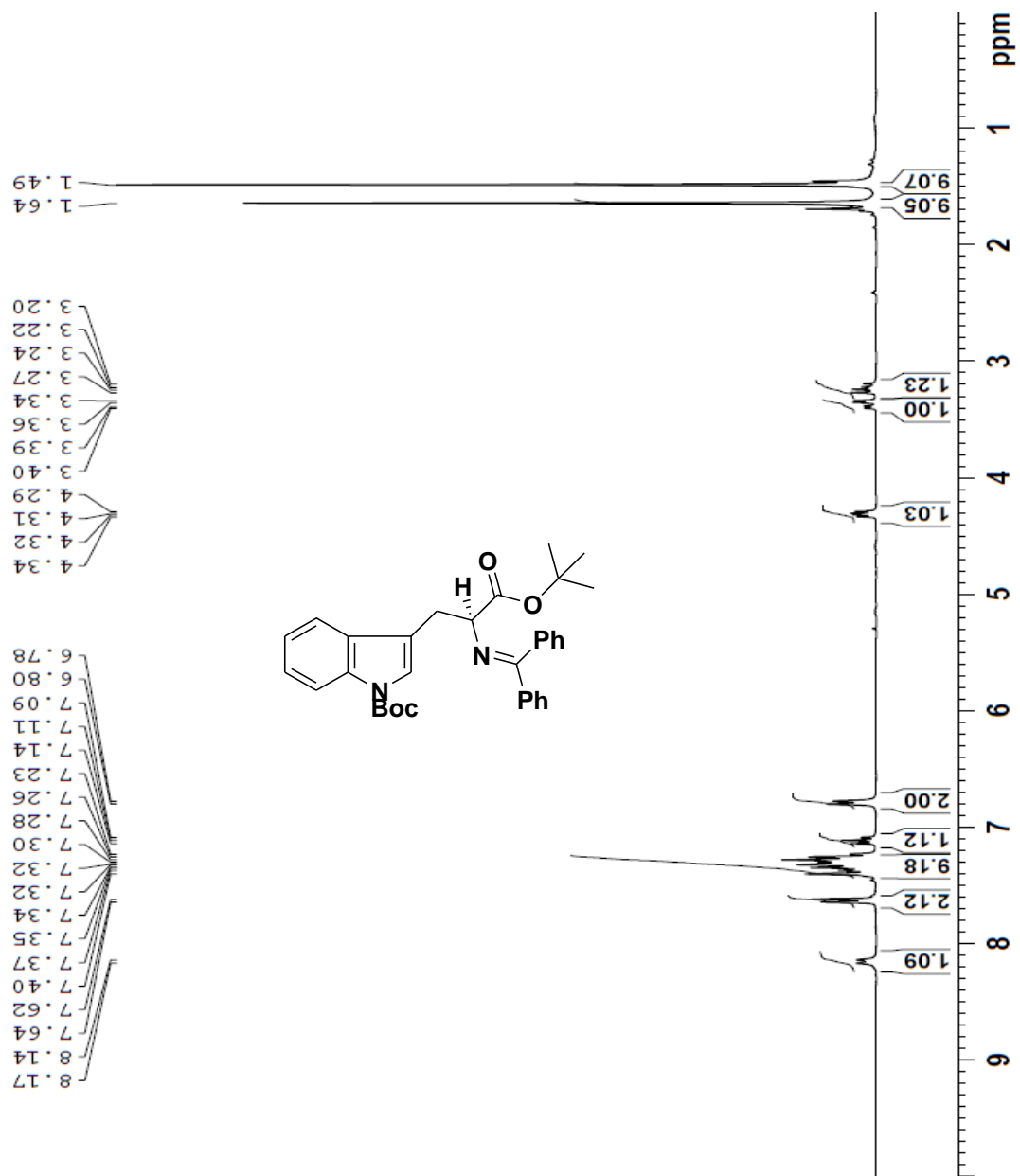
¹³C NMR Spectrum of Compound 4 in CDCl₃

28.08
28.18
28.96

66.08
76.68
77.10
77.52
81.22
83.17

115.00
116.99
119.17
122.24
124.13
124.23
127.65
127.94
128.15
128.28
128.80
130.17
130.70
135.36
136.16
139.55
149.65

170.46
170.88

ppm
50
100
150
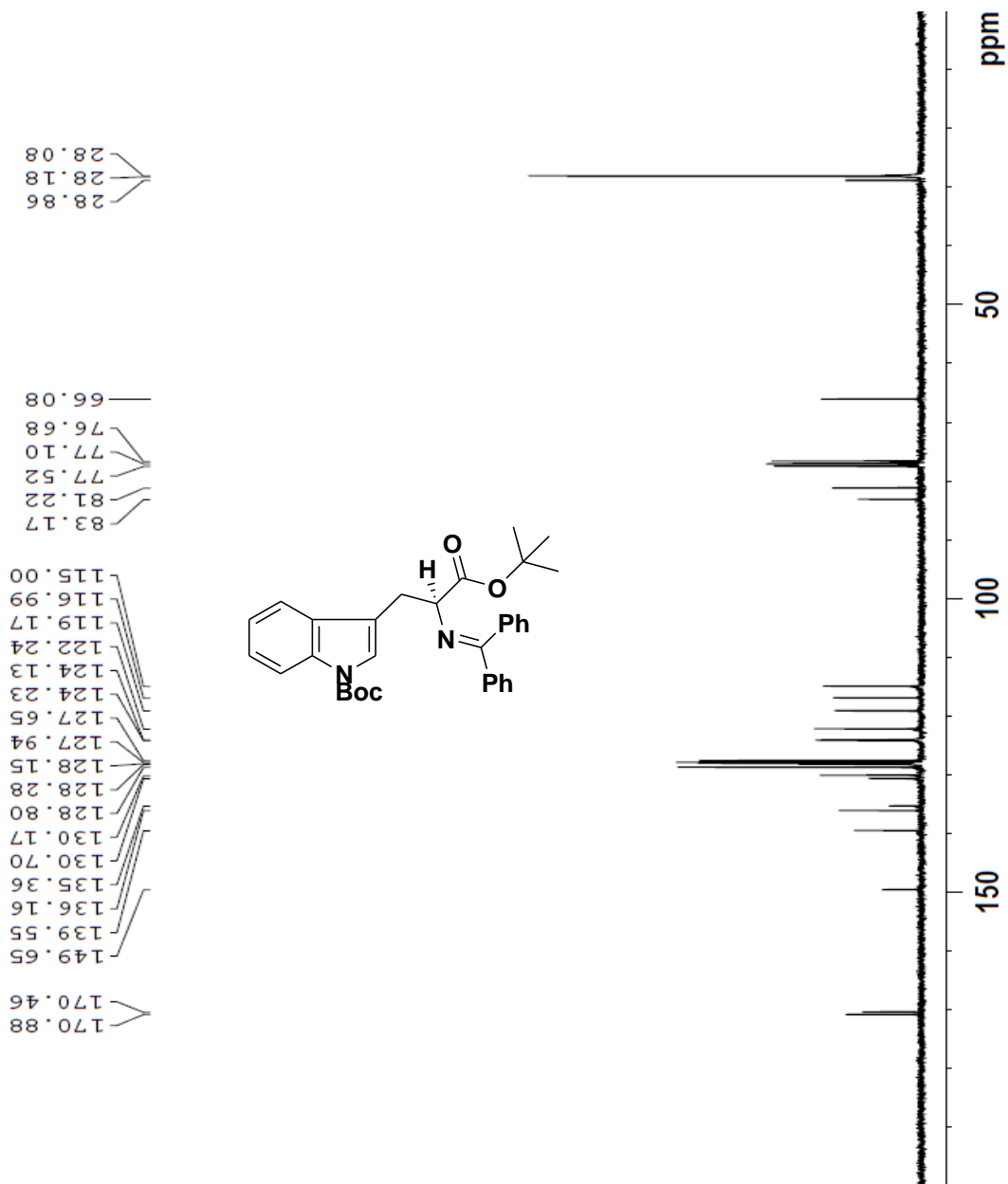
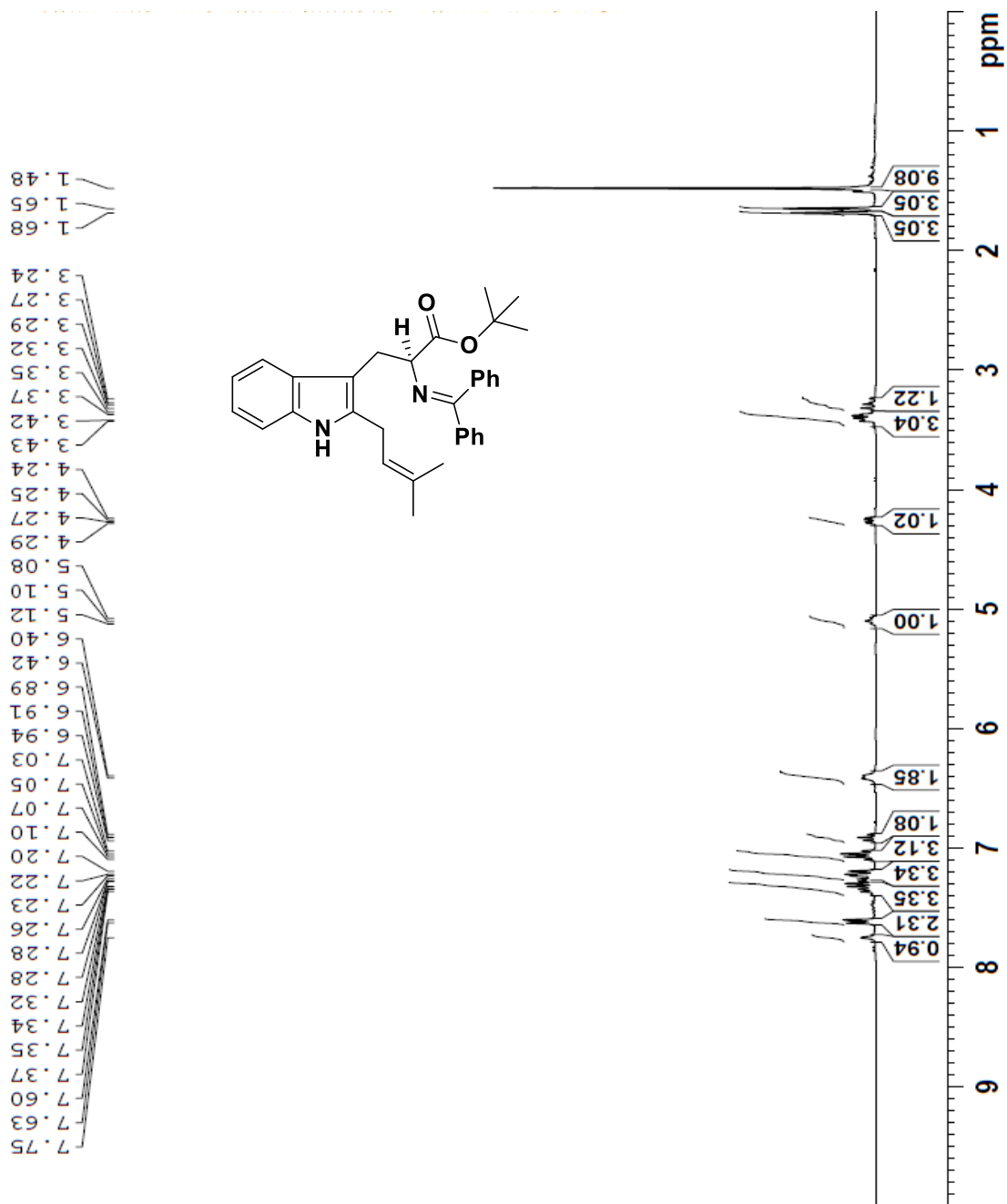# HRMS of Compound 4
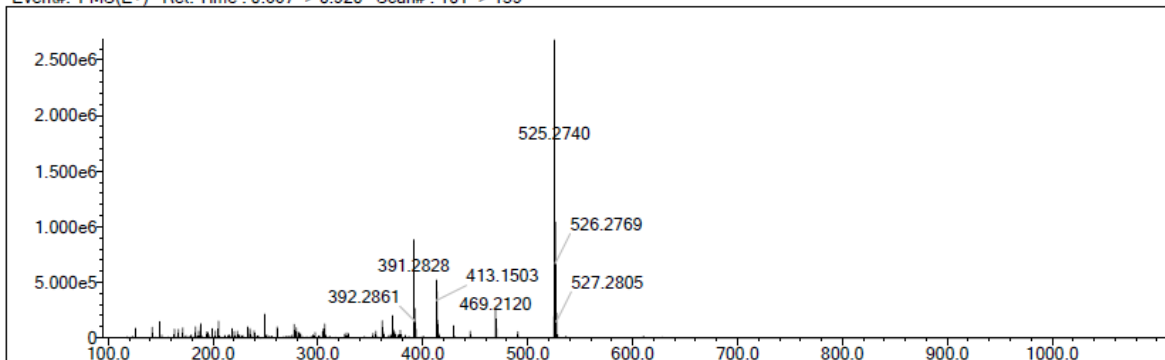
Measured region for 525.2738 m/z
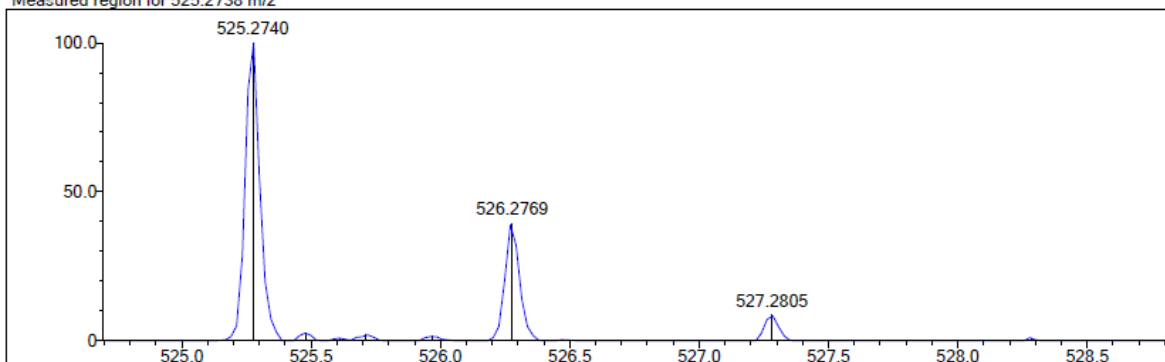
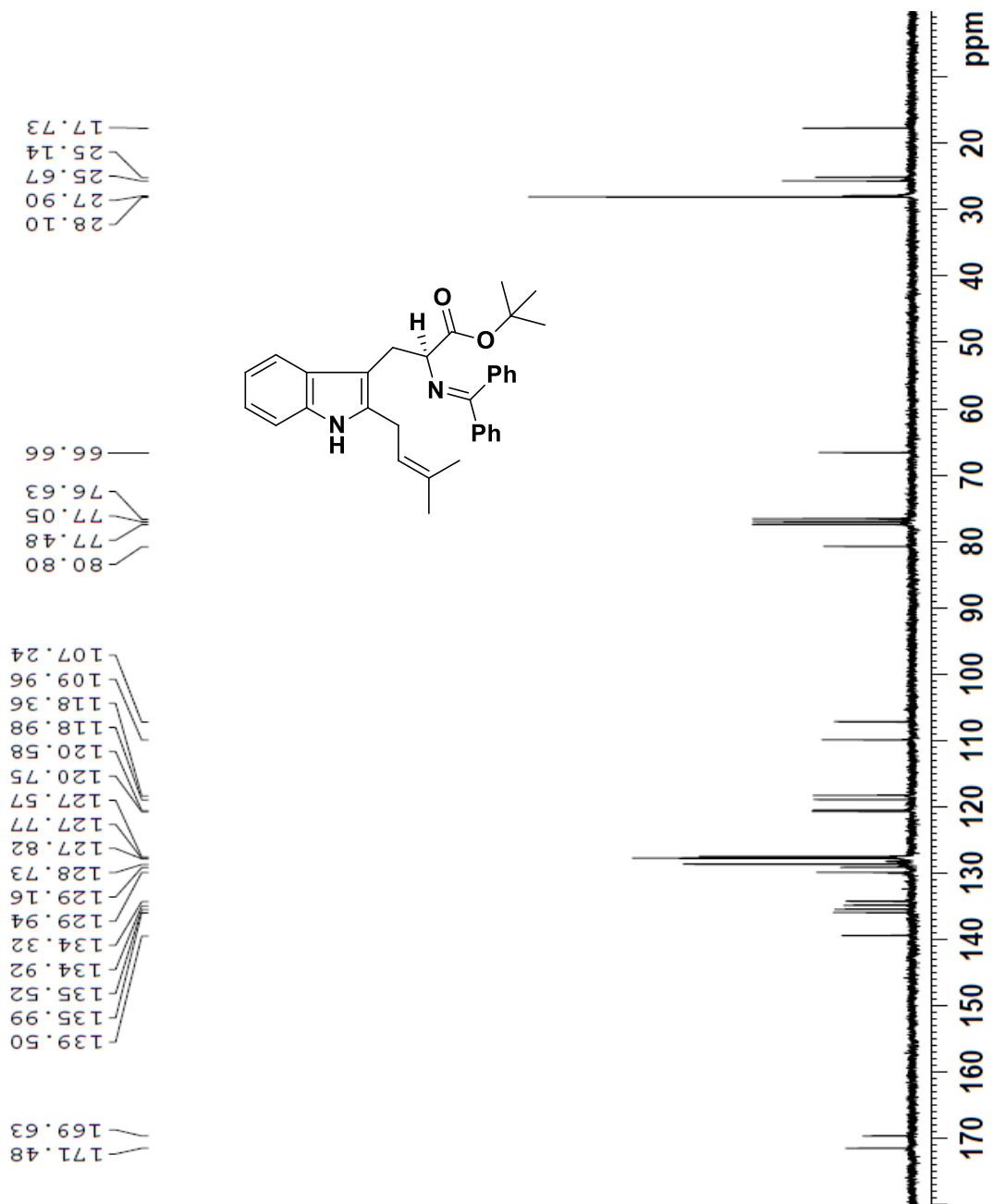C33 H36 N2 O4 [M+H]+ : Predicted region for 525.2748 m/z
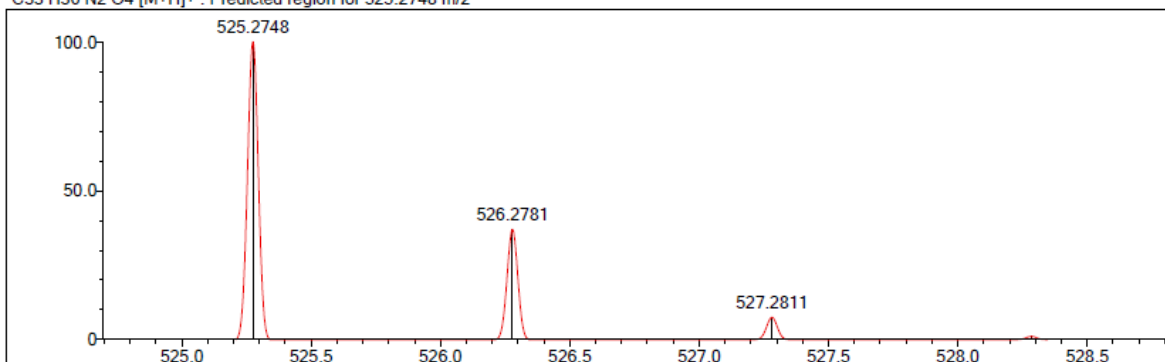
Rank	Score	Formula (M)	Ion	Meas. m/z	Pred. m/z	Df. (mDa)	Df. (ppm)	Iso	DBE
1	97.75	C33 H36 N2 O4	[M+H]+	525.2738	525.2748	-1.0	-1.90	100.00	17.0

^{1}H NMR Spectrum of Compound 6 in CDCl$_3$

1.59
1.76
1.81

3.15

4.36
4.39

5.22
5.29
5.32
5.34

7.16
7.19
7.21
7.24
7.26
7.29
7.94
8.01
8.03
8.09
8.12

9.35
3.15
3.03

6.03

2.06

2.05
1.07

2.26

1.03
1.14
1.00

ppm
1
2
3
4
5
6
7
8
9

^{13}C NMR Spectrum of Compound 6 in CDCl$_3$

19.47

26.44
28.08

48.40

58.64
61.51

76.83
77.26
77.68
84.96

107.61
110.89
115.15
120.30
123.80
125.16
129.83
130.54
135.00

148.82
148.91
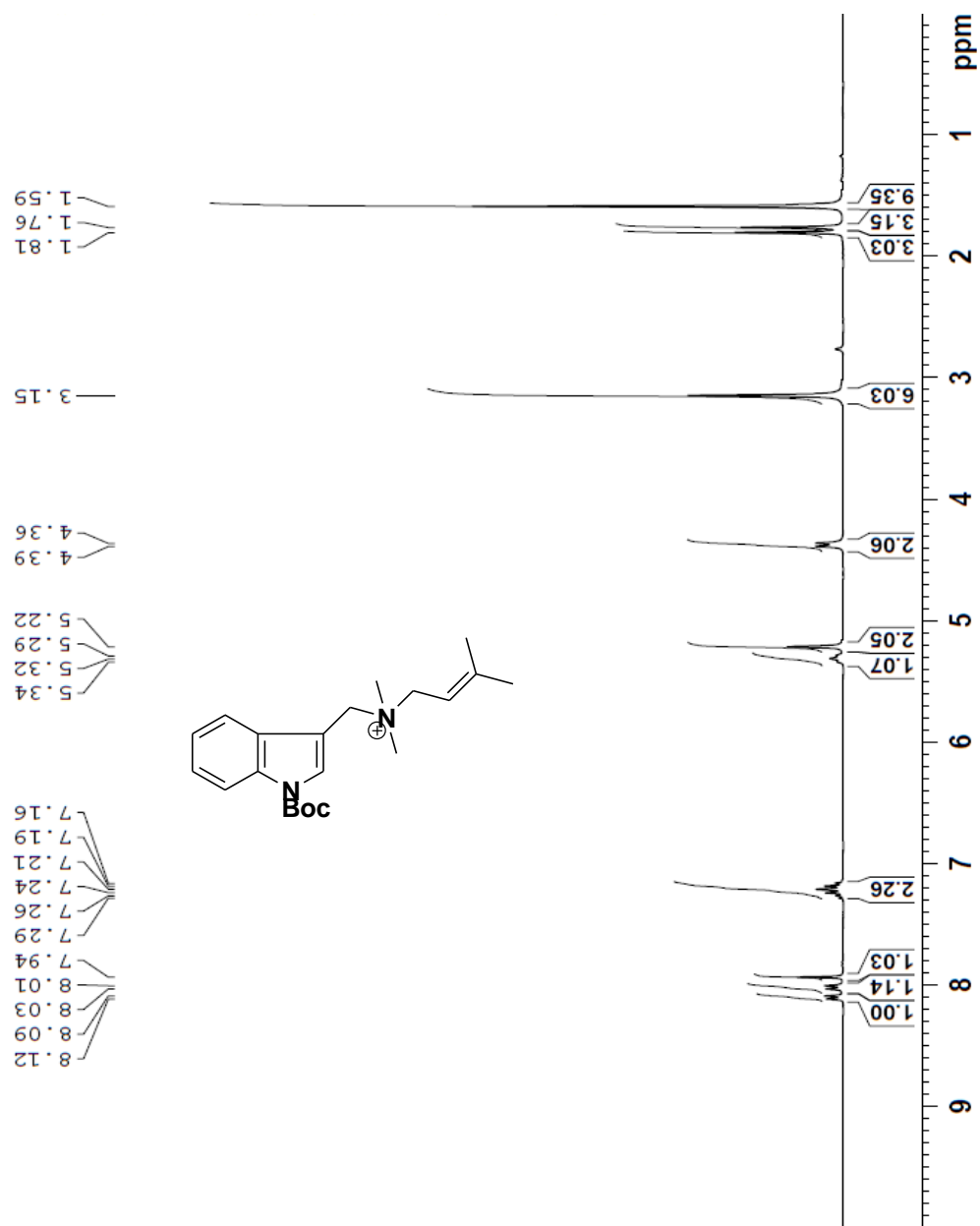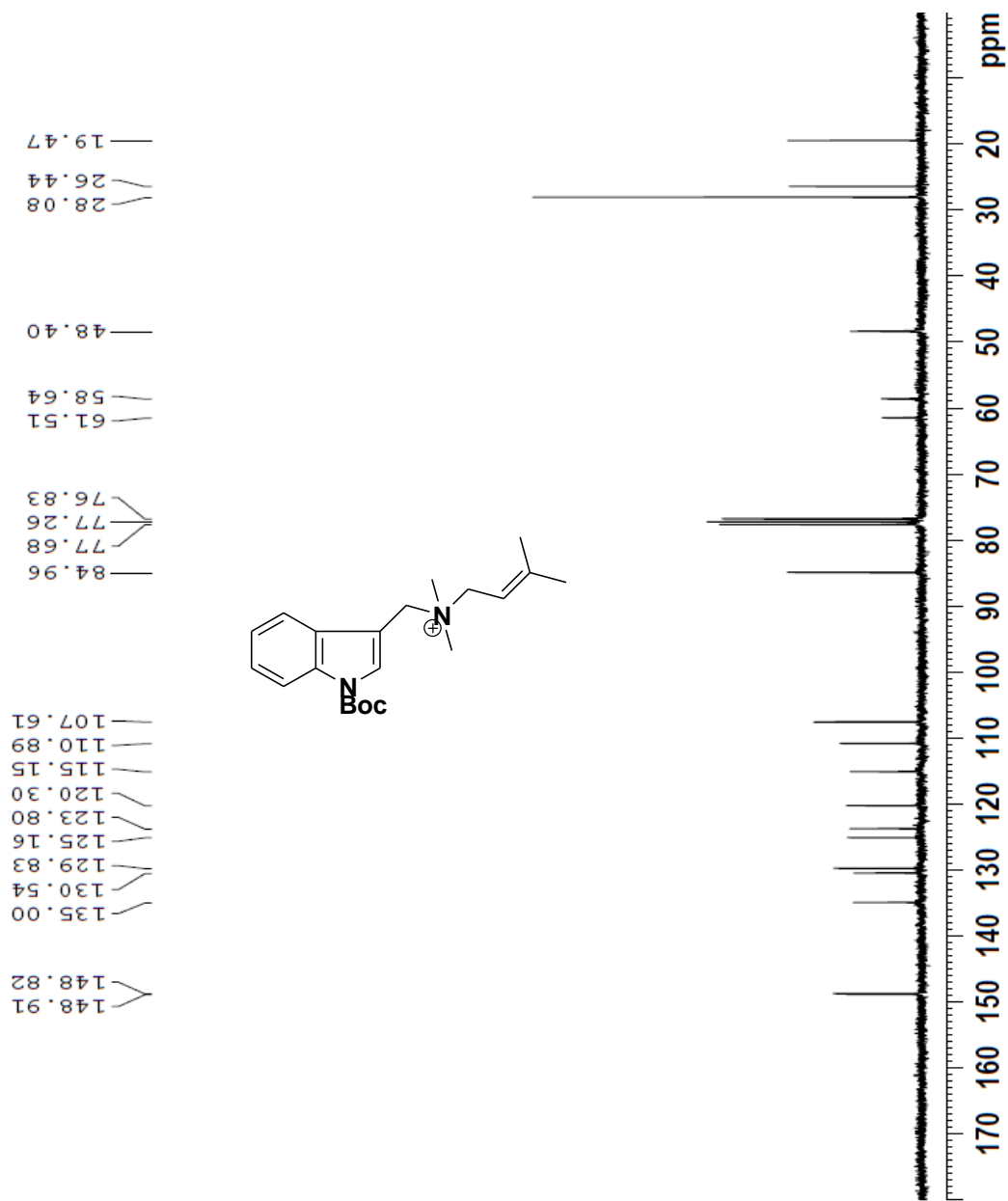
HRMS of Compound 6

Event#: 1 MS(E+)   Ret. Time : 0.613 -> 1.053 - 0.320 -> 0.452   Scan# : 93 -> 159 - 49 -> 69
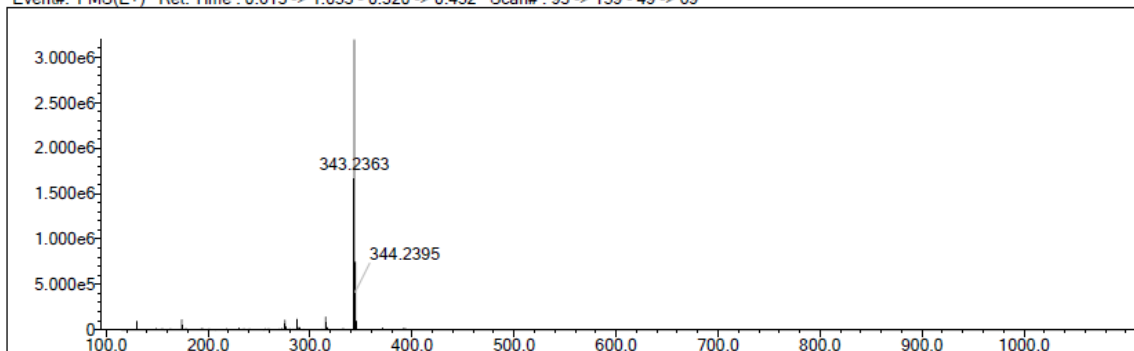
Measured region for 343.2363 m/z
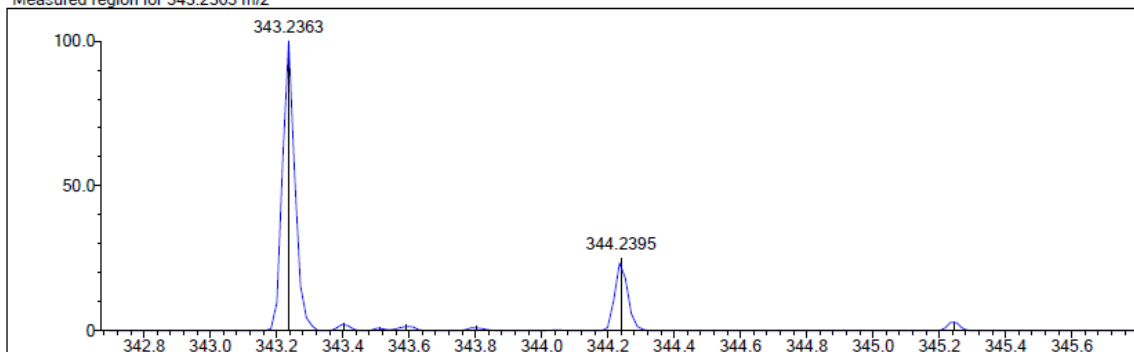
C21 H30 N2 O2 [M+H]+ : Predicted region for 343.2380 m/z
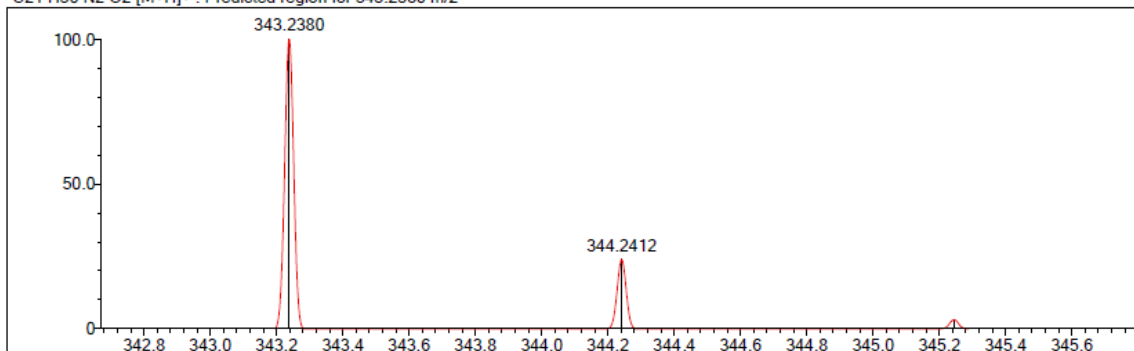
Rank	Score	Formula (M)	Ion	Meas. m/z	Pred. m/z	Df. (mDa)	Df. (ppm)	Iso	DBE
1	78.28	C21 H30 N2 O2	[M+H]+	343.2363	343.2380	-1.7	-4.95	86.86	8.0

^{1}H NMR Spectrum of Compound 4 in CDCl$_3$

^{13}C NMR Spectrum of Compound 4 in CDCl$_3$

28.07
29.14

66.65

76.79
77.04
77.30
80.94

110.81
112.31
118.97
119.10
121.71
123.04
127.61
127.77
127.93
128.00
128.09
128.78
130.07
135.99
136.18
139.66

170.09
171.28

ppm
20
30
40
50
60
70
80
90
100
110
120
130
140
150
160
170

^{1}H NMR Spectrum of Compound 7 in CDCl$_3$

1.67
1.80
1.88
1.93

3.17

3.91

4.55
4.57
5.04
5.27
5.31
5.36
5.39
5.41

7.30
7.32
7.33
7.35
8.06
8.09

12.31
3.13
3.11
3.18

6.00

1.71

2.08

1.02
2.07
1.19

2.44

2.08

ppm
1
2
3
4
5
6
7
8
9

¹³C NMR Spectrum of Compound 7 in CDCl₃

18.66
19.46
25.44
26.39
26.77
27.85

48.40

58.11
61.78

76.86
77.29
77.71
84.97

106.04
111.18
114.91
119.84
120.34
123.60
124.43
129.01
134.09
135.81

144.12
148.72
149.55

ppm
20
30
40
50
60
70
80
90
100
110
120
130
140
150

172

HRMS of Compound 7

Event#: 1 MS(E+) Ret. Time : 0.453 -> 0.973 Scan# : 69 -> 147
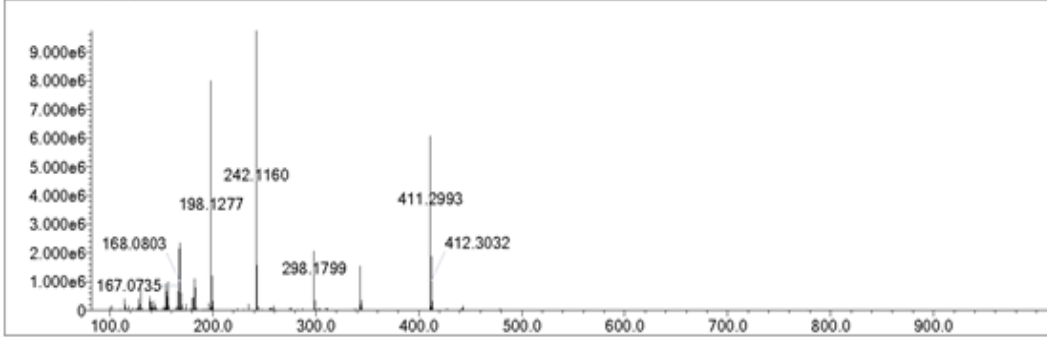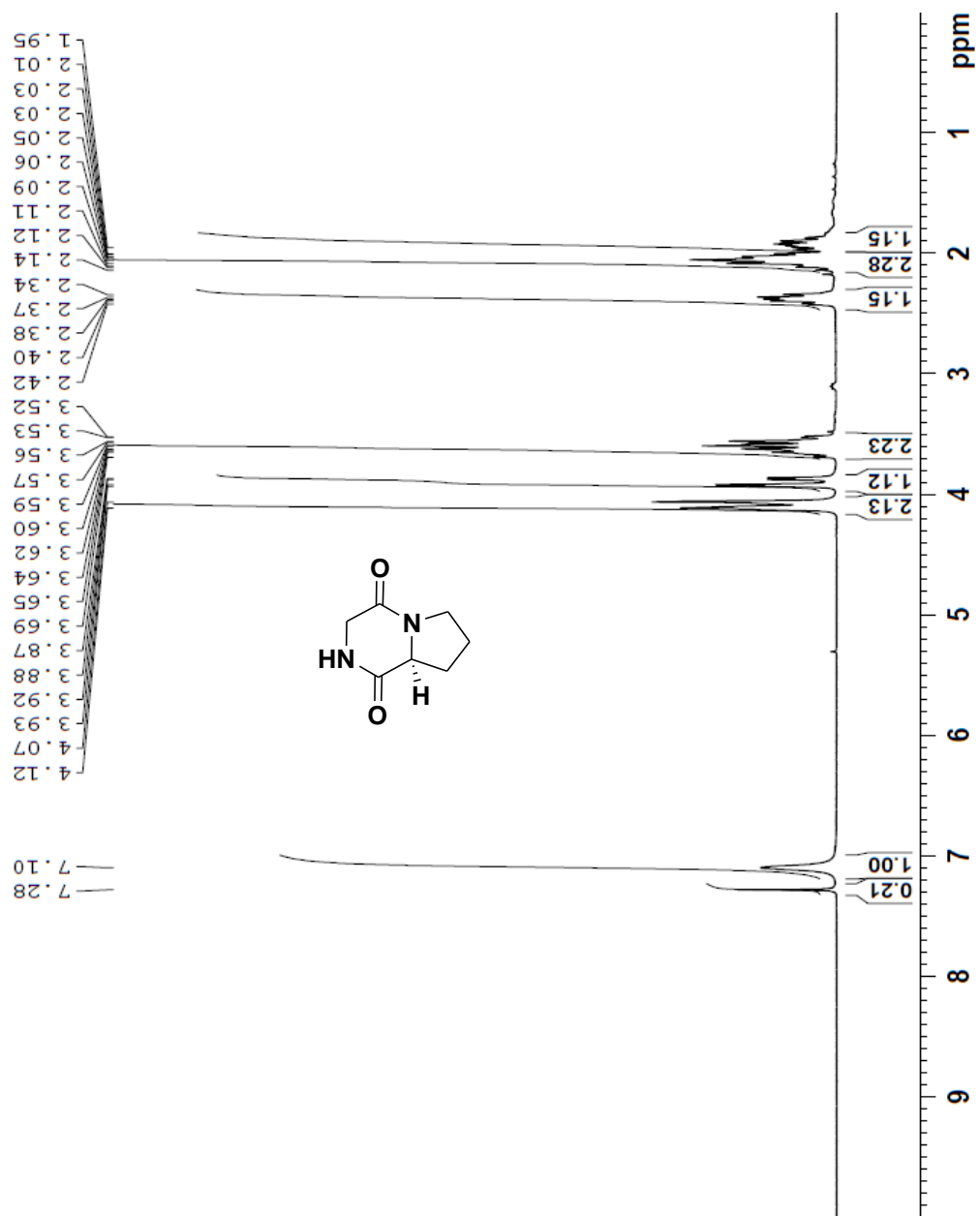
Measured region for 411.2993 m/z
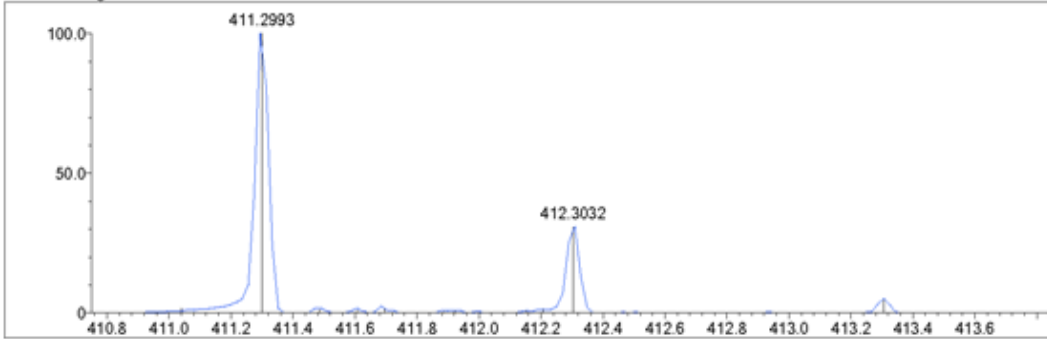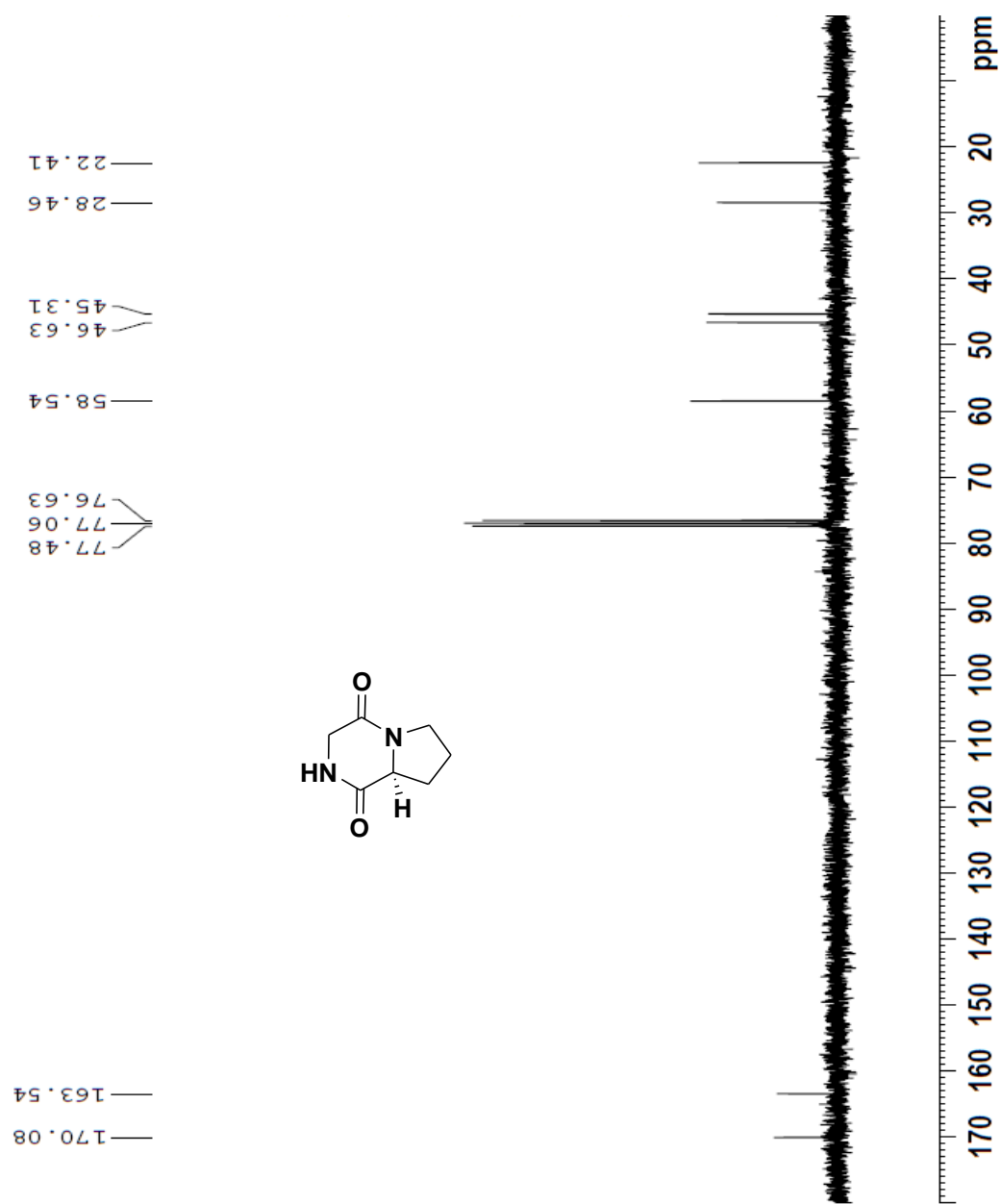
C26 H38 N2 O2 [M+H]+ : Predicted region for 411.3006 m/z
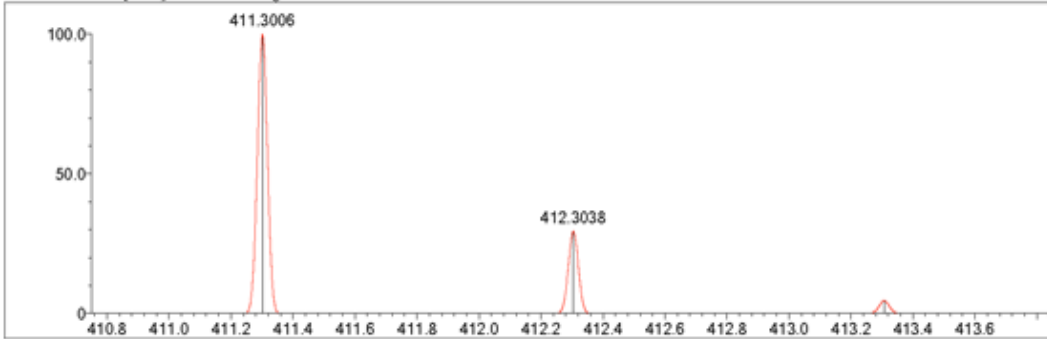
Rank	Score	Formula (M)	Ion	Meas. m/z	Pred. m/z	Df. (mDa)	Df. (ppm)	Iso	DBE
1	82.28	C26 H38 N2 O2	[M+H]+	411.2993	411.3006	-1.3	-3.16	86.98	9.0

Crystal Structure Data of Compound 7

CCDC 922382 DOI: 10.5517/ccdc.csd.cczyt8z

Blocks grown using slow diffusion method: Ethyl Acetate/Hexane

Analyzed by X-ray diffraction at UCSD with Arnold L. Rheingold

Unit Cell Dimensions: a=8.5784(2) Å; b=12.9668(3) Å; c=13.5267(3) Å
α=109.266(2)°; β=103.084(2)°; γ=107.596(2)°

Triclinic lattice, P1 space group, Z = 2 molecules per unit cell. R1 = 4.39%

^{1}H NMR Spectrum of Compound 8 in CDCl$_3$
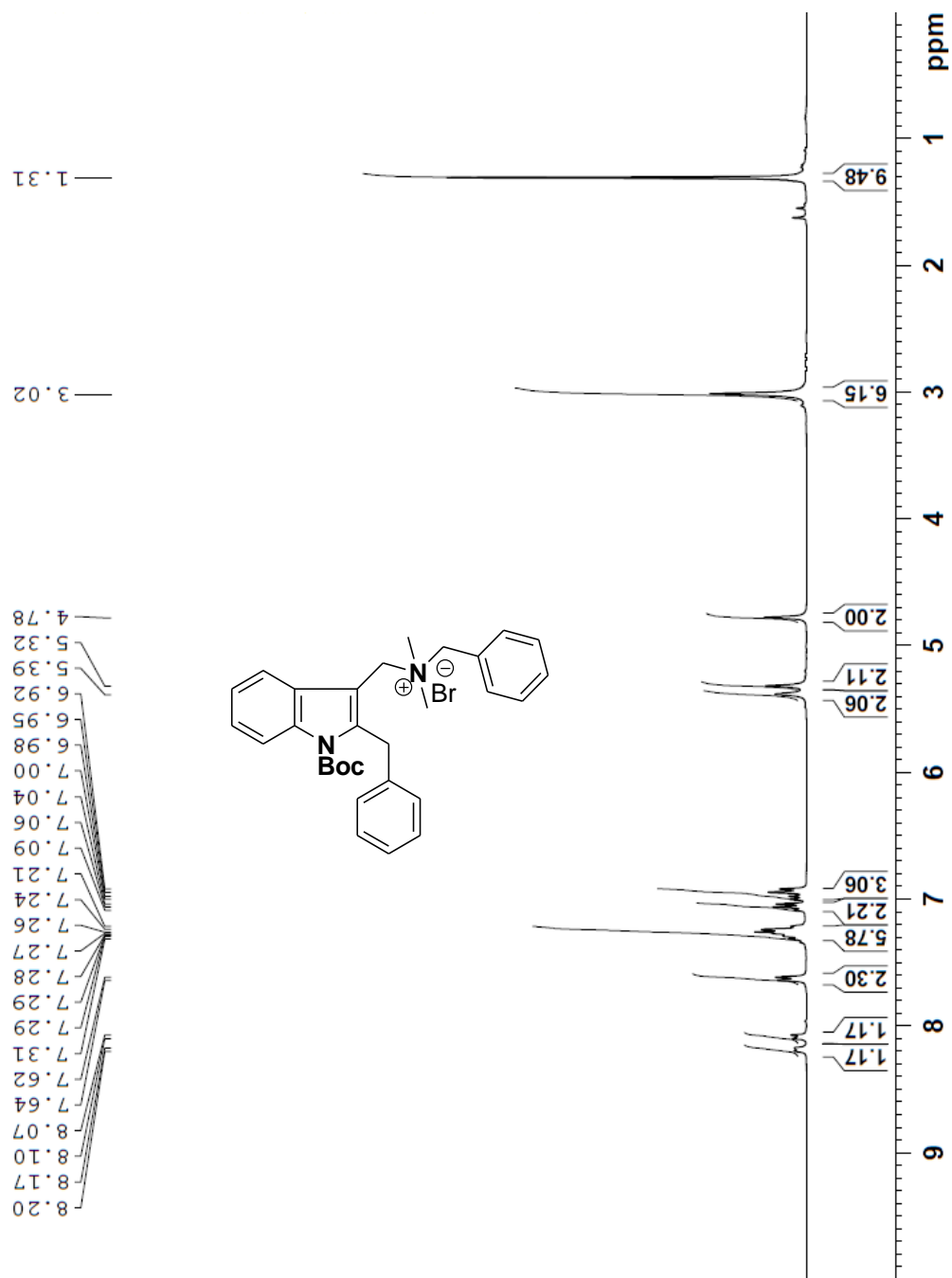
1.31
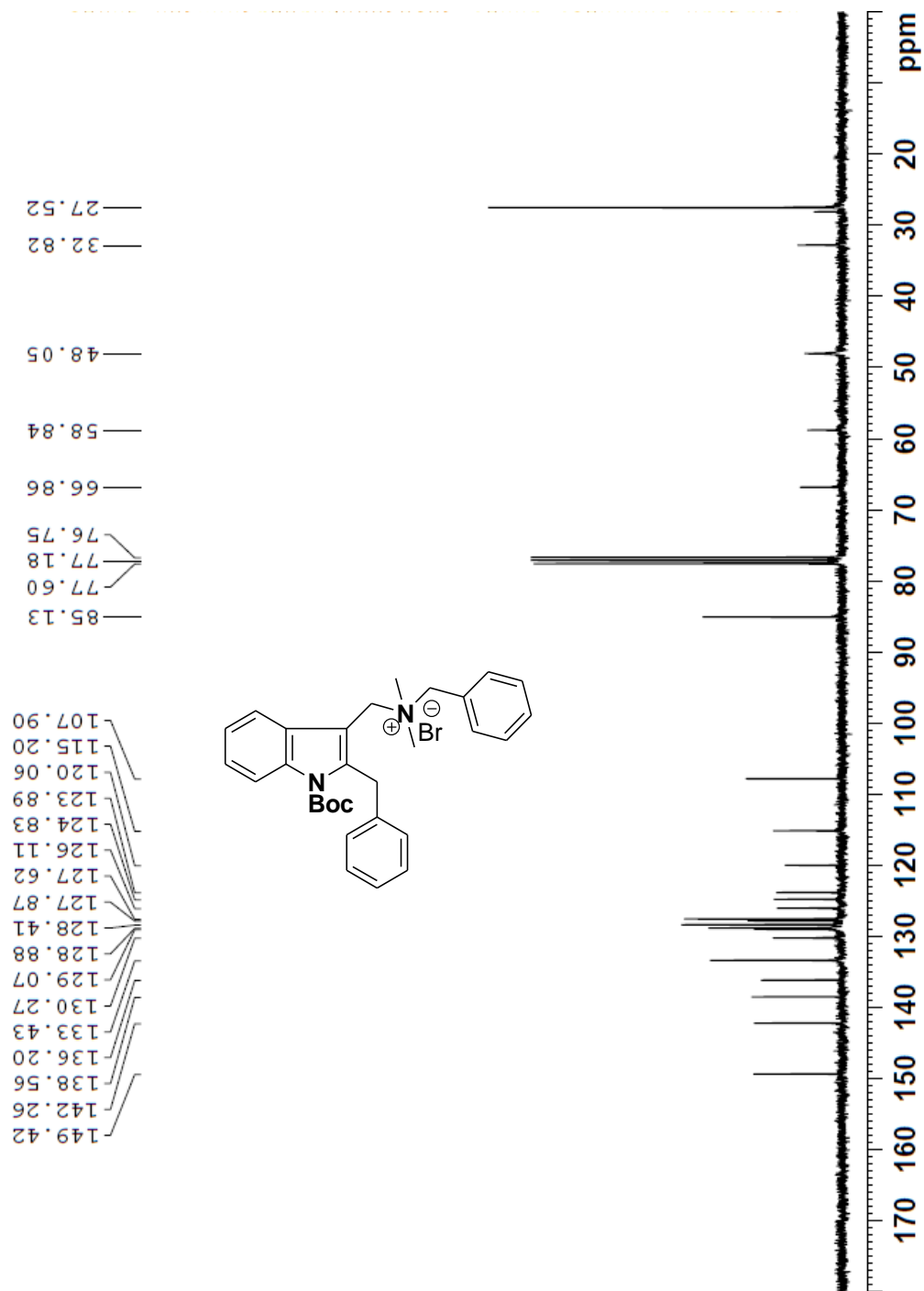
3.02

4.78
5.32
5.39
6.92
6.95
6.98
7.00
7.04
7.06
7.09
7.21
7.24
7.26
7.27
7.28
7.29
7.29
7.31
7.62
7.64
8.07
8.10
8.17
8.20

9.48

6.15

2.00
2.11
2.06

3.06
2.21
5.78
2.30
1.17
1.17

¹³C NMR Spectrum of Compound 8 in CDCl₃

27.52
32.82
48.05
58.84
66.86
76.75
77.18
77.60
85.13
107.90
115.20
120.06
123.89
124.83
126.11
127.62
127.87
128.41
128.88
129.07
130.27
133.43
136.20
138.56
142.26
149.42

HRMS of Compound 8
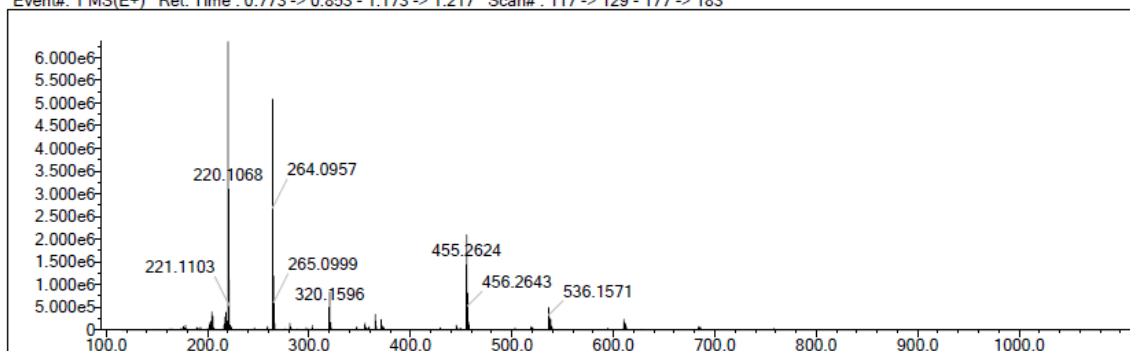
Measured region for 455.2624 m/z
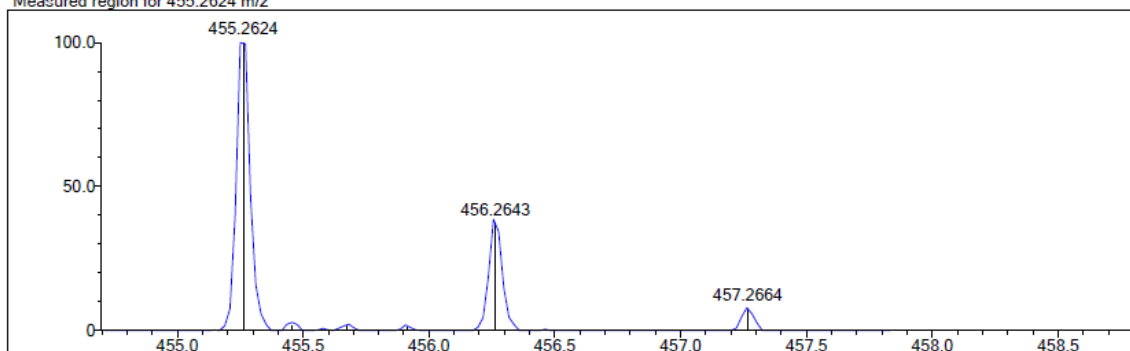
C30 H34 N2 O2 [M+H]+ : Predicted region for 455.2693 m/z
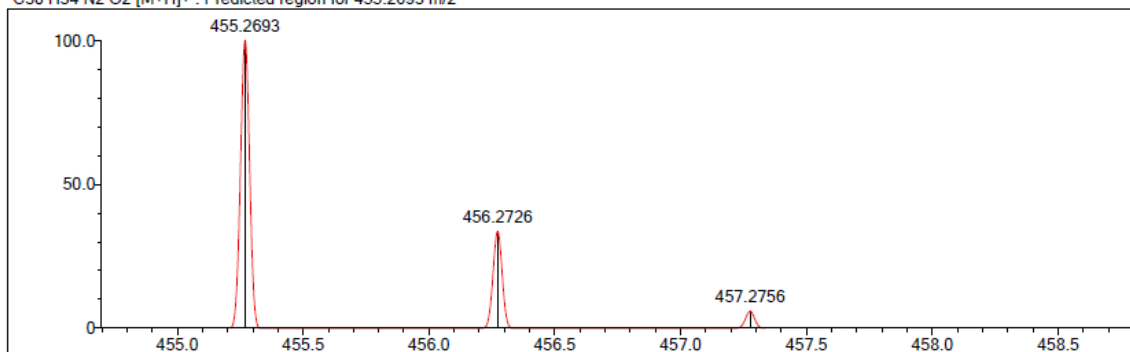
Rank	Score	Formula (M)	Ion	Meas. m/z	Pred. m/z	Df. (mDa)	Df. (ppm)	Iso	DBE
8	21.36	C30 H34 N2 O2	[M+H]+	455.2624	455.2693	-6.9	-15.16	81.42	15.0

1.48
1.65
1.68

3.24
3.27
3.29
3.32
3.35
3.37
3.42
3.43
4.24
4.25
4.27
4.29
5.08
5.10
5.12
6.40
6.42
6.89
6.91
6.94
7.03
7.05
7.07
7.10
7.20
7.22
7.23
7.26
7.28
7.28
7.32
7.34
7.35
7.37
7.60
7.63
7.75

9.08
3.05
3.05

1.22
3.04

1.02

1.00

1.85

1.08
3.12
3.34
3.35
2.31
0.94

ppm

^{13}C NMR Spectrum of Compound 9 in CDCl$_3$

17.73
25.14
25.67
27.90
28.10

66.99

76.63
77.05
77.48
80.80

107.24
109.96
118.36
118.98
120.58
120.75
127.57
127.77
127.82
128.73
129.16
129.94
134.32
134.92
135.52
135.99
139.50

169.63
171.48

HRMS of Compound 9

HPLC Data of Compound 9 (Racemic)
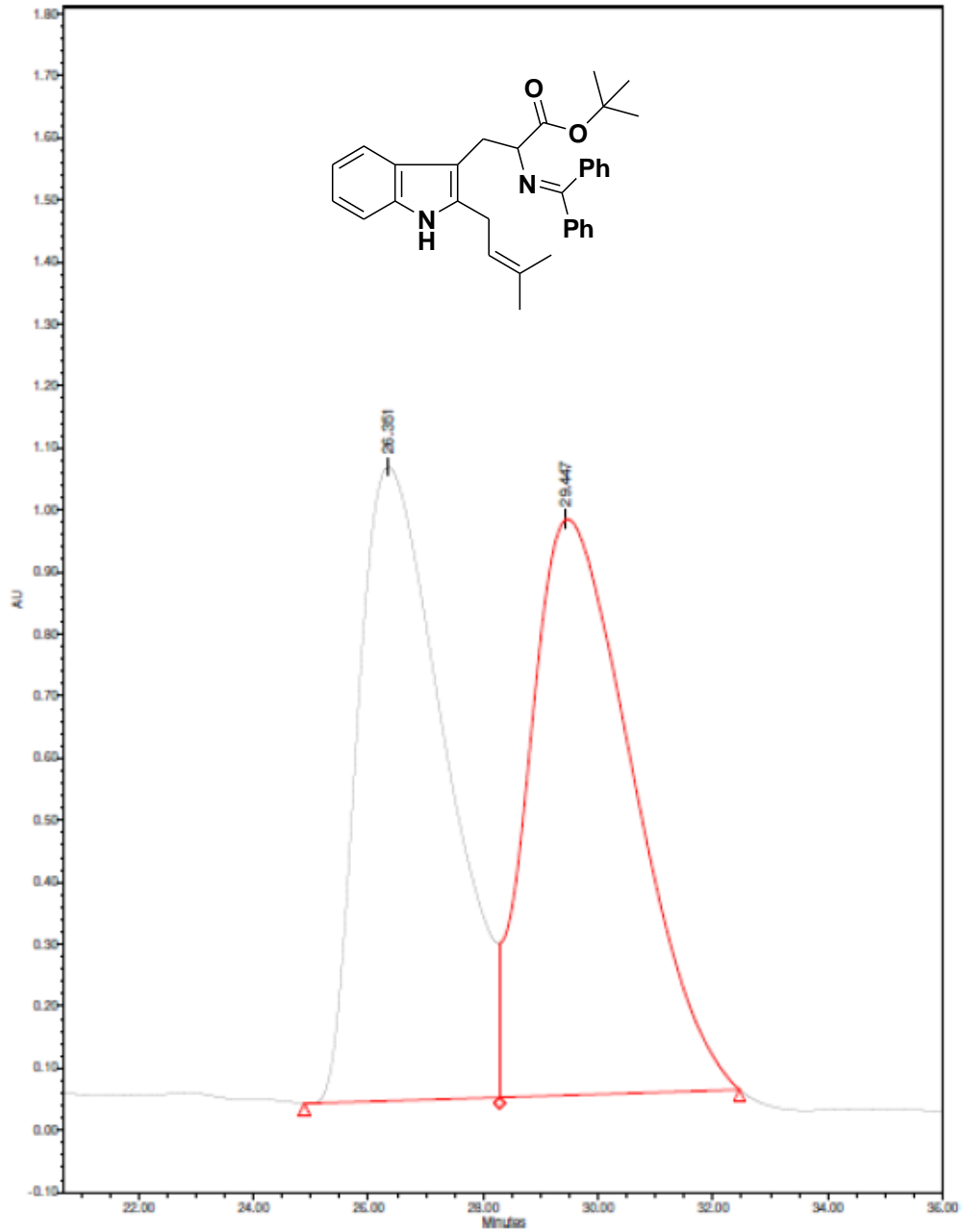
	RT (min)	Peak Type	Area (µV*sec)	% Area	Height (µV)	% Height	Integration Type	Response	Points Across Peak
1	26.351	Unknown	107905623	48.12	1022786	52.41	bV	1.080e+008	2040
2	29.447	Unknown	116317988	51.88	928704	47.59	Vb	1.164e+008	2504

HPLC Data of Compound 9 (Chiral)
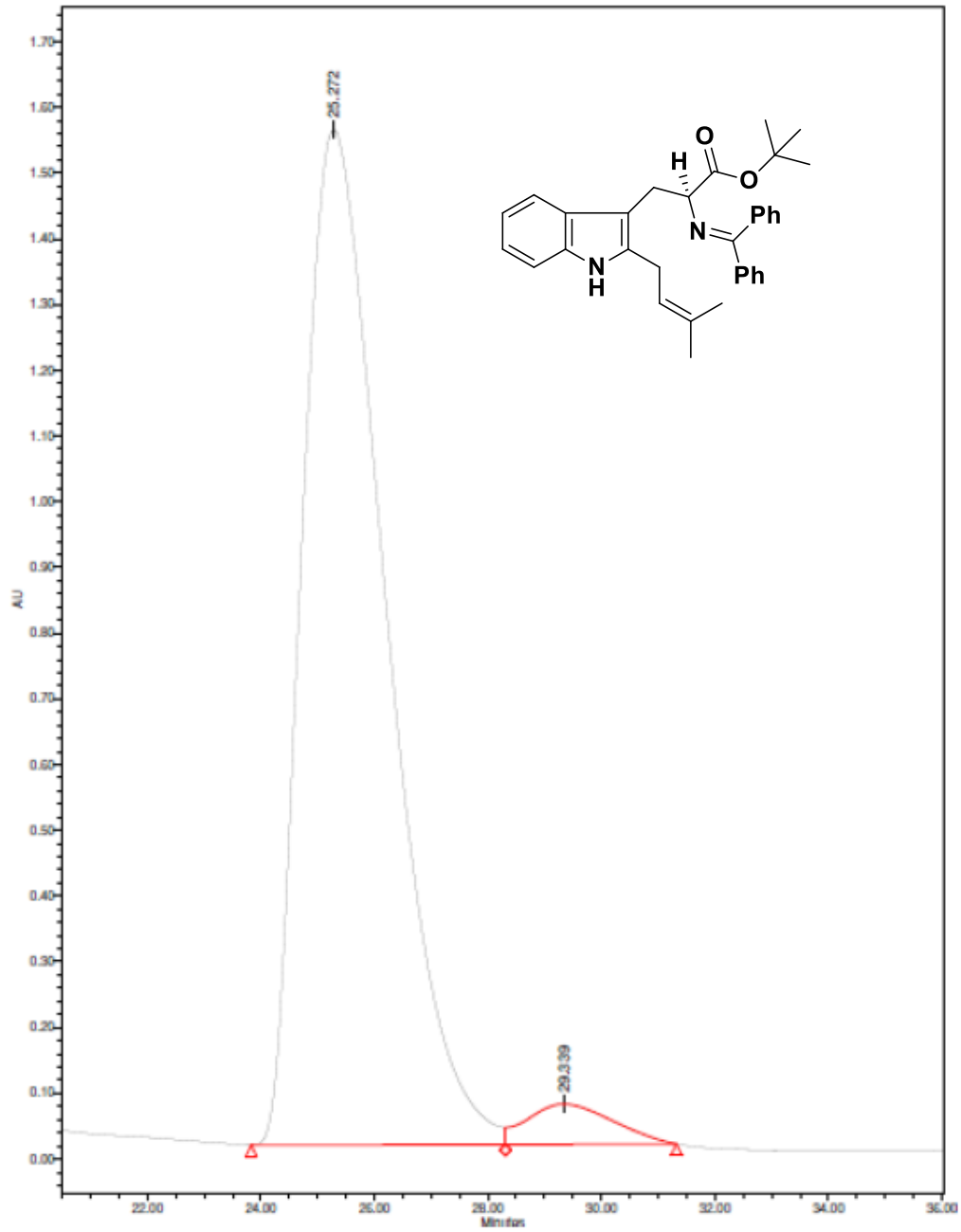
	RT (min)	Peak Type	Area (µV*sec)	% Area	Height (µV)	% Height	Integration Type	Response	Points Across Peak
1	25.272	Unknown	158038129	96.50	1544091	96.40	BV	1.591e+008	2701
2	29.339	Unknown	5734010	3.50	57647	3.60	Vb	7.819e+006	1666

^{1}H NMR Spectrum of Compound 10 in CDCl$_3$

1.46
1.78
1.96
2.87
2.90
2.92
2.95
3.22
3.24
3.27
3.29
3.48
3.50
3.73
3.74
3.76
3.77

5.29
5.32
5.34

7.08
7.10
7.11
7.13
7.15
7.25
7.27
7.57
7.60

8.52

9.46
6.01
2.20

1.22
1.21
2.12
1.16

1.03

2.31
1.37
1.16

1.00

ppm
1
2
3
4
5
6
7
8
9

^{13}C NMR Spectrum of Compound 10 in CDCl$_3$

17.95
25.32
25.78
28.04
30.54

55.93

76.87
77.30
77.73
81.01

106.57
110.59
118.23
119.21
120.68
121.06
128.80
134.14
135.40
136.02

174.58

ppm
20
30
40
50
60
70
80
90
100
110
120
130
140
150
160
170
180
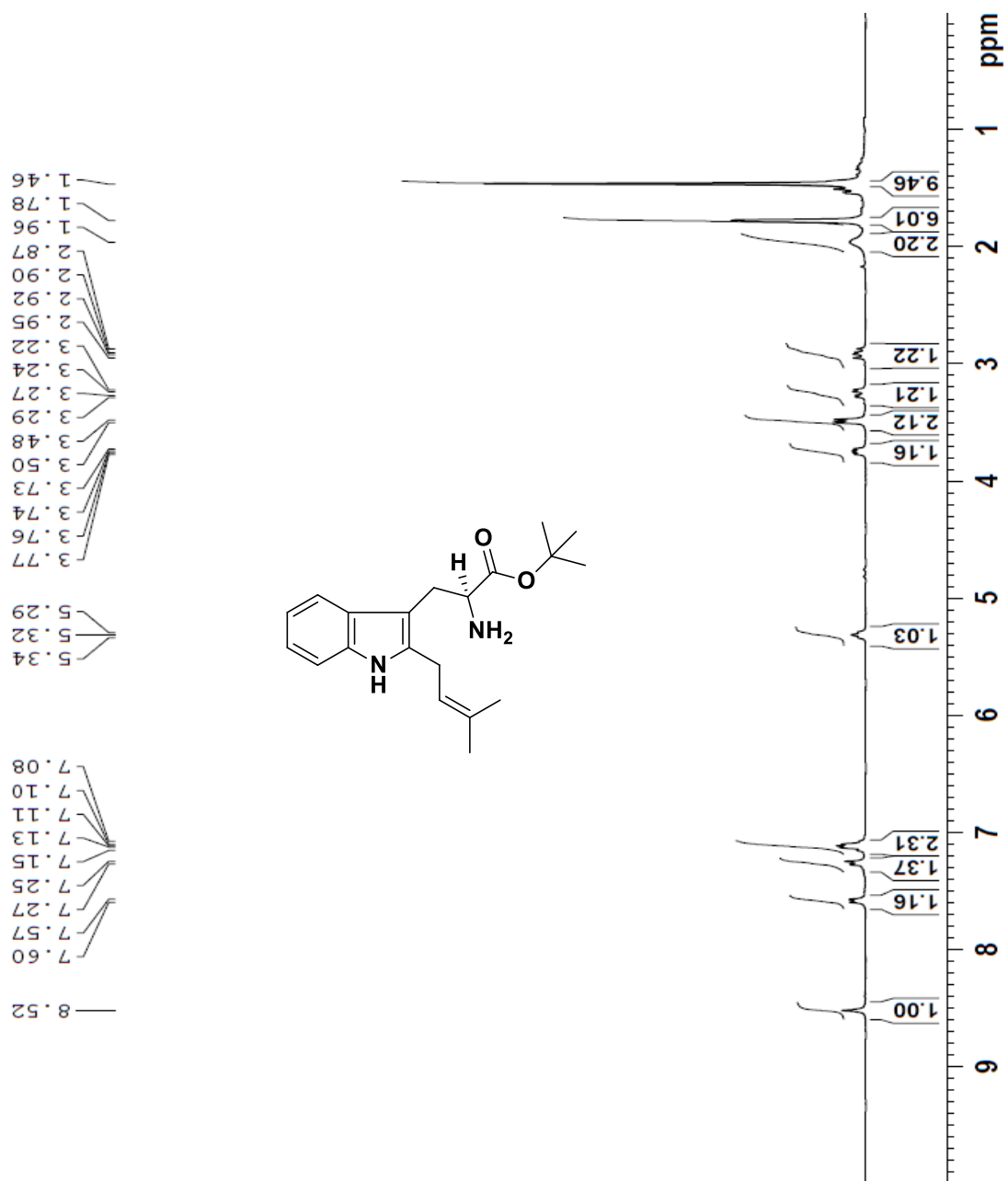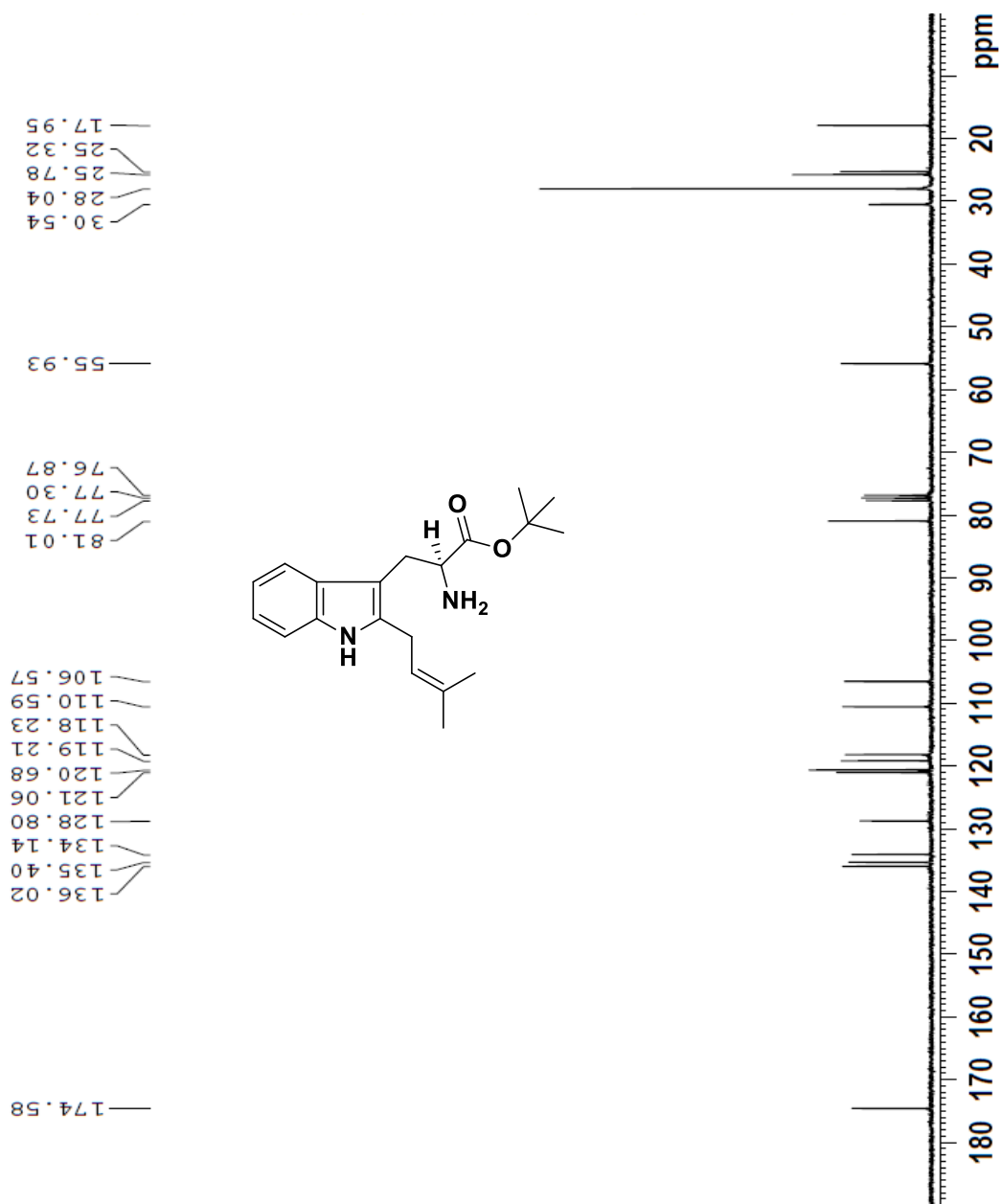
HRMS of Compound 10

^{1}H NMR Spectrum of Compound 12 in CDCl$_3$

1.36
1.61
1.63
1.65
1.68
1.70
1.78
1.80
2.02
2.89
2.90
2.91
2.92
2.94
2.96
2.98
3.00
3.16
3.17
3.18
3.21
3.23
3.48
3.50
3.53
3.68
3.70
3.71
3.73
4.71
4.73
5.34
7.03
7.05
7.06
7.07
7.08
7.09
7.09
7.11
7.24
7.27
7.27
7.28
7.53
7.56
7.96
8.00
8.03

9.17
3.04
3.37
3.31
1.37

2.21
2.33
2.05
1.20

1.12

1.03

2.36
1.34
1.14

1.00
0.80

ppm
1
2
3
4
5
6
7
8
9

^{13}C NMR Spectrum of Compound 12 in CDCl$_3$

17.94
25.24
25.79
27.16
27.89
30.42

46.99

53.46

60.19

76.62
76.84
77.04
77.25
77.46
77.68
81.64

105.94
110.28
118.44
119.14
120.16
121.00
129.12
134.86
135.04
135.66

171.28
173.60

ppm

20
30
40
50
60
70
80
90
100
110
120
130
140
150
160
170

HRMS of Compound 12

Event#: 1 MS(E+)   Ret. Time : 0.133 -> 0.333 - 0.013 -> 0.046   Scan# : 21 -> 51 - 3 -> 7
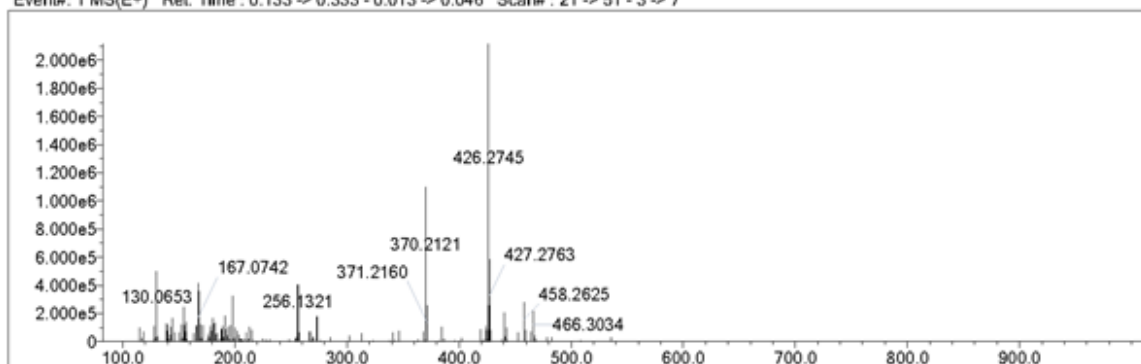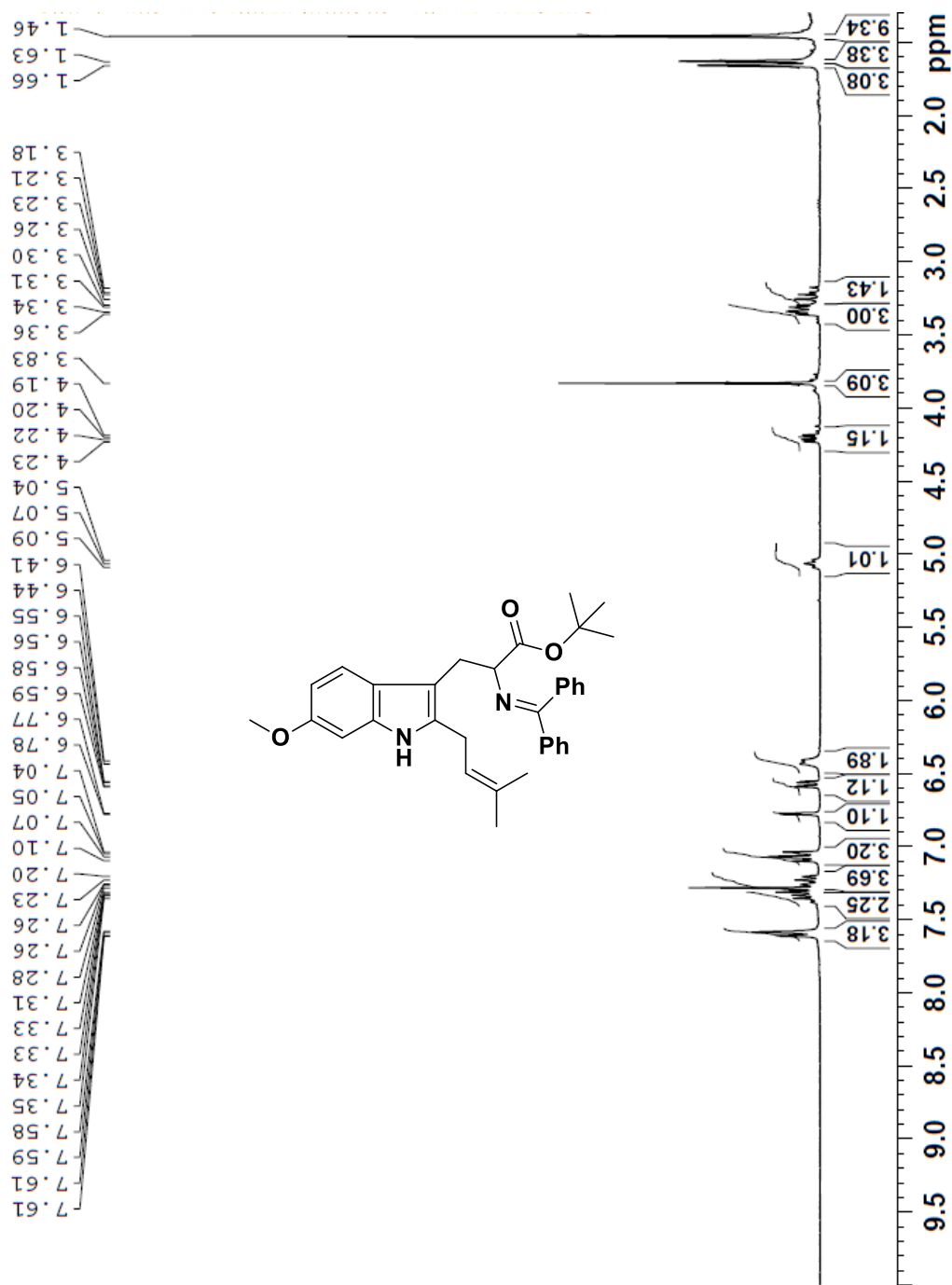
Measured region for 426.2745 m/z
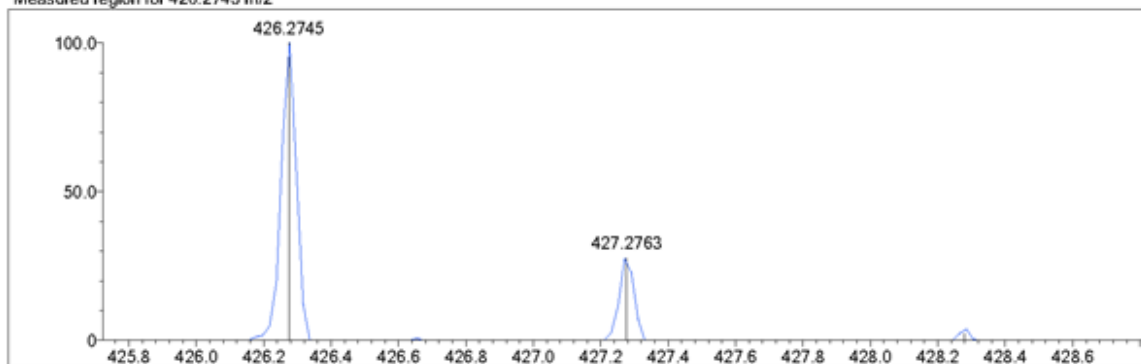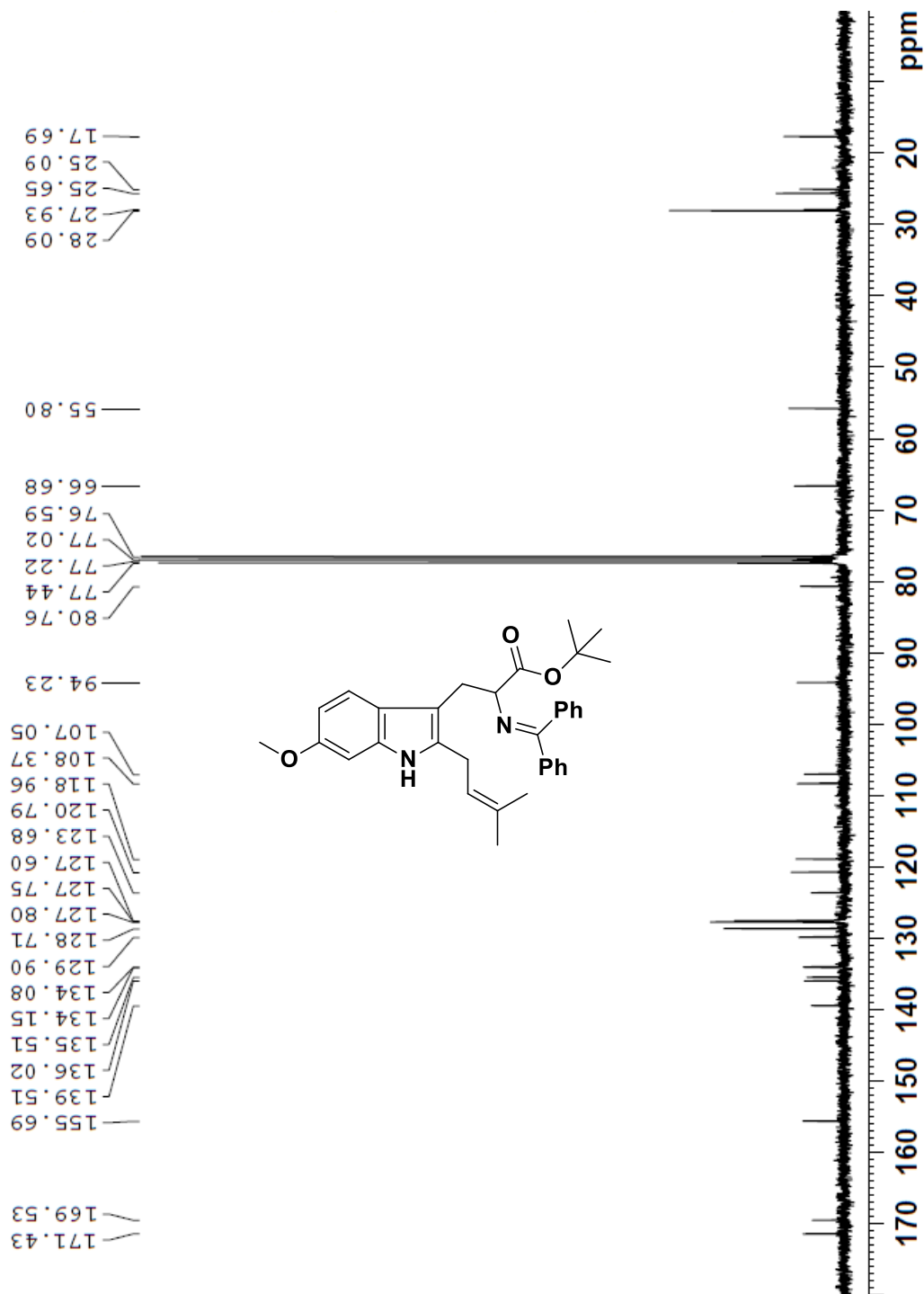
C25 H35 N3 O3 [M+H]+ : Predicted region for 426.2751 m/z
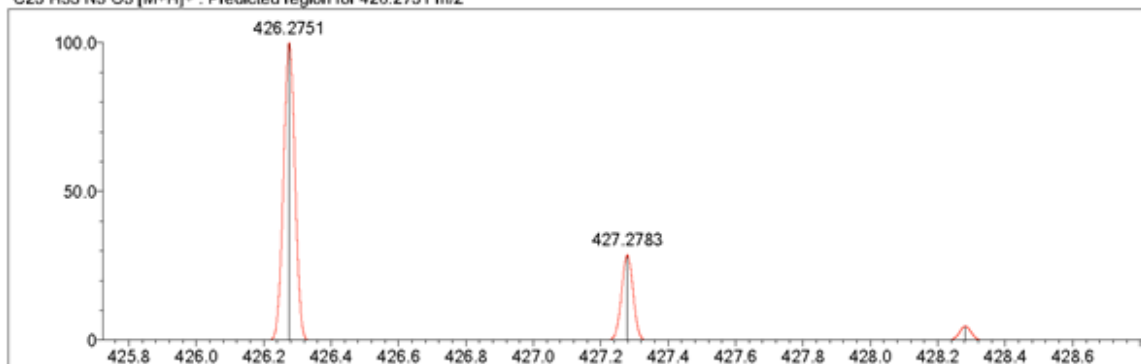
Rank	Score	Formula (M)	Ion	Meas. m/z	Pred. m/z	Df. (mDa)	Df. (ppm)	Iso	DBE
1	93.73	C25 H35 N3 O3	[M+H]+	426.2745	426.2751	-0.6	-1.41	94.70	10.0

^{1}H NMR Spectrum of Compound 15 in CDCl$_3$

1.95
2.01
2.03
2.03
2.05
2.06
2.09
2.11
2.12
2.14
2.34
2.37
2.38
2.40
2.42
3.52
3.53
3.56
3.57
3.59
3.60
3.62
3.64
3.65
3.69
3.87
3.88
3.92
3.93
4.07
4.12

7.10
7.28

1.15
2.28
1.15

2.23
1.12
2.13

1.00
0.21

ppm
1
2
3
4
5
6
7
8
9

^{13}C NMR Spectrum of Compound 15 in CDCl3

22.41
28.46
45.31
46.63
58.54
76.63
77.06
77.48
163.54
170.08

ppm
20
30
40
50
60
70
80
90
100
110
120
130
140
150
160
170

190

^{1}H NMR Spectrum of Tryprostatin B 16 in CDCl$_3$

1.78
1.81
1.92
1.93
2.02
2.03
2.03
2.05
2.06
2.34
2.35
2.91
2.95
2.98
2.98
3.00
3.48
3.49
3.51
3.61
3.62
3.63
3.63
3.67
3.68
3.69
3.71
3.71
3.72
4.08
4.37
4.38
4.39
4.40
5.32
5.33
5.66
7.10
7.12
7.13
7.16
7.18
7.19
7.28
7.33
7.34
7.49
7.51
8.03

3.30
3.00
1.39
2.39
1.26
1.25
2.14
1.34
2.31
1.07
1.04
1.24
1.01
1.38
1.29
1.45
1.30
1.08

9 8 7 6 5 4 3 2 1 ppm

^{13}C NMR Spectrum of Tryprostatin B 16 in CDCl$_3$

18.01
22.66
25.13
25.62
25.77
28.37

45.43

54.59
59.29

76.79
77.05
77.30

104.65
110.81
117.76
119.72
119.93
121.89
128.01
135.46
135.53
136.44

165.83
169.38

ppm
20
30
40
50
60
70
80
90
100
110
120
130
140
150
160
170

HRMS of Tryprostatin B 16

Event#: 1 MS(E+)   Ret. Time : 0.380 -> 0.780 - 0.153 -> 0.316   Scan# : 115 -> 235 - 47 -> 95
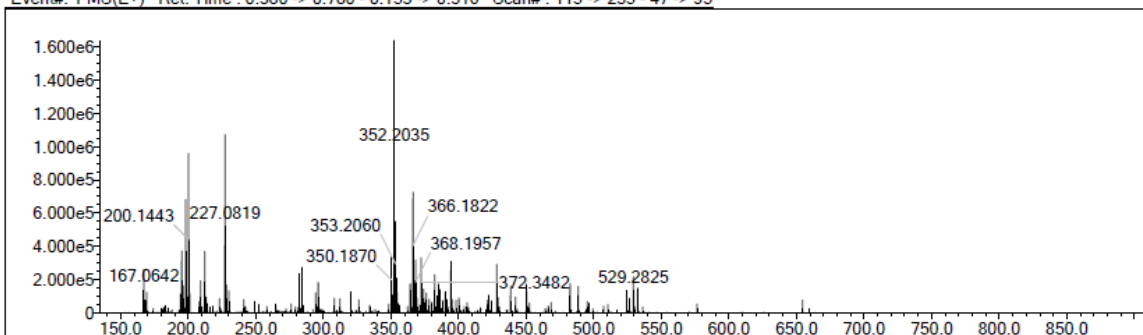
Measured region for 352.2035 m/z
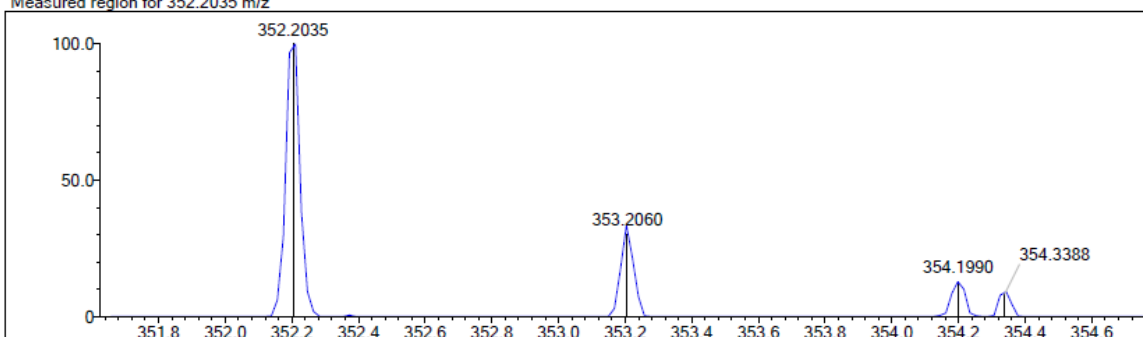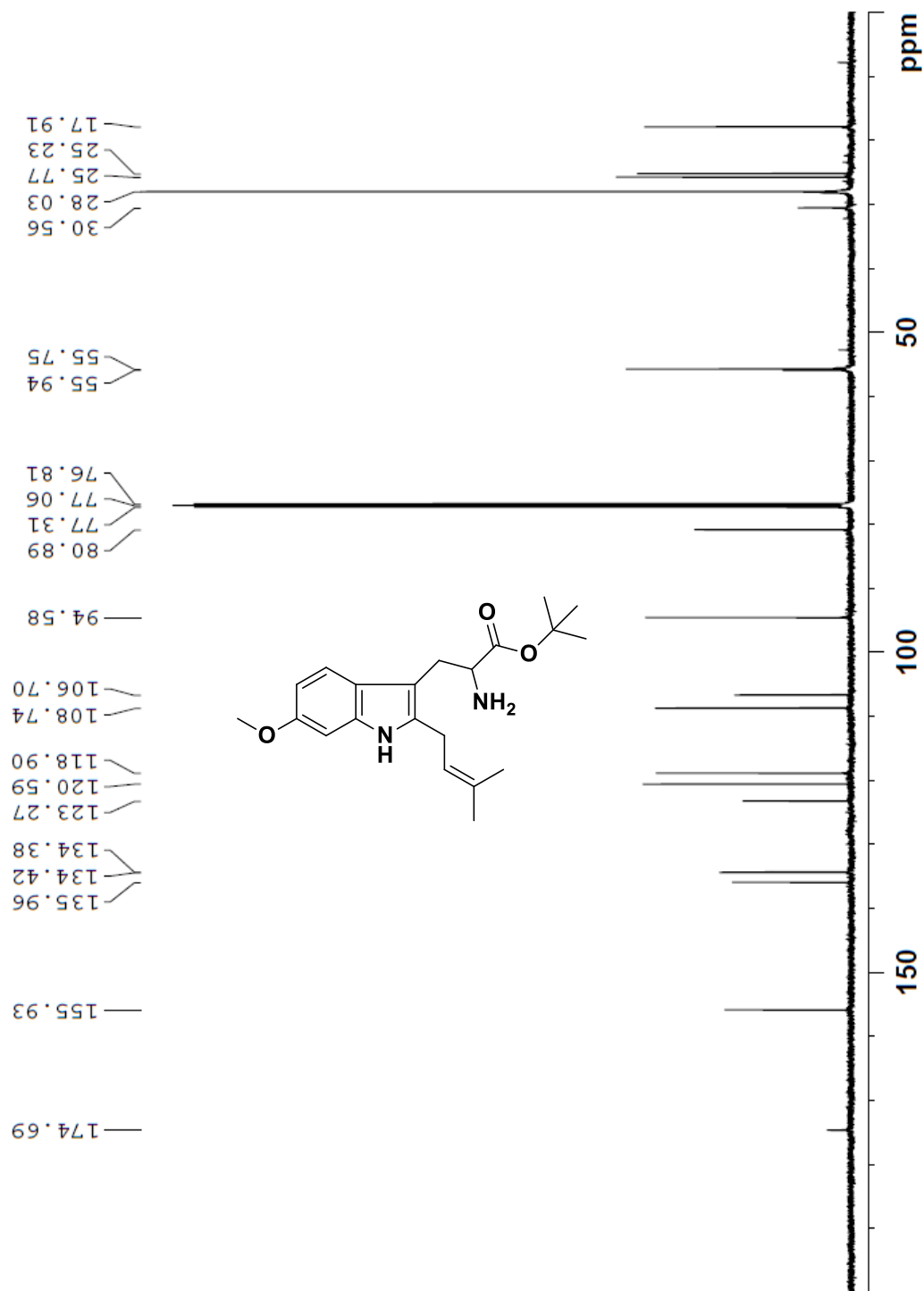
C21 H25 N3 O2 [M+H]+ : Predicted region for 352.2020 m/z
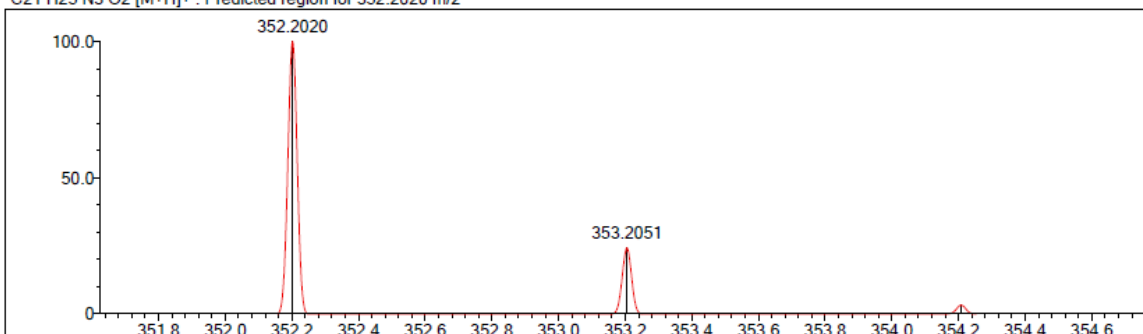
Rank	Score	Formula (M)	Ion	Meas. m/z	Pred. m/z	Df. (mDa)	Df. (ppm)	Iso	DBE
3	47.69	C21 H25 N3 O2	[M+H]+	352.2035	352.2020	1.5	4.26	51.92	11.0

^{1}H NMR Spectrum of Compound 17 in CDCl₃
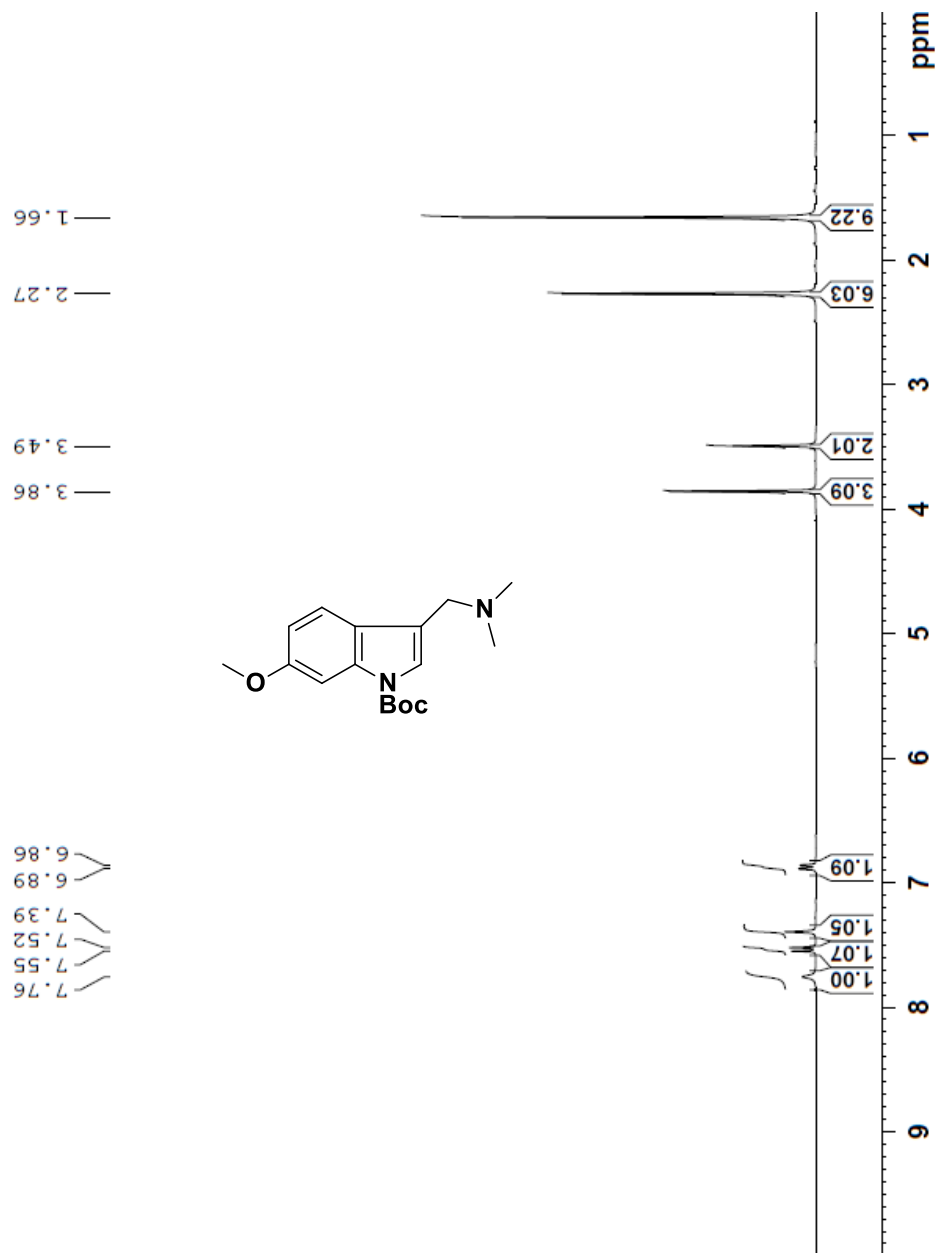
1.66
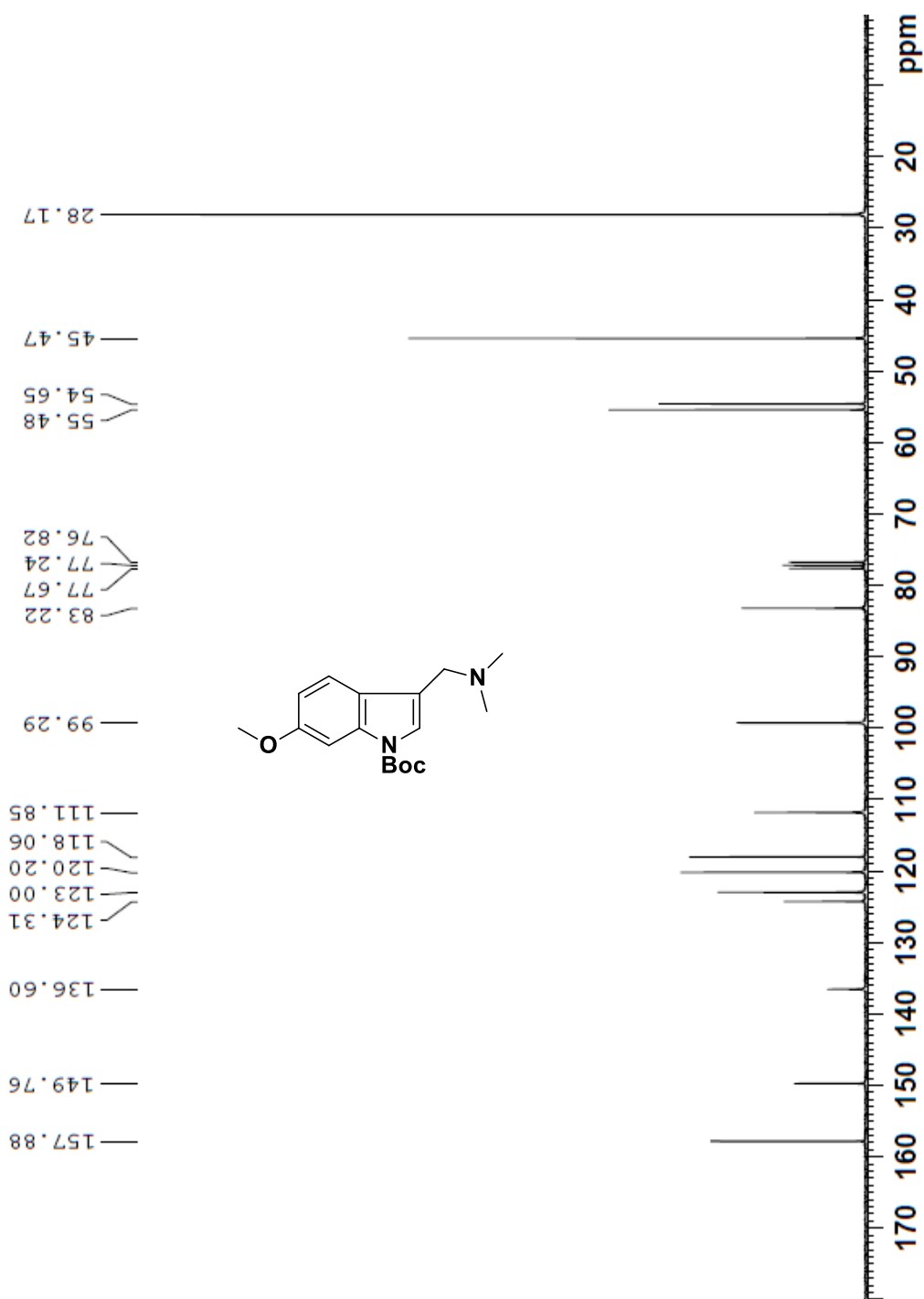
2.27

3.49

3.86

6.86
6.89

7.39
7.52
7.55
7.76

9.22

6.03

2.01

3.09

1.09

1.05
1.07
1.00

ppm

1 2 3 4 5 6 7 8 9

¹³C NMR Spectrum of Compound 17 in CDCl₃

28.17
45.47
54.65
55.48
76.82
77.24
77.67
83.22
99.29
111.85
118.06
120.20
123.00
124.31
136.60
149.76
157.88
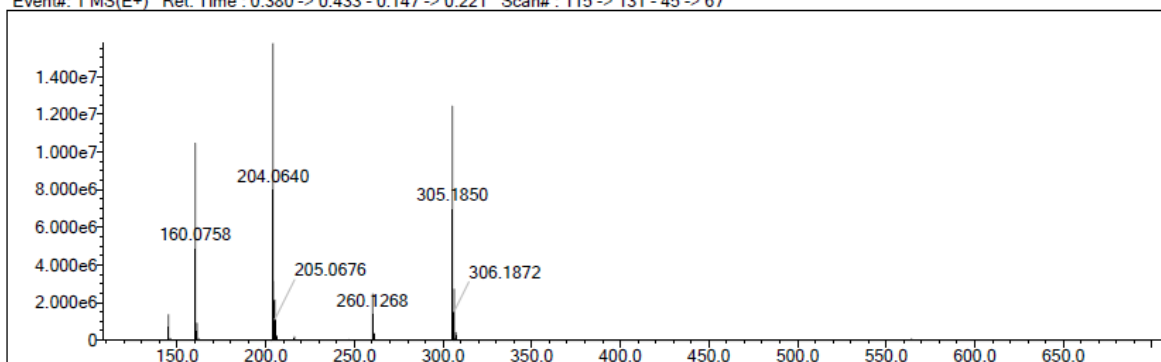
HRMS of Compound 17

Measured region for 305.1850 m/z
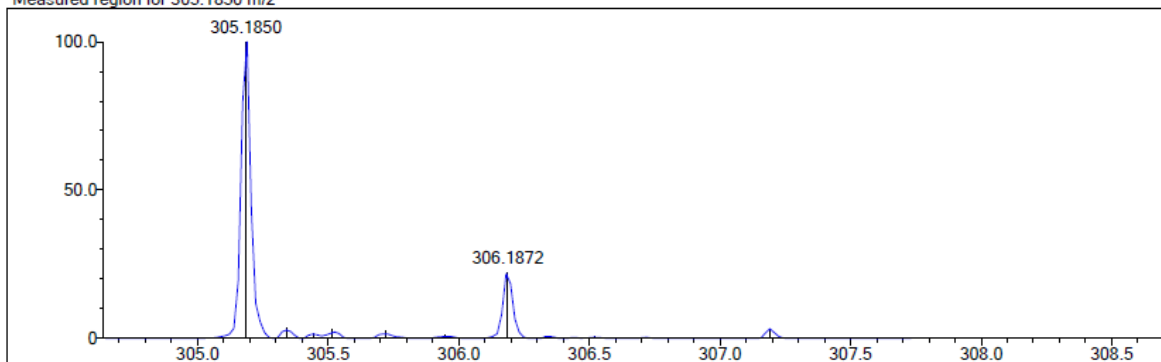
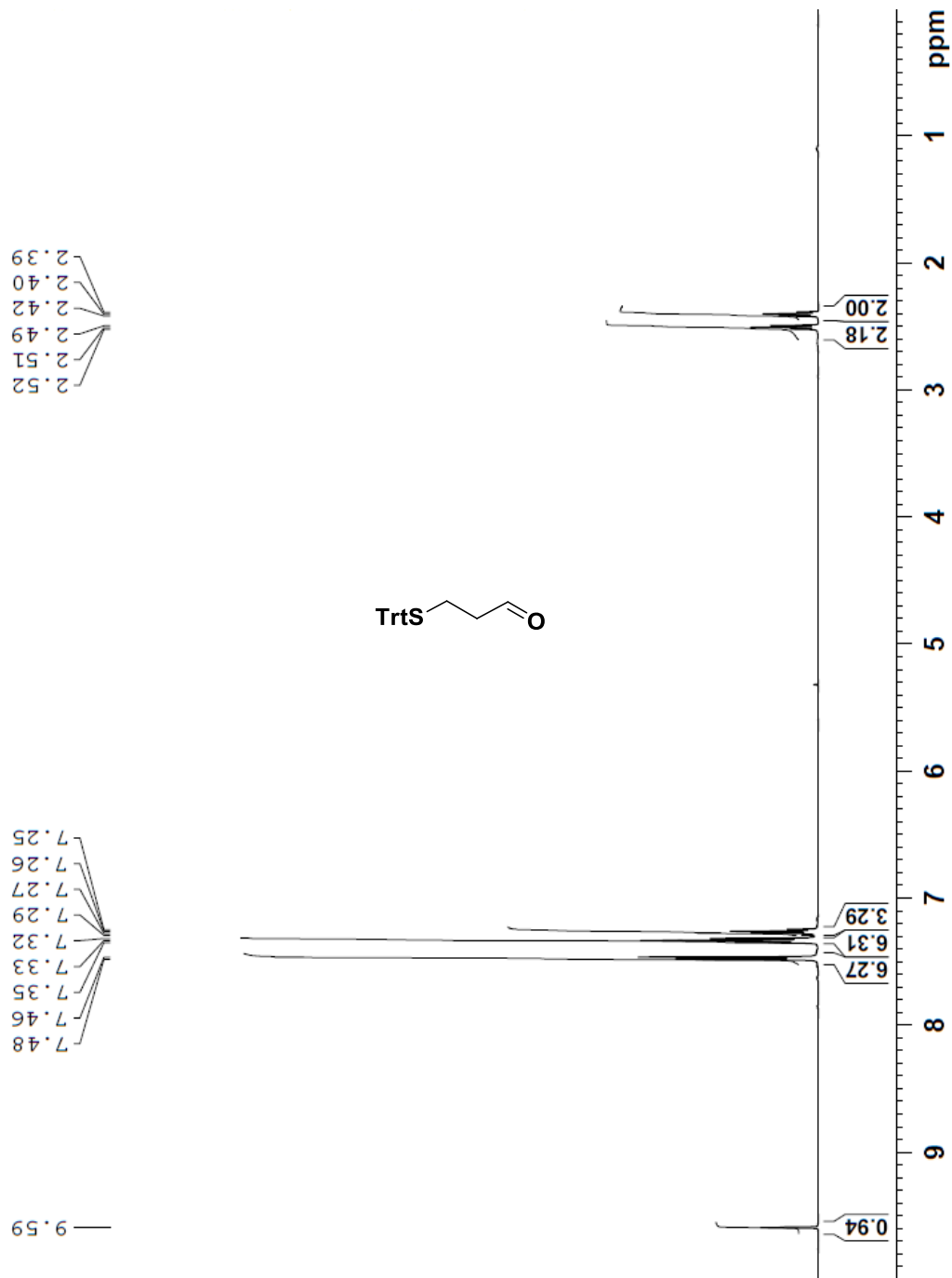C17 H24 N2 O3 [M+H]+ : Predicted region for 305.1860 m/z
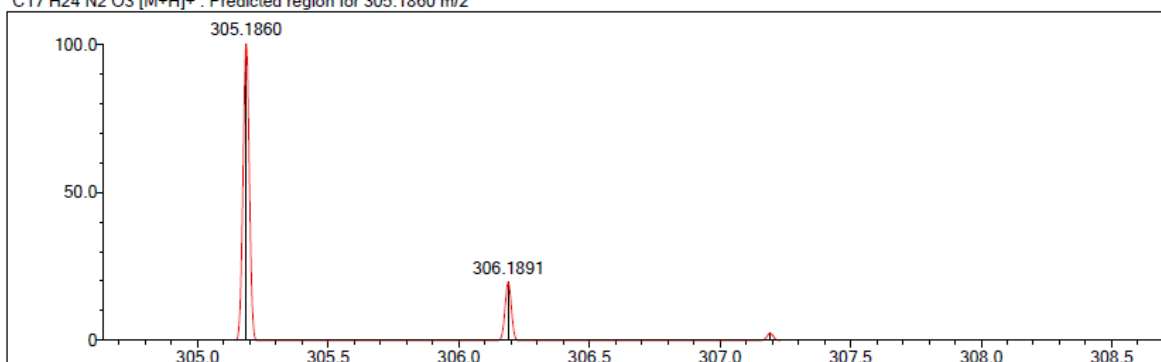
Rank	Score	Formula (M)	Ion	Meas. m/z	Pred. m/z	Df. (mDa)	Df. (ppm)	Iso	DBE
1	93.03	C17 H24 N2 O3	[M+H]+	305.1850	305.1860	-1.0	-3.28	98.65	7.0

^{1}H NMR Spectrum of Compound 18 in CDCl$_3$
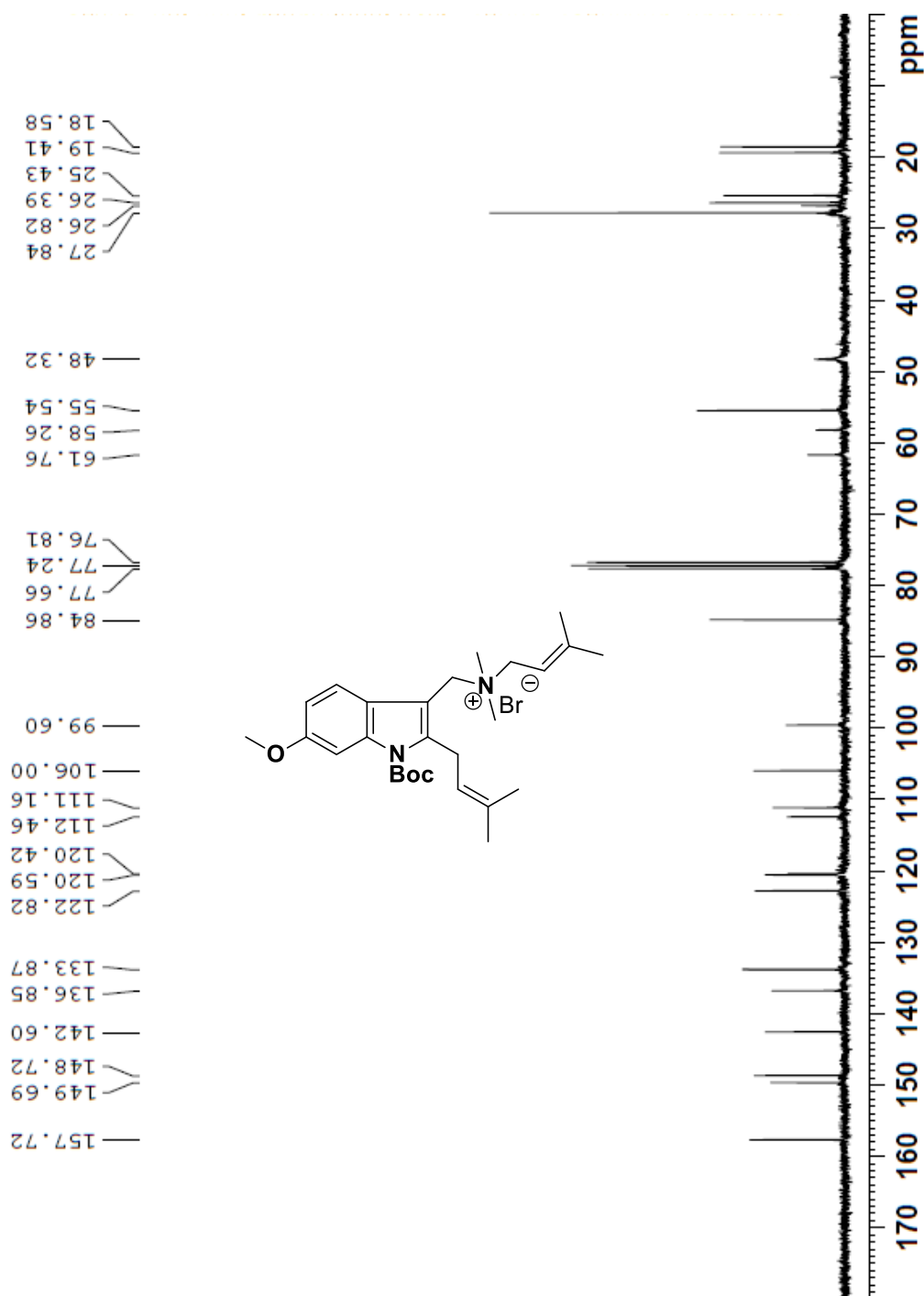
HRMS of Compound 18
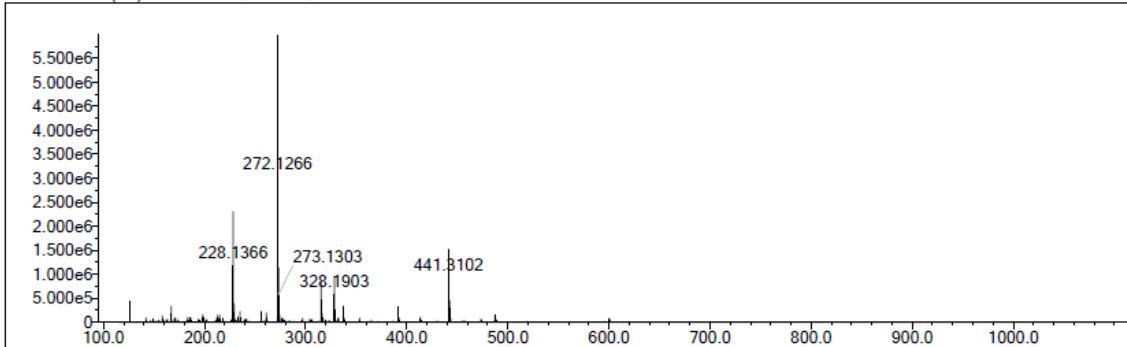
Measured region for 441.3102 m/z
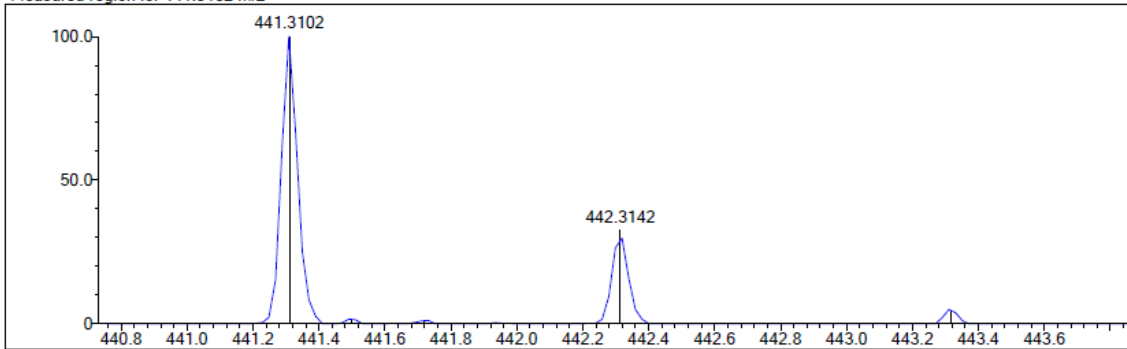
C27 H40 N2 O3 [M+H]+ : Predicted region for 441.3112 m/z
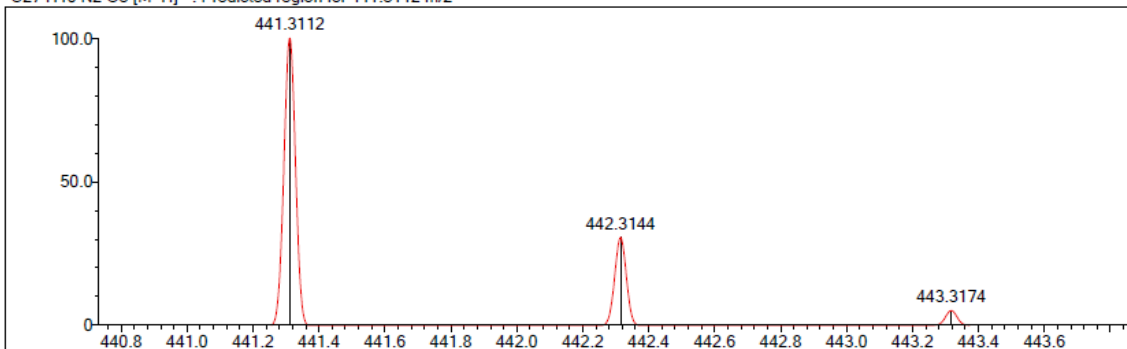
Rank	Score	Formula (M)	Ion	Meas. m/z	Pred. m/z	Df. (mDa)	Df. (ppm)	Iso	DBE
1	94.00	C27 H40 N2 O3	[M+H]+	441.3102	441.3112	-1.0	-2.27	97.08	9.0

199

^{1}H NMR Spectrum of Compound 19 in CDCl$_3$

9.34

3.38

3.08

1.43

3.00

3.09

1.15

1.01

1.89

1.12

1.10

3.20

3.69

2.25

3.18

ppm

2.0

2.5

3.0

3.5

4.0

4.5

5.0

5.5

6.0

6.5

7.0

7.5

8.0

8.5

9.0

9.5

1.46
1.63
1.66

3.18
3.21
3.23
3.26
3.30
3.31
3.34
3.36
3.83
4.19
4.20
4.22
4.23
5.04
5.07
5.09
6.41
6.44
6.55
6.56
6.58
6.59
6.77
6.78
7.04
7.05
7.07
7.10
7.20
7.23
7.26
7.26
7.28
7.31
7.33
7.33
7.34
7.35
7.58
7.59
7.61
7.61

^{13}C NMR Spectrum of Compound 19 in CDCl$_3$

17.69
25.09
25.65
27.93
28.09

55.80

66.89
76.59
77.02
77.22
77.44
80.76

94.23

107.05
108.37
118.96
120.79
123.68
127.60
127.75
127.80
128.71
129.90
134.08
134.15
135.51
136.02
139.51
155.69

169.53
171.43

ppm
20
30
40
50
60
70
80
90
100
110
120
130
140
150
160
170

HRMS of Compound 19

Event#: 1 MS(E+)   Ret. Time : 0.693 -> 0.867 - 0.440 -> 0.539   Scan# : 105 -> 131 - 67 -> 81
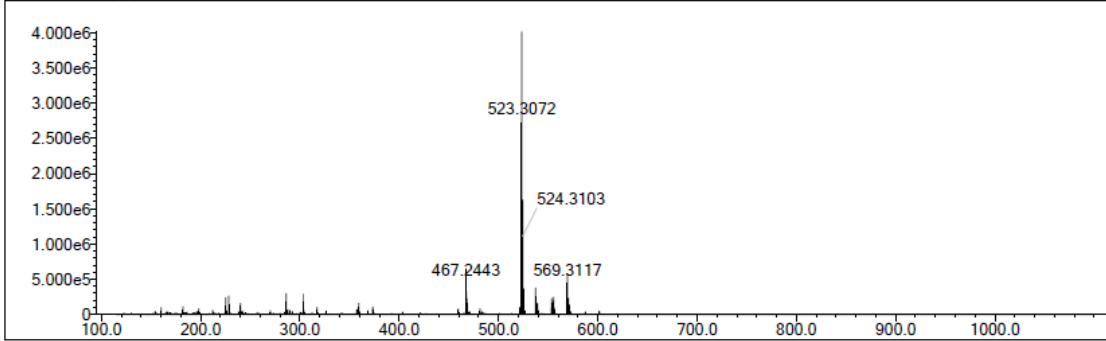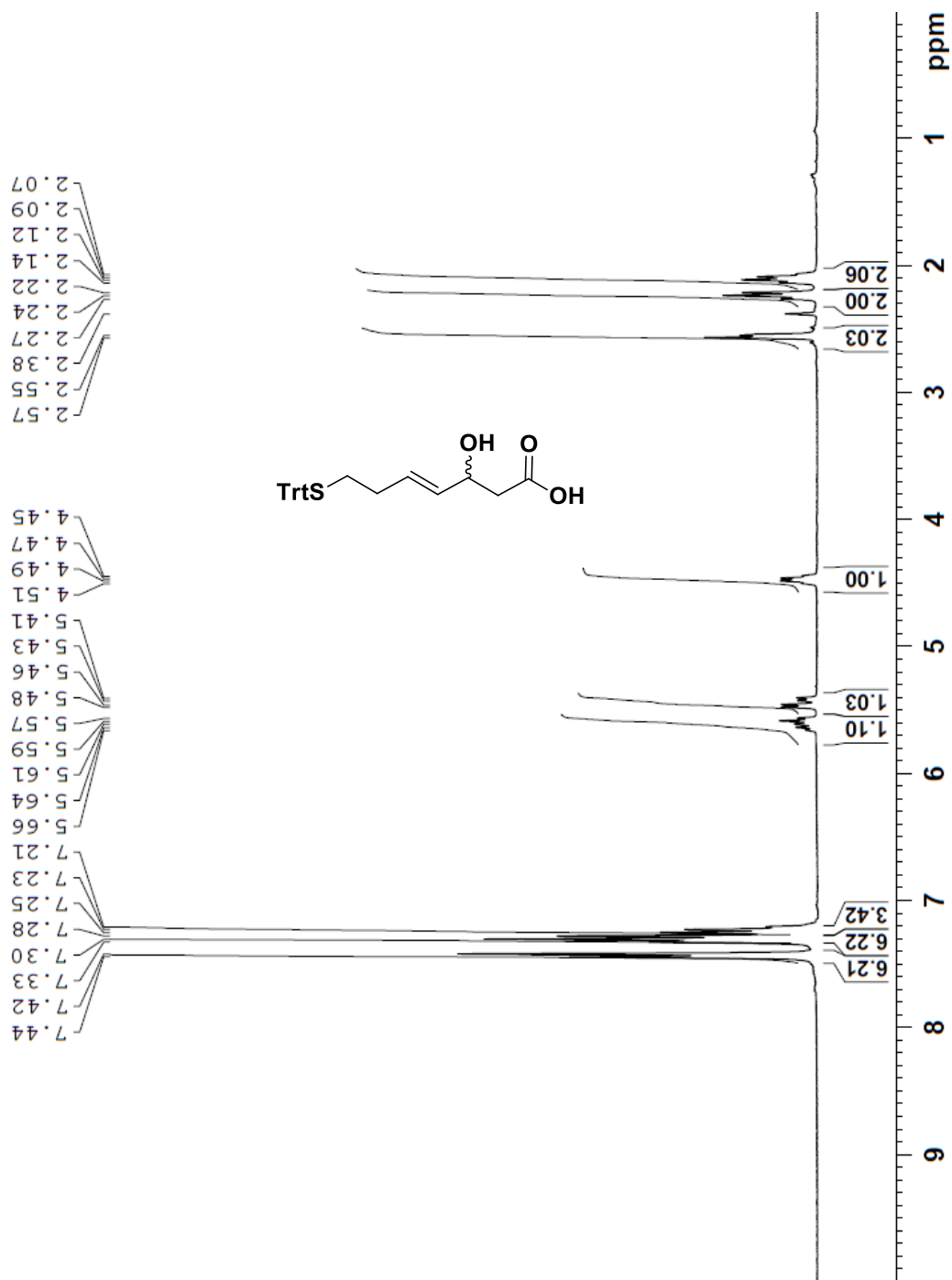

Measured region for 523.3072 m/z
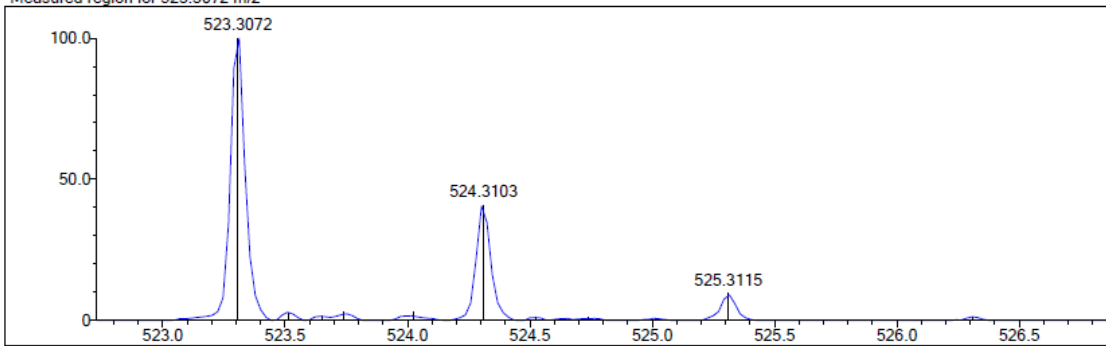
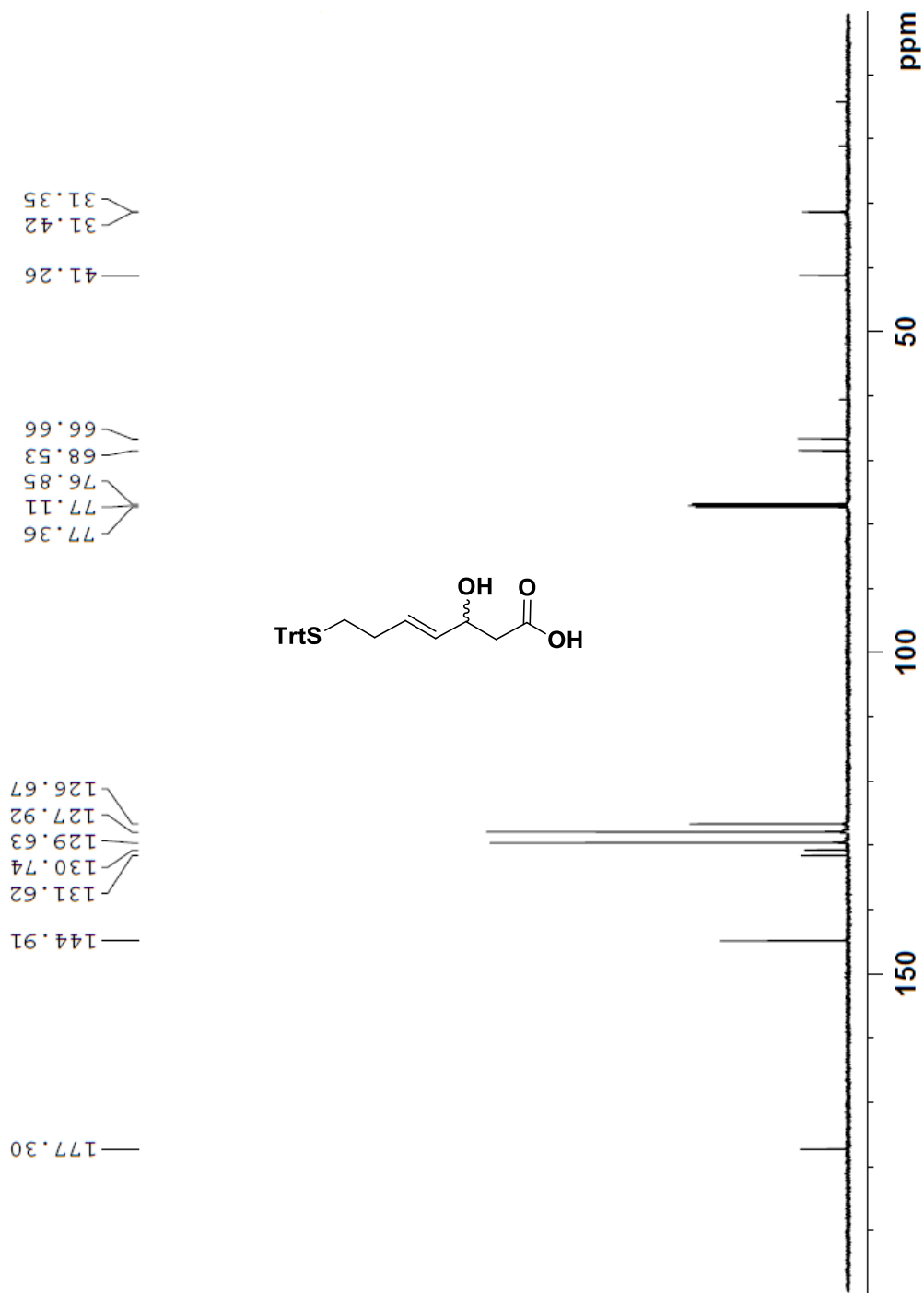C34 H38 N2 O3 [M+H]+ : Predicted region for 523.2955 m/z
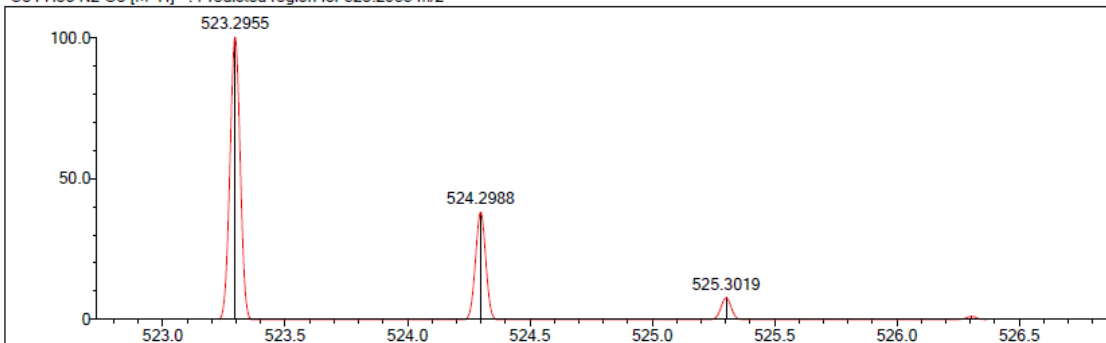
Rank	Score	Formula (M)	Ion	Meas. m/z	Pred. m/z	Df. (mDa)	Df. (ppm)	Iso	DBE
9	4.52	C34 H38 N2 O3	[M+H]+	523.3072	523.2955	11.7	22.36	64.19	17.0

202

^{1}H NMR Spectrum of Compound 20 in CDCl$_3$

1.44

1.77
1.79

2.82
2.84
2.85
2.87
3.16
3.17
3.19
3.20
3.46
3.48
3.67
3.69
3.84

5.30
5.31
5.33

6.76
6.77
6.82
7.29
7.43
7.44

7.87

9.00
3.13
3.01

1.05

1.05

2.01
1.08
3.04

1.08

1.05
1.03

0.47
1.15

1.02

ppm
1
2
3
4
5
6
7
8
9

^{13}C NMR Spectrum of Compound 20 in CDCl$_3$

17.91
25.23
25.77
28.03
30.56

55.75
55.94

76.81
77.06
77.31
80.89

94.58

106.70
108.74

118.90
120.59
123.27

134.38
134.42
135.96

155.93

174.69

ppm
50
100
150
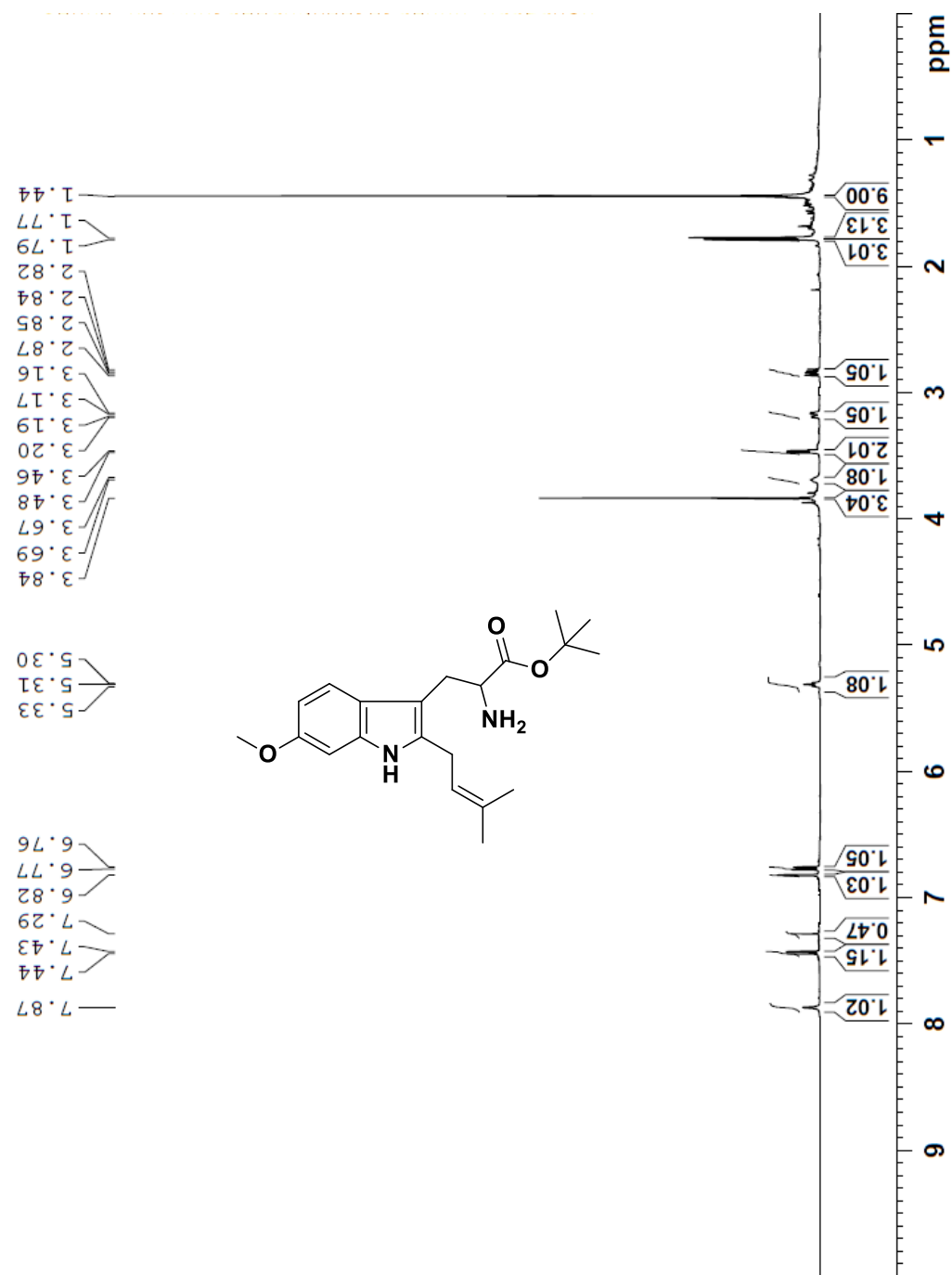
HRMS of Compound 20

Event#: 1 MS(E+) Ret. Time : 0.613 -> 1.027 - 0.347 -> 0.537 Scan# : 93 -> 155 - 53 -> 81
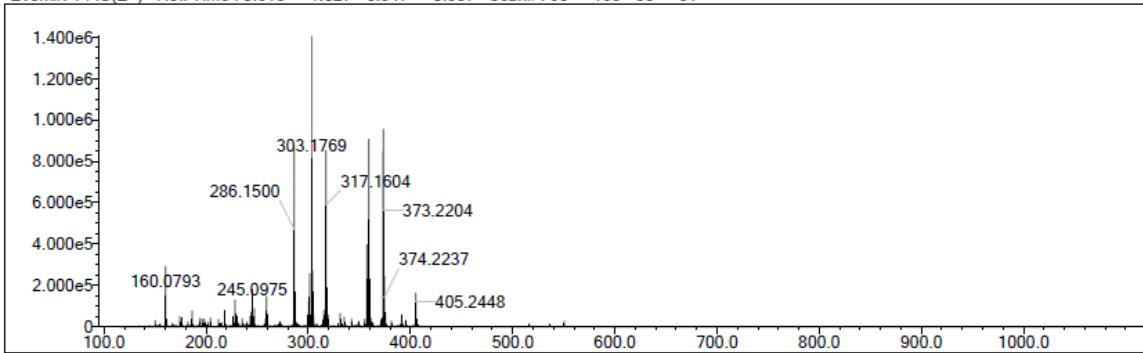
Measured region for 359.2404 m/z
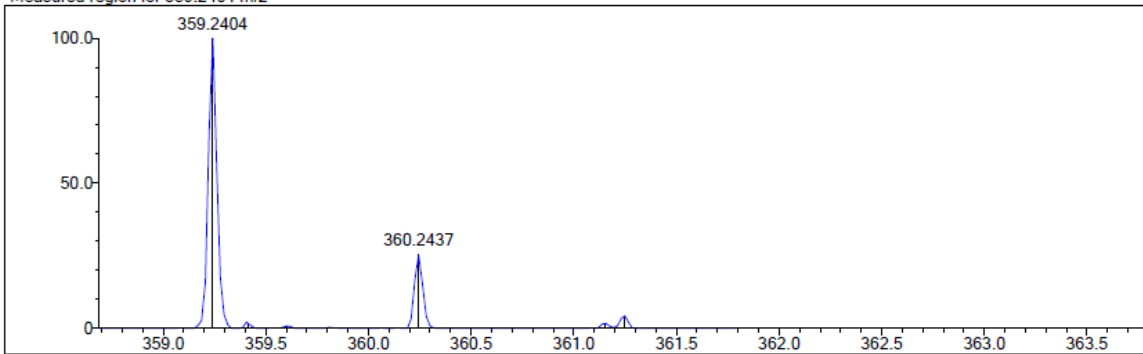
C21 H30 N2 O3 [M+H]+ : Predicted region for 359.2329 m/z
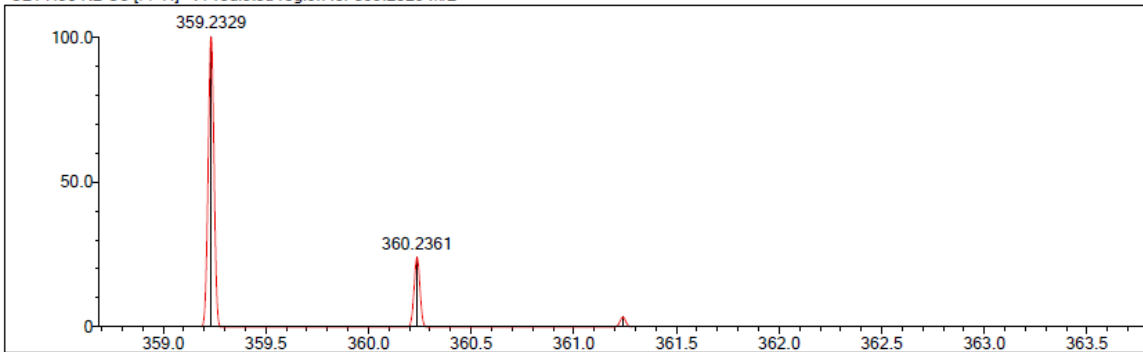
Rank	Score	Formula (M)	Ion	Meas. m/z	Pred. m/z	Df. (mDa)	Df. (ppm)	Iso	DBE
7	4.95	C21 H30 N2 O3	[M+H]+	359.2404	359.2329	7.5	20.88	45.09	8.0

PART II: SYNTHESIS AND BIOLOGICAL ASSESSMENT OF HISTONE DEACETYLASE INHIBITORS

Copies of ^{1}H NMR, ^{13}C NMR, and HRMS Spectral Data

^{1}H NMR Spectrum of Compound 3 in CDCl$_3$

2.39
2.40
2.42
2.49
2.51
2.52

7.25
7.26
7.27
7.29
7.32
7.33
7.35
7.46
7.48

9.59

TrtS\/\O

2.00
2.18

3.29
6.31
6.27

0.94

^{13}C NMR Spectrum of Compound 3 in CDCl$_3$

24.42 —

42.69 —

67.01 —
76.79
77.05
77.30

TrtS⌒⌒CHO

126.79
128.00
129.56

144.54 —

200.35 —

ppm

50

100

150

200

^{1}H NMR Spectrum of Compound 6 in CDCl$_3$

2.33
2.34
2.36
2.38
2.39

6.00
6.01
6.03
6.04
6.63
6.64
6.65
6.66
6.68
7.25
7.25
7.26
7.28
7.32
7.33
7.46
7.47

9.44
9.46
9.47
9.48

TrtS ⌒⌒⌒ O

4.36

1.00
1.03
3.46
6.25
6.46

1.02

ppm
1 2 3 4 5 6 7 8 9

^{13}C NMR Spectrum of Compound 6 in CDCl$_3$

30.05
31.75

67.02

76.81
77.06
77.32

126.82
128.01
129.56
133.66

144.59

155.80

193.78

ppm
50
100
150
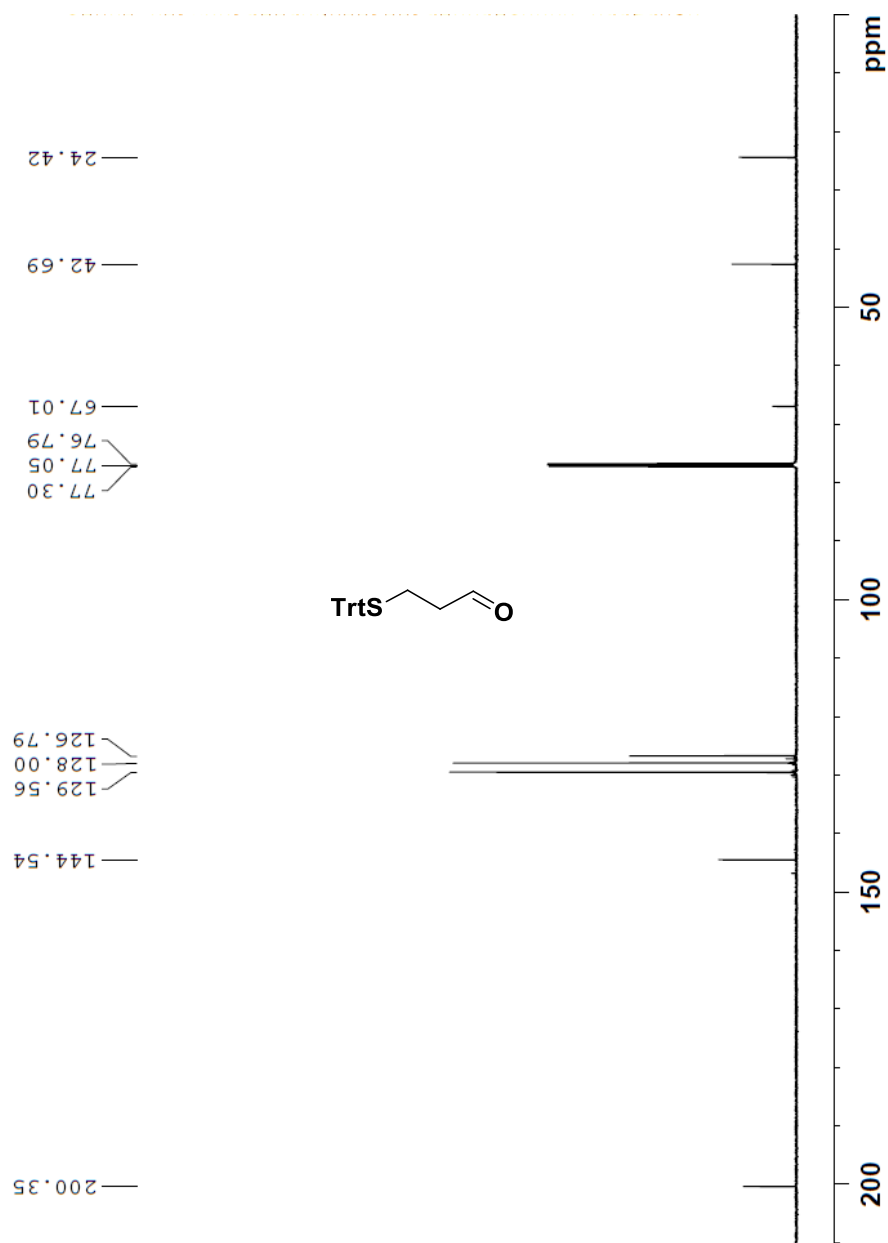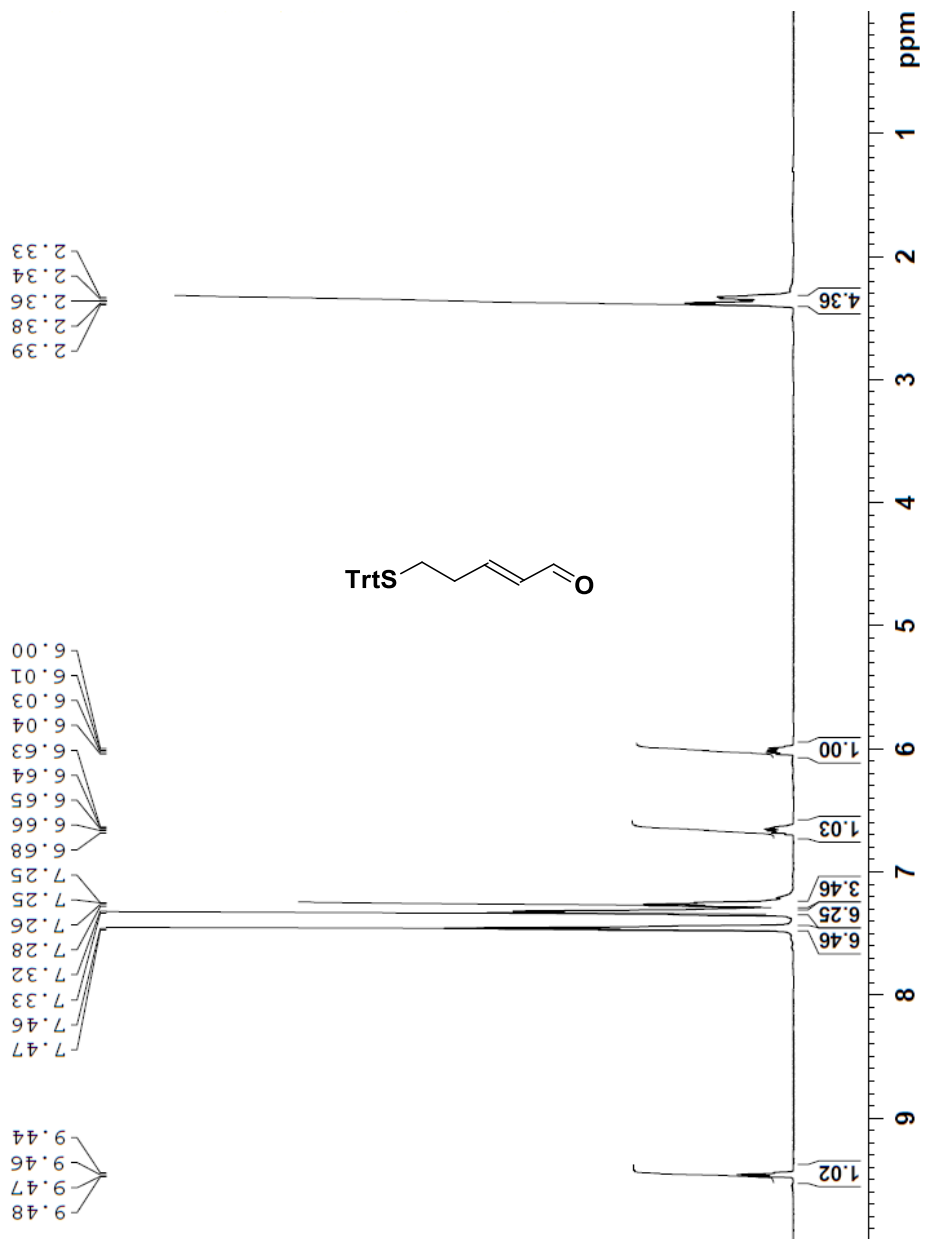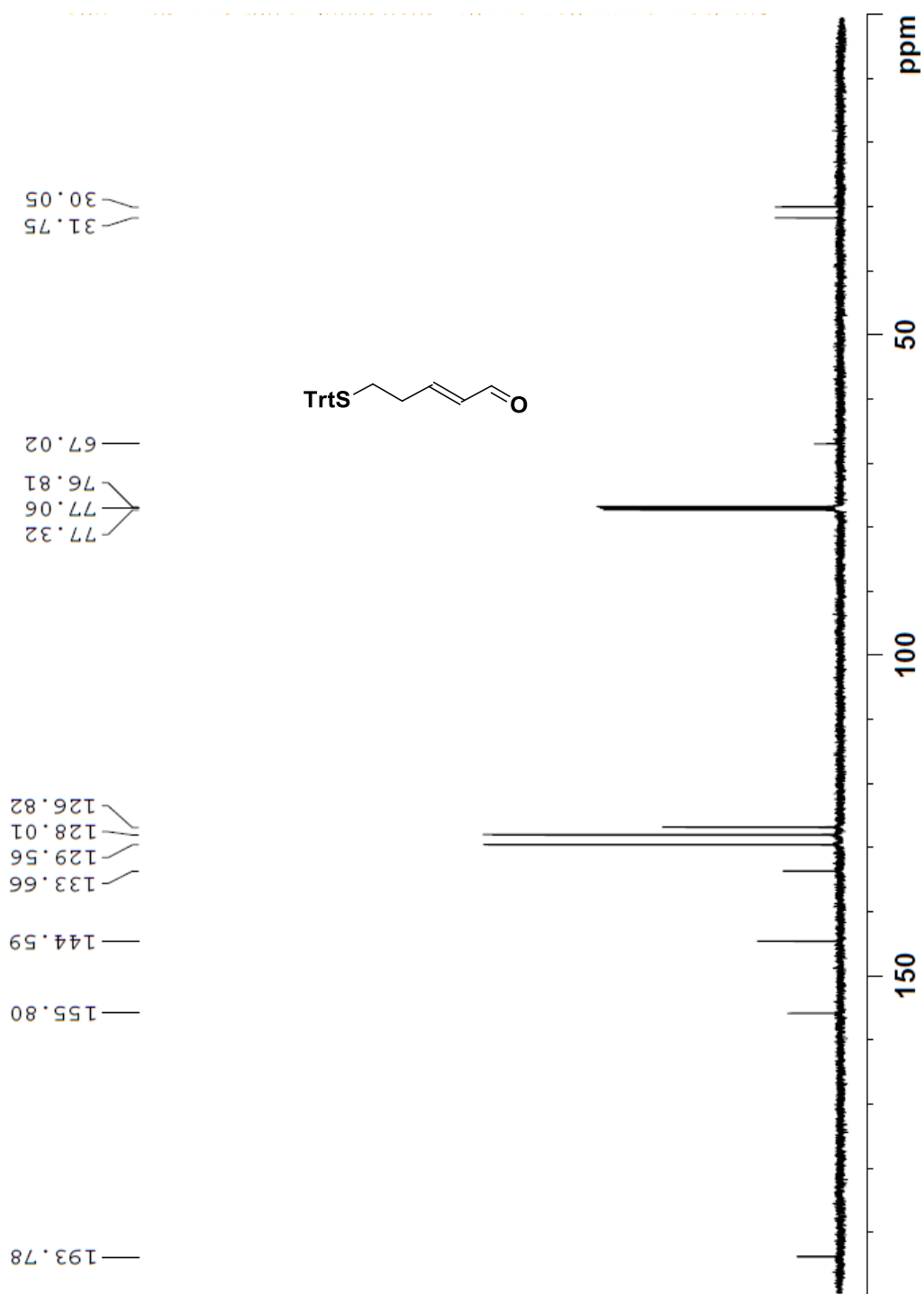
^{1}H NMR Spectrum of compound 9 in CDCl$_3$

^{13}C NMR Spectrum of Compound 9 in CDCl$_3$

28.16
31.42
31.52

42.40

66.61
68.72
76.86
77.11
77.37
81.38

126.64
127.90
129.63
129.94
132.10

144.94

171.84

ppm

50

100

150
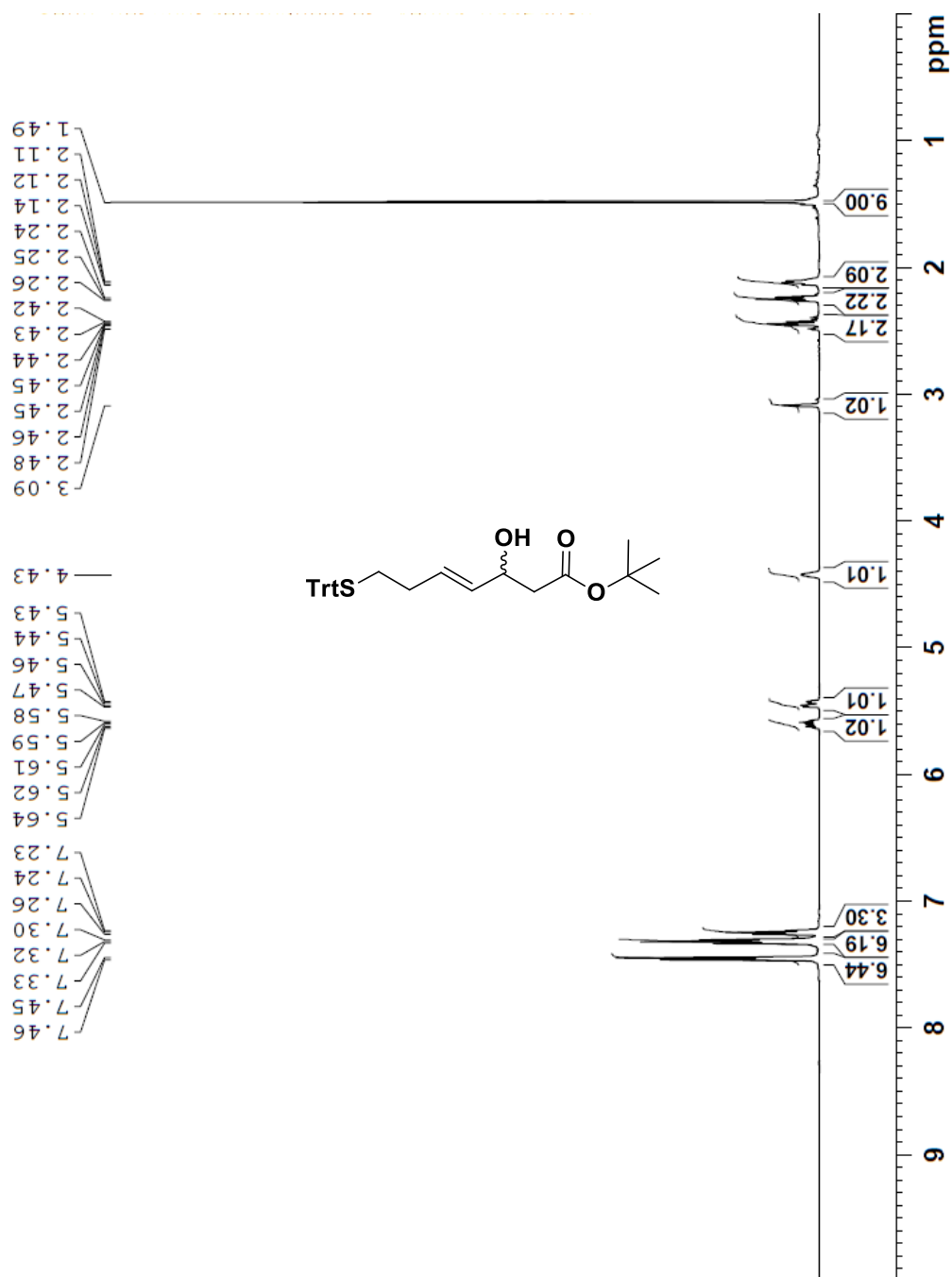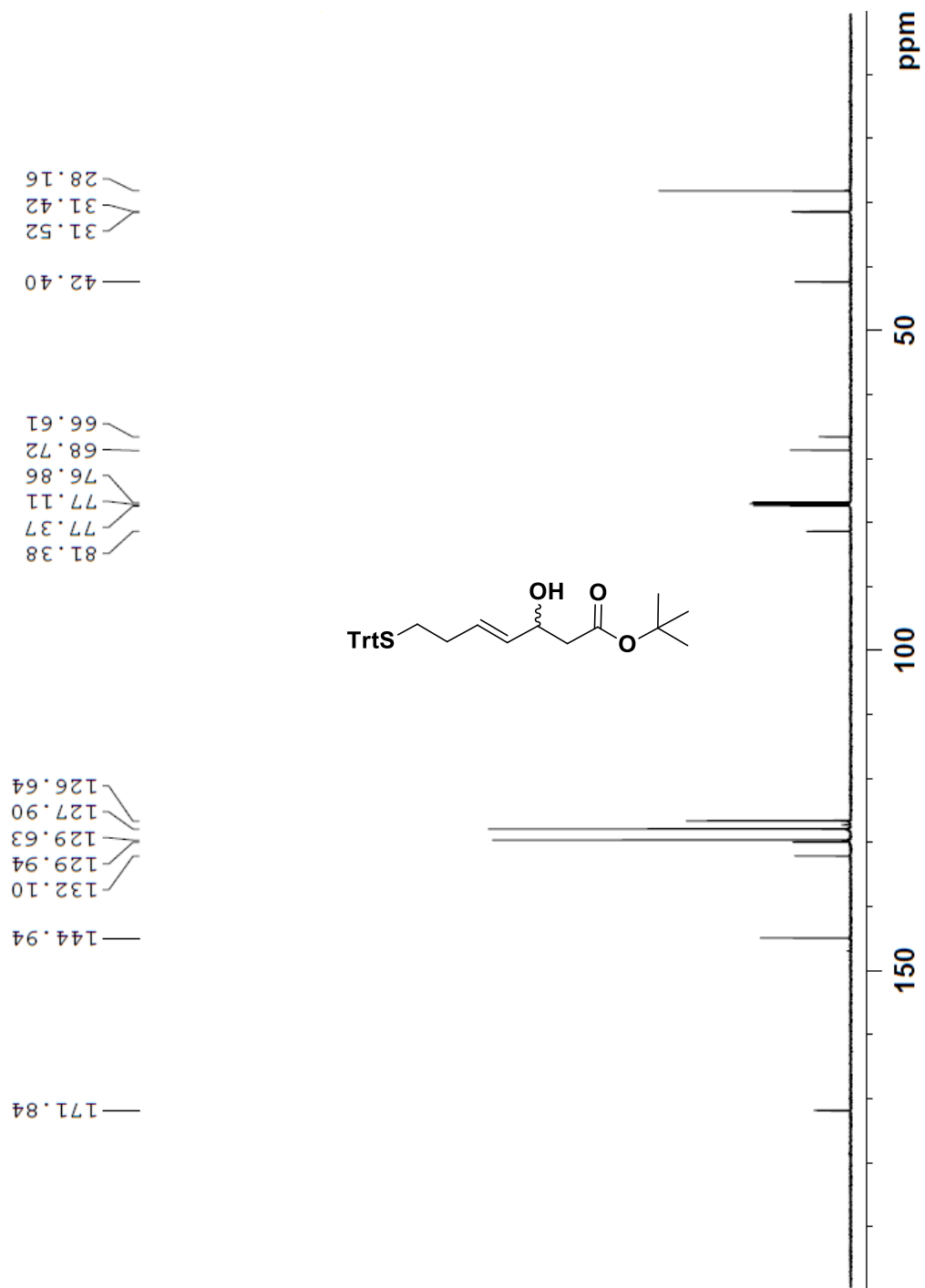
HRMS of Cpd 9

Event#: 1 MS(E+) Ret. Time : 0.400 -> 0.507 - 0.040 -> 0.099 Scan# : 61 -> 77 - 7 -> 15
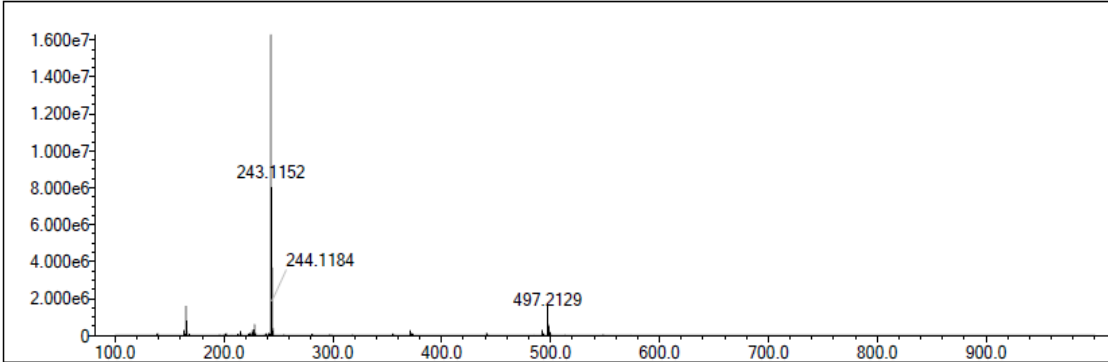
Measured region for 497.2129 m/z
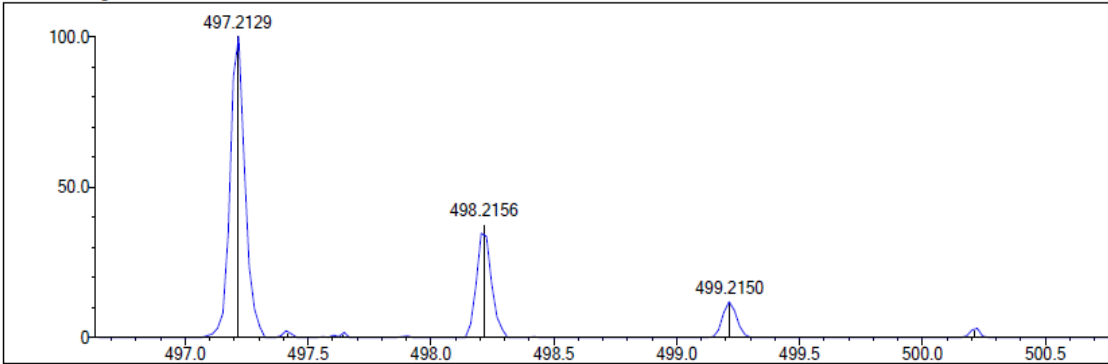
C30 H34 O3 S [M+Na]+ : Predicted region for 497.2121 m/z
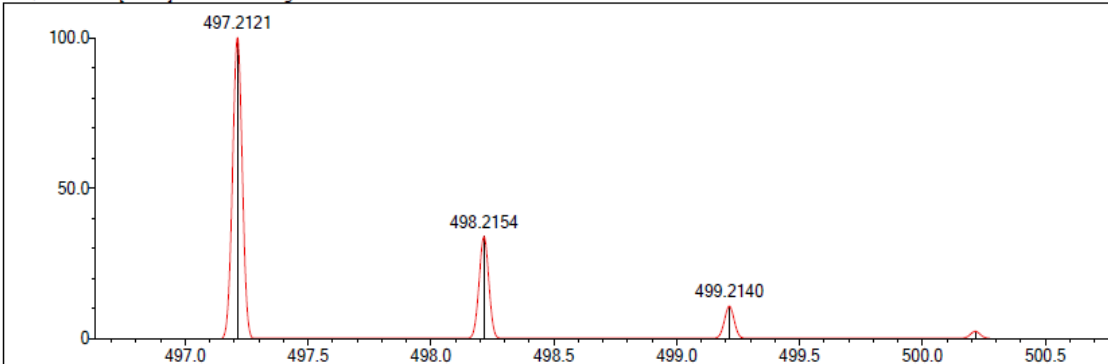
Rank	Score	Formula (M)	Ion	Meas. m/z	Pred. m/z	Df. (mDa)	Df. (ppm)	Iso	DBE
1	98.47	C30 H34 O3 S	[M+Na]+	497.2129	497.2121	0.8	1.61	100.00	14.0

^{1}H NMR Spectrum of Compound 10 in CDCl$_3$

2.07
2.09
2.12
2.14
2.22
2.24
2.27
2.38
2.55
2.57

4.45
4.47
4.49
4.51
5.41
5.43
5.46
5.48
5.57
5.59
5.61
5.64
5.66
7.21
7.23
7.25
7.28
7.30
7.33
7.42
7.44

2.06
2.00
2.03

1.00

1.03
1.10

3.42
6.22
6.21

^{13}C NMR Spectrum of Compound 10 in CDCl$_3$

31.35
31.42
41.26

66.99
68.53
76.85
77.11
77.36

126.67
127.92
129.63
130.74
131.62

144.91

177.30

^{1}H NMR Spectrum of Cpd 1' in CDCl$_3$

1.38

2.30
2.33
2.36
2.38
2.62
2.64
2.67

3.33

4.35
4.37
4.39
4.40

5.45
5.47
5.50
5.52
5.60
5.62
5.64
5.67
5.70

9.01

4.08
2.08

1.00

1.02

1.01
1.02

9 8 7 6 5 4 3 2 1 ppm

¹³C NMR Spectrum of Cpd 1' in CDCl₃

28.09
31.83
38.09
42.54

68.99
76.91
77.17
77.42
81.23

129.11
132.78

171.61

217
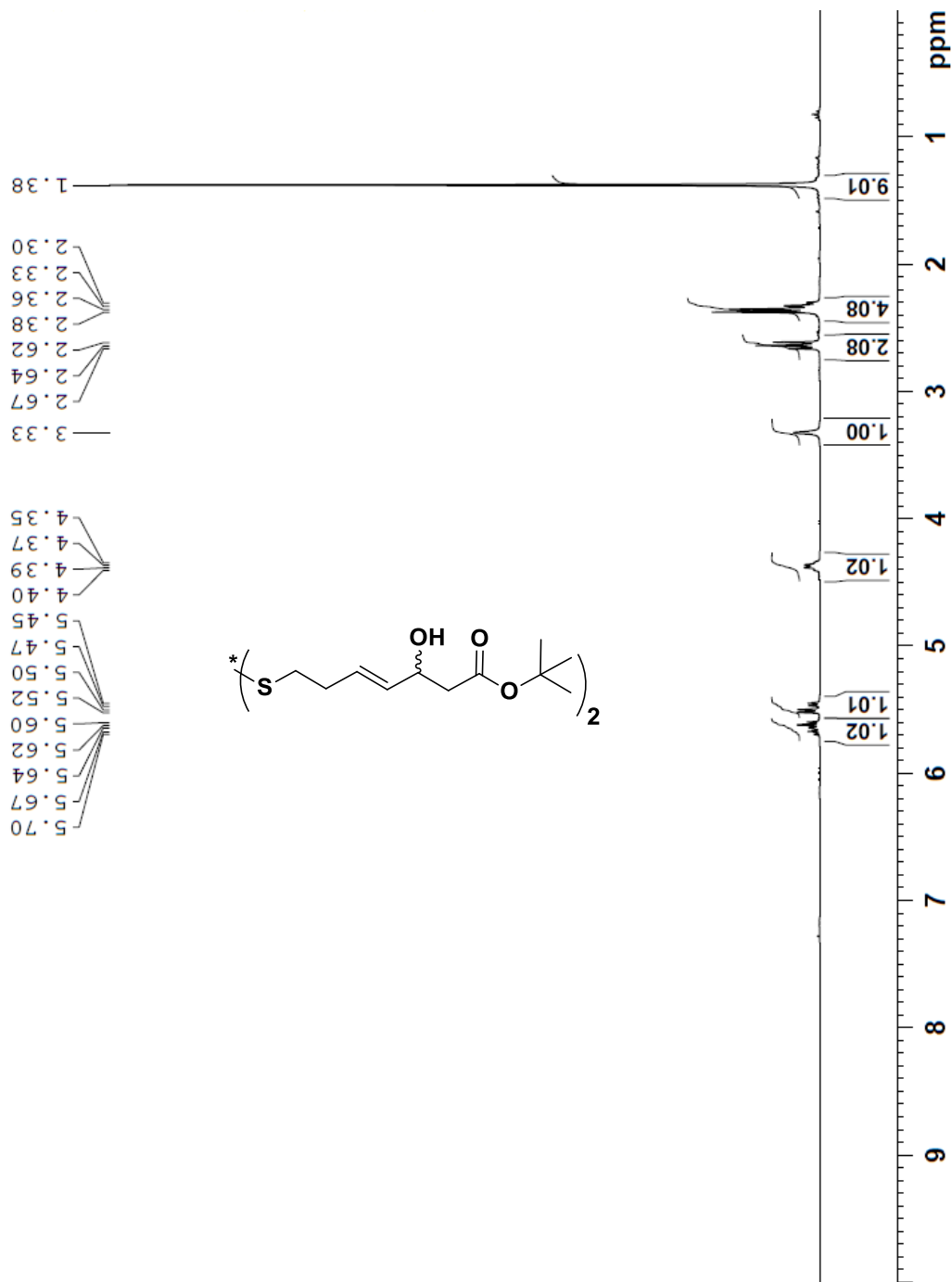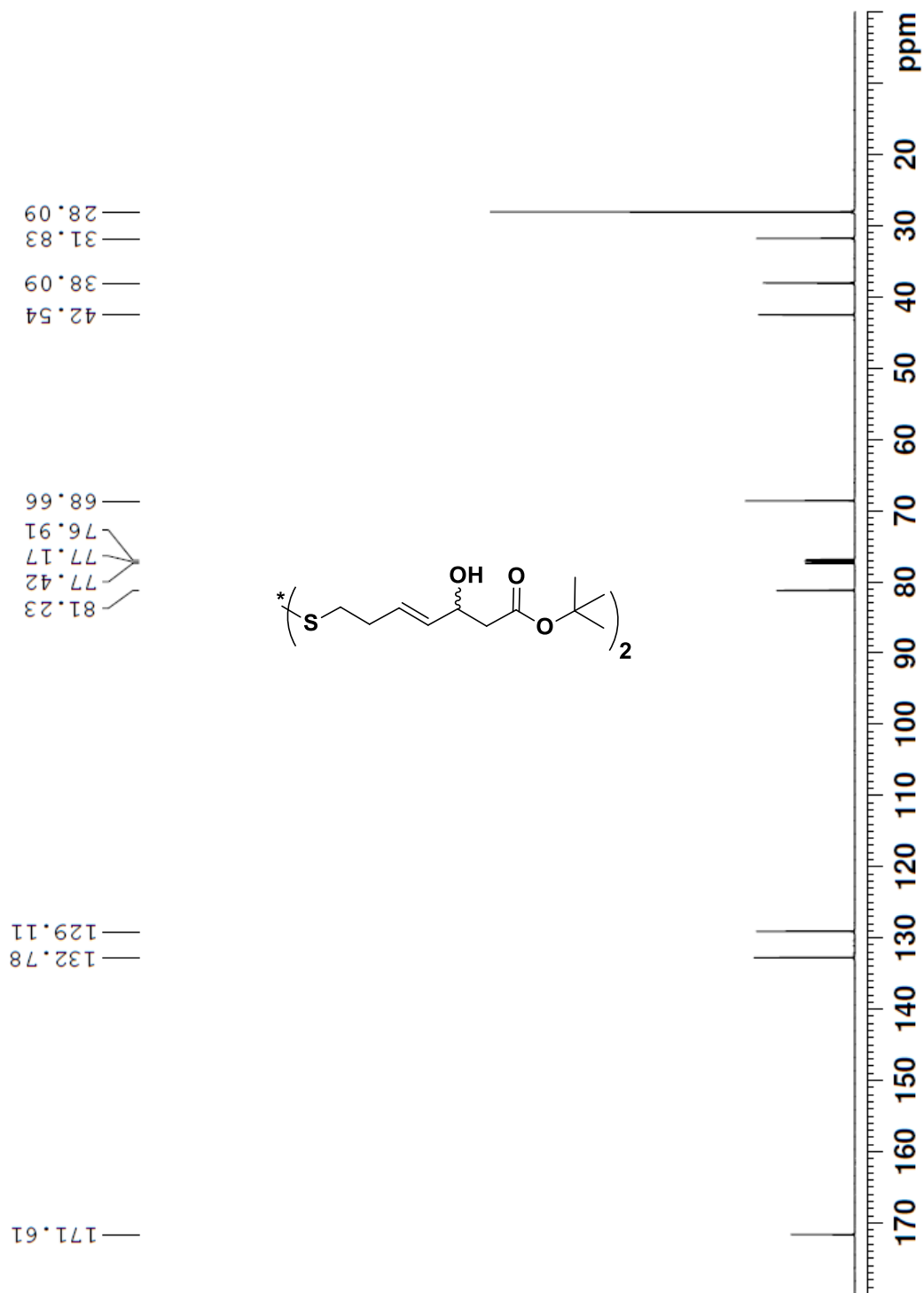
HRMS of Cpd 1'

Event#: 1 MS(E+) Ret. Time : 0.533 -> 1.280 - 0.333 -> 0.452 Scan# : 81 -> 193 - 51 -> 69

175.0416
315.0708
231.1032
333.0803
389.1449
445.2074
485.1995
486.2014
487.1977
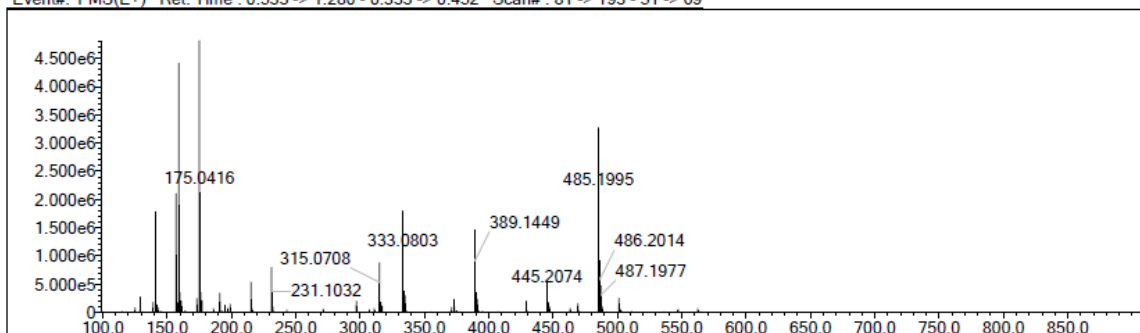
Measured region for 485.1995 m/z

485.1995
486.2014
487.1977
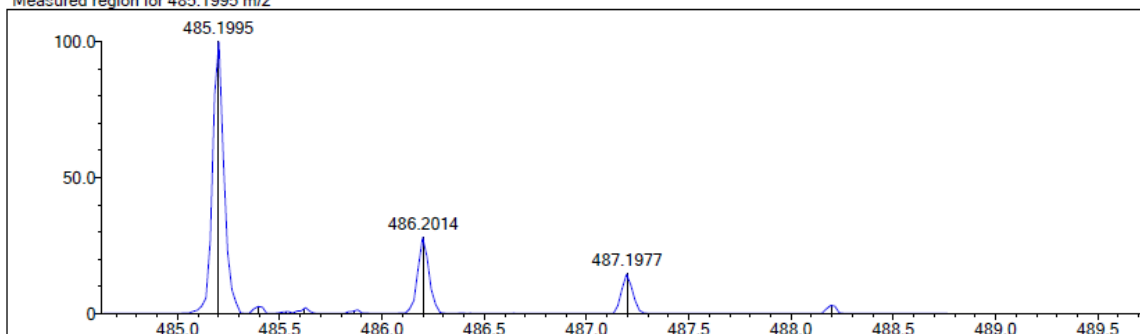
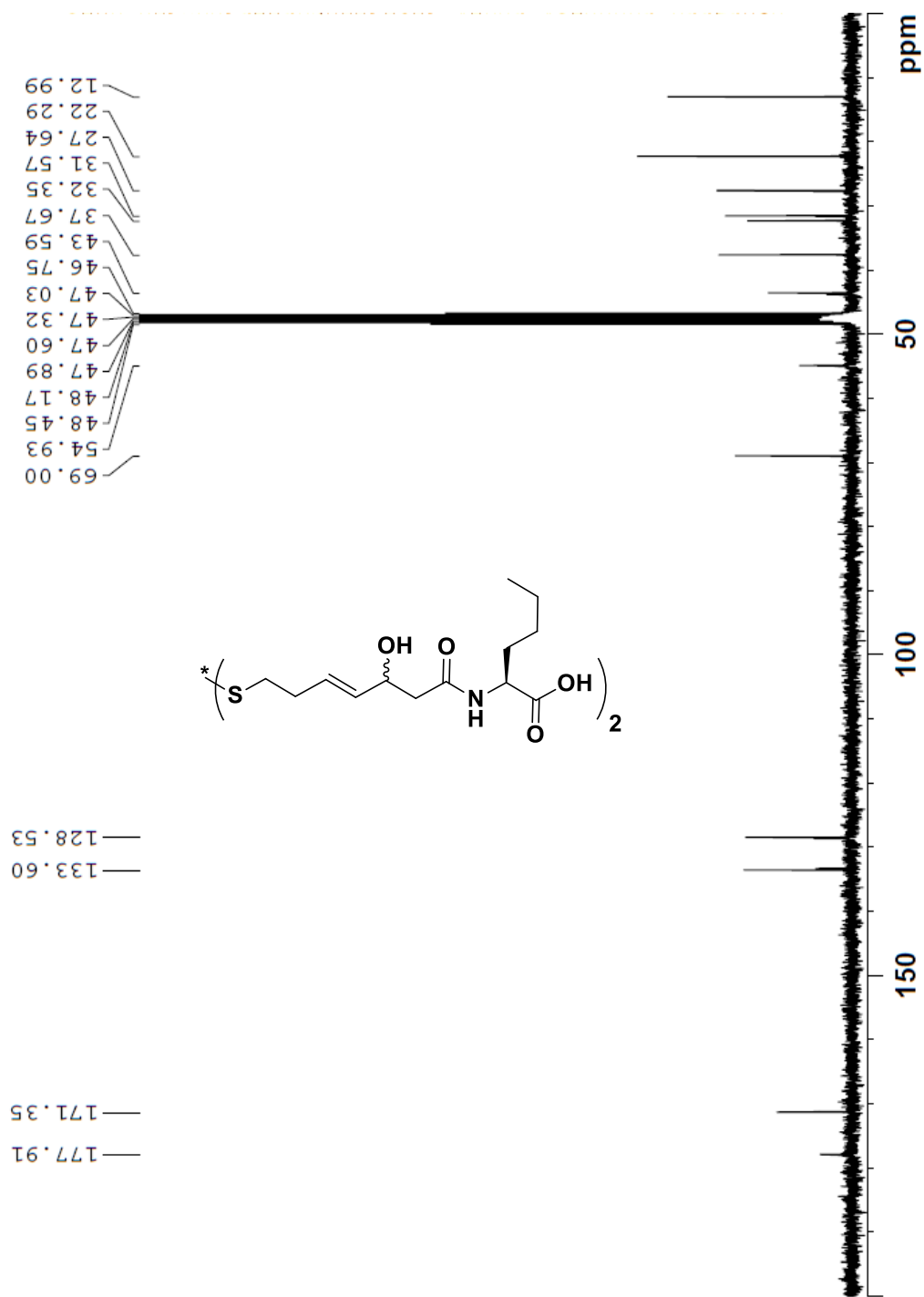C22 H38 O6 S2 [M+Na]+ : Predicted region for 485.2002 m/z

485.2002
486.2034
487.1993
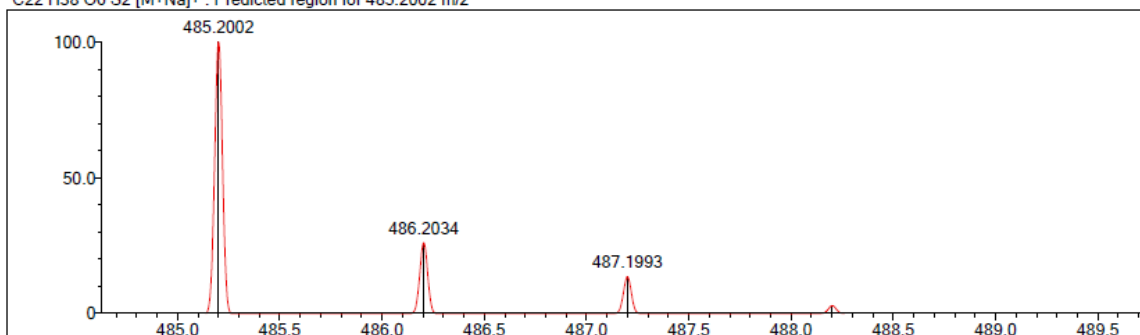
Rank	Score	Formula (M)	Ion	Meas. m/z	Pred. m/z	Df. (mDa)	Df. (ppm)	Iso	DBE
1	98.27	C22 H38 O6 S2	[M+Na]+	485.1995	485.2002	-0.7	-1.44	99.36	4.0

¹H NMR Spectrum of Cpd 1 in MeOD

2.43
2.45
2.47
2.49
2.73
2.76
2.78
3.32
3.33
3.33
4.45
4.47
4.49
4.51
4.97
5.58
5.60
5.63
5.65
5.71
5.73
5.75
5.78
5.80

4.24
2.00
0.46
1.01
2.89
1.00
1.05

ppm
1
2
3
4
5
6
7
8
9

^{13}C NMR Spectrum of Cpd 1 in MeOD

31.55
37.65
42.05
47.00
47.05
47.29
47.33
47.57
47.62
47.86
47.90
48.19
48.47
68.62

128.72
133.33

173.73

^{1}H NMR Spectrum of Compound 11 in CDCl$_3$

0.90
0.91
0.93
1.33
1.34
1.68
1.69
1.83
1.84
1.85
1.85
1.86
1.87
2.10
2.11
2.12
2.22
2.23
2.25
2.34
2.36
2.38
2.39
2.43
2.44
2.46
2.47
3.50
3.76
4.44
4.61
4.62
4.64
5.44
5.46
5.47
5.57
5.59
5.60
5.62
6.42
6.43
7.23
7.25
7.29
7.30
7.32
7.42
7.44

3.46
4.29
1.34
1.43
2.10
2.40
2.38
1.04
3.37
1.01
1.15
1.00
1.03
1.07
3.09
6.08
6.12

ppm
1
2
3
4
5
6
7
8
9

^{13}C NMR Spectrum of Compound 11 in CDCl$_3$

13.90

22.29
27.36
31.38
31.49
32.10

42.59

52.05
52.42

66.61
69.13
76.84
77.09
77.35

126.64
127.89
129.61
130.15
132.20

144.91

171.50
173.08

ppm
20
30
40
50
60
70
80
90
100
110
120
130
140
150
160
170

¹H NMR Spectrum of Compound 12 in CDCl₃

^{13}C NMR Spectrum of Compound 12 in CDCl$_3$

13.93

22.30
27.38
31.38
31.49
31.67

42.69

52.33

66.66
69.18
76.88
77.14
77.39

126.68
127.29
127.93
129.62

144.90
146.88

172.26
175.56

ppm

20
30
40
50
60
70
80
90
100
110
120
130
140
150
160
170
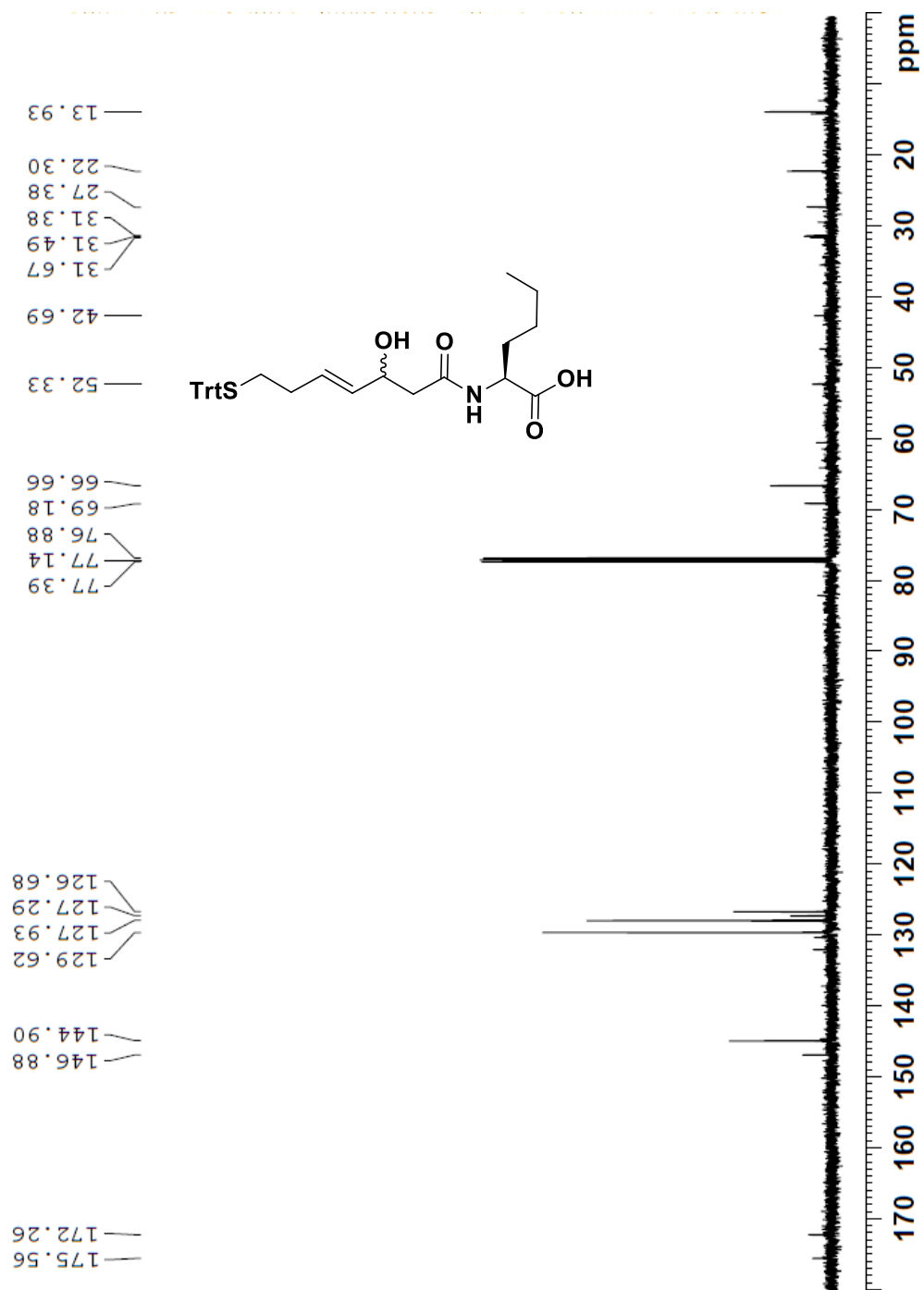
¹H NMR Spectrum of Cpd 5' in CDCl₃

¹³C NMR Spectrum of Cpd 5' in CDCl₃

13.84

22.24
27.48
31.73
31.83
38.23
42.93

52.19
52.39

69.20
76.82
77.08
77.33

129.27
132.93

171.78
173.26

ppm
50
100
150

HRMS of Cpd 5'

Measured region for 605.2914 m/z
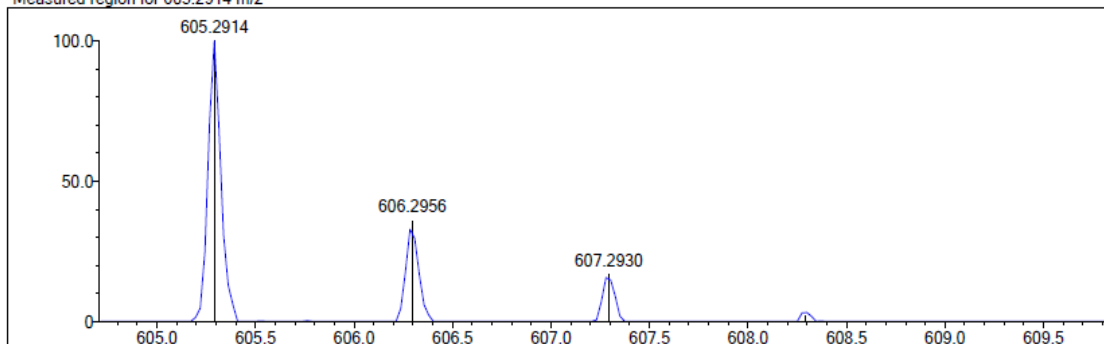
C28 H48 N2 O8 S2 [M+H]+ : Predicted region for 605.2925 m/z
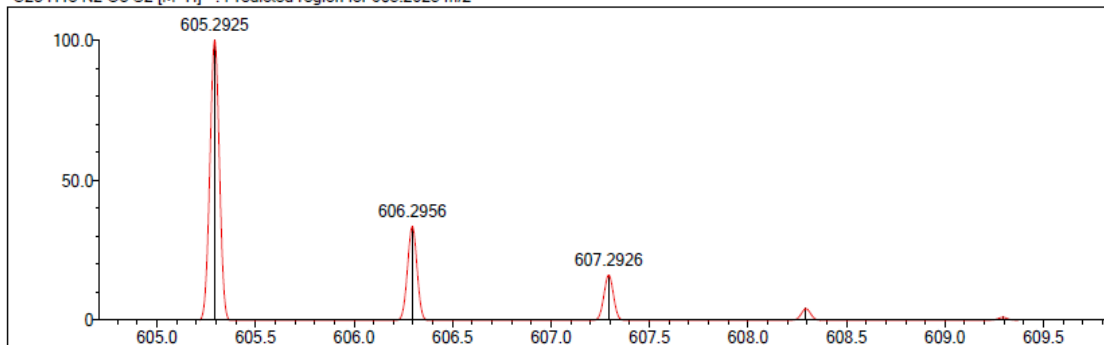
Rank	Score	Formula (M)	Ion	Meas. m/z	Pred. m/z	Df. (mDa)	Df. (ppm)	Iso	DBE
3	94.30	C28 H48 N2 O8 S2	[M+H]+	605.2914	605.2925	-1.1	-1.82	96.27	6.0

227

^{1}H NMR Spectrum of Cpd 5 in MeOD

^{13}C NMR Spectrum of Cpd 5 in MeOD

12.99
22.29
27.64
31.57
32.35
37.67
43.59
46.75
47.03
47.32
47.60
47.89
48.17
48.45
54.93
69.00

128.53
133.60

171.35
177.91

ppm
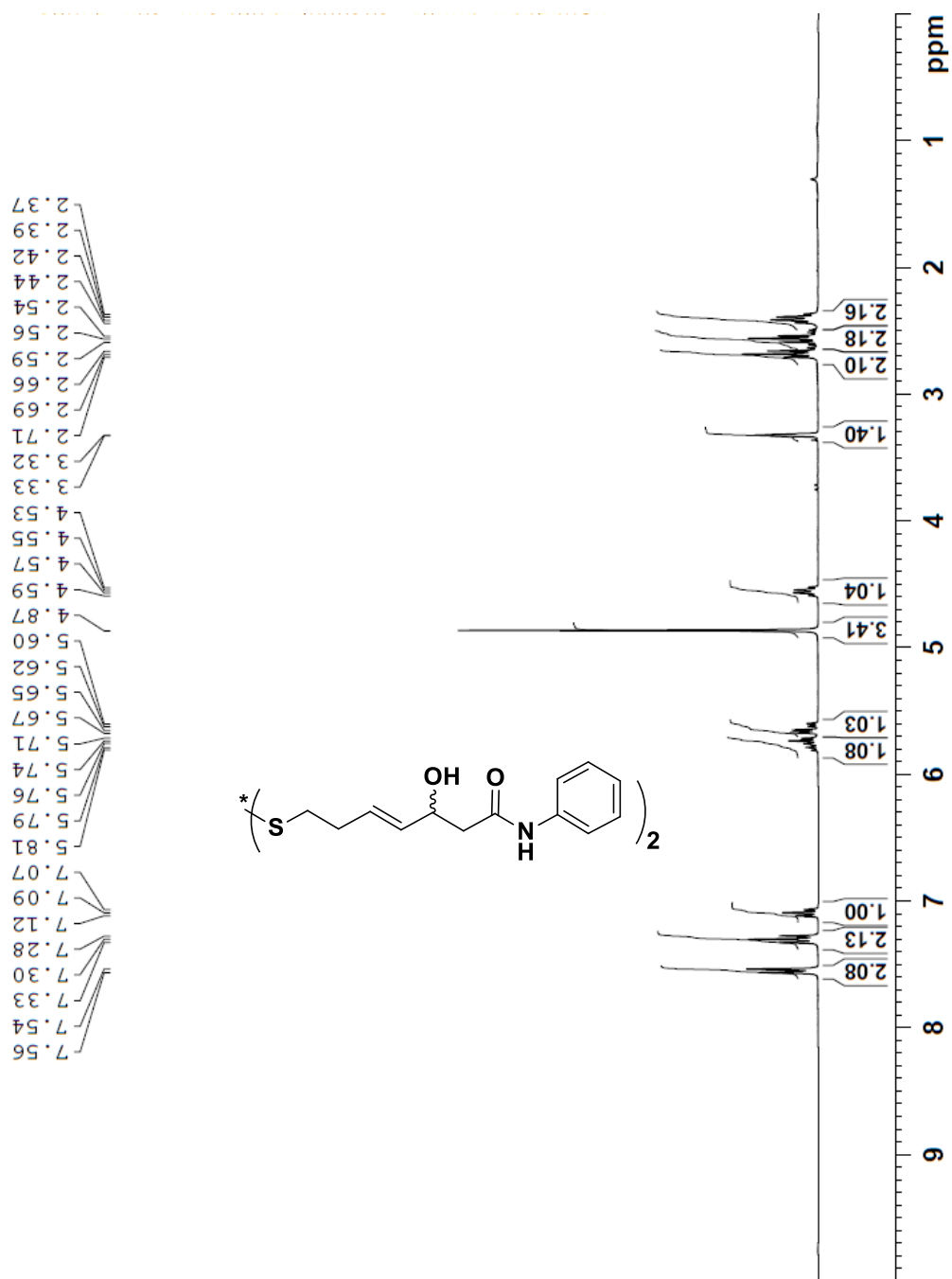
150

100

50
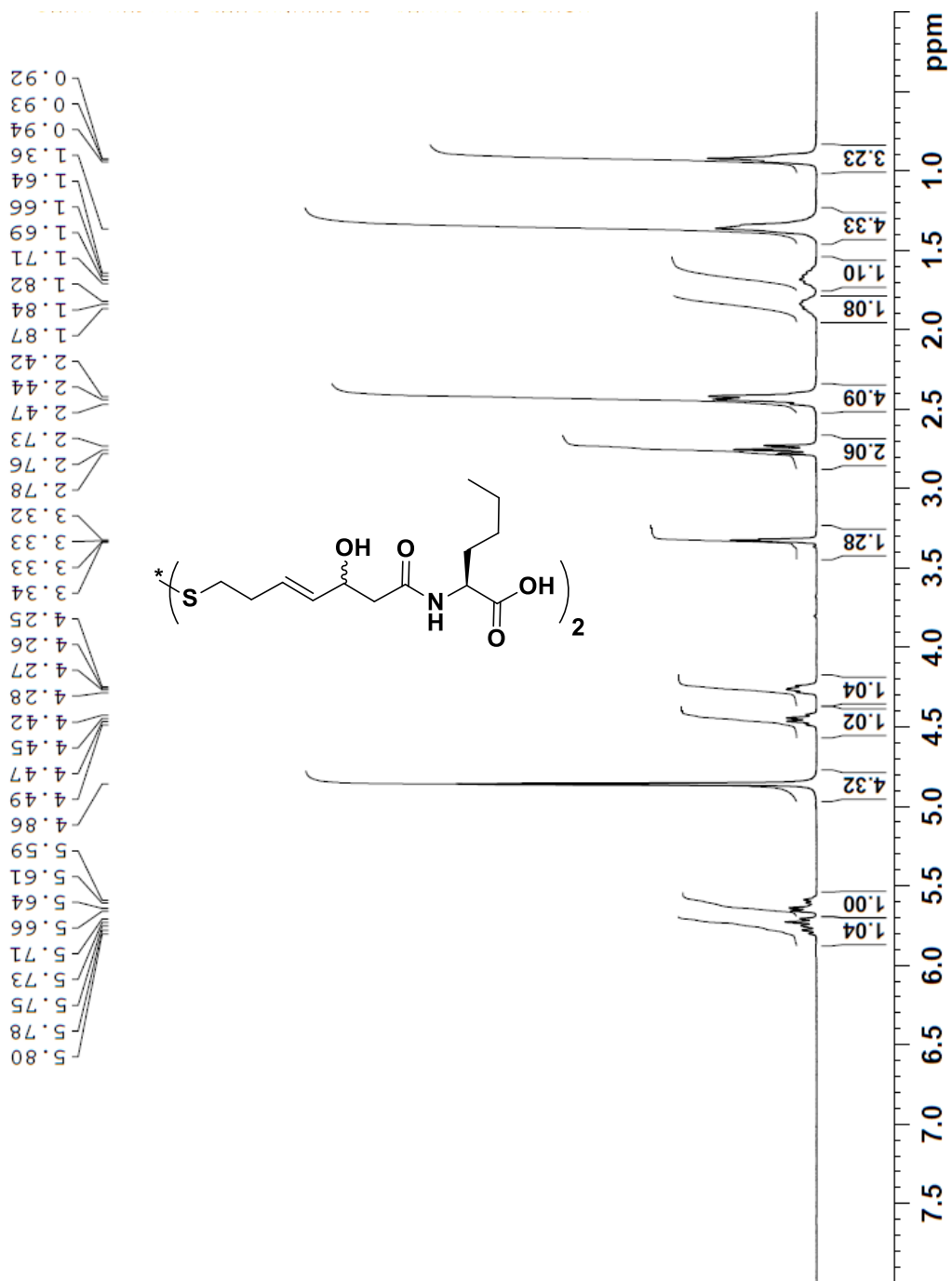
HRMS of Cpd 5

Event#: 1 MS(E+)   Ret. Time : 0.347 -> 0.467 - 0.027 -> 0.196   Scan# : 53 -> 71 - 5 -> 31
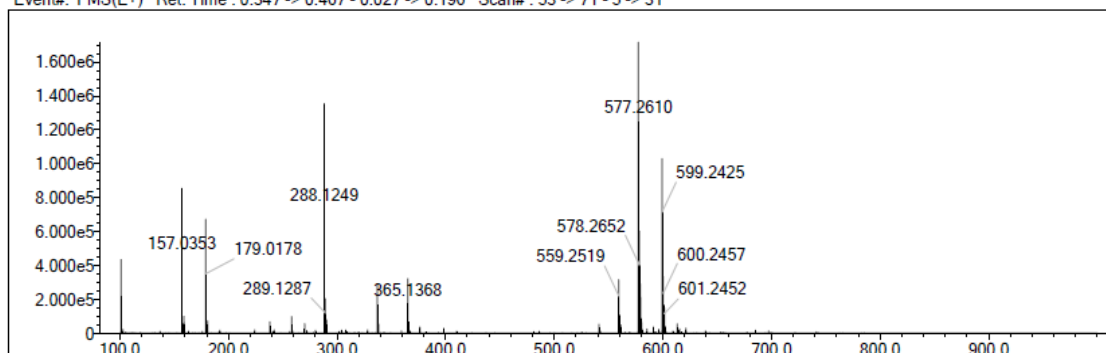
Measured region for 577.2610 m/z
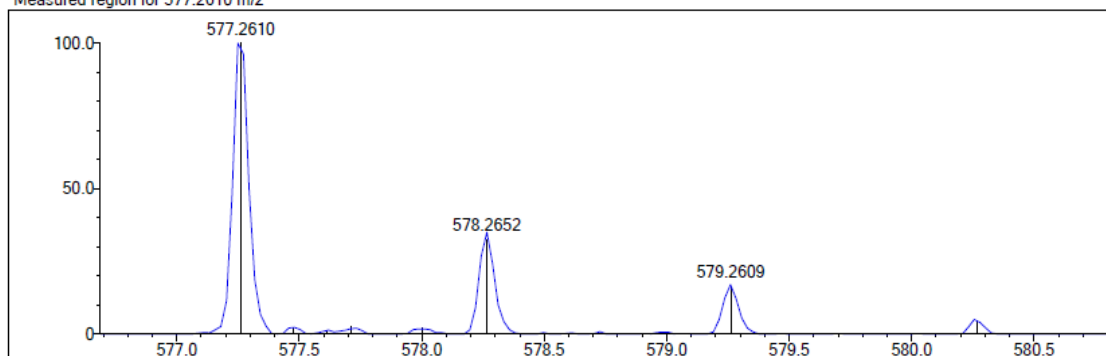
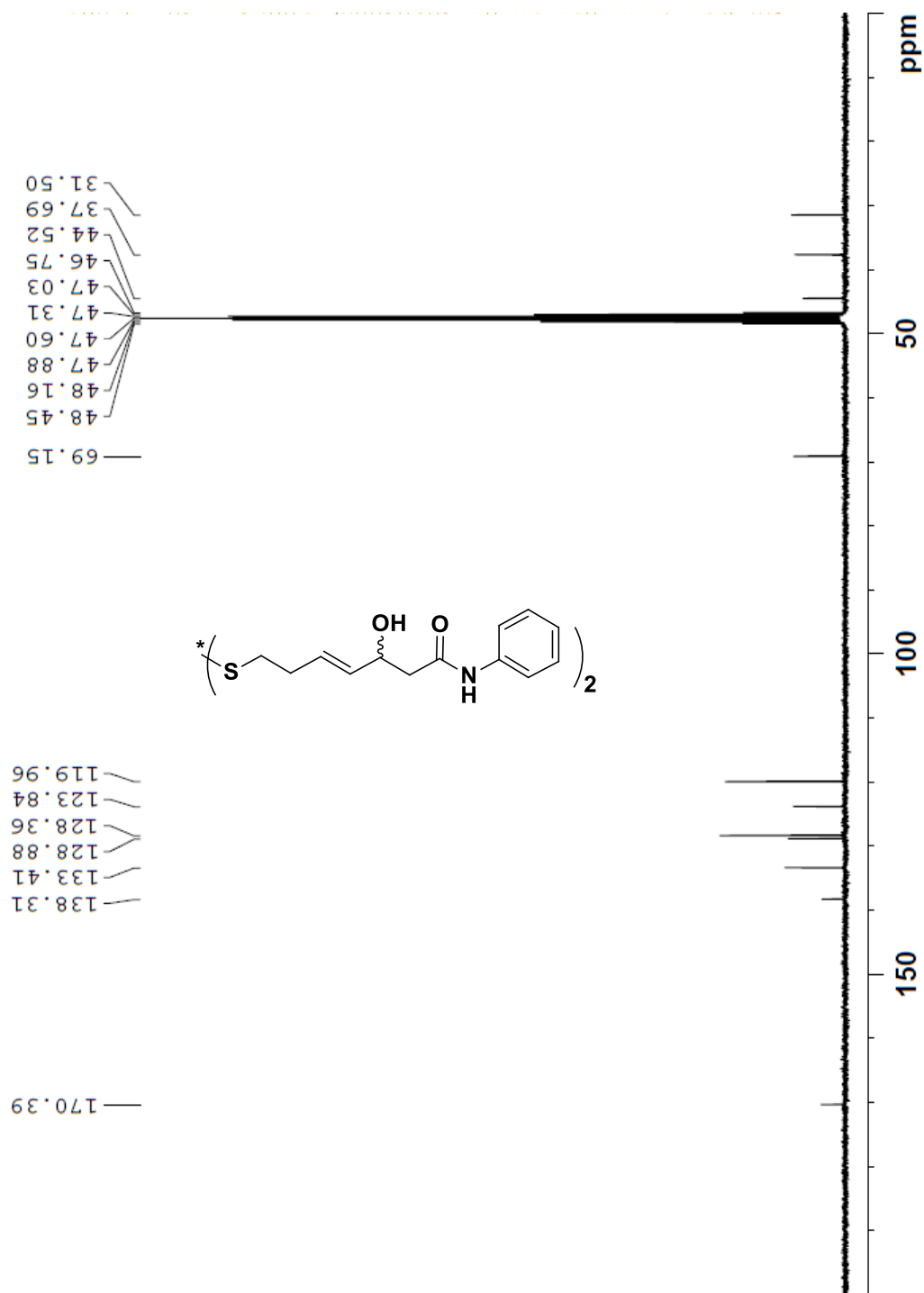
C26 H44 N2 O8 S2 [M+H]+ : Predicted region for 577.2612 m/z
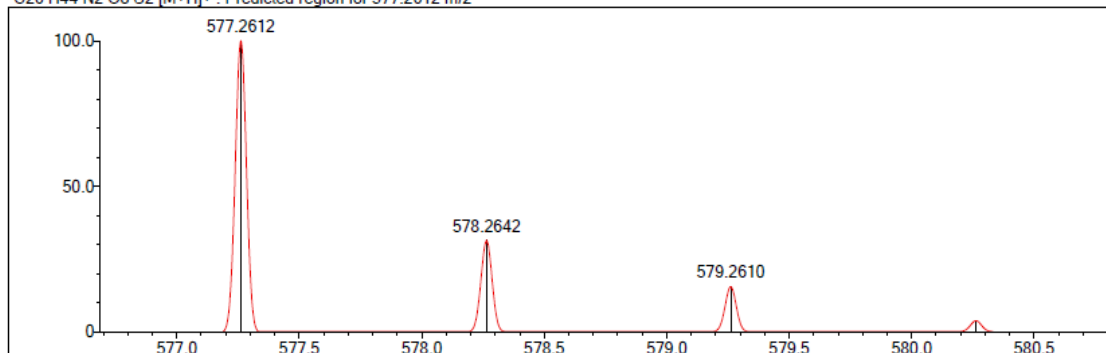
Rank	Score	Formula (M)	Ion	Meas. m/z	Pred. m/z	Df. (mDa)	Df. (ppm)	Iso	DBE
1	98.50	C26 H44 N2 O8 S2	[M+H]+	577.2610	577.2612	-0.2	-0.35	98.50	6.0

^{1}H NMR Spectrum of Compound 13 in CDCl$_3$

2.09
2.11
2.13
2.22
2.24
2.26
2.51
2.53
2.54
3.15

2.24
2.18
2.00

1.01

4.52
5.44
5.46
5.49
5.51
5.57
5.59
5.61
5.64
5.66
7.12
7.15
7.20
7.23
7.25
7.27
7.30
7.32
7.35
7.41
7.44
7.48
7.51
7.96

1.04

1.06
1.06

1.33
11.00
6.32
2.46

1.01

ppm
1
2
3
4
5
6
7
8
9

^{13}C NMR Spectrum of Compound 13 in CDCl$_3$

31.32
31.44

43.92

66.99
69.34
76.63
77.06
77.48

120.10
124.45
126.65
127.90
129.00
129.60
130.48
132.17
137.61
144.87

169.86
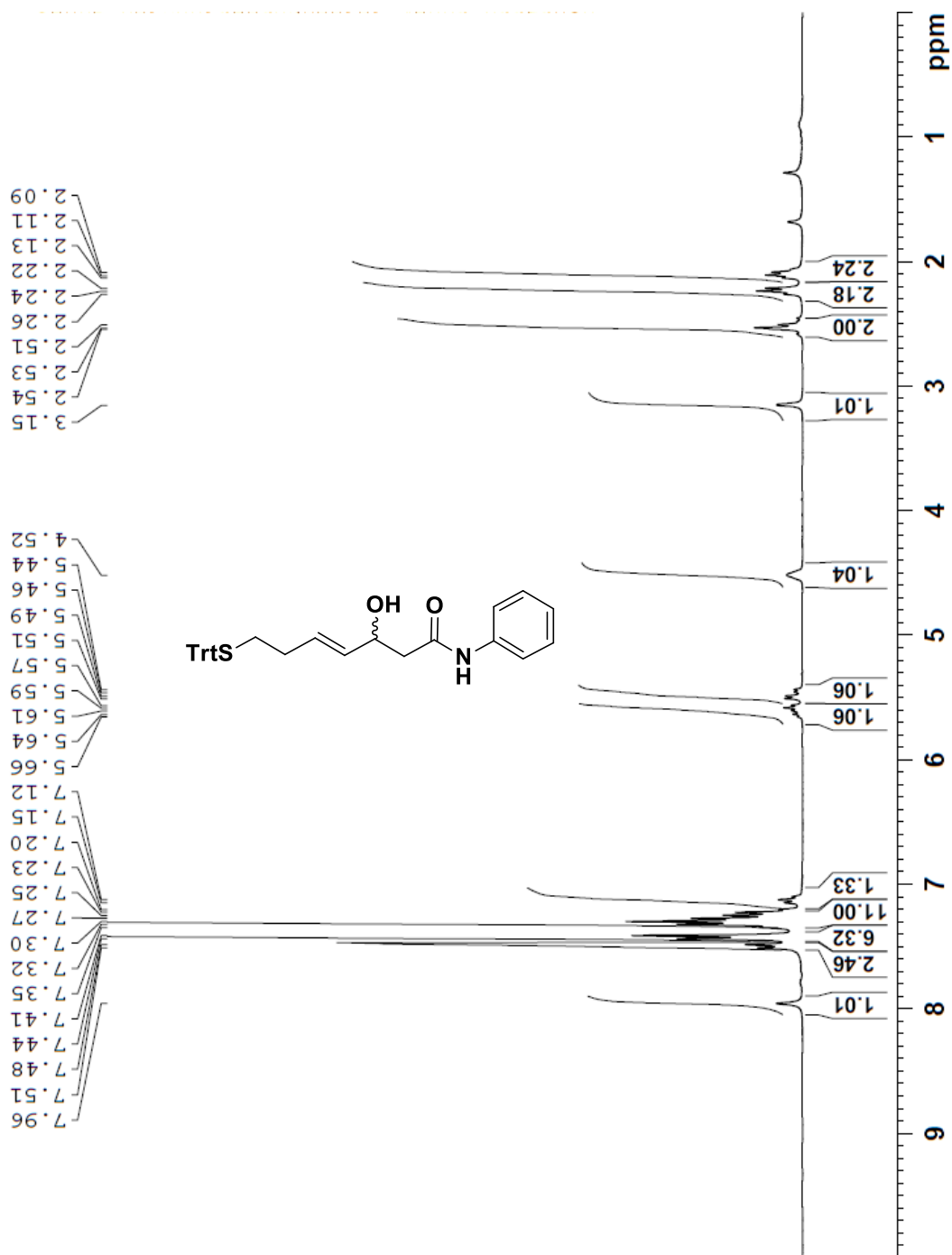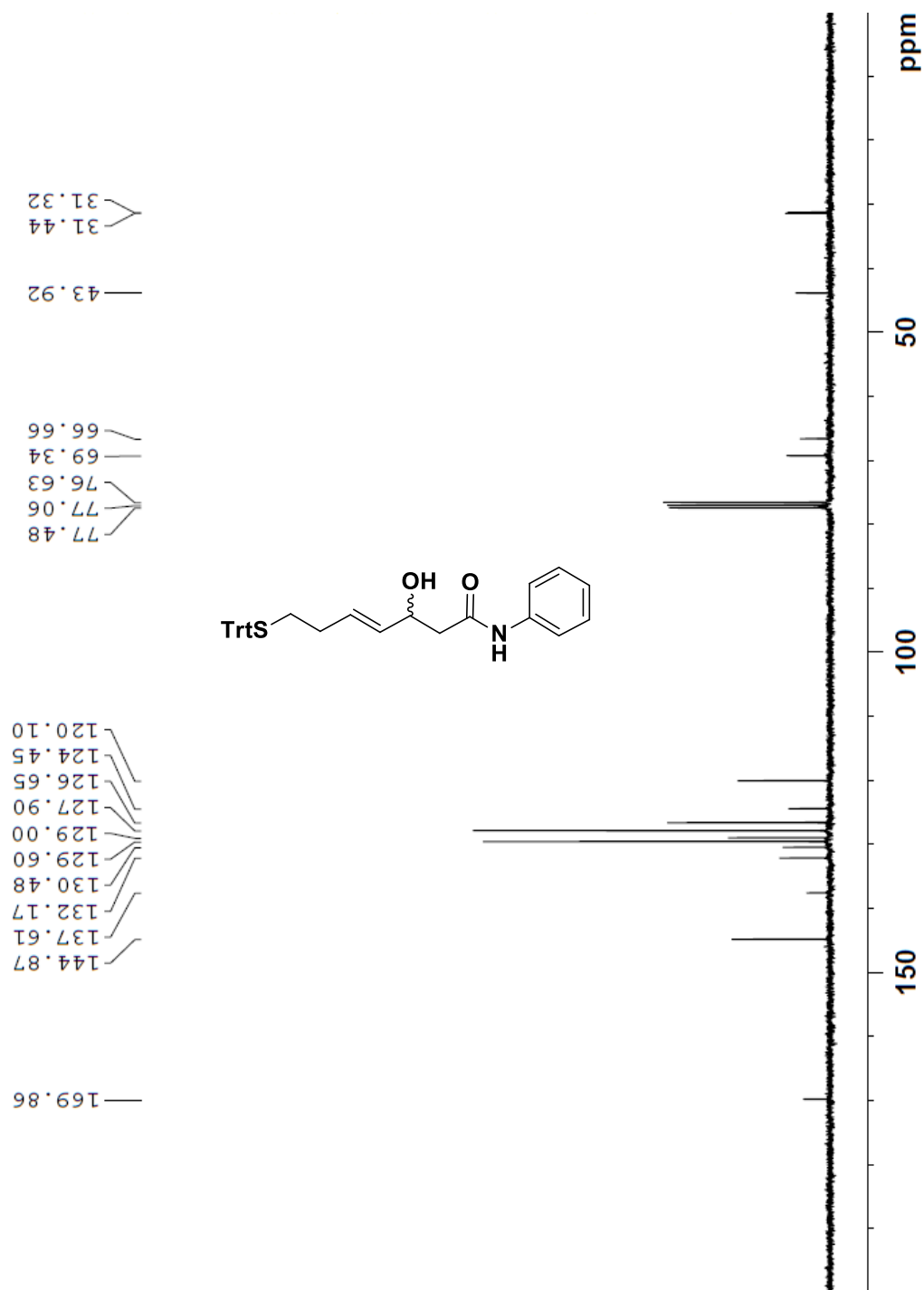
HRMS of Compound 13

Event#: 2 MS(E-) Ret. Time : 0.600 -> 1.187 - 0.200 -> 0.427 Scan# : 92 -> 180 - 32 -> 66
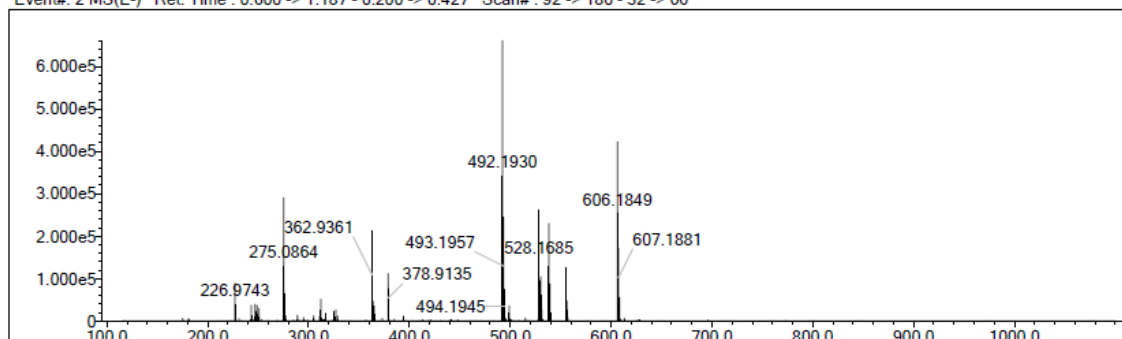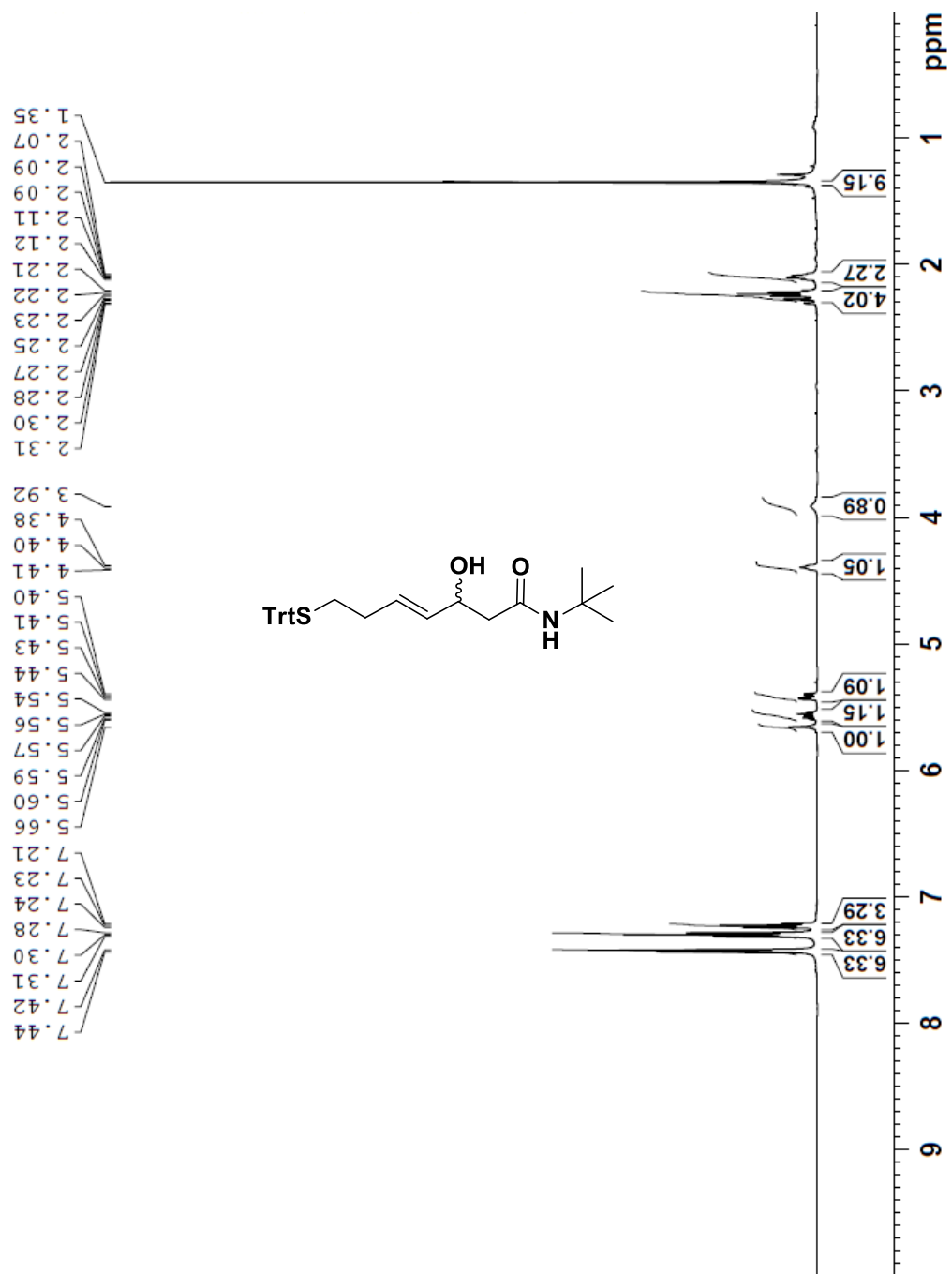
Measured region for 492.1930 m/z
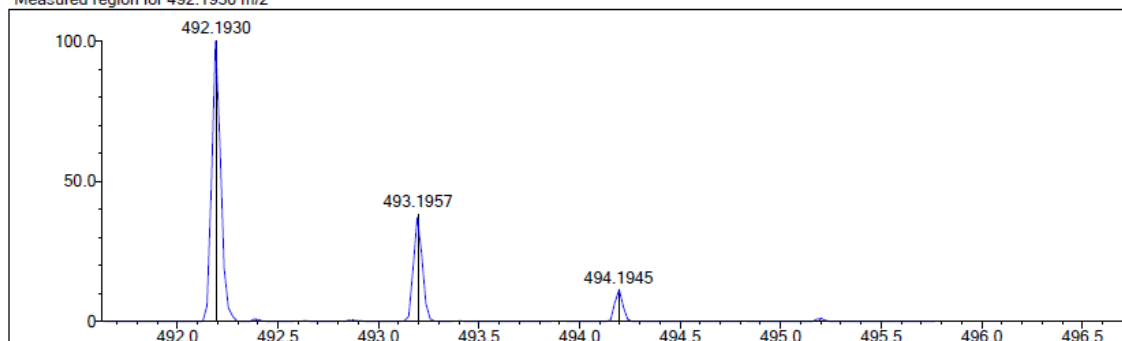
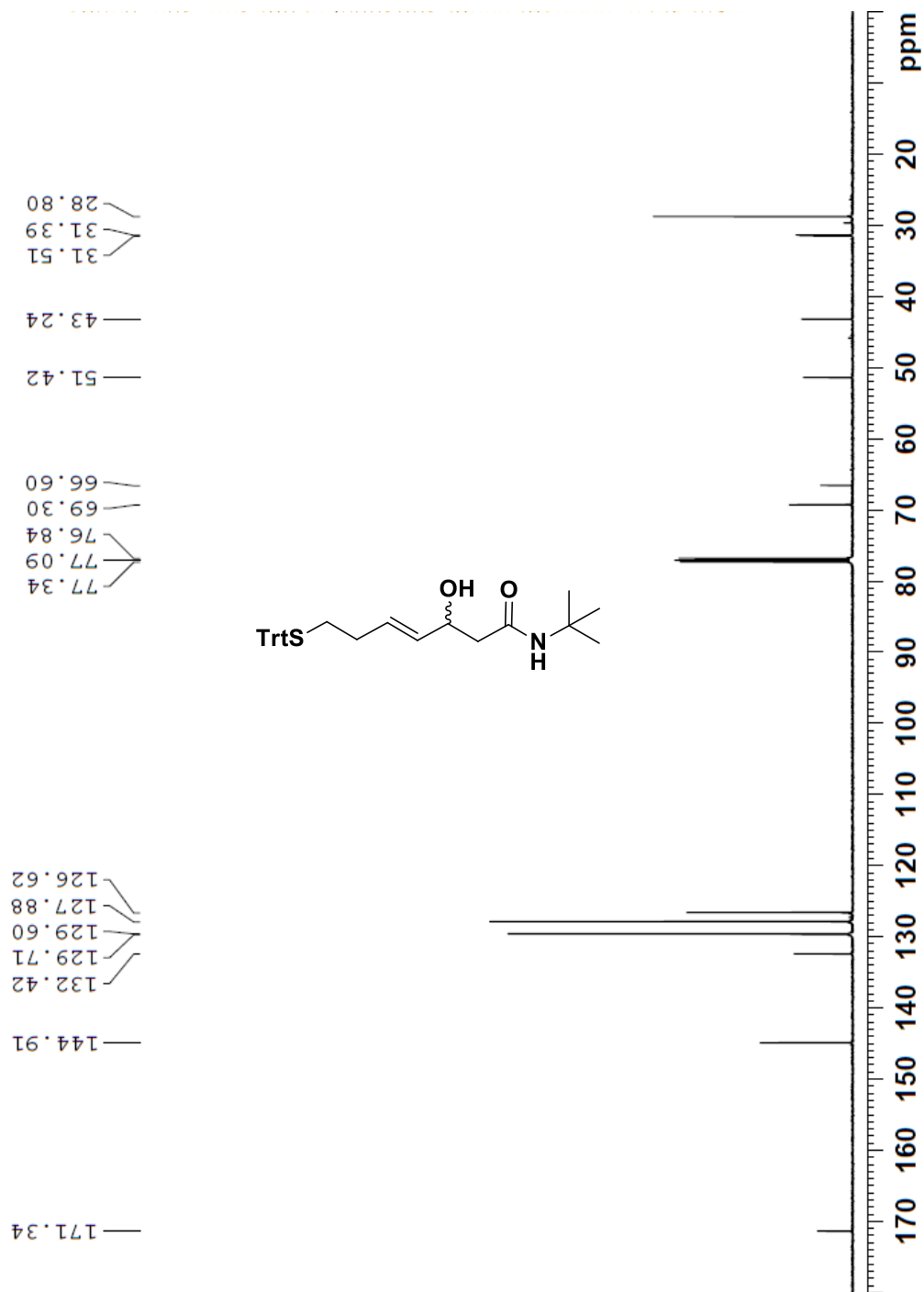C32 H31 N O2 S [M-H]- : Predicted region for 492.2003 m/z
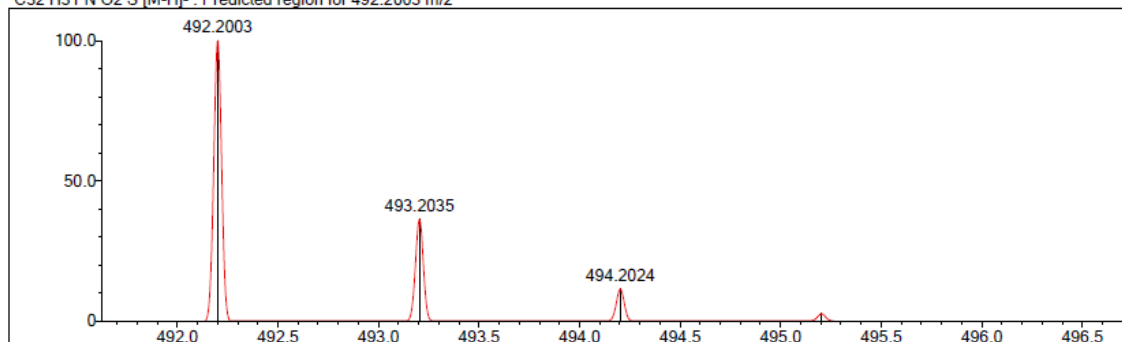
Rank	Score	Formula (M)	Ion	Meas. m/z	Pred. m/z	Df. (mDa)	Df. (ppm)	Iso	DBE
10	12.51	C32 H31 N O2 S	[M-H]-	492.1930	492.2003	-7.3	-14.83	46.14	18.0

^{1}H NMR Spectrum of Cpd 7 in CDCl$_3$

2.37
2.39
2.42
2.44
2.54
2.56
2.59
2.66
2.69
2.71
3.32
3.33
4.53
4.55
4.57
4.59
4.87
5.60
5.62
5.65
5.67
5.71
5.74
5.76
5.79
5.81
7.07
7.09
7.12
7.28
7.30
7.33
7.54
7.56

2.16
2.18
2.10
1.40
1.04
3.41
1.03
1.08
1.00
2.13
2.08

^{13}C NMR Spectrum of Cpd 7 in CDCl$_3$

31.50
37.69
44.52
46.75
47.03
47.31
47.60
47.88
48.16
48.45

69.15

119.96
123.84
128.36
128.88
133.41
138.31

170.39

ppm

50

100

150

HRMS of Cpd 7

Event#: 2 MS(E-)   Ret. Time : 0.600 -> 0.680 - 0.400 -> 0.498   Scan# : 92 -> 104 - 62 -> 76
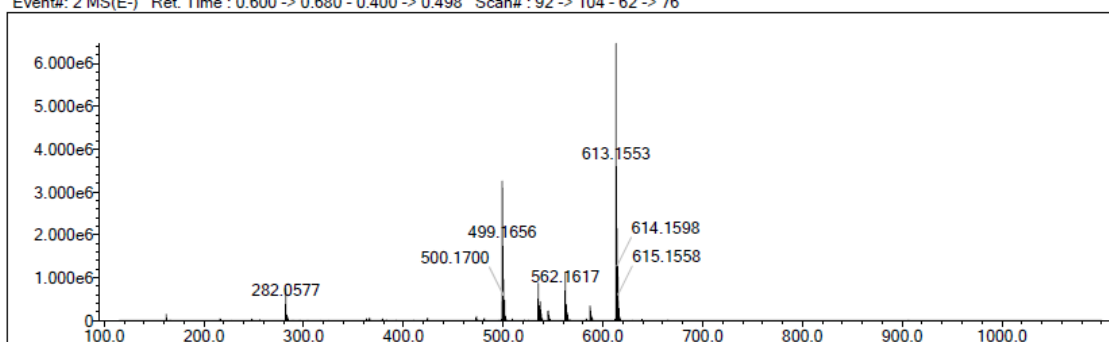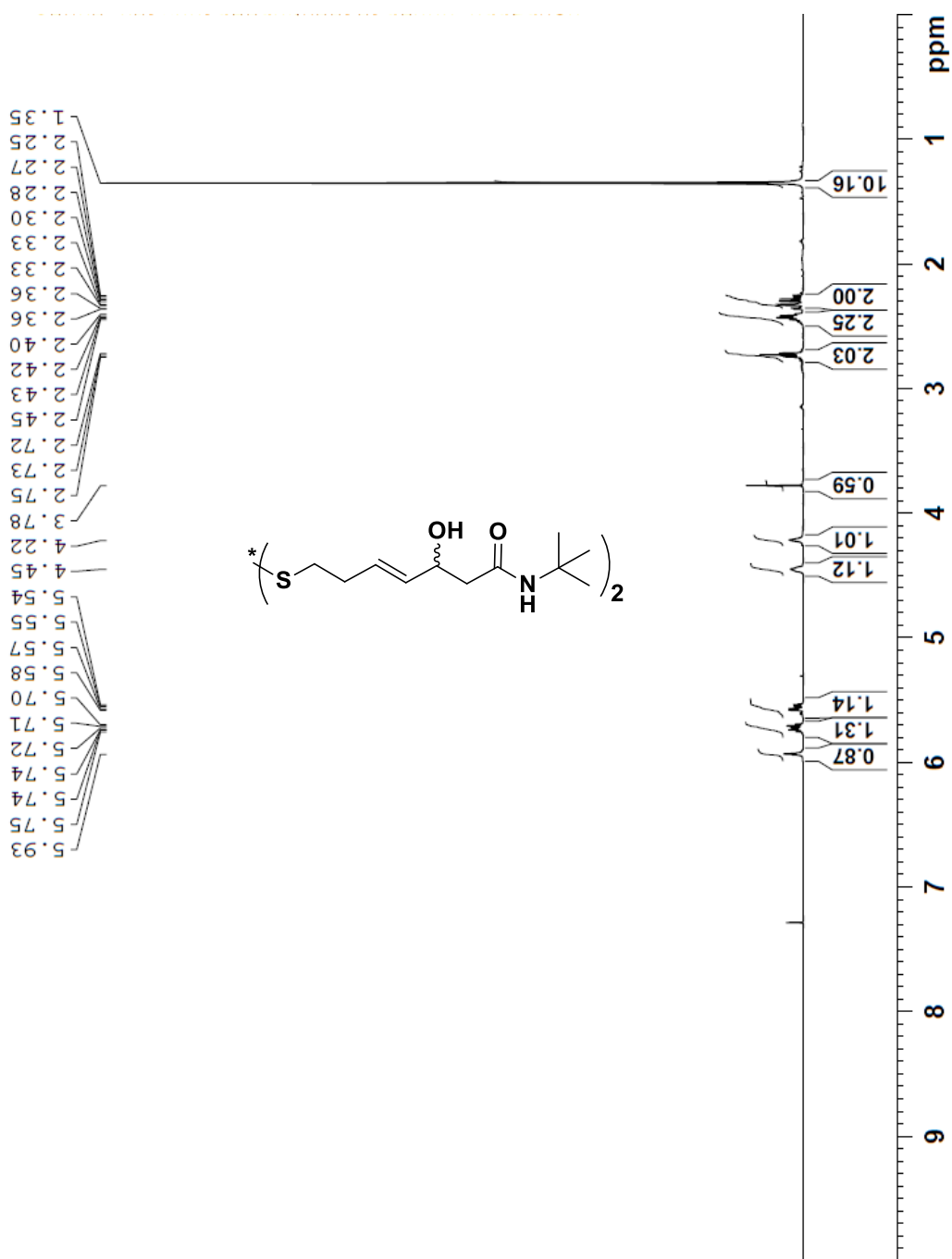
Measured region for 499.1656 m/z
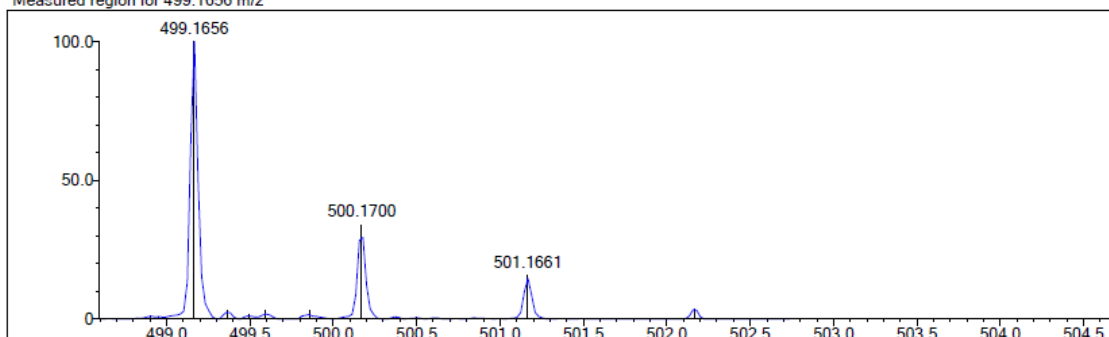
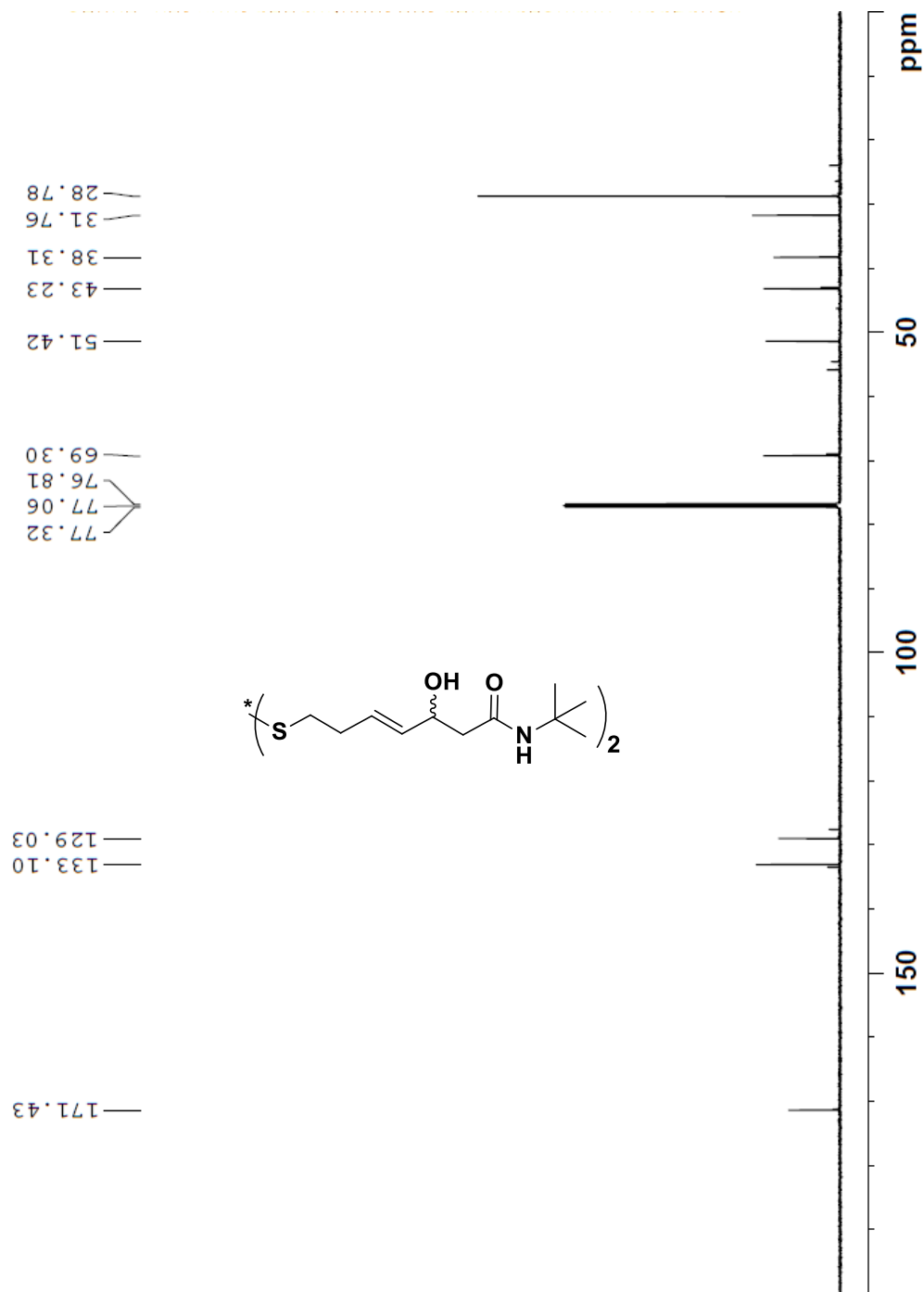C26 H32 N2 O4 S2 [M-H]- : Predicted region for 499.1731 m/z
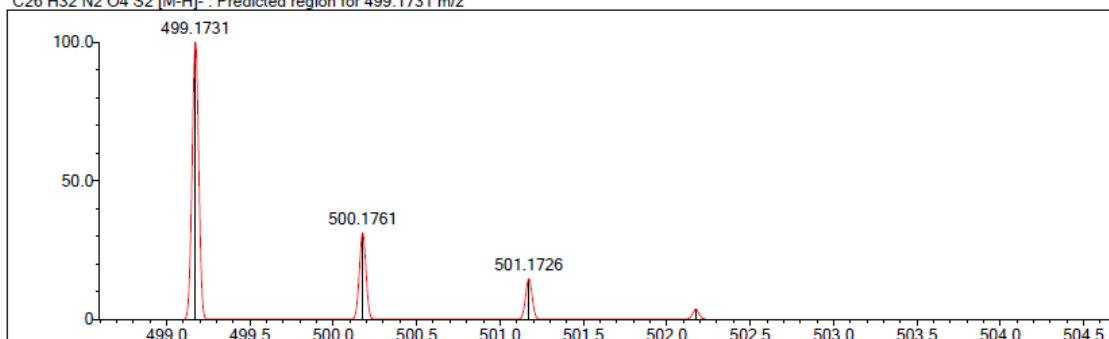
Rank	Score	Formula (M)	Ion	Meas. m/z	Pred. m/z	Df. (mDa)	Df. (ppm)	Iso	DBE
10	15.86	C26 H32 N2 O4 S2	[M-H]-	499.1656	499.1731	-7.5	-15.03	59.66	12.0

^{1}H NMR Spectrum of Compound 14 in CDCl$_3$

1.35
2.07
2.09
2.09
2.11
2.12
2.21
2.22
2.23
2.25
2.27
2.28
2.30
2.31

3.92
4.38
4.40
4.41
5.40
5.41
5.43
5.44
5.54
5.56
5.57
5.59
5.60
5.66
7.21
7.23
7.24
7.28
7.30
7.31
7.42
7.44

9.15
2.27
4.02
0.89
1.06
1.09
1.15
1.00
3.29
6.33
6.33

^{13}C NMR Spectrum of Compound 14 in CDCl$_3$

28.80
31.39
31.51

43.24

51.42

66.60
69.30
76.84
77.09
77.34

126.62
127.88
129.60
129.71
132.42

144.91

171.34

ppm
20
30
40
50
60
70
80
90
100
110
120
130
140
150
160
170

HRMS of Compound 14

Event#: 1 MS(E+) Ret. Time : 0.613 -> 1.080 - 0.227 -> 0.380 Scan# : 93 -> 163 - 35 -> 59
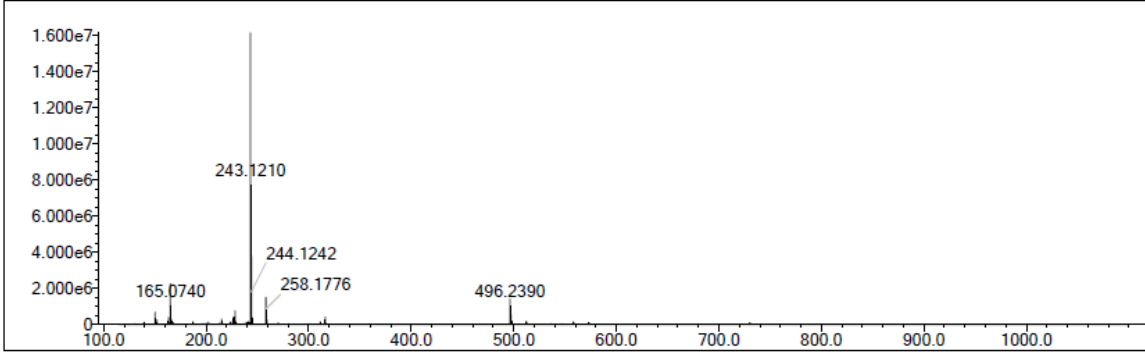
Measured region for 496.2390 m/z
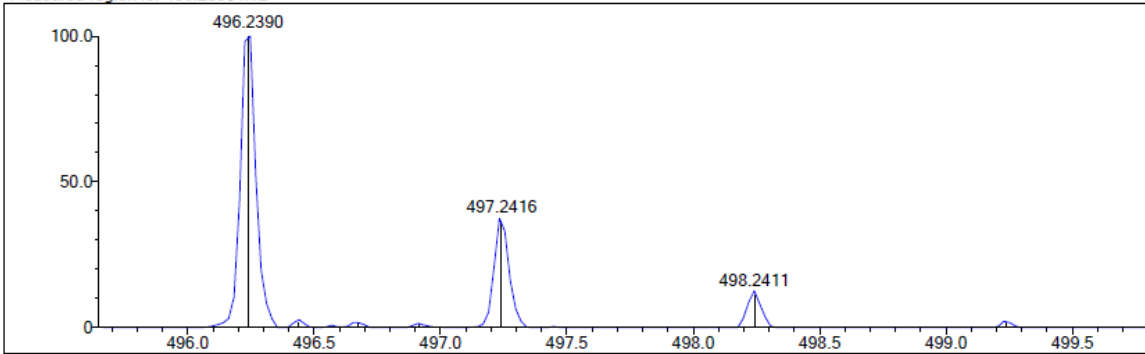
C30 H35 N O2 S [M+Na]+ : Predicted region for 496.2281 m/z
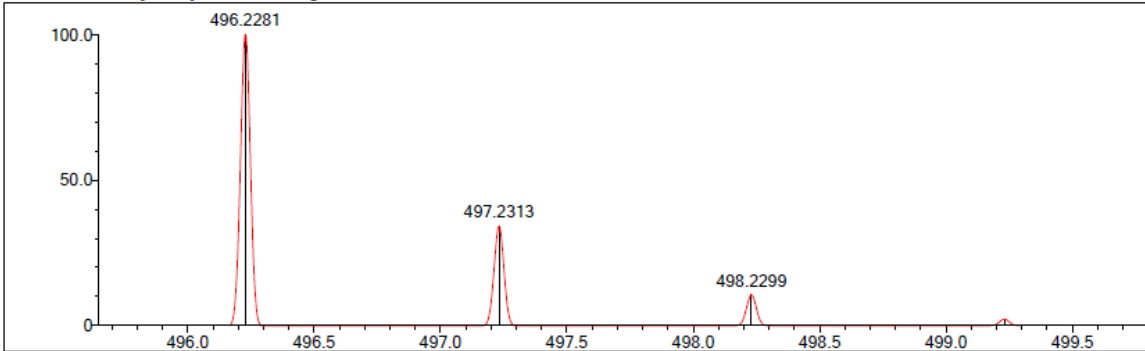
Rank	Score	Formula (M)	Ion	Meas. m/z	Pred. m/z	Df. (mDa)	Df. (ppm)	Iso	DBE
5	6.19	C30 H35 N O2 S	[M+Na]+	496.2390	496.2281	10.9	21.97	76.66	14.0

239

^{1}H NMR Spectrum of Cpd 8 in CDCl$_3$

1.35
2.25
2.27
2.28
2.30
2.33
2.33
2.36
2.36
2.40
2.42
2.43
2.45
2.72
2.73
2.75
3.78
4.22
4.45
5.54
5.55
5.57
5.58
5.70
5.71
5.72
5.74
5.74
5.75
5.93

10.16
2.00
2.25
2.03
0.59
1.01
1.12
1.14
1.31
0.87

ppm
1
2
3
4
5
6
7
8
9

^{1}H NMR Spectrum of Cpd 8 in CDCl$_3$

28.78
31.76
38.31
43.23
51.42

69.30
76.81
77.06
77.32

129.03
133.10

171.43

ppm

50

100

150

APPENDIX C

PART III: ACID CATALYZED REACTIONS OF AROMATIC KETONES WITH ETHYL DIAZOACETATE

Copies of ^{1}H NMR, ^{13}C NMR, and HRMS Spectral Data

^{1}H NMR Spectrum of Compound 3a (Keto-Enol Tautomer) in CDCl$_3$

1.18
1.20
1.23
1.27
1.30
1.32
1.87
2.21
4.16
4.18
4.19
4.21
4.21
4.23
4.23
4.24
4.25
4.26
4.71
7.16
7.17
7.17
7.18
7.19
7.19
7.28
7.29
7.31
7.32
7.32
7.33
7.33
7.34
7.36
7.36
7.38
7.39
7.40

13.15

3.35
3.20
3.00
3.00
3.96
0.91
1.91
8.01
0.95

ppm
1
2
3
4
5
6
7
8
9
10
11
12
13

¹³C NMR Spectrum of Compound 3a (Keto-Enol Tautomer) in CDCl₃

14.08
14.20
19.90

28.76

60.63
61.63
65.79

76.79
77.04
77.30

104.40

126.91
128.01
128.28
128.91
129.33
131.24
132.72
135.25

168.53
172.63
173.88

201.57

ppm

50

100

150

200
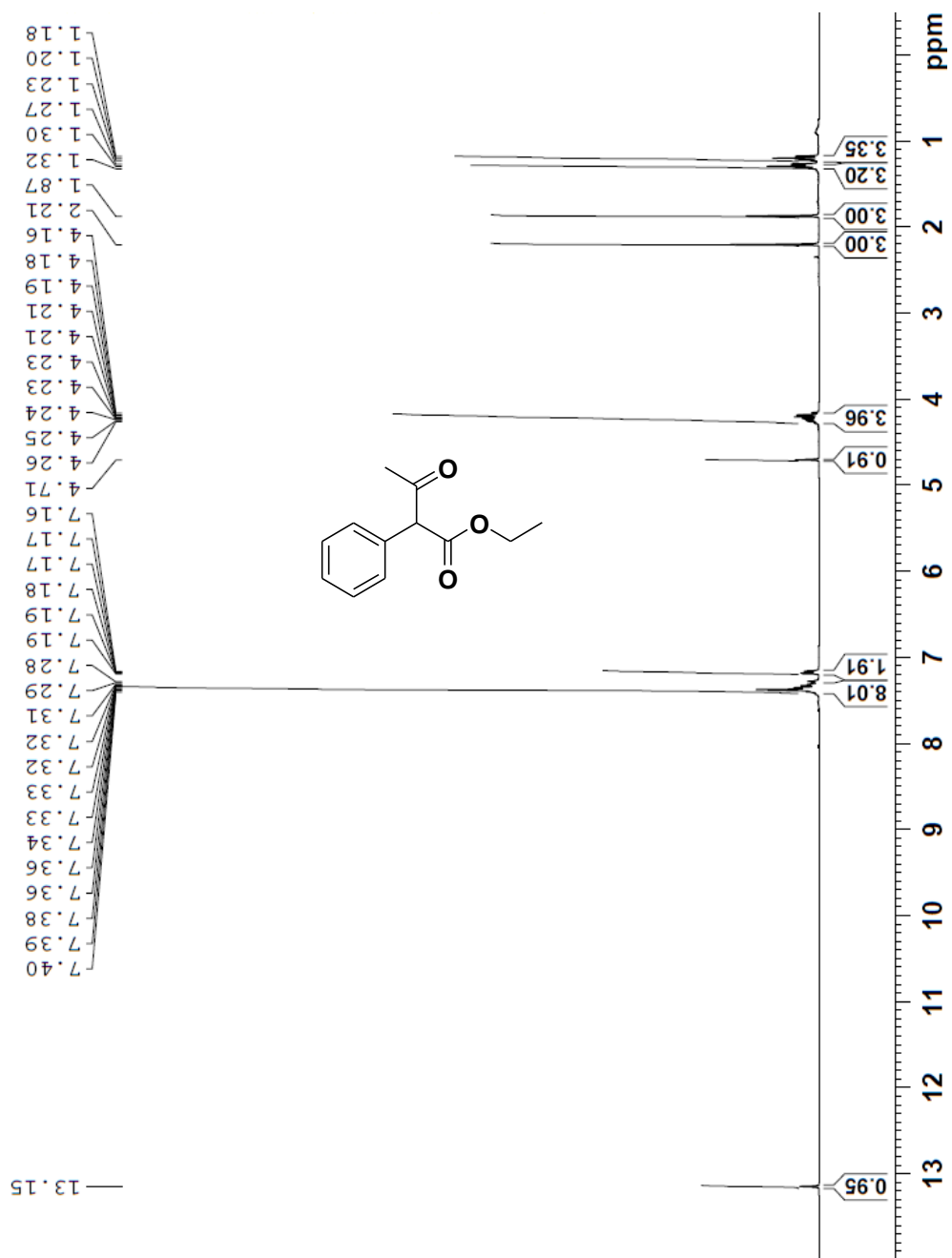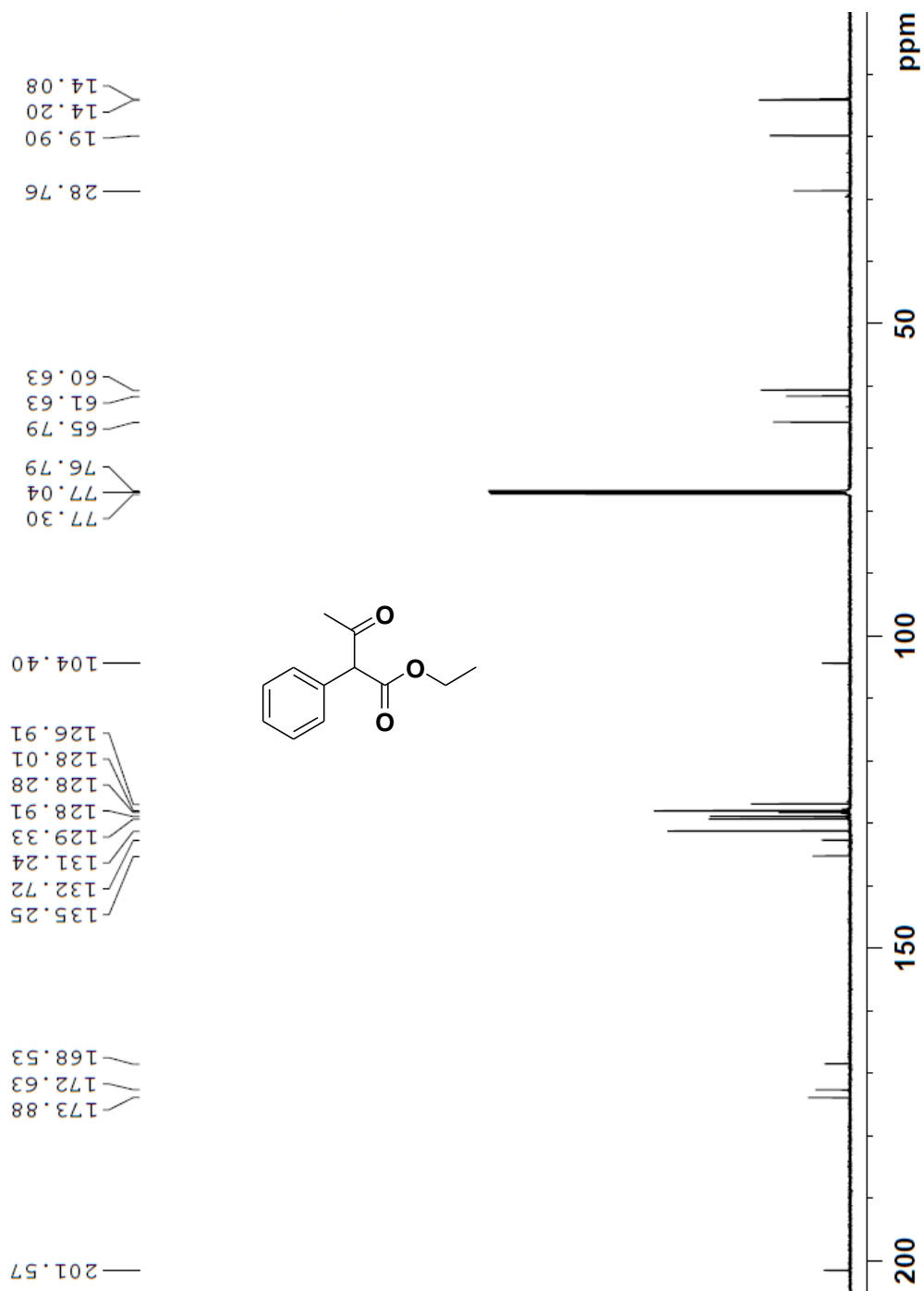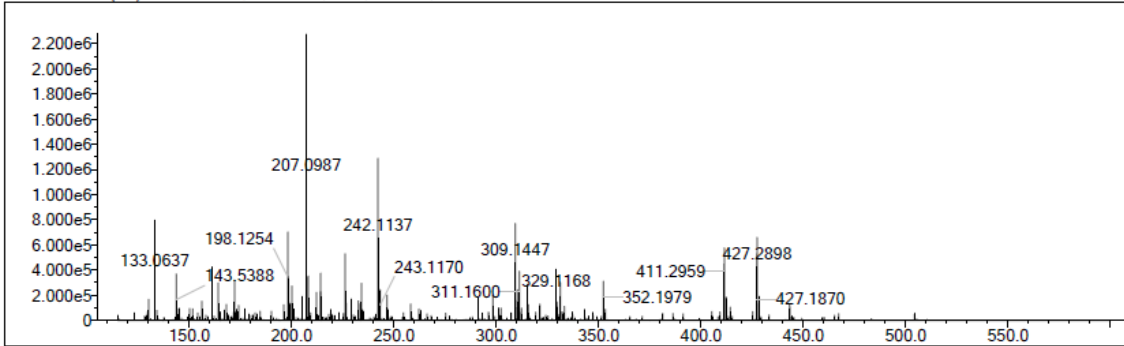
HRMS of Compound 3a

Measured region for 207.0987 m/z
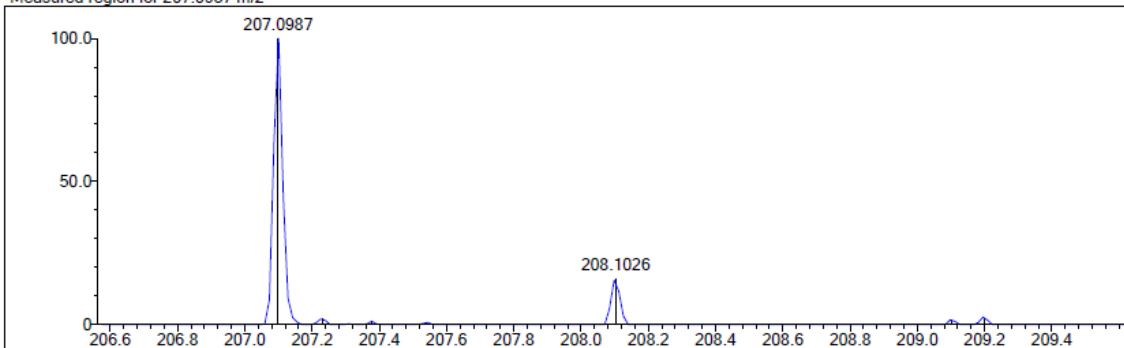
C12 H14 O3 [M+H]+ : Predicted region for 207.1016 m/z
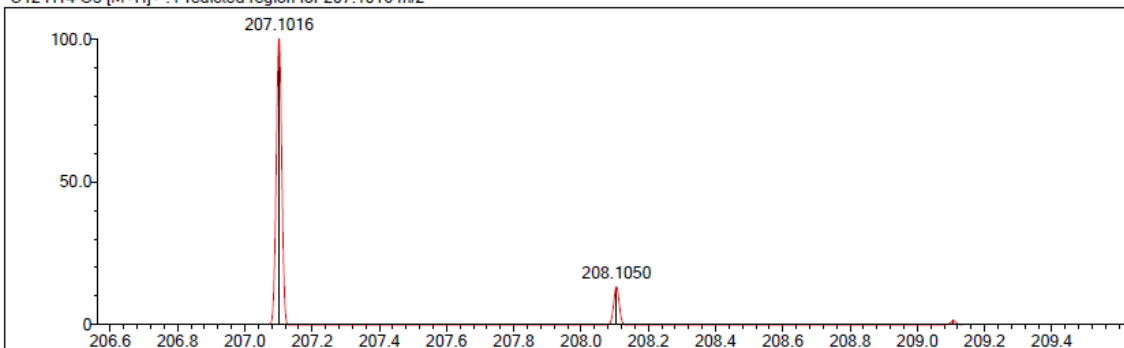
Rank	Score	Formula (M)	Ion	Meas. m/z	Pred. m/z	Df. (mDa)	Df. (ppm)	Iso	DBE
1	23.06	C12 H14 O3	[M+H]+	207.0987	207.1016	-2.9	-14.00	78.61	6.0
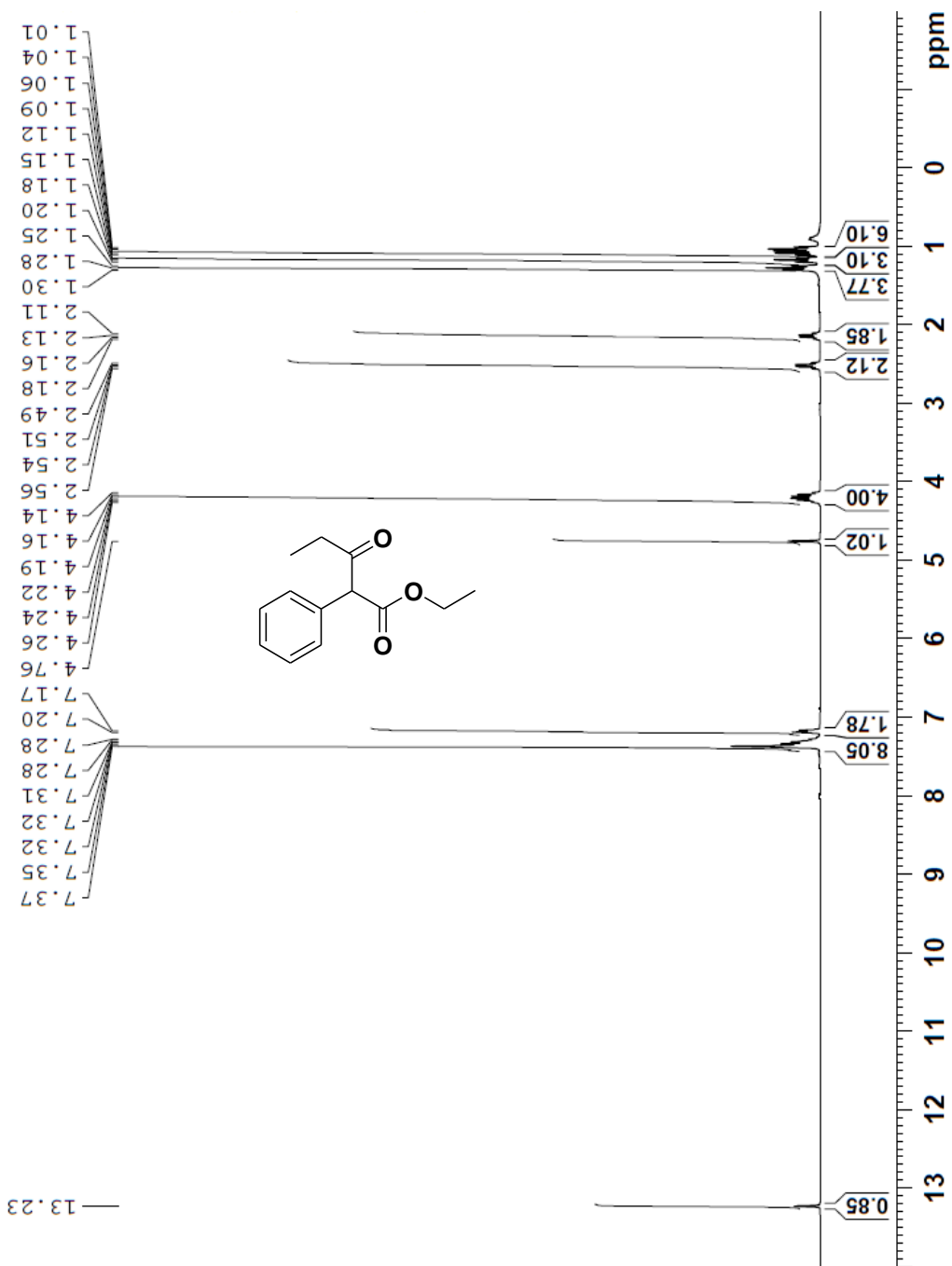
245

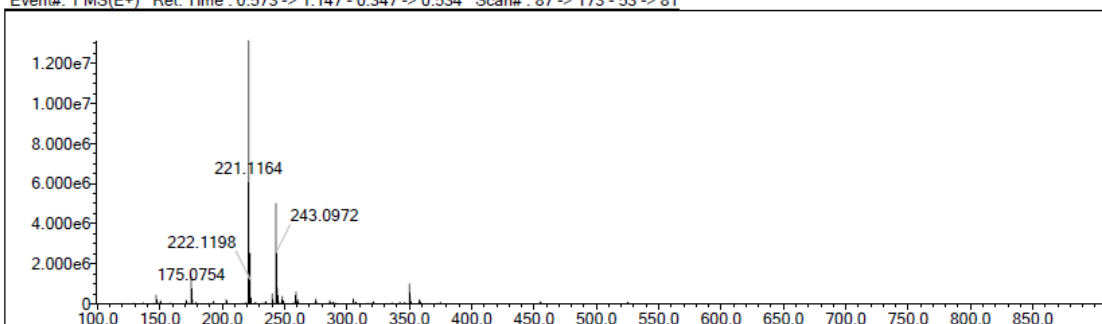# ^{1}H NMR Spectrum of Compound 3b (Keto-Enol Tautomer) in CDCl$_3$

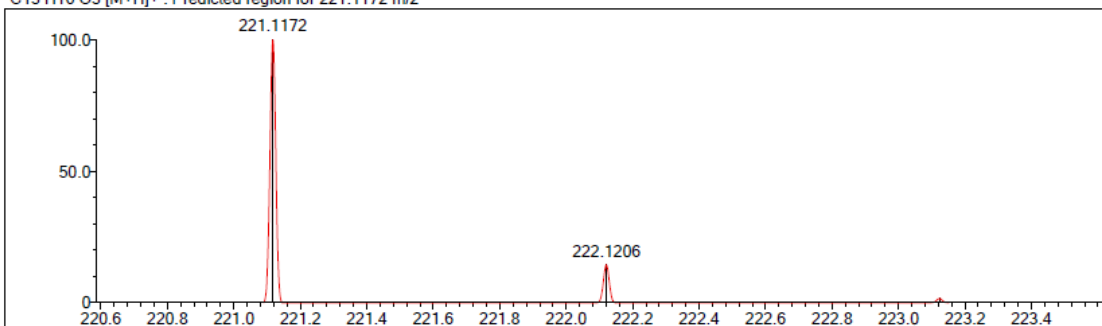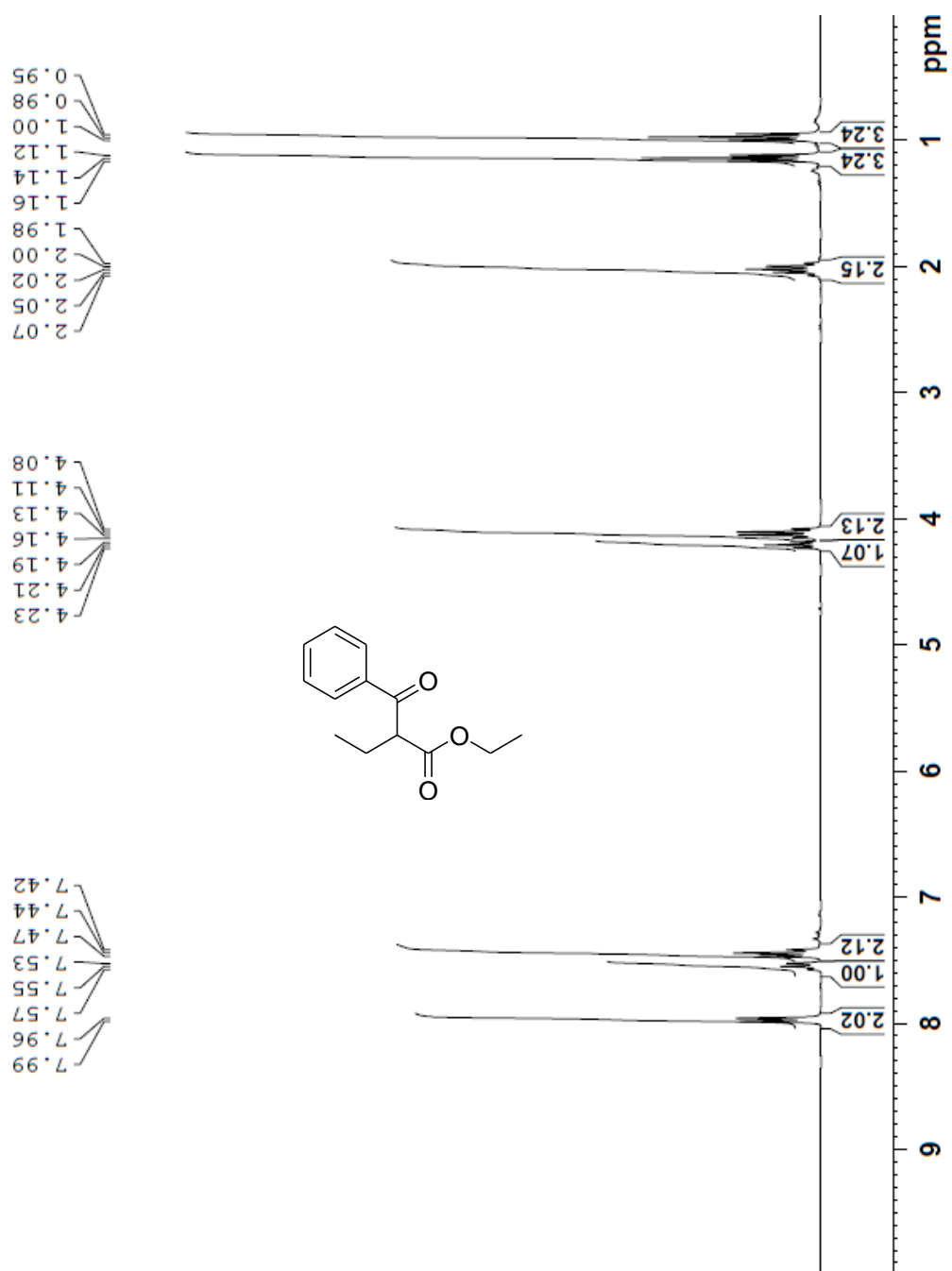# ¹³C NMR Spectrum of Compound 3b (Keto-Enol Tautomer) in CDCl₃

7.75
11.14
14.04
14.15

26.27

34.92

60.53
61.47
64.75

76.77
77.20
77.62

103.60

126.90
128.00
128.11
128.77
129.40
131.22
132.99
135.17

168.72
172.84
178.11

204.20

ppm
50
100
150
200

247
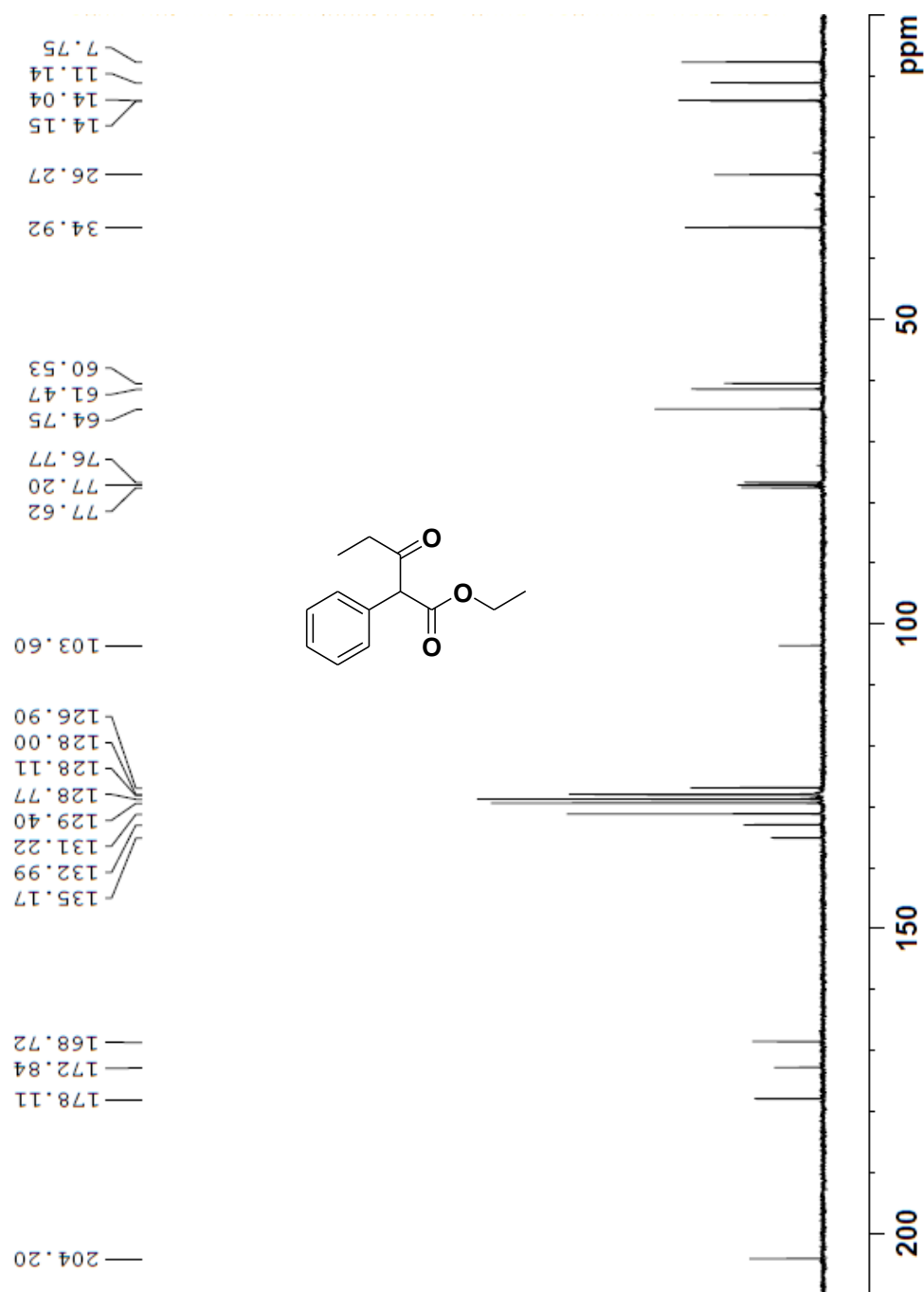
HRMS of Compound 3b

Measured region for 221.1164 m/z
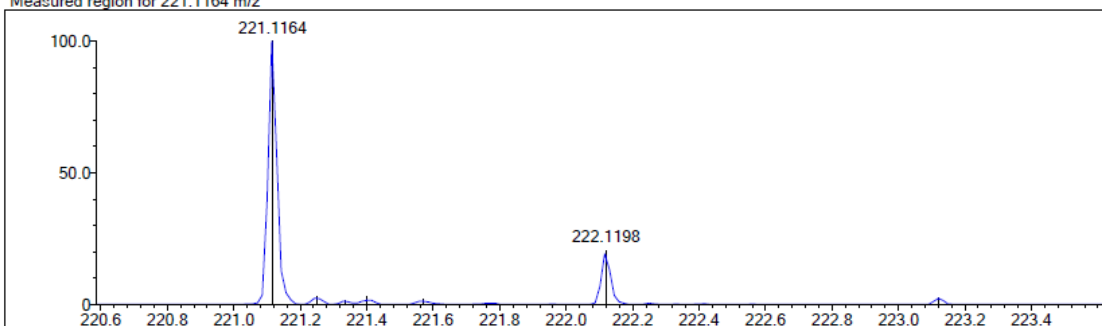
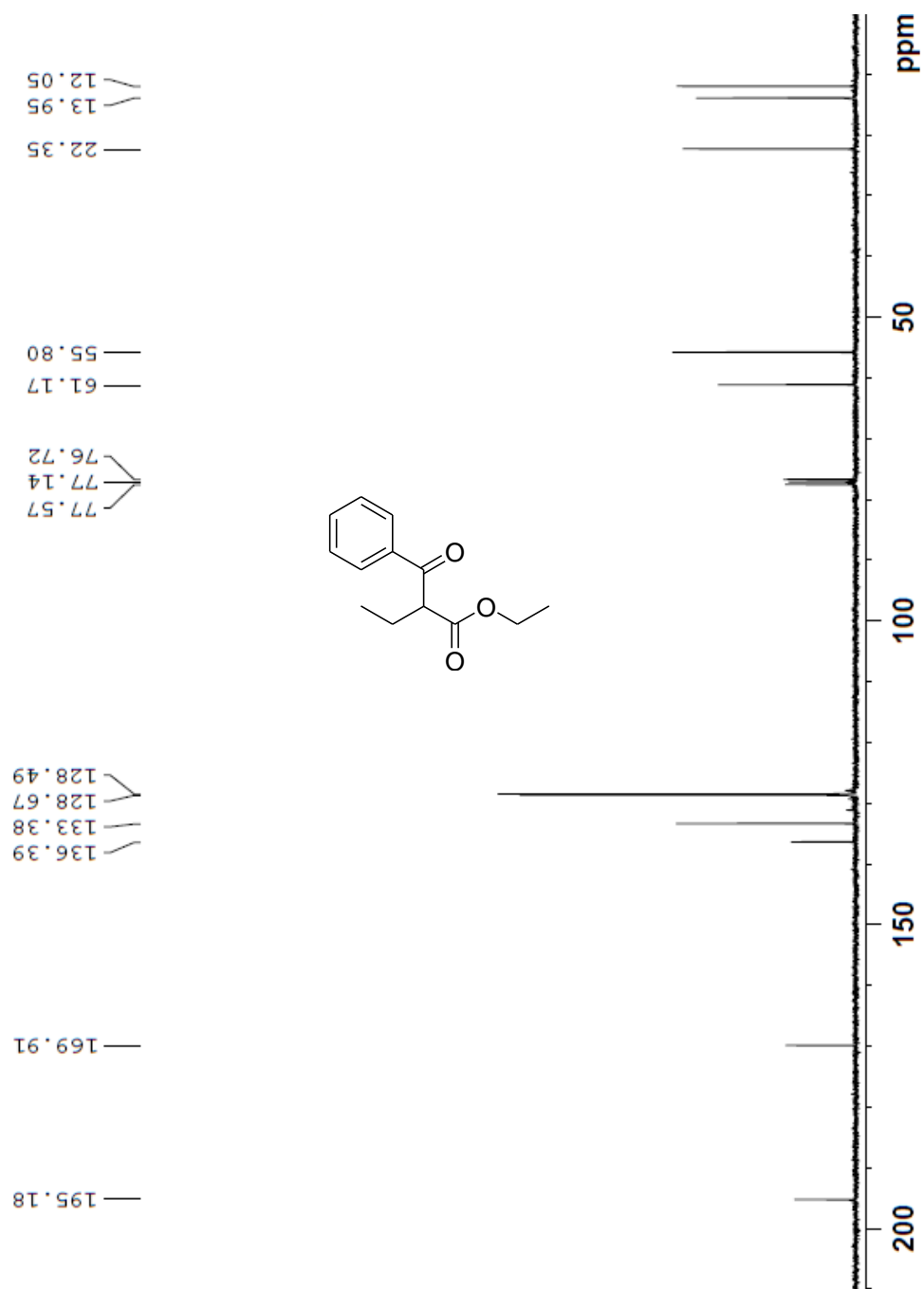C13 H16 O3 [M+H]+ : Predicted region for 221.1172 m/z

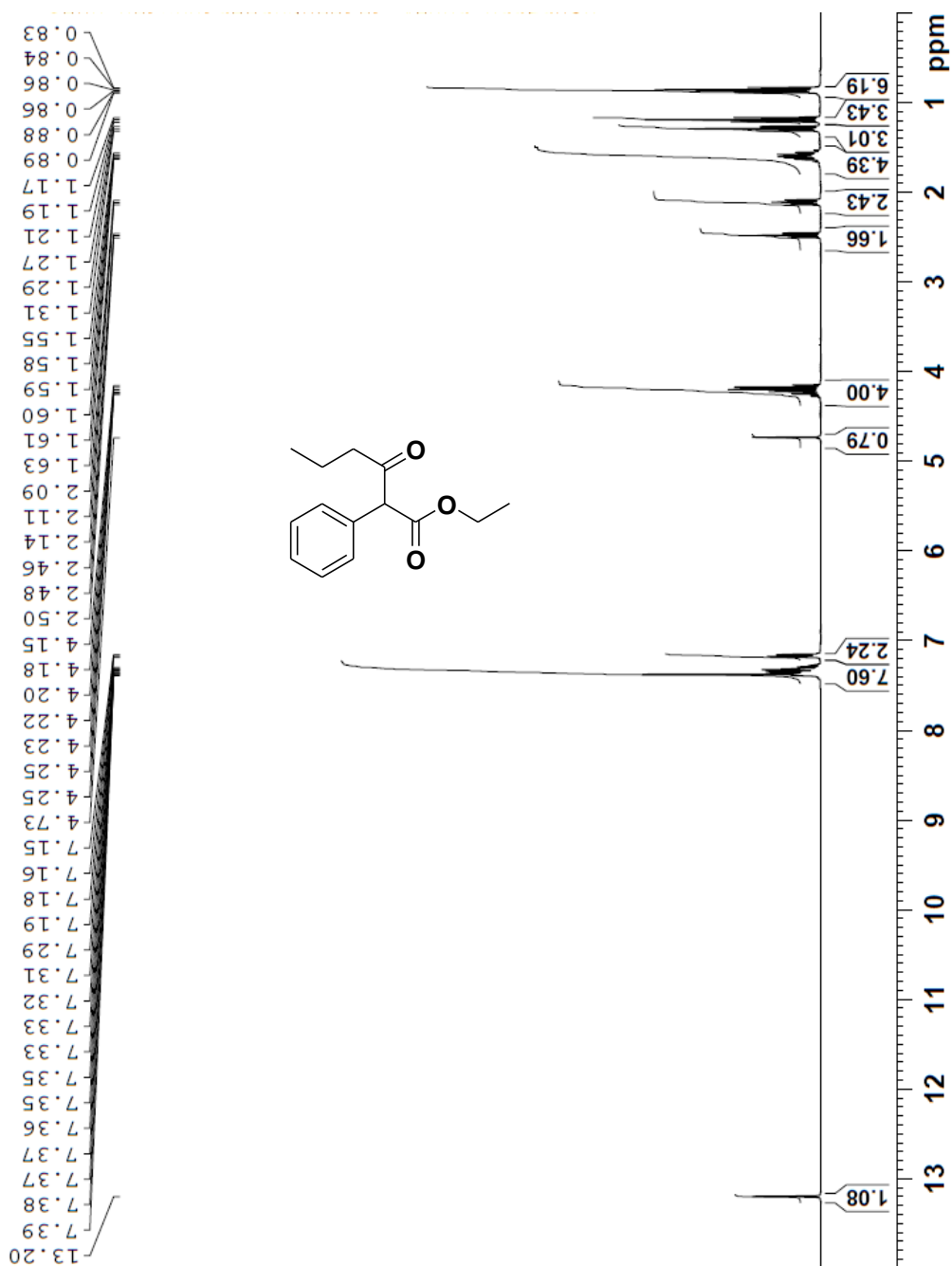| Rank	Score	Formula (M)	Ion	Meas. m/z	Pred. m/z	Df. (mDa)	Df. (ppm)	Iso	DBE
2	69.55	C13 H16 O3	[M+H]+	221.1164	221.1172	-0.8	-3.62	74.42	6.0

248

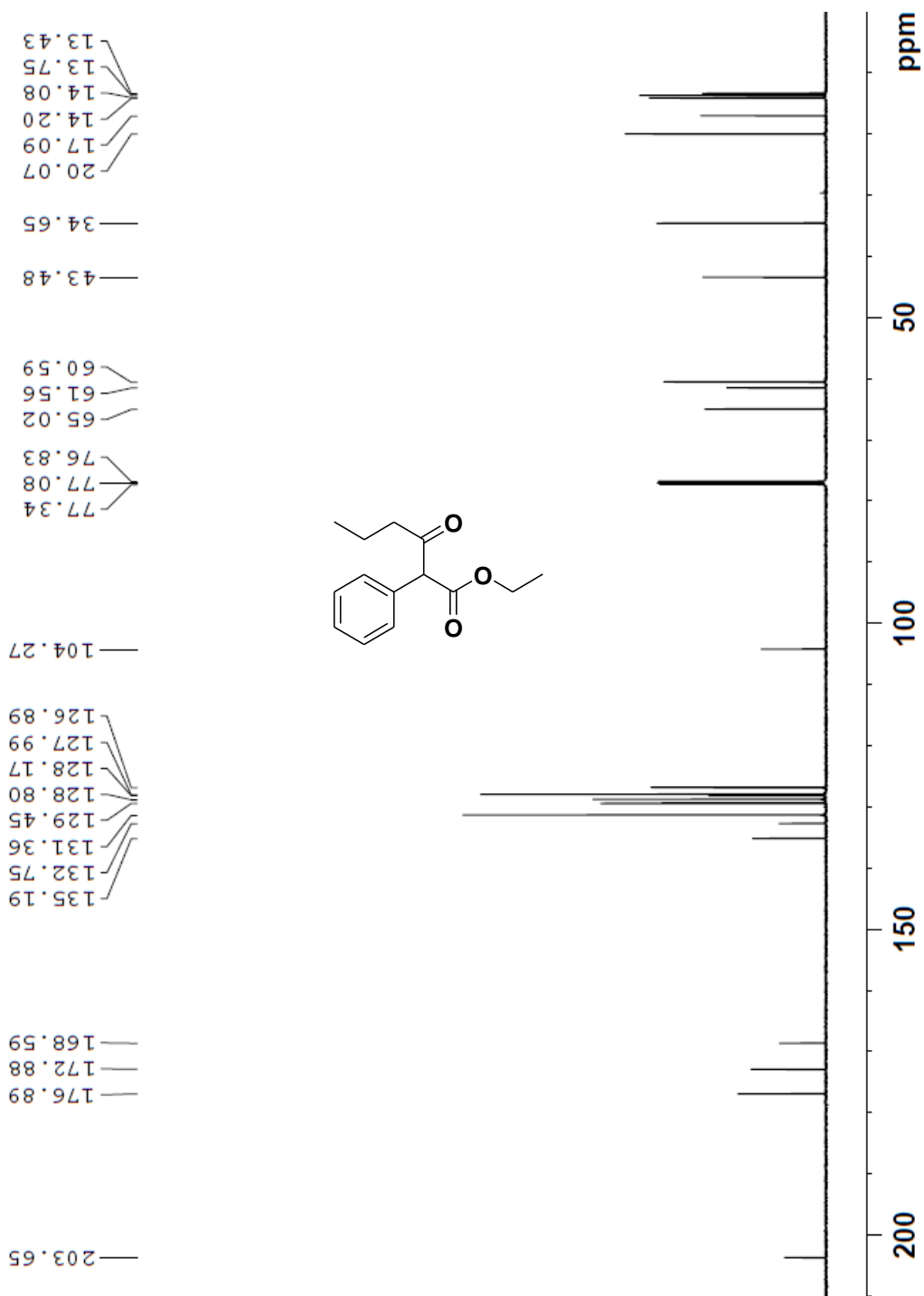# ^{1}H NMR Spectrum of Compound 3b' (Beta-Keto Ester) in CDCl$_3$

0.95
0.98
1.00
1.12
1.14
1.16
1.98
2.00
2.02
2.05
2.07
4.08
4.11
4.13
4.16
4.19
4.21
4.23
7.42
7.44
7.47
7.53
7.55
7.57
7.96
7.99

3.24
3.24
2.15
2.13
1.07
2.12
1.00
2.02

ppm
1 2 3 4 5 6 7 8 9

^{13}C NMR Spectrum of Compound 3b' (Beta Keto Ester) in CDCl$_3$

12.05
13.95
22.35
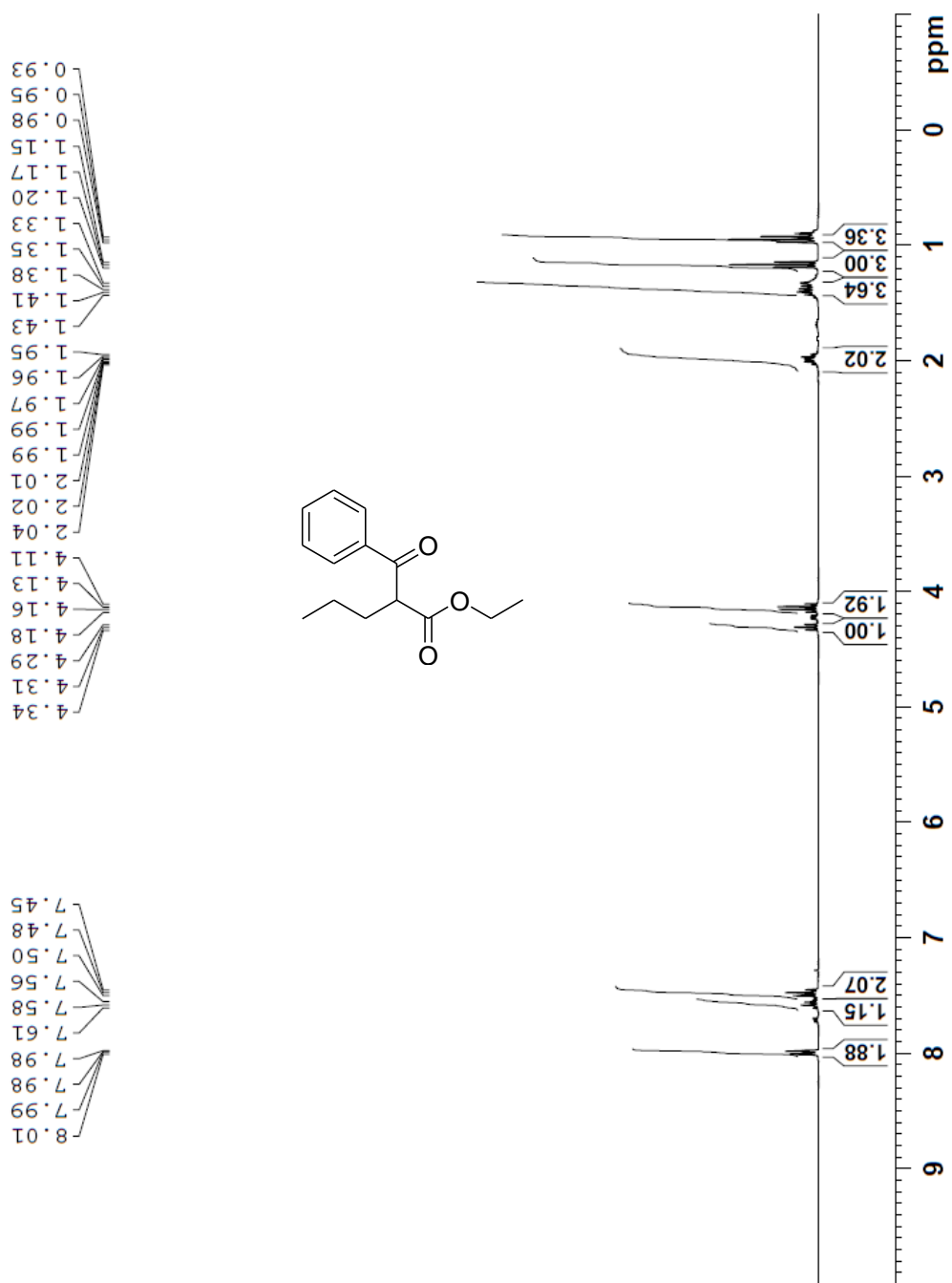
55.80
61.17

76.72
77.14
77.57

128.49
128.67
133.38
136.39

169.91

195.18

¹H NMR Spectrum of Compound 3c (Keto-Enol Tautomer) in CDCl₃

^{13}C NMR Spectrum of Compound 3c (Keto-Enol Tautomer) in CDCl$_3$

13.43
13.75
14.08
14.20
17.09
20.07

34.65

43.48

60.59
61.56
65.02

76.83
77.08
77.34

104.27

126.89
127.99
128.17
128.80
129.45
131.36
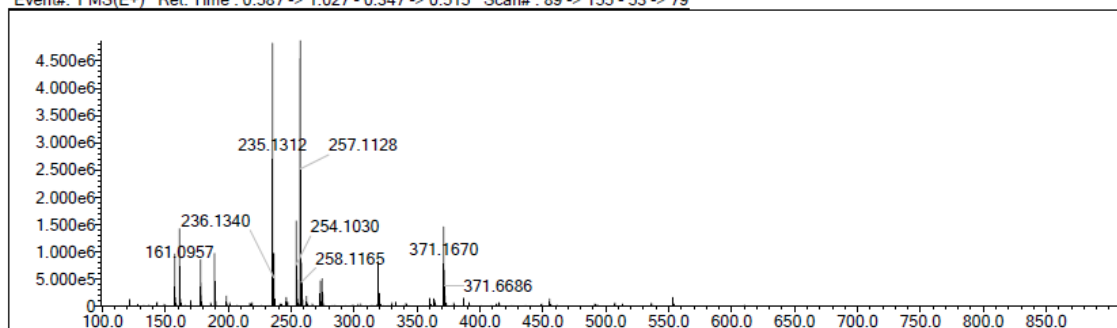132.75
135.19

168.59
172.88
176.89

203.65

ppm
50
100
150
200

^{1}H NMR Spectrum of Compound 3c' (Beta-Keto Ester) in CDCl$_3$
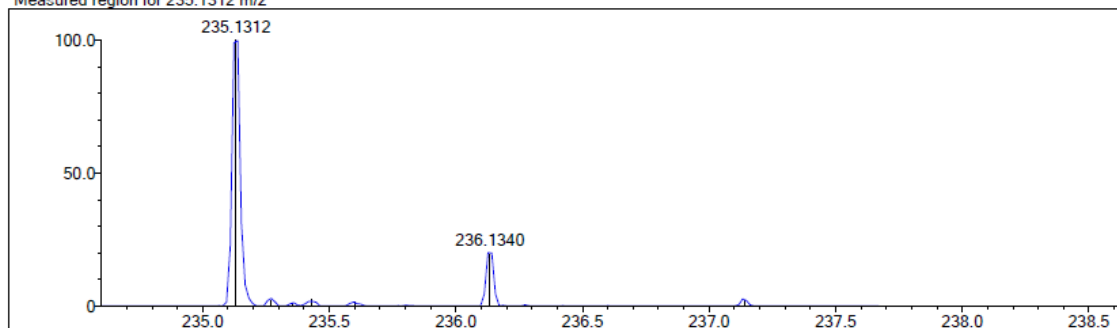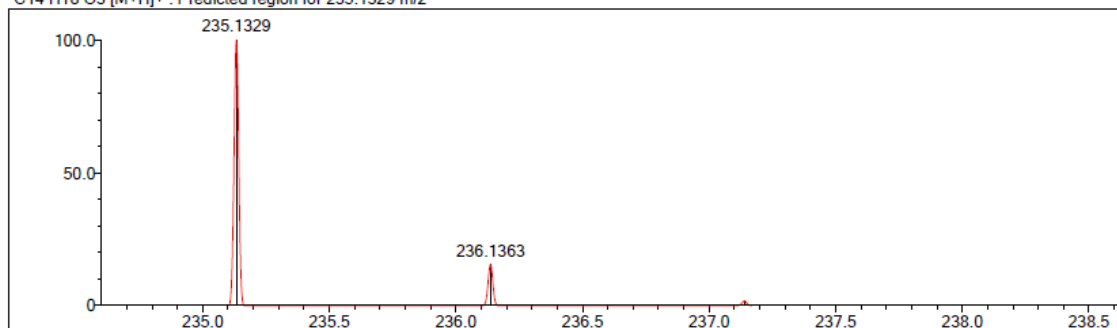
HRMS of Compound 3c'

Event#: 1 MS(E+) Ret. Time : 0.587 -> 1.027 - 0.347 -> 0.515 Scan# : 89 -> 155 - 53 -> 79
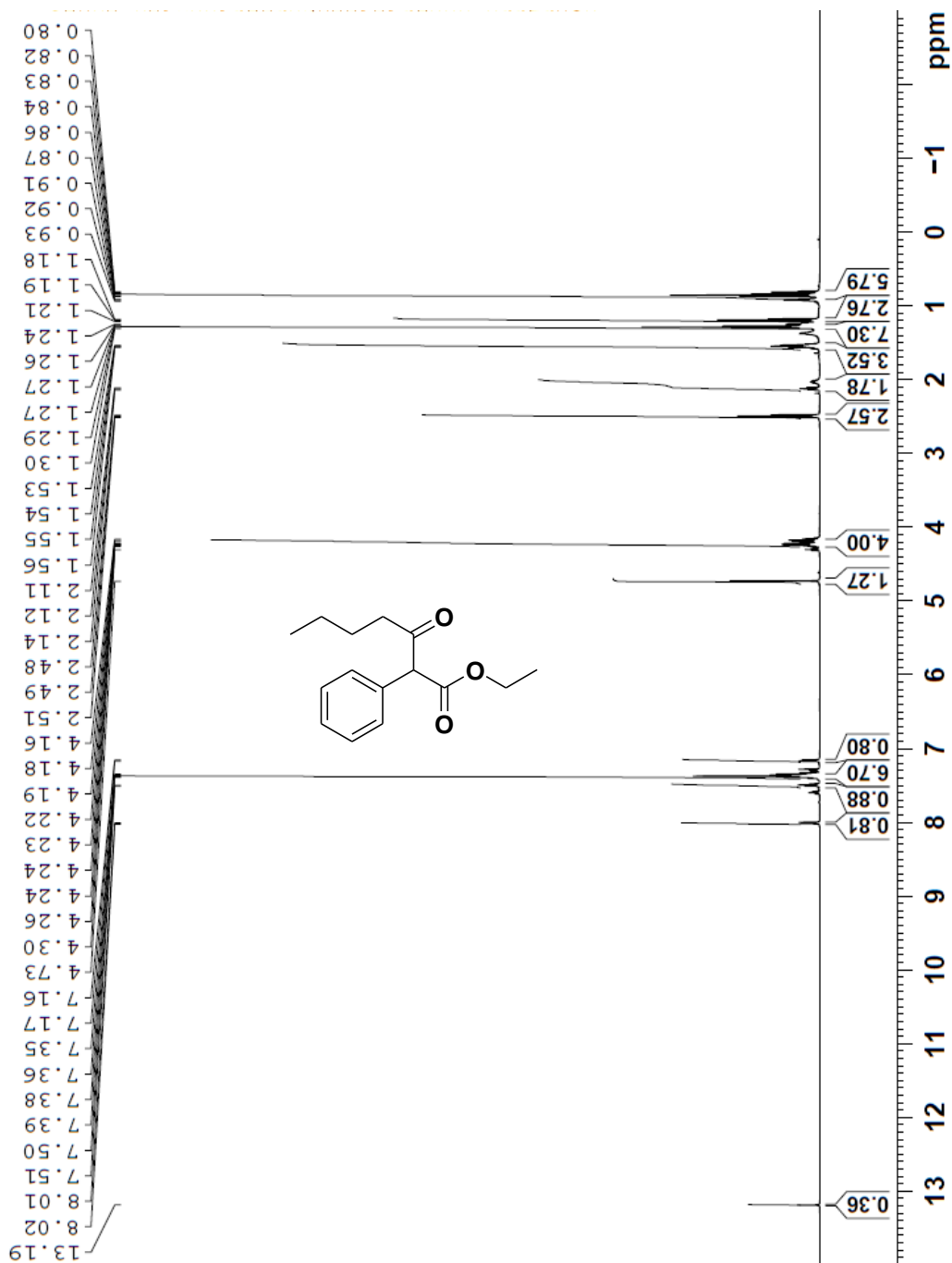

Measured region for 235.1312 m/z

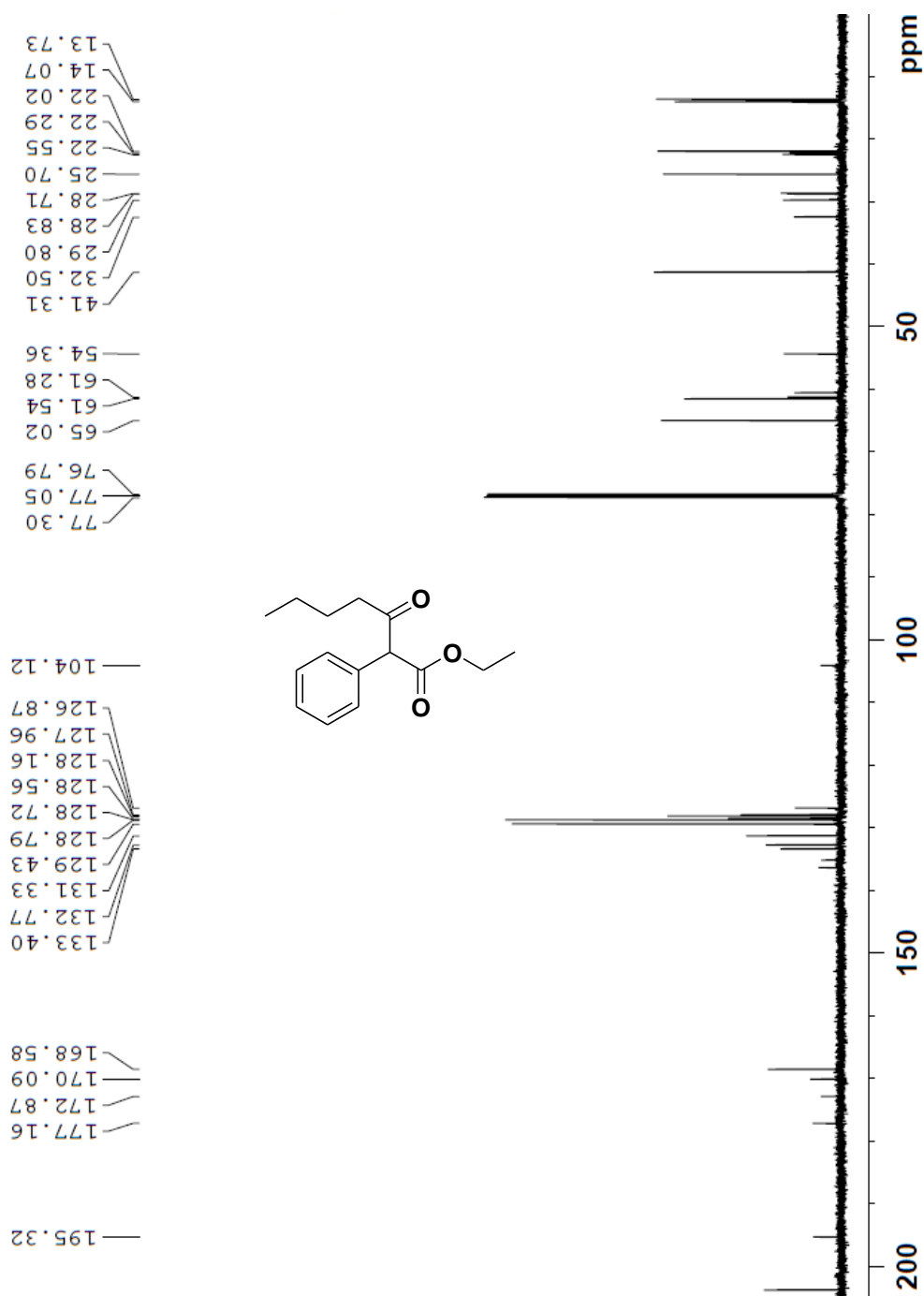C14 H18 O3 [M+H]+ : Predicted region for 235.1329 m/z

Rank	Score	Formula (M)	Ion	Meas. m/z	Pred. m/z	Df. (mDa)	Df. (ppm)	Iso	DBE
3	59.72	C14 H18 O3	[M+H]+	235.1312	235.1329	-1.7	-7.23	88.22	6.0

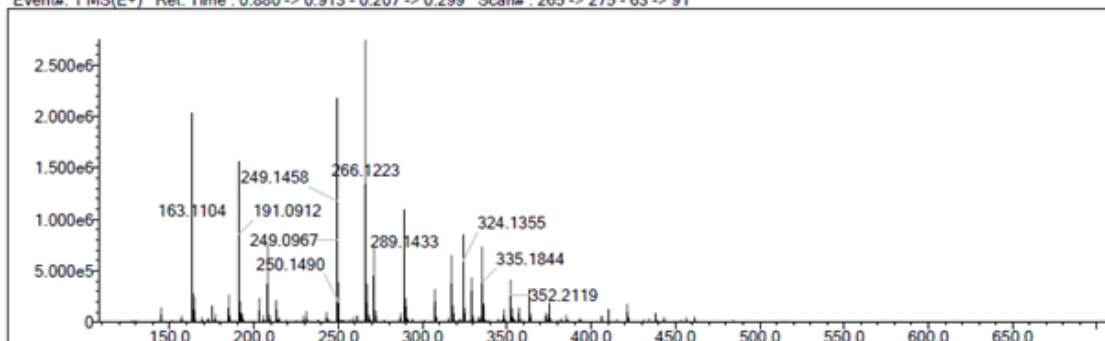# ^{1}H NMR Spectrum of Compound 3d (Keto-Enol Tautomer) in CDCl$_3$

^{13}C NMR Spectrum of Compound 3d (Keto-Enol Tautomer) in CDCl$_3$
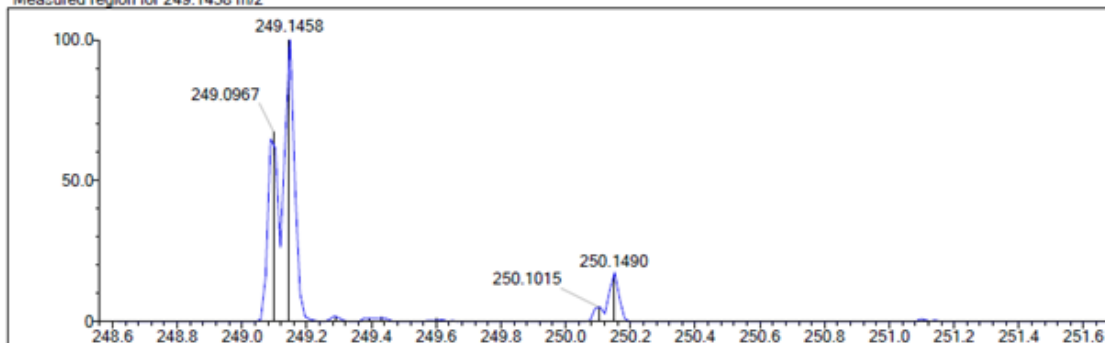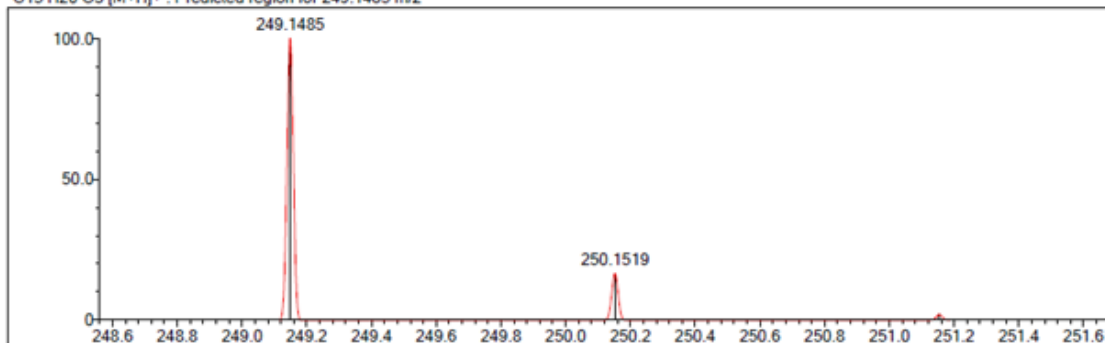
13.73
14.07
22.02
22.29
22.55
25.70
28.71
28.83
29.80
32.50
41.31

54.36
61.28
61.54
65.02

76.79
77.05
77.30

104.12

126.87
127.96
128.16
128.56
128.72
128.79
129.43
131.33
132.77
133.40

168.58
170.09
172.87
177.16

195.32

ppm

200
150
100
50

HRMS of Compound 3d

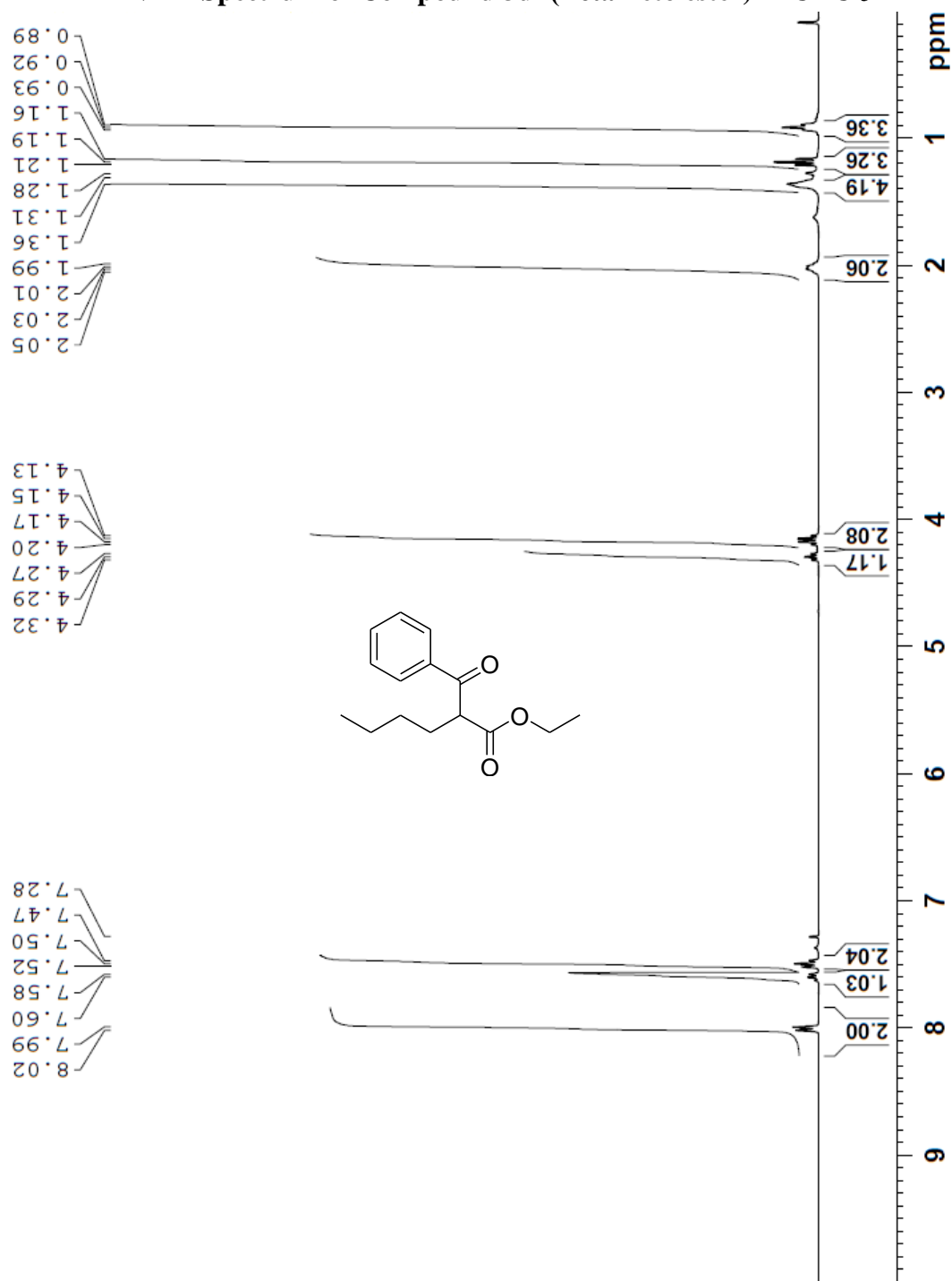Measured region for 249.1458 m/z

C15 H20 O3 [M+H]+ : Predicted region for 249.1485 m/z

Rank	Score	Formula (M)	Ion	Meas. m/z	Pred. m/z	Df. (mDa)	Df. (ppm)	Iso	DBE
3	24.79	C15 H20 O3	[M+H]+	249.1458	249.1485	-2.7	-10.84	65.64	6.0

^{1}H NMR Spectrum of Compound 3d' (Beta-keto ester) in CDCl$_3$

0.89
0.92
0.93
1.16
1.19
1.21
1.28
1.31
1.36
1.99
2.01
2.03
2.05

4.13
4.15
4.17
4.20
4.27
4.29
4.32

7.28
7.47
7.50
7.52
7.58
7.60
7.99
8.02

3.36
3.26
4.19
2.06
2.08
1.17
2.04
1.03
2.00

ppm
1
2
3
4
5
6
7
8
9

^{13}C NMR Spectrum of Compound 3d' (Beta-Keto Ester) in CDCl$_3$

13.81
14.00

22.53

28.70
29.79

54.36

61.28

76.59
77.01
77.44

128.55
128.70
133.39
136.39

170.10

195.33

^{1}H NMR Spectrum of Compound 3e (Keto-Enol Tautomer) in CDCl$_3$

0.83
0.85
0.87
0.89
1.15
1.17
1.20
1.22
1.23
1.24
1.26
1.28
1.30
1.54
1.56
1.59
1.61
1.63
2.12
2.14
2.17
2.48
2.51
2.53
4.14
4.16
4.19
4.20
4.21
4.22
4.24
4.25
4.26
4.77
7.17
7.19
7.20
7.28
7.29
7.30
7.30
7.31
7.32
7.34
7.37
7.38
7.39
7.41
13.26

6.00
14.36
4.07
2.39
1.57
4.01
0.78
2.33
7.64
1.16

ppm
1
2
3
4
5
6
7
8
9
10
11
12
13
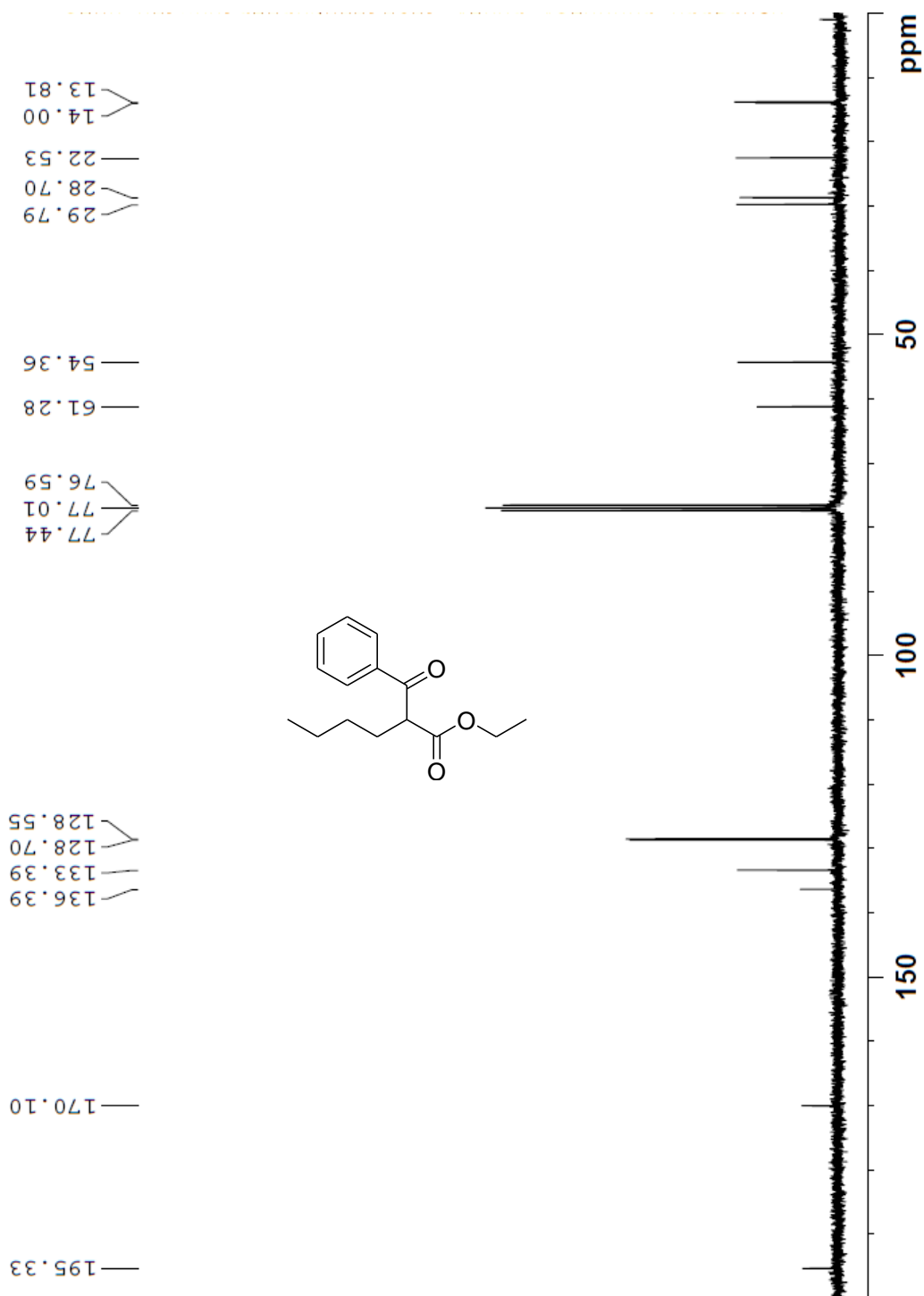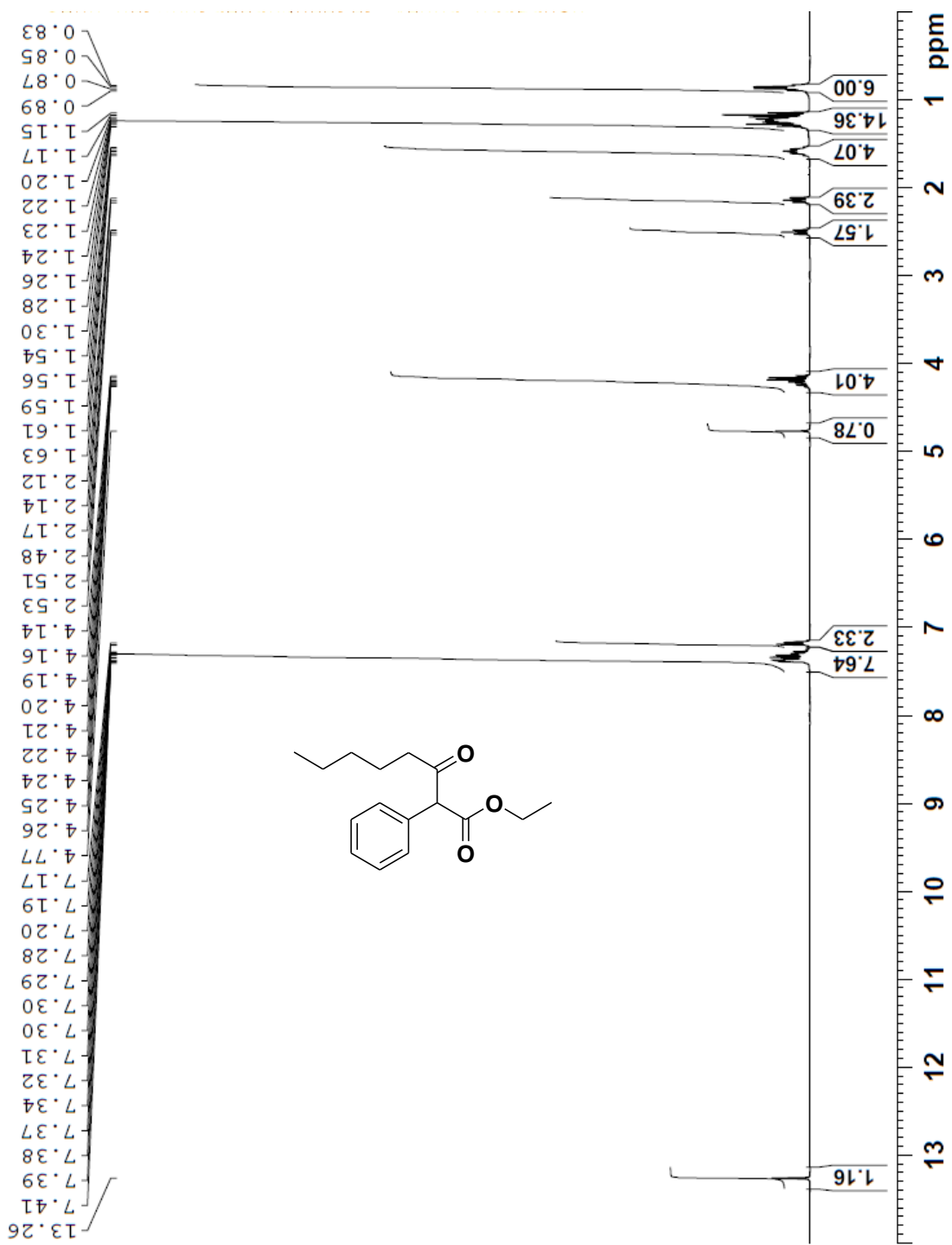
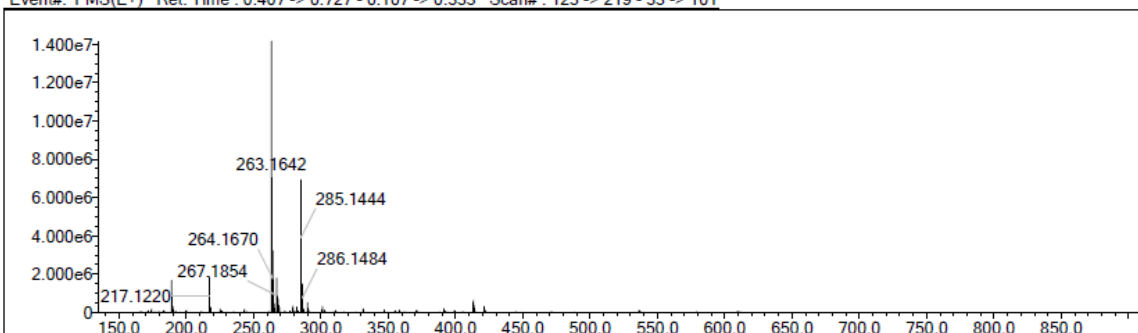# ¹³C NMR Spectrum of Compound 3e (Keto-Enol Tautomer) in CDCl₃
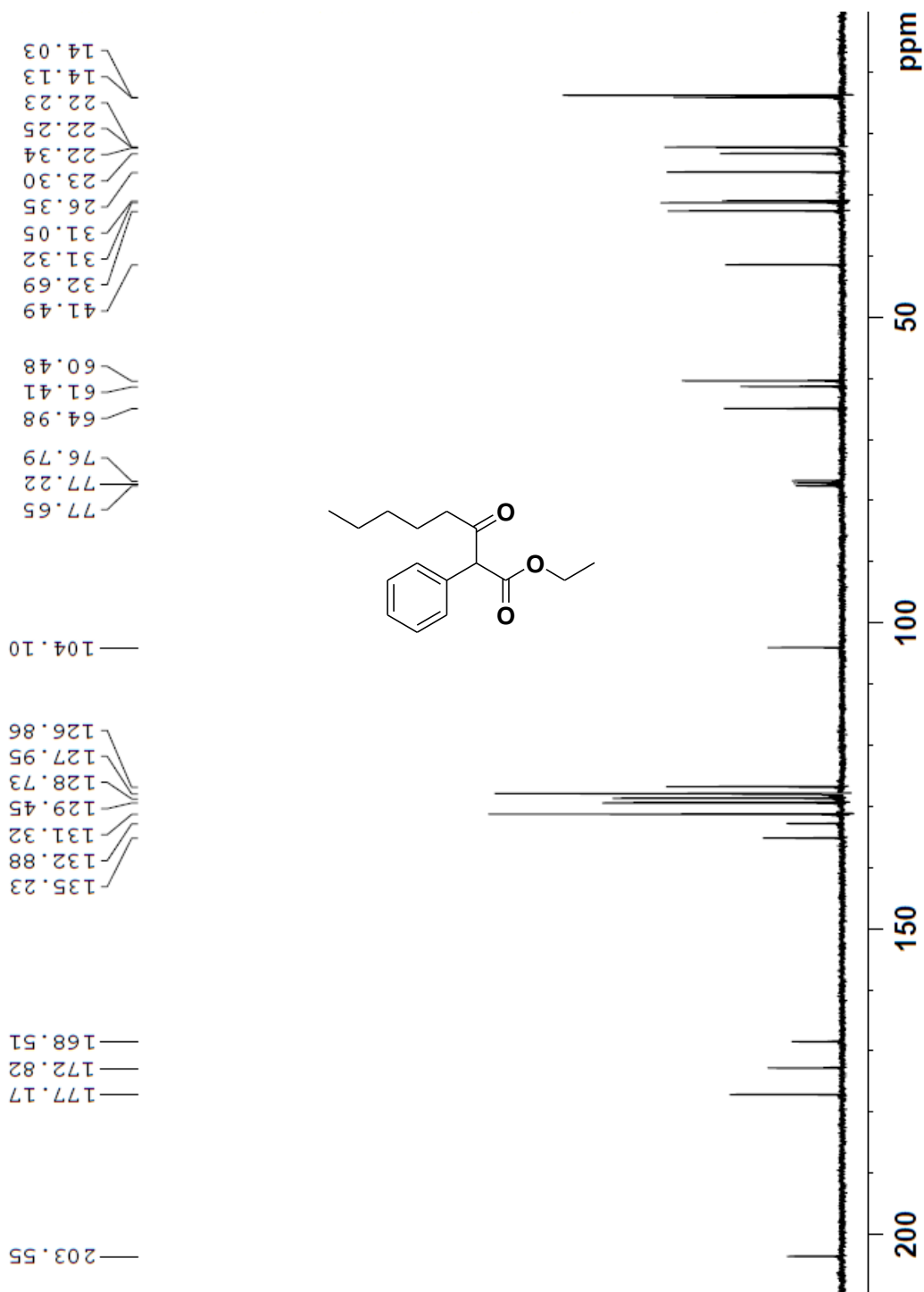
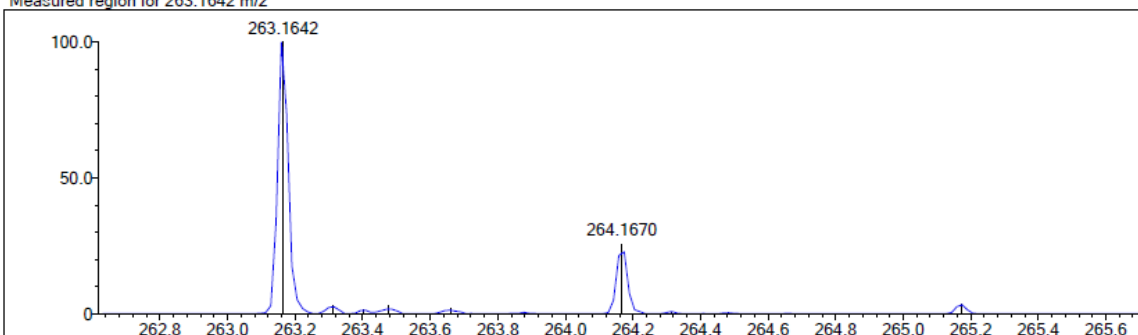# HRMS of Compound 3e

Event#: 1 MS(E+) Ret. Time : 0.407 -> 0.727 - 0.107 -> 0.333 Scan# : 123 -> 219 - 33 -> 101

217.1220
267.1854
264.1670
263.1642
285.1444
286.1484

Measured region for 263.1642 m/z

263.1642
264.1670

C16 H22 O3 [M+H]+ : Predicted region for 263.1642 m/z
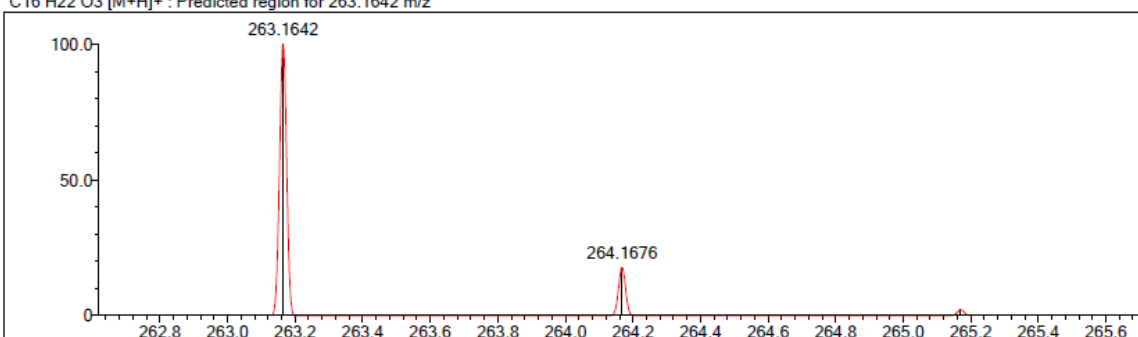
263.1642
264.1676

Rank	Score	Formula (M)	Ion	Meas. m/z	Pred. m/z	Df. (mDa)	Df. (ppm)	Iso	DBE
1	75.90	C16 H22 O3	[M+H]+	263.1642	263.1642	0.0	0.00	75.90	6.0

^{1}H NMR Spectrum of Compound 3e' (Beta-Keto Ester) in CDCl$_3$

0.86
0.89
0.91
1.16
1.18
1.21
1.27
1.28
1.32
1.34
1.39
1.98
2.00
2.02
2.03
2.05

4.12
4.15
4.17
4.20
4.27
4.30
4.32

7.46
7.49
7.51
7.57
7.60
7.62
7.99
8.02

3.39
3.08
6.16

2.09

2.07
1.13

2.06
1.00

2.00

ppm

¹³C NMR Spectrum of Compound 3e' (Beta-Keto Ester) in CDCl₃

HRMS of Compound 3e'

Event#: 1 MS(E+)   Ret. Time : 0.393 -> 0.720 - 0.193 -> 0.362   Scan# : 119 -> 217 - 59 -> 109
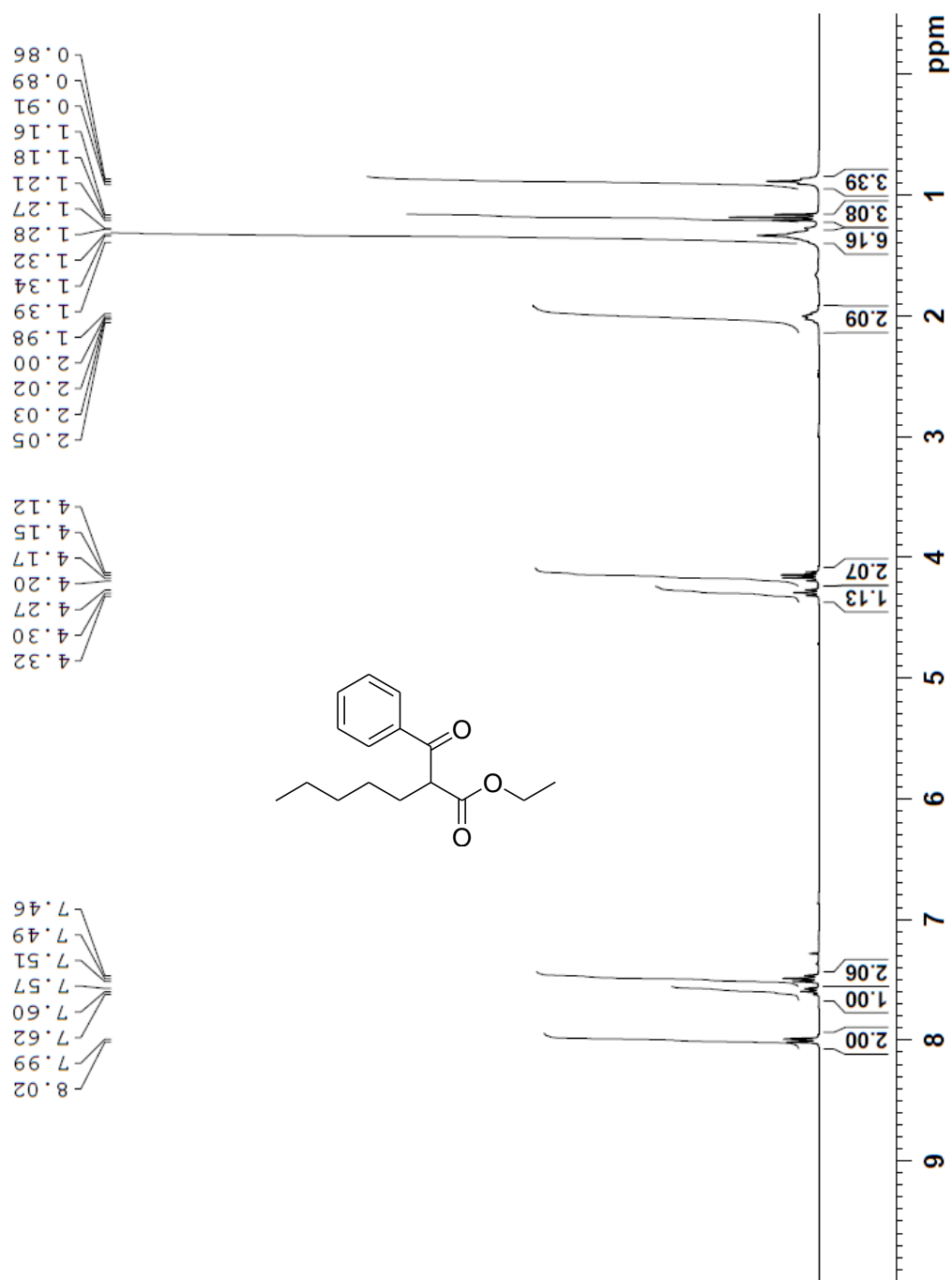
Measured region for 263.1649 m/z

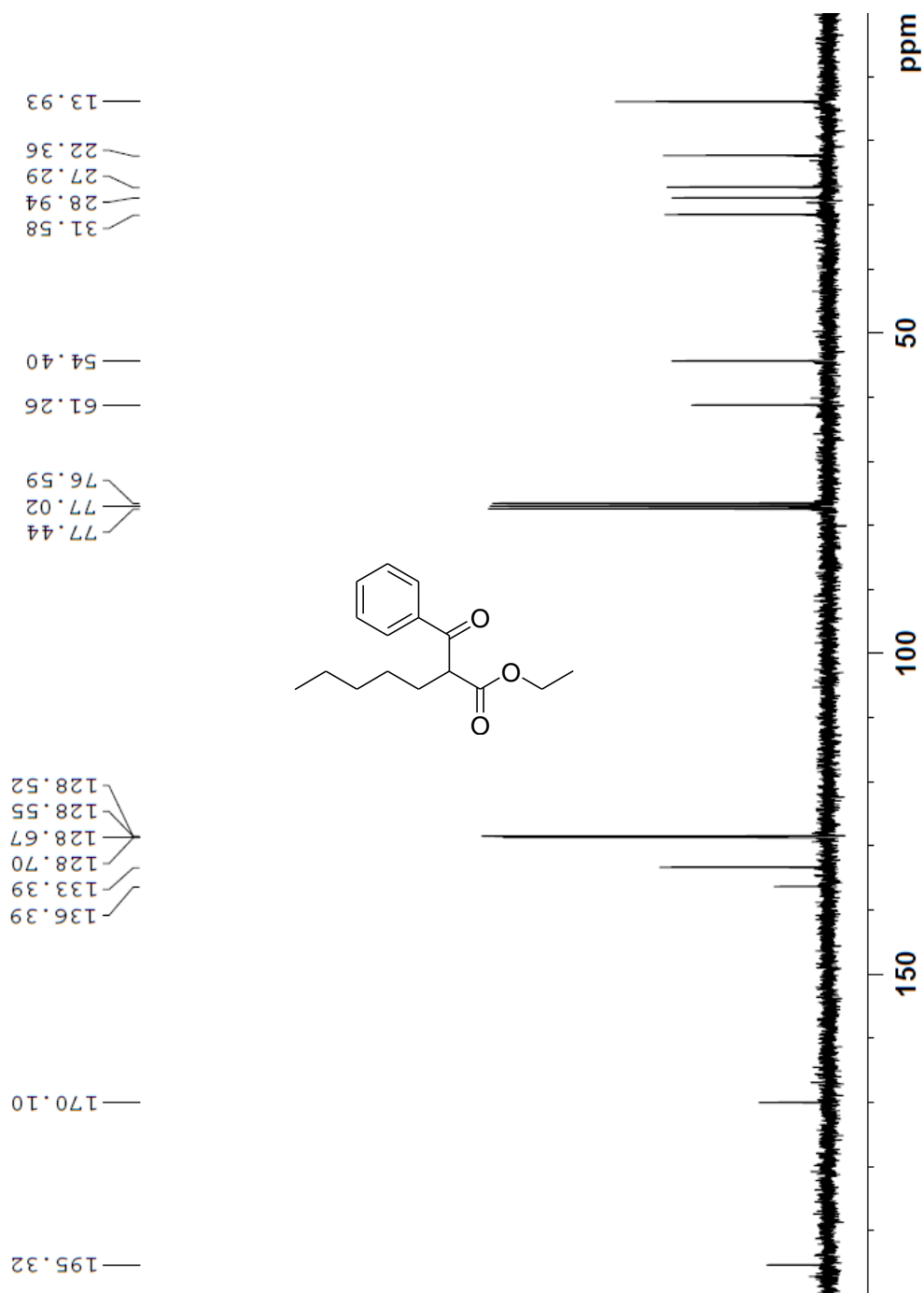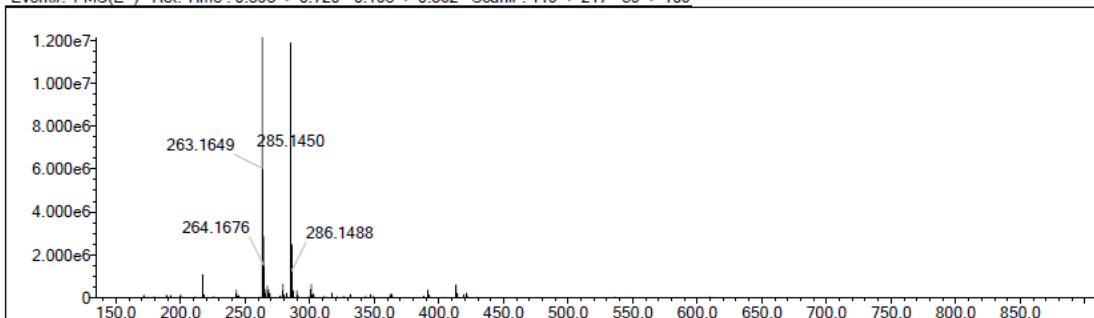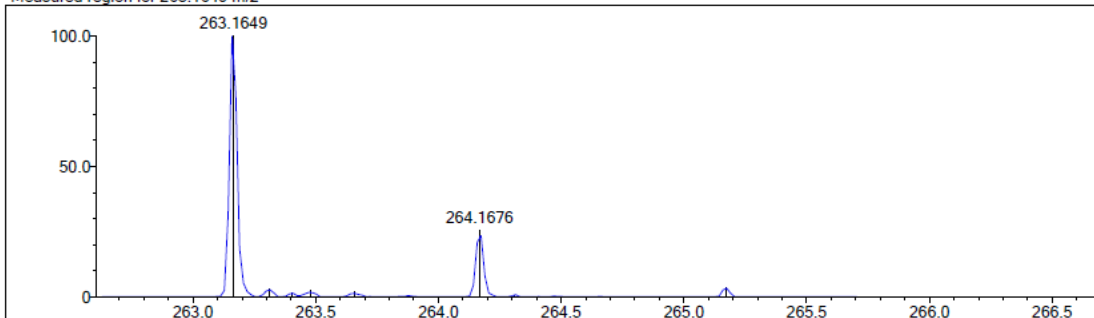C16 H22 O3 [M+H]+ : Predicted region for 263.1642 m/z
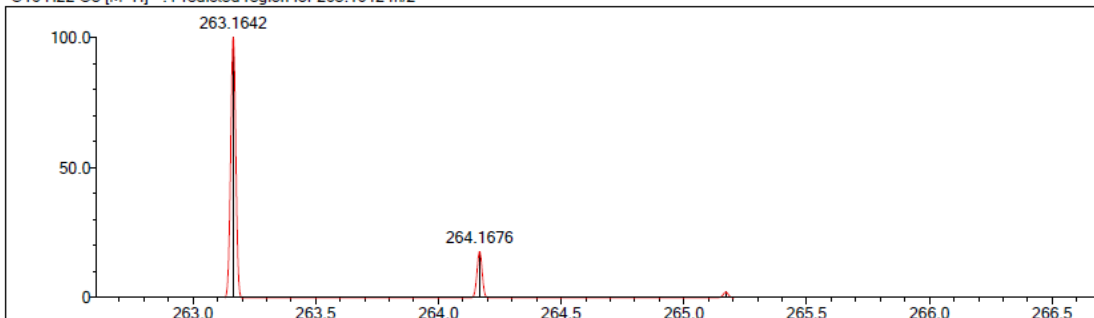
Rank	Score	Formula (M)	Ion	Meas. m/z	Pred. m/z	Df. (mDa)	Df. (ppm)	Iso	DBE
1	78.20	C16 H22 O3	[M+H]+	263.1649	263.1642	0.7	2.66	81.59	6.0

^{1}H NMR Spectrum of Compound 3f (Keto-Enol Tautomer) in CDCl$_3$

0.84
0.85
0.86
0.89
1.18
1.21
1.22
1.24
1.26
1.28
1.31
1.54
1.56
1.57
1.58
2.09
2.12
2.14
2.47
2.49
2.52
4.17
4.19
4.21
4.22
4.24
4.24
4.26
4.74
7.15
7.15
7.16
7.17
7.18
7.28
7.29
7.30
7.31
7.32
7.33
7.33
7.34
7.35
7.36
7.36
7.37
7.38
7.39
13.20

6.27
18.39
4.44
1.82
2.45

4.25
1.29

1.34
8.58

0.60

ppm
1
2
3
4
5
6
7
8
9
10
11
12
13

^{13}C NMR Spectrum of Compound 3f (Keto-Enol Tautomer) in CDCl$_3$

13.95
14.05
14.17
22.41
23.58
26.62
28.53
28.81
31.46
32.74
41.58

60.54
61.50
65.00

76.66
77.08
77.51

104.10

126.86
127.95
128.13
128.76
128.98
129.43
129.65
131.32
132.78
135.19

168.56
172.85
177.18

203.74

HRMS of Compound 3f

Event#: 1 MS(E+)   Ret. Time : 0.627 -> 0.973   Scan# : 95 -> 147
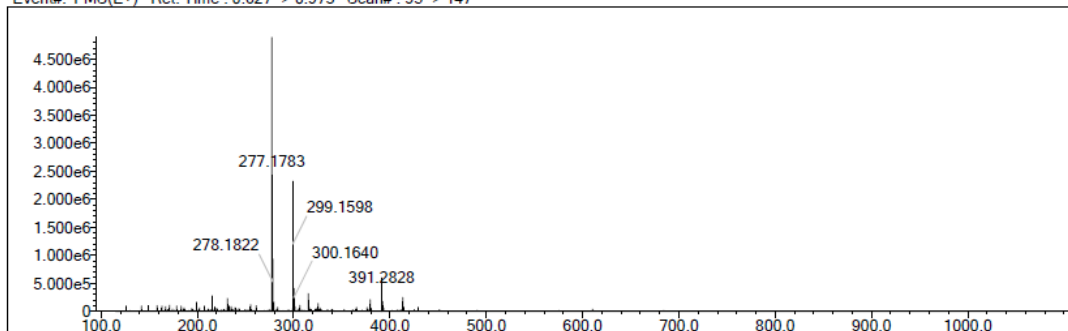
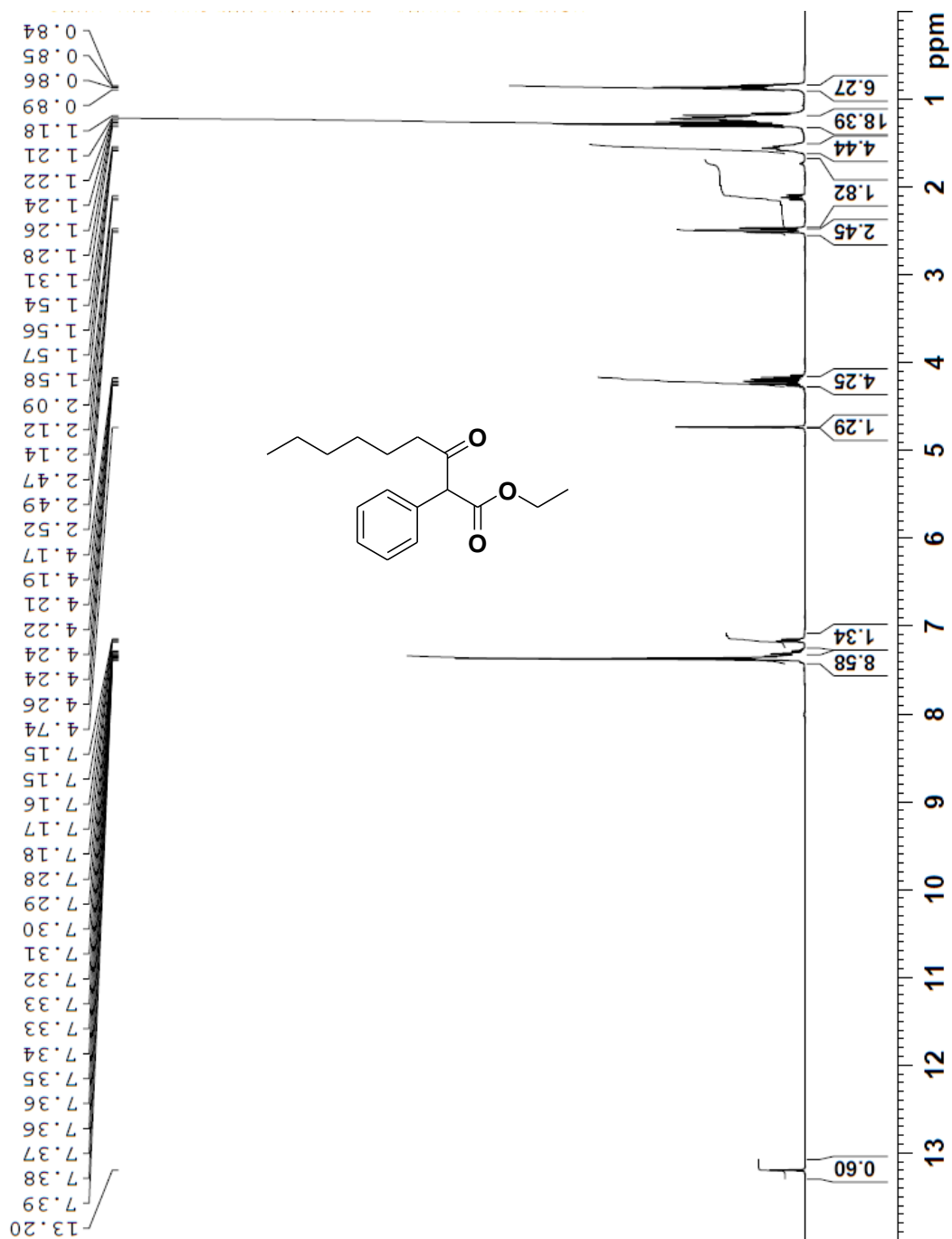Measured region for 277.1814 m/z
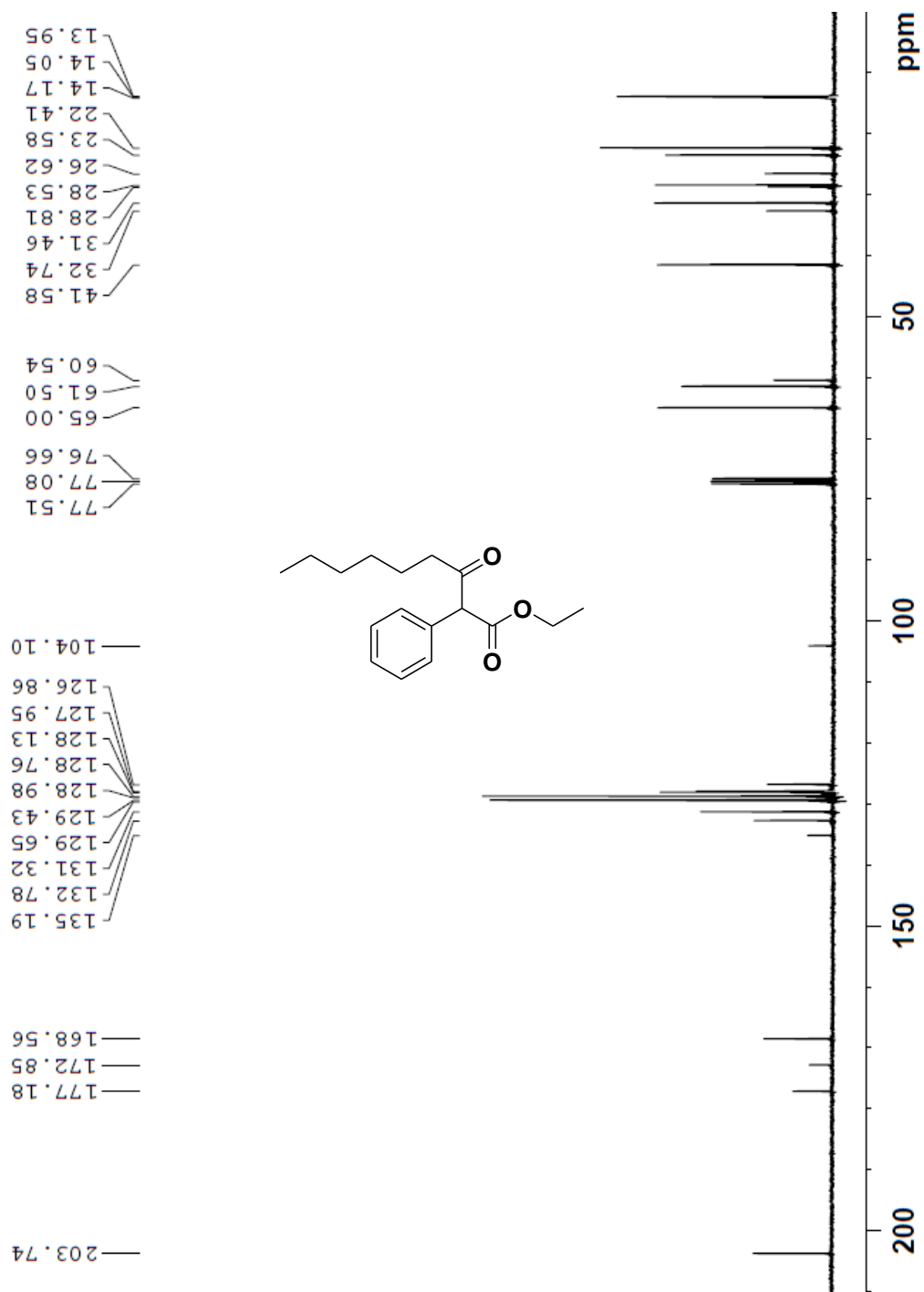

C17 H24 O3 [M+H]+ : Predicted region for 277.1798 m/z
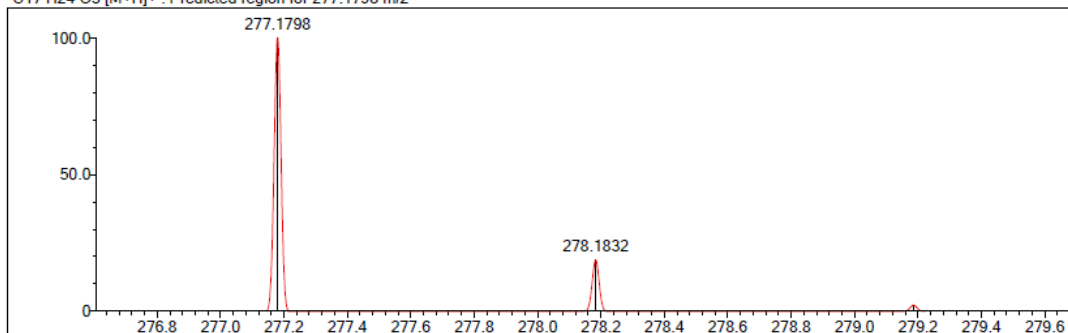
Rank	Score	Formula (M)	Ion	Meas. m/z	Pred. m/z	Df. (mDa)	Df. (ppm)	Iso	DBE
1	64.97	C17 H24 O3	[M+H]+	277.1814	277.1798	1.6	5.77	78.94	6.0

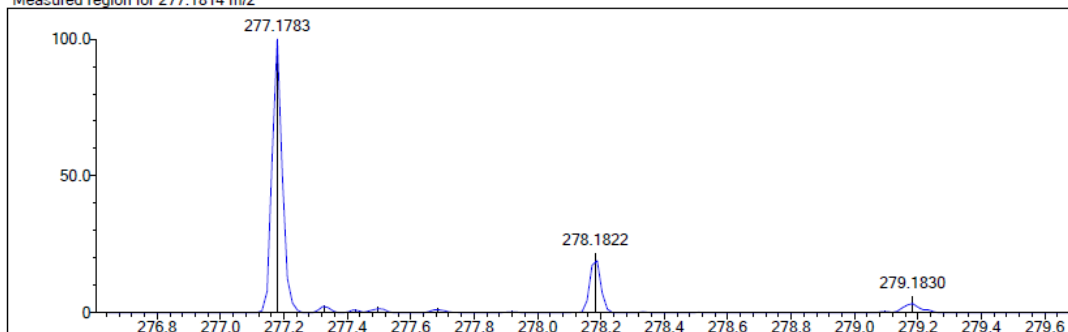# ^{1}H NMR Spectrum of Compound 3f' (Beta-Keto Ester) in CDCl$_3$

0.86
0.88
0.90
1.17
1.19
1.21
1.27
1.34
1.36
2.01
2.02

4.13
4.15
4.17
4.20
4.27
4.30
4.32

7.28
7.47
7.49
7.52
7.58
7.60
7.62
7.99
8.02

3.45
3.20
8.34
2.00
2.03
1.06
2.10
1.02
2.02

ppm
1
2
3
4
5
6
7
8
9

^{13}C NMR Spectrum of Compound 3f' (Beta-Keto Ester) in CDCl$_3$

14.01
22.52
27.59
28.99
29.08
29.69
31.52

54.40

61.28

76.59
77.02
77.22
77.44

128.55
128.70
133.39
136.38

170.10

195.33

ppm
50
100
150

HRMS of Compound 3f'

Event#: 1 MS(E+)   Ret. Time : 0.573 -> 1.160 - 0.347 -> 0.485   Scan# : 87 -> 175 - 53 -> 73
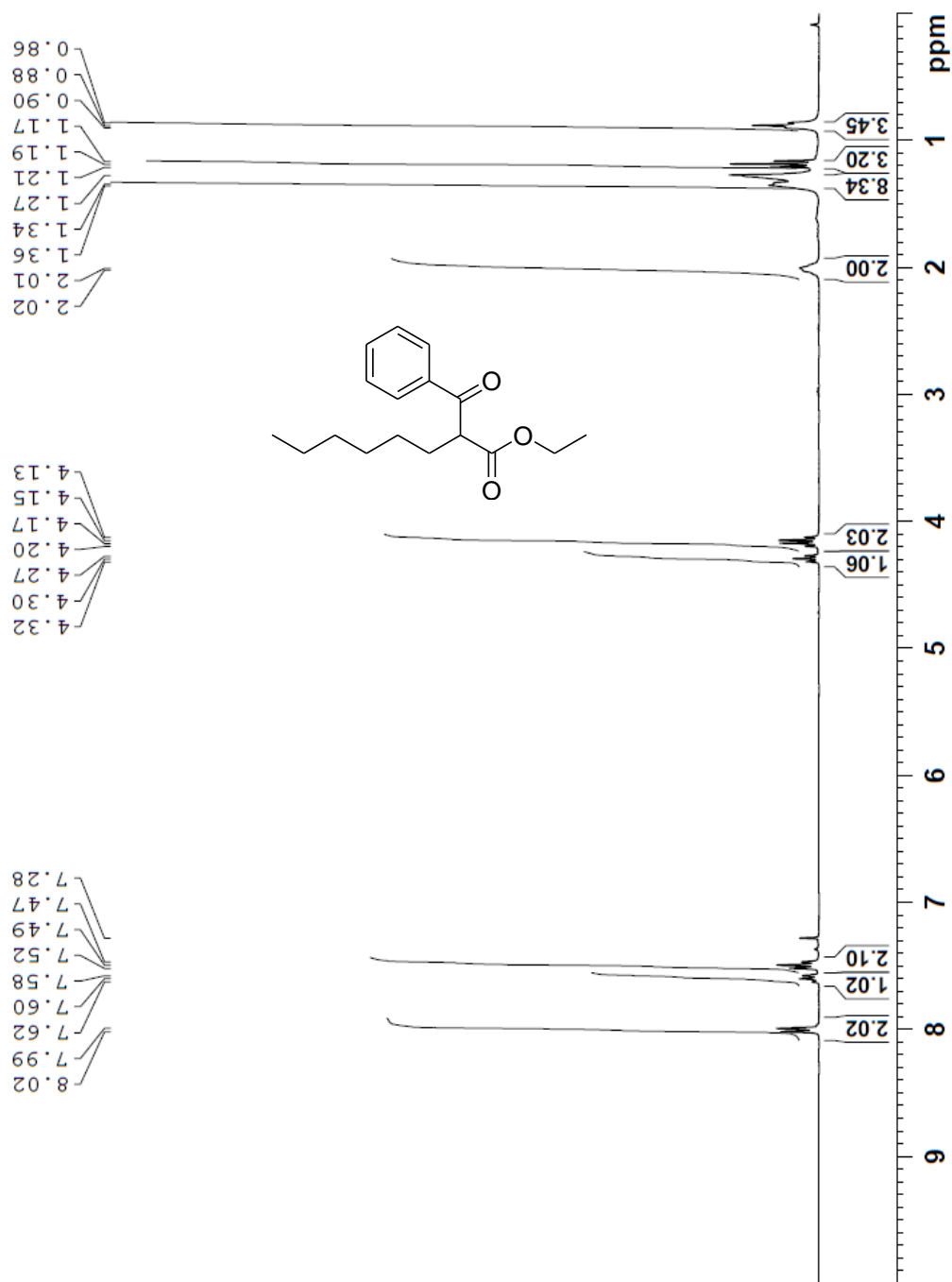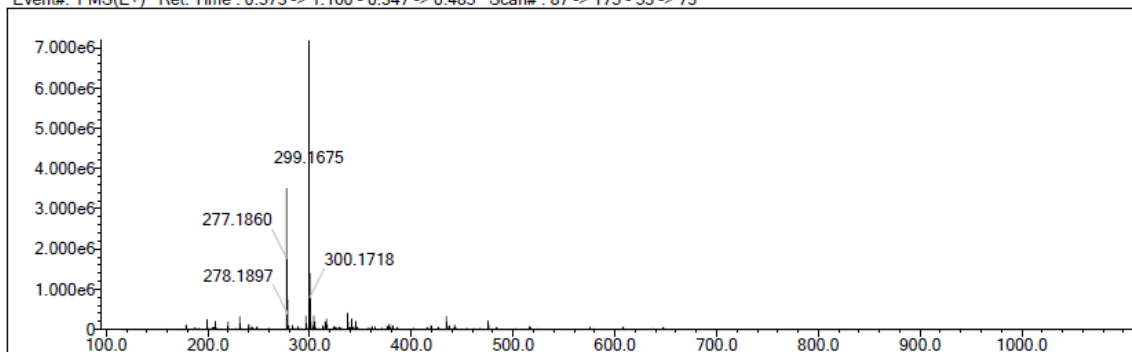

Measured region for 277.1860 m/z

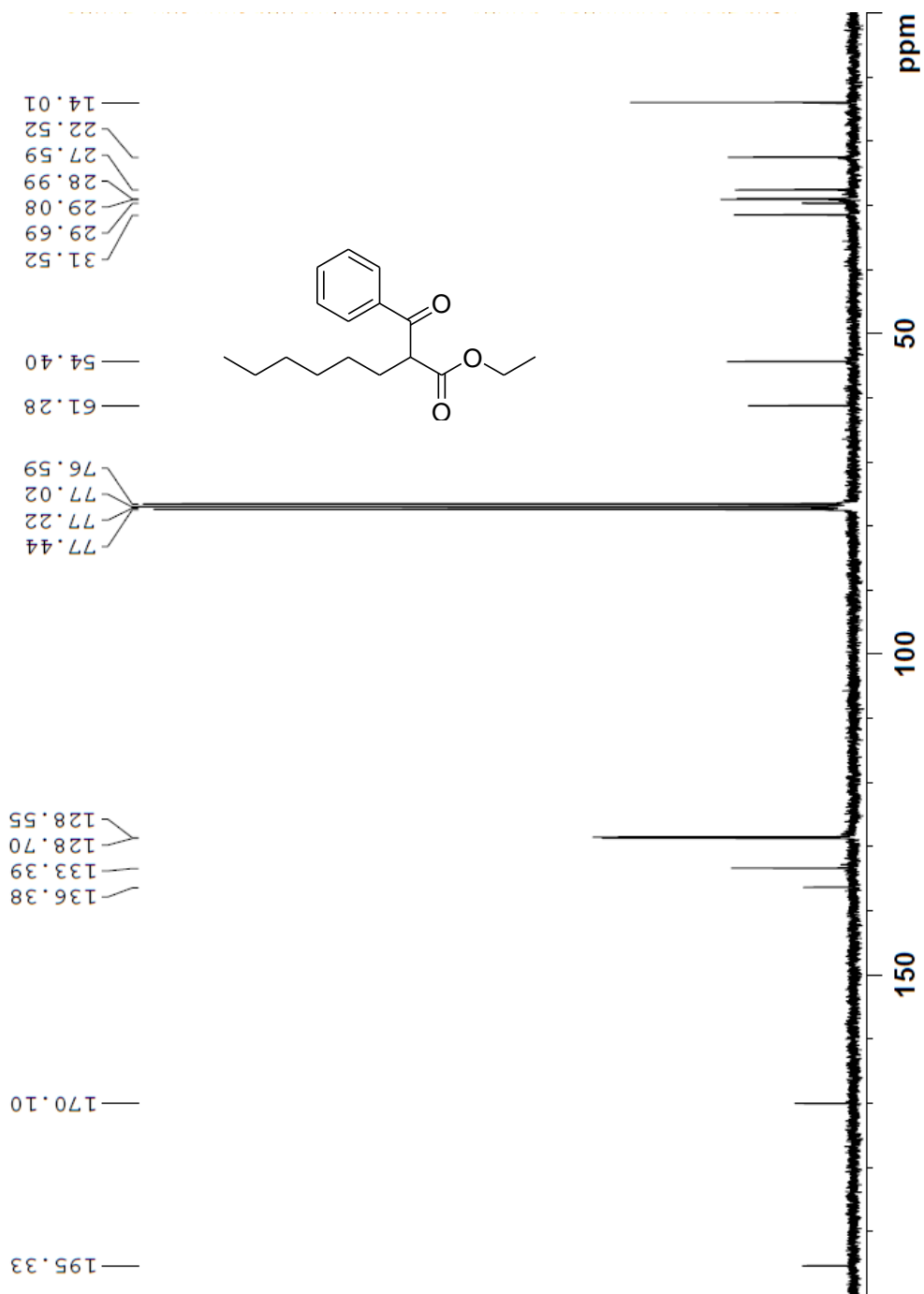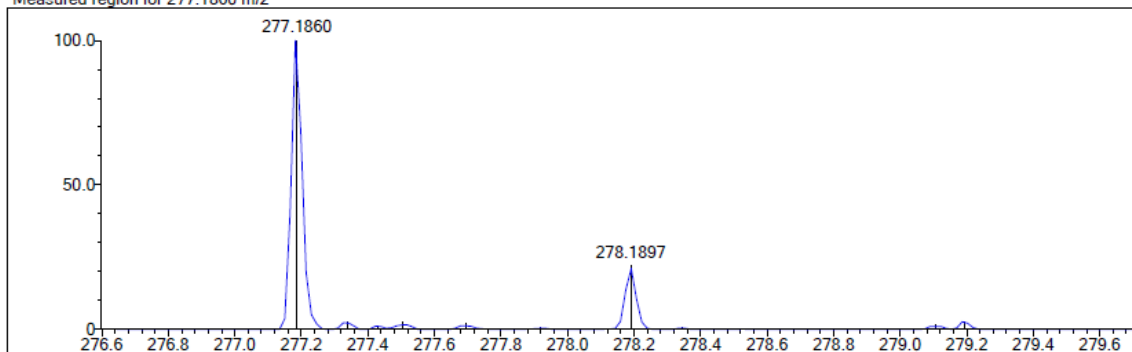C17 H24 O3 [M+H]+ : Predicted region for 277.1798 m/z
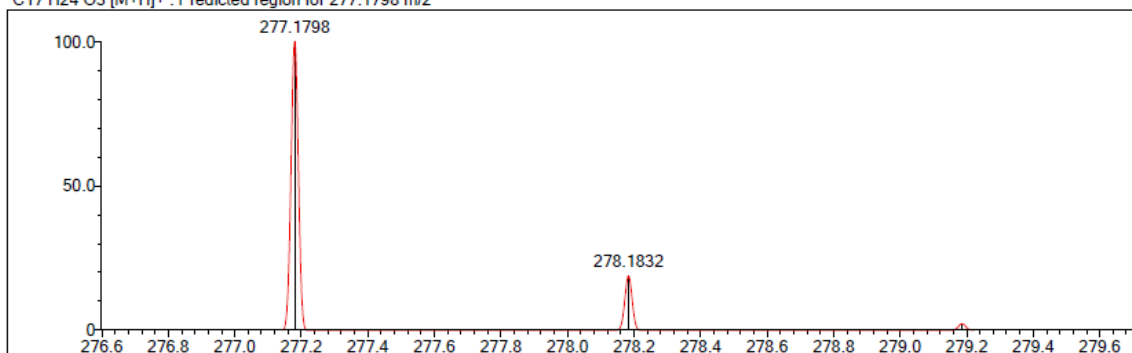
Rank	Score	Formula (M)	Ion	Meas. m/z	Pred. m/z	Df. (mDa)	Df. (ppm)	Iso	DBE
4	4.14	C17 H24 O3	[M+H]+	277.1860	277.1798	6.2	22.37	59.09	6.0

271

¹³C NMR Spectrum of Compound 3g (Keto-Enol Tautomer) in CDCl₃

Peak labels: 0.85, 0.87, 0.89, 1.17, 1.19, 1.23, 1.26, 1.28, 1.31, 1.55, 1.62, 2.09, 2.11, 2.14, 2.46, 2.49, 2.51, 4.15, 4.17, 4.20, 4.22, 4.24, 4.27, 4.73, 7.15, 7.17, 7.28, 7.32, 7.37, 13.18

Integrations: 6.09, 22.45, 4.00, 1.53, 2.32, 3.78, 1.12, 1.53, 8.25, 0.66

ppm axis: 0, 1, 2, 3, 4, 5, 6, 7, 8, 9, 10, 11, 12, 13

^{13}C NMR Spectrum of Compound 3g (Keto-Enol Tautomer) in CDCl$_3$

14.07
14.19
22.55
22.58
23.63
26.66
28.83
28.93
29.10
31.60
32.74
41.60

60.56
61.53
65.02

76.61
77.03
77.46

104.10

126.86
127.95
128.14
128.78
129.43
131.32
132.76
135.19

168.57
172.86
177.19

203.78

ppm

200 150 100 50

HRMS of Compound 3g

Event#: 1 MS(E+)   Ret. Time : 0.600 -> 1.240 - 0.160 -> 0.452   Scan# : 91 -> 187 - 25 -> 69
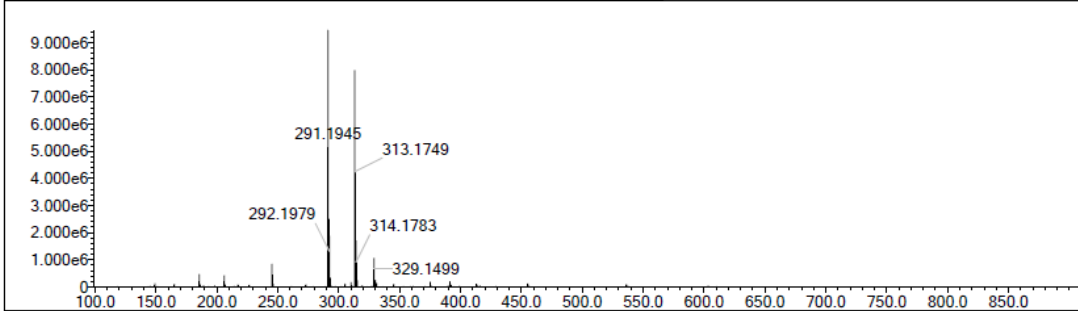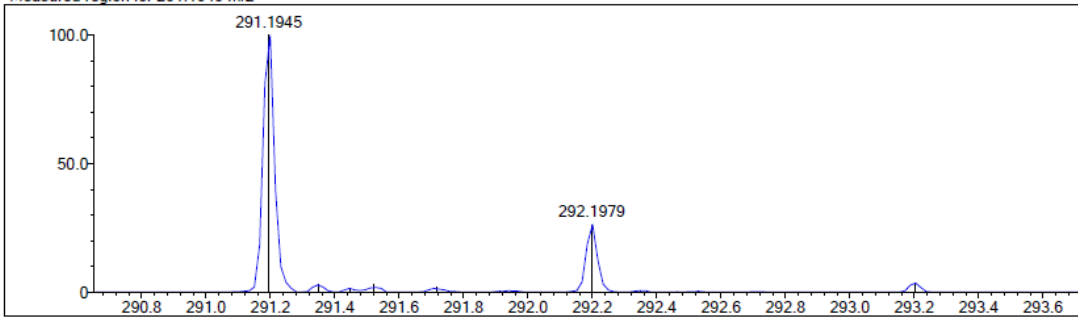
291.1945
313.1749
292.1979
314.1783
329.1499

Measured region for 291.1945 m/z

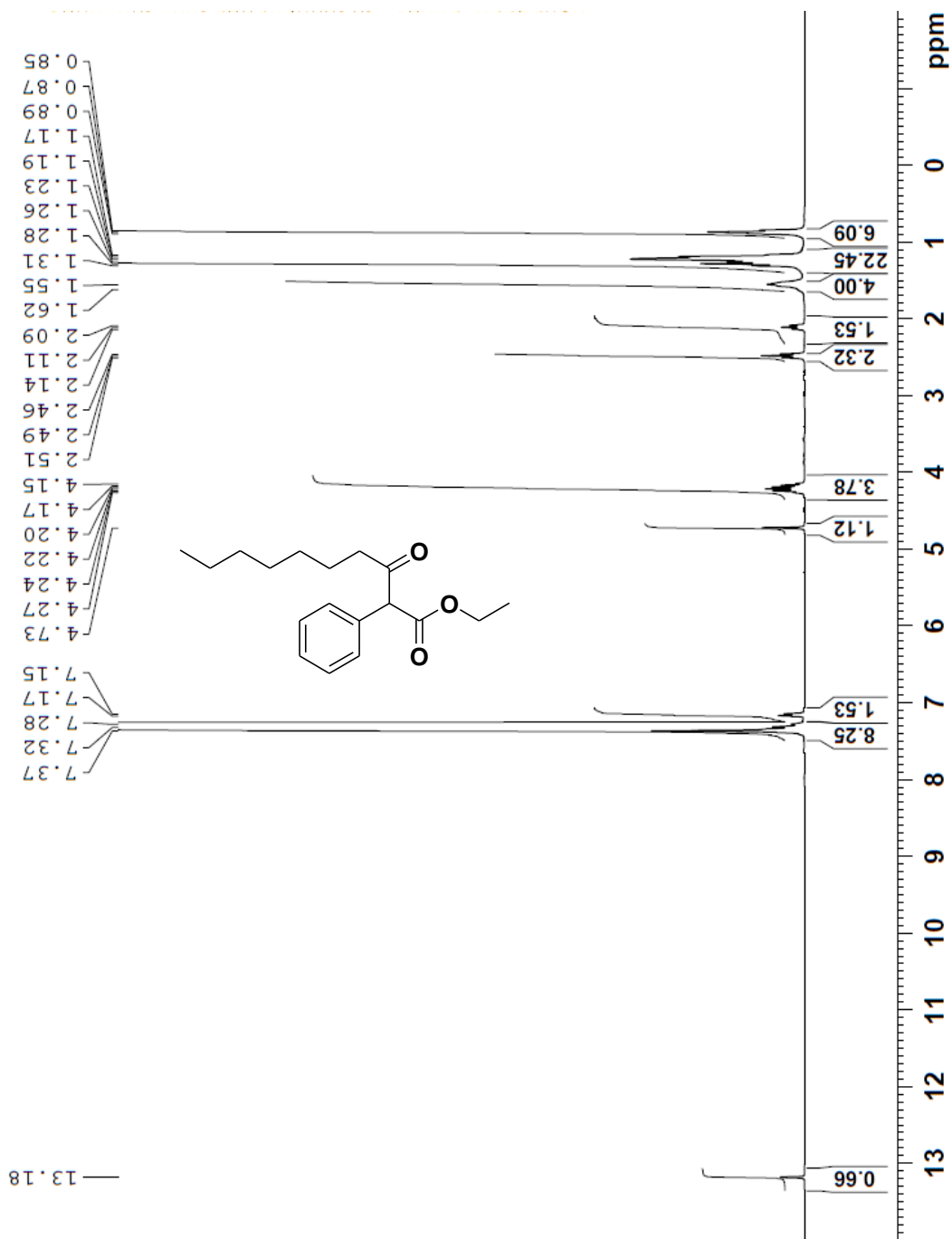291.1945
292.1979

C18 H26 O3 [M+H]+ : Predicted region for 291.1955 m/z
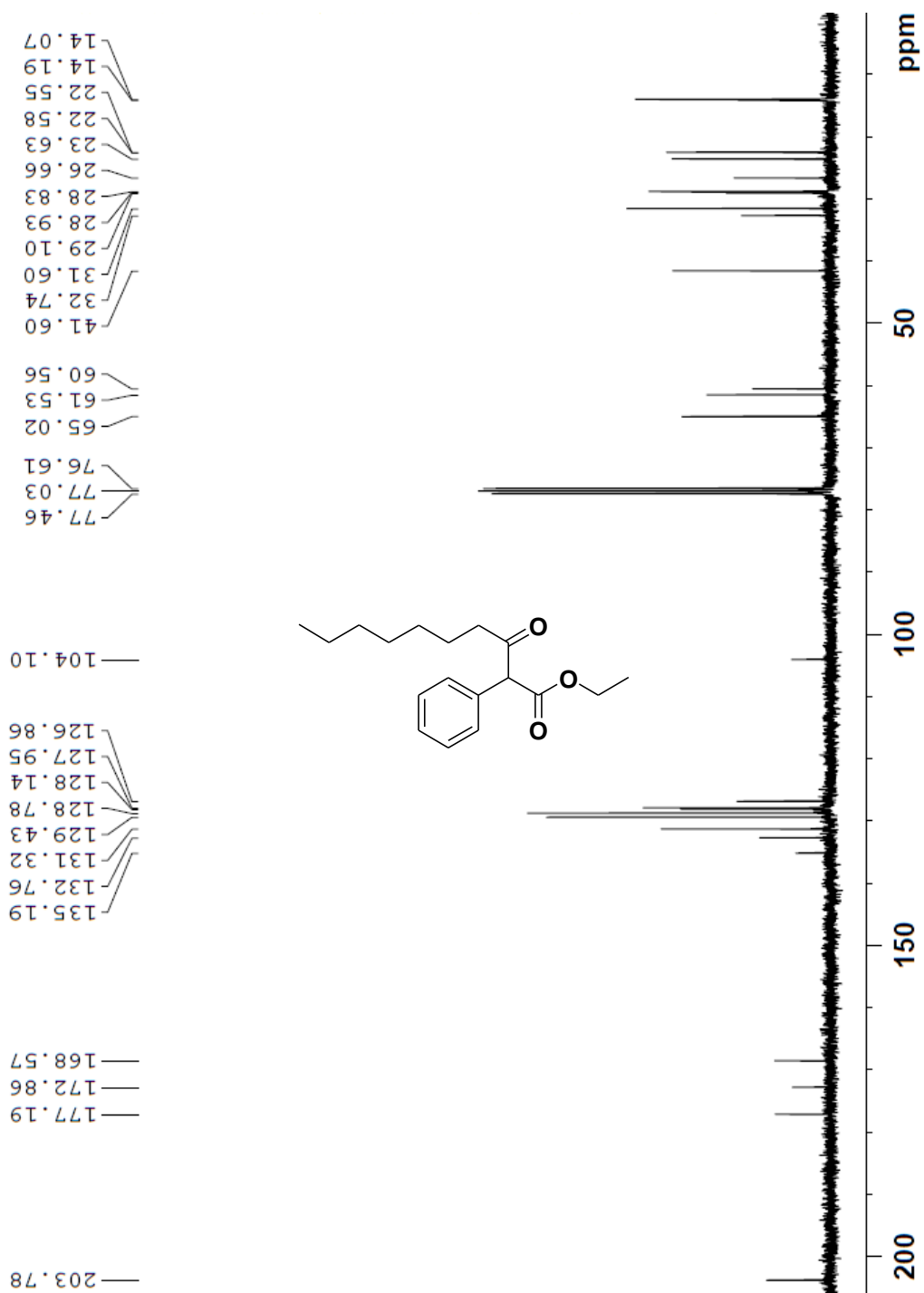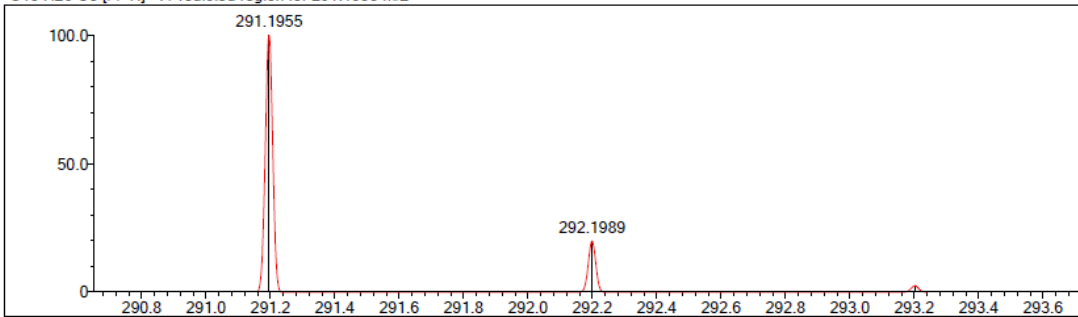
291.1955
292.1989

Rank	Score	Formula (M)	Ion	Meas. m/z	Pred. m/z	Df. (mDa)	Df. (ppm)	Iso	DBE
1	81.20	C18 H26 O3	[M+H]+	291.1945	291.1955	-1.0	-3.43	86.45	6.0

^{1}H NMR Spectrum of Compound 3g' (Beta-Keto Ester) in CDCl$_3$

^{13}C NMR Spectrum of Compound 3g' (Beta-Keto Ester) in CDCl$_3$

13.99
14.04
22.58
27.62
28.98
29.37
31.71

54.39

61.26

76.59
77.02
77.44

128.54
128.69
133.38
136.39

170.09

195.32

ppm
50
100
150

HRMS of Compound 3g'

Event#: 1 MS(E+) Ret. Time : 0.920 -> 1.133 - 0.200 -> 0.338 Scan# : 139 -> 171 - 31 -> 51
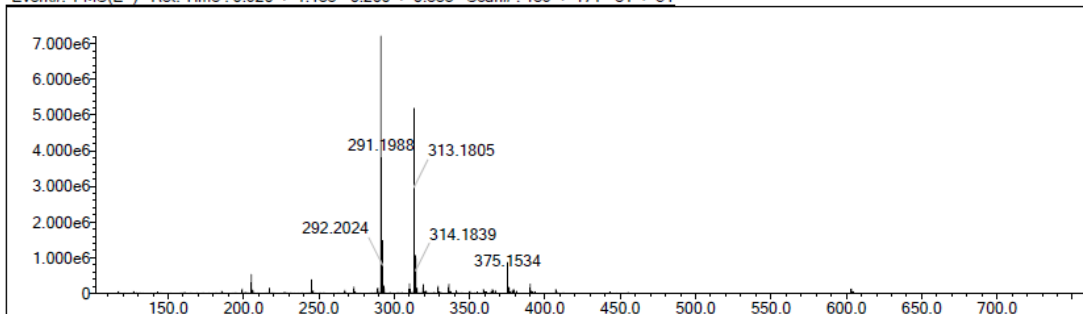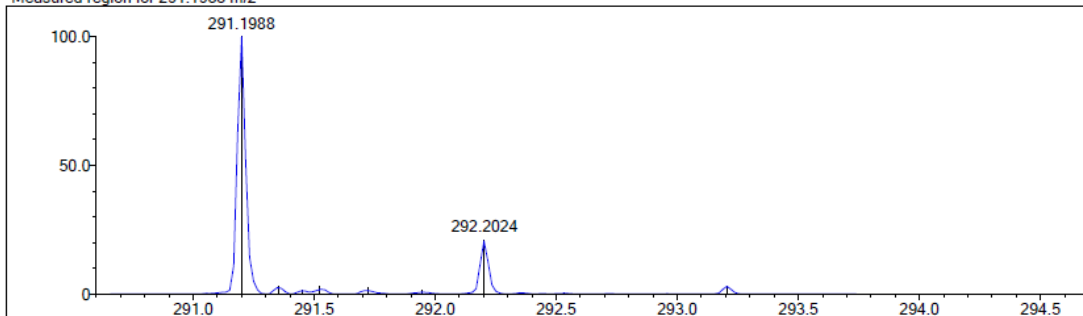
291.1988 313.1805
292.2024 314.1839
375.1534

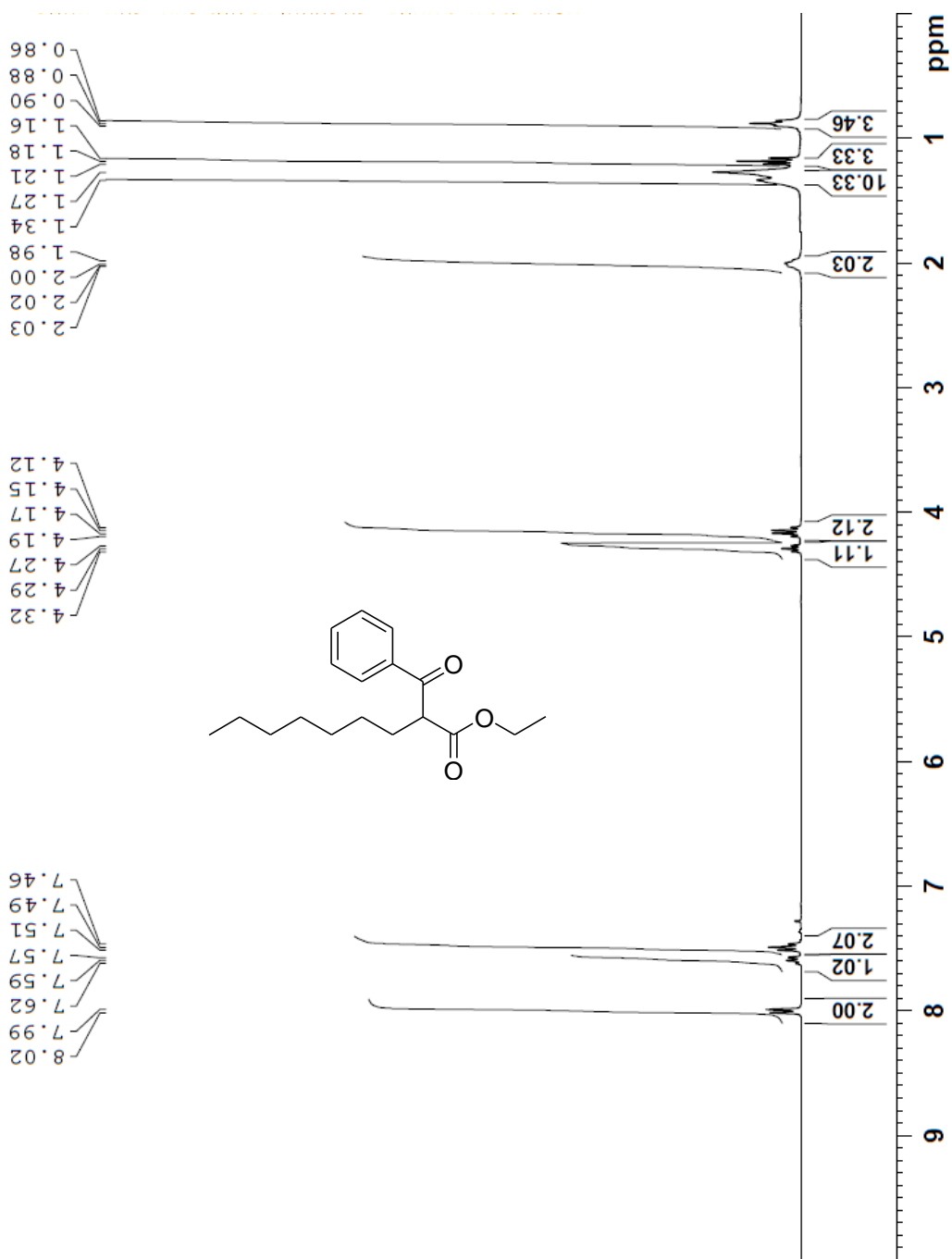Measured region for 291.1988 m/z

291.1988
292.2024

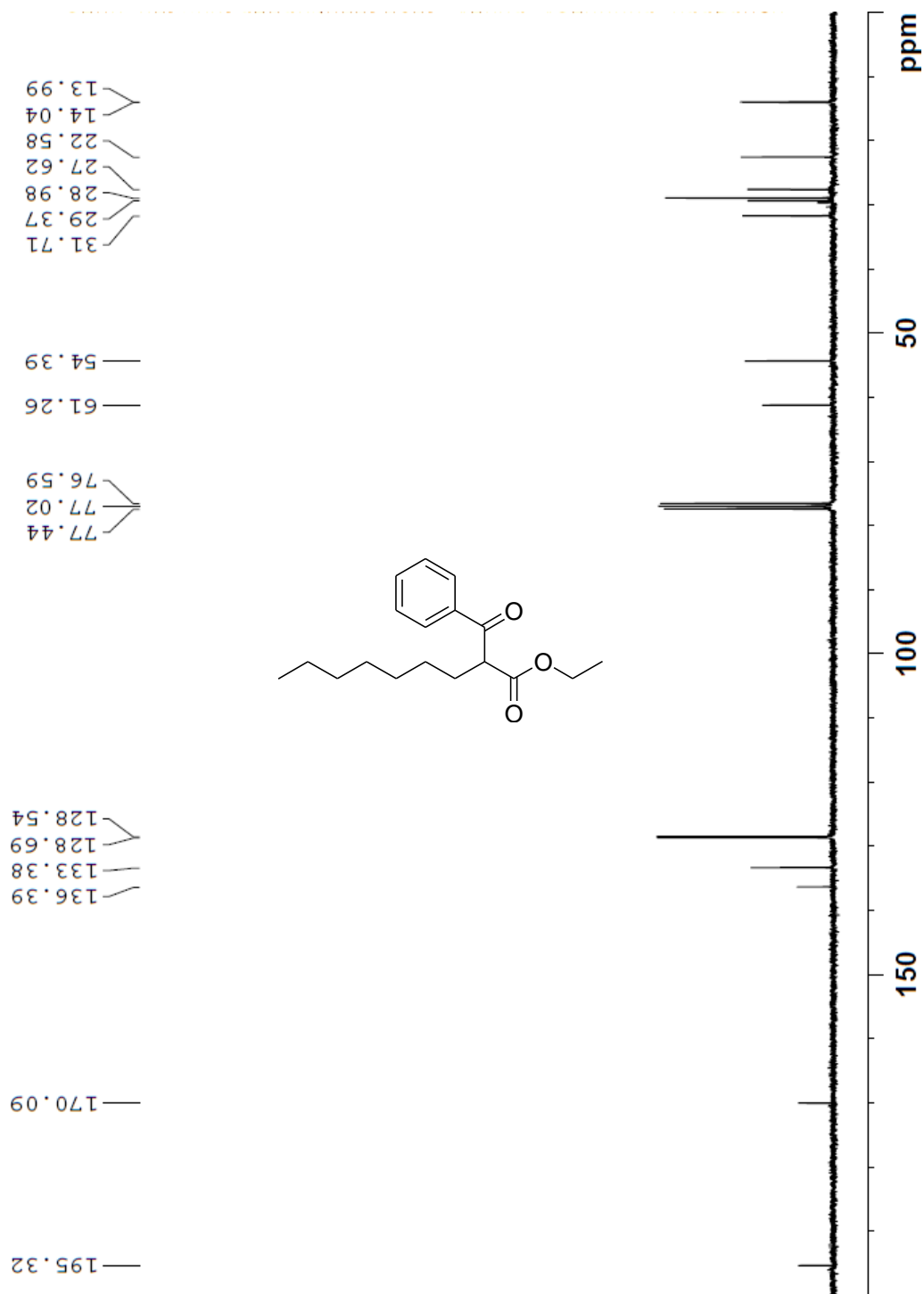C18 H26 O3 [M+H]+ : Predicted region for 291.1955 m/z
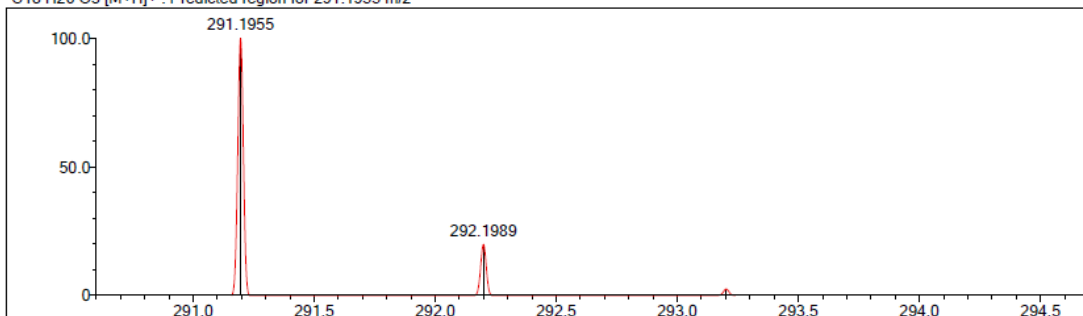
291.1955
292.1989

Rank	Score	Formula (M)	Ion	Meas. m/z	Pred. m/z	Df. (mDa)	Df. (ppm)	Iso	DBE
1	24.36	C18 H26 O3	[M+H]+	291.1988	291.1955	3.3	11.33	66.81	6.0

CURRICULUM VITAE

Mizzanoor Rahaman

Place of Birth: Rajshahi, Bangladesh.

EDUCATION

PhD in Organic Chemistry,

Department of Chemistry and Biochemistry, University of Wisconsin-Milwaukee, USA.

Dissertation Title: "Part I: A Concise Asymmetric Synthesis of Microtubule Inhibitor Tryprostatin B Part II: Synthesis and Biological Assessment of Histone Deacetylase (HDAC) Inhibitors Part III: Acid Catalyzed Reactions of Aromatic Ketones with Ethyl Diazoacetate"

Advisor: Professor M. Mahmun Hossain

MS in Organic Chemistry,

Department of Chemistry, University of Dhaka, Bangladesh.

Thesis: "Synthesis of Potential Bioactive Chromens by the Reaction of Arylideneacetophenones with Cyclic 1, 3-Diketones Using Acid Catalyst"

Advisor: Professor M. Giasuddin Ahmed

Result: First Class, 1st Place

BSc (Honors) in Chemistry,

Department of Chemistry, University of Dhaka, Bangladesh.

Project: "Optimization of Reaction Conditions for the Synthesis of Arylideneacetophenones"

Advisor: Professor M. Giasuddin Ahmed

Result: First Class, 8th Place

AWARDS & HONORS

University of Wisconsin-Milwaukee (UWM) Graduate School's Student Travel Award (2018 and 2019); ACS Milwaukee Section Student Travel Award (2018); Teaching Assistant of the Year Award (Department of Chemistry and Biochemistry, UWM) (2017); Department of Chemistry & Biochemistry Mentoring Travel Award (2016 and 2017); Summer Fellowship (Department of Chemistry & Biochemistry, UWM) (2014-2019); UWM Chancellor's Fellowship (2013-2017); Dr. Maleka-Al Razee Gold Medal for Obtaining Highest Grade in Organic Chemistry in MS, University of Dhaka, Bangladesh (2009).

RESEARCH EXPERIENCE

Experience Includes: Synthesis, Purification, and Characterization of Compounds

Extensive hands-on experience in multiple step organic syntheses using Schlenk lines techniques, glovebox technique, freeze-pump-thaw cycling, microwave reactor. Purification of synthetic compounds by extraction, distillation, crystallization-recrystallization, flash and gravity column chromatography, Yamazen C18 reversed-phase hi-flash column chromatography, preparative TLC, and preparative HPLC. Instrumentation including NMR, chiral HPLC, Shimadzu LCMS, HRMS, GC, FT-IR and UV-visible spectroscopy. Data analysis programs and software including SigmaPlot, ChemDraw, TopSpin, and Waters Breeze 2 HPLC software.

AFFILIATIONS

Member, American Chemical Society (ACS); Member, ACS-Division of Organic Chemistry; Member, Bangladesh Chemical Society (BCS); Member, Bangladesh Chemical and Biochemical Association in North America (BACABANA)

PROFESSIONAL SKILLS

Teaching Assistant: Department of Chemistry & Biochemistry, UWM (2013 to 2019)

Conducted Total 12 Semesters of Undergraduate Level Chemistry Discussions and Labs: Chemical Science (Chem 100), General Chemistry (Chem 102), Introductory Organic Chemistry Laboratory (Chem 342) and Organic Chemistry Laboratory (Chem 344).

Faculty: Bangladesh University of Textiles (2012-2013)

Conducted Undergraduate Level General Chemistry, Organic Chemistry and Lab Sections

Faculty: American International University- Bangladesh (2008-2012)

Conducted Undergraduate Level Introductory Chemistry, General Chemistry and Lab Sections

VOLUNTEER SERVICES

• Mentor, Department of Chemistry & Biochemistry at University of Wisconsin-Milwaukee (UWM) Newly Appointed Teaching Assistants (2016-2017)

• Vice President, Bangladesh Student Association at UWM (2014-2015)

• Judge, UWM Undergraduate Research Symposium (2019)

• Guide, During University Open House of UWM for the New Students and Their Family Members (2016-2017)

PUBLICATIONS

1   **Rahaman, M**.; Hossain, M. M. "Discussion Addendum for: Convenient Preparation of 3-Ethoxycarbonyl Benzofurans from Salicylaldehydes and Ethyl Diazoacetate." *Org. Synth.* **2019**, *96*, 98-109. (DOI: 10.15227/orgsyn.096.0098).

2   Huisman, M.[§]; **Rahaman, M**.[§]; Asad, S.; Oehm, S.; Novin, S.; Rheingold, A. L.; Hossain M. M. "Total Synthesis of Tryprostatin B: Synthesis and Asymmetric Phase-Transfer Catalyzed Reaction of Prenylated Gramine Salt." *Org. Lett.* **2019**, *21*, 134-137. (DOI: 10.1021/acs.orglett.8b03593). **[§]Huisman, M. and Rahaman, M contributed equally.**

3   Uddin, N.; **Rahaman, M**.; Alberch, E.; Asad, S. A.; Hossain M. M.; "Palladium (0)-Catalyzed Rearrangement of Allyl Enol Ether to Form Chiral Quaternary Carbon Center via Asymmetric Allylic Alkylation." *Tetrahedron Lett.* **2018**, *59*, 3401-3404. (DOI: 10.1016/j.tetlet.2018.07.065). **Highlighted** in the *Synfacts* (DOI: 10.1055/s-0037-1610954).

4   Ahmed, M. G; Romman, U. K. R.; Akhter, K.; **Rahaman, M.**; Nahar K. A.; "A One-pot Synthesis of Potential Bioactive Chromens by the Reactions of Aryledeneacetophenones with Cyclic 1, 3-Diketones." *J. Ban. Chem. Soc.* **2011**, *24*, 73-79.

5   **Rahaman, M**.; Hinz, H.; Ali, S.; Jahan, K.; Belayet, J.; Hopper, N.; Majinski, R.; Hossain, M. M. "Reactions of Carbonyl Compounds and Ethyl Diazoacetate: Synthetic Scope and Relative Migratory Aptitude Investigations." [*Manuscript in Preparation*]

6   **Rahaman, M**.; Belayet, J.; Steeber, D.; Frick, K.; Hossain, M. M. "Design, Synthesis and Biological Evaluation of Small, Potent Histone Deacetylase (HDAC) Inhibitors as Anti-Cancer Agents." [*Manuscript in Preparation*]

7   **Rahaman, M**.; Ali, S.; Jahan, K.; Belayet, J.; Hossain, M. M. "Formation of 3-Hydroxy Acrylates and Related *β*-keto esters: Mechanistic Study and Applications in Organic Chemistry (A Review)." [*Manuscript in Preparation*]

8   **Rahaman, M**.; Belayet, J.; Steeber, D.; Frick, K.; Hossain, M. M. "Potent Histone Deacetylase (HDAC) Inhibitors as a Potential Therapeutic Direction for Memory Enhancement in Alzheimer's disease". [*Work on Progress*]

9   **Rahaman, M**.; Jahan, K.; Hossain, M. M. "Alkylation at the C2-Position of the Indole Moiety by Direct Lithiation of the Boc-Protected Gramine". [*Work on Progress*]

10   Ali, S.; **Rahaman, M**.; Asad, S.; Belayet, J.; Hossain, M. M. "Asymmetric Total Synthesis of (-)-Coerulescine via Asymmetric Allylic Alkylation of Acrylates." [*Manuscript in Preparation*]

POSTERS

1   **Rahaman, M**.; Ali, S.; Hinz, D.; Jahan, K.; Belayet, J.; Hopper, N.; Majinski, R.; Hossain, M. M. "Reactions of Carbonyl Compounds and Ethyl Diazoacetate: Synthetic Scope and Mechanism" Poster in National Organic Chemistry Symposium (NOS) at Indiana University-Bloomington (2019).

2   **Rahaman, M**.; Huisman, M.; Hossain, M. M. "A Concise Asymmetric Total Synthesis of Tryprostatin A and B" Poster in 36th Annual Herbert C. Brown Lectures in Organic Chemistry at Purdue University (2019).

3   **Rahaman, M**.; Huisman, M.; Hossain, M. M. "Asymmetric Phase-Transfer Catalyzed Reaction of Prenylated Gramine Salt: Synthesis of Tryprostatin B", Poster in 256th ACS National Meeting & Expo (2018).

4   **Rahaman, M**.; Huisman, M.; Hossain, M. M. "Development and Optimization of Asymmetric Phase-Transfer Catalyzed Reaction of Prenylated Gramine Salt: Synthesis of Tryprostatin B" Poster in Bangladesh Chemical and Biochemical Association in North America (BACABANA) (2018).

5   **Rahaman, M**.; Ulicki, J.; Hossain, M. M. "Synthesis and Biological Evaluation of Histone Deacetylase (HDAC) Inhibitors as Anti-Cancer Agents" Poster in ACS-Milwaukee Section (2018).

6   **Rahaman, M**.; Ulicki, J.; Hossain, M. M. "Histone Deacetylase (HDAC) Inhibitors as Anti-Cancer Agents" Poster in 35th Annual Herbert C. Brown Lectures in Organic Chemistry at Purdue University (2018).

7   **Rahaman, M**. et al. Posters of My Research Outcomes in Annual Research Symposiums at UW-Milwaukee (2015-2019).

PRESENTATIONS

1   **Rahaman, M**. "Total Synthesis of Tryprostatin A and B", Oral Presentation in ACS-Great Lakes Regional Meeting (GLRM) in Lisle, Illinois (2019).

2   **Rahaman, M**. "Palladium Catalyzed Enantioselective C-H Activation in Organic Synthesis" Graduate Student Seminar, Department of Chemistry & Biochemistry, University of Wisconsin-Milwaukee (2014).